CHAPTER SEVEN

PLUTONIUM

David L. Clark, Siegfried S. Hecker, Gordon D. Jarvinen, and Mary P. Neu

7.1 INTRODUCTION

The element plutonium occupies a unique place in the history of chemistry, physics, technology, and international relations. After the initial discovery based on submicrogram amounts, it is now generated by transmutation of uranium in nuclear reactors on a large scale, and has been separated in ton quantities in large industrial facilities. The intense interest in plutonium resulted from the dual-use scenario of domestic power production and nuclear weapons – drawing energy from an atomic nucleus that can produce a factor of millions in energy output relative to chemical energy sources. Indeed, within 5 years of its original synthesis, the primary use of plutonium was for the release of nuclear energy in weapons of unprecedented power, and it seemed that the new element might lead the human race to the brink of self-annihilation. Instead, it has forced the human race to govern itself without resorting to nuclear war over the past 60 years. Plutonium evokes the entire gamut of human emotions, from good to evil, from hope to despair, from the salvation of humanity to its utter destruction. There is no other element in the periodic table that has had such a profound impact on the consciousness of mankind.

In 2005, approximately 2000 metric tons of plutonium exist throughout the world in the form of used nuclear fuel, nuclear weapons components, various nuclear inventories, legacy materials, and wastes (Albright and Kramer, 2004). This number grows every year by 70 to 75 metric tons through production in

irradiated nuclear fuels (Albright and Kramer, 2004). It is clear that the large inventories of plutonium must be prudently managed for many centuries. A complex blend of global political, socioeconomic, and technological challenges must be dealt with to manage these inventories efficiently and safely.

From physical, chemical, and technological perspectives, plutonium is one of the most complex and fascinating elements in the periodic table. The metal exhibits six solid allotropes at ambient pressure and its phases are notoriously unstable with temperature, pressure, chemical additions, and time. With little provocation, the metal can change its density by as much as 25%. It can be as brittle as glass or as malleable as aluminum; it expands when it solidifies, and its freshly machined surface will tarnish in minutes. It is highly reactive in air, has five chemical oxidation states (six if the metal is included), and can form numerous compounds and complexes in the environment and during chemical processing. Plutonium's continuous radioactive decay causes self-irradiation damage of the metal lattice, or modification of solutions containing plutonium ions. Plutonium sits near the middle of the actinide series, which marks the emergence of 5f electrons in the valence shell. Elements to the left of plutonium have delocalized (bonding) electrons, while elements to the right of plutonium exhibit more localized (nonbonding) character. Plutonium is poised in the middle, and in the δ-phase metal, the electrons seem to be in a unique state of being neither fully bonding nor localized, a property that leads to novel electronic interactions and unusual physical and chemical behavior. This position in the periodic table challenges our understanding of relativistic electronic interactions and the nature of chemical bonding in heavy element metals, compounds, and complexes. When the unique nuclear properties are also considered, the study of plutonium is inherently multidisciplinary in nature. The present discussion will be confined to the most recent aspects of the subject. Reviews describing aspects of the chemistry and physics of plutonium can be found by Keller (1971), Cleveland (1979), Wick (1980), Cooper and Schecker (2000), Hecker (2003), Hecker *et al.* (2004), and in the *Gmelin Handbook of Inorganic Chemistry* (Koch, 1972, 1976a,b).

7.2 HISTORICAL

When the first of the transuranium elements, neptunium (Chapter 6) was discovered, it was realized that the radioactive β decay of $^{239}_{93}$Np should lead to the formation of element 94. The scale of the experiments at that time, however, precluded its identification. Plutonium was first produced late in 1940 by Seaborg, McMillan, Kennedy, and Wahl (Seaborg *et al.*, 1946, 1949a) by bombarding uranium with deuterons to produce the isotope ^{238}Pu:

$$^{238}_{92}\mathrm{U} + {}^{2}_{1}\mathrm{H} \rightarrow {}^{238}_{93}\mathrm{Np} + 2\,{}^{1}_{0}\mathrm{n} \tag{7.1}$$

$$^{238}_{93}\mathrm{Np} \xrightarrow[2.1\mathrm{d}]{\beta^-} {}^{238}_{94}\mathrm{Pu}\ (t_{1/2} = 87.7\,\text{years}) \tag{7.2}$$

The short half-life of ^{238}Pu was conducive to tracer studies, and allowed Seaborg, Wahl, and Kennedy to obtain enough chemical information for subsequent separation and isolation of other plutonium isotopes. The isotope of major importance, ^{239}Pu, was discovered in 1941. Bombardment of $^{238}_{92}$U by neutrons produced $^{239}_{92}$U, which decayed to $^{239}_{93}$Np, and ultimately to $^{239}_{94}$Pu:

$$^{238}_{92}\mathrm{U} + {}^{1}_{0}\mathrm{n} \rightarrow {}^{239}_{92}\mathrm{U} + \gamma \tag{7.3}$$

$$^{239}_{92}\mathrm{U} \xrightarrow[23.5\ \mathrm{min}]{\beta^-} {}^{239}_{93}\mathrm{Np} \xrightarrow[2.36\,\mathrm{days}]{\beta^-} {}^{239}_{94}\mathrm{Pu}\,(t_{1/2} = 24,110\ \text{years}) \tag{7.4}$$

In 1941 Kennedy, Seaborg, Segré, and Wahl established the fissionability of ^{239}Pu with slow neutrons (Kennedy *et al.*, 1941). This crucial experiment revealed the potential of ^{239}Pu as a nuclear energy source. In March 1942, element 94 was christened 'plutonium' with the chemical symbol 'Pu' (Seaborg and Wahl, 1948a). Plutonium was named after the planet Pluto, following the pattern used in naming neptunium.

In August 1942, Cunningham and Werner, working at the wartime Metallurgical Laboratory at the University of Chicago, succeeded in isolating about 1 μg of $^{239}_{94}$Pu, which was prepared by cyclotron irradiation of 90 kg of uranyl nitrate (Cunningham and Werner, 1949a). This experiment made plutonium the first man-made element to be obtained (as Pu(IV) iodate) in a visible quantity. These same investigators carried out the first weighing of this man-made element using a larger sample size of 2.77 μg, on September 10, 1942.

Plutonium is now produced in much larger quantities than any other synthetic element. The large wartime chemical separation plant at Hanford, Washington, was constructed on the basis of investigations performed on the ultramicro chemical scale of investigation. The scale-up between ultramicro chemical experiments and the final Hanford plant corresponds to a factor of about 10^{10} (Seaborg, 1958). Seaborg and Cunningham give detailed first-hand accounts of the early history of plutonium in the *Proceedings of the 1963 Plutonium Chemistry Symposium* (1963). More recent descriptions of this fascinating history have been given by Seaborg (1977, 1978, 1979, 1980, 1983, 1992, 1995), Seaborg and Katz (1990), Seaborg and Loveland (1990), and by Hoffman *et al.* (2000).

7.3 NUCLEAR PROPERTIES

Numerous isotopes of plutonium have been synthesized, all of which are radioactive. These are listed in Table 7.l. The most recent isotope to be discovered is ^{231}Pu, which was reported in 1999 (Laue *et al.*, 1999). For data on nuclear masses the reader is referred to the compilation by Audi and Wapstra (1995),

Table 7.1 *Radioactive decay properties of plutonium isotopes*[a].

Mass number	*Half-life*	*Mode of decay*	*Main radiations* (MeV)	*Method of production*
228	1.1 s	α	α 7.772	^{198}Pt(^{34}S,4n)
229	–	α	α 7.460	^{207}Pb(^{26}Mg,4n)
230	2.6 min	EC, α	α 7.055	^{208}Pb(^{26}Mg,4n)
231	8.6 min	EC 90% α 10%	α 6.72	^{233}U(^{3}He,5n)
232	33.1 min	EC ≥80% α ≤20%	α 6.600 (62%) 6.542 (38%)	^{233}U(α,5n)
233	20.9 min	EC 99.88% α 0.12%	α 6.30 γ 0.235	^{233}U(α,4n)
234	8.8 h	EC 94% α 6%	α 6.202 (68%) 6.151 (32%)	^{233}U(α,3n)
235	25.3 min	EC >99.99% α 3×10^{-3}%	α 5.850 (80%) γ 0.049	^{235}U(α,4n)
236	2.858 yr 1.5×10^{9} yr	α SF 1.37×10^{-7}%	α 5.768 (69%) 5.721 (31%)	^{235}U(α,3n) ^{236}Np daughter
237	45.2 d	EC >99.99% α 4.24×10^{-3}%	5.356 (∼17.2%) 5.334 (∼43.5%)18 γ 0.059	^{235}U(α,2n) ^{237}Np(d,2n)
238	87.7 yr 4.77×10^{10} yr	α SF 1.85×10^{-7}%	α 5.499 (70.9%) 5.456 (29.0%)	^{242}Cm daughter ^{238}Np daughter
239	2.411×10^{4} yr 8×10^{15} yr	α SF 3.0×10^{-10}%	α 5.157 (70.77%) 5.144 (17.11%) 5.106 (11.94%) γ 0.129	^{239}Np daughter
240	6.561×10^{3} yr 1.15×10^{11} yr	α SF 5.75×10^{-6}%	α 5.168 (72.8%) 5.124 (27.1%)	multiple n capture
241	14.35 yr	β$^-$ >99.99% α 2.45×10^{-3}% SF 2.4×10^{-14}%	α 4.896 (83.2%) 4.853 (12.2%) β$^-$ 0.021 γ 0.149	multiple n capture
242	3.75×10^{5} yr 6.77×10^{10} yr	α SF 5.54×10^{-4}%	α 4.902 (76.49%) 4.856 (23.48%)	multiple n capture
243	4.956 h	β$^-$	β$^-$ 0.582 (59%) γ 0.084 (23%)	multiple n capture
244	8.08×10^{7} yr 6.6×10^{10} yr	α 99.88% SF 0.1214%	α 4.589 (81%) 4.546 (19%)	multiple n capture
245	10.5 h	β$^-$	β$^-$ 0.878 (51%) γ 0.327 (25.4%)	^{244}Pu(n,γ)
246	10.84 d	β$^-$	β$^-$ 0.15 (91%) γ 0.224 (25%)	^{245}Pu(n,γ)
247	2.27 d	β$^-$		multiple n capture

[a] See Appendix II.

and the update by Audi *et al.* (1997). A more detailed description of the nuclear properties of the individual plutonium isotopes may be found in the book by Hyde *et al*. (1964), in the *Table of Isotopes* (Firestone *et al.*, 1996, 1998), and in *Nuclear Data Sheets* (Tuli, 2004). As mentioned above, ^{238}Pu was the first of the plutonium isotopes discovered. Because of its relatively short half-life, it is a particularly useful tracer for plutonium. ^{238}Pu is readily obtained by neutron bombardment of ^{237}Np in the reaction:

$$^{237}\mathrm{Np}(\mathrm{n},\gamma)^{238}\mathrm{Np} \xrightarrow{\beta^-} {}^{238}\mathrm{Pu} \tag{7.5}$$

The ^{238}Pu is chemically separated from unreacted ^{237}Np by ion-exchange techniques (Burney, 1962; Tetzlaff, 1962; Coogler *et al.*, 1963; Burney and Thompson, 1972, 1974). ^{238}Pu may also be obtained from the α decay of ^{242}Cm and subsequent chemical separation from undecayed curium (Thompson, 1972). Because of its power density of 6.8–7.3 W cm^{-3} (specific power 0.57 W g^{-1}), ^{238}Pu has found important applications in radioisotope power systems – nuclear power systems that derive their energy from the spontaneous decay of radionuclides as distinguished from nuclear fission energy created in a nuclear reactor. Most radioisotope power systems utilize ^{238}Pu as an isotope heat source and an energy conversion system to partially transform the heat produced from ^{238}Pu radioactive decay into electricity (Lange and Mastal, 1994).

In the late 1960s, cardiac pacemakers suffered from early battery exhaustion, and the use of nuclear pacemakers whose battery life could outlive the patient was examined (Boucher and Quere, 1981; Pustovalov *et al.*, 1986). The first implantation of a ^{238}Pu-powered nuclear pacemaker was performed in France on April 27, 1970. Since that time, nuclear pacemakers powered by ^{238}Pu were implanted in patients in a number of countries. The overall results of these studies indicated that nuclear pacemakers required fewer follow-up operations and less maintenance, and were found to be safe and reliable. Subsequent advances in electronics in the intervening years rendered the plutonium-powered devices obsolete, and their use was discontinued. In 2004, there were still a number of living patients with ^{238}Pu pacemakers that had been functioning for over 30 years (Parsonnet *et al.*, 1990; Freedberg *et al.*, 1992; Parsonnet, 2004).

The most prevalent application for ^{238}Pu is as an important fuel for heat and power sources for space exploration (Lange and Mastal, 1994; Rinehart, 2001). For space exploration, heat source fuel is normally enriched to 83.5% in the ^{238}Pu isotope, and the oxygen atoms in $^{238}PuO_2$ are enriched in ^{16}O to reduce the neutron emission rate to as low as 6000 n s^{-1} g^{-1} ^{238}Pu. In freshly prepared fuel, the specific power is 0.4743 W g^{-1} Pu or 0.4181 W g^{-1} PuO_2. The ^{238}Pu isotope provides 99.9% of the thermal power in heat source fuel. Radioisotope thermoelectric generators (RTGs) have been used in the United States to provide electrical power for spacecraft since 1961 (Angelo and Buden, 1985). Early ^{238}Pu-fueled power sources employed Space Nuclear Auxiliary Power (SNAP) units to power satellites and remote instrument packages (DOE, 1987;

Lange and Mastal, 1994). SNAP units served as power sources for instrument packages on the five Apollo missions to the Moon, the Viking unmanned Mars Lander, and the Pioneer and Voyager probes to the outer planets (Jupiter, Saturn, Uranus, Neptune and beyond). The SNAP-3B and SNAP-9A systems were fueled with plutonium metal, the SNAP-19 and Transit systems were fueled with $^{238}PuO_2$–molybdenum cermets, and the SNAP-27 unit was fueled with $^{238}PuO_2$ microspheres (Rinehart, 2001). Voyager missions employed Multihundred Watt Radioisotope Thermoelectric Generators (MHW-RTGs) that consisted of 24 100-W heat sources of $^{238}PuO_2$ (Fig. 7.1) each enclosed in an iridium shell, a graphitic impact material, an ablative heat shield, and a thermoelectric material to convert the decay heat to electrical power at a design voltage of 30 V (Kelly, 1975; De Winter *et al.*, 1999).

The current systems employ General Purpose Heat Source-Radioisotope Thermoelectric Generators (GPHS-RTGs) fueled by $^{238}PuO_2$ pellets. Each GPHS consists of a hot-pressed 150 g pellet of $^{238}PuO_2$ encapsulated in an iridium alloy (iridium-0.3% tungsten) container or clad (Fig. 7.2). Each iridium

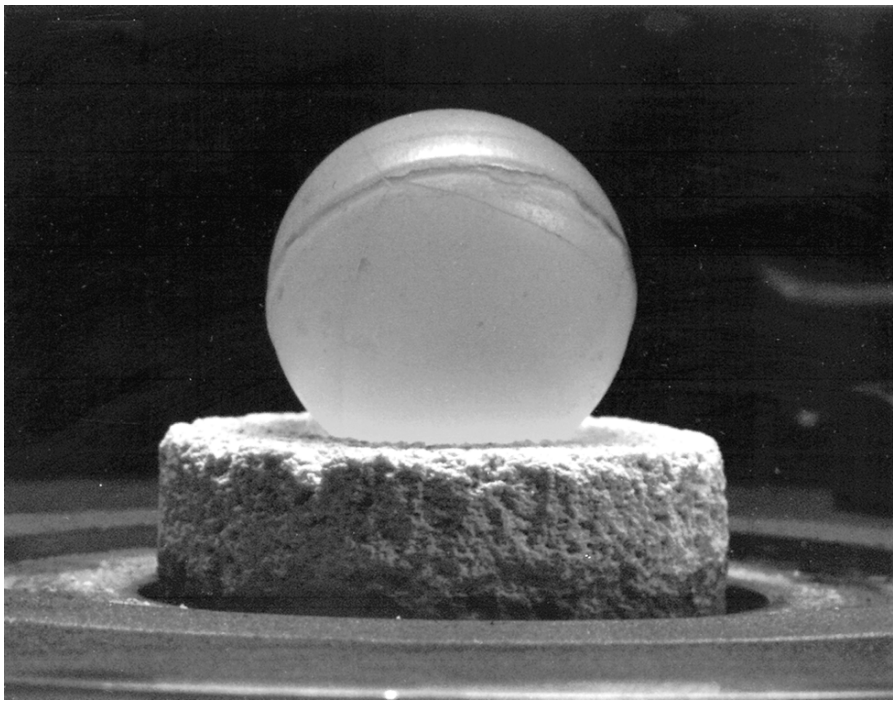

Fig. 7.1 *A* 100 W ^{238}*Pu heat source used in multihundred watt radioisotope thermoelectric generators* (*MHW-RTGs*) *employed in the Voyager space missions. The source contains* 250 g *of* $^{238}PuO_2$ *and was approximately* 3 cm *in diameter. The oxide glowed at red heat after being covered with an insulating ceramic blanket that was removed just before the photograph was taken* (*photograph courtesy of Los Alamos National Laboratory*).

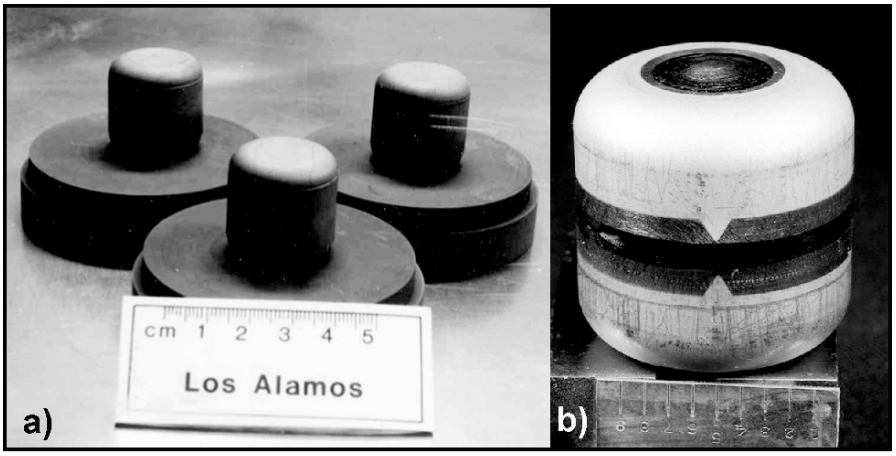

Fig. 7.2 *A modern* ^{238}*Pu general purpose heat source* (*GPHS*). *Hot pressed* 150 g *pellets of* $^{238}PuO_2$ *are* (*a*) *encapsulated in an iridium*-0.3% *tungsten alloy container, which is then encapsulated in* (*b*) *an iridium clad. Each iridium clad contains a sintered iridium powder frit vent designed to release the helium generated by the* α*-particle decay of the fuel. The iridium is compatible with plutonium dioxide at temperatures greater than* 1773 K, *and melts at* 2698 K. *Each GPHS produces* 62.5 *thermal watts* (*photographs courtesy of Los Alamos National Laboratory*).

clad contains a sintered iridium powder frit vent designed to release the helium generated by the α-particle decay of the $^{238}PuO_2$. The heat sources are packed in a tightly woven pierced fabric™ graphite aeroshell assembly that protects the fuel from impact, fire, or atmospheric reentry. The RTG consists of 72 GPHS pellets and a thermoelectric converter. The GPHS-RTGs flown on the Galileo, Ulysses, and Cassini spacecraft (3 RTGs per spacecraft) had a mass of 54 kg of PuO_2 and supplied 285 W of electrical power at the beginning of the mission from 4300 W of ^{238}Pu decay heat (Rinehart, 2001). These plutonium power sources have enabled huge advances in our scientific understanding of the solar system. The Cassini–Huygens spacecraft arrived at Saturn on June 30, 2004, and will provide vast amounts of new scientific data on the Saturnian system in the years to come.

Smaller Light Weight Radioisotope Heater Units (LWRHUs) are also used to maintain spacecraft equipment within their normal operating temperature range (Rinehart, 1992). The LWRHUs are cylindrical fueled clads consisting of a hot-pressed, 2.67 g pellet of $^{238}PuO_2$ encapsulated in a Pt-30%Rh container with a sintered platinum powder frit vent to release helium as shown in Fig. 7.3. As in the GPHS, the capsules are contained in a pyrolytic graphite insulator and aeroshell assembly (Rinehart, 2001). These smaller heater units have been employed on the Pioneer 10 and 11, Galileo, Mars Pathfinder, Mars Exploration Rovers (Spirit and Opportunity), and Cassini spacecraft, and are planned for use in many future missions.

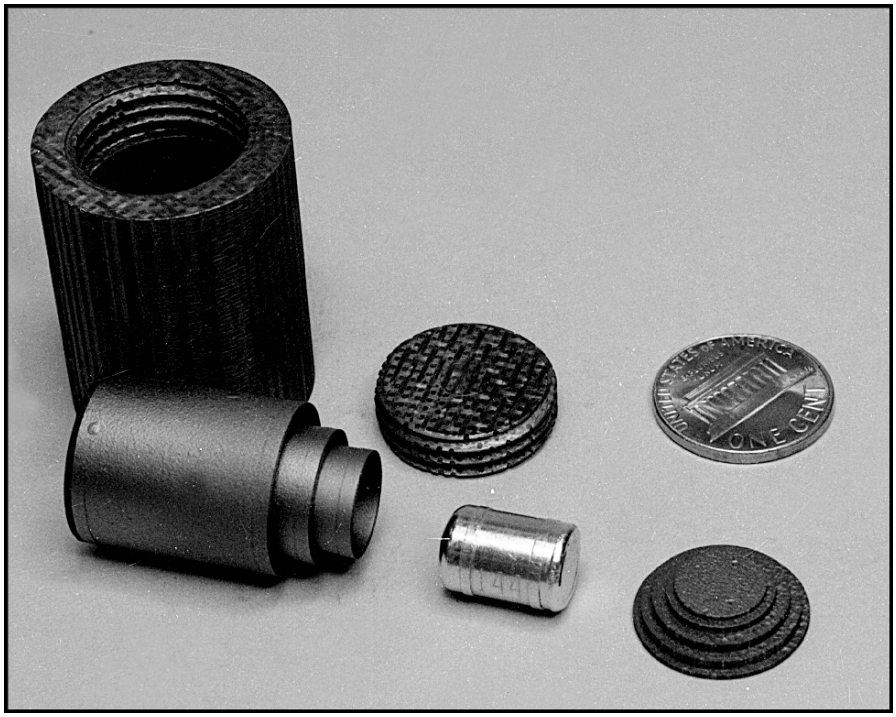

Fig. 7.3 *A* ^{238}*Pu lightweight radioisotope heater unit* (*LWRHU*) *before final assembly. The heat source consists of a fine weave pierced fabric graphite aeroshell, three inner layers of pyrolytic graphite thermal insulators, and a Pt-30% Rh-fueled clad containing a hot pressed* 2.67 g *pellet of* $^{238}PuO_2$ *that produces* 1 *thermal watt. The aeroshell serves as the primary heat shield to protect the interior components from aerodynamic forces and thermal heating during accidental atmospheric reentry as well as protecting the fueled clad from mechanical loads during ground impact. The pyrolytic graphite sleeves and plugs serve as thermal shields to keep the fueled clad from melting during an accidental reentry in the atmosphere* (*photograph courtesy of Los Alamos National Laboratory*).

Plutonium-239 is the most important isotope of plutonium. Its half-life (24,110 years) is sufficiently long to permit the preparation of this isotope in large-scale amounts, and to make it feasible to carry out conventional scientific studies. ^{239}Pu has a high cross-section for fission with slow neutrons, and is the isotope that serves as nuclear fuel for both nuclear power and nuclear weapons. By far the greatest portion of the knowledge of the chemical and physical properties of plutonium has been acquired by the use of ^{239}Pu. While its half-life is long enough to permit chemical studies, it is still short enough to present serious problems in handling. These difficulties are discussed in some detail below (Section 7.6). ^{239}Pu has a specific power of 2.2×10^{-3} W g^{-1}. In handling large quantities of ^{239}Pu, the criticality hazard caused by its fissionability becomes an additional problem. Amounts as small as 500 g may become critical

Table 7.2 *Minimum critical parameters of common forms of pure ^{239}Pu (Clark, 1981).*

metal	mass plutonium (kg)	5.0
	cylinder diameter (cm)	4.4
	slab thickness (cm)	0.65
oxide	mass plutonium (kg)	10.2
	mass PuO_2 (kg)	11.5
	cylinder diameter (cm)	7.2
	slab thickness (cm)	1.4
aqueous plutonium nitrate solution		
	plutonium mass (kg)	0.480
	concentration (g Pu L^{-1})	7.3
	H/Pu atomic ratio	3630
	cylinder diameter (cm)	15.4
	volume (L)	7.3

under certain conditions. In Table 7.2 some minimum critical parameters for pure ^{239}Pu obtained in various configurations have been summarized (Clark, 1981). Additional safety and criticality data are available in the compilations by Paxton (1975), Clark (1981), Knief (1985), and Paxton and Pruvost (1987).

The higher plutonium isotopes are formed as a result of successive neutron capture by the various plutonium isotopes:

$$^{239}\mathrm{Pu}(\mathrm{n},\gamma)^{240}\mathrm{Pu}(\mathrm{n},\gamma)^{241}\mathrm{Pu}(\mathrm{n},\gamma)\ \text{etc.} \tag{7.6}$$

The isotopic composition of plutonium produced in a nuclear reactor will therefore vary according to the length of time the plutonium formed is allowed to remain in the neutron flux. From this perspective it is noteworthy that the heavier isotopes ^{244}Pu, ^{245}Pu, and ^{246}Pu were originally discovered in the coral debris of the Mike thermonuclear test conducted in 1952, due to the extremely high neutron fluxes of the event. Hoffman, Ghiorso, and Seaborg described the events that led to the discoveries of these isotopes (Hoffman *et al.*, 2000). When ^{239}Pu targets were irradiated in a high-flux reactor to more than 90% burn-up, the residual plutonium was found to consist mainly of the higher isotopes ^{242}Pu and some ^{244}Pu. Many of the complications arising from the use of the relatively short-lived ^{239}Pu can be greatly ameliorated by the use of these long-lived isotopes of plutonium for fundamental scientific study.

Isotopically pure ^{240}Pu, ^{241}Pu, ^{242}Pu, and ^{244}Pu have become available from various sources. ^{240}Pu may readily be obtained by chemical separation from old ^{244}Cm samples. All the heavier plutonium isotopes have also been isotopically separated by electromagnetic separation in the Y-12 calutron plant in Oak Ridge (Love *et al.*, 1961; Love, 1973), but presently these calutrons have been placed in a standby condition. Gram quantities of these isotopes with isotopic purity above 99% were available from such separations. Russian scientists have

also been very successful in producing research quantities of higher plutonium isotopes using electromagnetic mass separation. Ultrapure ^{236}Pu and ^{237}Pu have been produced by Dmitriev and coworkers at the Joint Institute for Nuclear Research in Moscow (Dmitriev *et al.*, 1993, 1995, 1997), and Vesnovskii and Polynov at the Institute of Experimental Physics in Arzamas have been able to produce milligram to gram quantities of ^{240}Pu, ^{241}Pu, ^{242}Pu, and ^{244}Pu at greater than 99% isotopic purity (Vesnovskii and Polynov, 1992a,b). Milligram quantities of ^{244}Pu have been prepared at the IAEA Safeguards Analytical Laboratory in Austria using electromagnetic separation (Deron and Vesnovskii, 1999) and by selective ionization using a pulsed laser beam in Japan (Sasao and Yamaguchi, 1991).

The higher isotopes of plutonium possess interesting nuclear properties, which cannot be discussed in detail here. For further information see Hyde *et al.* (1964).

7.4 PLUTONIUM IN NATURE

Traces of plutonium are found all over the world, predominantly due to 'man-made' plutonium. In addition, two isotopes of plutonium (^{239}Pu and ^{244}Pu) can be found that are 'natural' in origin. Natural ^{239}Pu is produced in nature by nuclear processes occurring in uranium ore bodies, and minute traces of ^{244}Pu exist in nature as remnants of primordial stellar nucleosynthesis.

The presence of small amounts of plutonium in uranium of natural origin was first established in 1942 by Seaborg and Perlman (1948) and by Garner *et al.* (1948). These researchers were able to show that Canadian pitchblende and Colorado carnotite both contain a small amount of alpha activity due to a plutonium isotope, presumed to be ^{239}Pu at the time. Peppard *et al.* (1951) and Levine and Seaborg (1951) conclusively demonstrated the existence of ^{239}Pu in nature. Levine and Seaborg determined the plutonium content of a number of uranium ores, and Peppard and coworkers isolated microgram amounts of ^{239}Pu from uranium process wastes. Recent high-resolution thermal ionization mass spectrometry analyses of plutonium in uranium ore bodies have been described by Curtis *et al.* (1999) and by Dixon *et al.* (1997). The concentrations of plutonium in uranium ore bodies are collected in Table 7.3. No plutonium isotopes other than ^{239}Pu have been conclusively found in any of these experiments. More recently, ^{239}Pu has also been detected in granites from deep boreholes in Germany, and in salt brines from deep boreholes in the United States (Ganz *et al.*, 1991). Alpha pulse analysis and high-resolution mass spectrometry have been the experimental methods of choice for characterization of the isotopic composition of plutonium isolated from natural sources.

With the exception of the very long-lived ^{244}Pu, the half-lives of plutonium isotopes are so short that it is most unlikely that any plutonium except ^{244}Pu

Table 7.3 *Content of plutonium in natural uranium ore deposits.*

Ore	*Uranium content* (wt.%)	*Ratio* ^{239}Pu/U ($\times 10^{12}$)	*References*
Cigar Lake U deposit	31	6.4	Curtis *et al.* (1999)
Beaverlodge U deposit	7.09	14.3	Dixon *et al.* (1997)
Canadian pitchblende	13.5	7.1	Levine and Seaborg (1951)
Belgian Congo pitchblende	38	12	Levine and Seaborg (1951)
Colorado pitchblende	50	7.7	Levine and Seaborg (1951)
Brazilian monazite	0.24	8.3	Levine and Seaborg (1951)
N. Carolina monazite	1.64	3.6	Levine and Seaborg (1951)
Colorado furgusonite	0.25	<4	Levine and Seaborg (1951)
Colorado carnotite	10	<0.4	Levine and Seaborg (1951)

could have survived in nature from primordial times. It is overwhelmingly likely that ^{239}Pu arises in nature by nuclear reactions with ^{238}U and represents a steady-state concentration:

$$^{238}\mathrm{U}(\mathrm{n},\gamma)^{239}\mathrm{U} \xrightarrow{\beta^-} {}^{239}\mathrm{Np} \xrightarrow{\beta^-} {}^{239}\mathrm{Pu} \tag{7.7}$$

Neutrons necessary for the formation of ^{239}Pu from ^{238}U may arise from spontaneous fission of ^{238}U; by neutron multiplication in ^{235}U; from (α,n) reactions caused by the action of α particles (from the radioactive decay of uranium and daughters) on the nuclei of light elements in the ore (Li, B, Be, F, O, Si, Mg); and neutrons produced by cosmic rays. The neutrons from cosmic rays appear to be of negligible importance, since the neutron production from uranium by the capture of μ mesons is considerably less than 0.1% of the neutrons arising from spontaneous fission (Littler, 1952). Spontaneous fission in uranium occurs at the rate of (24.2 ± 0.5) fissions per gram per hour, which produces a neutron flux insufficient to account for the observed plutonium concentration. Neutron multiplication by capture of thermalized neutrons in ^{235}U and the production of fission neutrons will contribute to overcoming the deficiency. The contribution from this source will clearly depend on the uranium concentration, on the composition of the ore, and on the probability that a fission neutron will be slowed down to thermal energies. In all probability, the neutrons produced in (α,n) reactions account for a major portion of the neutrons required for ^{239}Pu formation. Fleming and Thode (1953a,b) found evidence that (α,n) and (α,p) reactions occur to a considerable extent in uranium minerals. This conclusion was reached from a study of the isotopic composition of argon obtained from uranium minerals. In thorium ores containing small amounts of uranium, the neutrons from (α,n) reactions predominate. The amount of plutonium created depends not only on the number of neutrons produced but also on their subsequent fate. Elements with high neutron-capture

cross-sections will compete for neutrons and decrease plutonium formation. In carnotite, potassium and vanadium atoms, and in fergusonite, tantalum atoms capture most of the available neutrons, thus accounting for the unusually low plutonium content found in these minerals (Table 7.3).

A fascinating example of the formation of ^{239}Pu by neutron multiplication in ^{235}U was found by French scientists in the uranium deposit at Oklo in the Gabon, Africa. From anomalies in the isotopic composition of rare earths (especially neodymium) and anomalies in the ^{235}U content, it was concluded that, in at least six different locations of this deposit, a self-sustaining nuclear chain reaction must have occurred (Bodu *et al.*, 1972; Neuilly *et al.*, 1972). It was found that, in these locations, a burn-up of part of the original ^{235}U had occurred, but the depletion found was not as great as one would have expected from the observed anomalies in the isotope composition of other elements. It is generally agreed that ^{239}Pu is formed through resonant capture of epithermal neutrons by the ^{238}U present in the matrix, and that subsequent radioactive decay of the ^{239}Pu again regenerates a fraction of the ^{235}U (Holliger and Devillers, 1981; Hidaka and Holliger, 1998; Hidaka, 1999). Since no plutonium has been found in the Oklo deposit, one may conclude that the self-sustaining chain reaction must have taken place around 1.9×10^9 years ago (Cowan, 1976).

A different situation exists with regard to ^{244}Pu, which is sufficiently long-lived to have survived from primordial times. In 1960, Kuroda postulated the existence of ^{244}Pu in the early solar system based on the Xe isotope ratios found in chondritic meteorites (Kuroda, 1960). In 1971, Alexander and coworkers measured the ratios of the Xe isotopes formed by spontaneous fission (SF) of ^{244}Pu and found they agreed with those found in chondritic meteorites, thus strongly supporting this hypothesis and SF decay of ^{244}Pu (Alexander *et al.*, 1971). The discovery of ^{244}Pu fission xenon in extraterrestrial samples such as the Moon (Kuroda and Myers, 1998), Martian (Marty and Marti, 2002), and other meteorites demonstrated that the transuranium elements were synthesized in exploding (supernovae) stars (Kuroda and Myers, 1998).

Conclusive proof for the occurrence of natural ^{244}Pu in a pre-Cambrian bastnasite ore was provided by Hoffman and coworkers (Hoffman *et al.*, 1971). Starting from approximately 85 kg of ore containing 10% bastnasite, these workers isolated 2×10^7 atoms (8×10^{-15} g) of ^{244}Pu corresponding to about 10^{-18} g of ^{244}Pu per gram of pure bastnasite. The presence of ^{244}Pu was conclusively identified using high-resolution mass spectrometry. Thus it seems most probable that this ^{244}Pu sample is a remnant of the stellar debris that coalesced to form the solar system.

That even the richest uranium deposits are not likely to supersede synthetic methods as a source of plutonium can be appreciated from the fact that the microgram amounts of plutonium isolated by Peppard and coworkers (Peppard *et al.*, 1951) required the residues of 100 metric tons of ore concentrate for each microgram of plutonium recovered.

7.5 SEPARATION AND PURIFICATION

7.5.1 Introduction

At the end of 2003, a little more than 60 years after the discovery of the first plutonium isotope in 1940, about 1855 metric tons of plutonium existed, principally within irradiated fuel from nuclear power plants (Albright and Kramer, 2004). About 225 metric tons of plutonium that had been separated and purified for recycling in commercial nuclear fuel cycles was in the unirradiated form. Roughly 260 metric tons of plutonium with a high ^{239}Pu content has been separated for use in nuclear weapons programs worldwide. Some of this weapons plutonium has been declared excess to military needs and will be incorporated into the commercial nuclear power system. Production of plutonium for military use had greatly decreased by early in the 21st century, but the total plutonium inventory will continue to increase as a consequence of nuclear power production for the foreseeable future. The rate of plutonium production in fuel of operating reactors was estimated at 70–75 metric tons per year at the end of 2003. Clearly, the separation of plutonium has been carried out on a large scale. The management of the separated plutonium and the large quantities of highly radioactive by-products of this production will continue to be a challenge in the decades to come.

Plutonium isotopes are produced mainly from neutron absorption by ^{238}U and the subsequent product nuclei as shown in the simplified scheme in Fig. 7.4. The major pathway to plutonium proceeds through absorption of a neutron to give ^{239}U followed by two successive β^- decays to give ^{239}Np and then ^{239}Pu. Neutron absorption by ^{239}Pu produces higher isotopes of plutonium and other transuranic elements, in competition with neutron-induced fission. Beta decay by ^{241}Pu and ^{243}Pu and further neutron absorption leads to the production of higher actinides, americium, curium, etc., but these steps are not shown in the diagram for the sake of clarity. As the scheme for the production of plutonium isotopes suggests, the isotopic composition of plutonium produced in a

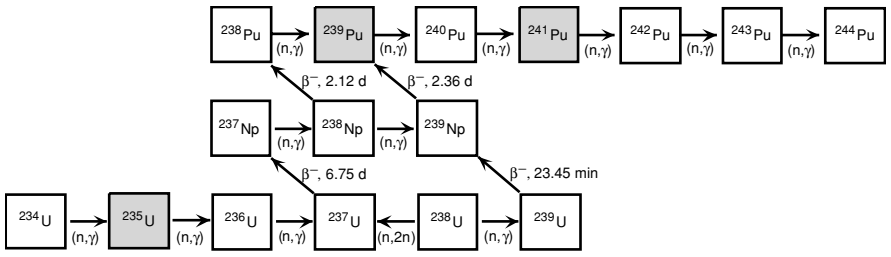

Fig. 7.4 *Major pathways for formation of plutonium isotopes by neutron absorption* (n, γ) *and beta decay* (β^-) *in uranium fuels or targets. Shaded boxes indicate most important isotopes undergoing neutron-induced fission in competition with neutron absorption.*

particular portion of the reactor fuel will be a complex function of the total flux and energy distribution of the neutrons that irradiate that fuel segment. The neutron flux and energy distribution will vary with irradiation time and the location of the fuel in the reactor.

The majority of nuclear power reactors around the world use low-enrichment uranium oxide fuels (^{235}U content of 3–5%) and light water (H_2O) to moderate the neutrons and act as the coolant for the system (Neeb, 1997). The uranium oxide fuel is fabricated into cylindrical pellets that are stacked inside a sealed container made of a cladding material such as a zirconium alloy to make a fuel pin. The plutonium content after 'burning' of these fuels amounts to about 1% of the mass of heavy metal content of the used fuel from a 'typical' light water reactor (LWR). Neutron-induced fission of the plutonium generated from neutron absorption by ^{238}U adds substantially to the total power production in commercial nuclear power plants (~40% of the total). The remaining mass of the used fuel consists of about 95% uranium, 4% fission products, and 0.1% all other transuranic actinides. It is the plutonium content in these 'spent' reactor fuels that provides most of the global plutonium inventory.

The build-up of the plutonium isotopes is accompanied by the production of a great variety of fission product elements. The fission process leads mostly to two product nuclei (only 0.2 to 0.3% of the fission events yield three fragments) that have an asymmetric statistical mass distribution with peaks at mass numbers of 95 and 138 for ^{235}U thermal (low energy) neutron-induced fission. The fission product nuclei commonly have excess neutrons relative to stable nuclei with the same atomic number and thus most are radioactive. The fission products decay primarily by beta/gamma chains to more stable nuclei. A calculation of the principal actinide and fission product isotopes present at the end of irradiation followed by 10 years of storage of a commercial reactor-type fuel is shown in Table 7.4. The burn-up of this fuel is higher than that used in most commercial plants to date, but the nuclear power industry trend is toward such higher burn-ups in the future. The list of fission product masses in Table 7.4 illustrates the two peaks in the fission product yield among the elements Zr through Pd and Xe through Nd. While the fission product masses do not change dramatically for most of the elements in the used fuel after 10 years of storage, the radioactivity has dropped more than two orders of magnitude and the ^{90}Sr and ^{137}Cs decay chains dominate the radioactivity of the used fuel from 10 years out to a few hundred years.

Inspection of Table 7.4 also illustrates that the fission products include elements from all the families of the periodic table. This considerably complicates the chemical problem of separation and purification of plutonium from the irradiated fuel. Additionally, the intense radioactivity requires facilities that use heavy shielding and remotely operated equipment to perform the separation processes. The mixture of plutonium isotopes present in the spent fuel is not so intensely radioactive and can be handled in a gloved box system once the fission products are removed. The term 'decontamination' is often applied to the

Table 7.4 *Actinide and fission product content of neutron-irradiated UO_2 fuel calculated using ORIGEN 2 code (Croff, 1980, 1983)*[a].

Element	*Weight at discharge* (g)	*Weight after* 10 yr *cooling* (g)	*Activity at discharge* (C_i)	*Activity after* 10 yr *cooling* (C_i)	*Major radioactive isotopes after* 10 yr *cooling and half-lives*
U-234	123	142	0.76	0.88	α, 2.46×10^5 yr
U-235	6 370	6 370	0.01	0.01	α, 7.04×10^8 yr
U-236	5 520	5 520	0.35	0.35	α, 2.34×10^7 yr
U-237	18	<0.1	1.47×10^6	2.76	β^-, 6.75 d
U-238	923 900	923 900	0.31	0.31	α, 4.47×10^9 yr
Np-237	1 020	1 050	0.72	0.74	α, 2.14×10^6 yr
Np-238	2	<0.1	5.23×10^5	0	β^-, 2.34 d
Np-239	100	<0.1	2.32×10^7	1.04×10^2	β^-, 2.34 d
Pu-238	236	242	3.99×10^3	4.09×10^3	α, 87.7 yr
Pu-239	4 900	5 000	3.01×10^2	3.07×10^2	α, 2.41×10^4 yr
Pu-240	2 070	2 130	4.57×10^2	4.70×10^2	α, 6.56×10^3 yr
Pu-241	1 820	1 130	1.85×10^5	1.15×10^5	β^-, 14.4 yr
Pu-242	579	579	2.3	2.3	α, 3.73×10^5 yr
Am-241	48	728	1.64×10^2	2.50×10^3	α, 432 yr
Am-242m	2	2	16.6	15.8	IT, 141 yr
Am-243	538	538	1.04×10^2	1.04×10^2	α, 7.37×10^3 yr
Cm-242	23	<0.1	7.75×10^4	13.0	α, 163 d
Cm-243	2	2	89.3	71.9	α, 29.1 yr
Cm-244	200	136	1.62×10^4	1.10×10^4	α, 18.1 yr
Cm-245	20	20	3.5	3.5	α, 8.5×10^3 yr
Cm-246	4	4	1.2	1.2	α, 4.76×10^3 yr
total An	**947 495**	**947 493**	**2.55×10^7**	**1.32×10^5**	
Se	85	85	9.6×10^5	0.58	Se-79 6.5×10^4 yr
Br	33	33	0	0	–
Kr	546	529	3.8×10^6	7.3×10^3	Kr-85 10.7 yr
Rb	520	537	5.4×10^6	<0.01	–
Sr	1 390	1 180	8.6×10^6	8.9×10^4	Sr-90 28.5 yr
Y	722	704	1.2×10^7	8.9×10^4	Y-90 64.1 h
Zr	5 480	5 630	1.0×10^7	2.8	Zr-93 1.5×10^6 yr
Nb	44	<0.01	1.5×10^7	1.1	Nb-93m 13.6 yr
Mo	5 090	5 210	0	0	–
Tc	1 220	1 230	1.2×10^7	21	Tc-99 2.1×10^5 yr
Ru	3 630	3 360	5.6×10^6	757	Ru-106 373 d
Rh	446	504	8.0×10^6	757	Rh-106 2.2 h
Pd	2 140	2 360	7.1×10^5	0.16	Pd-107 6.5×10^6 yr
Ag	73	71	9.4×10^5	0.33	Ag-110m 250 d
Cd	157	159	8.5×10^4	39	Cd-113m 13.7 yr
In	1	1	2.6×10^5	<0.01	–
Sn	76	75	1.5×10^6	1.1	Sn-126 2.5×10^5 yr
Sb	26	14	3.8×10^6	1.2×10^3	Sb-125 2.76 yr
Te	714	717	8.0×10^6	285	Te-125m 58 d
I	363	357	1.2×10^7	0.05	I-129 1.6×10^7 yr
Xe	8 190	8 190	9.0×10^6	<0.01	–
Cs	4 140	3 340	8.6×10^6	1.5×10^5	Cs-137 30.2 yr, Cs-135 2.3×10^6, Cs-134 2.07 yr

Table 7.4 (*Contd.*)

Element	*Weight at discharge* (g)	*Weight after* 10 yr *cooling* (g)	*Activity at discharge* (C_i)	*Activity after* 10 yr *cooling* (C_i)	*Major radioactive isotopes after* 10 yr *cooling and half-lives*
Ba	2 310	3 100	1.0×10^7	1.2×10^5	Ba-137m 2.5 mo
La	1 880	1 870	1.0×10^7	<0.01	–
Ce	4 170	3 690	8.1×10^6	190	Ce-144 284 d
Pr	1 690	1 730	7.0×10^6	193	Pr-144 17.3 mo
Nd	5 770	6 220	1.7×10^6	<0.01	–
Pm	100	7	1.8×10^6	6.9×10^3	Pm-147 2.63 yr
Sm	1 150	1 240	9.6×10^5	1.4×10^3	Sm-151 90 yr
Eu	309	243	6.2×10^5	1.3×10^4	Eu-155 4.73 yr, Eu-154 8.5 yr
Gd	237	309	8.1×10^3	<0.01	–
Tb	3	2	4.8×10^3	<0.01	–
Dy	2	2	1.4×10^3	<0.01	–
total FP	**52 700**	**52 700**	$\mathbf{1.8 \times 10^8}$	$\mathbf{4.8 \times 10^5}$	

[a] Based on an initial uranium loading of 4.25% ^{235}U enrichment (957.5 kg ^{238}U, 42.5 kg ^{235}U, 0.293 kg ^{234}U), burn-up of 50 000 MW-days (metric ton)$^{-1}$ (Hill, 2005).

process of removing the fission products from the plutonium, uranium, or other actinides of interest in the irradiated fuel or target material. The decontamination factor measures the extent to which the concentration of fission products has been removed relative to the original level in the spent fuel at the time processing begins. To allow the product plutonium to be handled by personnel using a gloved box without undue exposure to fission product radioactivity, the decontamination factor required for some fission products is on the order of 10^8. Clearly, the required decontamination factors will vary with the cooling time of the fuel before processing begins.

The fission products and actinides produced from the irradiated uranium fuel are dispersed intimately in the fuel matrix (Neeb, 1997). The fission product nuclei dissipate their kinetic energy after traveling on average 5–10 μm through the uranium oxide matrix, leaving an ionization track and displacement cascade that ultimately generates most of the heat that is used to generate electricity. Atomic mixing occurs from both radiation-induced and thermal mass transport processes. In a typical LWR fuel each atom of the fuel is displaced from its lattice site an average of once a day. Some segregation of the fission product elements occurs under reactor conditions (Neeb, 1997). For example, inert gases such as xenon and krypton can form bubbles in the fuel matrix and even escape into the gas space inside a fuel pin, and some transition elements (Mo, Ru, Rh, Pd, Tc) form small metal inclusions in the uranium oxide. However, the bulk of the fission products and transuranic elements are

dispersed fairly homogeneously within the uranium fuel. The uranium matrix must be dissolved into a suitable solution or converted into a volatile compound to allow the fission product and actinide 'impurities' to be separated from the uranium.

The methods used to recover plutonium (and other actinides) from irradiated fuels or targets can be divided into two major groups, aqueous and nonaqueous processes, depending on the primary phase used for the separation process. The major classes of aqueous processes are liquid–liquid extraction (solvent extraction), ion exchange, and precipitation. Examples of nonaqueous processes are electrorefining (ER) in molten salts and fluoride volatility. The separation methods use differences in the chemical properties of the various elements present to segregate some components preferentially between the primary phase and a secondary phase that can be a solid, liquid, or gas. Separation of the two phases partitions the components of the original single phase for further processing steps. These next steps can be additional stages of the same separation method (e.g., a bank of centrifugal contactors for extraction) or a different method (e.g., ion exchange followed by precipitation).

Nearly all of the separation methods take advantage of the multiple oxidation states that plutonium can adopt in its various chemical forms. The chemical properties of plutonium (and other metal ions) change to a large extent depending on the oxidation state. If conditions can be adjusted to obtain various metal ions in a mixture in different oxidation states, the separation of these metals is often straightforward. For example, in aqueous acid solutions it is possible to have uranium in the hexavalent oxidation state (as UO_2^{2+}), neptunium in the pentavalent state (as NpO_2^{+}), plutonium in the tetravalent state, and americium in the trivalent state. The complexes formed by ions in these different oxidation states in solution are quite different, so that separation by a number of methods is possible. In the case of an irradiated fuel with fission products present, if the chemical behavior of a fission product resembles that of plutonium in one oxidation state, it can be quite different when the plutonium oxidation state or the fission product element oxidation state is changed. The use of oxidation state changes to improve separations will be illustrated in the discussion of specific separation methods below.

The large-scale separation and purification of plutonium has been primarily accomplished using the Plutonium, Uranium, Reduction, EXtraction (PUREX) liquid–liquid extraction process. This process was first developed for separating plutonium from metallic uranium fuels irradiated to produce plutonium for nuclear weapons applications, but has since been adapted to separate uranium and plutonium from many kinds of fuels and targets, including commercial power reactor fuels. While a variety of other processes have been used to separate and purify plutonium from irradiated fuels, many of these are now of only historical interest. More detailed information on the separation technology for plutonium and the other actinides can be found in Chapter 24 of this work, *Actinide Separation Science and Technology*, including extensive

documentation of the separation literature. The goal in this chapter is to present the main features of selected separation methods of particular importance to plutonium and to illustrate major factors guiding development of plutonium separation processes. Only brief references to the history of plutonium separations will be made here.

Processes for separation of plutonium from neutron-irradiated uranium metal, uranium oxide, or other irradiated target materials are one important group of plutonium separation and purification methods, but there are additional separation needs. Separated plutonium must be converted into the forms required for various applications, for example, purification of PuO_2 to meet all the specifications for mixed oxide (MOX) fuel fabrication. Recovery and recycle of plutonium from the process and waste streams of these conversion operations constitute another important group of separation processes. A wider variety of separation methods can be employed to accomplish these separations because the high radiation levels of the fission products are not present and the amount of material to be processed is typically much smaller. There is also a need for separation processes to remove plutonium from items that have been contaminated by plutonium-containing materials resulting from normal operations or accidental release to the environment, e.g. equipment, concrete, soils, etc. These types of operations are commonly referred to as decontamination methods; the radioactive contaminant is plutonium in this case rather than a fission product. Finally, a large number of separation methods and reagents have been used to preconcentrate or remove interfering components in analytical procedures for plutonium-containing samples to improve detection limits and accuracy of the results.

As the above discussion indicates, many processes have been developed for separating plutonium from a variety of matrices. There are often variations for a particular method and many combinations of methods possible for accomplishing a specific separation goal. The chosen process can be a result of many factors at a particular facility including available equipment and expertise, safety and operational limits, product specifications, national regulatory requirements, waste management, cost, and schedule. It is possible in some processes to vary operating conditions over a wide range and still obtain a desired result. In the discussion of separation methods that follow, variations in process conditions are common. Defining an 'optimum' process depends on factors like those mentioned above, which can vary even at a single facility over its lifetime. Operational details of this kind are beyond the scope of this chapter.

7.5.2 Introduction to aqueous-based separation methods

Before discussing aqueous separation processes for plutonium in more detail, a brief overview of actinide chemistry in aqueous solution is useful because most actinide separations have been performed using aqueous acid solutions.

The separation of actinides from basic aqueous solutions has been employed less often because the low solubilities of the hydroxides or oxyhydroxides of the high-valent actinide metal ions greatly limit the amount of material that can be processed in a given volume except where strongly complexing ligands, such as carbonate or peroxide, are present. More detailed information on the solution chemistry of plutonium (see Section 7.9) and the other actinide metal ions can be found in the appropriate sections of the chapters for each element and in other chapters of this work.

As noted above, the separation of plutonium and the other early actinides (Th–Am) from fission products and from each other is generally accomplished by adjusting the oxidation state of the actinide ion in aqueous solution to make the coordination chemistry of the actinide ion substantially different from the other species to be separated. The actinides are highly electropositive metals and form cationic species in aqueous solutions. These cations are 'hard' Lewis acids and form strong complexes in solution with hard anions such as hydroxide and fluoride. The oxidation states from III to VI are accessible in aqueous acid solutions of uranium, neptunium, and plutonium. After plutonium the actinides become more lanthanide-like with the coordination chemistry of the trivalent metal ion dominating. The pentavalent and hexavalent actinide ions are found in aqueous solutions as linear dioxo cations, e.g. NpO_2^+ and PuO_2^{2+}. These 'actinyl' species have no close analogs in transition metal oxo complexes and are also hard Lewis acids. Water and other ligands bind to these linear cations in a ring-shaped equatorial region around the metal ion between the two tightly bound oxoanions. The coordination numbers and geometries for the actinide ions are highly variable and reflect the largely ionic bonding in these complexes: generally, 6–12 for An(IV), 6–9 for An(III), and 4–6 in the equatorial ring of AnO_2^+ or AnO_2^{2+}. The trivalent actinides exhibit a slightly stronger bonding to ligands containing soft donor atoms (e.g. sulfur, nitrogen, chloride) than the corresponding lanthanides and this property can be used as a basis for separating these groups of elements.

For plutonium the oxidation states from III to VII are accessible in aqueous solution. The species Pu(III), Pu(IV), and Pu(VI) (PuO_2^{2+}) are most important in acidic aqueous solution. The pentavalent ion PuO_2^+ disproportionates rapidly in acidic solution at moderate plutonium concentrations and is usually a very minor species in acidic aqueous separation systems. Stabilizing Pu(VII) requires strongly complexing ligands such as hydroxide, fluoride, or carbonate in basic solution and, thus, Pu(VII) has not been used in any separation systems.

7.5.3 Precipitation and crystallization methods

As noted above, the oxidation states of the actinide ions in solution produce large differences in coordination chemistry facilitating separation by a variety of methods. An example of this is shown in Table 7.5 which lists the qualitative solubility behavior of the actinides in oxidation states III–VI with some common

Table 7.5 *Precipitation reactions characteristic of various actinide oxidation states* (*aqueous solution,* 1 M H^+)[a].

Anion	M^{3+}	M^{4+}	MO_2^+	MO_2^{2+}
OH^-	I	I	I	I
F^-	I	I	I[b]	S
IO_3^-	I	I	S	S
O_2^{2-}	–	I	–	–
$C_2O_4^{2-}$	I	I	I	I
CO_3^{2-}	(I)[c]	I[c]	I[d]	S
$CH_3CO_2^-$	S	S	S	I[e]
PO_4^{3-}	I	I	I[f]	I[g]
$Fe(CN)_6^{4-}$	I	I	S	I

I = insoluble, S = soluble.
[a] Unless otherwise stated (the OH^- and CO_3^{2-} precipitations occur in alkaline solution).
[b] At pH = 6, $RbPuO_2F_2$ and $NH_4PuO_2F_2$ may be precipitated by addition of RbF or NH_4F, respectively.
[c] Complex carbonates are formed.
[d] Solid $KPuO_2CO_3$ precipitates on addition of K_2CO_3 to Pu(V) solution.
[e] From solution of Pu(VI) in CH_3CO_2H, $NaPuO_2(CH_3CO_2)_3$ precipitates on addition of Na^+.
[f] Addition of $(NH_4)_2HPO_4$ to Pu(V) solution yields $(NH_4)HPuO_2PO_4$.
[g] On addition of H_3PO_4, $HPuO_2PO_4{\cdot}xH_2O$ precipitates.

anions. These precipitations are very useful for separating mixtures of the actinides and for recovery of solid products from an aqueous stream after using another separation process such as ion exchange or solvent extraction. They are generally not selective enough to be used as the primary process for separation of plutonium or other actinides from all the fission products in irradiated fuel or targets. This is illustrated by a study (Winchester and Maraman, 1958) that used precipitation of Pu(III) oxalate, Pu(IV) oxalate, Pu(III) fluoride, and Pu(IV) peroxide to recover plutonium directly from an irradiated plutonium-rich alloy dissolved in nitric acid. The decontamination factors reported in Table 7.6 indicate that none of the precipitation processes achieved high enough fission product or corrosion product (Fe and Co) removal for use as a primary separation process. However, as will be described below, coprecipitations with other metal ion species such as bismuth phosphate were used in the first large-scale separations of plutonium from irradiated uranium. These processes were replaced in time by more efficient solvent extraction processes.

The distinction between crystallization and precipitation is quite often based on the speed of the process and the size of the solid particles produced. The term precipitation commonly refers to a rapid crystallization that gives small crystals that may not appear crystalline to the eye, but still may give very distinct X-ray diffraction (XRD) peaks. Precipitation often involves a relatively irreversible reaction between an added reagent and other species in solution whereas

Table 7.6 *Decontamination factors for plutonium using various precipitation methods.*

Element	*Pu(III) oxalate*	*Pu(IV) oxalate*	*Pu(IV) peroxide*	*Pu(III) fluoride*
Fe	33	10	50	1.4
Co	47	>95	30	8.6
Zr	3.5	>44	1	1.1
Mo	>13	>15	>140	1.1
Ru	>38	33	>14	36
Ce	1	1	6	1.1

crystallization products can usually be redissolved using relatively simple means such as heating or dilution. The details of the precipitation or crystallization process can be very important to produce a pure product and one that separates well from the liquid phase. Thus, the order and speed of reagent addition, the temperature, and the 'aging' time before filtration or centrifugation can all be important parameters in a precipitation or a crystallization process. The Pu(IV) oxyhydroxide 'polymer' that readily forms in relatively low acid solutions of Pu(IV) is an infamous example of a 'difficult' precipitate that can complicate the processing of plutonium aqueous solutions. The characteristics of this polymer will be described in more detail in Section 7.9.1.d.

(a) Coprecipitation methods

Coprecipitation processes were the first to be used for the recovery of plutonium. The tiny amounts of plutonium present in the first preparations were too small to be precipitated directly, so coprecipitation or 'carrier' precipitations were used to purify and deduce the chemical properties of plutonium and many other radioactive elements. In general, plutonium will coprecipitate if the anion contained in the bulk precipitate forms an insoluble salt with plutonium in the same oxidation state or states present in the solution. Useful carrier precipitation methods for plutonium have been reviewed (Sorantin, 1975). Coprecipitation methods have also been used to purify plutonium in microgram amounts and for recovery on a production scale.

(*i*) *Lanthanum fluoride*

Precipitation of lanthanum fluoride or other lanthanide fluorides from acid solutions carries trivalent and tetravalent actinides, but not the pentavalent and hexavalent ions. The lanthanide and yttrium fission products coprecipitate, but most of the other fission products remain in solution. The behavior of

neptunium and plutonium in lanthanum fluoride precipitation was used to establish the existence of two oxidation states of these elements before weighable quantities were available (Seaborg and Wahl, 1948b). The lanthanum fluoride carrier precipitation was also a key step in the first isolation of a weighable plutonium compound to be described below.

Cunningham and Werner isolated a PuO_2 sample that weighed 2.77 μg, the first weighable quantity of any synthetic element, on September 10, 1942 at the Metallurgical Laboratory of the University of Chicago (Cunningham and Werner, 1949b). The plutonium had been separated from about 90 kg of uranyl nitrate hexahydrate that had been irradiated for 1 to 2 months with neutrons produced by bombarding a beryllium target with deuterons at the cyclotron facility at Washington University in St. Louis. The separation of plutonium was accomplished through oxidation state adjustments and a series of LaF_3 precipitations that carried Pu(IV) and Np(IV) but not Pu(VI) or Np(VI). The brief overview that follows provides an example of a coprecipitation separation method and also illustrates the painstaking effort required in these first explorations of plutonium chemistry.

About 90 kg of irradiated $UO_2(NO_3)_2 \cdot 6H_2O$ was mixed with 100 L of diethyl ether to yield about 120 L of ether solution containing uranyl nitrate solvate, $UO_2(NO_3)_2[O(CH_2CH_3)_2]_2$, and a small amount of fission products and 8 L of an aqueous phase that consisted of about 50 wt % uranyl nitrate hydrate with most of the fission products and transuranic elements, principally neptunium and plutonium. This was essentially a solvent extraction step that partitioned most of the U(VI) to the ether phase along with a small amount of the fission products.

The aqueous phase was diluted to 20 L, made 2 M in nitric acid and 0.014 M in La(III) and then HF was added to give a solution 4 M in HF. The resulting 40 g of LaF_3 precipitate contained the transuranium elements and about 25% of the original fission product activity (mostly the lanthanide and yttrium fission products). The separated LaF_3 precipitate was heated in concentrated sulfuric acid to distill HF and then dissolved in and diluted to 5 L with 2 M nitric acid. The Pu(IV) was oxidized to Pu(VI) by using $K_2S_2O_8$ and Ag(I) as a catalyst. The solution was then made 4 M in HF which produced about 40 g of LaF_3 precipitate that was separated by filtration. The LaF_3 precipitate contained most of the remaining fission product activity, while the solution contained the Pu(VI) and Np(VI). The addition of a 6% SO_2 solution to the filtrate and washings reduced the Pu(VI) and Np(VI) and the excess peroxydisulfate. Addition of 2 g of $La(NO_3)_3$ in solution precipitated LaF_3 that carried the tetravalent plutonium and neptunium. Repeated cycles of precipitation with progressively smaller amounts of LaF_3 were used to further decontaminate the plutonium and neptunium. For two of the LaF_3 precipitation cycles, $KBrO_3$ was employed as the oxidizer to selectively oxidize neptunium, but not plutonium. This allowed the separation of the neptunium into the filtrate solutions while plutonium was carried with the LaF_3. These additional cycles of smaller

precipitations eventually yielded a 120 μL solution of 1.7 M HNO_3 and 5 M HF that was fumed in a platinum crucible and treated with 10 M ammonium hydroxide to precipitate Pu(VI) hydroxide. The washed precipitate of plutonium hydroxide contained about 40 μg of plutonium. The microliter-scale solution manipulations were performed in a specially designed glass apparatus viewed with a microscope. Additional purification steps yielded a 50 μL solution of plutonium in nitric acid. Ten μL of this solution were placed on a platinum weighing pan, dried, and heated to give the oxide. This sample provided the first weighable quantity of plutonium that is now displayed in the Lawrence Hall of Science at Berkeley, California.

(*ii*) *Bismuth phosphate process*

The bismuth phosphate process was used for the first large-scale purification of plutonium from neutron-irradiated uranium at the Hanford site during the Manhattan Project, and after the war until the 1950s when it was replaced by solvent extraction processes. More detail on the bismuth phosphate process and its replacement by solvent extraction processes can be found in Chapter 24. The precipitation of $BiPO_4$ from acid solutions carries the trivalent and tetravalent actinides, and especially Pu(IV), but not the pentavalent and hexavalent ions. Bismuth phosphate is quite insoluble in moderately concentrated nitric and sulfuric acids. This is an important property because addition of sulfuric acid to a nitric acid solution of neutron-irradiated uranium could be used to keep the relatively large quantity of U(VI) in solution as a sulfate complex while bismuth phosphate was precipitated and carried the plutonium. The $BiPO_4$ precipitate carried only small amounts of the fission products, and could be redissolved in concentrated nitric acid; thus simplifying the process relative to use of a lanthanum fluoride carrier that is difficult to redissolve. A series of oxidation state adjustments and precipitations of $BiPO_4$ from solutions of neutron-irradiated uranium in nitric acid separated the plutonium from the uranium, neptunium and fission products in a scheme that resembles the lanthanum fluoride process described above. In fact, cycles of lanthanum fluoride precipitation from nitric acid were incorporated into the bismuth phosphate process to concentrate and further purify plutonium.

Thompson and Seaborg first developed the bismuth phosphate process (Thompson and Seaborg, 1956). The scale-up of the process from the laboratory to an operating plant by a factor of 10^8 in a short time is a remarkable story (Hill and Cooper, 1958). An overall decontamination factor from the fission products of 10^7 was obtained at Hanford for the plutonium. The disadvantages of the process included discarding the uranium with the fission products, generation of large volumes of high salt wastes, and batch operation. Continuous solvent extraction processes based on extraction of uranium and plutonium from nitric acid solutions of dissolved fuel have replaced the bismuth phosphate process.

(b) Precipitation and crystallization methods for conversion chemistry of plutonium

Solvent extraction processes have displaced the original bismuth phosphate coprecipitation method for production scale plutonium separation from neutron-irradiated uranium fuels and targets. However, precipitation and crystallization from aqueous solutions have always been important processes for preparing and purifying solid compounds for the various applications of plutonium. The major products are plutonium metal for irradiation targets and fuels, weapons components, or storage and PuO_2 for MOX fuels, heat sources (when the ^{238}Pu content is high), and storage.

The bulk of the aqueous processing of plutonium takes place in nitric or hydrochloric acid solutions and most plutonium solids are precipitated from these solutions (Cleveland, 1980; Christensen *et al.*, 1988). The most common precipitations use oxalate, peroxide, hydroxide, and fluoride. The typical reasons for using these precipitations are:

- Good recovery of plutonium can be obtained in the solid in a form suitable for preparing metal or oxide.
- Relatively concentrated plutonium nitrate or chloride solutions can be largely or partially purified from many cationic impurities.
- Precipitation from relatively dilute solutions provides a very quick and convenient method for concentrating plutonium.
- Calcination at 500–800°C readily converts properly precipitated Pu(III) and Pu(IV) oxalates to PuO_2 that is suitable for direct oxide reduction (DOR) with calcium to the metal, or hydrofluorination to PuF_4 that is then reduced to metal (see Section 7.7.2).
- Precipitation of plutonium or americium hydroxides from waste solutions such as oxalate or peroxide filtrates generally provides an effective method to recycle the plutonium and americium in the separated precipitate and to dispose of the alkaline filtrate to low-level waste treatment operations.

This group of common precipitation methods will be briefly reviewed. The detailed procedures used at different facilities vary widely because of the many facility-specific factors that enter into the process design as discussed briefly in Section 7.5.1. Both batch and continuous processes have been developed for these precipitations.

(*i*) *Plutonium(III) oxalate precipitation*

Since the time of the Manhattan Project, researchers have found it useful to precipitate the easily filterable turquoise-blue $Pu_2(C_2O_4)_3 \cdot 10H_2O$ by reducing plutonium to the trivalent state in low acid solution and carefully adding an oxalic acid solution. Directly adding solid oxalic acid will produce a crystalline precipitate with a smaller average particle size (Christensen *et al.*, 1988). The solubility of $Pu_2(C_2O_4)_3 \cdot 10H_2O$ can be approximated by the expression

$[Pu(mg\,L^{-1})] = 3.24[H^+]^3[H_2C_2O_4]^{-3/2}$ (Harmon and Reas, 1957). However, the typical filtrate from a production run will have somewhat higher concentrations of plutonium (0.1–0.5 g L^{-1}) left in solution than that calculated from this equation. The precipitation is useful over a wide range of conditions when the Pu(III) concentration is more than 1 g L^{-1} and with less than 4 M acid. The Pu(III) oxalate precipitation gives good decontamination factors from such impurities as Al(III), Fe(III), and U(VI). There is less decontamination from sodium, potassium, and calcium and none from Am(III). Plutonium(III and IV) can be scavenged from very dilute solutions using Ca(II) or Pb(II) oxalates as carriers (Maraman *et al.*, 1954; Akatsu, 1982; Akatsu *et al.*, 1983).

(*ii*) *Plutonium*(*IV*) *oxalate precipitation*

Plutonium(IV) precipitates as the tan solid $Pu(C_2O_4)_2 \cdot 6H_2O$ from low acid solutions upon addition of oxalic acid, but it is usually a very fine tacky solid at room temperature (Christensen *et al.*, 1988). Precipitation at elevated temperatures can greatly improve the filterability of the solid. Typical losses of plutonium to the filtrate in practical operations are 0.2–0.5 g L^{-1}. The precipitation is used over a wide range of conditions with Pu(IV) concentrations greater than 1 g L^{-1} and acid concentrations between 1 and 5 M. The decontamination factors for impurities such as Al(III), Fe(III), and U(VI) are typically higher than for the Pu(III) oxalate method. There is no decontamination from Am(III).

(*iii*) *Plutonium*(*IV*) *peroxide precipitation*

Plutonium(IV) peroxide is an olive-green solid formed by the addition of hydrogen peroxide solutions to acid solutions of Pu(IV). The typical range of acid concentration is 2.5–5.5 M. The solutions are often cooled to 10–15°C to reduce the decomposition of hydrogen peroxide. High levels of iron, copper, manganese, or nickel catalyze the decomposition of the H_2O_2 and interfere with precipitation. At higher acid concentrations and with careful H_2O_2 addition, a very filterable hexagonal form of plutonium(IV) peroxide precipitates. At lower acidities a gelatinous cubic form precipitates that is difficult to filter. Plutonium(IV) peroxide is not a stoichiometric compound and its O:Pu ratio may approach 3.5 (Cleveland, 1979, 1980), but does not reach 4.0 as is suggested by the formula $Pu(O_2)_2$. Anions such as nitrate, chloride, and sulfate, if present in the solution, are incorporated into the solid. Indeed, sulfate is added in some processes at a concentration of 0.1–0.3 M to nitric acid solutions to improve the filterability of the peroxide precipitate.

The Pu(IV) peroxide precipitation is a powerful method for purification of plutonium from many impurity elements except those such as thorium, neptunium, and uranium that form similar peroxides under these conditions. Unlike the oxalate precipitations, Am(III) is removed to a high degree. The excellent

decontamination factors obtained for many elements and the use of one reagent that is easily decomposed to water and oxygen in subsequent operations are the major advantages of using this process. The disadvantages are greater losses of plutonium in the filtrate (typically 0.1–0.5%) and violent decomposition of H_2O_2 that can occur during precipitations in the presence of high concentrations of iron and other metal ion catalysts for the decomposition reaction.

(*iv*) *Plutonium*(III) *fluoride precipitation*

Addition of aqueous HF to a solution of Pu(III) in nitric or hydrochloric acid precipitates blue-violet $PuF_3 \cdot xH_2O(x \sim 0.75)$ (Christensen *et al.*, 1988). The Pu(IV) concentration should be kept low because the hydrated PuF_4 precipitate is very gelatinous and much more soluble than the trifluoride. Significant Pu(IV) content will thus increase filtering time and plutonium losses to the filtrate. Reducing agents such as hydroxylamine, sulfamic acid, or ascorbic acid are commonly used. With careful oxidation state control, losses of plutonium to the filtrate are very low (0.05–0.1%). A disadvantage of preparing any fluorine-containing compound of plutonium is increased production of neutrons from α-n reactions relative to the oxygen-, carbon-, and nitrogen-based precipitants. The trifluoride precipitation does not give decontamination factors from cationic impurities that are as high as the oxalate or especially the peroxide precipitations. It gives moderate decontamination from many impurities including iron, but not from aluminum, zirconium, and uranium. Dried PuF_3 can be roasted in oxygen to produce a mixture of PuF_4 and PuO_2 that can be directly reduced with calcium metal to give 95–97% yields of plutonium metal (See Sections 7.7.1 and 7.7.2).

(*v*) *Plutonium hydroxide precipitation*

Hydroxide precipitation is quite useful to produce a filtrate with very low levels of plutonium. Sodium or potassium hydroxide solutions are commonly added to precipitate the gelatinous green Pu(IV) hydroxide (Christensen *et al.*, 1988). If Pu(III) is present, it will slowly oxidize to Pu(IV). Many other metal ions will precipitate as hydroxides as well or be carried by the plutonium hydroxide so that this is not a useful purification procedure. The hydroxide is generally difficult to filter. If large amounts of magnesium or calcium are present, the voluminous hydroxide precipitates of these metal ions make filtration especially difficult, unless they are avoided by carefully controlling the pH. The dried hydroxide cake can be recycled for plutonium recovery by dissolving it in acid. The formation of the Pu(IV) oxyhydroxide polymer should be avoided because this material behaves quite differently from the hydroxide precipitate and can be quite difficult to redissolve in acid. The formation and properties of the polymer are described in more detail in Section 7.9.1.d.

(*vi*) *Miscellaneous precipitations*

Other precipitation methods have been tested for plutonium processing operations, but have not been deployed or as widely used as those reviewed above. These include $CaPuF_6$ and Cs_2PuCl_6 from acid solutions for metal production operations (Christensen *et al.*, 1988; Muscatello and Killion, 1990) and $(NH_4)_4PuO_2(CO_3)_3$ or mixed $(NH_4)_4(Pu, U)O_2(CO_3)_3$ from alkaline solution for the preparation of MOX fuels (Roepenack *et al.*, 1984).

7.5.4 Solvent extraction separation processes

Liquid–liquid (or solvent) extraction partitions solutes between two immiscible liquid phases. The two phases are generally intimately mixed to improve the rate of transfer of solutes between them. The use of a laboratory separatory funnel by a synthetic chemist illustrates the operation of a single stage of liquid–liquid extraction. The two immiscible phases, commonly an organic and an aqueous phase, are shaken vigorously for some time to approach the equilibrium distribution of solutes between the phases and then the phases are allowed to coalesce and reform layers that can be separated. On an industrial scale, the labor-intensive separatory funnel is replaced by a wide variety of equipment that pumps, mixes and separates the phases in a continuous operation so that multiple stages of extraction and back-extraction can be accomplished in an efficient manner. Solvent extraction is a very versatile and useful industrial separation method and has proven to be very important for the recovery and purification of plutonium and other actinides. In fact, as discussed in Chapter 24 of these volumes, the industrial practice of solvent extraction advanced considerably because of the new development work needed to solve the separation challenges of processing neutron-irradiated fuels and targets for military and industrial applications.

In the case of plutonium and other actinide metal ions, the two immiscible phases used in solvent extraction processes are usually an aqueous acid solution and an organic solvent containing components that stabilize certain metal ion complexes in the organic phase. Nitric acid is the most common acidic solution used; hydrochloric acid has seen more limited application. Acids with more strongly complexing anions such as sulfuric, phosphoric, or hydrofluoric acids can have problems with limited solubilities of actinide ions (see Table 7.5) and also some fission product metal ions and are used less commonly. In some cases, these acids with more strongly complexing anions are used in controlled amounts in the acidic aqueous phase as 'masking agents' to hold certain metal ions in the aqueous phase and to improve the selectivity of the extraction into the organic phase. They can also be deployed in an aqueous phase to 'strip' or back-extract metal ions from an organic phase that has been 'loaded' with metal ions in a previous step of the process.

The organic phases used for actinide extractions comprise a wide range of solvents (or diluents) and organic-soluble compounds (extractants) that stabilize metal complexes in an organic phase. Aliphatic and aromatic hydrocarbons, chlorinated hydrocarbons, ethers, and ketones represent some of the major solvent groups. In some cases the solvent and the extractant are the same. For example, chemists used diethyl ether to extract uranyl nitrate from aqueous solutions long before the nuclear age dawned. The influence of the solvent on the extraction system is manifested in various ways such as the solubility of the extractant and metal ion species, the overall thermodynamic activity of the extractant, and the concentration of water in the organic phase (Cox and Flett, 1983).

Metal ions can be stabilized in the organic phase in a variety of structures. While uncharged individual metal ion complexes are solvated in the organic phase in many cases, ion-pairs, reverse micelles, and other aggregated structures are observed, especially as higher concentrations of metal ions are loaded into the organic phase (Borkowski *et al.*, 2003; Chiarizia *et al.*, 2003). For many extraction systems, a third phase can form if the metal ion concentration becomes too high in the organic phase (Rao and Kolarik, 1996). This is a situation to be avoided because the extraction equipment is designed to separate two liquid phases, not three, and any solid phase is particularly troublesome. Phase-modifying reagents are sometimes added to the organic solvent to inhibit third-phase formation and to allow higher levels of metal loading.

When two or more extractant compounds are combined in a single solvent they may act independently or the extraction equilibrium for a metal ion can be enhanced over what each extractant would give independently. This effect is referred to as synergism. It is most typically observed when an acidic extractant is combined with a neutral donor extractant and the major extractant complex contains both extractants bound to the metal ion (Cox and Flett, 1983).

The range and combinations of compounds that have been used in organic solvents to extract plutonium is very extensive and cannot be reviewed here. The extractant compounds can be generally divided into two large groups: compounds with donor atoms that form organic-soluble complexes with the metal ion, and ion-pair reagents that stabilize a charged metal ion complex in the organic phase. Given the hard Lewis acid character of the actinide metal ions, it is not surprising that most of the ligand-type extractants have one or more oxygen donor atom sites that coordinate to the metal ion in the organic phase. The major actinide extractant classes are alkyl and aryl phosphates, $(RO)_3P{=}O$, phosphonates, $(RO)_2RP{=}O$, phosphinates, $(RO)R_2P{=}O$, and phosphine oxides, $R_3P{=}O$; alkyl and aryl phosphoric, $(RO)_2PO_2H$, phosphonic, $(RO)RPO_2H$, and phosphinic acids, R_2PO_2H; ethers, R_2O; ketones, $R_2C{=}O$; 1,3-diketones, $RC(O)CH_2C(O)R$; amides, $RC(O)NR_2$, malonamides, $R_2NC(O)CHRC(O)NR_2$, and carbamoylmethylphosphine oxides, $(RO)_2P(O)CH_2C(O)NR_2$ (the R groups in the formulas can all have different or identical alkyl or aryl functionality). The major ion-pair extractant classes

for actinides are tetraalkylammonium salts, $R_4N^+X^-$, and protonated tertiary amines, $R_3NH^+X^-$. More detail on the classes of solvent extraction systems and their use for actinide separations is found in Chapter 24. Tri(*n*-butyl) phosphate (TBP), $(n\text{-BuO})_3P{=}O$, is of particular importance for plutonium separations as the key component of the PUREX process and will be discussed below.

(a) The PUREX process

As mentioned previously, nearly all of the roughly 500 metric tons of plutonium that has been separated to date has been recovered using the PUREX solvent extraction process. The use of TBP to extract nitrate complexes of uranium and other actinides was examined as early as 1944 during the Manhattan Project (Orlemann, 1944; Spedding *et al.*, 1945; Warf, 1945) and a patent application for a solvent extraction process for plutonium based on TBP and other trialkylphosphates was submitted in 1947 – the patent was not issued until 1960 because of security concerns (Anderson and Asprey, 1960). The development work leading to deployment of the process started in the late 1940s principally at Oak Ridge National Laboratory (Coleman and Leuze, 1978). The PUREX process was first used in 1954 at the Savannah River site of the U.S. Atomic Energy Commission and then in 1956 at the Hanford site (Swanson, 1990). With many variations in operational details, the process has since been used around the world as the principal method to separate plutonium and uranium from used reactor fuel and neutron-irradiated actinide materials (McKay *et al.*, 1990). The key to this process is the selective extraction of U(VI) and Pu(IV) from a nitric acid solution of dissolved irradiated fuel into an aliphatic hydrocarbon solvent containing TBP while leaving most of the fission products in the acid solution. The plutonium and then the uranium can be back-extracted separately from the loaded organic solvent into an aqueous strip phase. Additional solvent extraction stages with TBP can be used to further purify the uranium and plutonium or another method such as ion exchange can be used. Most PUREX operations target very pure uranium and plutonium products with high decontamination factors from the fission products of about 10^8 and high recovery (typically about 99.9%).

The following equilibrium equations represent the major separation steps of the PUREX process:

$$Pu^{4+}_{(aq)} + 4NO^-_{3\,(aq)} + 2TBP_{(org)} \rightleftharpoons Pu(NO_3)_4(TBP)_{2\,(org)} \tag{7.8}$$

$$UO^{2+}_{2\,(aq)} + 2NO^-_{3\,(aq)} + 2TBP_{(org)} \rightleftharpoons UO_2(NO_3)_2(TBP)_{2\,(org)} \tag{7.9}$$

$$HNO_{3\,(aq)} + TBP_{(org)} \rightleftharpoons TBP \cdot HNO_{3\,(org)} \tag{7.10}$$

The subscripts (aq) and (org) refer to species present in the aqueous and organic phases, respectively. The distribution coefficient (D) in liquid–liquid

extraction is defined as the ratio of the concentration of the solute in the organic phase to that in aqueous phase under a particular set of conditions, e.g. volume ratio of the aqueous to organic phase, temperature, extractant concentration, pH, metal ion concentration. Tetravalent and hexavalent actinide ions are selectively extracted under the PUREX conditions (typically 1–3 M nitric acid and 20–30 vol % TBP in an aliphatic hydrocarbon diluent) but the trivalent and pentavalent oxidation states of the actinides and most of the fission products are poorly extracted. This is illustrated by the data in Table 7.7 that lists the single-stage distribution coefficients for U(VI), Pu(VI), Pu(IV), Pu(III), and a group of fission products for TBP and two other compounds, hexone [$CH_3C(O)CH_2CH(CH_3)_2$] and dibutylcarbitol [$CH_3(CH_2)_3O(CH_2)_2O(CH_2)_2O(CH_2)_3CH_3$] that were the basis for two other competing solvent extraction processes, REDOX and BUTEX (Peterson and Wymer, 1963). The REDOX and BUTEX processes were used for a time at Hanford and in the United Kingdom, respectively, but eventually were replaced by the PUREX process. The data in Table 7.7 illustrate that the modest D values like those for uranium of 1.5–8.1 can be exploited for high recovery by using multiple stages of extraction. The data in the table also show that the bulk of the fission product have very low D values, but there are exceptions (Zr, Ru, and Tc). These fission product contaminants can be removed in various ways during the additional uranium and plutonium purification operations.

The equations shown above for Pu(IV) and U(VI) extraction indicate that higher nitrate concentrations in the aqueous phase and higher TBP concentrations in the organic phase should increase the D values for these metal ions. This is indeed observed as long as the activities of the various species are taken into account and metal ion concentrations are low. However, the extraction of nitric acid by TBP indicated in (7.10) competes with metal ion extraction for the TBP and limits the increase in the D value with increasing nitric acid concentration. The D values will continue to increase at a low fixed nitric acid concentration if nitrate salts are added to the aqueous phase rather than nitric acid. Pure TBP is

Table 7.7 *Distribution coefficients of uranium, plutonium, and some fission products using TBP, hexone, and Butex extractants.*

Solvent	*U(VI)*	*Pu(VI)*	*Pu(IV)*	*Pu(III)*	*Fission products*[a]
hexone[b]	1.6	2.9	0.84	4.5×10^{-4}	0.03
TBP[c]	8.1	0.62	1.55	0.008	0.001
Butex[d]	1.5	1.8	7	<0.01	~ 0.02

[a] Combined β emitters (without Zr, Ru, Ca).
[b] From 0.3 M HNO_3/1.0 M $Al(NO_3)_3$/(U,Pu) into hexone at 25°C, or from 0.25 M HNO_3/1.5 M $Al(NO_3)_3$/ΣFP into hexone at 25°C.
[c] From 3.0 M HNO_3 into 30 vol.% TBP in kerosene at 25°C.
[d] From 4 M HNO_3 into dibutylcarbitol (Butex).

a liquid and can be used as the organic phase in an extraction, but it is quite viscous. PUREX plants typically operate with 20–30 vol % TBP in an aliphatic hydrocarbon diluent (Swanson, 1990).

Adjusting the oxidation state of plutonium from Pu(IV) to Pu(III) is the most commonly used way of selectively stripping plutonium from the loaded organic phase. As shown in Table 7.7, the D value of Pu(III) is quite low and it will preferentially distribute to the aqueous nitric acid phase. Reducing agents that have been used to strip plutonium from the TBP phase are Fe(II), hydroxylamine, and U(IV). The addition of ferrous sulfamate in the aqueous acid solution used to strip the plutonium has given some of the best results as indicated by the purity of the uranium and plutonium products that result (Miles *et al.*, 1990). The overall equation for the Fe(II) reduction and stripping reaction is:

$$Pu(NO_3)_4(TBP)_{2\,(org)} + Fe^{2+}_{(aq)} \rightarrow Pu^{3+}_{(aq)} + 4NO^{-}_{3\,(aq)} + Fe^{3+}_{(aq)} + 2TBP_{(org)} \tag{7.11}$$

After the removal of plutonium, the uranium can be stripped from the TBP phase with a dilute acid solution. The TBP solution can then be reused to extract more uranium and plutonium. A generalized PUREX flow sheet is shown in Fig. 7.5.

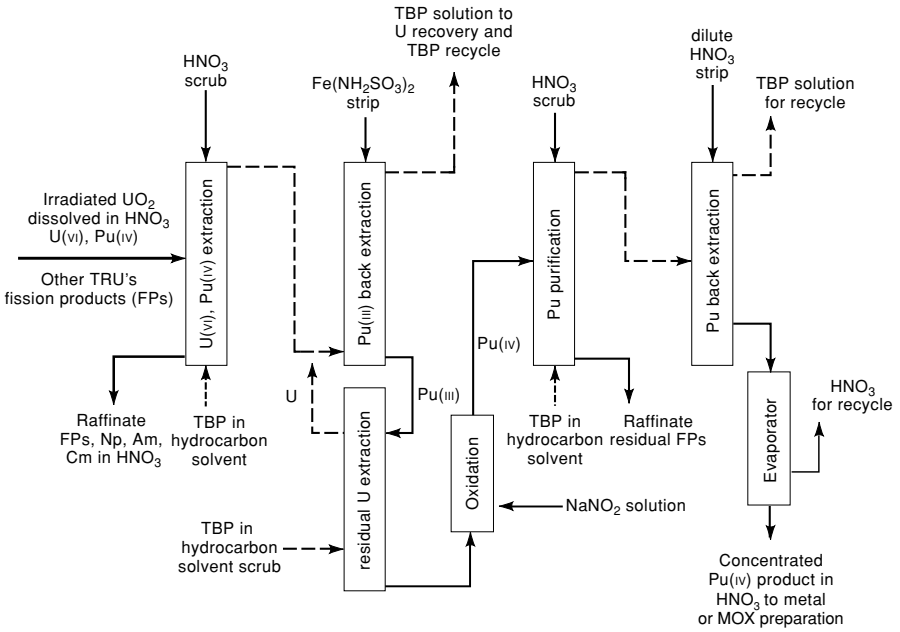

Fig. 7.5 *A generalized PUREX flow sheet where the dashed line indicates the organic stream.*

Of course, there are many other operations needed for running an actual PUREX plant that are not indicated by the simple extraction equations above. A few will be mentioned here and the references can be consulted for more detail. The decladding and dissolution of the fuel in nitric acid in a highly shielded facility are major operations that prepare the feed for the PUREX process. During the extraction process, the organic solvent and TBP undergo degradation reactions because of reactive species produced by the high level of ionizing radiation, particularly in the first extraction cycle where all the fission products are present. Some of the degradation products of TBP, dibutylphosphoric and monobutylphosphoric acids can cause problems by forming solids and modifying the D values for certain metal ions. This is dealt with by adding a washing operation to keep the concentration of these compounds below certain levels. The slight solubility of TBP and any entrainment of organic phase droplets in the aqueous phase also cause losses that must be replaced. Maintaining the oxidation states of various actinide and fission product metal ions in the intense radiation field requires careful adjustments at various points in the process. To improve process efficiency and to minimize wastes, evaporators are used to recover nitric acid and concentrate solutions at various points in the process. Finally, the products and wastes from all the operations must be handled properly and transported to their next destination.

During more than 50 years of use around the world, the PUREX process has undergone many improvements. Enhancements continue to be made at operating plants and new plants that will begin operations in the future. As options are considered for advanced nuclear fuel cycles, additional separations operations are under development for potential deployment in PUREX-type plants (see Chapter 24, section 4). Among these operations are solvent extraction processes for recovery of neptunium, americium, and curium to allow their transmutation in advanced reactor systems and for technetium, cesium, and strontium to allow these fission products to be disposed of more efficiently. Solvent extraction systems are certainly the most developed separation processes to accomplish these goals in the near future. The use of other separation approaches to augment or replace solvent extraction in advanced nuclear fuel cycles will require large technology development efforts.

(b) Extraction chromatography and supported liquid membranes

Liquid–liquid extraction can be deployed in forms other than the typical methods of mixing and separating the immiscible liquid phases. In extraction chromatography, the extractant and solvent (in some cases) are prepared in a thin layer on a solid support that usually consists of small spherical particles of a polymer or inorganic material. Inorganic materials such as silica require a surface treatment to generate a relatively hydrophobic surface that will be compatible with the organic extraction components. Aqueous solutions are contacted with the solid and metal ions are extracted into the thin surface

layer much as occurs in a liquid–liquid extraction system. However, the composition of the surface layer can be quite different from that of the liquid–liquid system and this must be taken into account when predicting extraction behavior. Extraction chromatography materials are used most commonly for analytical separations of plutonium and other actinides and have been deployed for a limited number of gloved box scale process operations. These materials generally do not have the radiation stability or capacity for use in large-scale processing of irradiated fuels. However, such an approach has been proposed and tested at a small scale with a spent fuel solution using some silica-based extraction materials by Wei and coworkers (Wei *et al.*, 2002).

Supported liquid membranes consist of a liquid phase that separates two fluid phases: two gases, two liquids, or a gas and a liquid. Components in the fluid phases can be separated by differential transport through the liquid membrane phase driven by the chemical potential gradients. For metal ion separations, the fluid phases on each side of the membrane are usually aqueous solutions and the membrane consists of a porous solid support with an organic extractant solution filling the pores. Supported liquid membranes have been demonstrated on the laboratory scale to be an efficient separation method for metal ions, but have seen relatively few industrial applications because of long-term stability problems. With time, the components of the liquid membrane are lost to the aqueous phases and the membrane fails. Many approaches have been considered to overcome this problem, but none have yet seen widespread industrial use (Sastre *et al.*, 1998).

In the extraction chromatography and supported liquid membrane systems the active extractant is not chemically bound to the support. Solids that do contain such chemically bound groups that can selectively bind plutonium and other actinides will be discussed under ion-exchange processes (see Section 7.5.5).

7.5.5 Ion-exchange processes

Ion-exchange materials are insoluble solid materials with groups of one charge fixed in a three-dimensional solid matrix and mobile or exchangeable ions of the opposite charge associated with these fixed sites that balance the charge in the solid. In contact with a liquid phase that contains dissolved ions, the mobile ions will be exchanged for ions of like charge in the solution if the overall free energy of the system is lowered after the exchange. The relative affinity of the ion-exchange material for various cations or anions can be used to separate particular ions from solution. By using a regeneration solution under different conditions, it is usually possible to recover the adsorbed ions from the ion-exchange material (often in more concentrated and pure form) and prepare the ion-exchanger for additional cycles of exchange and regeneration. Both inorganic solids and organic polymers, including natural materials such as clays and zeolites, can function as ion exchangers. Ion exchange has long been an important process for water treatment. One of the first industrial

applications of ion exchange described in 1905 was the use of synthetic sodium aluminosilicates (zeolites) to exchange Ca^{2+} from hard water with Na^{+} (Simon, 1991).

Ion exchangers are commonly deployed in industrial processes as a packed bed of small particles to obtain a high surface area and accessible exchange sites with minimal diffusion path lengths to the sites. In the loading phase, liquid feed solution is passed through the bed until the mobile ions in the solution have been exchanged for mobile ions in the solid to the extent that the target ion or ions are no longer being removed from solution to the required level. If the ions loaded on the exchanger are to be recovered as a product (e.g. plutonium), one or more wash solutions may be passed through the bed to improve the final purity by removing residual feed solution and exchanging more weakly held ions. In the elution phase a different solution is passed through the column to recover the product ions. The conditions during the elution phase are changed (pH, ion concentration or type, temperature, etc.) so that the target ions bound during the loading phase are exchanged back into the solution. After elution the ion exchanger may be ready for reuse directly or may require an additional regeneration step. Most ion-exchange processes are operated in such a batch mode with separate loading and elution or regeneration steps. Continuous ion-exchange processes have also been developed, but are not as widely used as batch operations (Simon, 1991).

Ion-exchange processes for metal ion separation most commonly use an organic polymer solid phase (often referred to as an ion-exchange 'resin') containing charged functional groups fixed to the polymer structure to selectively bind metal ions or complexes of metal ions with a net opposite charge from an aqueous solution. The organic polymer is usually prepared in the form of small spherical particles or beads with a large internal porosity. The structure of the polymer greatly affects the final ion-exchange properties and the synthetic conditions are adjusted to control properties such as the degree of crosslinking, the number of ion-exchange sites, the size distribution of the pores, and the bead size. The polymer structure in most commercial ion-exchange materials is formed from styrene (vinyl benzene)–divinylbenzene copolymers with the fixed charged groups attached to the phenyl rings. The most common functional groups are sulfonic acid and carboxylic acid groups with protons that exchange for cations (cation exchangers) and alkylamine, alkanolamine, and tetraalkylammonium groups that act as anion exchangers. Other polymer structures have been used to make ion exchangers including polyacrylates and polyvinylpyridines (Simon, 1991; Harland, 1994).

(a) Plutonium ion-exchange separations

Both cation- and anion-exchange processes have been used for concentrating and purifying plutonium from aqueous solutions that result from processing operations ranging from solvent extraction (e.g. PUREX) to recovery of

plutonium leached from scrap or debris material. Ion exchange is generally not used as the primary step to separate plutonium and other actinides from fission products in nuclear fuel or neutron-irradiated targets because the intense radiation field degrades the polymer matrix too rapidly. However, organic ion exchangers are very useful for separations in acidic solutions where the radiation dose comes mostly from plutonium and other actinides. Inorganic ion exchangers are generally more radiation-resistant than organic exchangers, but have other problems for large-scale processing such as limited stability over wide pH ranges, difficulty in obtaining reproducible behavior from batch to batch, and the greater difficulty of preparing particles of suitable size and shape for processing (Pekarek and Marhol, 1991).

Plutonium in any of its oxidation states can be taken up onto cation exchangers from dilute acid solutions with weakly binding anions such as nitric, hydrochloric, or perchloric acids. The strength of the binding of the oxidation state decreases in the order $Pu^{4+} > Pu^{3+} > PuO_2^{2+} > PuO_2^{+}$ as expected with the decreasing net charge on the cation. The ion-exchange process on a strong acid cation exchanger can be represented by the reaction:

$$Pu^{n+}_{(aq)} + nRH_{(org)} \rightarrow Pu(R)_{n\,(org)} + nH^{+}_{(aq)} \tag{7.12}$$

where RH represents a proton exchange site on the organic resin (usually a sulfonic acid site) and $n+$ is the net charge on the plutonium species. Separations can be made based on the ionic charge alone, but the greater utility of ion exchange results from using the exchange material in combination with complexants in the aqueous solution that bind the various oxidation states of plutonium and other metal ions differently. For example, in dilute hydrofluoric acid, Pu(III) will bind to a cation-exchange resin more strongly than Np(IV), in apparent disagreement with the expected order based on oxidation state alone. This is because Np(IV) forms complexes with fluoride to a greater extent than Pu(III) thereby reducing its overall net charge, e.g. NpF_3^{+} and NpF_2^{2+} (Zagrai and Sel'chenkov, 1962). Measuring the change in the ion-exchange equilibrium as a function of metal ion binding in the aqueous phase is one method for determining stability constants and can be particularly useful for radioactive metal ions like plutonium that can be analyzed at low concentrations.

The formation of anionic complexes of plutonium, especially by Pu(IV) and Pu(VI), is the basis for separations using anion-exchange resins. For example, in moderate concentrations of hydrochloric acid (~6 M) both Pu(IV) and Pu(VI) absorb strongly on a Dowex 1 resin (quaternary ammonium exchange sites), but Pu(III) shows no significant uptake even in concentrated HCl. Spectroscopic and ion-exchange capacity data indicate that the anionic species bound in the resin are $PuCl_6^{2-}$ and $PuO_2Cl_4^{2-}$ (Ryan, 1975). If high concentrations of chloride salts (e.g. 10 M LiCl) are used with a relatively low acid concentration, Pu(III) can also be taken up on Dowex 1 as an anionic complex. The absorbed plutonium species can be eluted from the resin by using low concentrations of HCl.

Anion exchange of Pu(IV) from moderate concentrations of nitric acid or nitrate salts is a particularly useful separation method for plutonium and has been applied from the process scale to the analytical scale. Applications range from concentrating and purifying the plutonium product stream from PUREX plants, to recovering and purifying plutonium dissolved from a wide range of scrap, residue, and debris materials, to preparation of analytical samples. The basis for the separation is the strong adsorption of Pu(IV) onto the anion-exchange resin from moderate concentrations of nitric acid or nitrate salts. Few other elements are significantly retained under these conditions by an anion exchanger and large separation factors can be obtained (Faris and Buchanan, 1964). The III, V, and VI oxidation states of plutonium and other actinides are also not bound strongly. Fig. 7.6 shows the Pu(IV) distribution coefficients (K_d) onto Dowex 1×4 resin plotted as a function of nitrate concentration for HNO_3 and $Ca(NO_3)_2$ solutions at 25 and 60°C (Ryan, 1959). The high distribution coefficients for Pu(IV) near 7 M nitric acid when combined with

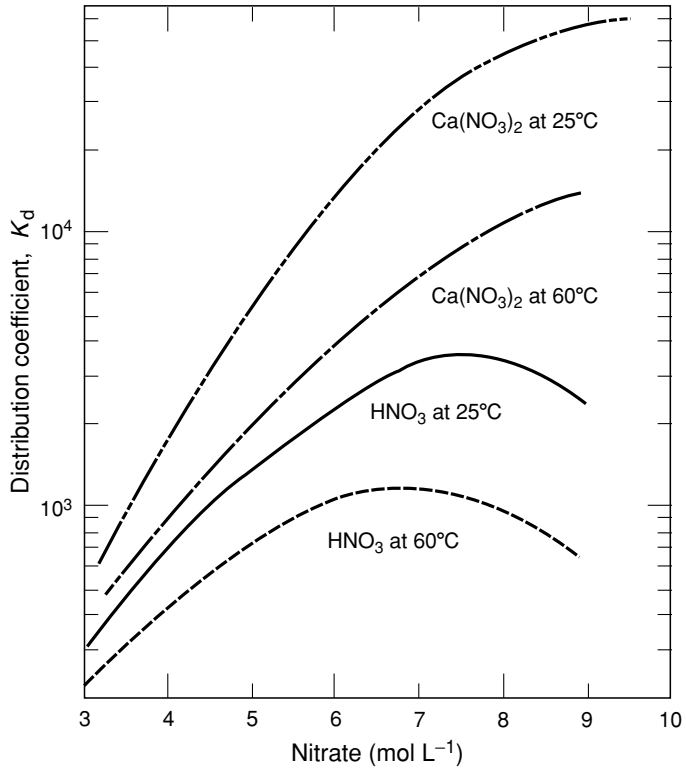

Fig. 7.6 *Plutonium(IV) distribution coefficients from nitric acid and calcium nitrate onto Dowex* 1 × 4 *anion-exchange resin* (*Ryan*, 1959).

an efficient elution method make large concentration factors possible. Elution of the plutonium is usually accomplished using a low nitric acid concentration alone or a low concentration of nitric acid and a reducing agent that generates Pu(III). The data in Fig. 7.6 show that the K_d values are lower at higher temperature, however, the kinetics of loading and elution are faster at higher temperature and this factor can be used as an advantage in process design (Ryan, 1975).

Visible absorption spectroscopy and resin capacity data show that Pu(IV) is absorbed on anion exchangers from nitric acid or nitrate salt solutions as the hexanitrato complex, $Pu(NO_3)_6^{2-}$ (Ryan, 1960, 1975). This has been confirmed by recent extended X-ray absorption fine structure (EXAFS) studies of anion exchange resins loaded with plutonium (Marsh *et al.*, 2000). Visible absorption, nuclear magnetic resonance (NMR), and EXAFS spectra of Pu(IV) and Th(IV) in nitric acid have also refined the information on the complexes formed in nitric acid solution (Veirs *et al.*, 1994; Allen *et al.*, 1996b; Berg *et al.*, 1998, 2000). At low nitric acid concentrations (~0.1 to 3 M) Pu^{4+}, $Pu(NO_3)^{3+}$, and $Pu(NO_3)_2^{2+}$ are the major species present (water molecules fill the rest of the plutonium coordination sphere in these complexes). At high nitric acid concentrations (>10 M), $Pu(NO_3)_6^{2-}$ is the dominant complex. At intermediate nitric acid concentration, in addition to $Pu(NO_3)_2^{2+}$ and $Pu(NO_3)_6^{2-}$, one major additional species is present that has been assigned as $Pu(NO_3)_4$. The trinitrato and pentanitrato complexes do not appear to be present at levels that can be easily observed (See Section 7.9.1.e). The concentration profile of the putative $Pu(NO_3)_4$ complex peaks at about 7 M nitric acid and correlates well with the distribution coefficient profile for Pu(IV) on anion-exchange resins from nitric acid (Marsh *et al.*, 1991). This observation suggests that the uncharged $Pu(NO_3)_4$ species might be important to the mechanism of uptake for Pu(IV) on an anion exchanger, but further work will be needed to verify this.

A general flow sheet for the operation of an anion-exchange process for plutonium recovery is illustrated in Fig. 7.7 (Christensen *et al.*, 1988). The oxidation state of plutonium dissolved in the nitric acid feed solution is carefully adjusted to maximize the amount of Pu(IV) because plutonium in other oxidation states is not retained on the exchanger. A variety of methods can be used for the oxidation state adjustment based on the composition of the feed. If fluoride is present in the feed solution, aluminum may be added to preferentially complex the fluoride and improve plutonium recovery. The nitric acid concentration is adjusted to 7 M and the solution is pumped through the packed bed of anion exchange beads so that $Pu(NO_3)_6^{2-}$ binds to the exchanger. The loaded resin is washed with 7 M nitric acid to remove impurities. Nitric acid at low concentration (0.35–0.6 M) is then pumped through the bed to elute the Pu(IV), or a solution of hydroxylammonium nitrate (or another suitable reducing agent) in dilute nitric acid is used to elute Pu(III). The plutonium in the eluate is commonly precipitated as an oxalate complex of either Pu(III) or Pu(IV) and the washed and dried oxalate solid is calcined to give a PuO_2 product.

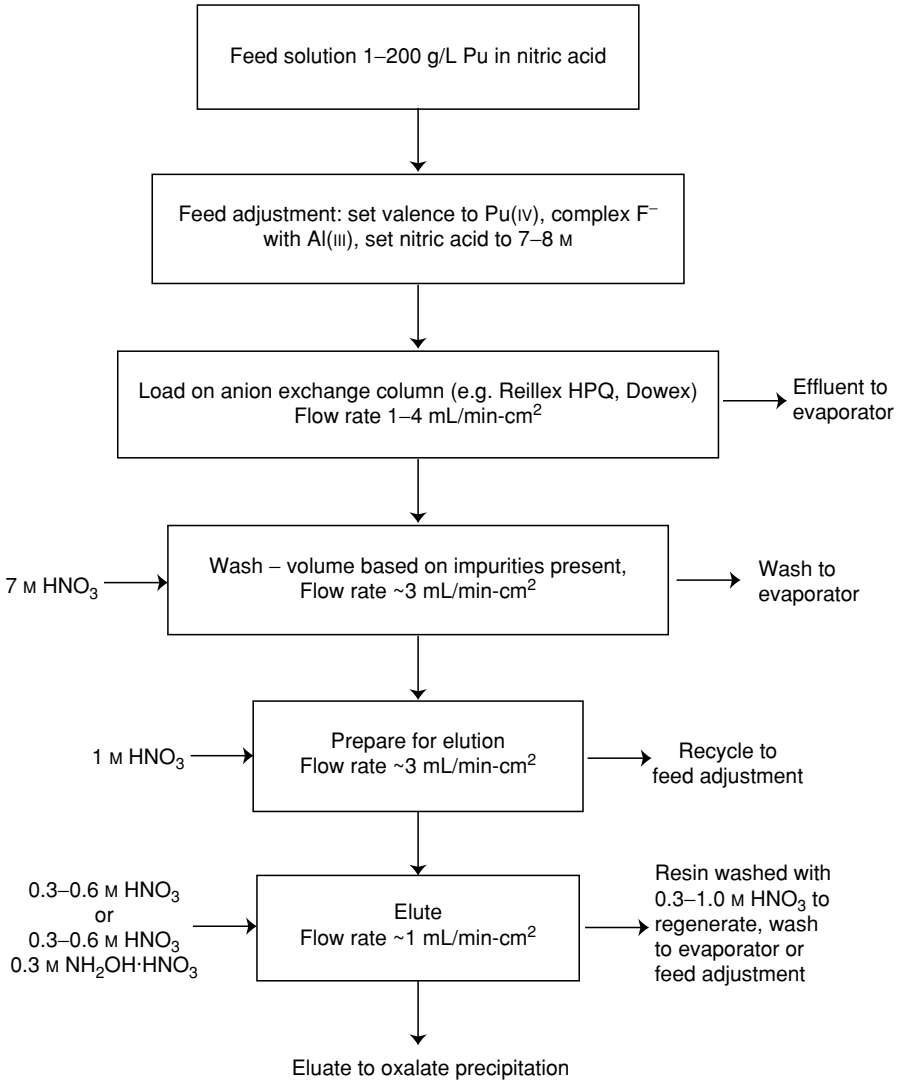

Fig. 7.7 *General flow sheet for operation of Pu(IV) anion-exchange purification process in nitric acid.*

There are a number of important features that must be controlled to safely and efficiently operate such an anion-exchange process for plutonium purification. Some of these features will be mentioned here. More detail can be found in the references (Cleveland, 1980; Christensen *et al.*, 1988). The batch size and the geometry of the packed bed are set up so that criticality cannot occur during

normal operation. During elution of plutonium from the column, the nitric acid concentration should not drop so low as to allow the formation of the Pu(IV) polymer (see Section 7.9.1.d) as this material can clog the column and can be difficult to redissolve. The nitric acid–organic resin system can undergo a runaway oxidation reaction if temperatures are allowed to reach an initiation point around 160–180°C. A variety of safety devices and operating procedures are used to avoid this situation. For example, in using anion exchange to purify plutonium with a high percentage of the ^{238}Pu isotope for radioisotope heat sources, smaller batch sizes and columns are used to allow removal of the additional heat generated by decay of ^{238}Pu in comparison to 'regular' plutonium with a high ^{239}Pu content (Pansoy-Hjelvik *et al.*, 2001).

Ion exchange has been employed for separating plutonium and studying its chemistry since its discovery of more than 60 years ago. Considerable advances have been made in the processes used to manufacture ion-exchange materials during this time, partly driven by the need to separate plutonium and other actinides more efficiently. Highly uniform ion-exchange beads with reproducible behavior are now standard. The development of methods to synthesize macroporous polymer structures in the beads has reduced swelling and shrinkage of the bed as a function of changing solution conditions while retaining good kinetics of absorption (Simon, 1991). The organic ion-exchange polymers are degraded by radiation-induced reactions as noted above, including the alpha-induced radiolysis reactions of plutonium solutions in nitric acid. Anion exchange polymers made from 4-vinylpyridine crosslinked with divinylbenzene (e.g. Reillex HPQ) were demonstrated to be substantially more resistant to radiation-induced degradation than related polystyrene-based anion exchangers while maintaining excellent properties for plutonium processing (Marsh *et al.*, 1991; Buscher *et al.*, 1999). Reillex HPQ has thus replaced the polystyrene-based materials for plutonium recovery operations at some facilities.

Of course, improvements in ion-exchange technology will continue. Exchange columns that consist of a microporous polymer monolith with uniform flow paths and relatively short diffusion pathways compared to packed beds of beads have been developed. These materials could greatly improve future ion-exchange processes (Buchmeiser, 2001; Viklund *et al.*, 2001). Inorganic ion exchangers are continuing to become more versatile and should see wider applications. Membrane-based ion-exchange processes are also seeing wider application and offer potentially very efficient separation operations, but generally will require membrane materials with better long-term stability, including radiation stability, to replace the more common column method.

(b) Liquid ion exchangers and chelating ion exchangers

The solvent extraction processes discussed in Section 7.5.4 that use organic-soluble tetraalkylammonium salts or trialkylamines to extract anionic metal ion complexes as ion pairs are ion-exchange processes as well. These extractants

are sometimes referred to as 'liquid anion exchangers.' Liquid cation exchangers are also used, for example, aliphatic and aromatic sulfonic acid compounds. Also, many types of functional groups have been placed on polystyrene and other polymer supports that can bind directly to the inner coordination sphere of a metal ion and help to stabilize a complex of the metal ion on the solid phases. This includes essentially all of the oxygen donor functionalities that were discussed in Section 7.5.4 (e.g. phosphates, phosphonates, phosphinates, and phosphine oxides). These polymers containing fixed ligand sites resemble solid versions of solvent extraction systems. However, fixing of the ligand to the polymer structure can considerably alter the metal ion-binding properties relative to an analogous ligand in solution. These kinds of materials are often referred to as 'chelating ion-exchange polymers' or resins, but it must be recognized that more than exchange of ion pairs is occurring in such materials and the thermodynamics of complex formation must be included in determining the selectivity and strength of the metal ion binding in these polymers. The use of chelating ion-exchange materials for separations of actinides is reviewed in Chapter 24 and a more general review for metal ion separations was published by Beauvais and Alexandratos (1998).

7.5.6 Separations in aqueous alkaline solutions

As noted in the brief discussion of aqueous actinide chemistry above, alkaline solutions are generally not used for actinide processing because the hydroxide complexes are quite insoluble. Large amounts of high-level caustic waste containing small amounts of actinides have been generated at Hanford and Savannah River as a result of neutralizing nitric acid solutions from PUREX recovery operations. A large body of work has been performed to better define the speciation of the actinides and to examine some potential processes for removing actinides from highly caustic tank wastes, including plutonium removal with various precipitants and absorbents. An overview of this work with references to the extensive literature has been published (Clark and Delegard, 2002).

Alkaline solutions containing strong ligands that can compete with hydroxide such as carbonate, fluoride, and peroxide can give high solubility to actinides in some oxidation states and even stabilize unusual oxidation states such as Pu(VII). The relatively small amount of work that has been done on extraction of actinides from alkaline solutions is reviewed in Chapter 24 (Section 3.7). One method to produce MOX fuels uses crystallization of Pu(VI) and U(VI) from ammonium carbonate solutions as $(NH_4)_4PuO_2(CO_3)_3$ or $(NH_4)_4UO_2(CO_3)_3$, respectively. The ammonium plutonyl and uranyl carbonates can be crystallized separately and blended or coprecipitated as the mixed carbonate (Roepenack *et al.*, 1984). An alkaline processing scheme for separation of the components of spent fuel in sodium carbonate/bicarbonate has been proposed and tested at a small scale on uranium and nonradioactive fission product elements (Asanuma *et al.*, 2001).

7.5.7 Nonaqueous separation processes

As noted above, the recovery of plutonium from irradiated uranium fuels has been dominated by the PUREX process, which requires dissolution of the fuel matrix in nitric acid. Alternative fluid media have been used or are under study to dissolve the uranium matrix and allow separation of the fission products from uranium, plutonium, and the other actinides, but none of these methods have been deployed on a large scale. The types of fluid media used include molten salts, molten metals, volatile halide compounds, ionic liquids, and supercritical fluids. The potential advantages for separation processes using these types of media compared to aqueous-based separations include: (1) greater resistance to radiation damage relative to water and organic solvents, (2) fewer and sometimes less complex steps to obtain products, (3) smaller highly shielded processing area, (4) smaller waste volumes that may also allow ready preparation for disposal, (5) simpler criticality control with reduced amounts of neutron moderating and reflecting materials, and (6) new separation selectivity. The separation selectivity for some of the nonaqueous processes are lower on a per stage basis relative to some of the aqueous technology, but that is not always a disadvantage when considering that more impurities may be acceptable in future reactor fuels and that safeguards benefits may result from keeping some components of the original mixture together. The advantages listed above do not apply to every process, but serve to give an indication of why there is continuing interest around the world in nonaqueous processing for advanced nuclear power systems.

The nonaqueous separation methods have disadvantages as well. The major disadvantage has already been mentioned, in that these processes have not been developed as extensively as the aqueous methods and thus have less well-defined costs, safety envelopes, and operational experience. The chemistry of these nonaqueous separation methods is presented in more detail in Chapter 24, especially as they apply to advanced methods for partitioning of spent nuclear fuel. In this chapter, we will briefly review the nonaqueous separation methods most relevant to plutonium processing.

(a) Pyrochemical separation and conversion processes

After plutonium has been separated from the fission products, pyrometallurgical operations have been used since the days of the Manhattan Project to prepare and purify metallic plutonium from various compounds (Hammel, 1998). Plutonium is a very electropositive and reactive metal, and preparation and purification methods based on molten salts and molten metals under inert atmospheres were adapted from industrial practice with adjustments required for actinide-specific factors such as radioactivity and criticality. The major pyrochemical processes used to prepare and purify plutonium metal (bomb

reduction of PuF_4, direct oxide reduction (DOR) of PuO_2, molten salt extraction (MSE) of americium, electrorefining (ER), and pyroredox) are discussed in Sections 7.7.1 and 7.7.2. The pyrochemical operations occur in mixtures of molten Group 1 or 2 chloride or fluoride salts at temperatures of 700–900°C, although temperature spikes near 2000°C may occur during the bomb reduction of PuF_4 with calcium metal. Preparing the feed materials for these pyrochemical operations using aqueous processing operations is reviewed in Section 7.5.3(b).

A wide variety of pyrochemical processes have been considered to separate the components of spent nuclear fuels in advanced nuclear fuel cycles. The processes range from early work on use of molten metals such as silver, cadmium, zinc, and magnesium that are immiscible with molten uranium as extractants for plutonium (Dwyer *et al.*, 1959; Wiswall *et al.*, 1959) to recent work on the pyroelectrochemical deposition of PuO_2 and UO_2 from molten chloride salts for direct fabrication by vibropacking into fast reactor fuel elements (Grachev *et al.*, 2004). An entire reactor system, the Molten Salt Reactor Experiment, based on a molten BeF_2 and ^7LiF core containing fissile UF_4 and fertile ThF_4 was studied at Oak Ridge National Laboratory in the 1960s. Reviews of these processes, both historical and those under development, have been published (Long, 1978; Bychkov and Skiba, 1999).

(b) Room temperature ionic liquids

Room temperature ionic liquids (RTILs) are salts that are liquid at or near room temperature. The RTILs currently under study consist of an organic cation (e.g. quaternary ammonium, $R_1R_2R_3R_4N^+$, or alkylpyridinium) paired with a wide variety of inorganic and organic anions (e.g. $AlCl_4^-$, PF_6^-, $CF_3CO_2^-$). The RTILs are under study for a wide array of applications, such as organic synthesis, battery electrolytes, catalyst systems, and metal ion separations (Rogers and Seddon, 2002). It should be noted that the RTILs and the inorganic molten salts discussed above under pyrochemistry are part of the larger class of ionic liquids. The inorganic salts generally have much higher melting points, but that situation may change to some extent as new classes of ionic liquids are investigated. For example, the sodium/potassium nitrate eutectic has a melting point near 170°C.

Potential applications of RTILs to plutonium and actinide separations are under development in two main areas: use as low temperature ionic liquid solvents for electrochemical deposition of metal or oxide and as liquid–liquid extractants for actinide metal ions from aqueous solutions. A research team led by the Queen's University of Belfast and British Nuclear Fuels, Ltd. has also proposed using RTILs to process spent nuclear fuel (Baston *et al.*, 2002; Pitner *et al.*, 2003). It is not yet known if the present generation of organic-containing RTILS is sufficiently radiation resistant for the processing of spent fuel.

(c) Halide volatility processes

The isotopic separation of volatile UF_6 using processes such as gaseous diffusion or gas centrifugation has been practiced at a large scale since the 1940s. In 1949, Sheft, Andrews, and Katz proposed a separation process for irradiated nuclear fuel based on fluorination using liquid interhalogen compounds. This was the beginning of an extensive research and development program into what is commonly called the fluoride volatility process (Sheft *et al.*, 1949). In this type of process, the irradiated fuel (uranium oxide, uranium alloys, even fuel assemblies with cladding intact) is dissolved in a liquid fluorinating solution, a molten salt sparged with fluorine, or fluorinated directly in a fluidized bed. The volatile UF_6 (along with NpF_6 and PuF_6 depending on the process details) and fission product fluorides such as TcO_3F, RuF_6, NbF_6, and MoF_6 are collected and separated using volatility differences and differences in reactivity of the fluorides with beds of solid reagents. In some proposed fluoride volatility processes, neptunium and plutonium are left with the nonvolatile fission product fluorides and separated by another method such as solvent extraction (Amano *et al.*, 2004).

The major advantages of the fluoride volatility process are relatively simple chemistry, radiation resistance of the reagents, high decontamination factors, and separation of uranium in a form suitable for re-enrichment. The disadvantages are the use of extremely corrosive reagents and the attendant corrosion of materials of construction, the criticality concerns associated with the high reactivity of hexafluorides, especially PuF_6, and controlling their deposition in the process equipment. Investigations of variants of fluoride volatility continue today, but these processes have not yet been deployed on a large scale. A fluoride volatility process for recovery of plutonium from certain scrap materials was demonstrated at the Rocky Flats Plant on a pilot scale, but was never deployed as a regular plant operation (Standifer, 1968).

Chloride volatility processes for separating the components of spent fuels have also been investigated (Bohe *et al.*, 1997). In general, this appears to be a less selective process because of the greater number of volatile fission product chlorides that could accompany the volatile actinide species, but the separation of the various volatile chloride species has not received as much effort as the fluoride system. The removal of zirconium alloy cladding materials by chlorination with HCl or Cl_2 and collection of the volatile $ZrCl_4$ has also been examined (Gens, 1961). This process could potentially provide an attractive alternative to mechanical decladding methods and could allow recycling of the slightly radioactive zirconium.

(d) Supercritical fluid extraction processes

Supercritical fluids, principally carbon dioxide, have been investigated to extract actinides from waste materials, for separating actinides and fission products from spent nuclear fuels, and as an alternative to conventional

liquid–liquid extraction. Reagents required for forming metal ion complexes (which include complexing agents, acids, and/or redox reagents) such as 1,3-diketones or TBP · HNO_3 are dissolved in supercritical carbon dioxide and this fluid phase is contacted with a solid material (e.g. uranium oxides or a waste solid) or an aqueous phase. The extracted metal ions can be recovered by a number of methods: changing the pressure to modify solubility and filtering a solid product, removing the carbon dioxide as a gas to leave a solid or liquid product, or back-extracting the metal ions into an aqueous phase. The bulk of the studies in this area with actinides have used uranium and thorium, but some work with plutonium and other transuranic elements has appeared. Extraction of U(VI) and Pu(IV) from aqueous nitric acid solutions into supercritical CO_2 solutions of TBP has been studied as a function of temperature and pressure (Iso *et al.*, 2000). Some data on the dissolution of oxides with TBP · HNO_3 dissolved in supercritical CO_2 have been reported for PuO_2 and solid solutions of $(Pu,U)O_2$ and $(Pu,Am,U)O_2/Eu_2O_3$ (Trofimov *et al.*, 2004). The use of chelating agents dissolved in supercritical CO_2 or liquid CO_2 with modifiers such as pyridine or water for decontamination of various solid materials including stainless steel, rubber, cotton, plastic, and soil from plutonium and other radionuclides has been studied (Murzin *et al.*, 2002b). The solubility of some 1,3-diketone complexes of U(VI), Np(IV), Pu(IV), and Am(III) in supercritical CO_2 has been measured (Murzin *et al.*, 2002a,b). Removal of plutonium and americium from soil using TBP and thenoyltrifluoroacetone (TTA) or hexafluoroacetone in supercritical CO_2 has been investigated (Mincher *et al.*, 2001; Fox and Mincher, 2002). The studies of supercritical fluid extraction for actinides are reviewed extensively in Chapter 24 (section 3.10).

(e) Combination processes

A great variety of aqueous, nonaqueous, and combined aqueous and nonaqueous processes have been proposed for partitioning of spent fuel. As described above, to prepare and purify plutonium metal, a combination of aqueous (PUREX and precipitation-crystallization methods) and nonaqueous (pyrochemical) processes has been used. A few recent examples proposed in the literature will be briefly described to indicate that combination processes are being considered in future separation facilities for processing used nuclear fuels. Amano and coworkers proposed the use of fluoride volatility on irradiated fuel to separate uranium for re-enrichment. Some volatile fission product fluorides such as technetium would also be collected separate from the uranium. The residual solid would then be dissolved in nitric acid for PUREX-type solvent extraction to separate plutonium and other transuranic actinides from the fission products to recycle the actinides to a fast reactor system, the so-called FLUOREX process (Amano *et al.*, 2004). Another group in Japan has proposed separating uranium, neptunium, and plutonium from spent fuel dissolved in nitric acid by oxidizing the neptunium and plutonium to the hexavalent state

and then cooling the nitric acid solution to crystallize out the mixed nitrate complex $(U, Np, Pu)O_2(NO_3)_2 \cdot xH_2O$ (Kikuchi *et al.*, 2003). A variety of other combined aqueous/nonaqueous processes that have been proposed for processing irradiated fuels are reviewed in Chapter 24.

7.6 ATOMIC PROPERTIES

Plutonium, like all of the heaviest elements, has a very complex electronic structure. The free atom and free ion spectra of plutonium are among the richest and most thoroughly studied of any chemical element. The complexity of the electronic structure is apparent in the spectral properties, such as X-ray absorption and emission spectra, and arc, spark, and discharge emission spectra. Early measurements were made with electrodeless discharge lamps and large grating spectrographs such as the 9.15 m Paschen–Runge spectrograph at Argonne National Laboratory (ANL). Very high-resolution grating spectrographs have been replaced by Fourier transform (FT) spectrometers such as those at the Laboratoire Aimé Cotton (LAC) (built in 1970) and at the Kitt Peak National Solar Observatory. The plutonium free atom, Pu^0, designated Pu I, has 94 electrons of which 86 electrons are in filled shells as found in the radon atom. It is customary in discussing the actinide series to only list the electrons in shells outside the radon core. The outermost electrons of the free actinide atoms and ions outside the radon core are found in the 7s, 7p, 6d, and 5f shells. For example, the ground state (lowest energy) configuration for Pu I is $5f^67s^2$. Identified excited configurations of Pu I within the first 3 eV ($\sim$24,000 cm^{-1}) of the ground state include $5f^56d7s^2$, $5f^66d7s$, $5f^56d^27s$, $5f^67s7p$, $5f^57s^27p$, and $5f^56d7s7p$. In the free atoms and ions, many low-lying configurations interact strongly with each other, giving rise to a large number of electronic states, and tens of thousands of spectral lines. A detailed discussion and review of the spectra of actinide free atoms and ions can be found in Chapter 16, and in reviews by Blaise *et al.* (1983a, 1986), Reader and Corliss (1980), and Blaise and Wyart (1992).

7.6.1 Optical emission spectra of Pu I and Pu II

The emission spectrum of neutral (Pu I) and singly ionized (Pu II) plutonium, which can be excited by arc, spark, hollow cathode, or inductively coupled plasmas, has been extensively studied. The first measurements of plutonium were conducted in 1943 by Rollefson and coworkers (Rollefson and Dodgen, 1943; Dodgen *et al.*, 1944, 1949) who measured the wavelengths and intensities of about 125 spectral lines. In the initial publications of plutonium spectra, only the wavelengths and intensities of unidentified transitions were reported. In 1959, McNally and Griffin reported the first energy level analysis

for Pu II, where seven levels of the lowest terms of the $5f^6 7s$ (^8F and ^6F) electronic configuration were determined (McNally and Griffin, 1959). In 1961, Bovey and Gerstenkorn determined the five lowest levels of $5f^6 7s^2$ (^7F) for Pu I (Bovey and Gerstenkorn, 1961). In 1961, a collaboration was formed between scientists at ANL, LAC, and Lawrence Livermore National Laboratory (LLNL) to continue studies of the term analyses of Pu I and Pu II spectra. In 1970, the FT spectrometry at LAC was used to record the spectra of ^{240}Pu and of a mixture of ^{240}Pu, ^{242}Pu, and ^{244}Pu isotopes up to 3.59 μm. A portion of one of these spectra is shown in Fig. 7.8. The high resolution and extension into the infrared spectral region greatly enhanced the spectral analysis and allowed the connection between the lowest odd and even levels (Blaise *et al.*, 1983a).

The first comprehensive description of Pu I and Pu II spectra became available in 1983, when Blaise, Fred, and Gutmacher collected wavelengths, wavenumbers, intensities, classifications, and isotope shift data in a 612 page ANL report (Blaise, 1983b). In 1992, Blaise and Wyart published all known energy levels of the actinide elements that had been analyzed up to that time and listed ionization stage, energies, intensities, *J*-values, and level assignments of selected lines (Blaise and Wyart, 1992). The contents of that compilation are available on an updated database at LACs website (www.lac.u-psud.fr).

At the time of this writing (2005), 9500 isotope shifts have been measured, and half of them are in the IR region. More than 31,000 lines of the Pu I and Pu II spectra have been observed, of which 52% have been classified as transitions between pairs of levels (Blaise *et al.*, 1983a, 1986; Blaise and Wyart, 1992). With the aid of Zeeman and isotope-shift data, a total of 606 even and 589 odd levels for Pu I, and 252 even and 746 odd levels for Pu II, have been identified. For all

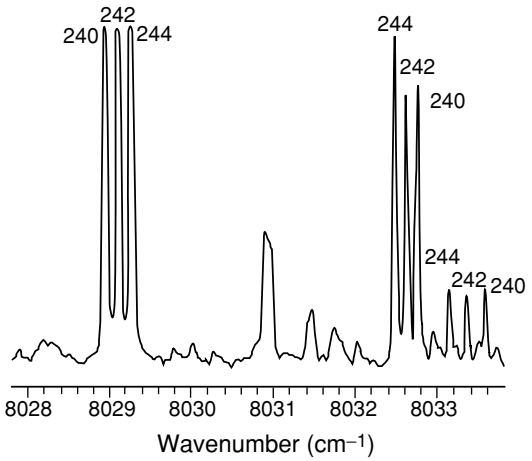

Fig. 7.8 *Fourier transform spectrum of a mixture of ^{240}Pu, ^{242}Pu, and ^{244}Pu isotopes* (*Blaise* et al., 1983a).

these levels the quantum number J has been assigned, and for many levels Landé g-factors are given. To date, levels belonging to 14 different electronic configurations in Pu I, and 9 electronic configurations in Pu II have been identified. The lowest levels of these configurations are given in Table 7.8 along with the Landé g-factors and experimental isotope shifts (Blaise *et al.*, 1983a; Blaise and Wyart, 1992).

The full-term analysis of plutonium spectra is still not yet complete because, even in 2005, a detailed quantum-mechanical treatment is hindered by the extreme complexity of the spectra. Even though the emission spectra of plutonium are still not completely assigned, they are among the best-understood spectra of the heavy elements.

7.6.2 Ionization potentials

The first ionization potential (IP) is a fundamental physical and chemical property of an element, and it is directly connected to the atomic spectra. Its accurate determination is important for identifying systematic trends within the actinide series of elements. In 1973 and 1974, Sugar derived values for the ionization energies of neutral plutonium and other actinides by using interpolated spectral properties of the atoms (Sugar, 1973, 1974). For neutral plutonium, the first IP was calculated to be 6.06(2) eV or 48,890(200) cm^{-1}. Worden *et al.* (1993) measured the first IP of ^{239}Pu by laser resonance techniques requiring as much as 2 g of ^{239}Pu. The photoionization threshold value for the ^{239}Pu I IP was determined to be 48,582(30) cm^{-1}, and the more accurate value from the Rydberg series measurements was 48,604(1) cm^{-1} or 6.0262(1) eV. In 1998, Erdmann and coworkers reported the first IP of ^{239}Pu using resonance ionization mass spectrometry (RIMS), a technique that requires only a few hundred picograms of material. In this approach, one- or two-step resonant laser excitation in a well-defined electric field promotes the atoms to a highly excited state, and ionization is obtained by scanning the wavelength of an additional tunable laser across the threshold, and extrapolation to zero field strength. From RIMS data, the first IP was found to be 48,601(2) cm^{-1} or 6.0258(2) eV (Erdmann *et al.*, 1998; Waldek *et al.*, 2001).

7.6.3 X-ray spectra

Plutonium X-ray spectra have been studied in detail by several authors (Cauchois *et al.*, 1954; Cauchois and Manescu, 1956; Shacklett and DuMond, 1957; Merrill and DuMond, 1958, 1961; Nelson *et al.*, 1969, 1970), and detailed wavelength and energy tables have been published by Bearden (Bearden, 1967; Bearden and Burr, 1967). The reader is also referred to the *Gmelin Handbook* (Koch, 1973c). The K and L series of the Pu X-ray spectra are known, and a few lines of the M and N series have been measured (Cauchois *et al.*, 1963a,b; Bonnelle, 1976). The L edges of the X-ray absorption spectra have been used

Table 7.8 *The lowest energy level of each electronic configuration of neutral Pu I and monovalent Pu II with their corresponding term symbol, energy, Landé g-values, and isotope shifts* (*Blaise and Wyart*, 1992).

Configuration	*Parity*	*Term*	*Energy* (cm^{-1})	*g*	*IS* (240–239) (10^{-3} cm^{-1})	*References*
Pu I						
$5f^6 7s^2$	even	$^7F_0$	0.000	–	465	Bovey and Gerstenkorn (1961)
$5f^5 6d 7s^2$	odd	$^7K_4$	6 313.886	0.487	653	Bauche *et al.* (1963b)
$5f^6 6d 7s$	even	$^9H_1$	13 528.246	−0.59	253	Bauche *et al.* (1963b)
$5f^5 6d^2 7s$	odd	$^9L_4$	14 912.011	0.496	488	Bauche *et al.* (1963b)
$5f^6 7s 7p$	odd	$^9G_0$	15 449.472	–	336	Brewer (1971a)
$5f^5 7s^2 7p$	even	$^7I_3$	17 897.119	0.450	698	Bauche *et al.* (1963b) and Blaise *et al.* (1983a)
$5f^5 6d 7s 7p$	even	$^9L_4$	20 828.477	0.352	467	Bauche *et al.* (1963b)
$5f^7 7s$	odd	$^9S_4$	25 192.231	1.768	273	Blaise *et al.* (1983a,b)
$5f^6 7s 8s$	even	$^9F_1$	31 572.610	2.403	446	Bauche *et al.* (1963b)
$5f^6 6d^2$	even	$^9I_2$	31 710.912	0.200	115	Blaise *et al.* (1983a)
$5f^6 7s 7p$	odd	$^9I_2$	33 070.58	0.673	293	Blaise *et al.* (1983a, unpublished)
$5f^4 6d^2 7s^2$	even	$^7M_6$	36 050.562	0.83	535	Brewer (1971a)
$5f^5 6d^2 7p$	even	$^9M_5$	37 415.524	0.980	403	Blaise *et al.* (1983a, unpublished)
$5f^5 6d 7s 8s$	odd	$^9K_3$	39 618.16	0.27	503	Blaise *et al.* (1986)
Pu II						
$5f^6 7s$	even	$^8F_{1/2}$	0.000	3.150	381	McNally and Griffin (1959)
$5f^5 7s^2$	odd	$^6H_{5/2}$	8 198.665	0.415	896	Fred *et al.* (1966)
$5f^5 6d 7s$	odd	$^8K_{7/2}$	8 709.640	0.310	555	Brewer (1971b) and Blaise *et al.* (1983a)
$5f^6 6d$	even	$^8H_{3/2}$	12 007.520	−0.019	77	Bauche *et al.* (1963b)
$5f^5 6d^2$	odd	$^8L_{9/2}$	17 296.88	0.494	242	Brewer (1971b) and Blaise *et al.* (1983a)
$5f^6 7p$	odd	$^8G_{1/2}$	22 038.95	0.345	287	McNally and Griffin (1959) and Brewer (1971b)
$5f^5 7s 7p$	even	$^8I_{5/2}$	30 956.36	0.650	424	Brewer (1971b) and Blaise *et al.* (1983a)
$5f^5 7s 7p$	even	$^8L_{9/2}$	33 793.30	0.795	208	Blaise *et al.* (1983a)
$5f^4 6d^2 7s$	even	$^8M_{11/2}$	37 640.78	0.70	813	Brewer (1971b) and Blaise *et al.* (1983a)

for plutonium oxidation state determination through the X-ray absorption near edge structure (XANES) in a variety of matrices (Conradson *et al.*, 1998, 2004a; Duff *et al.*, 1999; Richmann *et al.*, 1999; Fortner *et al.*, 2002; Antonio *et al.*, 2004; Lechelle *et al.*, 2004).

7.6.4 Core-level spectra

A few core-level spectra on plutonium compounds have been measured and comprehensively reviewed by Teterin and Teterin (2004). Core-level spectra that probe plutonium 4d, 4p, 4f, 5d, 5p, 6s, and 6p levels have been applied to determination of oxidation states and local environment, the magnetic properties of compounds, the nature of the chemical bonding, and secondary electronic processes that accompany photoemission. The use of fine structure spectral parameters, together with the electron binding energies and line intensities, significantly extends the scope of application of the X-ray photoelectron spectroscopy (XPS) method in structural studies. We mention only a few recent applications of core-level spectra.

Kotani and coworkers examined 4f core XPS of PuO_2 and other actinide dioxides and employed the Anderson impurity model to show that PuO_2 is a strongly mixed-valent compound and that a crossover between Mott–Hubbard and charge-transfer insulators occurs near NpO_2 (Kotani and Ogasawara, 1993; Kotani *et al.*, 1993). Allen and coworkers examined Pu 4f XPS of the α, β, γ, and δ phases of plutonium metal. They found that the 4f core-level spectra display features that vary systematically for the α, β, γ, and δ phases. For all phases they observed a sharp feature at binding energy 422 eV and a much broader shoulder that is approximately 2.5 eV higher. Application of an Anderson impurity model indicates that these features represent well-screened ($5f^6$) and poorly screened ($5f^5$) final states, respectively (Allen *et al.*, 1996a; Cox *et al.*, 1999). More recently, Gouder *et al.* (2002) employed 4f core-level spectroscopy to demonstrate dramatic changes in the electronic structure of ultrathin layers of α-Pu, and suggest that the surface of α-Pu should have δ-Pu character.

7.6.5 Mössbauer spectra

It is possible to obtain Mössbauer spectra on plutonium using excited states of ^{238}Pu, ^{239}Pu, and ^{240}Pu. In the case of ^{238}Pu, the β decay of ^{238}Np yields the 44 keV excited state of ^{238}Pu, which decays to the ground state with $T_{1/2} = 183$ ps and E2 dipole radiation. The 44 keV γ-ray may be used in resonance absorption measurements. A disadvantage is the short half-life of the 44 keV level (170 ps), which causes line broadening, and the relatively short half-life (2.1 days) of the source nuclide ^{238}Np, which makes it difficult to prepare sufficient amounts of the latter for a Mössbauer spectroscopy source.

For ^{239}Pu, the β decay of ^{239}Np produces a 57.3 keV state of ^{239}Pu, which decays through E2 γ radiation, which may be used in resonance fluorescence

spectroscopy. Gal *et al.* (1972) studied the resonance fluorescence of the 57.3 keV γ ray using a $^{239}NpO_2$–ThO_2 source and ^{239}Pu as the absorber. At 4.2 K, a resonance with a half-width of (5.13 $\pm$ 0.10) cm s^{-1} was observed. Assuming a Debye temperature of (250 $\pm$ 50) K for PuO_2, they calculated a natural linewidth of (473 $\pm$ 0.25) cm s^{-1}. This corresponds to a half-life of (101 $\pm$ 5) ps, in agreement with the lifetime of rotational levels, which decay by E2 transitions.

For ^{240}Pu, the α decay of ^{244}Cm yields a 42.9 keV state in ^{240}Pu in 23.3% of all occurring α decays. This state decays to the ground state with $T_{1/2} = 164$ ps. The 42.9 keV transition has an internal conversion coefficient of $\alpha_T = 920$. The use of this transition for Mössbauer spectroscopy was first demonstrated by Kalvius *et al.* (1978), who studied tetravalent $^{240}PuO_2$ and hexavalent $^{240}PuO_2C_2O_4$. In the tetravalent system, at 4.2 and 77 K, a single resonance line was found with a width of about 20% larger than the natural width of about 40 mm s^{-1}. In the hexavalent plutonyl oxalate, $PuO_2C_2O_4$, at 4.2 K a quadrupole interaction $|e^2qQ| = 95$ mm s^{-1} was found, but no isomer shifts were detected.

7.7 PLUTONIUM METAL AND INTERMETALLIC COMPOUNDS

Plutonium metal, alloys, and intermetallic compounds have important technological applications principally because of the nuclear properties of isotope 239. Plutonium metals and alloys are the materials of choice for the nuclear explosive in nuclear weapons and for fuel elements for some advanced reactor designs. The metallic properties of plutonium are important not only for nuclear weapons design, but also for the safe storage and disposition of excess weapons-grade plutonium. Plutonium alloys were used in some early reactor concepts (Anderson *et al.*, 1960; Kiehn, 1961; Burwell *et al.*, 1962) and are under development for advanced designs such as the Integral Fast Reactor (Keiser *et al.*, 2003). Much of the early work on plutonium metal and alloys was done in secrecy in the declared nuclear weapons states (mostly in the United States, Soviet Union, U.K., and France). President Eisenhower's Atoms for Peace initiative, which was launched with his December 8, 1953 speech to the United Nations brought most of the scientific work and many of the engineering properties into the open through a series of international conferences, starting with the first Atoms for Peace Conference in Geneva in 1955. Today, the threats of proliferation and terrorism cause concern about the amount of practical information regarding the construction of nuclear devices available in the open literature. Over the years, the U.S. government has taken the position that the fundamental scientific and engineering properties of plutonium be treated as open information. However, practical manufacturing methods, including those specific to weapons manufacture and the performance of nuclear weapons, remain classified. These guidelines are followed in this chapter.

In addition to its technological importance, plutonium in condensed matter also proves to be fascinating scientifically. The unusual nature of plutonium in the solid state is the result of its peculiar electronic structure. It lies near the middle of the actinide series – precisely at a transition point between the 5f electrons participating in bonding or being localized and chemically inert. Exploring the properties of plutonium and its compounds is an area of great interest in condensed matter physics. From a metallurgical perspective, the peculiarities associated with plutonium's electronic structure cause plutonium to defy most conventional metallurgical wisdom. These peculiarities, along with much of the interesting chemistry of plutonium, have been the subject of several recent reviews (Guerin, 1996; Cooper and Schecker, 2000; Terminello *et al.*, 2001; Hanrahan *et al.*, 2003; Jarvinen, 2003). In this section, we focus on the basic properties of plutonium, but we also explore properties of the neighboring actinides to better understand plutonium within the context of the entire actinide series.

Although our focus is on properties, we state at the outset that to delineate plutonium's metallic behavior it is imperative to understand what is called in the materials science community the processing–structure–properties relationship. Metallurgical practitioners routinely adjust properties by tailoring structure through careful control of chemistry and processing of metals and alloys. By structure we mean crystal structure, grain structure, and defect structure on the nano- and microscale. Plutonium is notoriously unstable with respect to temperature, pressure, and chemical additions, and its surface is reactive, especially in the presence of hydrogen or water. The synthesis and processing of plutonium are quite complex. There is considerable concern over lot-to-lot variations in processing and structure because criticality considerations limit the production of plutonium metal and alloys to small lots (at most on the order of kilograms). Also, microcracks, surface reactions, inclusions from impurities, and retained second phases can affect sample properties. In addition, the self-irradiation of plutonium (especially the prevalent isotopes ^{239}Pu and ^{238}Pu) causes microstructural changes that may affect its properties as it ages. Hence, the age of plutonium samples, or the time elapsed since the material was last molten or heat treated, can affect the properties. Unfortunately, most publications on plutonium properties provide little structural information, and detailed descriptions of processing conditions or sample age are typically limited.

We will draw attention to those cases for which the properties are especially sensitive to structure, processing, and age. The reader is also advised to examine reported density data and X-ray crystal structure information as both provide a good indication of what phases were present in the samples studied.

7.7.1 Preparation of plutonium metal

Plutonium metal may be obtained by a number of reduction reactions of plutonium compounds. Summaries of the various reactions have been given by Harmon *et al.* (1961), Leary and Mullins (1966), McCreary (1955),

Christensen and coworkers (Christensen and Mullins, 1983; Christensen *et al.*, 1988), Coops *et al.* (1983), and Baldwin and Navratil (1983). Not all of the reactions that produce plutonium metal are ideally suited for metal preparation in production work. For production processes, the chemical reactions must (a) produce a dense, coherent mass of pure plutonium in high yield; (b) generate sufficient heat to melt both the metal and the resulting slag; (c) result in a slag that stays molten and nonviscous long enough to allow the plutonium to coalesce; and (d) work on the scale desired (a reaction suitable for microgram-scale reductions might be less useful for gram- or multigram-scale reductions and vice versa). In reactions where one of the conditions (a–d) is not initially fulfilled, modified process conditions may still make the technique usable. For example, if the heat of reaction for a Ca reduction is insufficient (condition b), then addition of an iodine booster or use of a laser can provide sufficient heat to make the overall process usable. The resulting CaI_2 in turn helps to improve condition (c).

The pyrochemical preparation of plutonium metal is best carried out by reduction of PuF_4, PuF_3, $PuCl_3$, PuO_2, or a PuO_2–PuF_4 mixture with calcium metal in a high-temperature molten salt. Quite often a booster (such as iodine) initiates the reaction and provides sufficient energy to ensure the complete reaction:

$$PuF_4 + 2Ca^0 \rightarrow Pu^0 + 2CaF_2 \tag{7.13}$$

$$2PuCl_3 + 3Ca^0 \rightarrow 2Pu^0 + 3CaCl_2 \tag{7.14}$$

$$PuO_2 + 2Ca^0 \rightarrow Pu^0 + 2CaO \tag{7.15}$$

These methods of preparation do not produce any purification (Leary and Mullins, 1966); they simply produce metallic plutonium. Of these approaches, the reduction of PuO_2 has become the preferred route for preparation of plutonium metal. $PuCl_3$ is extremely hygroscopic, which poses handling difficulties, particularly for large quantities of material. The plutonium fluorides (PuF_4, PuF_3) are neutron emitters (due to α-n reactions), and working with plutonium fluorides requires considerable protective shielding. A related lithium reduction of PuO_2 has been developed as a pyrochemical process for the recycle of oxide fuels (Usami *et al.*, 2002).

Hydriding and dehydriding or hydriding followed by oxidation can recover plutonium metal scraps adhering to other metal surfaces (Haschke, 1991; Flamm *et al.*, 1998). Even at room temperature, plutonium metal reacts reversibly with hydrogen to form a metallic PuH_x powder (see Section 7.8.1).

$$2Pu^0 + xH_2 \rightleftharpoons 2PuH_x \tag{7.16}$$

The hydride spalls off the inert substrate and subsequent heating of the hydride product in a vacuum recovers the plutonium metal.

7.7.2 Modern pyrochemical preparation and refining

Over time, the general process for obtaining, preparing, and refining plutonium has evolved based on the kinds of feed materials available. Historically, plutonium was first produced in production reactors; extracted, concentrated, and converted to either an oxide or fluoride; and then reduced to metal. The resulting metal was used for fabrication of various parts and components. The fabrication process itself generates major quantities of waste and scrap plutonium that must then be recovered and recycled. In modern times, the feed material for preparation and refining of metallic plutonium has evolved to recovery and recycle of residues and scrap material. This in turn drives the current technology selection for metal preparation and refining. In addition, the technology selection must take nuclear material safeguards, accountability, criticality safety, and radiation exposure into consideration. The major pyrochemical processes that are currently employed in large facilities are bomb reduction of PuF_4, DOR, MSE, anode casting, ER, and pyroredox, and these techniques are integrated into a general processing flow diagram, such as the Los Alamos approach indicated in Fig. 7.9. As the figure shows, each operation produces residues that are treated either by pyrochemical or aqueous means to recover plutonium. We will discuss these pyrochemical processes in some detail.

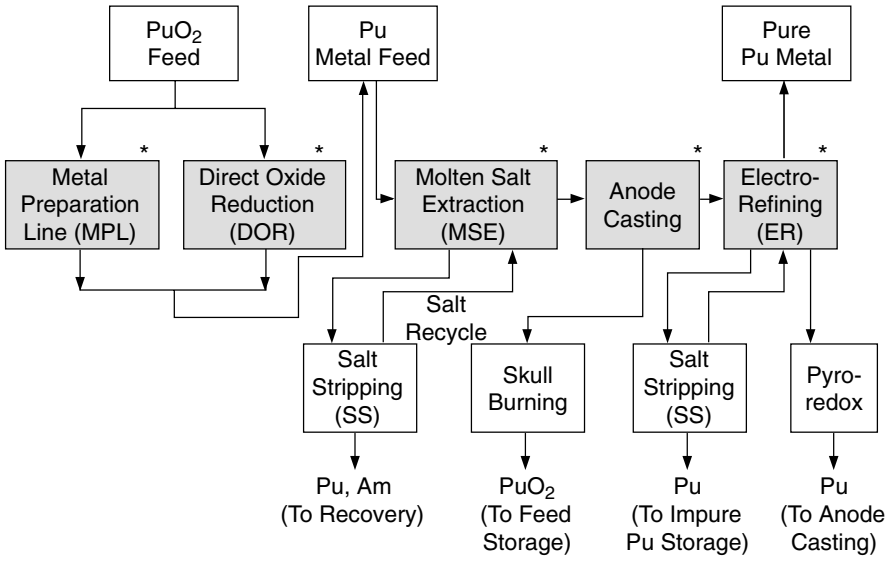

Fig. 7.9 *A general integrated pyrochemical processing system for plutonium metal preparation* (*Christensen* et al., 1988).

(a) Fluorination and reduction

The fluorination and reduction process produces plutonium metal from PuF_4 by the high-pressure reaction between the fluoride and calcium metal (Baker, 1946). Plutonium dioxide is converted to PuF_4 with HF in a hydrofluorination reaction, or by direct fluorination with F_2 (see Section 7.8.6.a). After fluorination of oxide, a chemical booster, such as iodine, initiates the reduction reaction:

$$PuO_2 + 4HF \rightarrow PuF_4 + 2H_2O \tag{7.17}$$

$$PuO_2 + 2F_2 \rightarrow PuF_4 + O_2 \tag{7.18}$$

$$PuF_4 + 3Ca^0 + I_2 \rightarrow Pu^0 + 2CaF_2 + CaI_2 \tag{7.19}$$

An illustration of a typical bomb reduction furnace is shown in Fig. 7.10. The PuF_4, calcium metal, and MgO (magnesia) slag are thoroughly mixed in a molded, open-porosity magnesia crucible. Iodine, added before the equipment is assembled and heated, acts as an initiator and reaction booster. At approximately 325°C, calcium and iodine react exothermically to rapidly raise the temperature. At 600°C, the PuF_4 reduction reaction begins and the system temperature rises rapidly to nearly 2000°C. The slag remains molten while the liquid plutonium sinks to the bottom of the crucible and solidifies. After the equipment has cooled, the crucible is broken to recover the metal button, which is mechanically separated from the slag (Christensen *et al.*, 1988). Little or no purification occurs during the process, and the metal purity is similar to that of the feed material. If the reagents are of high purity, and sufficiently pure plutonium feed is used, then the resulting metal is satisfactory for high-purity applications. Yields usually range from 97 to 99% (Baker and Maraman, 1960). This reaction can be carried out on a relatively large scale, and up to 6 kg batches of plutonium metal are not uncommon.

(b) Direct oxide reduction (DOR)

In the DOR process, plutonium dioxide is reduced with calcium metal to produce plutonium metal and calcium oxide (Mullins *et al.*, 1982; Mullins and Foxx, 1982; Christensen and Mullins, 1983). The reaction takes place in a molten $CaCl_2$ or $CaCl_2$–CaF_2 solvent, which dissolves the resulting CaO and allows the plutonium metal to coalesce in the bottom of the crucible to form a metal button. The PuO_2, calcium metal, and fused $CaCl_2$ are loaded into a vitrified magnesia crucible. The $CaCl_2$ is cast before use and contains no detectable water. The generic DOR apparatus is shown in Fig. 7.11 (Christensen and Mullins, 1983). The crucible is heated in a resistance furnace to 800°C. Once the $CaCl_2$ is molten, a Ta stirrer and a Ta–Ni thermocouple sheath are lowered in the melt. The reaction typically begins at about 820°C with a temperature

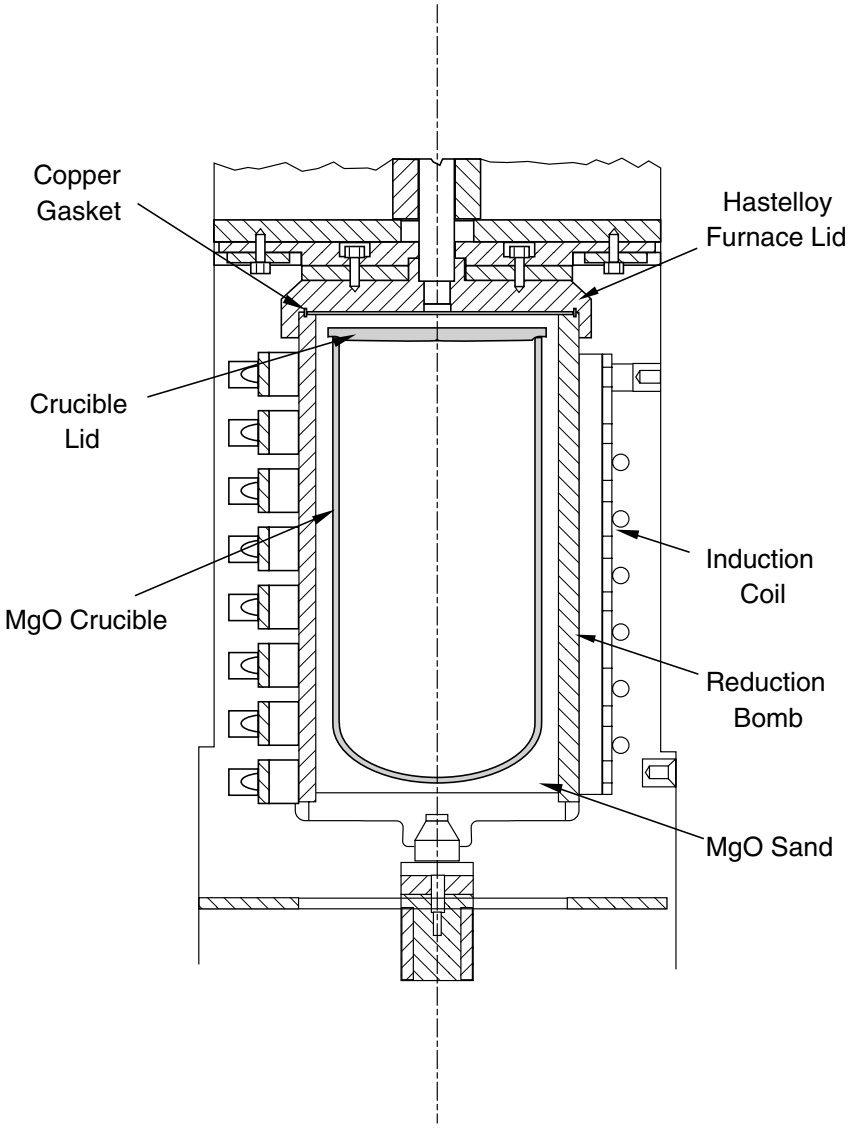

Fig. 7.10 *A furnace assembly for plutonium metal production by reduction of* PuF_4 (*Christensen* et al., 1988).

spike to 875°C. The reaction is complete within 15 min. The reaction proceeds to completion when excess calcium is present, sufficient $CaCl_2$ is available to dissolve the CaO that is produced, and rapid stirring is applied. While stirring, the reaction is monitored with a thermocouple. After completion of the

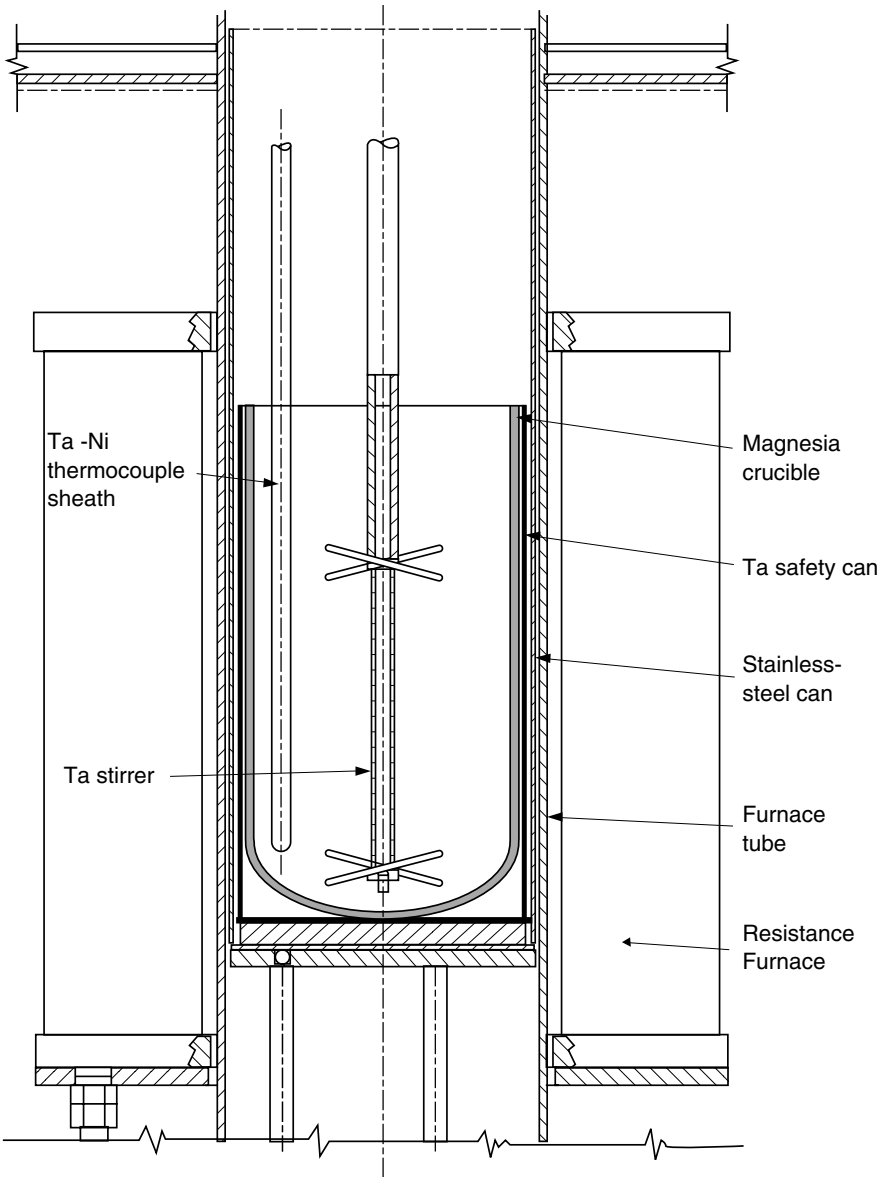

Fig. 7.11 *A general furnace assembly for direct oxide reduction* (*DOR*), *molten salt extraction of americium* (*MSE*) *and pyroredox operations* (*Christensen* et al., 1988).

reaction, the thermocouple well and stirrer are retracted, and the melt is allowed to settle and cool. Almost all the plutonium forms a metal button at the bottom of the crucible, and a typical DOR reaction product is shown in Fig. 7.12. The salt immediately above the button contains a layer of metal shot, and the bulk of

Fig. 7.12 (*a*) *A photograph of a DOR breakout showing the MgO crucible, residues, and metal product at the bottom.* (*b*) *The DOR metal button* (*top*) *and residues* (*photographs courtesy of Los Alamos National Laboratory*).

the salt solidifies above the metal. The plutonium button is mechanically separated, and the shot is recovered by reheating the shot-rich (usually with calcium present) material above the melting point to consolidate the metal. Product yields are greater than 95% (Mullins *et al.*, 1982).

(c) Molten salt extraction (MSE)

The plutonium metal produced in PuF_4 and PuO_2 reduction is impure and needs to be refined. The MSE process is specifically designed to reduce the americium content of plutonium metal (^{241}Am spontaneously grows into plutonium as a result of ^{241}Pu β-decay), but it also separates the more reactive elements, such as rare-earths, alkali-metals, and alkaline-earth metals (Knighton and Steunenberg, 1965; Knighton *et al.*, 1976; Coops *et al.*, 1983). The general principle of MSE is to oxidize the americium to Am(III) to extract it into the salt phase, leaving plutonium in the metallic phase. The extraction procedure is identical to the DOR process and uses essentially the same apparatus shown in Fig. 7.11, with the exception that a reusable tantalum vessel replaces the magnesia crucible, an oxidant is added, and the stirring time is typically 30 min instead of only a few minutes. To run the reaction, workers place impure plutonium metal in contact with a ternary salt, consisting of

$MgCl_2$ as the oxidizing agent in a NaCl/KCl eutectic. The major reactions are (Mullins *et al.*, 1968; Leary and Mullins, 1974):

$$2Am^0 + 3MgCl_2 \rightarrow 2AmCl_3 + 3Mg^0 \tag{7.20}$$

$$2Pu^0 + 3MgCl_2 \rightarrow 2PuCl_3 + 3Mg^0 \tag{7.21}$$

$$Am^0 + PuCl_3 \rightarrow AmCl_3 + Pu^0 \tag{7.22}$$

A typical batch size is 4.5 kg with a 12-h temperature cycle to 750°C. (The actual reaction time is only 30 min.) After the equipment has cooled to room temperature, the fused salt containing the americium and other impurities is separated from the plutonium metal button and crucible. Usually, each feed button goes through two batch extractions. In a typical 4.5-kg run containing 3000 ppm americium, 90% of the americium is oxidized at the expense of ca. 100 g plutonium. A typical product weighs 4.4 kg and contains 98% of the feed plutonium (Christensen and Mullins, 1983; Christensen *et al.*, 1988).

(d) Vacuum melting and casting

After the americium is extracted from the impure metal, the plutonium metal must be cast into a cylindrical geometry that is compatible with the ER cell (Anderson and Maraman, 1962). The ER operation is typically carried out with 6 kg of plutonium, in which case the high-density α phase must be avoided due to nuclear criticality concerns. This requires alloying with sufficient gallium to bring the density from >19 to <16.5 g cm^{-3}. Casting is accomplished by mixing about 6 kg of impure metal with an appropriate amount of gallium in a tantalum pour crucible as shown in Fig. 7.13 (Christensen *et al.*, 1988). The metal and gallium mix upon melting and are bottom-poured from the tantalum crucible into a graphite mold. A casting residue, or "skull", always forms and contains light element impurities, oxide films (thorium, americium, alkali metals, alkaline-earth, and rare-earth metals) or other high melting contaminants. A typical ingot is shown in Fig. 7.14 with yields generally averaging more than 90%.

(e) Electrorefining (ER)

In the ER process, liquid plutonium oxidizes from the anode ingot into a molten-salt electrolyte (Mullins *et al.*, 1960, 1963a,b, 1982; Mullins and Leary, 1965; Mullins and Morgan, 1981). The resulting Pu(III) ion is transported through the salt to the cathode, where it is reduced back to metal. The process is carried out at 740°C in a molten salt consisting of an equimolar mixture of NaCl/KCl containing a small amount of $MgCl_2$ as an oxidizing agent. The $MgCl_2$ reacts with the impure plutonium metal to charge the electrolyte with Pu(III) before a current is passed and ensures the initial reduction of plutonium at the cathode.

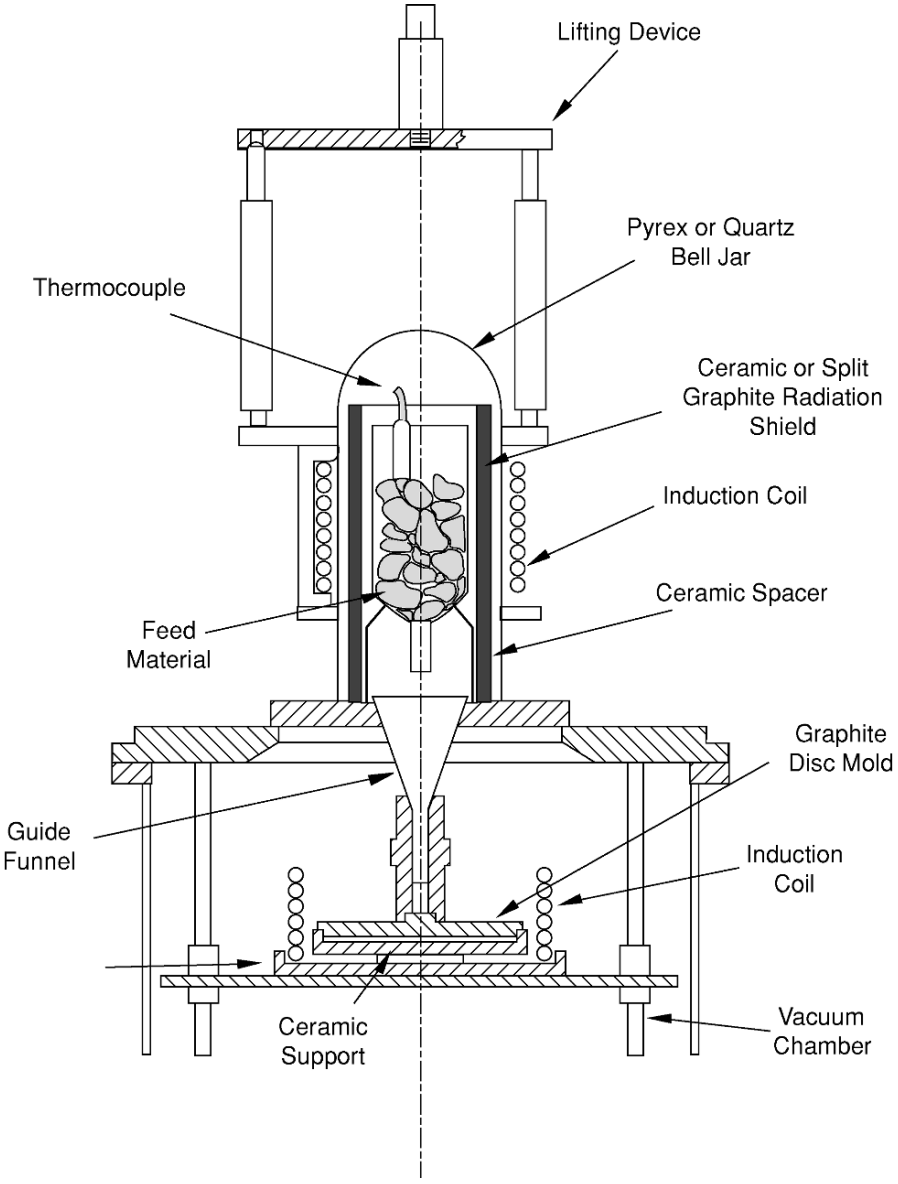

Fig. 7.13 *A general furnace assembly for vacuum casting of plutonium metal* (*Christensen* et al., 1988).

The process is performed in a double-cupped, vitrified magnesia crucible as shown in Fig. 7.15 (Mullins and Morgan, 1981). The inner cup contains the impure metal ingot that serves as the anode material. The electrolyte salt casting is placed on top of the ingot. The crucible is placed inside a tantalum safety can

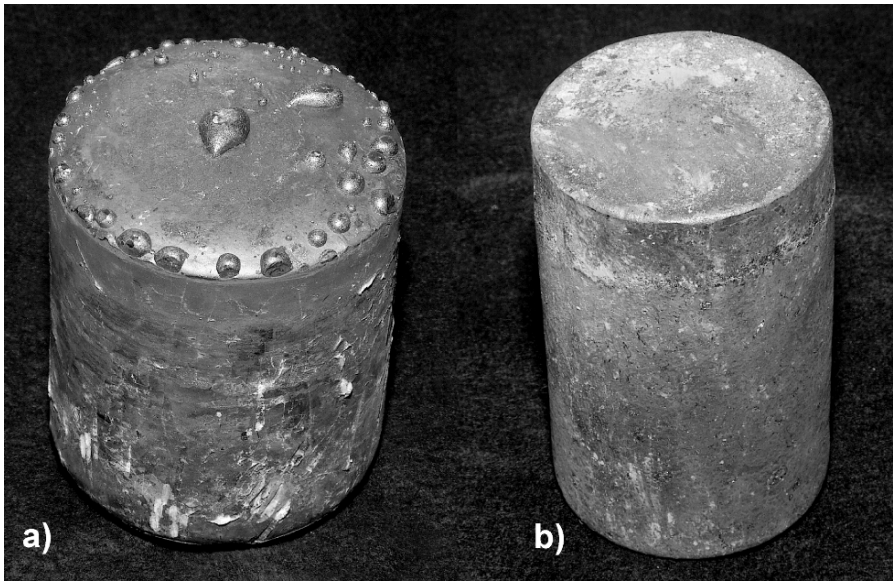

Fig. 7.14 *Photographs of plutonium ingots from vacuum casting.* (*a*) *Metal feed for electrorefining, and* (*b*) *for double electrorefining* (*photographs courtesy of Los Alamos National Laboratory*).

and placed inside the furnace. The assembly is heated using a resistance furnace (the entire assembly is shown in Fig. 7.16). A tantalum or vitrified magnesia stirrer stirs both the impure metal and the molten salt electrolyte. A tungsten rod is suspended in the impure metal pool to serve as the anode rod, and electrically insulated from the salt by a magnesia sleeve. A cylindrically shaped sheet of tungsten is suspended in the annular space between the two cups and serves as the cathode. Stirring and passing a dc current between the anode and cathode accomplish the process. Plutonium oxidizes at the anode and reduces back to metal at the cathode. The liquid metal drips off the cathode and into the annular space. After cooling to room temperature, the cell is broken apart and the plutonium recovered as an annular metal casting, or 'ER ring,' as shown in Fig. 7.17. The product yield from a Pu-1 wt % Ga alloy is greater than 80%. Approximately 10% of the residual plutonium remains in the anode as a very impure anode heel. The rest of the plutonium remains in the salt either as uncoalesced metal shot or as Pu(III), both of which can be recovered and recycled.

(f) Pyroredox or anode recovery

The pyroredox process recovers the plutonium from impure scrap materials and has found application in recovering plutonium from the spent anode heels from

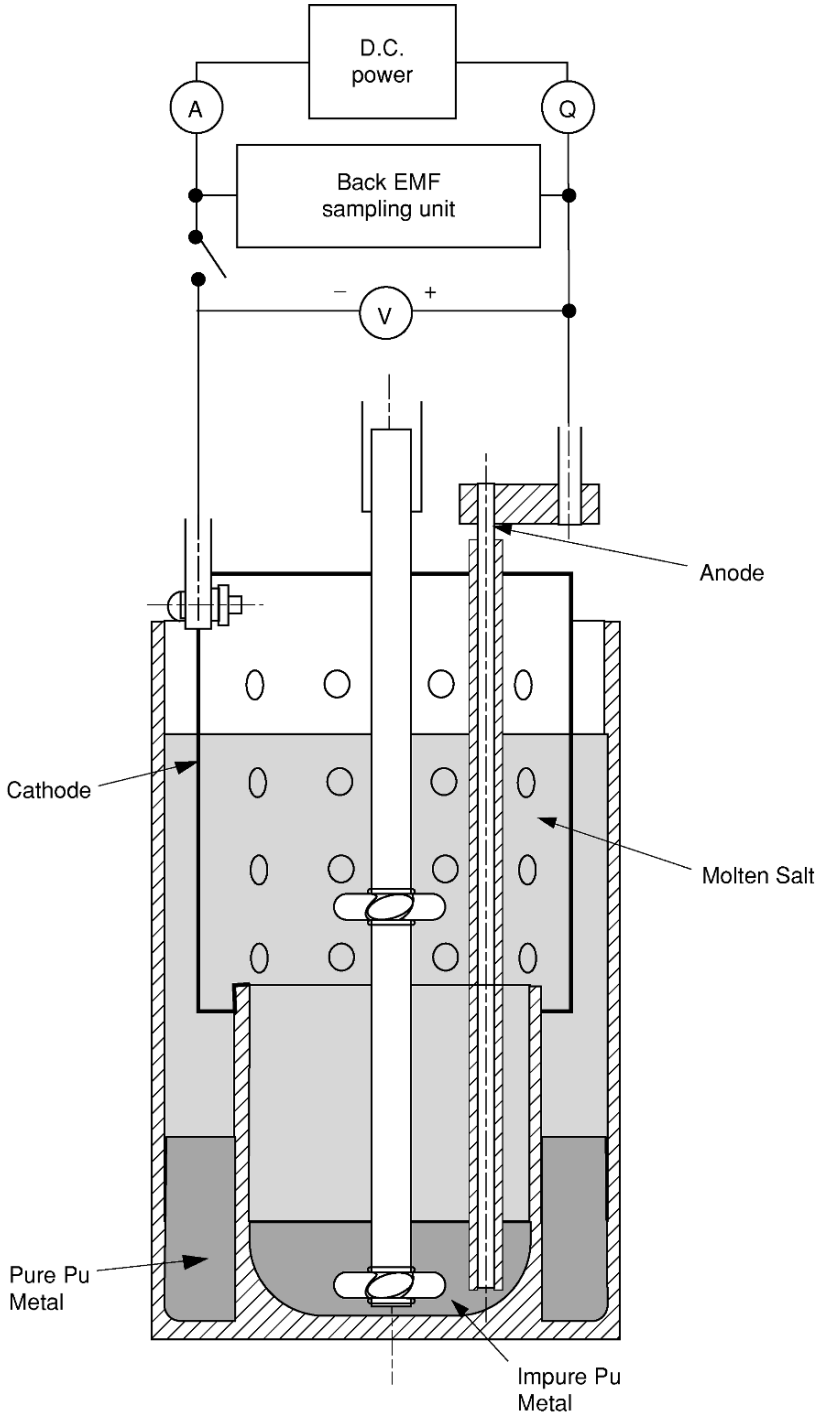

Fig. 7.15 *A general schematic of an electrorefining* (*ER*) *cell showing major features* (*Christensen* et al., 1988).

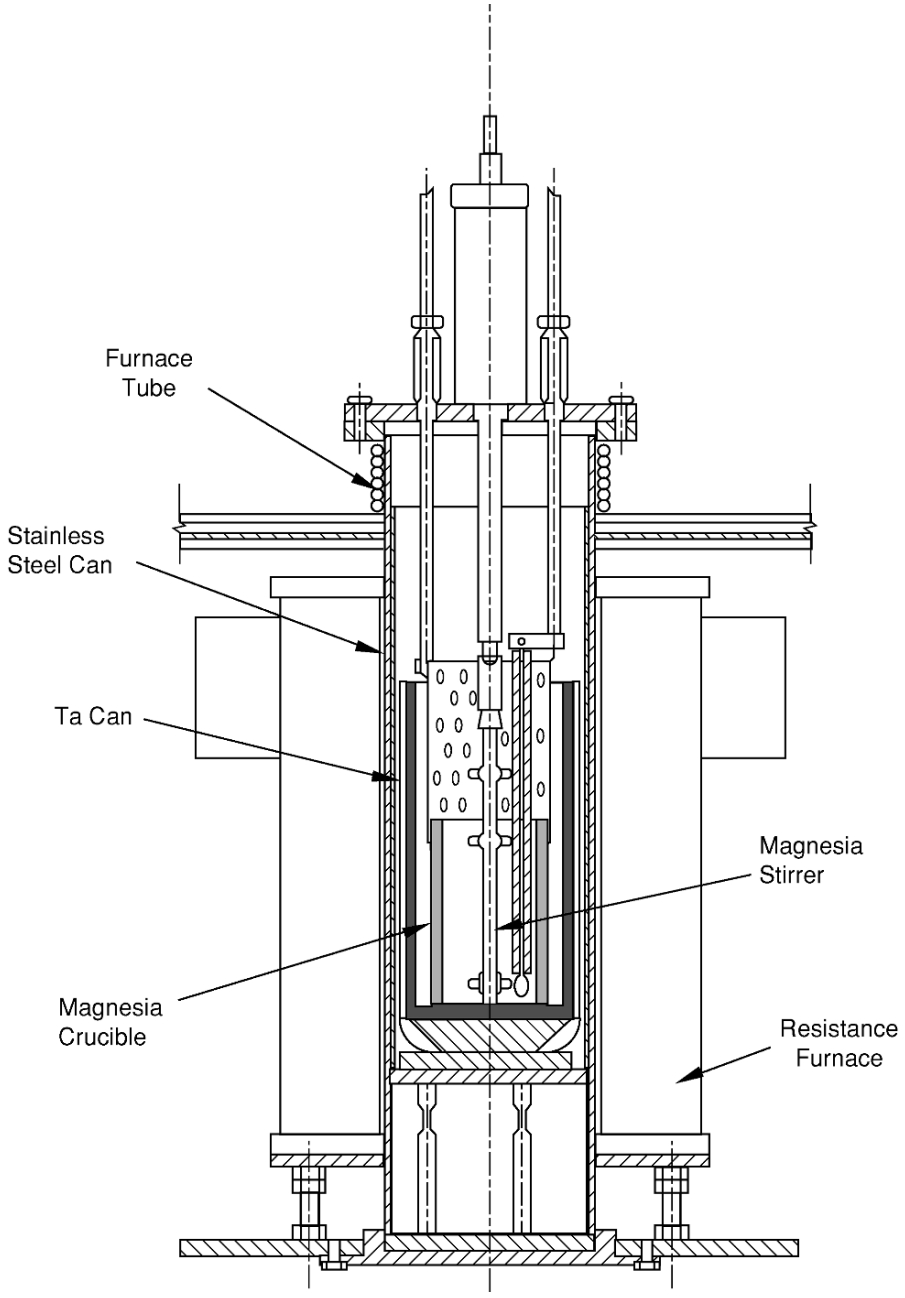

Fig. 7.16 *A general schematic of an electrorefining (ER) furnace apparatus showing major features* (*Christensen* et al., 1988).

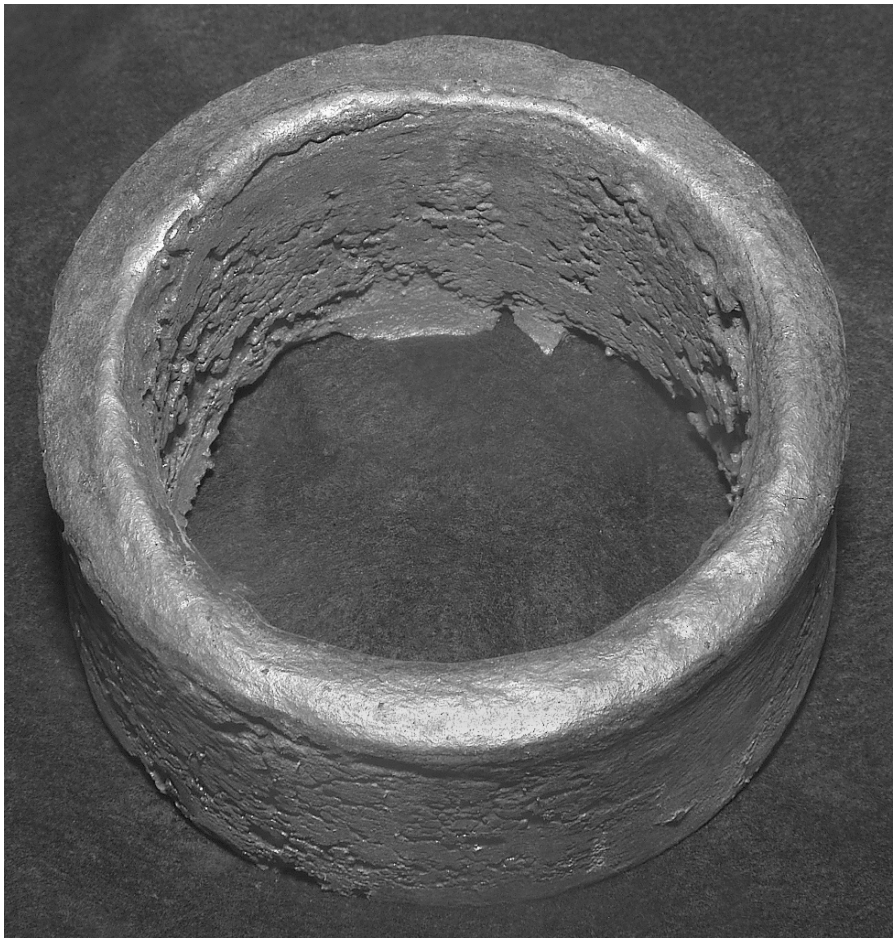

Fig. 7.17 *Photograph of a plutonium product ring from electrorefining* (*ER*) (*photograph courtesy of Los Alamos National Laboratory*).

the ER process (Baldwin and Navratil, 1983; Coops *et al*., 1983; McNeese *et al*., 1986; Christensen *et al*., 1988). The process equipment is identical to that used in DOR (Fig. 7.11). In the pyroredox process, workers initially polish the spent anode with calcium to ensure that all the plutonium is present as metal. The metal is then oxidized to Pu(III) with $ZnCl_2$ dissolved in KCl at 750°C with stirring. After an hour, the mixture is heated to 850°C to promote phase separation. In addition to plutonium, all other elements more active than zinc are oxidized into the salt phase. This process forms a zinc button that may be mechanically separated from the salt and discarded. For the reduction step, the salt containing $PuCl_3$ is crushed and mixed with a $Ca/CaCl_2$ mixture, pressed into an ingot, and placed back into a magnesia crucible and inserted into the

furnace assembly. The vessel is heated to 850°C with stirring, and then allowed to cool after removing the stirrer. The chemical reactions are:

$$2Pu^0 + 3ZnCl_2 \rightarrow 2PuCl_3 + 3Zn^0 \tag{7.23}$$

$$2PuCl_3 + 3Ca^0 \rightarrow 2Pu^0 + 3CaCl_2 \tag{7.24}$$

The reaction product is a salt phase above a two-phase metal button. The salt phase is mechanically separated and discarded. The bottom, denser metal phase is composed of plutonium and small quantities of calcium and zinc. The upper phase is typically 50% plutonium with the remainder being primarily zinc. Several buttons are allowed to coalesce at 850°C for 6 h to separate the ingots into a plutonium-rich lower phase suitable for ER and a less-pure upper phase that is recycled back to the oxidation step.

(g) Zone-refining of small research samples

Plutonium metal that has been doubly electrorefined is considered of high purity for most applications but still contains small amounts of Fe, U, Mg, Ca, Ni, Al, K, Si, O, C, and H. For small-scale research applications, it can be further purified via levitation zone-refining using a floating molten zone to minimize introduction of impurities from crucible materials. Tate and Anderson (1960) originally observed the phenomenon when they reported that zone melting promoted a reduction of impurity elements within a plutonium rod. Spriet (1965) conducted a more detailed investigation to include quantification of rates and impurity analyses. In more recent work, levitation zone-refining in concert with levitation distillation at reduced pressure has proven to be quite successful at producing ultrahigh purity specimens (Blau, 1998; Lashley *et al.*, 1999). Levitation zone-refining targets metals and metalloids while levitation vacuum-distillation targets daughter products and gases. In the levitation apparatus, radio frequency (rf) power-induced electric current flows into a crucible while the crucible acts as a transformer, inducing a current in the opposite direction to the current in the crucible. Magnetic fields in the crucible and the plutonium are opposed, causing repulsion and levitation of the plutonium a small distance from the crucible walls. Magnetic levitation of plutonium metal rods between 700 and 1000°C enables purification while eliminating plutonium-crucible interactions and minimizing the contact with other elements. The magnetic levitation is the fundamental operating basis for both the zone-refining apparatus and the distillation apparatus.

The zone-refining process involves casting a rod of unalloyed plutonium and then serially passing a molten zone through the rod in one direction at a slow rate. Impurities travel in the same or opposite direction to the direction of motion of the zone, depending on whether it lowers or raises the melting point of the plutonium. Consequently, impurities are swept and become concentrated in the ends of the rod, thereby leaving the remainder purified. The degree of

separation approaches an infinitesimal limit as the number of passes increases. Recent work has shown that ten passes through a molten zone can result in the reduction of impurities in double-electrorefined and vacuum-cast unalloyed plutonium from 727 to 184 ppm through levitation zone-refining (Blau, 1998; Lashley *et al.*, 1999).

Since americium exhibits a high vapor pressure relative to plutonium it is possible to remove ^{241}Am daughters from plutonium samples via vaccum distillation. The ^{241}Am is separated when plutonium metal is heated to the liquid state under reduced pressure (10^{-7} Torr). The molten plutonium is levitated while ^{241}Am is distilled off and condensed onto a cold finger. The plutonium is cooled and solidifies. Recent results from levitation distillation show that the concentration of ^{241}Am was reduced from 1100 to 500 ppm (Lashley *et al.*, 1999). These general principles have been combined into a floating zone refining followed by an *in situ* distillation, alloying, and casting technique for high-purity research samples of δ-Pu. In the procedure, a mixture of α-Pu is first levitation zone-refined. The α-Pu and gallium are then added to a levitation crucible. The mixture is heated to the melt while suspended in a magnetic levitation field. As the gallium mixes with the plutonium in the melt, it will stabilize the δ phase upon solidification. While in the melt, ^{241}Am is distilled from the plutonium and collected on a water-cooled condenser. Next, the furnace power is reduced, and plutonium is cast directly from the electromagnetic field into a ceramic mold. The apparatus is illustrated in Fig. 7.18.

7.7.3 Phase stability – allotropes, crystal structures, and transformations

It is important to understand the different allotropic phases of plutonium and the limits of stability with temperature, pressure, chemical additions, and time. We describe the stability of unalloyed plutonium along with the characteristics of its phases as a function of temperature and pressure in this section. We deal with the effects of chemical additions and time subsequently.

C. S. Smith and his Manhattan Project team of metallurgists and chemists were the first to come to grips with the unstable nature of this enigmatic element (Hammel, 1998). During their initial work in 1944, they routinely found the densities of their freshly prepared plutonium samples to vary by more than a factor of two. They quickly determined that unalloyed plutonium has at least five allotropes (a sixth was eventually found) over a very narrow temperature range and that it exhibits large volume changes at the various phase transitions during cooling from the melt, making it difficult to cast. Smith soon found that most of the transformations and the large volume changes could be avoided by alloying pure plutonium with a few atomic percent aluminum or gallium. Such alloying additions retained the high-temperature face-centered cubic (fcc) δ-phase, which is less dense, weak, and ductile, in contrast to the typical room temperature α-phase, which is very dense, strong, and brittle. The profound influence of chemical additions to plutonium on phase stability and the

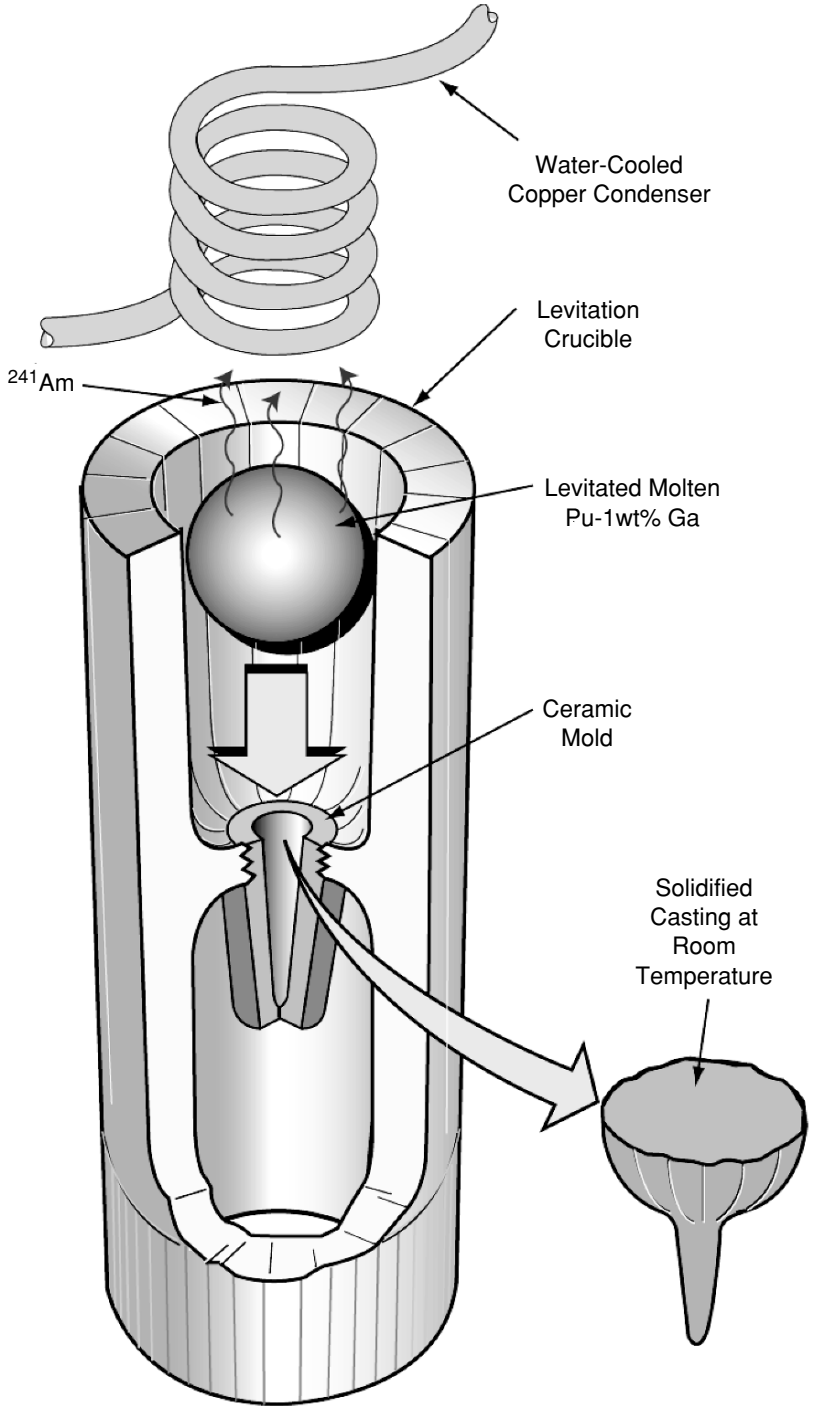

Fig. 7.18 In situ *americium distillation, alloying, and chill casting apparatus* (*Lashley* et al., 1999).

dramatic differences in properties exhibited by the different plutonium allotropes must be kept firmly in mind when considering plutonium and its properties. Moreover, phase transformations between the different allotropes are difficult to avoid during sample preparation, especially if samples are heated, cooled, worked, ground, or polished.

Zachariasen (1944) was the first to suggest that the large density and property variations in the early separated plutonium samples were due to crystallographic modifications of plutonium. Five solid allotropes designated by the Greek symbols α, β, γ, δ, and ϵ were identified during the early studies. A sixth, designated by the symbol δ', was discovered in 1954 by Cramer (Cramer *et al.*, 1961) in high-purity plutonium. An idealized thermal expansion curve is shown for pure plutonium in Fig. 7.19 (Miner and Schonfeld, 1980), along with the crystal structures and densities of the solid phases and the liquid phase. The stability ranges and crystal structure data for the individual allotropes are shown in Table 7.9. The transformation temperatures of the α, β, and γ phases are only approximate because the transformations are kinetically sluggish. The limits represent the approximate transformation temperatures as obtained by dilatometry and thermal analysis at slow heating or cooling rates of 1 to 1.5°C min^{-1}. The actual heating and cooling curves show significant hysteresis.

The data shown in Fig. 7.19 and Table 7.9 demonstrate the idiosyncratic behavior of plutonium. The six solid allotropes at ambient pressure (a seventh was found under pressure by Morgan (1970)) are the most of any element in the periodic table. Plutonium has an unusually low melting point of 640°C, and it contracts upon melting. The maximum density difference between the phases is a very large 20%. Moreover, the classical close-packed fcc phase is the least dense (less dense than the liquid). The two low-temperature phases are low-symmetry monoclinic structures, atypical of metals. The thermal expansion coefficients of these phases are very large and positive, whereas that of the fcc phase is negative.

The low-density, high-temperature phases of plutonium are easily transformed to the higher density phases under hydrostatic pressure as shown in Fig. 7.20 (Liptai and Friddle, 1967). Morgan (1970) clearly demonstrated the existence of a seventh phase at high pressure, designated ζ phase, as shown in Fig. 7.21. Its structure has yet to be determined. Elliott (1980) pointed out the similarity of the new ζ phase to the η phase in the Pu–U and Pu–Np systems. As shown in Fig. 7.20, at 3.0 GPa the ζ phase and all other high-volume phases collapse to the two low-temperature α and β allotropes.

The low-symmetry monoclinic ground-state α phase of plutonium results from the peculiar nature of the 5f electron bonding in plutonium as discussed below. Zachariasen and Ellinger (1957, 1963a) and Zachariasen (1961a) demonstrated that the α phase is a simple monoclinic crystal structure ($P2_1/m$) with 16 atoms per unit cell and eight unique atom positions. All 16 atoms lie in the reflection planes with coordinates $\pm$ (x,¼,z). Several views of the crystal structure of α plutonium are shown in Fig. 7.22. The 16 structural parameter values

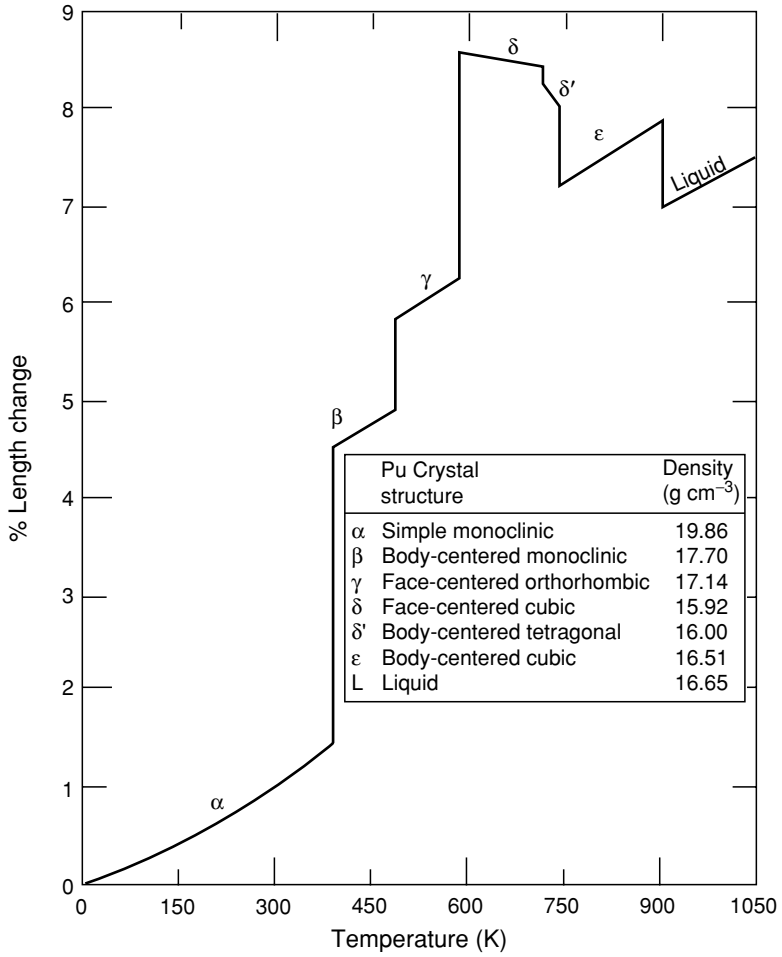

Fig. 7.19 *Thermal expansion of unalloyed plutonium. This idealized curve was generated by Schonfeld and Tate* (1996) *based on the best available expansion data. Of particular relevance is the correction to the α-Pu thermal expansion, as detailed in Fig.* 7.44.

are listed in Table 7.10 along with the bond lengths. The monoclinic structure of α plutonium is a slight distortion from a hexagonal lattice. This similarity was used by Crocker (1971) in modeling the crystallographic relationships of phase transformations involving the α phase. In addition, the bonding characteristics of the eight atom positions are markedly different. Position 1 has the greatest number of short bonds, whereas position 8 has the fewest short bonds (as shown in Table 7.11). All positions have the same point symmetry. The bonding characteristics are important in determining how the α phase accommodates

Table 7.9 *Crystal structure data for plutonium.*

Phase	*Stability range* (K)	*Crystal lattice and space group*	*Unit cell dimensions* (Å)	*Atoms per unit cell*	*X-ray density* ($g\ cm^{-3}$)	*Transformation temperature* (K)[b]
α	below 397.6	simple monoclinic $P2_1/m$	at 294 K $a = 6.183(1)$ $b = 4.822(1)$ $c = 10.963(1)$ $\beta = 101.79°(1)$	16	19.85	
β	397.6 – 487.9	body-centered monoclinic $I2/m$[a]	at 463 K $a = 9.284(3)$ $b = 10.463(4)$ $c = 7.859(3)$ $\beta = 93.13°(3)$	34	17.71 (α→β)	397.6
γ	487.9 – 593.1	face-centered orthorhombic F*ddd*	at 508 K $a = 3.159(1)$ $b = 5.768(1)$ $c = 10.162(2)$	8	17.15 (β→γ)	487.9
δ	593.1 – 736.0	face-centered cubic F*m*3*m*	at 593 K $a = 4.6371(4)$	4	15.92 (γ→δ)	593.1
δ′	736.0 – 755.7	body-centered tetragonal I4/*mmm*	at 738 K $a = 3.34(1)$ $c = 4.44(4)$	2	16.03 (δ→δ′)	736.0
ϵ	755.7 – 913.0	body-centered cubic I*m*3*m*	at 763 K $a = 3.6361(4)$	2	16.51 (δ′→ϵ) m.p.	755.7 913.0

[a] Although space group $I2/m$ is not one of the 'standard' space groups tabulated in the International Union of Crystallography, *International Tables for X-ray Crystallography,* vol. 1, Kynoch Press, Birmingham, its notation is retained to obtain a β angle of approximately 90° (data from Miner and Schonfeld, 1980).
[b] Data from Lemire *et al.* (2001). The reader is cautioned that the transformation temperatures vary between sources, and are sensitive to heating and cooling rates and metal purity.

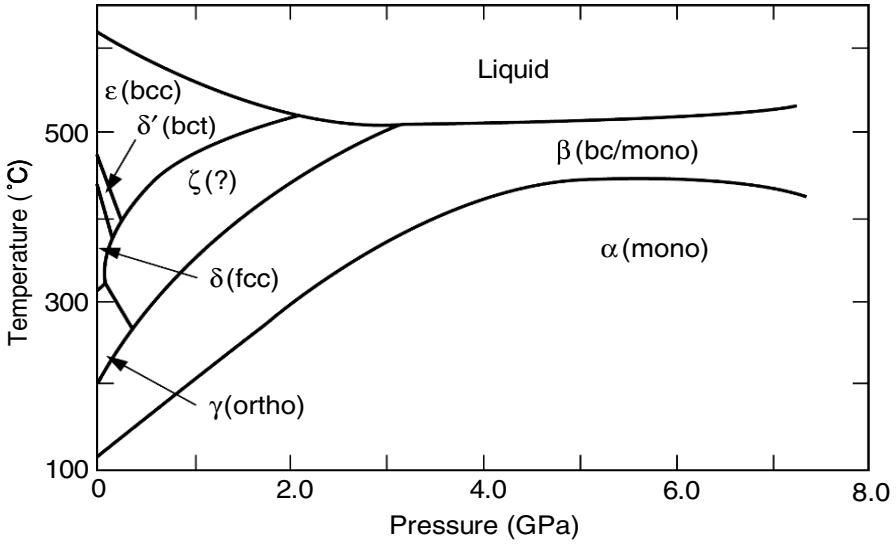

Fig. 7.20 *Pressure–temperature phase diagram of unalloyed plutonium from Liptai and Friddle* (1967).

impurity atoms. Lawson *et al.* (1996) pointed out that with eight unique atom positions, α plutonium looks like a self-intermetallic, much like α manganese. The low-symmetry monoclinic structure of the α phase has a profound influence on its properties; it has no macroscopic ductility, and most properties are highly directional.

The β phase is a body-centered monoclinic (*I2/m*) and equally complex. The atomic coordinates, the structural parameters, and the bond lengths are shown in Table 7.12 (Zachariasen and Ellinger, 1963b). It is considerably less dense than the α phase (17.7 g cm^{-3} compared to 19.85 g cm^{-3}), and it has 34 atoms per unit cell with seven unique atom positions. Properties are also quite anisotropic. The crystal structure of the β phase is compared to the other five allotropes in Fig. 7.23.

The γ phase is a face-centered orthorhombic (*Fddd*) with eight equivalent atoms per unit cell and a density of 17.14 g cm^{-3} (Zachariasen and Ellinger, 1955, 1959; Crocker, 1971). Each atom has four neighbors at 3.026 Å, two at 3.159 Å, and four at 3.228 Å. Roof (cited by Miner and Schonfeld, 1980) pointed out that placing the origin at the center of symmetry places the positions of the eight atoms of the unit cell at ± (1/8,1/8,1/8) + (0,0,0; 0,½, ½; ½,0, ½; ½,½,0). The crystal structure of the γ phase is shown along with the other allotropes in Fig. 7.23.

The δ phase is fcc (*Fm3m*) with four equivalent atoms per unit cell as shown in Fig. 7.23. It is the least dense of the plutonium allotropes at 15.92 g cm^{-3}. Each

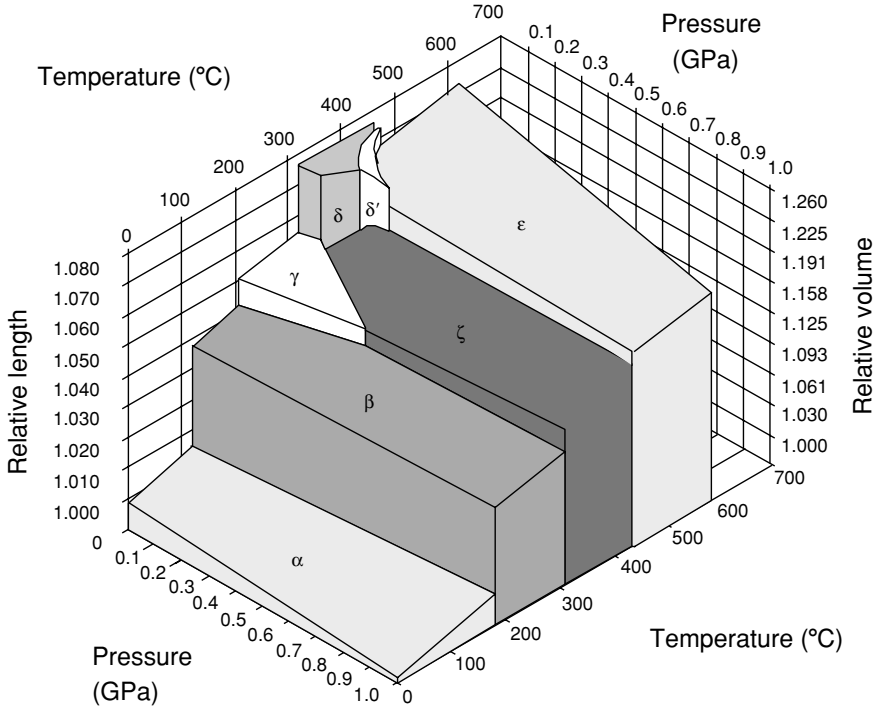

Fig. 7.21 *Pressure–temperature phase diagram from Morgan* (1970) *showing the existence of a seventh phase,* ζ.

atom has 12 neighbors at 3.279 Å in the standard fcc arrangement (0,0,0; 0,½,½; ½,0,½; ½,½,0). The δ′ phase is described by Ellinger (1956) as body-centered tetragonal (*I4/mmm*) with two atoms per unit cell at (0,0,0) and (½,½,½), with a density of 16.00 g cm^{-3}. He pointed out that the structure can be alternatively described as a face-centered tetragonal cell containing four atoms per unit cell, derived from the close-packed arrangement by a slight compression along the [001] direction. The ϵ phase is body-centered cubic (bcc) (*Im3m*) with two equivalent atoms per unit cell at (0,0,0) and (½,½,½). Each atom has eight neighbors at 3.149 Å.

As shown in Figs. 7.20 and 7.21, a seventh solid allotrope, the ζ phase, appears with the application of hydrostatic pressure at elevated temperatures. Very little is known about the precise crystal structure of this phase. However, Elliott (1980) suggested a similarity of this structure with the η phase of the PuU and PuNp systems.

The local coordination and interatomic distances for the four higher-temperature allotropes are shown in Table 7.13. Based on the crystal structure

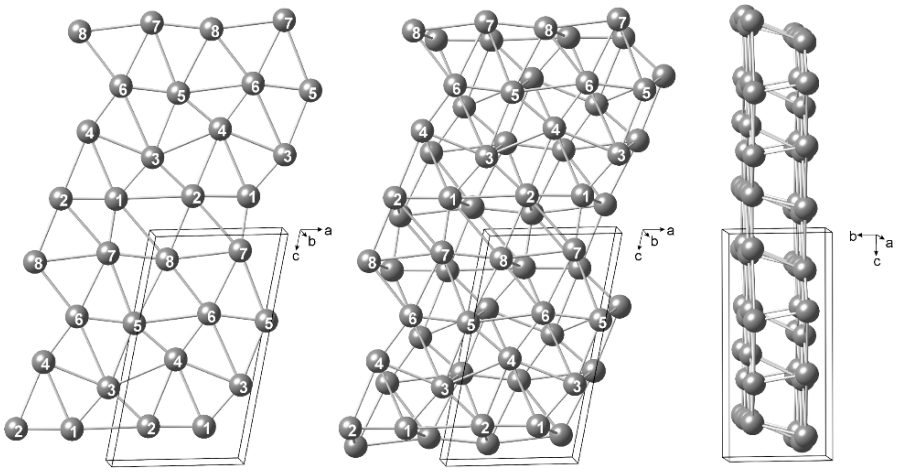

Fig. 7.22 *Several views of the monoclinic α-phase structure of plutonium with* 16 *atoms per unit cell and eight different atom positions.*

Table 7.10 *Structural parameters and bond lengths for α plutonium* (*Miner and Schonfeld*, 1980).

			Short bonds (Å)		*Long bonds* (Å)		*All bonds* (Å)	
Atom	*x*	*z*	*No.*	*Range*	*No.*	*Range*	*No.*	*Mean*
1	0.345(4)	0.162(2)	5	2.57–2.76	7	3.21–3.71	12	3.10
2	0.767(4)	0.168(2)	4	2.60–2.64	10	3.19–3.62	14	3.21
3	0.128(4)	0.340(3)	4	2.58–2.66	10	3.24–3.65	14	3.18
4	0.657(5)	0.457(3)	4	2.58–2.74	10	3.26–3.42	14	3.13
5	0.025(5)	0.618(3)	4	2.58–2.72	10	3.24–3.51	14	3.19
6	0.473(4)	0.653(2)	4	2.64–2.74	10	3.21–3.65	14	3.22
7	0.328(4)	0.926(2)	4	2.57–2.78	10	3.30–3.51	14	3.15
8	0.869(4)	0.894(2)	3	2.76–2.78	13	3.19–3.71	16	3.32

Table 7.11 *Bond characteristics for the eight different atom positions in the α-plutonium structure.*

Atom	*Short bonds*[a]	*Average length* (Å)
1	5	2.67
2–7	4	2.64
8	3	2.77

[a] The short bonds range from 2.57 to 2.78 Å and the long bonds from 3.19 to 3.71 Å. The point symmetry is the same for all eight atom positions.

Table 7.12 *Structural parameters for β plutonium* (*Zachariasen and Ellinger*, 1963*b*).

			Crystallographic parameters			*Bond lengths*			
Type	*No.*	*General atom positions*	*x*	*y*	*z*	*No.*	*Short bonds* (Å)	*No.*	*Long bonds* (Å)
1	2	(0, 0, 0)	0	0	0	4	2.97	8	3.15–3.26
2	4	±(x, 0, z)	0.146(4)	0	0.387(5)	3	3.03–3.10	11	3.26–3.55
3	4	±(x, 0, z)	0.337(4)	0	0.082(5)	4	2.79–3.03	9	3.15–3.43
4	4	±(x, 0, z)	0.434(4)	0	0.672(5)	4	2.79–3.01	8	3.16–3.48
5	4	±(1/2, y, 0)	0.500	0.220(3)	0	4	2.80–2.84	10	3.36–3.63
6	8	±(x, y, z), (x, $\bar{y}$, z)	0.145(3)	0.268(2)	0.108(3)	4	2.91–3.10	10	3.16–3.55
7	8	±(x, y, z), (x, $\bar{y}$, z)	0.167(3)	0.150(2)	0.753(4)	5	2.59–3.05	7	3.14–3.63

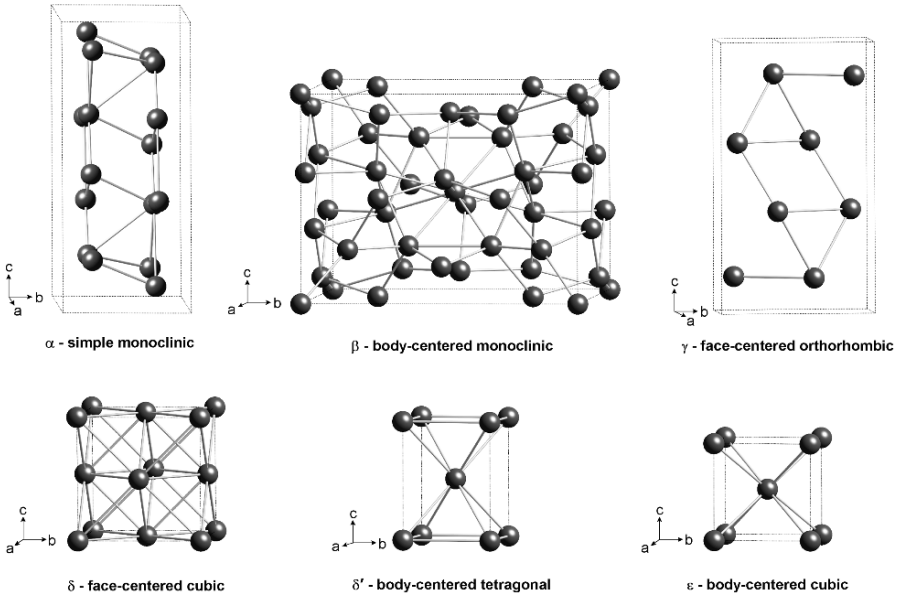

Fig. 7.23 *Crystal structures of all six solid phases of plutonium.*

information presented above, Zachariasen (1961b, 1973) derived metallic radii by normalizing the radii to coordination number 12 and extrapolating the high-temperature data to room temperature. His results are shown in Table 7.14. Zachariasen and others also calculated the valences for the plutonium allotropes. We do not present these here because we do not consider these estimates to be useful in considering the complexity of the f-electron bonding. We also list Dormeval's (2001) compilation of atomic volumes for the various allotropes in Table 7.14.

The liquid phase of plutonium is denser than the three highest-temperature solid phases. Density as a function of temperature is listed in Table 7.15, based on the work of Herrick *et al.* (1959) and Serpan and Wittenberg (1961). Extrapolation of the data in Table 7.15 yields a density of 16.65 g cm^{-3} at the melting point of 640°C. Hence, plutonium contracts approximately 2.5% upon melting. Plutonium liquid has a high surface tension and high viscosity.

The transitions (or, in metallurgical terms, phase transformations) between the various allotropes are important. Most studies of such transformations in unalloyed plutonium were conducted before 1970. A typical thermal expansion curve from Goldberg and Massalski (1970) for high-purity, electrorefined plutonium heated and cooled at 4.5°C min^{-1} is shown in Fig. 7.24. The sluggish nature of the transformation among the lower temperature phases results in

Table 7.13 *Coordination and interatomic distances of the higher plutonium allotropes* (*Ellinger* et al., 1956).

Phase	*Symmetry*	*Coordination*	*Distance* (Å)	*Effective coordination number*	*Average distance* (Å)	*Temperature* (°C)
γ	orthorhombic	Pu–4Pu Pu–2Pu Pu–4Pu	3.021 3.160 3.286	10	3.155	210
		Pu–4Pu Pu–2Pu Pu–4Pu	3.026 3.159 3.288	10	3.157	235
		Pu–4Pu Pu–2Pu Pu–4Pu	3.041 3.154 3.294	10	3.165	310
δ	face-centered cubic	Pu–12Pu	3.279	12	3.279	320
		Pu–12Pu	3.275	12	3.275	440
δ′	body-centered tetragonal	Pu–8Pu Pu–4Pu	3.249 3.327	12	3.275	465
		Pu–8Pu Pu–4Pu	3.239 3.347	12	3.275	485
ϵ	body-centered cubic	Pu–8Pu	3.149	8	3.149	490
		Pu–8Pu	3.156	8	3.156	550

Table 7.14 *Metallic radii* (*Zachariasen*, 1961*b; Zachariasen and Ellinger*, 1963*b*) *and volumes* (*Dormeval*, 2001) *of plutonium atoms.*

Phase	*Temperature* (°C)	*Radius* (Å)	*Radius at* 25°C (Å)	*Atomic volume* (Å^3)
α	25	1.580	1.580	20.00
β	93	1.600	1.590	22.43
γ	235	1.601	1.589	23.14
δ	320	1.640	1.644	24.93
δ′	465	1.638	1.644	24.69
ϵ	490	1.622	1.594	24.00

significant hysteresis, compared with the idealized curve shown in Fig. 7.19, and makes it difficult to conclusively determine the transformation temperatures. These temperatures depend on metal purity, microstructural variables (such as grain size and dislocation density), heating or cooling rates, applied stress,

Table 7.15 *Density of liquid plutonium* (g cm^{-3}).

Temperature (°C)	*Serpan and Wittenberg* (1961)[a]	*Olsen* et al. (1955)[b]
664	16.62	16.604
691	16.58	16.554
728	16.52	16.511
746	16.50	16.485
752	16.49	16.476
771	16.46	16.488
788	16.43	16.424

[a] Density equation $\rho = (17.63 - 1.52 \times 10^{-3}\ T) \pm 0.04$; temperature in °C
[b] Density equation $\rho = (17.567 - 0.001451\ T) \pm 0.021$; temperature in °C

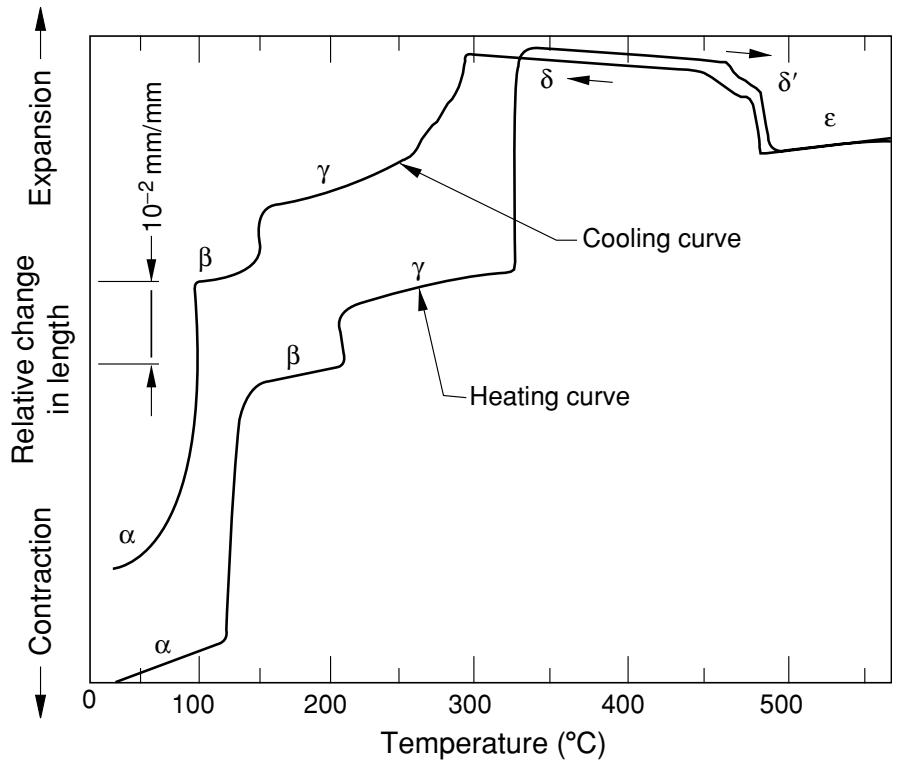

Fig. 7.24 *Experimental thermal expansion curve for heating and cooling of unalloyed plutonium showing typical hysteresis* (*after Goldberg and Massalski,* 1970).

sample size and shapes (resulting in stress effects), and prior transformation history.

Lemire *et al.* (2001) compared various phase transformation studies and compiled the best estimates of transformation temperatures and stability ranges

for the various allotropes listed in Table 7.9. Precise transformation temperatures are difficult to measure not only because they depend on the variables mentioned above, but also because all transformations exhibit significant time dependence. The isothermal (as opposed to athermal, where no thermal activation is needed) nature of the $\alpha \rightarrow \beta$ and $\beta \rightarrow \alpha$ transformations is best illustrated by the so-called time–temperature–transformation (TTT) diagram shown in Fig. 7.25 (after Nelson (1980)). The 'C-curve' shape of the transformation demonstrates how the temperature for the onset of transformation depends on the cooling rate. By determining the curves for both transformations, Nelson was able to establish the equilibrium transformation temperature as 112°C (compared with the average transformation temperature of 122°C during heating at relatively slow rates reported in Table 7.9).

Significant uncertainty still exists about the nature of the transformation mechanisms among the allotropes of plutonium (Hecker, 2000). The transformations among the high-temperature allotropes (δ, δ', and ϵ) are generally considered to be of a diffusion-controlled (diffusive) nature. However,

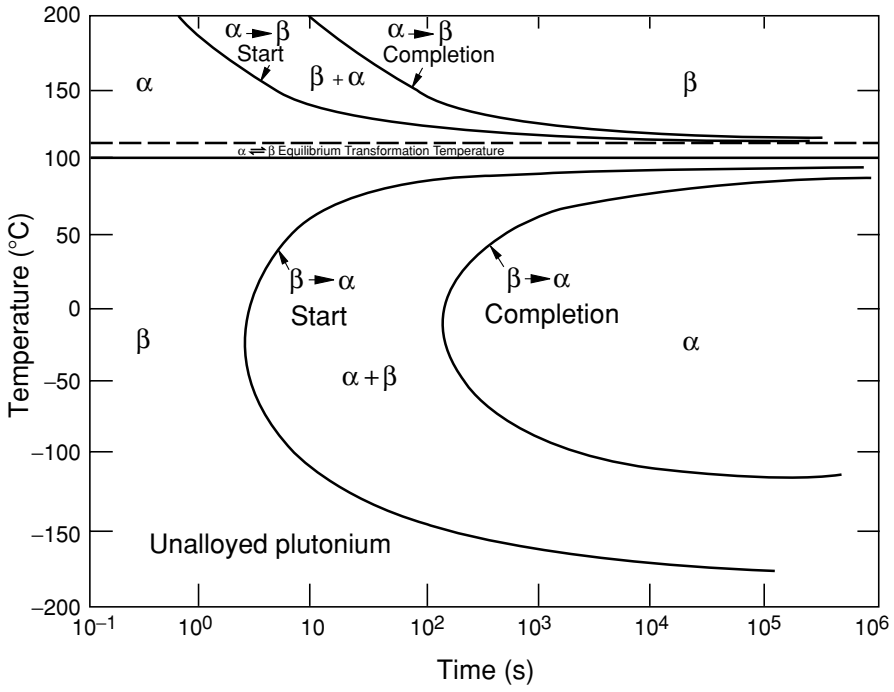

Fig. 7.25 *Representative time–temperature-transformation (TTT) curves of the $\beta \rightarrow \alpha$ and $\alpha \rightarrow \beta$ transformations in high-purity, electrorefined plutonium. The sample was taken to the β phase for* 45 min *at* 170°C (*from Nelson*, 1980).

transformations at lower temperatures among the δ, γ, β, and α phases show signs of diffusive and diffusionless, shear-type transformations. Shear transformations (of a martensitic nature) involve cooperative shear motion of the atoms and typically result in specific crystallographic relationships between the parent and the transformed phases. The evidence for such relationships was reviewed by Nelson (1980) and by Goldberg and Massalski (1970), who described the highly textured α-phase transformation product that can be formed when the β→α transformation is induced by cooling under applied stress.

Microcracking is difficult to avoid in most unalloyed plutonium as it cools from the melt or from annealing at elevated temperatures. The volume fraction of microcracks can range from 0.1 to 3%. High purity, large sample size, and slow cooling rates result in more extensive microcracking. Thermal cycling between the α and β allotropes greatly exacerbates the microcracking problem and results in sample distortion and surface rumpling (Hecker, 2000). On the other hand, quenching samples from the β phase to –80°C minimizes microcracking. Nelson pointed out that α-phase densities greater than 19.65 g cm^{-3} are generally considered to be good-quality plutonium. Densities around 19.8 g cm^{-3} have been achieved by cooling through the β→α transformation under pressure or by hydrostatic extrusion and concurrent recrystallization (Merz, 1970).

Another important consideration in sample preparation and subsequent property determination is the amount of retained high-temperature phases at ambient temperature. As noted in Figs. 7.24 and 7.25, the transformation from β→α is time-dependent and, hence, not necessarily complete at room temperature, resulting in retained β phase (or sometimes retained γ or δ phases). Impurities generally shift the onset of transformation (the 'C-curve' in Fig. 7.25) to the right. Spriet (1967) demonstrated that the onset of transformation was retarded by a factor of ten as the purity level changed from 200 to 400–1000 ppm. The impurities Ti, Hf, Zr, and U retard the β→α transformation and lead to greater β-phase retention at ambient temperature (Oetting *et al.*, 1976; Hecker, 2000). The impurities Ga, Al, and Si favor retention of the δ phase (Hecker, 2000). The most convenient method to determine the presence of retained high-temperature phases in α plutonium is to measure the density. The best way to identify the retained phases is by XRD; however, by using XRD it is difficult to identify retained phases at the level of less than a few volume percent.

Thermodynamic properties related to phase transformations can be measured directly by calorimetry or estimated from phase diagrams. Such properties are summarized in Table 7.16 along with the best estimates of the equilibrium transformation temperatures and volume changes. The scatter is quite large for reasons mentioned above. Nevertheless, these values are important to help guide the theory and modeling activities. Transformation enthalpies for the pressure-induced ζ phase are shown in Fig. 7.26, as derived from the data of Morgan (1970).

Table 7.16 *Entropies and enthalpies of transformations of the plutonium allotropes.*

Phase transformation	ΔS^a (J K^{-1} mol^{-1})	ΔS^b (J K^{-1} mol^{-1})	ΔH^c (J mol^{-1})	ΔH^d (J mol^{-1})	ΔH^e (J mol^{-1})
$\alpha \rightarrow \beta$	9.55	8.66	3430	3600	3706 ± 100
$\beta \rightarrow \gamma$	1.38	1.34	565	586	478 ± 20
$\gamma \rightarrow \delta$	1.05	0.88	586	649	713 ± 40
$\delta \rightarrow \delta'$	0.04	0.04	84	41	84 ± 20
$\delta' \rightarrow \epsilon$	2.47	2.46	1841	1859	1841 ± 100
$\epsilon \rightarrow$liquid	3.09	3.18	2824	2847	2824 ± 100

[a] Wick (1980); [b] Wittenberg *et al.* (1970); [c] Oetting *et al.* (1976); [d] Deloffre (1997); [e] Lemire *et al.* (2001).

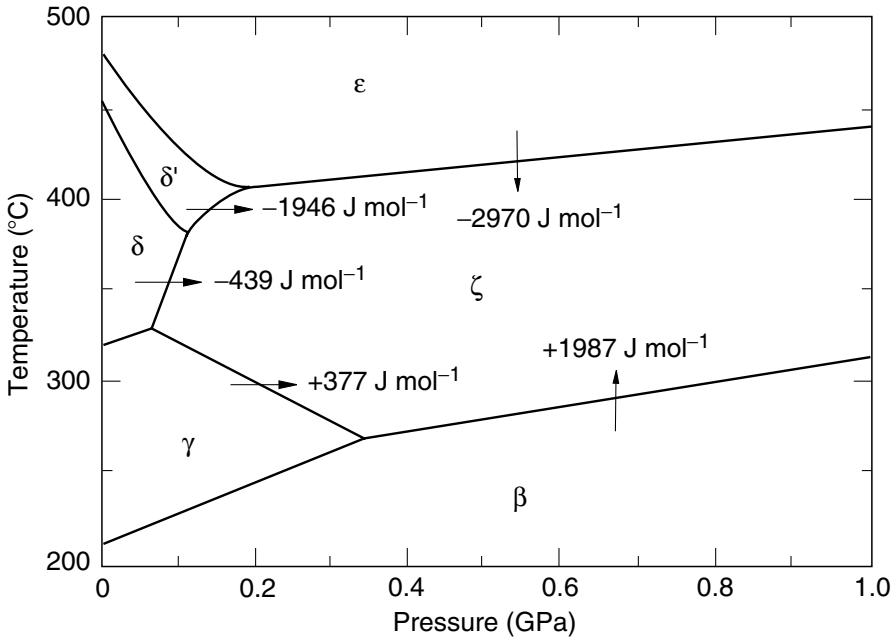

Fig. 7.26 *Transformation enthalpies of ζ plutonium calculated from the Clapeyron equation and slopes from Fig.* 7.21 (*Morgan*, 1970).

7.7.4 Alloys and phase transformations

Equilibrium phase diagrams provide a map of phase stability as a function of chemical concentration and temperature (most of the work of this nature has been done at ambient pressure and for binary alloy systems). All of the early work on phase diagrams of plutonium done during and after the Manhattan Project was classified. It was not until President Eisenhower launched the

'Atoms for Peace' initiative that much of that work was declassified and published. The Russian research group associated with A. A. Bochvar (Konobeevsky, 1955) published the first series of plutonium phase diagrams (with elements Be, Pb, V, Mn, Fe, Ni, and Os, as well as the ternary Pu–U–Fe) at a Moscow conference during the summer of 1955 in the preface to the first Conference on Peaceful Uses of Atomic Energy held in Geneva that fall. The U.S., U.K., and France rapidly followed suit. The Russian group added the Pu–Cu, Pu–Al, Pu–Bi, Pu–Zr, Pu–Mo, Pu–Th, and Pu–U systems at the second Geneva conference held in 1958 (Bochvar *et al.*, 1958). Coffinberry *et al.* (1958), and Schonfeld *et al.* (1959) published plutonium phase diagrams based on their work at Los Alamos Scientific Laboratory. Waldron *et al.* (1958) and Cope *et al.* (1960) published the U.K. results and Hocheid *et al.* (1967) the French results.

By 1968, most of the binary phase diagrams of plutonium were determined and published in the classic report of Ellinger *et al.* (1968b). Additional compilations were published in the *Plutonium Handbook*, edited by Wick (1980) and in the *Plutonium Metallurgy Handbook* (Hasbrouk and Burns, 1965). The most recent compilation is presented by Peterson and Kassner (1988). We review the salient features of binary plutonium phase diagrams below. The reader is referred to the reviews mentioned above for a discussion of available ternary plutonium diagrams. We also note that Blank provides a comprehensive compilation of phase diagram data in Table 2/1 of the *Gmelin Handbook of Inorganic Chemistry* (Blank, 1976). In addition, Blank (1976, 1977) provides a comprehensive treatment of the properties of plutonium alloys.

(a) Elements that expand the δ-phase field

Chemical additions (or alloying) significantly affect plutonium phase stability with temperature and pressure. The dramatic effects of the addition of a few atomic percent gallium to plutonium on its thermal behavior are demonstrated in Fig. 7.27. The addition of gallium retains the attractive feature of expansion during solidification while avoiding all of the large volume perturbations during cooling because the addition of gallium retains the fcc δ phase to room temperature. The thermal expansion is essentially zero, or 'Invar-like,' (Hecker, 2004) making Pu–Ga alloys much easier to cast. Moreover, the soft and ductile nature of the fcc δ phase makes these alloys much easier to shape than unalloyed plutonium. Consequently, most of the detailed work on properties of plutonium alloys has focused on systems that retain the δ phase. However, interest in metallic reactor fuels (Keiser *et al.*, 2003) has also resulted in work on β-phase retainers and on lean plutonium alloys involving uranium.

The complexity of chemical alloying is demonstrated in Fig. 7.28 for the Pu–Ga system. In addition to the six allotropes of plutonium, several new binary phases and 11 intermetallic compounds are formed. The fcc δ phase is retained to room temperature over a substantial range of gallium concentrations.

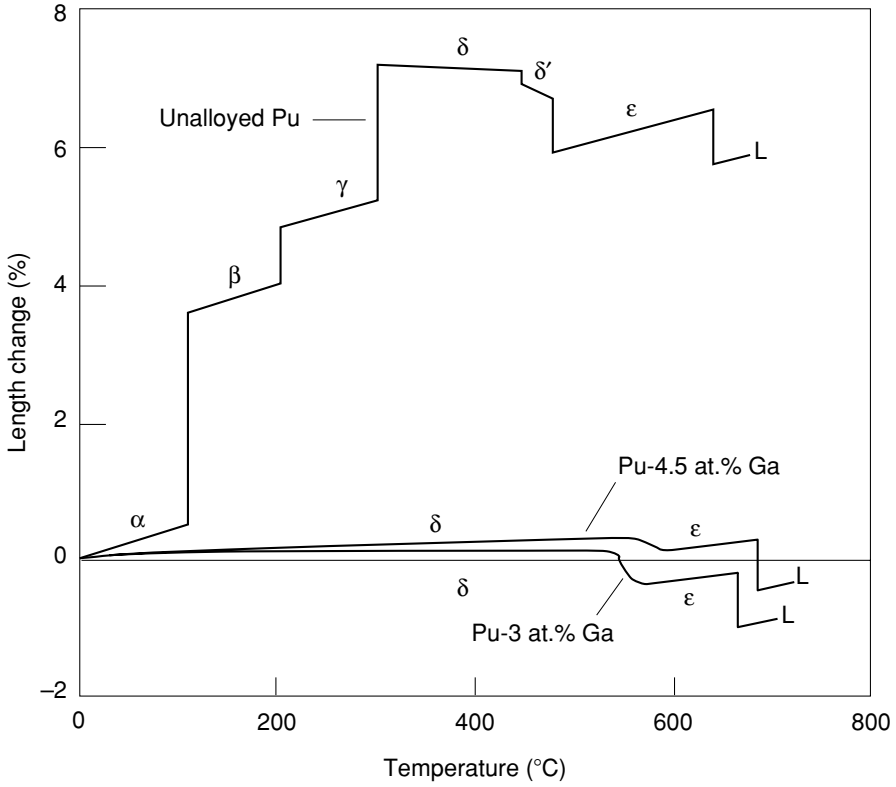

Fig. 7.27 *Length changes for unalloyed plutonium compared to Pu*-3.0 at.% *Ga and Pu*-4.5 at.% *Ga alloys.*

The question of whether the retained δ phase is stable or metastable was resolved only recently when Hecker and Timofeeva (2000) reconciled the U.S. (as well as the U.K. and French) and Russian versions of the Pu–Ga phase diagram. A comparison of the two versions of this fundamental phase diagram is shown in Fig. 7.29. They now believe that the Russian diagram (Fig. 7.29b), which shows an eutectoid point at 97°C and 7.9 at.% Ga, is the true equilibrium phase diagram (or as close a representation as possible, recognizing that radioactive decay in plutonium precludes true equilibrium). This diagram indicates that the δ phase should decompose below 97°C into α-Pu + Pu_3Ga. Such decomposition has never been observed because the kinetics are too slow. Timofeeva (2001) built her case on a clever set of experiments that demonstrated conclusively that the phase boundaries just above the eutectoid temperature clearly point to a decomposition (Hecker and Timofeeva, 2000). In fact, Timofeeva (2001) estimated that such decomposition requires more than 10,000 years at room temperature because the kinetics of the decomposition are exceedingly slow.

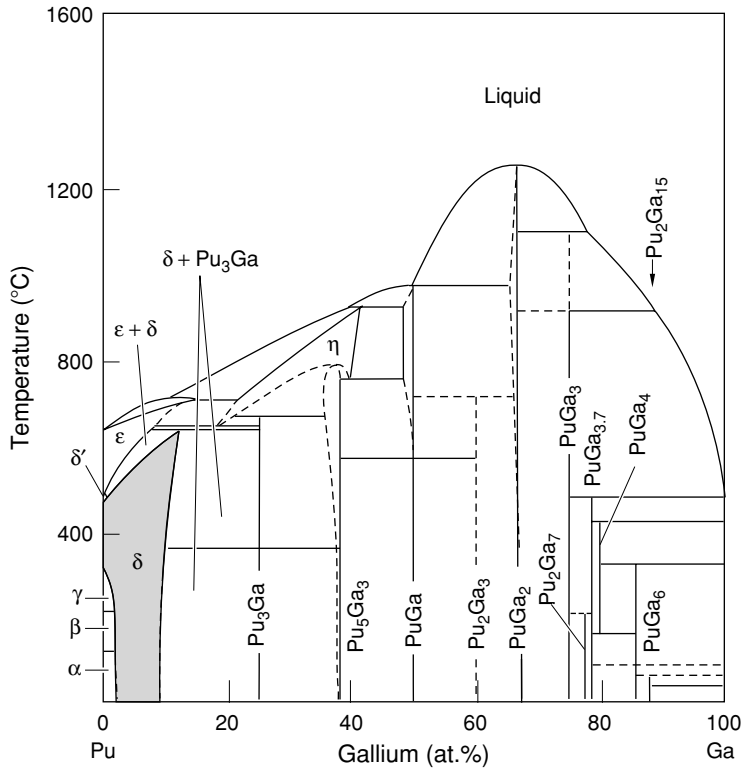

Fig. 7.28 *The Pu–Ga phase diagram at ambient pressure (from Peterson and Kassner*, 1988).

Therefore, the U.S. version (Fig. 7.29a), in which the δ phase is retained at least down to room temperature, represents an adequate 'working' diagram. Blank (1977), in his Table 2/105, presented the most complete table of crystal structures, atom positions, and atomic distances.

Timofeeva (2001) also demonstrated that the Pu–Al system undergoes a similar eutectoid decomposition near 100°C. The plutonium-rich end of the U.S. and Russian diagrams are shown in Fig. 7.30. In addition to the difference in findings related to the stability of the δ phase, Timofeeva also concluded that the intermetallic compound Pu_3Al does not extend to room temperature at thermodynamic equilibrium but rather only to 380°C. The eutectoid decomposition below 93°C is to α-Pu + PuAl (Timofeeva, 2001, 2003a). This finding differs from the conclusions of both the prior U.S. work reported by Ellinger *et al.* (1968b) and the prior Russian work reported by Bochvar *et al.* (1958). Timofeeva (2001) pointed out that the differences result because of slow kinetics. Her experiments allowed for sufficient time to demonstrate that PuAl is the intermetallic compound stable at room temperature.

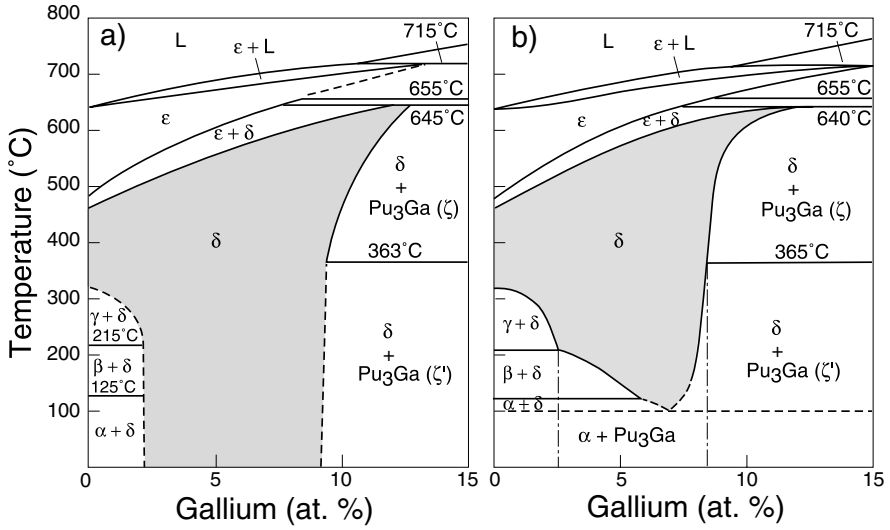

Fig. 7.29 *Comparison of* (*a*) *US and* (*b*) *Russian Pu–Ga phase diagrams from Hecker and Timofeeva* (2000).

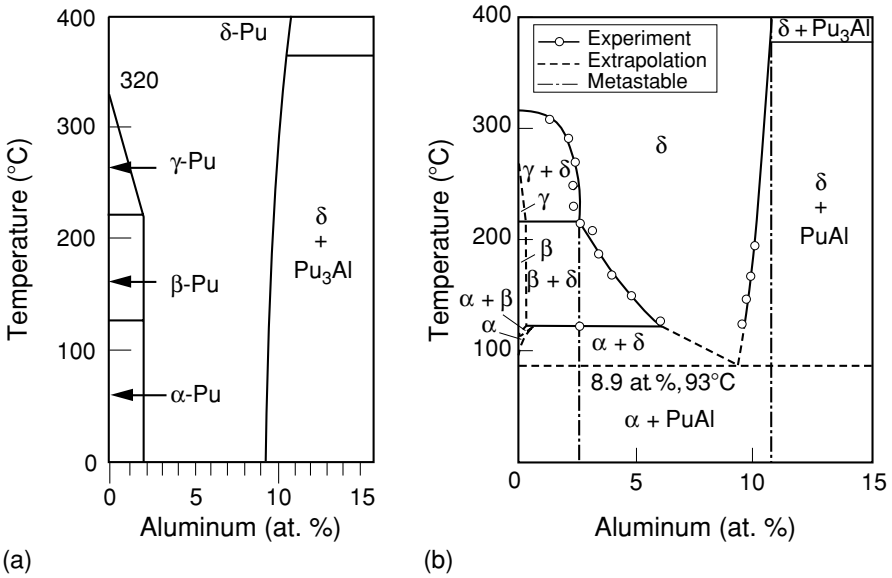

Fig. 7.30 *US* (*a*) *and Russian* (*b*) *versions of the Pu-rich side of the Pu–Al phase diagram. The US version is from Ellinger* et al. (1962*b*), *and the Russian version is from Hecker and Timofeeva* (2000).

Timofeeva (2003a) recently published data on 53 eutectoid transformations found in 30 binary plutonium phase diagrams. Eutectoid transformations are observed in binary systems of plutonium with transition metal elements (12), lanthanides (7), actinides, and elements of group IIIB (4 each). Only one eutectoid transformation exists with the elements of groups II, IV, and V. An interesting set of results is shown in Fig. 7.31 for four elements that expand the δ-phase field, Al, Ga, In, and Tl. Timofeeva demonstrated that the compositional range of the δ-phase field decreases and the eutectoid temperature increases monotonically with increasing atomic number of the alloying element. Additions of most trivalent elements expand the δ-phase field (Hecker, 2000), and in addition to Al, Ga, In, and Tl listed above, Ellinger *et al.* (1968b) showed that Sc, Ce, and Am also retain the δ phase. However, as discussed above, the retention appears to be metastable for most of these elements. It is likely that only Am results in a thermodynamically stable δ phase at room temperature. Timofeeva (2003a) reports a eutectoid transformation in Pu–Ce, and Pu–Sc systems that appears not to have received the same scrutiny as the other elements, so its status remains inconclusive.

In addition to the elements that readily retain the δ phase to room temperature (Al, Ga, Ce, Am, Sc, In, and Tl), there is a second class of elements (Si, Zn, Zr, and Hf) that retain the δ phase in a metastable state under conditions of rapid cooling. There are also some indications that the δ phase in Pu–Th alloys can be retained by rapid quenching (Gschneidner *et al.*, 1960).

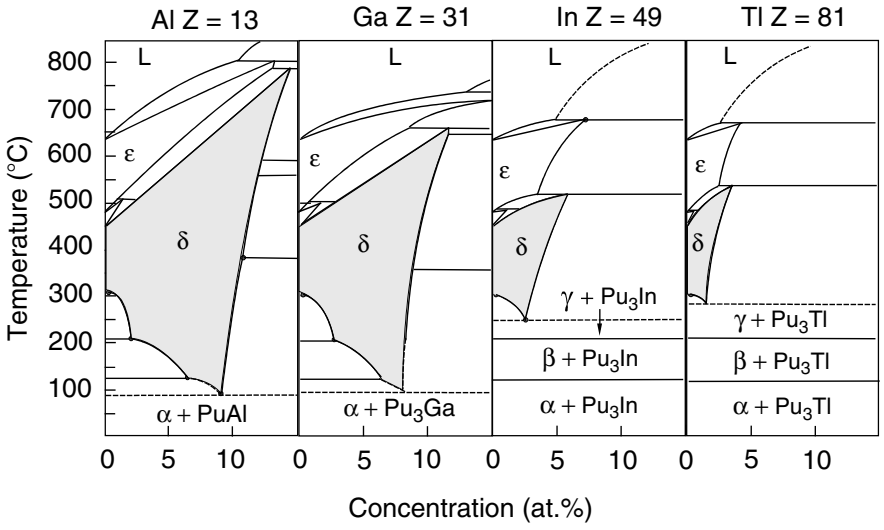

Fig. 7.31 *Phase diagrams of plutonium with several group* III*B elements show the eutectoid parameters and δ-phase region dependence* (*from Timofeeva,* 2003b).

Gschneidner *et al.* (1960) also found a number of the trivalent lanthanides (Dy, Er, Tm, Lu, and possibly Tb) to favor δ-phase retention, but their phase diagrams exhibit no δ-phase stability. Elliott and coworkers (Elliott and Giessen, 1975; Giessen *et al.*, 1975) demonstrated that retention of the δ phase and the bcc ϵ-phase can be extended in a metastable manner by splat cooling (rates from 10^6 to 10^8 s^{-1}). For example, both of these phases can be retained in splat-cooled Pu–Ti alloys. In Pu–Ga alloys, the maximum solubility of gallium in plutonium at room temperature is extended from 12.5 to 20 at.%. In Pu–Ce alloys, fcc δ phases can be retained across the entire range of cerium additions by splat cooling.

(b) α-Phase and β-phase stabilizers

Only neptunium has been found to expand the α-phase field. No other element is known to have any equilibrium solubility in the monoclinic α phase. Neptunium is also the only element that significantly expands the β-phase region. However, limited solubility of U, Hf, and Zr has been found in the β phase. Also, additions of Ti, Hf, and Zr will retain the β phase to room temperature and below by rapid quenching. Neptunium and uranium lower the melting point of plutonium slightly. The elements Hf, Zr, and Ti raise it significantly, even with small additions.

(c) Eutectic-forming elements

Additions of Mn, Fe, Co, or Ni lower the melting point of plutonium substantially. These elements form a low-melting eutectic much as does lead alloyed with tin to make solder. For example, the Pu–Fe phase diagram, shown in Fig. 7.32, exhibits the eutectic decomposition at 410°C and close to 10 at.% Fe from the liquid to δ-Pu + Pu_6Fe. This eutectic alloy was used in the first metallic plutonium fuel elements in the Los Alamos Molten Plutonium Reactor (LAMPRE) in the late 1940s (Kiehn, 1961; Burwell *et al.*, 1962). The elements Mn, Co, and Ni exhibit eutectic temperatures at approximately, 525°C, 405°C, and 465°C, respectively. These elements decompose to the intermetallic compounds $PuMn_2$, Pu_6Co, and PuNi, respectively. Other elements form eutectics but at somewhat higher temperatures. These include Si, Mn, Os, Ru, Rh, and Th. Eutectic-forming elements such as Mn, Fe, Ni, or Co are of special significance because they limit the useful temperature range of plutonium and its alloys. For example, plutonium metal heated above 410°C contained in steel will melt through the steel by forming the eutectic. Even when present in small amounts in plutonium, the alloying elements can segregate to grain boundaries, enriching the local alloying concentration and causing local melting or embrittlement at temperatures close to the eutectic temperature. Blank (1977) presented a thorough review of the properties of plutonium alloys and intermetallics with the eutectic-forming elements.

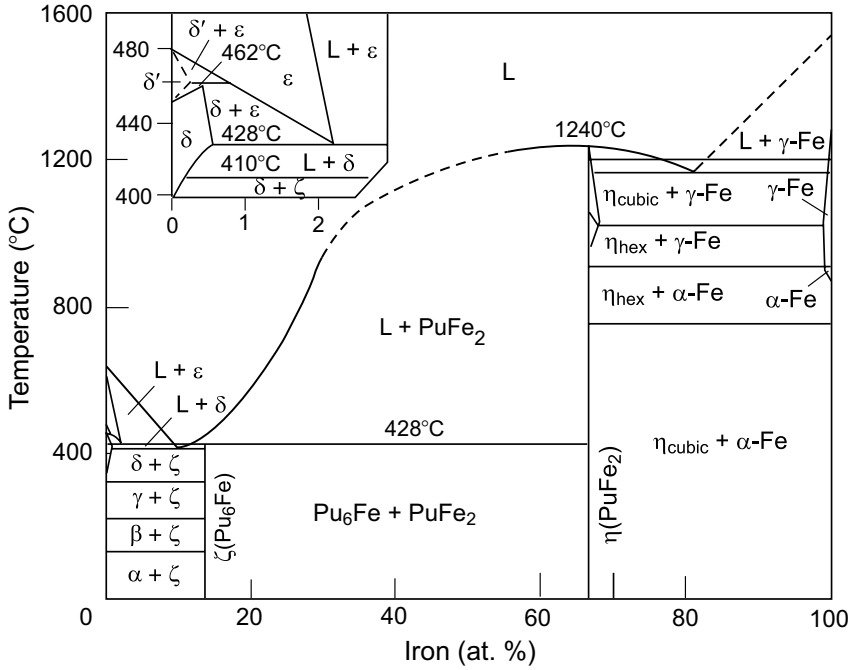

Fig. 7.32 *The Pu–Fe phase diagram at ambient pressure from Ellinger* et al. (1968*b*) *and first reported by Schonfeld* (1961).

(d) Interstitial compounds

When nonmetallic elements with very small radii are alloyed with metals, they tend to form interstitial solid solutions. A general rule of thumb is that if the radius of the nonmetallic element is <0.59 that of the metallic element, then an intermetallic compound with a simple structure (often fcc or hcp) forms. If the ratio is greater, then compounds with complex structures form. The most important nonmetallic elements for plutonium in the solid state are O, C, N, and H. None of these elements shows any solubility in the equilibrium phase diagrams. The Pu–O phase diagram is shown in Fig. 7.90. The elements O, C, and N all form several high-melting, refractory ceramic compounds. The structure and properties of these ceramic compounds will be discussed in greater detail in Section 7.8. Hydrogen also has a tendency to form compounds, but these readily decompose, rather than being refractory.

(e) The rest of the elements

Most other elements show only limited solubility in the δ phase, while some elements such as Ba, Sr, and Ca are immiscible. Most elements increase the

melting point. Some have shallow eutectics before the melting point increases. More than half of the elements, namely Th, Np, U, Ti, Ru, Rh, Pt, Os, and most lanthanides, show solubility in the ϵ phase.

Detailed X-ray crystal structure data are presented for many intermetallic compounds of plutonium in Table 7.17.

(f) Microsegregation in δ-phase alloys

Since alloys in which the fcc δ phase is retained to room temperature are of particular interest, we discuss the problem of microsegregation, which can dramatically influence the properties of δ-phase alloys. We use the Pu–Ga system shown in Fig. 7.33 for the purpose of illustration. During solidification and cooling, alloys within the range of gallium content to 13 at.% must cool through the liquid + ϵ and ϵ + δ two-phase regions. In a two-phase region, assuming gallium diffusivity is infinite in both phases, the composition of each phase is given by the phase boundaries at that temperature (the lever rule), giving rise to possible microsegregation. We track the gallium content through the ϵ + δ two-phase field in Fig. 7.33a. As the temperature reaches point A, the first δ phase to form has the gallium concentration shown at point B. As the temperature is lowered, the gallium concentration in the δ phase moves along the line BD, whereas the gallium concentration in ϵ moves along the line AC – if diffusion is sufficiently rapid to allow migration of gallium consistent with the imposed cooling rate. (Of course, the average gallium concentration in the alloy must be the initial concentration.) The diffusion rate of gallium is approximately 10^4 faster in the ϵ phase (because of its open bcc structure) than the δ phase, thereby not allowing equilibration in the δ phase for typical cooling rates. As a consequence, the gallium concentration of the remaining ϵ phase is pushed to lower values as cooling proceeds, resulting in increased segregation over that expected from equilibrium conditions.

As a result, the microstructure of a typical as-cast δ-phase alloy exhibits a range of gallium concentrations between points B and C. The interior of the δ-phase grains reflects the gallium concentration at point B and the grain boundaries may have very little gallium because they are the last ϵ-phase areas to transform with gallium at or below point C. The resulting microstructure appears heavily 'cored' or segregated as shown in Fig. 7.33b. It consists of gallium-rich δ phase in the center, a gallium-lean δ-phase shell (dark areas) at the core boundaries, and a gallium-lean intercore region that transformed to the α phase during cooling because of insufficient gallium. This type of microsegregation typically occurs during cooling through liquid + solid two-phase regions because diffusion in the liquid is so much faster than in the solid. However, the anomalously high diffusion rate in ϵ-plutonium avoids the problem in the liquid + ϵ region, only to have it reappear in the ϵ + δ two-phase region. Equilibrating the gallium concentration requires a sustained return to temperatures high in the δ-phase region, typically hundreds of hours, to achieve

Table 7.17 *X-ray crystal structure data for selected intermetallic compounds of plutonium.*

Phase	*Structure type*	*Symmetry*	*Space group*	*Lattice parameters* a_0(Å)	b_0(Å)	c_0(Å)	*Angle* (deg)	*Units per cell*	*X-ray density* (g cm^{-3})	*References*
$PuAg_3(\zeta)$		hexagonal	P6/*m*	12.730(3)		9.402(5)		16	11.33	Ellinger *et al.* (1968b), Miner (1970), Kutaitsev *et al.* (1967), and Runnalls (1956)
				12.72(5)		9.39(3)				Freeman and Darby (1974) and Blank *et al.* (1962)
$PuAg_{3.6}$	$GdAg_{3.6}$	hexagonal	P6/*m*	12.727(6)		9.392(4)			11.15	Ellinger *et al.* (1968b) and Miner (1970)
$PuAg_2$										Miner (1970)
Pu–Ag phase diagram										Ellinger *et al.* (1968b) and Kutaitsev *et al.* (1967)
$Pu_3Al(\zeta)$	$SrPb_3$	tetragonal	P4/*mmm*	4.499(1)		4.536(1)		1	13.45	Ellinger *et al.* (1968b), Freeman and Darby (1974), Blank *et al.* (1962), and Bochvar *et al.* (1958)
	Ti_3Cu			4.499(2)		4.538(2)			13.45	Coffinberry and Miner (1961)
		cubic		4.500						Ellinger *et al.* (1962b)
				4.530		4.575				
$PuAl(\eta)$	related to CsCl	bcc		10.769(1)				29	10.25	Ellinger *et al.* (1968b), Freeman and Darby (1974), Blank *et al.* (1962), and Bochvar *et al.* (1958)
				10.769					10.253	Kay and Waldron (1967)
$PuAl_2(\theta)$	Cu_2Mg	cubic	F*d*3*m*	7.831(5)				8	8.09	Ellinger *et al.* (1968b), Freeman and Darby (1974), Blank *et al.* (1962), and Runnalls (1956)
				7.840(1)(Pu-rich)						Bochvar *et al.* (1958)
				7.836(1)(Al-rich)						Bochvar *et al.* (1958)
				7.874						Ellinger *et al.* (1962b)
				7.838(1)(Pu-rich)					8.06	Coffinberry and Miner (1961)
				7.848(1)(Al-rich)						Coffinberry and Miner (1961)

				7.833				8.095	Kay and Waldron (1967)
$PuAl_3(\iota)$	$PuAl_3$	hexagonal(6H)	$P6_3/mmc$	6.08(1)		14.40(3)			Ellinger *et al.* (1968b), Freeman and Darby (1974), Blank *et al.* (1962), and Runnalls (1956)
				6.084(1)		14.427(2)	6	6.8	Bochvar *et al.* (1958)
				6.10(2)		14.47(4)		6.84	Larson *et al.* (1957)
		hexagonal		6.083		14.410		6.643	Kay and Waldron (1967)
		cubic(3H)	$Pm3m$	4.262				6.604	Kay and Waldron (1967)
		rhomb($9H_\beta$)	$R\bar{3}m$	7.879			$\alpha = 45.94$	6.657	Kay and Waldron (1967)
		rhomb($9H_\alpha$)		7.901			$\alpha = 45.81$	6.634	Kay and Waldron (1967)
$PuAl_4(\kappa)$	UAl_4	orthorhombic	*Imma*	4.42(2)	6.26(2)	13.66(3)			Ellinger *et al.* (1968b), Freeman and Darby (1974), and Blank *et al.* (1962)
				4.387(2)	6.262(2)	13.714(4)	4	6.02–6.11	Bochvar *et al.* (1958)
				4.41	6.29	13.79			Ellinger *et al.* (1968b)
α-$PuAl_4$		orthorhombic	*Imma*	4.396(1)	6.266(1)	13.708(2)	3.6	5.680	Kay and Waldron (1967)
β-$PuAl_4$		orthorhombic	*Imma*	4.396(1)	6.266(1)	13.708(2)		5.680	Kay and Waldron (1967)
(α- and β-$PuAl_4$ differ by the distribution of lattice vacancies)									
Pu–Al phase diagram, see Fig. 7.30									Kay and Waldron (1967), Bochvar *et al.* (1958), Waldron *et al.* (1958), Ellinger *et al.* (1962b), and Moeller and Schonfeld (1950)
Pu–Am system, no compounds, phase diagram known									Ellinger *et al.* (1966)
Pu–As system, see Section 7.8, Table 7.33									
$Pu_xAu_y(\eta)$									Ellinger *et al.* (1968b) and Kay and Waldron (1967)
$PuAu(\zeta)$									Ellinger *et al.* (1968b) and Kay and Waldron (1967)

Table 7.17 (*Contd.*)

Phase	*Structure type*	*Symmetry*	*Space group*	*Lattice parameters* a_0(Å)	b_0(Å)	c_0(Å)	*Angle* (deg)	*Units per cell*	*X-ray density* (g cm^{-3})	*References*
$PuAu_2$(ι)										Ellinger *et al.* (1968b) and Kay and Waldron (1967)
Pu_xAu_y(κ)										Ellinger *et al.* (1968b) and Kay and Waldron (1967)
$PuAu_3$(λ)		hexagonal	P6/*m*	12.710		9.210		16	17.11	Ellinger *et al.* (1968b), Kay and Waldron (1967), and Kutaitsev *et al.* (1967)
$PuAu_4$(μ)										Ellinger *et al.* (1968b) and Kay and Waldron (1967)
$PuAu_5$(ν)										Ellinger *et al.* (1968b) and Kay and Waldron (1967)
Pu–Au phase diagram										Ellinger *et al.* (1968b), Kay and Waldron (1967), and Kutaitsev *et al.* (1967)
Pu–B system, see Section 7.8, Table 7.28										
Pu–Ba system, no compounds										(Seaborg *et al.* 1946, 1949b), Ellinger *et al.* (1968b), and Bochvar *et al.* (1958)
$PuBe_{13}$	$NaZn_{13}$	cubic	F*m*3*c*	10.284(1)(Be-rich)				8	4.35	Runnalls (1956)
				10.278(1)(Pu-rich)						Runnalls (1956)
				10.274(2)					4.36	Seaborg *et al.* (1946) and Bochvar *et al.* (1958)
				10.282(1)(Be-rich)					4.35	Coffinberry and Miner (1961)
Pu–Be phase diagram										Seaborg *et al.* (1946, 1949b), Konobeevsky (1955), Ellinger *et al.* (1968b), and Bochvar *et al.* (1958)

Pu–Bi system, see Section 7.8, Table 7.33									
Pu–Bi phase diagram									Seaborg *et al.* (1946, 1949b), Ellinger *et al.* (1968b), and Bochvar *et al.* (1958)
Pu–C system, see Section 7.8, Table 7.29									
Pu–Ca system, no compounds									Seaborg *et al.* (1946, 1949b), Ellinger *et al.* (1968b), and Bochvar *et al.* (1958)
$PuCd_2(\zeta)$									Etter *et al.* (1965)
$PuCd_4(\eta)$									Etter *et al.* (1965)
$PuCd_6(\theta)$	$CeCd_6$	cubic	I*m*3	15.59(1)				9.61	Etter *et al.* (1965) and Johnson *et al.* (1965)
$PuCd_{11}(\iota)$	$BaHg_{11}$	cubic	P*m*3*m*	9.282(2)			3	10.25	Etter *et al.* (1965) and Johnson *et al.* (1965)
Pu–Cd phase diagram									Ellinger *et al.* (1968b), Etter *et al.* (1965), and Johnson *et al.* (1965)
Pu–Ce system, no compounds, phase diagram known									Wilkinson (1960), Ellinger *et al.* (1968b), and Selle and Etter (1964)
$Pu_6Co(\zeta)$	U_6Mn	tetragonal	I4/*mcm*	10.45(1)		5.32(1)	4	17.6	Bochvar *et al.* (1958)
				10.46(2)		5.33(1)	4	17.00	Coffinberry and Miner (1961)
$Pu_3Co(\eta)$	Al_2CuMg	orthorhombic	C*mcm*	3.501(3)	11.03(3)	9.23(15)(Pu-rich)		14.7	Poole and Nichols (1961)
				3.477(3)	10.99(3)	9.20(15)(Co-rich)			Poole and Nichols (1961)
				3.470	10.939	9.196		14.76	Coffinberry and Miner (1961)
				3.475(4)	10.976(10)	9.220(8)		14.65	Larson *et al.* (1963)
$Pu_2Co(\theta)$	Fe_2P	hexagonal	P321	7.902(4)(Pu-rich)		3.549(2)	3	14.0	Coffinberry and Miner (1961)
				7.763(2)(Co-rich)		3.648(3)			Coffinberry and Miner (1961)
				7.803(8)(Pu-rich)		3.606(5)			Poole and Nichols (1961)
				7.732(8)(Co-rich)		3.654(5)			Poole and Nichols (1961)
$PuCo_2(\iota)$	Cu_2Mg	cubic	F*d*3*m*	7.075(5)			8	13.39	Runnalls (1956)
				7.083(10)(Pu-rich)					Bochvar *et al.* (1958)
				7.066(10)(Co-rich)					Bochvar *et al.* (1958)
				7.081(1)(Pu-rich)					Coffinberry and Miner (1961)
				7.095(5)(Pu-rich)					Poole and Nichols (1961)

Table 7.17 (*Contd.*)

Phase	*Structure type*	*Symmetry*	*Space group*	*Lattice parameters* a_0(Å)	b_0(Å)	c_0(Å)	*Angle* (deg)	*Units per cell*	*X-ray density* (g cm^{-3})	*References*
				7.023(5)(Co-rich)						Poole and Nichols (1961)
$PuCo_3(\kappa)$	$PuNi_3$	rhombohedral (hexagonal setting)		8.635(10) 8.327(5)			$\alpha = 33°40'$	3	11.74	Poole and Nichols (1961)
$Pu_2Co_{17}(\lambda)$	Th_2Ni_{17}	hexagonal	$P6_3/mmc$	8.325(2) 8.327(5)	8.104(3) 8.107(5)			2	10.10	Bochvar *et al.* (1958) Poole and Nichols (1961)
Pu–Co phase diagram										Seaborg *et al.* (1946, 1949b) and Poole and Nichols (1961)
Pu–Cr system, no compounds, phase diagram known										Ellinger *et al.* (1968b), Bochvar *et al.* (1958), and Bowersox and Leary (1968)
Pu–Cs system, no compounds										Seaborg *et al.* (1946, 1949b) and Bochvar *et al.* (1958)
$PuCu_2(\zeta)$	$CeCu_2$	orthorhombic	*Imma*	4.332(2) 4.32(2)	6.686(1) 6.69(2)	7.376(1) 7.38(2)		4	11.20	Pons *et al.* (1972) Lataillade *et al.* (1971)
$PuCu_4(\eta)$		orthorhombic		4.320(1) 4.37(2)	8.264(3) 8.37(2)	9.226(3) 9.32(2)		4	10.12	Pons *et al.* (1972) Lataillade *et al.* (1971)
$Pu_4Cu_{17}(\theta)$										Lataillade *et al.* (1971)
$PuCu_6(\iota)$	$CeCu_6$	orthorhombic	*Pnma*	8.50(3) 8.16	5.025(3) 5.14	10.059(6) 10.06		4	10.12	Kutaitsev *et al.* (1967) Wittenberg and Grove (1964)
Pu–Cu phase diagram										Ellinger *et al.* (1968b), Grison *et al.* (1960), and Kutaitsev *et al.* (1967)
Pu–Dy system, miscibility gap, no compounds										Ellinger *et al.* (1968b)
Pu–Er system, miscibility gap, no compounds										Ellinger *et al.* (1968b)
Pu–Eu system, immiscibility, no compounds										Ellinger *et al.* (1968b)
$Pu_6Fe(\zeta)$	U_6Mn	tetragonal	$I4/mcm$	10.41(1)		5.359(4)		4		Mardon *et al.* (1957)

				10.404(4)	5.355(2)	4	17.07	Coffinberry and Miner (1961)
				10.403	5.347		17.10	Konobeevsky (1955)
				10.405(5)	5.349(3)			Bowersox and Leary (1966)
				10.40(2)	5.345(5)			Coffinberry and Waldron (1956)
$PuFe_2(\eta_{cub})$	Cu_2Mg	cubic	F*d*3*m*	7.150(5)('preparation a')			12.74	Runnalls (1956)
				7.190(5)('preparation b')			12.53	Runnalls (1956)
				7.191(1)(Pu-rich)		4	12.53	Coffinberry and Miner (1961)
				7.178			12.59	Konobeevsky (1955)
				7.189				Mardon *et al.* (1957)
$PuFe_2(\eta_{hex})$	$MgNi_2$	hexagonal		5.64	18.37			Avivi (1964)
Pu–Fe phase diagram								Ellinger *et al.* (1968b) and Grove (1966)[f]
Pu–Ga(η)		cubic	$I2_13$	7.207(18%Ga)			16	Blank and Lindner (1976)
			$I2_1$	7.167(41.6%Ga)				Chebotarev (1976)
		bcc pseudo-cell		3.58				Ellinger *et al.* (1964)
α-$Pu_3Ga(\zeta')$	$SrPb_3$	tetragonal	P4/*mmm*	4.470	4.523	1	14.45	Blank and Lindner (1976)
				4.469(1)	4.527(2)	1	14.45	Ellinger *et al.* (1964)
				4.492	4.555			Hocheid *et al.* (1965)
β-$Pu_3Ga(\zeta)$	$AuCu_3$	cubic	P*m*3*m*	4.514(Pu-rich)		1	14.27	Blank and Lindner (1976)
				4.497(Ga-rich)				
				4.507(2)		1	14.27	Ellinger *et al.* (1964)
				4.500				Hocheid *et al.* (1965)
$Pu_5Ga_3(\theta)$	W_5Si_3	tetragonal	I4/*mcm*	11.736	5.559	4	12.29	Blank and Lindner (1976)
		tetragonal	I4/*mcm*	11.735(3)	5.511(2)	4	12.29	Ellinger *et al.* (1964)
		fcc		5.570				Hocheid *et al.* (1965)
α-PuGa		cubic	I*m*3*m*	3.53		2		Hocheid *et al.* (1965)
β-PuGa(ι)		tetragonal	I4/*mm*	6.641	8.069	8	11.52	Blank and Lindner (1976)
				6.666	7.985(Pu-rich)			Blank and Lindner (1976)
				6.640(1)	8.066(1)	8	11.53	Ellinger *et al.* (1964)
Pu_2Ga_3 (κ)		hexagonal		4.378	3.792			Blank and Lindner (1976)
$PuGa_2(\lambda)$	AlB_2	hexagonal	P6/*mmm*	4.248(1)	4.120	1	9.76	Ellinger *et al.* (1964)
				4.258	4.120			Hocheid *et al.* (1965)
				4.248	4.107(Pu-rich)	1	9.77	Blank and Lindner (1976)
				4.258	4.139(Ga-rich)			Blank and Lindner (1976)
α-$PuGa_3(\mu)$	Ni_3Sn	rhombohedral	$R\bar{3}m$	6.173	27.99	12	9.66	Blank and Lindner (1976)

Table 7.17 (*Contd.*)

Phase	*Structure type*	*Symmetry*	*Space group*	*Lattice parameters* a_0(Å)	b_0(Å)	c_0(Å)	*Angle* (deg)	*Units per cell*	*X-ray density* (g cm^{-3})	*References*
				6.178(1)		28.031(4)				Larson *et al.* (1965)
				(10.001)			($\alpha = 35°59'$)	12	9.63	Larson *et al.* (1965)
β-$PuGa_3$(μ′)	Mg_3Cd	hexagonal	$P6_3/mmc$	6.299		4.513		2	9.61	Blank and Lindner (1976)
	Ni_3Sn	hexagonal	$P6_3/mmc$	6.300(1)		4.514(1)		2	9.59	Ellinger *et al.* (1964)
~Pu_2Ga_7(?)		tetragonal		4.253		9.695				Blank and Lindner (1976)
Pu_3Ga_{11}–Pu_4Ga_{15}										Blank and Lindner (1976)
$PuGa_4$(ν)	UAl_4	orthorhombic	*Imma*	4.380(1)	6.290(1)	13.673(4)		4	9.13	Land *et al.* (1965a) and Ellinger and Zachariasen (1965)
			Imma	4.387	6.297	13.663		4	9.11	Blank and Lindner (1976)
α-$PuGa_6$										Blank and Lindner (1976)
β-$PuGa_6$(ζ)	$PuGa_6$	tetragonal	P4/*nbm*	5.942(1)		7.617(1)		2	8.11	Land *et al.* (1965a) and Ellinger and Zachariasen (1965)
			P4/*mbm*	5.941		7.621		2	8.12	Blank and Lindner (1976)
~Pu_2Ga_{15}		tetragonal		6.206		8.332		1	7.88	Blank and Lindner (1976)
Pu–Ga phase diagram										Ellinger *et al.* (1964), Hocheid *et al.* (1965), and Akhachinskii and Bashlykov (1970)
Pu–Al–Ga phase diagram										Blank and Lindner (1976)
Pu–Gd system, miscibility gap, no compounds										Kutaitsev *et al.* (1967)
Pu_3Ge										Coffinberry and Miner (1961)
Pu_3Ge_2										Coffinberry and Miner (1961)
Pu_2Ge_3	AlB_2	hexagonal	P6/*mmm*	3.975(2)		4.198(2)		0.5	10.16	Coffinberry and Miner (1961)
$PuGe_2$	$ThSi_2$	bc tetragonal	I4/*amd*	4.102(2)		13.81(1)		4	10.98	Coffinberry and Miner (1961)
$PuGe_3$	$AuCu_3$	cubic	P*m*3*m*	4.223(1)				1	10.07	Coffinberry and Miner (1961)
Pu–Ge phase diagram unknown										Ellinger *et al.* (1968b)
Pu–H system, see Section 7.8, Table 7.26										

$Pu_{28}Hf(\zeta)$	$Pu_{28}Zr$	bc tetragonal	$I4_1/a$	18.19		7.851	4	17.57	Zachariasen and Ellinger (1970)
									Ellinger and Land (1968)
$\sim Pu_{15.7}Hf(\theta)$									
$\sim Pu_{10}Hf(\zeta)$		hexagonal		3.205(1)	5.100(1)			17.07	Kutaitsev *et al.* (1967)
$\sim Pu_9Hf(\theta)$		orthorhombic		10.415(5)	10.428(5)	11.245(5)		17.7	Kutaitsev *et al.* (1967)
Pu–Hf phase diagram									Ellinger *et al.* (1968b), Kutaitsev *et al.* (1967), and Ellinger and Land (1968)
$PuHg_3(?)$	$UHg_3(?)$								Coffinberry and Miner (1961)
$PuHg_4$		pseudo-cubic		3.61(1)					Coffinberry and Miner (1961)
Pu_5Hg_{21}	γ-brass	distorted bcc	$D8_{1-3}$	21.78(1)			16	13.90	Berndt (1966)
Pu–Hg phase diagram									Seaborg *et al.* (1946, 1949b) and Ellinger *et al.* (1968b)
Pu–Ho system, no compounds									Ellinger *et al.* (1968b)
$Pu_3In(\zeta)$	$AuCu_3$	cubic	P*m*3*m*	4.702(1)(Pu-rich)			1		Bochvar *et al.* (1958)
				4.705(Pu-rich)				13.34	Ellinger *et al.* (1965)
				4.722(In-rich)				12.96	Ellinger *et al.* (1965)
				4.750					Hocheid *et al.* (1965)
				4.703(2)			1	13.3	Coffinberry and Miner (1961)
η phase									Ellinger *et al.* (1965)
PuIn(θ)	AuCu	tetragonal	P4/*mmm*	4.811(1)		4.538(1)	2	11.19	Ellinger *et al.* (1965)
$Pu_3In_5(\iota)$									Ellinger *et al.* (1965)
$PuIn_3(\kappa)$	$AuCu_3$	cubic	P*m*3*m*	4.607(1)					Bochvar *et al.* (1958)
				4.6096(2)				9.22	Ellinger *et al.* (1965)
				4.6185(Pu-rich)					Ellinger *et al.* (1965)
				4.6088(In-rich)					Ellinger *et al.* (1965)
Pu–In phase diagram									Hocheid *et al.* (1965) and Ellinger *et al.* (1965)
Pu_5Ir_3	W_5Si_3	tetragonal	I4/*mcm*	11.0438		5.6115	4	17.18	Beznosikova *et al.* (1974)
				11.043		5.611			Beznosikova *et al.* (1974)
				11.012(3)		5.727(2)	4	16.94	Cromer (1977a)
				11.015		5.621(Ir-rich)			Beznosikova *et al.* (1974)
Pu_5Ir_4	Pu_5Ir_4	orthorhombic	P*nma*	7.245	14.60	7.455	4	16.54	Blank and Lindner (1976)
$PuIr_2$	Cu_2Mg	fcc	F*d*3*m*	7.512(1)–7.528(1)			8		Kutaitsev *et al.* (1967)
				7.518					Erdmann and Keller (1973)

Table 7.17 (*Contd.*)

Phase	*Structure type*	*Symmetry*	*Space group*	*Lattice parameters* a_0(Å)	b_0(Å)	c_0(Å)	*Angle* (deg)	*Units per cell*	*X-ray density* (g cm^{-3})	*References*
Pu–Ir phase diagram, no information										Erdmann and Keller (1973)
Pu–K system, no compounds										Ellinger *et al.* (1968b)
Pu–La system, miscibility gap, no compounds										Grison *et al.* (1960), Kutaitsev *et al.* (1967), and Ellinger *et al.* (1967)
Pu–Li system, no compounds										Ellinger *et al.* (1968b)
Pu–Lu system, no information										
$PuMg_2(\zeta)$	CaF_2	fcc	F*m*3*m*	7.34(1)				4	4.83	Coffinberry and Miner (1961) and Ellinger *et al.* (1968b)
$PuMg_{2+x}$		hexagonal		13.8(1)		9.7(1)				Coffinberry and Miner (1961) and Ellinger *et al.* (1968b)
Pu–Mg phase diagram										Ellinger *et al.* (1968b) and Knoch *et al.* (1969)
$PuMn_2$	Cu_2Mg	fcc	F*d*3*m*	7.290(5)(Pu-rich)				8	11.96	Runnalls (1956)
				7.292(1)(Pu-rich)					11.95	Coffinberry and Miner (1961)
				7.29(Pu-rich)						Konobeevsky (1955)
				7.26(Mn-rich)						Konobeevsky (1955)
Pu–Mn phase diagram										Konobeevsky (1955), Ellinger *et al.* (1968b), Bochvar *et al.* (1958), and Grove (1966)
Pu–Mo system, no compounds, phase diagram established										Ellinger *et al.* (1968b), Grison *et al.* (1960), and Bochvar *et al.* (1958)
Pu–N system, see Section 7.8, Table 7.33										
Pu–Na system, no compounds										Ellinger *et al.* (1968b)
Pu–Nb system, no compounds, phase diagram established										Ellinger *et al.* (1968b) and Bochvar *et al.* (1958)
Pu–Nd system, miscibility gap, no compounds, phase diagram established										Ellinger *et al.* (1968a,b) and Kutaitsev *et al.* (1967)

PuNi(ζ)	TlI	orthorhombic	C*mcm*	3.59(1)	10.21(2)	4.22(1)		4	12.78	Cromer and Roof (1959)
$PuNi_2$(η)	Cu_2Mg	fcc	F*d*3*m*	7.16(1)				8	13.1	Runnalls (1956)
				7.141(1)(Pu-rich)						Coffinberry and Miner (1961)
				7.115(1)(Ni-rich)						
				7.14						
$PuNi_3$(θ)	$PuNi_3$	rhombohedral	R$\bar{3}$*m*	8.615			$\alpha = 33°44'$	3	11.8	Cromer and Olsen (1959)
$PuNi_4$(ι)	$PuNi_4$	monoclinic	C2/*m*	4.87(1)	8.46(2)	10.27(2)	$\beta = 100°$	6	11.33	Ellinger *et al.* (1968b) and Cromer and Larson (1960)
$PuNi_5$(κ)	$CaZn_5$	hexagonal	P6/*mmm*	4.875(5)		3.970(5)		1	10.8	Runnalls (1956)
				4.872(2)(Pu-rich)		3.980(1)				Coffinberry and Miner (1961)
				4.861(2)(Ni-rich)		3.982(1)				Coffinberry and Miner (1961)
Pu_2Ni_{17}(λ)	Th_2Ni_{17}	hexagonal	P6_3/*mmc*	8.30(1)		8.00(1)				Runnalls (1956)
				8.29(2)		8.01(2)		2	10.3	Coffinberry and Miner (1961)
Pu–Ni phase diagram										Ellinger *et al.* (1968b) and Wensch and Whyte (1951)
Pu–Np										
η phase		orthorhombic		10.86	10.67	10.43		54		Mardon *et al.* (1961) and Cope *et al.* (1960)
Pu–Np phase diagram										Mardon *et al.* (1961) and Cope *et al.* (1960)
Pu–O system, see Section 7.8, Table 7.37										
$Pu_{19}Os$(ζ)	related to β-Pu	orthorhombic	P*nna*	15.839(5)	7.819(3)	9.151(3)		52	18.02	Cromer (1979b)
$Pu_{19}Os$(η)		orthorhombic	C*mca*	5.345(5)	14.884(14)	10.898(15)		2	18.12	Cromer (1978)
Pu_3Os										Konobeevsky (1955)
Pu_3Os(η′)										Ellinger *et al.* (1968b)
Pu_5Os_3(θ)	W_5Si_3	tetragonal	I4/*mcm*	10.8818		5.6645		4	17.48	Beznosikova *et al.* (1974) and Cromer *et al.* (1975)
$PuOs_2$(ι)	$MbZn_2$	hexagonal	P6_3/*mmc*	5.337		8.683		4	19.2	Konobeevsky (1955)
Pu–Os phase diagram										Konobeevsky (1955), Ellinger *et al.* (1968b), and Miner (1970)

Table 7.17 (*Contd.*)

Phase	*Structure type*	*Symmetry*	*Space group*	*Lattice parameters* a_0(Å)	b_0(Å)	c_0(Å)	*Angle* (deg)	*Units per cell*	*X-ray density* (g cm^{-3})	*References*
Pu–P system, see Section 7.8, Table 7.33										
$Pu_3Pb(\zeta)$	Cu_3Au	cubic	P*m*3*m*[a]	4.737(1)				1	14.56	Wood *et al.* (1969)
$Pu_5Pb_3(\eta)$	W_5Si_3	tetragonal	I4/*mcm*	12.310(2)		6.084(1)			13.07	Wood *et al.* (1969)
$Pu_5Pb_4(\theta)$	Ti_5Ga_4	hexagonal	$P6_3/mcm$	9.523(4)		6.482(3)			13.31	Wood *et al.* (1969)
$Pu_4Pb_5(\iota)$	Pu_4Pb_5(?)[b]	hexagonal	$P6_322$	16.52(1)		6.440(3)				Wood *et al.* (1969)
$PuPb_2(\kappa)$[c]	$HfGa_2$	tetragonal	$I4_1/amd$	4.621(5)		31.29(3)			12.99	Wood *et al.* (1969)
$PuPb_3(\lambda)$	Cu_3Au	cubic	P*m*3*m*	4.8084(Pu-rich)				1		Wood *et al.* (1969)
				4.8077(Pb-rich)					12.86	Wood *et al.* (1969)
				4.808(1)				1	12.86	Bochvar *et al.* (1958) and Wood *et al.* (1969)
				4.81						Coffinberry and Miner (1961), Konobeevsky (1955), and Bochvar *et al.* (1958)
Pu–Pb phase diagram										Bochvar *et al.* (1958) and Wood *et al.* (1969)
Pu_5Pd_4 (probably identical with PuPd)										Kutaitsev *et al.* (1967)
PuPd	FeB	orthorhombic	P*nma*	7.036(4)	4.550(2)	5.663(2)		4	12.65	Cromer (1975)
				7.028(5)	4.571(1)	5.658(2)		4	12.6	
Pu_3Pd_4	Pu_3Pd_4	rhombohedral	$R\bar{3}$	7.916			$\alpha = 114.2$			Kutaitsev *et al.* (1967)
		(hexagonal setting)		13.304		5.783		2	12.8	Kutaitsev *et al.* (1967)
				13.344(2)		5.744(2)			12.85	Cromer *et al.* (1973)
Pu_3Pd_5	Ga_5Zr_3	orthorhombic	C*mcm*	9.201	7.159	9.771		4	12.89	Cromer (1976)
$PuPd_3$	$AuCu_3$	cubic	P*m*3*m*	4.077–4.119				1	13.41[d]	Kutaitsev *et al.* (1967)
				4.095						Erdmann and Keller (1973)
Pu–Pd phase diagram										Ellinger *et al.* (1968b) and Kutaitsev *et al.* (1967)

Pu–Pr system, no compounds, miscibility gap, phase diagram established									Ellinger *et al.* (1968a,b) and Kutaitsev *et al.* (1967)
$Pu_5Pt_3(\zeta)$	Mn_5Si_3	hexagonal	P$6_3/mcm$	8.490		6.094	2		Beznosikova *et al.* (1974)
				8.490(2)		6.084(2)	2	15.57	Cromer and Larson (1975)
$Pu_{31}Pt_{20}(\eta)$	$Pu_{31}Pt_{20}$	tetragonal	I4/*mcm*	11.302(5)		37.388(23)	4	15.73	Cromer and Larson (1977)
PuPt(θ)	TaB	orthorhombic	C*mcm*	3.816	10.694	4.428		15.95	Kutaitsev *et al.* (1967), Cromer and Roof (1959)
$PuPt_2(\iota)$	Cu_2Mg	fcc	F$d3m$	7.633			8	18.69	Erdmann and Keller (1973)
				7.631–7.653					Kutaitsev *et al.* (1967)
α-$PuPt_3(\kappa)$	$AuCu_3$	cubic	P$m3m$	4.107			1	19.75	Kutaitsev *et al.* (1967)
				4.105					Erdmann and Keller (1973)
β-$PuPt_3(\kappa')$	PNi_3	bc tetragonal	$I\bar{4}$	10.39(1)		4.60(3)			Land *et al.* (1978)
$PuPt_4(\lambda)$	defect $PuPt_5$	orthorhombic	C*mmm*	5.258(15)	8.759(29)	4.563(13)			Land *et al.* (1978)
$PuPt_5(\mu)$	$CaCu_5$	hexagonal	P6/*mmm*	5.262(8)		4.393(8)			Land *et al.* (1978)
	$SmPt_5$	orthorhombic		5.314	9.100	26.51			Erdmann and Keller (1973)
Pu–Pt phase diagram									Kutaitsev *et al.* (1967) and Land *et al.* (1978)[f]
Pu–Rb system, no compounds									Ellinger *et al.* (1968b)
$PuRe_2$	$MgZn_2$	hexagonal	P$6_3/mmc$	5.396(1)		8.729(1)	4	18.45	Coffinberry and Miner (1961)
Pu–Re phase diagram unknown									
$Pu_2Rh(\zeta)$									Kutaitsev *et al.* (1967)
$Pu_5Rh_3(\eta)$		tetragonal	P4/*ncc*	10.94		6.020	4		Kutaitsev *et al.* (1967) and Beznosikova *et al.* (1974)
$Pu_{31}Rh_{20}(\theta)$	$Pu_{31}Pt_{20}$	tetragonal	I4/*mcm*	11.076(1)		36.933(12)	4	13.87	Cromer and Larson (1977)
$Pu_5Rh_4(\iota)$		orthorhombic	P*nma*	7.276(2)	14.332(4)	7.419(2)	4	13.79	Cromer (1977b)
				7.263	14.48	7.464	4	13.59	Blank and Lindner (1976)
PuRh(κ)									Kutaitsev *et al.* (1967)
$Pu_3Rh_4(\lambda)$									Kutaitsev *et al.* (1967)
$PuRh_2(\mu)$	Cu_2Mg	fcc	F$d3m$	7.488			8	14.07	Kutaitsev *et al.* (1967) and Erdmann and Keller (1973)
$PuRh_3(\nu)$	$AuCu_3$	cubic	P$m3m$	4.009–4.040			1	13.95	Kutaitsev *et al.* (1967)
				4.042					Erdmann and Keller (1973)
Pu–Rh phase diagram									Kutaitsev *et al.* (1967) and Land *et al.* (1978)

Table 7.17 (*Contd.*)

Phase	*Structure type*	*Symmetry*	*Space group*	*Lattice parameters* a_0(Å)	b_0(Å)	c_0(Å)	*Angle* (deg)	*Units per cell*	*X-ray density* (g cm^{-3})	*References*
$Pu_{19}Ru(\zeta_2)$	$Pu_{19}Os$(?)									Ellinger *et al.* (1968b) and Miner (1970)
$Pu_3Ru(\eta)$		(ortho?)		(6.216)	(6.924)	(8.093)		(4)	(15.60)	Berndt (1962)
$Pu_5Ru_3(\theta)$	W_5Si_3	tetragonal	I4/*mcm*	10.7685		5.7473		4	14.93	Beznosikova *et al.* (1974)
				10.745(3)		5.719(2)		4	15.07	Cromer *et al.* (1975)
$PuRu(\iota)$	CsCl	cubic	P*m*3*m*	3.363(1)				1	14.87	Coffinberry and Miner (1961)
				3.3635(6)					14.84	Kutaitsev *et al.* (1967)
$PuRu_2(\kappa)$	Cu_2Mg	fcc	F*d*3*m*	7.476(1)				8	14.06	Coffinberry and Miner (1961)
				7.472(1)–7.476(1)					14.03	Coffinberry and Miner (1961)
				7.4737(1)(Ru-rich)						Kutaitsev *et al.* (1967)
Pu–Ru phase diagram										Seaborg *et al.* (1946, 1949b), Kutaitsev *et al.* (1967), and Cope (1960)
Pu–S system, see Section 7.8, Table 7.39										
'$Pu_{11}Sc_9$'(ζ)		hexagonal	P6_3/*mmc*	3.310(Pu-rich)		10.717		4	10.5	Kutaitsev *et al.* (1967)
				3.308(Sc-rich)		10.709				
'Pu_5Sc_4'										Kutaitsev *et al.* (1967)
Pu–Sc phase diagram										Ellinger *et al.* (1968b), Miner (1970), and Kutaitsev *et al.* (1967)
Pu–Se system, see Section 7.8, Table 7.39										
Pu–Si system, see Section 7.8, Table 7.32										
Pu–Sm phase diagram										Ellinger *et al.* (1968a,b)[f]
Pu_3Sn	$AuCu_3$(?)	fcc		4.680						Ellinger *et al.* (1968b)
$PuSn_2$	$HfGa_2$	tetragonal	I4_1/*amd*	4.43(2)		31.0(1)				Wallace and Harvey (1974)
$PuSn_3$	$AuCu_3$	fcc	P*m*3*m*	4.630(1)				1	9.96	Coffinberry and Miner (1961)
				4.654(2)						Akhachinskii and Bashlykov (1970)

Pu–Sn phase diagram unknown								
Pu–Sr system, no compounds								Ellinger *et al.* (1968b)
Pu–Ta system, no compounds, phase diagram established								Ellinger *et al.* (1968b)
Pu–Tc system, no information								
Pu–Tb system, no compounds								Ellinger *et al.* (1968b)
Pu–Te system, see Section 7.8								
$Pu_{13}Th_6$		orthorhombic	9.820	8.164	6.681	6		Poole *et al.* (1957)
			7.90	8.43	9.79	8		Bochvar *et al.* (1958)
Pu–Th phase diagram								Seaborg *et al.* (1946, 1949b), Ellinger *et al.* (1968b), Bochvar *et al.* (1958), and Poole *et al.* (1957)
Pu–Ti system, no compounds, phase diagram established								Ellinger *et al.* (1968b) Grison *et al.* (1960) Kutaitsev *et al.* (1967)
Pu_3Tl	$AuCu_3$	cubic	4.723				14.5	Bochvar *et al.* (1958)
$PuTl_3$	disordered							
	Mg	hexagonal	3.458		5.519		12.4	Bochvar *et al.* (1958)
Pu–Tl system, phase diagram not yet established								
Pu–Tm system, no compounds								Bowersox and Leary (1966)
Pu–U(ζ)		primitive cubic						
35 at.%U			10.60(2)					Waldron *et al.* (1958)
35 at.%U			10.692				18.5	Ellinger *et al.* (1959)
50 at.%U			10.61(1)					Waldron *et al.* (1958)
50 at.%U			10.664					Ellinger *et al.* (1959)
65 at.%U			10.65(1)					Waldron *et al.* (1958)
70 at.%U			10.651			58	18.8	Waldron *et al.* (1958)
Pu–U(η)		tetragonal						
25 at.%U			10.57(5)		10.76(5)	52	17.3	Ellinger *et al.* (1959)
20 at.%U			10.44		10.73	56	18.5	Bochvar *et al.* (1958)
Pu–U phase diagram								Coffinberry and Miner (1961) and Ellinger *et al.* (1959)

Table 7.17 (*Contd.*)

Phase	*Structure type*	*Symmetry*	*Space group*	*Lattice parameters* a_0(Å)	b_0(Å)	c_0(Å)	*Angle* (deg)	*Units per cell*	*X-ray density* (g cm^{-3})	*References*
Pu–V system, no compounds, phase diagram established										Konobeevsky (1955), Ellinger *et al.* (1968b), and Bowersox and Leary (1967)
Pu–W system, no compounds, phase diagram established										Ellinger *et al.* (1968b)
PuY system, no compounds, phase diagram established										Ellinger *et al.* (1968b), Kutaitsev *et al.* (1967), and Wittenberg and Grove (1963)
Pu–Yb system, no compounds										Ellinger *et al.* (1968b)
$PuZn_2(\zeta)$	Cu_2Mg	bc tetragonal	F*d*3*m*	7.760(1)(Pu-rich) 7.747(1)(Zn-rich)				8	10.54 10.5	Cramer *et al.* (1960)
$Pu_2Zn_{\sim 9}(\eta)$		hexagonal	$P6_3/mmc$ (?)	28.86(2)		14.14(1)			9.05	Larson and Cromer (1967)
$Pu_{13}Zn_{58}$	subcell of $Pu_2Zn_{\sim 9}$	hexagonal	$P6_3/mmc$ or $P6_3mc$	(14.43)		(14.14)		2	8.98	Larson and Cromer (1967)
$Pu_3Zn_{22}(\theta)$		bc tetragonal	$I4_1/amd$	8.85		21.18		4	8.71	Johnson *et al.* (1967)
$Pu_2Zn_{17}(\iota)$	Th_2Zn_{17}	rhombohedral (hexagonal setting)	$R\bar{3}m$	8.95		13.1			8.5	Cramer and Wood (1967)
'Pu_2Zn_{17}'(κ)[e]		hexagonal	P6/*mmm*	8.9		17.7				Cramer and Wood (1967)

'Pu_2Zn_{17}'(κ')[e]		hexagonal	$P6_3/mmc$	8.98		8.85			Cramer and Wood (1967)
'Pu_2Zn_{17}'(λ)[e]		hexagonal	$P6_322$	8.98		8.85			Cramer and Wood (1967)
Pu–Zn phase diagram									Cramer *et al.* (1960) and Albrecht (1964)
$Pu_{28}Zr(\zeta)$	related to β-Pu	bc tetragonal	$I4_1/a$	18.1899(3)		7.8576(2)	4		Cromer (1979a)
				18.19(1)		7.851(3)		17.444	Zachariasen and Ellinger (1970)
$\sim Pu_6Zr$		orthorhombic		10.39	10.44	11.18	8	16.7	
$Pu_4Zr(\iota)$		tetragonal	$P4/ncc$	10.893(3)		14.889(7)	16	15.76	Berndt (1967)
$PuZr_{2-3}(\kappa)$	UZr_2	hexagonal	$P6/mmm$	5.060		3.119	1		Bochvar *et al.* (1958)
				5.055		3.123			Marples (1960)
Pu–Zr phase diagram									Bochvar *et al.* (1958) and Johnson (1954)

[a] No superstructure observed (Pu_3Pb).
[b] Preliminary analysis (Pu_4Pb_5).
[c] Low-temperature modification($PuPb_2$).
[d] For 75 at.% Pu ($PuPd_3$).
[e] Assignments to phase regions at the zinc-rich end of the phase diagram (Pu_2Zn_{17}).
[f] Also, F. H. Ellinger, C. C. Land, and K. A. Johnson, unpublished work, Los Alamos Scientific Laboratory.

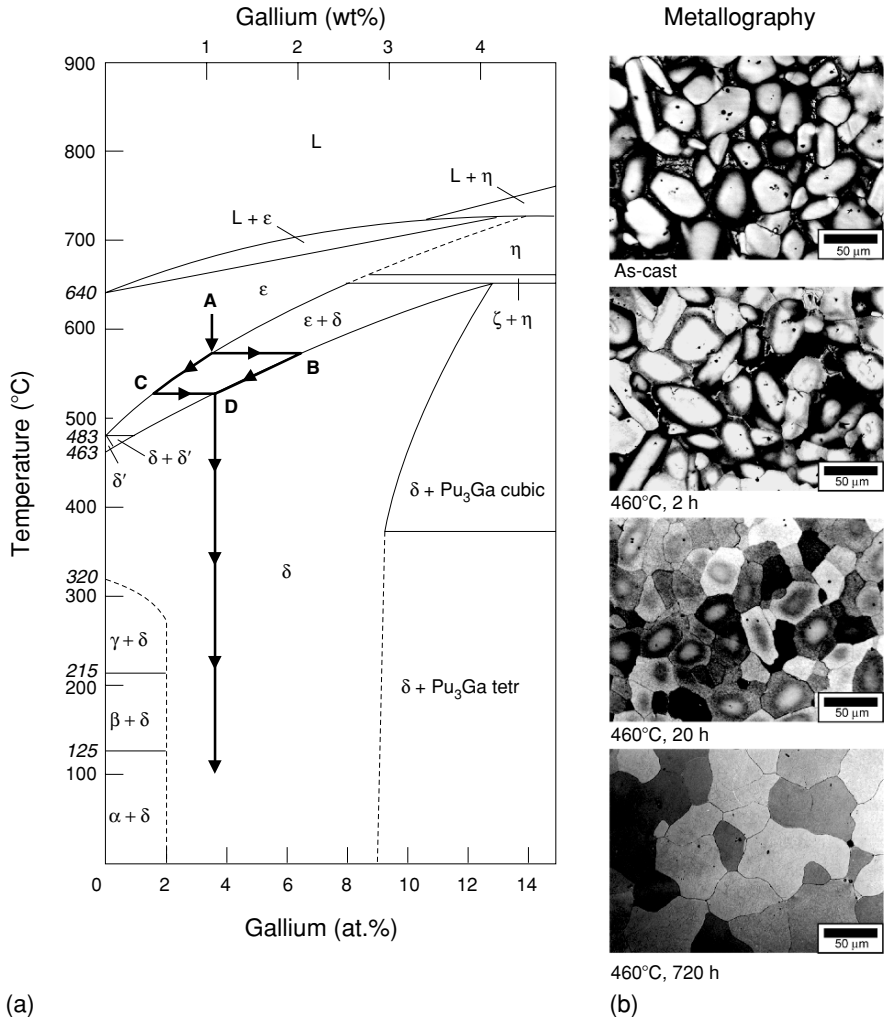

Fig. 7.33 (*a*) *The Pu-rich side of the Pu–Ga phase diagram depicting a typical gallium segregation path.* (*b*) *Typical optical microstructures of a Pu*-3.4 at. *% Ga alloy for various conditions* (*from as-cast to annealed at* 460°C *for* 720 h) (*Mitchell* et al., 2001).

a uniform gallium concentration. The progression of gallium 'homogenization' and consequent change in microstructure are also shown for a homogenization temperature of 460°C in Fig. 7.33(b).

Such microsegregation can occur with any of the alloying elements that retain the δ phase to room temperature. The extent of microsegregation depends on the cooling rate and on the shape of the two-phase field. A typical gallium

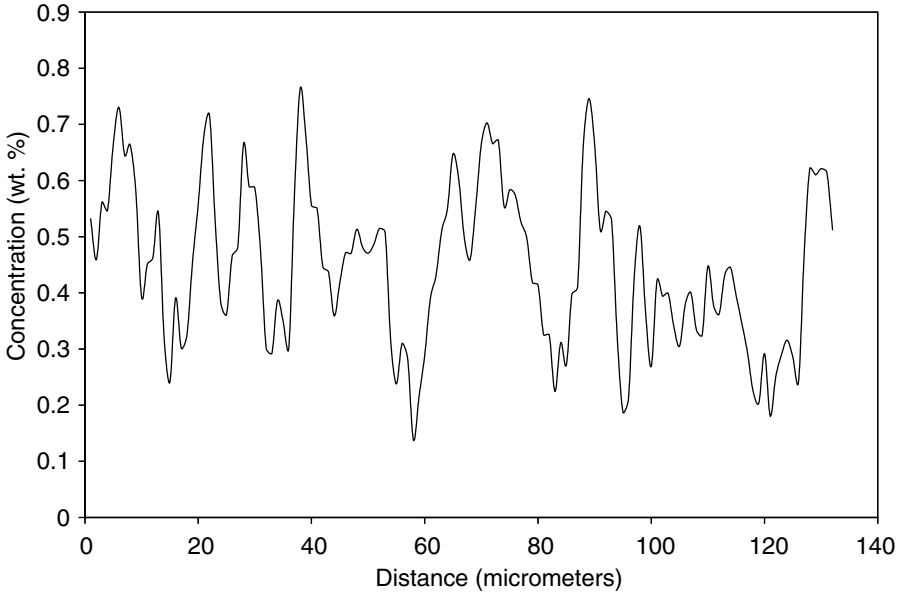

Fig. 7.34 *A typical gallium concentration profile for a nominal Pu*-1.7 at. *% Ga* (0.5 wt. *% Ga*) *alloy by electron microprobe. The grain size was roughly* 30 μm (*from unpublished work of one of the authors, S. S. Hecker*).

profile taken with an electron microprobe is shown in Fig. 7.34 for Pu–1.8 at.% Ga cooled at a rate of $\sim$5°C min^{-1}. At such rates, all areas with $<$1.4 at.% Ga transform to the α phase upon cooling to room temperature. If initial cooling rates are rapid, and homogenization times of hundreds of hours at 460°C are employed, then the δ phase can be retained to room temperature with as little as 1 at.% Ga. However, the retained δ phase is metastable and will transform at low temperatures and/or hydrostatic compression. Hence, proper homogenization treatments for δ-phase alloys are important in studying plutonium alloys. If not properly homogenized, such alloys exhibit continuously varying gallium gradients (on the scale of the grain size as shown in Fig. 7.34), or they may consist of two-phase mixtures. Either one of these conditions can significantly affect the properties of the alloy.

(g) Phase transformations in δ-phase alloys

Hecker *et al.* (2004) and Deloffre (1997) presented comprehensive overviews of phase transformations in δ-phase plutonium alloys. During cooling the retained fcc δ phase transforms to the monoclinic α phase (sometimes through an intermediate phase such as the β phase or γ phase). The transformation behavior as monitored in a dilatometer is shown for a constant cooling rate for several

Pu–Ga alloys (Hecker *et al.*, 2004) in Fig. 7.35. The transformation is martensitic, that is, diffusionless and displacive (shear). The transformation start temperature depends strongly on the gallium concentration (all three alloys shown were thoroughly homogenized before cooling) as shown in Fig. 7.35. The transformation behavior depends on cooling rate and is, therefore, characterized as an isothermal martensitic transformation. Orme *et al.* (1976) determined the TTT kinetics for Pu–Ga alloys as illustrated by the double C-curves shown in Fig. 7.36. Thermal activation appears to be necessary to nucleate the transformation before the martensite transformation product grows by a shear mechanism at sonic velocities. The C-curve kinetics result from insufficient

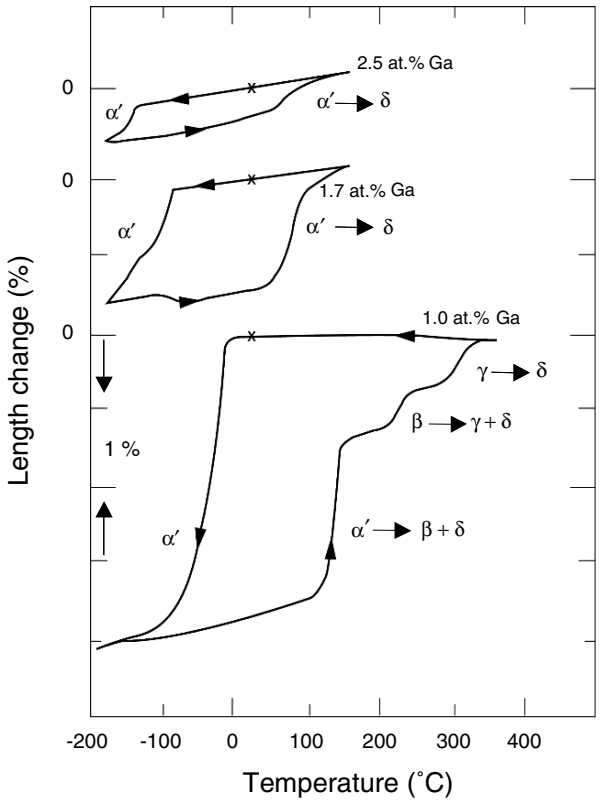

Fig. 7.35 *Thermally induced δ→α′ and reverse transformations for Pu–Ga alloys during cooling and heating. The zero is offset for the three curves as shown. The α′ phase in the* 2.4 *and* 1.7 at. *% Ga alloys revert back to the δ phase. The α′ phase in the Pu-*1 at. *% Ga alloy reverts along a more complex path to mostly β, then γ and finally to the δ phase with a small amount of the α′ phase reverting directly to the δ phase as the rest transforms to the β phase. The x in each of the three figures denotes the onset of the cooling and the end point after heating and cooling* (*Hecker* et al., 2004).

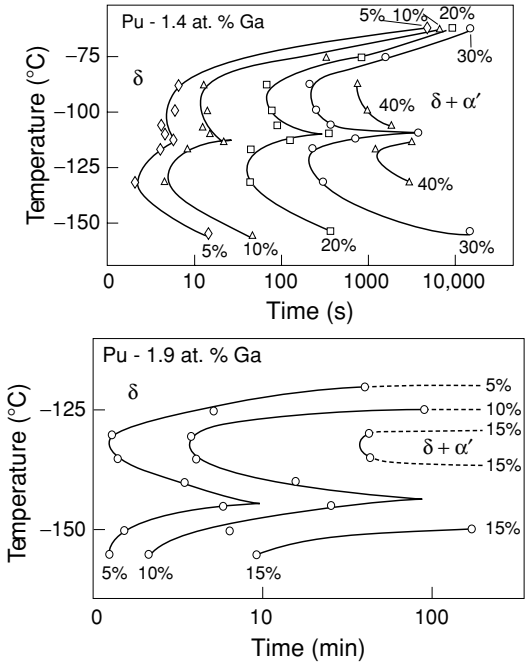

Fig. 7.36 *Time–temperature-transformation curves for* (*top*) *Pu*-1.4 at. *% Ga and* (*bottom*) *Pu*-1.9 at. *% Ga alloys* (*Orme* et al., 1976). *Transformation curves are shown for* 5, 10, 20, *and* 30% *transformation in* (*top*) *and for* 5, 10, *and* 15% *transformation in* (*bottom*) (*from Hecker* et al., 2004).

driving force at the higher temperatures and insufficient thermal activation at the lower temperatures. The overall kinetics is shown to be dependent on gallium concentration.

Similar transformation behavior is observed for δ-phase Pu–Al alloys as demonstrated by Hecker *et al.* (2004) and shown in Fig. 7.37. The well-homogenized Pu–2 at.% Al alloys begin to transform at approximately –130°C during cooling. After cooling to liquid nitrogen temperature and heating back to room temperature, metallographic and X-ray examination showed that the resulting microstructure (shown in Fig. 7.37) consisted of 25% α′ phase (in the form of martensite platelets) and 75% residual δ phase. The α′-phase designation is used here to indicate that the aluminum or gallium atoms, which have no equilibrium solubility in the α phase, are trapped by the martensitic transformation and expand the lattice of the α phase (Hecker *et al.*, 2004). During hydrostatic compression at room temperature, the δ phase collapses just below 0.4 GPa (as shown in Fig. 7.37), transforming martensitically first to the β′ followed by the α′ phase. The microstructure is more complex as shown in Fig. 7.37. If such

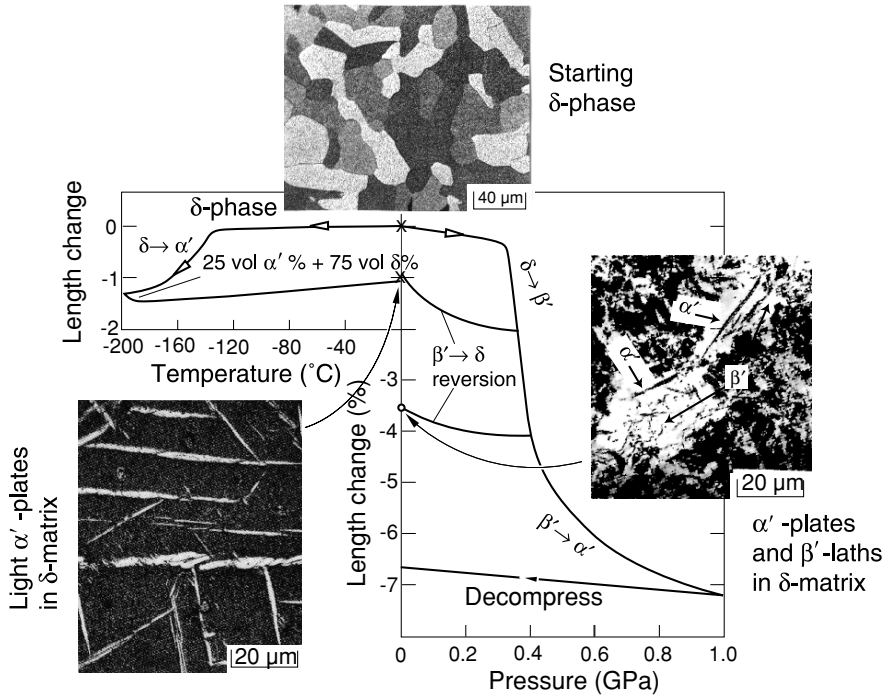

Fig. 7.37 *Temperature and pressure-induced transformations in Pu*-2.0 at. *% Al alloys* (*Zukas* et al., 1981*; Hecker* et al., 1982). *The starting δ-phase microstructure is shown on top and the transformed microstructures on the left and right for temperature and pressure-induced transformations, respectively.*

samples are compressed only partially, then both product phases appear in the residual δ-phase matrix.

Adler and coworkers (Olson and Adler, 1984; Adler *et al.*, 1986) modeled the crystallography of the δ→α′ transformation during cooling. Zocco *et al.* (1990) subsequently confirmed their predictions by transmission electron microscopy (TEM) and determined the lattice correspondence between the parent and product phases and the α′-phase habit plane. The details of the experimental and theoretical results are reviewed by Hecker *et al.* (2004). Heating the transformed α′ phase above room temperature for Pu–Ga alloys results in the transformation behavior shown in Fig. 7.35. The low-gallium alloys transform from α′→β→γ, whereas the higher-gallium alloys transform directly from α′→δ at temperatures significantly lower than the α→β transformation temperature.

Complex stress states such as those found during cold rolling, machining, or mechanical polishing all trigger the δ→α′ transformation. Machining most likely produces a complex mixture of α′ and α-phases (that is, expanded and

unexpanded) because of the heat generated. Mechanical polishing is especially effective in promoting the γ'-phase as an intermediary phase (Zukas *et al.*, 1983). These authors also observed that samples that had previously undergone a $\delta \rightarrow \alpha$ transformation were susceptible to the reverse $\alpha' \rightarrow \delta$ transformation at the crack tip of tensile specimens. Hydrostatic tension favors the larger volume δ phase. Hecker and Stevens (2000) reported this behavior for both transformed samples and for unalloyed α plutonium. The reversion results reinforce the importance of the sign and magnitude of the hydrostatic stress component in triggering martensitic transformations in plutonium.

The complex nature of the transformation behavior for plutonium and its alloys must be taken into account during sample synthesis and preparation. In plutonium alloys, the slightest mechanical polishing or machining procedures can leave a layer of transformation product that may influence the properties to be measured. Such transformation products can be avoided or removed, but only if sufficient care is taken. For example, electropolishing is quite effective to remove surface products. Heating is also effective but must be done with care so as to not introduce new artifacts or changes in structure (this is especially true for aged samples in which helium has been generated by self-irradiation damage).

7.7.5 Electronic structure, theory, and modeling

The complex electronic structure of plutonium has been a subject of intense study for theorists and modelers for more than 50 years. Arko *et al.* (2006) present the most recent review of electronic structure in the actinides, including plutonium, in Chapter 21 of this work. As mentioned above, the actinides mark the filling of the 5f atomic subshell much like the rare earths mark the filling of the 4f subshell. Yet, the 5f electrons of the light actinides behave more like the 5d electrons of the transition metals than the 4f electrons of the rare earths. The peculiar properties described in Section 7.7.3, and shown in Fig. 7.19, are telltale signs of novel interactions and correlations among electrons, which result in behavior that cannot be explained by the one-electron band theory of metals. Boring and Smith (2000) point out that such novel interactions typically result from a competition between itinerancy (bonding electrons that form bands in metals) and localization (electrons with local moments that magnetically order at low temperature). In these elements, we find that such novel interactions occur in the d- and f-electron metals near iron, at cerium, and near plutonium. Based on these considerations, Smith and Kmetko (1983) rearranged the periodic table for the transition metals, the rare earths, and the actinides as shown in Fig. 7.38. This representation shows that most transition metals, lanthanides, and actinides have predictable ground states and become either superconducting or magnetic as the temperature is lowered. The elements along the diagonal have two or more partially filled bands that are close in energy. One of the bands is typically relatively narrow with a high density of states (DOS) at the Fermi

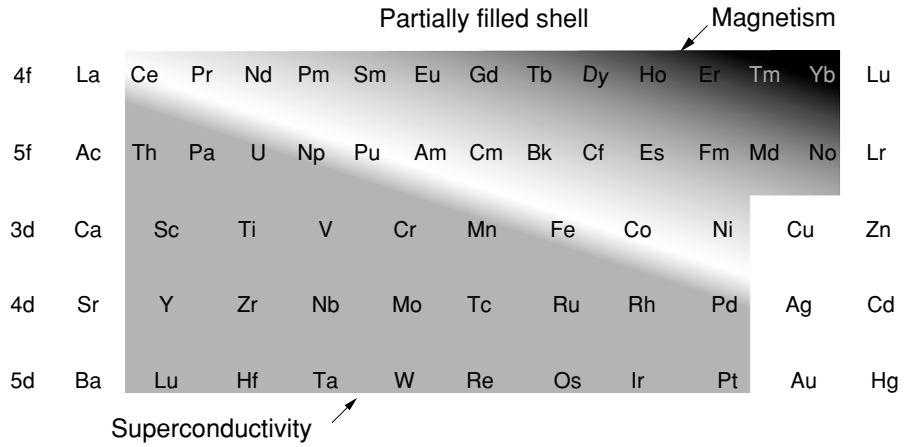

Fig. 7.38 *Smith and Kmetko* (1983) *rearranged periodic table that highlights the transition in electronic behavior from localized electrons* (*resulting in magnetism*) *to itinerant electrons* (*resulting in superconductivity*).

energy (the f-bands are 2 to 4 eV wide and the d-bands span 5 to 10 eV). Narrow bands tend to mix or hybridize with other bands close in energy. The electrons in these narrow bands can be strongly correlated, but still bonding. They spend much more of their time close to their atomic cores than do the 'free' (valence) s-electrons. The electrons in the narrow bands are highly sensitive to small perturbations, which enhances polymorphism and causes instability in the solid state. Smith and Boring point out that in addition to exhibiting multiple crystal structures, the elements along the diagonal also exhibit strong catalytic activity, have a great affinity for hydrogen, and spark easily when struck. Moreover, the behavior of the elements can easily be moved across the diagonal by changes in temperature, pressure, or by alloying.

The electronic configuration of isolated plutonium atoms is $7s^2 5f^6$ (see Section 7.6). In the metallic state the electronic configuration is $7s^2 6d^1 5f^5$. The atomic volumes in the solid state change abruptly across the actinide series at plutonium, as shown in Fig. 7.39. This change indicates a major electronic transition between the light and the heavy actinides. In the light actinides up to plutonium, each additional 5f electron (like each d-electron in the transition metals) goes into the conduction band, where it increases the chemical bonding forces, pulling the atoms closer together and resulting in a decrease in atomic volume. Beginning at americium, the 5f electrons behave like the 4f electrons of the rare earths, localizing at each lattice site and becoming chemically inert. With no 5f contribution to bonding, the atomic volume suddenly increases at americium, and contracts only slightly with increasing atomic number because the 5f electrons remain localized in the remainder of the series. As shown in

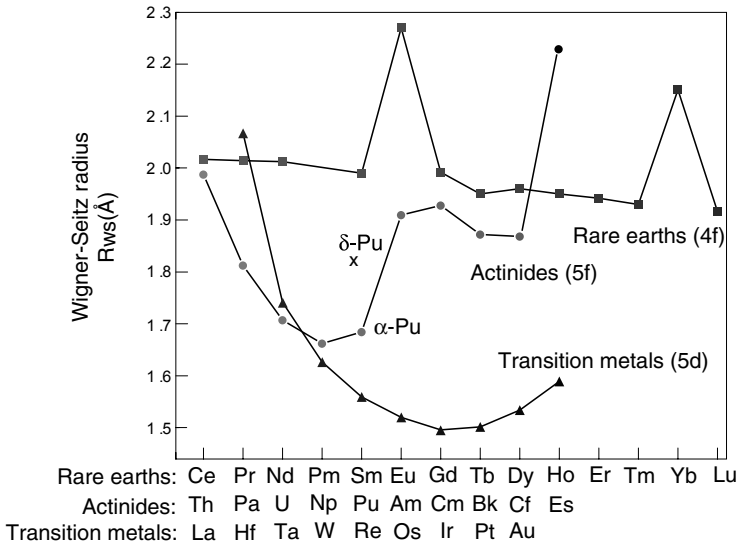

Fig. 7.39 *Wigner–Seitz radii for the actinides compared to the lanthanides and 5d transition metals. The actinides include the data for Es* (*Haire* et al., 2004), *which is divalent with a large volume, much like Eu in the lanthanides.*

Fig. 7.39, this behavior is similar to the lanthanides. The large jump in atomic volume at Es is due to divalent behavior similar to that for Eu and Yb for the lanthanides. The pattern of local moments, another strong indicator of what the electrons are doing, confirms this general picture. The light actinides show no local moments, as expected if all the valence electrons are in the conduction band, whereas the heavy actinides and the lanthanides generally exhibit local moments.

In the α phase, the 5f electrons appear to be bonding (although Savrasov *et al.* (2001) claim that the f-electrons are already strongly correlated in the α phase), whereas in americium the 5f electrons are clearly localized. It is interesting to note here that americium was found to be an ordinary superconductor with no hint of a magnetic moment although it is on the 'magnetic' side of the diagonal in Fig. 7.38 (Smith and Haire, 1978). This is a consequence of the $5f^6$ electronic configuration resulting in a total angular momentum $J = 0$, so that no moment is present even in the free ion limit. As shown by the atomic volumes in Fig. 7.39, the δ phase in pure plutonium falls between the plutonium α phase and the americium dhcp phase. The plutonium δ phase is a state that appears to be unique among the elements. Before addressing the δ phase, we will first consider the α phase ground state.

First-principles total-energy calculations based on density-functional theory (DFT) successfully predict electronic structure and bonding properties of simple

metals and the transition metals (Skriver, 1985). With the advent of high-performance computing, it has become possible during the past 10 to 15 years to extend such calculations to the actinides by incorporating low-symmetry crystal structures, relativistic effects, and electron–electron correlations. The complicated electron–electron exchange term arising from the Pauli exclusion principle and electron–electron electrostatic interactions are incorporated through a local density approximation (LDA) or a generalized gradient approximation (GGA), which incorporates the local electron density and the density gradient. Wills and Eriksson (2000), who summarized their efforts and those of their colleagues, successfully predicted the structures and volumes of the low-symmetry ground states of the light actinides, including plutonium. These calculations show that in α plutonium all eight valence electrons are in the conduction band. However, the 5f bands are very narrow – that is, each 5f electron is nearly localized on an atomic site and, hence, spends a long time near this site before it jumps to the next site. Because the bands are narrow, they exhibit a very high DOS. As the number of 5f electrons populating the band increases across the actinide series, the specific properties of the band begin to dominate the bonding properties of the metal.

Wills and Eriksson demonstrated that the α phase is the stable ground state of plutonium because special conditions favor lattice distortions. Specifically, the very narrow band of the 5f electrons with a high DOS at or very near the Fermi energy split the band in certain regions, thereby lowering the total energy through a Jahn–Teller/Peierls-like distortion. We recall that in iron the degeneracy of the d-conduction band is lifted by the electron spins causing the d-band to split spontaneously into spin-up and spin-down bands. In plutonium the degeneracy of the f-band is lifted by a lattice distortion leading to lower energy. Also, because the narrow 5f band overlaps the s, p, and d bands, a number of electronic configurations have nearly equal energy, leading to multiple allotropes in the light actinides and to their great sensitivity to external influences such as temperature, pressure, and chemical additions. Before the insight gained from the calculations of Wills and Eriksson, the low-symmetry ground state in metallic plutonium was attributed to directional or covalent-like bonding, resulting from the angular characteristics of f-electron orbitals (somewhat analogous to molecular bonding, see Section 7.9.3) (Boring and Smith, 2000; Hecker, 2000). Although total-energy electronic structure calculations apply only at zero temperature, they have been remarkably successful in predicting the ground-state properties of the actinides, both at ambient and elevated pressures. In addition, energy differences for various structures can be calculated to give an indication of whether these are thermally accessible. Wills and Eriksson (2000) point out that including temperature effects is not a simple task. One possibility is to integrate existing molecular dynamics or Monte Carlo simulations with electronic structure calculations. It may also be possible that accurate calculations of the phonon spectra of different allotropes may enable reliable calculations of the free energy as a function of temperature.

We now turn to the fcc δ phase, which is the most desirable from an engineering standpoint but the least understood from a physics standpoint. As shown in Fig. 7.39, the volume (the Wigner–Seitz radius is actually plotted) of the δ phase falls between that of α plutonium and americium. The 5f electrons appear to be in some mixed state, neither fully itinerant nor fully localized. Above, we pointed out that the δ phase has other unusual properties, such as a negative thermal expansion coefficient and an unusually large low-temperature electronic specific heat. Unfortunately, even the best calculations based on standard DFT with some LDA do not adequately predict the δ-phase volume or elastic constants in unalloyed plutonium. This failure has spawned numerous attempts to go beyond the LDA. Wills and Eriksson (2000) found that they had to 'constrain' their calculations by localizing four of the five 5f electrons in the δ phase to predict the correct atomic volume using the same formalism as for the ground state of the light actinides. The constrained 5f electrons cannot hop from site to site and do not hybridize with other electrons. In essence, the constrained calculations combine knowledge of DFT and atomic theory. Hecker *et al.* (2004) review other recent attempts to explain the peculiarities of the δ phase. However, none of them currently provide an adequate explanation. The approach of Wills and Eriksson provides the best current guidance for understanding the δ phase and the alloying behavior of plutonium. This is clearly an area where we can expect significant advances in our understanding over the coming decade.

(a) Alloy theory and modeling

Before discussing the alloying behavior, it is instructive to view the behavior of plutonium in context of the other actinides. Fig. 7.40 shows the connected binary alloy phase diagrams of the actinides through curium. At the beginning of the actinides, there is little f-electron influence and, hence, one finds typical metallic crystal structures, few allotropes, and high melting points. As more f-electrons are added (up to plutonium) and participate in bonding (that is, they are itinerant), the crystal structures become less symmetric, the number of allotropes increases, and the melting points decrease. At americium and beyond, crystal structures typical of metals return, the number of allotropes decrease, and the melting points rise – all indications of the f-electrons becoming localized or inert. So we see that the peculiar properties of plutonium are not a single anomaly, but rather the culmination of a systematic trend across the actinides. And, the transition occurs not between plutonium and americium, but right at plutonium – between the ground-state α phase and the elevated-temperature δ phase.

To predict plutonium alloy phase diagrams, we need to know the Gibbs free energy of all the phases and compounds as a function of alloy concentration and temperature. We must calculate the internal energy and the entropy (electronic, vibrational, and configurational). To predict δ-phase stability, we must be able

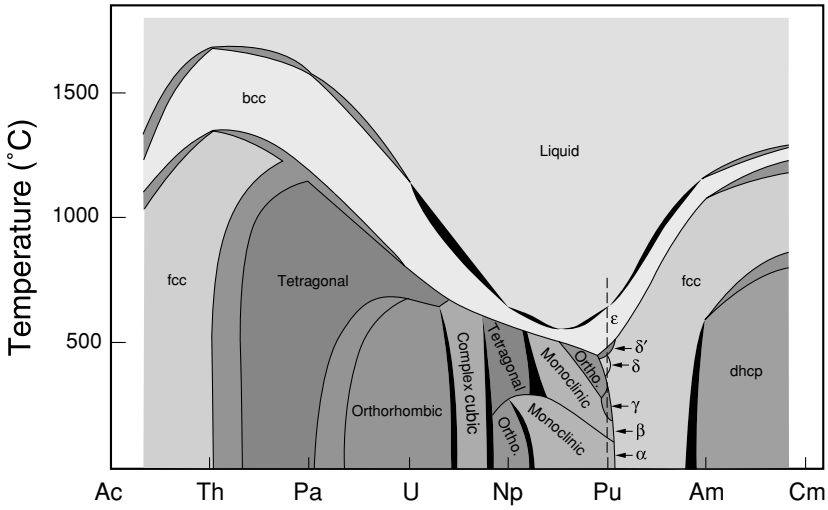

Fig. 7.40 *The experimentally determined, connected binary alloy phase diagram of adjacent actinide elements* (*Smith and Kmetko,* 1983).

to calculate the internal energy of a random substitutional alloy from first principles, which is an immense challenge. So, it is not surprising that semiempirical and phenomenological approaches have guided metallurgical practitioners for many decades. The Hume–Rothery rules, recently reviewed by Massalski (1996) and Gschneidner (1980), relate limits of solid solubility as well as the stability and extent of transition element intermediate phases to three factors:

1. If the atomic size differences of A and B are greater than 15%, solid solubility will be restricted. Significant experimental data support this rule. From a theoretical point of view, large size differences result in large elastic strain energies. The atomic size rule is primarily a 'negative' rule stressing that size differences will restrict solid solution formation. Within favorable size ranges, size differences become only of secondary importance.
2. High chemical affinity of A for B (usually denoted by large differences in electronegativity) helps promote intermetallic compounds and, therefore, limits solid solubility.
3. The relative valence rule stresses the importance of electron concentration, which is typically taken as the ratio of all valence electrons to the number of atoms (e/a).

Darken and Gurry (1953) developed a map that predicts solubility for size differences less than 15% and electronegativity differences of less than 0.4.

Gschneidner (1980) achieved best overall agreement on a large number of known binary alloys by relating solubility to size and similar electronic structures (for which he used the crystal structure as a first approximation) of the constituents. The Darken and Gurry maps for plutonium alloys have been discussed by Blank (1977).

We have not found any of these approaches, or the more sophisticated methods developed by Pettifor (1996) (using tight-binding approximation models) or by Miedema and coworkers (Miedema, 1973, 1976) (using a two-parameter model based on the work function, which is closely related to electronegativity, and on electron density) helpful in predicting solid solubility in δ-phase plutonium. Given the complex electronic structure of plutonium, especially the δ phase, this is not surprising. It is difficult to imagine that these simple approaches would capture the essence of how the electronic structure of plutonium changes with the addition of other elements. However, the Hume–Rothery size rule appears to set a reasonable upper limit on solubility.

Brewer (1965, 2000) developed models based on chemical binding insight to relate phase stability primarily to the total number of valence electrons per atom. Ferro and Cacciamani (2002) recently reviewed the work of Brewer and colleagues on the classification and mapping of alloying patterns. Brewer (1970, 1983) provided some useful insights and general guidance on solubility, melting points, and thermodynamic properties of plutonium and the actinides. For example, he predicted little mutual solubility between plutonium and the alkali metals, the alkaline-earth metals from calcium through radium, and europium and ytterbium. Also, he predicted little solubility of the 4d and 5d transition metals in plutonium, but somewhat greater solubility of the 3d transition metals. He also offered an explanation of the low melting point of plutonium based on the unusually stable liquid phase. He pointed out that plutonium exhibits four or more electronic configurations of comparable energy in the metal. Consequently, atoms of plutonium have different sizes that are readily accommodated in the liquid and pack to very high density. The strain energy resulting from trying to accommodate different-sized atoms into structures such as bcc and fcc with equivalent atom sites destabilizes these structures compared to the liquid. The stability of the liquid, according to Brewer, results from the increased entropy of mixed valence in the liquid state.

A more quantitative, phenomenological approach to predicting phase diagrams was developed by Kaufman and coworkers (Kaufman and Bernstein, 1970; Chang *et al.*, 2002; Kaufman, 2002). The success of CALPHAD (calculation of phase diagrams), a computational thermodynamics approach to predicting phase diagrams of multicomponent alloy systems based on the work of Kaufman and coworkers, was recently reviewed by Turchi *et al.* (2002). Applications of computational thermodynamic modeling to plutonium and its alloys is being developed, but is limited by the lack of good thermodynamic data on plutonium, its alloys, and its compounds. Adler (1991) assessed the Pu–Ga diagram with a calculation using FACT (Facility for the Analysis of Chemical

Thermodynamics, A. Pelton) and retrieved the excess free energy consistent with the Russian phase diagram. Turchi *et al.* (2004) applied the CALPHAD methodology to study the stability and the kinetics of phase transformation and evolution in plutonium-based alloys. They report very good agreement with the thermodynamic properties of pure, unalloyed plutonium. They also predict eutectoid decompositions for both the Pu–Ga and Pu–Al alloy systems.

This brings us back to the first-principles calculations for random alloy systems. In pure materials and perfectly ordered systems, the solution of the many-body Schrödinger equation is simplified by Bloch's theorem that allows us to solve the equation for one cell and use translational symmetry. Random substitutional alloys are disordered by definition and, hence, require some short-range order approximation, typically using an Ising-like cluster expansion. Colinet (2002) recently reviewed the state of the art of deriving phase diagrams by combining quantum mechanics and statistical thermodynamics contributions. Local chemistry affects both the internal energy and the configurational entropy. Statistical treatments of short- or long-range order in solid solutions can use the cluster variation method (CVM) or Monte Carlo simulations. The cluster interactions are either derived experimentally or from first-principles calculations. Local relaxations around the solute atoms are important but also difficult to treat theoretically (Zunger *et al.*, 1990; Abrikosov *et al.*, 1998). Although significant progress has been made in some of the well-studied alloy systems, first-principles calculations of phase stability or phase diagrams are still beyond our grasp. For plutonium, the difficulty is exacerbated by the fact that the parent δ phase is not well understood theoretically and key experimental measurements are sparse.

Baskes (2000) recently extended his semiempirical atomistic embedded-atom method (which is based on DFT) to plutonium. He found reasonable agreement of the calculated energetics and volumes of the phases of plutonium with experimental data. With this method, it is possible to calculate the properties of perfect and defect-containing bulk metal as a function of temperature and pressure. Baskes *et al.* (2003) extended the modified embedded-atom method to model the Pu–Ga phase diagram. They found that a subregular solid solution model is required to describe the properties of the δ phase. They were able to predict the eutectoid decomposition of the δ phase, in qualitative agreement with the Russian phase diagram. However, the accuracy of the calculated temperature and composition of the eutectoid point is limited by inadequate thermodynamic data on Pu_3Ga.

For now, the calculations of Wills and Eriksson (2000) provide good insight into δ-phase stability and alloying. They demonstrated that the low-symmetry ground states in plutonium and the other light actinides require the special conditions of narrow bands and high DOS at or very near the Fermi energy (a natural consequence of the oddity of an f-electron conduction band). It seems reasonable then that anything that destroys these special conditions favors the retention of high-symmetry structures. Their calculations show that energy can

be gained (that is, the total energy lowered) either through bonding energy gained from a structural distortion, or through correlation energy gained by localization of the electrons. Plutonium is exactly at that position in the periodic table where either process leads to about the same energy gain. However, alloying or defects disturb the coherence of the 5f bands, thus reducing the bonding energy and leading to at least partial localization of the 5f electrons. Hence, we believe that the fcc δ phase is favored at high temperature in unalloyed plutonium because of 'bond stretching' (in addition to entropy considerations) and in alloys because of 'bond breaking.' Hence, we may expect any alloy addition without bonding 5f electrons to favor the δ phase, assuming it can be dissolved in plutonium. Likewise, defects such as vacancies, vacancy clusters, dislocations, and grain boundaries may favor the retention of the δ phase locally.

Sadigh and Wolfer (2005) recently suggested another mechanism based on their DFT calculations, which showed that the volume decrease that occurs with gallium additions to the δ phase is primarily the result of the reduction in size of the plutonium host atoms. This reduction accounts for roughly two-thirds of the experimentally measured value. The other third is split between the misfit of the gallium in the δ-phase lattice and the elastic strains. The large volume reduction of the plutonium is accompanied by a negative heat of mixing. Their calculations showed that the enthalpy of transformation from the δ→α phase at absolute zero decreases substantially with the addition of gallium solutes. They conclude this reduction accounts for the retention of the δ phase. Clearly one must then invoke a different mechanism for the existence of the δ phase in unalloyed plutonium at high temperature. For example, it could be a combination of entropy effects and possible changes in electronic structure, such as those observed by Manley *et al.* (2001) for uranium. The calculations of Sadigh and Wolfer (as those of Söderlind (2001)) require large local spin moments in the δ phase to get the volume correct.

Considerable debate still exists over these calculational techniques because no local moments have been found experimentally (as recently reviewed by Lashley (2005). The search for magnetic moments has been so elusive, Söderlind explains, because his calculations predict a near zero-ordered moment as the spin and orbital moments are close in magnitude but antiparallel. However, Shick *et al.* (2005), using the *around-the-mean-field* version of the LDA+U method, predict a nonmagnetic ground state for the δ phase. They claim the nonmagnetic character results from $S = 0$ and $L = 0$, rather than the cancellation of spin and orbital parts of the momentum. They claim good agreement with experimental measurements of δ-phase plutonium properties. Shorikov *et al.* (2005) used the LDA+U+SO method to predict nonmagnetic ground states with zero values of spin, orbital, and total moments in both δ-phase and α-phase plutonium. We look forward to future advances in electronic structure theory that provide satisfactory explanations to the enigma surrounding plutonium.

(b) Lattice effects and local structure

We now examine in greater detail some of the interesting electronic structure effects observed in binary plutonium alloys. Binary alloys of plutonium with Am, Ce, Ga, and Al solutes were studied recently by Dormeval *et al.* (2003). Fig. 7.41 shows the approximate range of the δ-phase fields at room temperature for these solutes and the variation in the δ-phase plutonium lattice parameters. The addition of americium or cerium expands the plutonium lattice, whereas gallium and aluminum shrink it. All of them show some deviation from the ideal solution behavior described by Vegard's law, which is not surprising considering the complex electronic interactions expected in plutonium alloys.

In americium, the 5f electrons are completely localized. Substituting large americium atoms into the smaller δ-phase lattice expands the plutonium lattice and causes the 5f electrons in plutonium to become more localized, thereby stabilizing the δ phase over the entire range of americium concentrations. Also,

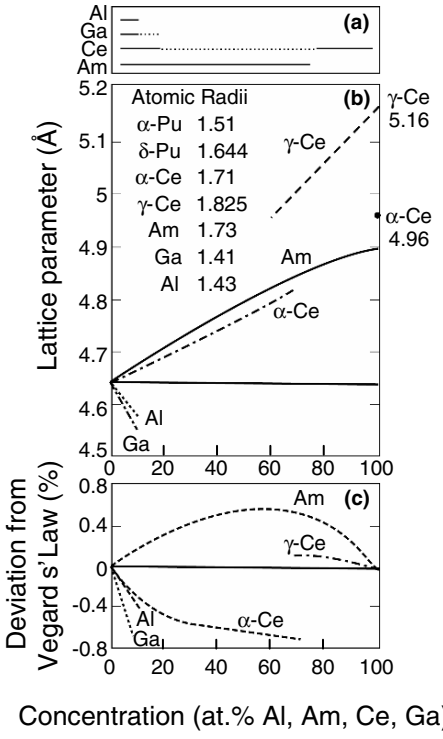

Fig. 7.41 (*a*) *Approximate solubility ranges at room temperature for the δ phase alloyed with Al, Ga, Ce, and Am.* (*b*) *Lattice parameters for these alloys.* (*c*) *Deviation from Vegard's Law* (*Dormeval,* 2001*; Hecker* et al., 2004).

the increased localization of the 5f electrons in plutonium causes the plutonium atoms themselves to increase in size, resulting in a positive deviation from Vegard's law. If a transition from itinerant (bonding) 5f electrons to localized 5f electrons were to suddenly occur in plutonium atoms as the americium concentration is increased, then we would expect a sudden increase in lattice parameter. As seen in Fig. 7.41, no discontinuities in lattice parameters are observed across the entire americium concentration range. This behavior demonstrates that the limited stability of the δ phase in unalloyed plutonium is just the tip of the iceberg for δ-phase stability upon alloying. This is shown most convincingly by looking more closely at the connected binary Np–Pu–Am phase diagrams shown in Fig. 7.42.

In contrast to additions of americium, neptunium stabilizes the α phase of plutonium. In fact, the Pu–Np phase diagram looks strikingly like the plutonium temperature–pressure phase diagram also shown for comparison in Fig. 7.42. Hence, adding neptunium has the same effect as applying pressure to the plutonium lattice, whereas adding americium is equivalent to applying hydrostatic tension.

As shown in Fig. 7.41, the addition of cerium also expands the δ-phase plutonium lattice. The range of stability for the fcc phase was extended across the entire concentration range of cerium by splat cooling (as indicated by the

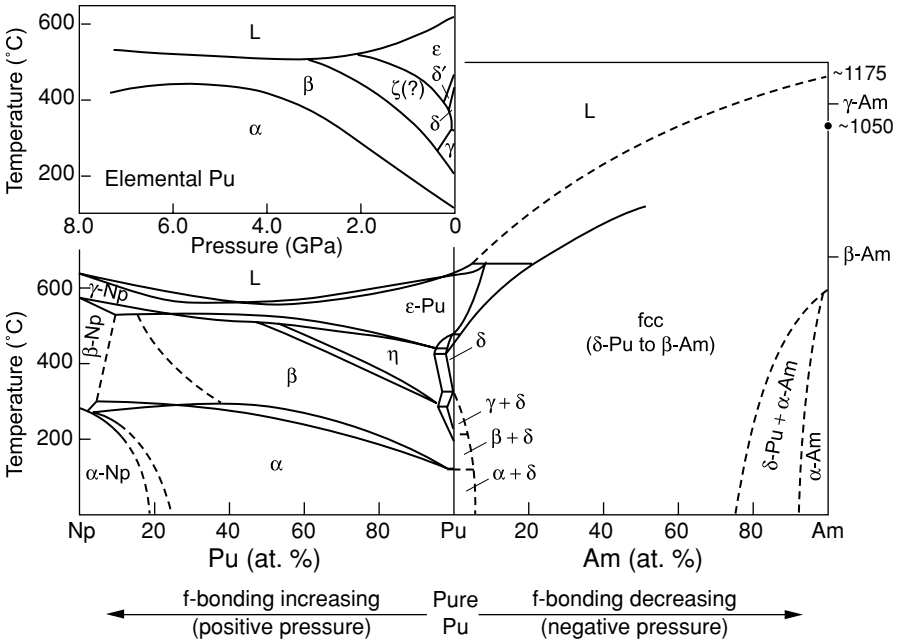

Fig. 7.42 *Plutonium pressure–temperature phase diagram compared to connected Np–Pu–Am binary ambient-pressure phase diagrams* (*Hecker,* 2004).

dotted lines in Fig. 7.41a). In addition to retaining the stable fcc phases of δ plutonium and γ cerium, Giessen *et al.* (1975) were able to retain the metastable fcc α-cerium phase at intermediate concentrations. Unlike americium, which behaves as a rigid sphere because the 5f electrons are well-localized, cerium is a 'soft' sphere, whose diameter adapts to its surroundings. When squeezed into the smaller δ-phase plutonium lattice at the plutonium-rich end, cerium's 4f electrons become delocalized and it takes on the α-phase radius ($r = 1.71$ Å). At 75 at.% Ce, an abrupt transition is observed to γ-cerium (with $r = 1.825$ Å). When viewed from the cerium end, the smaller plutonium atoms substitute in the γ-cerium lattice, until at 25 at.% Pu the pressure is sufficient to collapse the unstable cerium atom to its α-phase radius. Using EXAFS spectroscopy, Conradson (2003) showed that the cerium solute atom was accommodating in the plutonium lattices. It readily adapted its size to fit either into the δ-phase lattice or the even smaller α-plutonium lattice (when trapped in the α lattice under metastable conditions).

Dormeval *et al.* (2003) calculated the deviation of lattice constants from Vegard's law by considering two different limits in the law. As a result of the pressure imposed by the δ-plutonium lattice, cerium is α-like at concentrations below 75 at.% Ce and γ-like above that level. Hence, on the cerium end, there are two different limits corresponding to α-cerium and γ-cerium extrapolated to room temperature and pressure. Following this approach, Dormeval *et al.* found the deviation from Vegard's law to be negative on the plutonium-rich end, while slightly positive at the cerium-rich end as shown in Fig. 7.41c. Based on measurements of lattice constants, electrical resistivity, and magnetic susceptibility, Dormeval *et al.* suggested that the principal cause of the complex alloying behavior of cerium in plutonium is not the plutonium itself but the unstable nature of the cerium atom.

The addition of aluminum or gallium shrinks the δ-phase plutonium lattice (Fig. 7.41). Both show negative deviations from Vegard's law, with the gallium deviation being more than twice that of aluminum. As mentioned above, several investigators have probed the local structure of Pu–Ga alloys using EXAFS (Cox *et al.*, 1995; Faure *et al.*, 1996; Conradson, 2000; Allen *et al.*, 2002). These EXAFS results show that the first-neighbor Pu–Ga bond is 0.13 Å, or 3.7% (the experimental measurements vary from 3.5 to 4%) shorter than the Pu–Pu bond in dilute alloys. Scheuer and Lengeler (1991) and Massalski (1996) pointed out that local distortions in substitutional alloys may bear little or no relation to macroscopic distortions of the unit cell. The local distortions can vary greatly in magnitude and in sign compared to the average change in lattice parameters. The contraction in Pu–Ga is at the upper end of that found in substitutional alloys. Scheuer and Lengeler reported that the change in the next-nearest-neighbor and more distant shells is typically small for substitutional alloys. Conradson (2000) found contractions in the second and third nearest-neighbor shells in Pu–Ga to be almost negligible (0.05 and 0.01 Å, respectively). He also reported a significant change in local order in Pu–Ga alloys as the gallium

concentration increases beyond roughly 3.5 at.% Ga. He found the Pu–Ga distance to remain constant with gallium addition, whereas Faure *et al.* (1996) found it to first increase and then decrease. Resolution of the differences in local Pu–Ga arrangements must await additional experiments. However, Ravat *et al.* (2003) recently reported results similar to those of Conradson; that is, the first shell distance for the Pu–Ga bond is 0.1 Å shorter than the Pu–Pu bond, and the second shell bonds are close to the Pu–Pu bond length. We must also heed the caution expressed by Scheuer and Lengeler that alloy additions of roughly 2% or more typically cause complex local ordering effects.

A lattice contraction with the addition of gallium or aluminum to plutonium is expected from purely elastic considerations because the atomic radii of aluminum and gallium are considerably smaller than the radius of δ-phase plutonium. The atoms tend to relax toward their natural bond length rather than retain their average spacing. Harrison (2001) pointed out that each solute atom eliminates 12 f–f bonds in δ-phase plutonium. The f–f bond cutting should counter the elastic contraction of the solutes. However, Harrison's calculations for Pu–Ga alloys showed that the experimentally observed negative deviation from Vegard's law results from a coupling between the core d-states in gallium and the unoccupied d-states in plutonium. Faure *et al.* (1996) suggested that negative deviation to Vegard's law is proof of delocalization. They assume that this negative deviation results from the f–p bonding between Pu 5f and Ga 4p electrons. Thus, in the Pu–Ga alloys the solutes delocalize some of the 5f electrons in alloyed δ plutonium compared to the pure δ plutonium, which, in turn, promotes more bonding and smaller atomic volumes. As pointed out above, using DFT (with spin polarization for the δ phase), Sadigh and Wolfer (2005) predicted that the δ-lattice volume decrease results primarily from the reduction in size of the plutonium host atoms. All of these analyses indicate that electronic effects play a major role in determining the alloying characteristics of plutonium.

Another interesting electronic effect in plutonium is the behavior of alloying elements such as gallium and aluminum in α-phase plutonium. Ellinger *et al.* (1968b) showed that there is no measurable equilibrium solubility of these elements in the α phase. However, as pointed out by Hecker *et al.* (2004), lean δ-phase Pu–Ga and Pu–Al alloys transform to the α phase upon cooling below 0°C or with hydrostatic pressure at ambient temperature and below. Adler *et al.* (1986) and Olson and Adler (1984) concluded that the temperature-induced δ→α transformations are martensitic. Zukas *et al.* (1981) concluded that the pressure-induced δ→α transformations are also martensitic – that is, displacive with no compositional change. Hence, the solute atoms are trapped in the monoclinic α lattice. The crystal structure, as shown in Fig. 7.22, has 16 atoms per unit cell, with eight unique lattice sites and with variable bond lengths.

Hecker *et al.* (2004) reported that XRD measurements and immersion-density measurements of the transformed α phase clearly showed that the gallium is in substitutional lattice positions in the monoclinic lattice, but that

it expanded the α lattice (the expanded lattice is called the α′ phase). All three-crystal axes expand, whereas the monoclinic angle remains nearly constant. The volume expansions in the α′ phase with the addition of gallium or aluminum are shown in Fig. 7.43 and contrasted with the volume contractions in the δ phase with alloying additions. With the addition of gallium, the α-phase volume expands ~0.9% per at.% Ga, whereas the δ-phase volume decreases by ~0.6% per at.% Ga.

These results are a most interesting manifestation of the peculiar electronic effects in plutonium. As explained above, the gallium atom, which is 14.2% smaller than the δ-plutonium atom, contracts the lattice significantly more than expected because it is believed to make the plutonium atoms contract in its presence. In other words, the addition of gallium causes more of the 5f electrons in plutonium to bond. This result is conceptually consistent with the calculations of Wills and Eriksson (2000), which indicated that only one of the five 5f electrons appears to be bonding in the unalloyed δ phase. Also, Sadigh and Wolfer (2005) predict the decrease in the size of the plutonium atoms quantitatively.

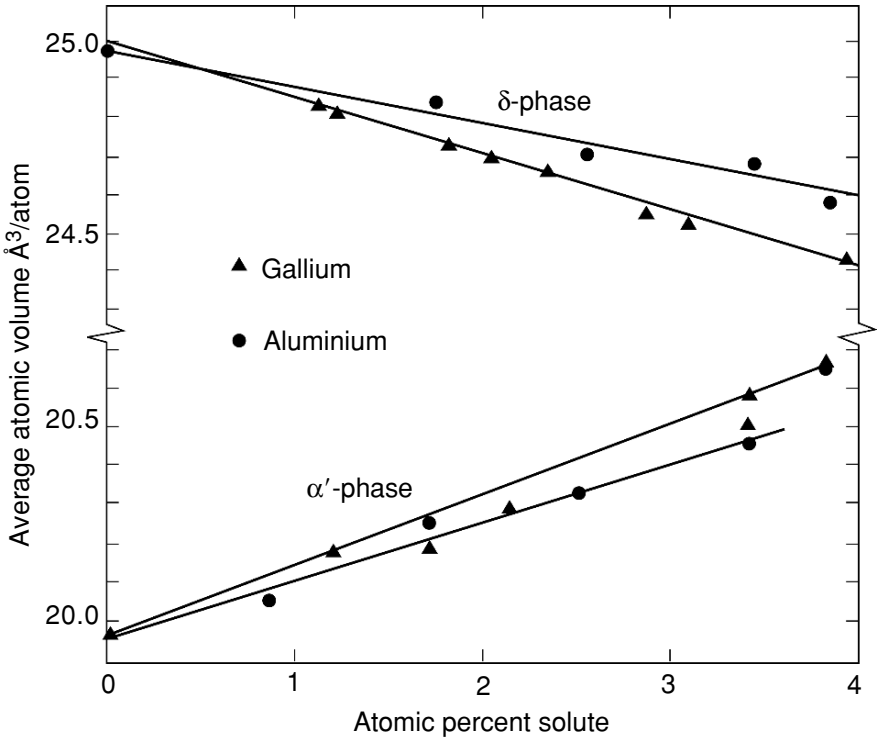

Fig. 7.43 *Atomic volumes of Pu–Ga and Pu–Al alloys in the δ and α′ phases.*

On the other hand, the gallium atom, although 7% smaller than the α-plutonium atom, expands the α lattice, indicating that in the α phase the presence of gallium localizes more of the 5f electrons. The calculations of Wills and Eriksson (2000) showed that all five 5f electrons bond in the α phase, hence it is quite likely that the solute additions disrupt the bonding, causing the volume to expand. Hecker *et al.* (2004) also showed that the lattice expansion in the α′ phase disappears slowly with time at ambient temperature and quite rapidly at slightly elevated temperatures. During the martensitic transformation, the solute atoms are trapped randomly in the α′ lattice, causing it to expand.

However, the eight different lattice sites have different bond lengths as shown in Fig. 7.22. Hecker *et al.* (2004) suggested that there is a strong driving force to rearrange the solute atoms into preferred sites, namely lattice site 8, because it has the fewest number of short bonds (Table 7.l0). Based on their recent calculations, Sadigh and Wolfer (2005) showed that site 8 is by far the most favorable substitutional position for gallium. Furthermore, they found that the unit cell of the α phase is not expanded when gallium occupies site 8, while significant expansions are exhibited when gallium is substituted in other sites, with the largest expansion for site 1 occupancy. The energies for gallium substitution correlate with this volume expansion, with a maximum difference of 1.5 eV between site 1 and site 8, confirming the suggestion of Hecker *et al.* (2004) that gallium entrapped in sites other than site 8 will tend to order to this site and in the process contract the unit cell of the α′ phase.

These results demonstrate that plutonium atoms, like cerium atoms, readily change their electronic configurations and adjust their size as their lattice environment changes. It is no surprise then that alloying of plutonium is so complex.

7.7.6 Physical and thermodynamic properties

The physical and thermodynamic properties of plutonium are of great practical interest and present significant engineering challenges; they also represent some of the most puzzling features of solid-state behavior.

(a) Densities and lattice parameters

The densities of the six solid plutonium allotropes and liquid plutonium are summarized in Table 7.18. Of particular note is the fact that the density of liquid plutonium exceeds that of the three high-temperature allotropes and that the δ phase, which is also the closest-packed crystal structure, exhibits a particularly low density compared to the other allotropes. As pointed out above, full density is difficult to achieve in the α phase of unalloyed plutonium because of the propensity for microcracking during cooling and the retention

Table 7.18 *Typical densities for plutonium allotropes, alloys, and compounds.*

Material	*Density* (g cm^{-3}); *References calculated*[a]		*Density* (g cm^{-3}); *References experimental*	
α-Pu	19.86;	Zachariasen and Ellinger (1963a)	19.82;	Merz (1974)
β-Pu	17.69;	Zachariasen and Ellinger (1963b)		
γ-Pu	17.15;	Zachariasen and Ellinger (1955)		
δ-Pu	15.92;	Ellinger (1956)		
δ′-Pu	16.00;	Ellinger (1956)		
ϵ-Pu	16.51;	Ellinger (1956)		
liquid Pu	16.65;	Miner and Schonfeld (1980)		
Pu-1.24 at.% Ga	15.86		15.83;	Gardner (1965)
Pu-1.7 at.% Ga	15.85		15.82;	Hecker (unpublished)
Pu-2.61 at.% Ga	15.827		15.78;	Gardner (1965)
Pu-3.35 at.% Ga	15.806		15.76;	Hecker (unpublished)
Pu-4.22 at.% Ga	15.787		15.73;	Gardner (1965)
Pu-5.0 at.% Ga	15.77		15.69;	Hecker (unpublished)
Pu-1.2 at.% Al	15.82		15.80;	Elliott *et al.* (1962)
Pu-2 at.% Al	15.76		15.70;	Hecker *et al.* (1982)
Pu-3.4 at.% Al	15.66		15.56;	Elliott *et al.* (1962)
Pu-5 at.% Al	15.55		15.50;	Rosen *et al.* (1969)
Pu-11 at.% Al	15.135		15.19;	Rosen *et al.* (1969)
Pu-5 at.% Ce	15.47		15.45;	Elliott *et al.* (1962)
Pu-10 at.% Ce	15.03		14.93;	Elliott *et al.* (1962)
Pu-18 at.% Ce	14.34		14.24;	Elliott *et al.* (1962)
Pu-5 at.% Am	15.75;	Ellinger *et al.* (1966)		
Pu-10 at.% Am	15.61;	Ellinger *et al.* (1966)		
Pu-15 at.% Am	15.45;	Ellinger *et al.* (1966)		
Pu_6Fe	17.10;	Ellinger *et al.* (1968b)		
Pu_3Ga (cubic)	14.27;	Ellinger *et al.* (1968b)		
Pu_3Ga (tetragonal)	14.45;	Ellinger *et al.* (1968b)		
PuO_2	11.46;	Ellinger *et al.* (1968b)		
Pu_2O_3 (hexagonal)	11.47;	Ellinger *et al.* (1968b)		
PuC_{1-x}	13.6;	Ellinger *et al.* (1968b)		
PuN	14.22;	Ellinger *et al.* (1968b)		

[a] From X-ray data.

of lower-density phases during processing. Merz (1974) achieved exceptionally high density (19.82 g cm^{-3}) in α-phase plutonium by extrusion and concurrent recrystallization, which resulted in very fine grain size (on the order of micrometers). Alpha phase plutonium samples with densities >19.7 g cm^{-3} are typically considered as sound samples.

Alloying plutonium with elements such as aluminum and gallium, which promote δ-phase retention to room temperature, yields densities close to that of the unalloyed high-temperature δ phase. The densities of some δ-phase alloys are also compared to that of the plutonium allotropes and common plutonium compounds in Table 7.18. The densities reported in the middle column were calculated by the authors from the lattice parameters measured by XRD by a number of investigators. Experimental densities are typically measured by liquid immersion techniques. The experimental densities for the δ-phase alloys are usually lower than the calculated densities from X-ray measurements because of impurities and inclusions. Experimental densities higher than X-ray densities are almost always the result of transforming the surfaces of test samples from the δ phase to the α phase during sample preparation (such as punching, machining, filing, or polishing). The compounds Pu_6Fe, PuO_2, PuC, and PuN are common inclusions found in plutonium metal and alloys of typical purity. PuO_2, PuC, and PuN have also been considered for reactor fuels. The compound Pu_3Ga is the most plutonium-rich compound in the Pu–Ga system. Figs. 7.41 and 7.43 show how the lattice parameters of δ-phase plutonium alloys decrease with increasing alloy content.

(b) Thermal expansion

Thermal expansion of the unalloyed α, β, and γ phases of plutonium is large and positive. Thermal expansion of these allotropes is also anisotropic because of their low-symmetry crystal structures. Table 7.19 lists the coefficients of thermal expansion for all allotropes, including coefficients for different lattice directions for the low-symmetry allotropes. The values shown in Table 7.19 were taken primarily from X-ray measurements because of the variability of dilatometric results. Schonfeld and Tate (1996) recently reviewed available thermal expansion results for unalloyed plutonium. We have chosen to present their best fits to the available dilatometric data, as shown in Fig. 7.19. The low-temperature behavior of α-phase plutonium is quite nonlinear, as reported by Cramer *et al.* (1961) and Lallement (1963). On page 37 of the *Plutonium Handbook*, Miner and Schonfeld (1980) show an inflection in thermal expansion near 60 K. However, more recently, Schonfeld and Tate (1996) argued convincingly that the slight lattice expansion in α-phase plutonium reported below 60 K results from self-irradiation damage. Schonfeld and Tate replotted all available thermal expansion data for α-phase plutonium, as shown in Fig. 7.44. They list the average thermal expansion coefficient between 0 and 393 K as 37.8×10^{-6} K^{-1} and that between 294 and 377 K as 53.8×10^{-6} K^{-1} (by dilatometry) and 54×10^{-6} K^{-1}

Table 7.19 *Linear thermal expansion of plutonium.*[a]

Phase	*Principal coefficient*	*Temperature range* (°C)	*Mean coefficient* (10^{-6}°C^{-1})	*Method*	*References*
α	$\bar{\alpha}_p$ (average)	−186 to 101	42.3	dilatometry	Cramer *et al.* (1961)
	$\bar{\alpha}_1 \perp c$-axis	21 to 104	60	X-ray	Zachariasen and Ellinger (1963a)
	$\bar{\alpha}_2 = \bar{\alpha}_b$		75		
	$\bar{\alpha}_3 = \bar{\alpha}_c$		29		
	$\bar{\alpha}_p$ (average)		54		
β	$\bar{\alpha}_1$	93 to 190	94	X-ray	Zachariasen and Ellinger (1963b)
	$\bar{\alpha}_2 = \bar{\alpha}_b$		14		
	$\bar{\alpha}_3 \perp (10\bar{1})$		19		
	$\bar{\alpha}_p$ (average)		42		
γ	$\bar{\alpha}_a$	210 to 310	-19.7 ± 1.0	X-ray	Zachariasen and Ellinger (1955)
	$\bar{\alpha}_b$		39.5 ± 0.6		
	$\bar{\alpha}_c$		84.3 ± 1.6		
	$\bar{\alpha}_p$ (average)		34.6 ± 0.7		
δ	$\bar{\alpha}$	320 to 440	-8.6 ± 0.3	X-ray	Ellinger (1956)
δ′	$\bar{\alpha}_a$	452 to 480	444.8 ± 12.1	X-ray	Elliott and Larson (1961)
	$\bar{\alpha}_c$		-1063.5 ± 18.2		
	$\bar{\alpha}_p$ (average)		-65.6 ± 10.1		
ϵ	$\bar{\alpha}$	490 to 550	36.5 ± 1.1	X-ray	Ellinger (1956)
liquid	$\bar{\alpha}_v$	664 to 788	93[b]	pycnometry	Serpan and Wittenberg (1961)

[a] For low symmetry allotropes, coefficients are given for different lattice directions.
[b] Mean coefficient of volume expansion.

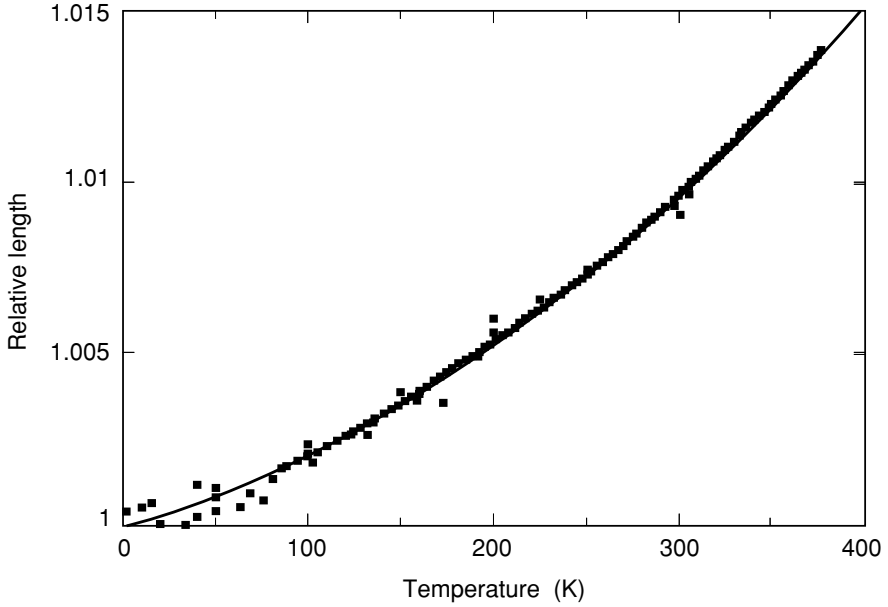

Fig. 7.44 *Thermal expansion of unalloyed α-phase plutonium over most of its temperature region of stability. The curve is a composite generated by Schonfeld and Tate* (1996) *based on data from several references* (*Sandenaw,* 1960*b; Cramer* et al., 1961*; Lee* et al., 1965*a; Lallement and Solente,* 1967*; Miner and Schonfeld,* 1980*; Lawson* et al., 1994).

(by X-ray measurements). The low-temperature results of Schonfeld and Tate are incorporated into the overall thermal expansion curve shown in Fig. 7.19.

The expansion of the high-temperature δ and ϵ phases is isotropic. However, the δ and δ′ phases exhibit negative thermal expansion. Thermal expansion of the δ′ phase is also highly anisotropic. The explanation of this unusual behavior has been a contentious issue since the late 1950s. In δ-phase alloys, the thermal expansion coefficient varies from slightly negative to positive, depending on the amount of alloying addition. A graphic example of this behavior is shown for Pu–Ga alloys in Fig. 7.45 (Goldberg *et al.*, 1970). We also show the thermal expansion behavior of various δ-phase plutonium alloys in Fig. 7.46 (taken mostly from the work of Elliott *et al.* (1960) and Lawson *et al.* (2002)). All alloying additions move the coefficient of thermal expansion to more positive values from that of the unalloyed δ phase; that is, alloying results in thermal expansion behavior closer to that observed in normal metals. As shown in Fig. 7.46, significantly less aluminum or gallium is required to increase the coefficient compared to cerium. The properties of Pu–Am alloys were estimated from the measurements of Shumakov *et al.* (1990).

The peculiar thermal expansion behavior of δ-phase plutonium alloys was reviewed by Lawson *et al.* (2002). A negative thermal expansion is associated

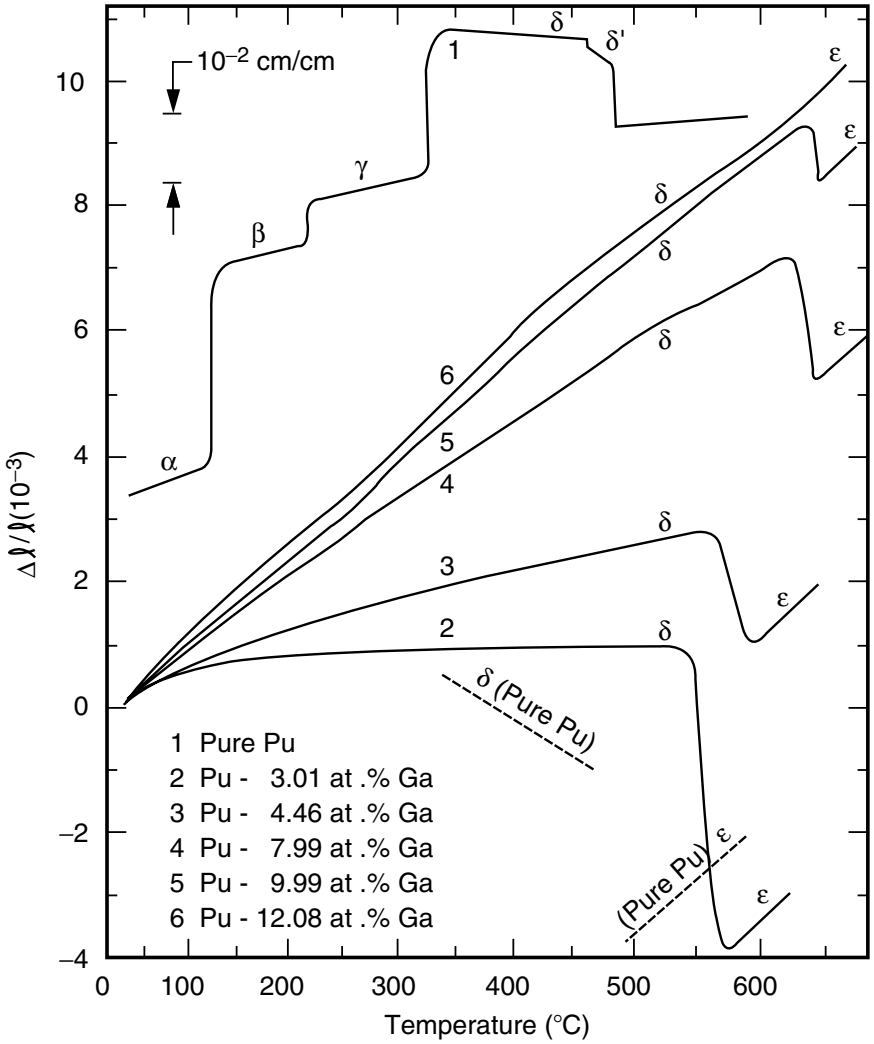

Fig. 7.45 *Corrected dilatometric heating curve* (*at* 4.5°C min^{-1}) *for a series of δ-phase Pu–Ga alloys. The curve for unalloyed* (*pure*) *plutonium is based on a scale of one-tenth* (*as shown in insert*) *that used for the alloys. The dashed curves for unalloyed* (*pure*) *plutonium are portions redrawn on the same scale used for the alloys. The scale on the ordinate refers only to the alloys* (*Goldberg* et al., 1970).

with increasing disorder (higher entropy) at higher pressures according to the Maxwell relation $(\partial V/\partial T)_p = -(\partial S/\partial P)_T$, in contrast with the behavior found in ordinary metals. However, for some complex solids with negative thermal expansion, such as the recently discovered ZrW_2O_8, increasing pressure has

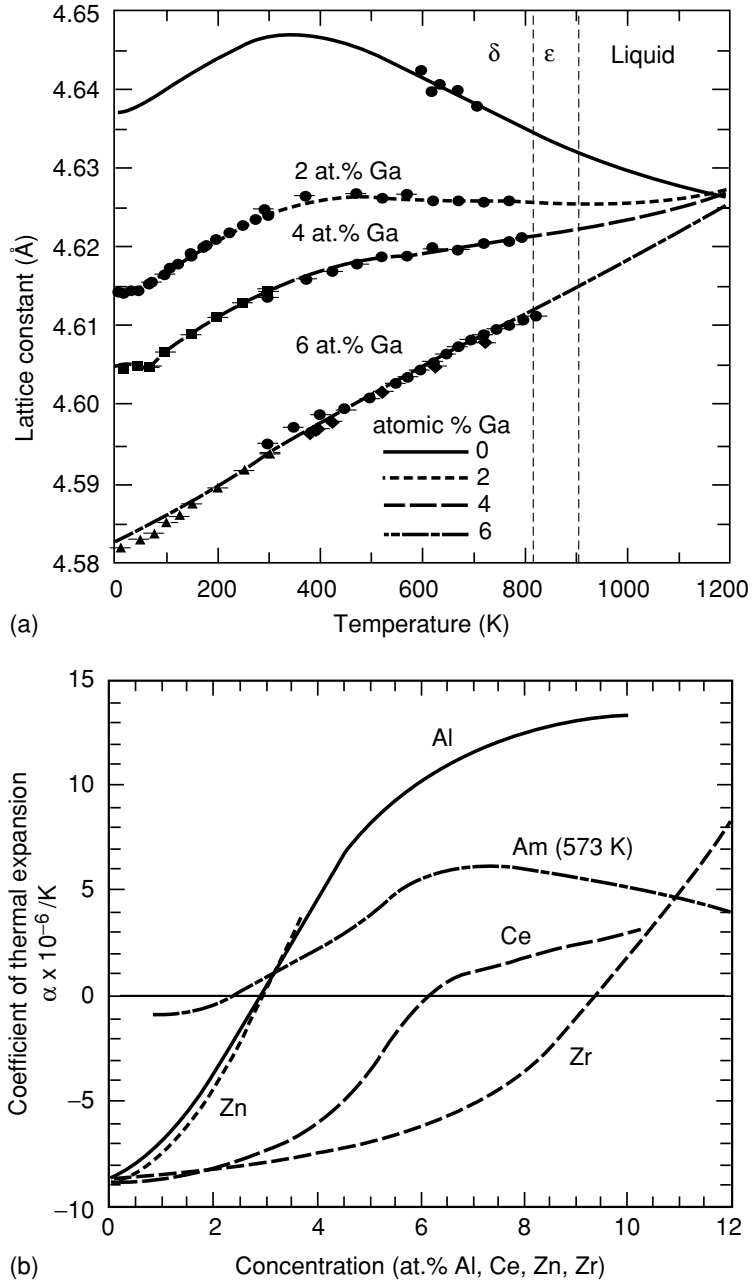

Fig. 7.46 (*a*) *Lattice constants of δ-phase Pu–Ga alloys measured by neutron diffraction by Lawson* et al. (2002). *The line through the data is a fit by the 'Invar' model proposed by Lawson* et al. (*b*) *Coefficient of thermal expansion as a function of solute content for δ-phase plutonium alloys* (*Elliott* et al., 1960). *The results for Pu–Am alloys were estimated from the measurements of Shumakov* et al. (1990) *taken at* 573 K, *where the range of solid solution across the Pu–Am diagram is complete.*

been shown to increase the vibrational entropy of the molecular modes (Evans *et al.*, 1996; Mary *et al.*, 1996; Mittal *et al.*, 2001). For fcc δ plutonium there are no internal vibrational modes, so Lawson *et al.* looked for an electronic degree of freedom whose entropy variation with pressure determines the thermal expansion. They believe zero thermal expansion (Invar-like behavior) of some of the alloys results from a thermal transfer of plutonium atoms from a lower-energy, higher-volume δ_1 state to a higher-energy, lower-volume δ_2 state, comparable to the Weiss two-level model used to explain the Invar behavior in Fe–Ni alloys (Weiss, 1963).

For ordinary metals that follow Grüneisen's law, the thermal expansion behavior can be used to estimate the temperature dependence of the bulk modulus (or the sound speed or Debye temperature); namely, $dB/dT = -\gamma\beta B$, where B is the bulk modulus, γ the Grüneisen parameter, and β the volume thermal expansion. The δ-phase plutonium alloys, however, do not follow this relationship since the thermal expansion is small – or even negative – and dB/dT is large. For these alloys it is necessary to assume that the elastic stiffness is intrinsically temperature dependent, independent of volume. For unalloyed α-phase plutonium, a recent review by Ledbetter (2004) and by Ledbetter and Migliori (2005) of Grüneisen parameters shows large variations from values of 3.1 to 7.0. They believe the best value is ~3.5. We also note that Hasbrouk and Burns (1965) provide additional listings of thermal expansion in various plutonium allotropes and in several alloys.

(c) Elastic constants and sound velocities

Early elastic constant measurements for unalloyed plutonium and several plutonium alloys by various investigators were compiled by Hasbrouk and Burns (1965). As pointed out by Fisher (1974) in a later compilation, reported elastic constant measurements (particularly the bulk modulus) exhibit significant scatter because of difficulties in fabricating quality samples. Acoustic measurements typically yield the most reliable elastic constants. Calder *et al.* (1981) reported elastic constants of α plutonium and δ-phase Pu–3.4 at.% Ga alloys at elevated temperatures. Migliori *et al.* (2004, 2006) and Ledbetter *et al.* (2004, 2005) recently performed the most accurate acoustic measurements to date on high-quality, high-purity, unalloyed plutonium (with a density >19.7 g cm^{-3}), and Pu–Ga alloys using the resonant ultrasound technique (Migliori *et al.*, 2000). Their room-temperature results are summarized in Table 7.20. Unalloyed α plutonium is soft elastically – its bulk modulus is nearly 50% less than that of α uranium. As shown in Table 7.20, the δ-phase Pu–Ga alloys exhibit substantially reduced elastic constants compared to α plutonium. Typical sound velocities are also listed in Table 7.20.

The temperature dependence of the elastic modulus (Young's modulus), the shear modulus, bulk modulus, and Poisson's ratio is shown for unalloyed

plutonium in Fig. 7.47. All but Poisson's ratio are quite sensitive to temperature. The ratio of the bulk modulus at 0 K to the bulk modulus at 300 K for α plutonium is 1.303, compared to 1.104 for lead, 1.03 for iron, and 1.075 for aluminum. There are no single-crystal elastic constant measurements in the literature for α plutonium because of the difficulty of making single crystals of unalloyed plutonium. In addition, making elastic constant measurements of the monoclinic structure of the α phase with 13 independent elastic constants is a daunting task. Moment (2000) and Lashley *et al.* (2000) describe techniques used to prepare single crystals of δ-phase plutonium alloys. Ledbetter and Moment (1976) reported elastic constant measurements on a single crystal δ-phase Pu–3.4 at.% Ga alloy. As shown in Fig. 7.48, the elastic constants are highly anisotropic. The single crystals are stiff in tension and compression and soft in shear in the [111] direction and vice versa in the [100] direction. In fact, the Zener anisotropy ($Z = 2c_{44}/c_{11}–c_{12}$), where c_{ij} are the typical elastic constants is 7.03; whereas lead, the next elastically most anisotropic fcc metal, is roughly 4 and aluminum is nearly isotropic at slightly over 1.0. The elastic constants for a polycrystalline δ-phase Pu–3.35 at.% Ga alloy reported by Calder *et al.* (1981) and shown in Fig. 7.49, exhibit a greater reduction in elastic constants with temperature than that for unalloyed α plutonium. Poisson's ratio for the δ-phase alloy increases monotonically with temperature as is typical for fcc metals.

In addition to providing stiffness data, elastic constants also play an important role in determining the overall mechanical response of materials (Hecker and Stevens, 2000). The Debye temperature at 0 K can be determined by correcting for the temperature dependence of the elastic constants. We will compare these results to the Debye temperatures from specific heat measurements in a subsequent section. Sound velocities provide a convenient way to determine elastic constants. They are also important in dynamic and shock responses of materials. The sound velocities for α plutonium and Pu–Ga alloys are presented in Table 7.20. We also note that Rosen *et al.* (1969) measured elastic properties ultrasonically at low temperatures and found no discontinuities in the elastic constants at low temperature (at the time they were looking for a possible magnetic transition) for α plutonium, and δ-phase Pu–Al and Pu–Ce alloys. However, they observed a sharp peak in the longitudinal wave attenuation accompanied by a normal temperature dependence of the transverse attenuation. Cornet and Bouchet (1968) measured the elastic properties of unalloyed plutonium with temperature, including the bcc ϵ phase (the room-temperature density was 19.1 g cm^{-3}, indicating that the samples contained many microcracks). They reported detailed results for Young's modulus for the δ, δ′, and ϵ phases. They found the ϵ phase to exhibit a large compressibility (0.16 GPa^{-1} at 758 K) and a low Young's modulus (11 GPa at 703 K). As indicated above, however, the sample quality was questionable because of its low density.

Table 7.20 *Elastic constants and sound velocities for plutonium and plutonium alloys at room temperature.*

Material	*Temperature* (°C)	*Density* (g cm^{-3}) *at* 25°C	*Bulk modulus* (GPa)	*Shear modulus* (GPa)	*Young's modulus* (GPa)	*Poisson's ratio*	*Sound speed* (km s^{-1}) (*longitudinal*)	*Sound speed* (km s^{-1}) (*transverse*)	*References*
unalloyed α Pu (high purity)	27	>19.70	54.4	43.7	103.4	0.183	2.39	1.49	Migliori *et al.* (2004) and Ledbetter *et al.* (2005)
unalloyed α Pu (high purity)	~25	19.71	53.43	42.26	100.66	0.186	–	–	Linford quoted in Gardner (1980)
Pu-2.36 at.% Ga	27	15.795	31.2 ± 0.1	16.6 ± 0.01	42.4	0.274	1.86	1.04	Migliori *et al.* (2004)
Pu-2.4 at.% Ga	25	15.75	30.6 ± 0.1	16.3 ± 0.05	41.8 ± 0.1	0.272	–	–	Migliori *et al.* (2006)
Pu-3.3 at.% Ga	27	15.76	29.7 ± 0.4	16.74 ± 0.02	42.3	0.263	1.82	1.03	Migliori *et al.* (2004)
Pu-3.35 at.% Ga	25[a]	15.9	–	15.7	40.5	~0.295	–	–	Calder *et al.* (1981)
Pu-4.64 at.% Ga	27	15.70	30.9	17.1	43.0	0.267	1.86	1.04	Migliori *et al.* (2004)
Pu-5 at.% Al	~25	15.5	–	18.28	45.4	0.24	–	–	Rosen *et al.* (1969)
Pu-6 at.% Al	20	–	–	18.5	46.8	0.264	–	–	Taylor *et al.* (1965)

[a] Extrapolated.

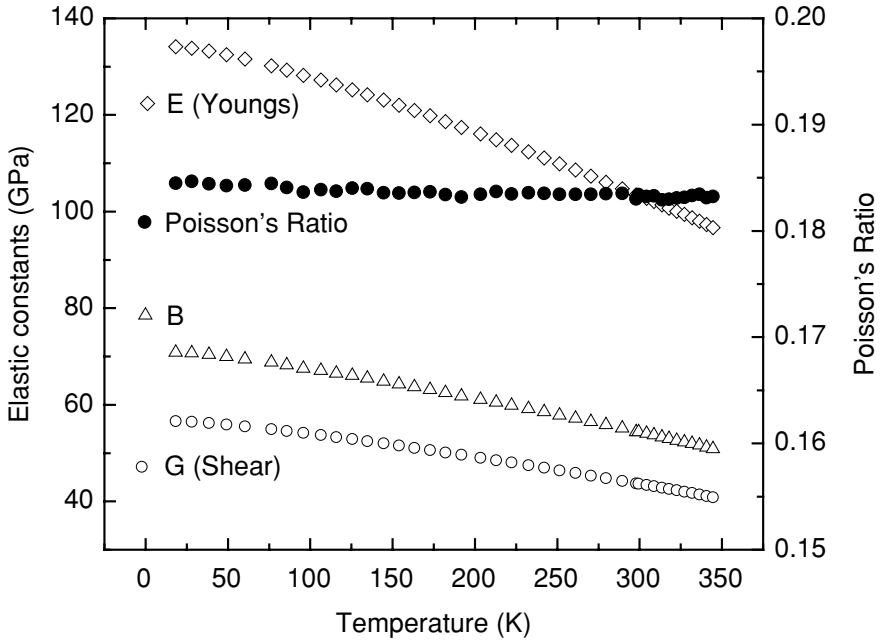

Fig. 7.47 *Elastic moduli of a high-purity, unalloyed α-plutonium polycrystal. Error bars are much smaller than the data points. The primary error is in the determination of density, computed from the dimensions and mass. E denotes Young's modulus, G, the shear modulus, and B, the bulk modulus* (*data from Ledbetter* et al., 2004; *Migliori* et al., 2004).

(d) Heat capacity

In 1976, Oetting *et al.* (1976) reviewed the early heat capacity measurements on plutonium. Low-temperature measurements of the heat capacity in ^{239}Pu, the most readily available plutonium isotope, have been plagued by self-heating (typically 2.2×10^{-3} W g^{-1} for ^{239}Pu) and by self-irradiation damage, which is especially pronounced at low temperatures where little if any healing of lattice damage occurs (Hecker and Martz, 2001). Although several investigators (Sandenaw and Gibney, 1971; Gordon *et al.*, 1976) minimized the effects of self-irradiation damage by using ^{242}Pu, they still had difficulty in obtaining sufficiently low temperatures to accurately measure the electronic specific heat. Lashley *et al.* (2003b) also reviewed previous low-temperature measurements and extended the measurements to ~2 K on ^{242}Pu using a thermal relaxation method and a specially designed sample mount (Lashley, 2003).

Lashley *et al.* demonstrated conclusively that previously reported anomalies in the heat capacity of plutonium resulted from the effects of self-irradiation damage. They also showed that anomalies in some of the δ-phase plutonium

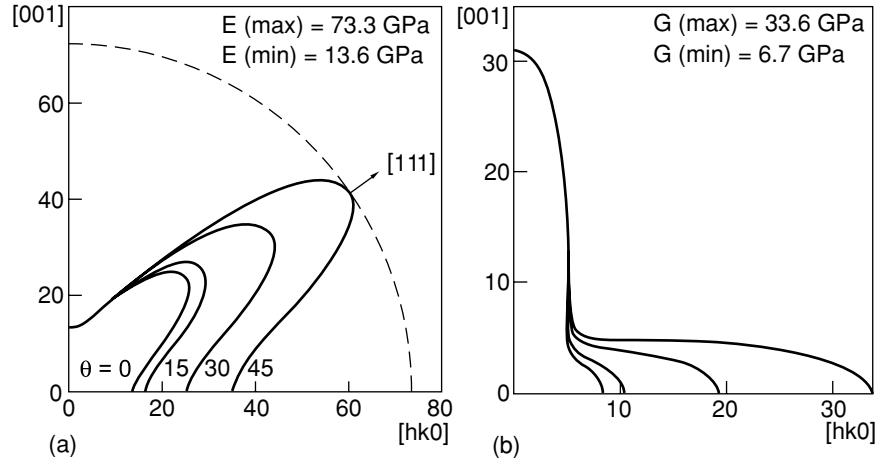

Fig. 7.48 *Elastic constants measured by Ledbetter and Moment* (1976) *on a δ-phase Pu*-3.4 at. *% Ga single crystal.* (*a*) *Young's modulus, E, as a function of crystal direction and* (*b*) *torsion modulus, G, as a function of direction.*

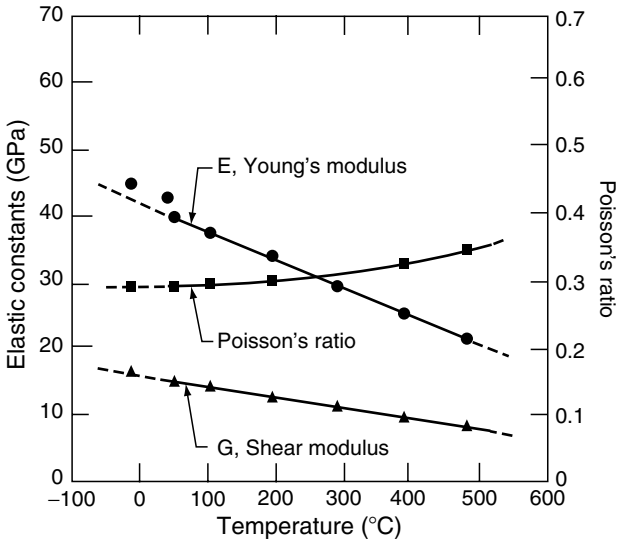

Fig. 7.49 *Elastic moduli of polycrystalline δ-phase Pu*-3.35 at. *% Ga as a function of temperature* (*after Calder* et al., 1981).

alloys at low temperatures resulted from martensitic transformations incurred in such samples when cooled to cryogenic temperatures. The results of Lashley *et al.* for very pure, zone-refined α-phase ^{242}Pu (<200 ppm impurities) are shown in Fig. 7.50 and compared to those reported by Gordon *et al.* (1976).

The electronic contribution to the specific heat can be measured at low temperatures where the phonon contribution is small. It is represented by equation (7.25)

$$(C_p/T) = \gamma + \alpha T^2 + \delta T^4 + \ldots \tag{7.25}$$

where γT and $\alpha T^3 = (12\pi^4 RT^3)/(5\theta_D{}^3)$ are the electronic and phonon contributions to C_p and θ_D is the Debye temperature. The results of Lashley *et al.* (2003b) for low-temperature heat capacity measurements on high-purity ^{242}Pu and a ^{242}Pu–5 at.% Ga alloy are shown in Fig. 7.51. The intercept at $T = 0$, γ, is a measure of the electronic DOS. The low-temperature fit yields $\gamma = (17 \pm 1)$ mJ K^{-2} mol^{-1}, which is within the range of 16 to 23 reported by Gordon *et al.* (1976), but less than the values of 22 to 25 reported by Stewart and Elliott (1981).

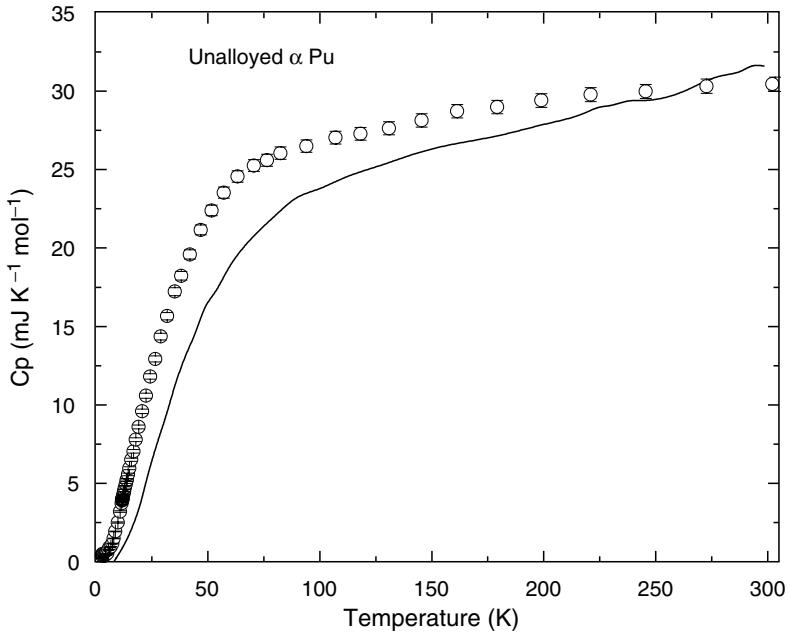

Fig. 7.50 *Heat capacity of unalloyed ^{242}Pu (solid line from Gordon* et al., 1976) *and high-purity, unalloyed ^{239}Pu (symbols) from Lashley* et al. (2003*b*) *who took extraordinary care to avoid self-irradiation damage at low temperatures.*

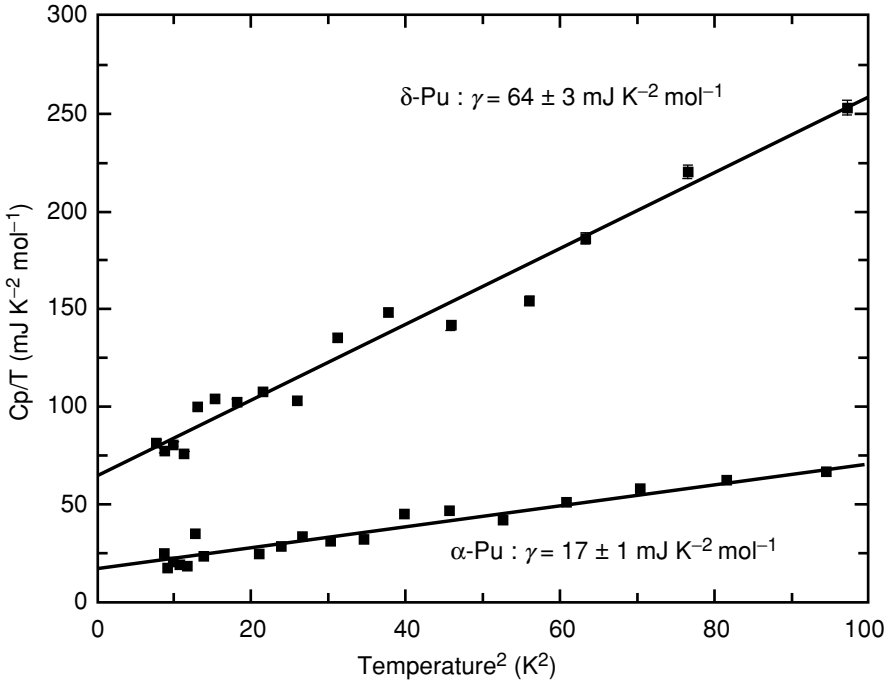

Fig. 7.51 *The low-temperature specific heat of unalloyed α plutonium and a δ-phase Pu-*5.1 at. *% Al alloy. These data represent the lowest temperature specific heat measurements reported on plutonium* (*after Lashley* et al., 2003*a,b*).

Since Lashley *et al.* reached the lowest temperatures, it is likely that their values are the most accurate. In any case, γ for plutonium is larger than that of any other element (Kittel and Kroemer, 1980). The δ-phase Pu–Al alloy has an even more remarkable γ of (64 ± 3) mJ K^{-2} mol^{-1}. Stewart and Elliott measured γ for Pu–Al alloys of varying aluminum concentration and found γ to vary from 44 to 63 mJ K^{-2} mol^{-1}. Extrapolation of the alloy data to zero alloy content yields $\gamma = 53$ mJ K^{-2} mol^{-1} for pure plutonium in the δ phase. Hence, the δ phase of plutonium, which is known to have less participation by the 5f electrons in bonding than the α phase, nevertheless has three times the electronic DOS at the Fermi energy.

Lashley *et al.* (2003b) calculated a Debye temperature, θ_D, of 153 K for α plutonium. On the other hand, Migliori *et al.* (2004, 2005) report the Debye temperature ($T = 0$ K) as 205 K based on the extrapolation of their elastic constant measurements to absolute zero. This method typically yields more accurate estimates of the Debye temperatures because it is less susceptible to the effects of self-irradiation damage. The literature values for α plutonium as determined from heat capacity, elastic constant, EXAFS, and neutron

scattering Debye–Waller measurements (Sandenaw, 1961, 1962; Taylor *et al.*, 1965; Lee *et al.*, 1965b; Gordon *et al.*, 1976; Stewart and Elliott, 1981; Lawson *et al.*, 1994; Lashley *et al.*, 2003b) vary from 118 to 205 K. On the other hand, the Debye temperature for the δ-phase plutonium alloys are reported to vary much less; namely, from 100 to 130 K (Ledbetter and Moment, 1976; Stewart and Elliott, 1981; Lashley *et al.*, 2003b).

Heat capacity measurements below and above room temperature as reported by Oetting and Adams (1983), Taylor *et al.* (1968), and Lashley (2005) for unalloyed plutonium, and by Lashley *et al.* (2003a), Lashley (2005), and Rose *et al.* (1970) are shown in Table 7.21. The heat capacity measurements above room temperature are not affected by self-irradiation damage because defects are sufficiently mobile to heal the damage. As pointed out by Oetting *et al.* (1976) and others, no anomalies in the paramagnetic susceptibility with temperature have been observed, thus the magnetic contribution to heat capacity is negligible, as confirmed by Lashley (2005).

Oetting and coworkers (Oetting *et al.*, 1976) present a comprehensive listing of the thermodynamic functions – enthalpy and entropy – along with the enthalpies of transformation between the various plutonium allotropes. The heat capacity of unalloyed plutonium as a function of temperature taken from Lashley *et al.* (2003b) and Kay and Loasby (1964) is shown in Fig. 7.52. The enthalpies and entropies of transformation are listed for unalloyed plutonium in Table 7.16.

(e) Magnetic behavior

Fig. 7.53 shows the molar magnetic susceptibilities of unalloyed plutonium and a Pu–6 at.% Ga alloy as a function of temperature. The plots are taken from Lashley (2005). The data for unalloyed plutonium above 300 K are those of Comstock, published by Sandenaw (1961) with additional details provided by Olsen *et al.* (1992). These data were obtained by the Gouy method on large samples of ^{239}Pu with a purity of 99.9%. The low-temperature data for the unalloyed α plutonium and all of the data for the alloy is that of Méot-Reymond and Fournier (1996). Their plutonium alloy samples were of high purity, electrorefined, with ferromagnetic impurities constituting <10 ppm. In the plot shown in Fig. 7.53, Lashley *et al.* align Méot-Reymond and Fournier's high- and low-temperature alloy data at 300 K because of the concerns expressed by Méot-Reymond and Fournier about their high-temperature technique.

We note that the susceptibilities of unalloyed plutonium and the alloy are similar – both are quite large, similar to the magnetic susceptibility of manganese. Unlike manganese, which orders antiferromagnetically at 95 K, plutonium shows no anomaly in its susceptibility at low temperatures. Magnetic susceptibilities on the order of those exhibited by plutonium are characteristic of metals with relatively strong paramagnetism caused by electronic band magnetism (such as that for palladium). Lashley *et al.* (2004) recently concluded that a

Table 7.21 *Experimental heat capacities (C_p) at various temperatures for α plutonium and δ-phase Pu–Ga alloys.*

	C_p (*unalloyed α-Pu*) (mJ K^{-1} mol^{-1})			C_p (δ-*Pu alloys*) (mJ K^{-1} mol^{-1})	
				Pu-1.7 at.% *Ga*	*Pu*-3.3 at.% *Ga*
T (K)	*Oetting and Adams* (1983)	*Lashley* (2005)	*Taylor* et al. (1968)	*Lashley* et al. (2003b) *and Lashley* (2005)	*Rose* et al. (1970)
2.78		0.227			
3		0.236			
3.5		0.317			
3.7				0.3201	
4		0.414		0.36968	
4.5		0.477		0.46436	
5		0.52		0.58135	
5.5		0.714		0.71759	
6		0.87049		0.87265	
6.5		0.93806		1.05475	
7		1.02		1.24524	
8		1.5		1.70936	
10		2.6		2.81808	
12		4.02757		4.15583	
15		5.92989		6.41797	
20		9.14411	3.65	10.37966	
22		10.36358		11.90103	
25		12.16125		14.26709	
30		14.80288		17.8891	
35		17.10077		21.10807	

40		18.85255		23.92317	
45		20.5505		25.89824	
50		21.95556	16.68	27.62289	
65		24.72443		31.5921	
70		25.19762		32.49775	
75		25.51758		33.19174	
80		25.86718		33.63288	
90		26.33692		34.84199	
100		26.73917	24.09	35.84115	
125		27.46718		34.99518	
150		28.3027		34.62373	
200		29.42604	28.66	33.40867	
250		30.04106		30.59754	
300	31.57	30.43499	32.18	30.80206	31.97
340	33.66				
380	35.16				32.43 (373 K)
400	32.64				
440	33.16				
480	33.69				33.81 (473 K)
500	33.50				
540	34.42				
580	35.34				36.12 (573 K)
600	34.96				
640	35.40				
680	35.83				39.30 (673 K)
700	36.04				
773					43.41
863					33.94
903					33.94

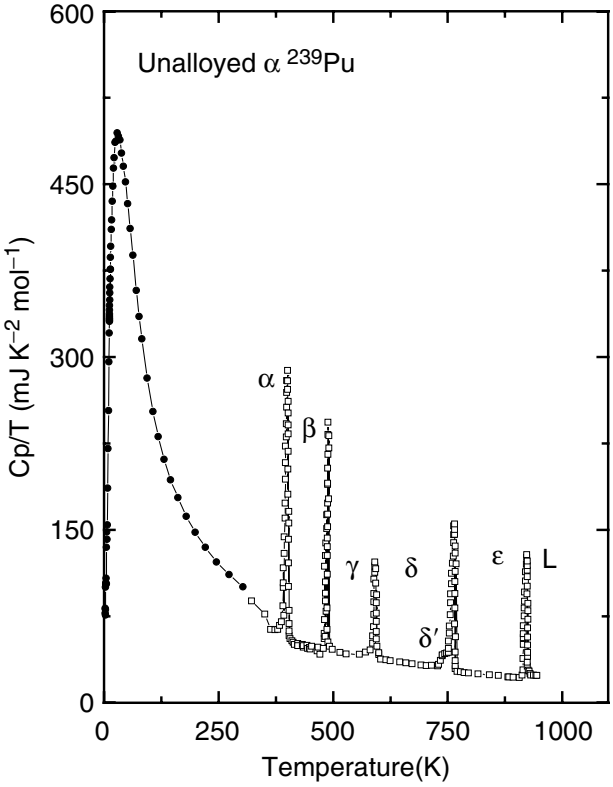

Fig. 7.52 *Heat capacity divided by temperature for high-purity, unalloyed α-phase plutonium. Open symbols are from Kay and Loasby* (1964) *and the solid symbols are unpublished work from Lashley* (2004).

thorough review of experimental data for plutonium (both in the unalloyed α phase and in the alloyed δ phase) provides no evidence for localized magnetic moments. They concluded that neither temperature nor magnetic-field dependencies of measured susceptibilities show evidence for ordered or disordered moments. They reinforce their conclusions with the results of other experimental probes, such as specific heat and NMR.

Magnetic moments and atomic volume are indicators of what the electrons are doing. As shown in Fig. 7.39, the atomic volumes of the actinides exhibit a huge expansion right at plutonium (between the α and δ phases, with an additional expansion at americium). In their review of actinide theory related to magnetic behavior, Lashley *et al.* (2004) show that the consensus among theorists is that a localization of the 5f electrons is required to explain the large volume expansion between the α phase and the δ phase, which leads inexorably

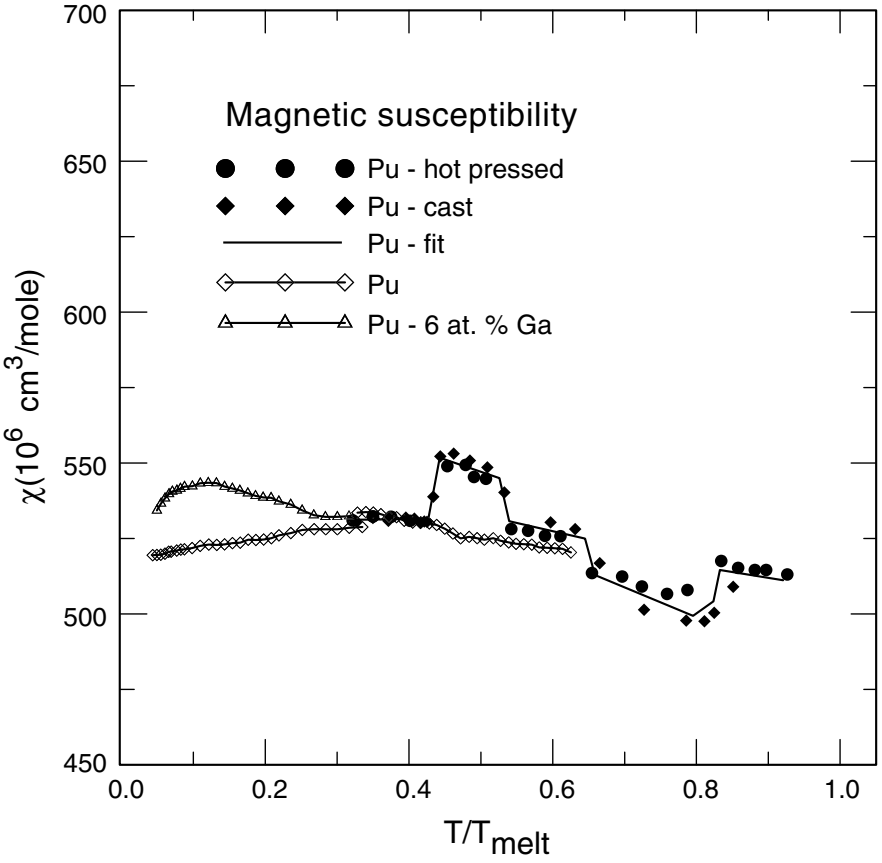

Fig. 7.53 *Molar susceptibility of unalloyed plutonium and δ-phase Pu-*6 at. *% Al alloy plotted as a function of temperature scaled by the melting point* (*from Lashley* et al., 2004). *See text for details of data.*

to magnetic ordering in the δ phase. Some theorists also predict magnetic order in the α phase. The magnetic moments are predicted to be large in both cases. Some of the theoretical treatments have suggested a partial cancellation between the spin and the orbital parts of the moments. However, even with such cancellation, magnetic moments of the order of 1 to $2\mu_B$ are predicted. Yet, the experimental evidence points overwhelmingly to the conclusion reached by Lashley *et al.* namely, neither ordered nor disordered local moments exist. Recent theoretical treatments by Shick *et al.* (2005) and Shorikov *et al.* (2005) predict reasonable volumes without any magnetic moments.

The reader is referred to the *Plutonium Handbook* (Miner and Schonfeld, 1980) and the *Gmelin Handbook of Inorganic Chemistry* (Lesser and Peterson,

1976; Blank, 1977) for additional references to magnetic susceptibility measurements and to the Hall effect in plutonium and its alloys. Recent magnetic susceptibility measurements on plutonium alloys, including Pu–Am and Pu–Ce, are also reported by Dormeval (2001) and Dormeval *et al.* (2000, 2003).

(f) Electrical resistivity, thermal conductivity, thermal diffusivity, and thermoelectric power

The unusual electrical resistivity of unalloyed plutonium is shown in Fig. 7.54 from Sandenaw and Gibney (1958). Unlike most normal metals that exhibit a linear decrease in resistivity at low temperatures, plutonium exhibits an increase and a maximum in resistivity at ~105 K. This low-temperature anomaly was initially believed to result from antiferromagnetic ordering. However, as pointed out above, no magnetic ordering has been found in plutonium or its alloys. Méot-Reymond and Fournier (1996) and Dormeval *et al.* (2000) suggest that the resistivity maximum is an indication of a Kondo effect in plutonium and its alloys. Boring and Smith (2000) make a convincing argument that the resistivity behavior along with other properties (such as the enhanced low-temperature specific heat) is an indication of strong electron–electron correlations involving spin and charge interactions. The resistivity maximum in plutonium is at the level of 150 μΩ cm, which means that an electron is scattered by roughly every atom in the lattice. As pointed out by Boring and Smith (2000), this type of scattering is considered the highest possible simple resistance that a

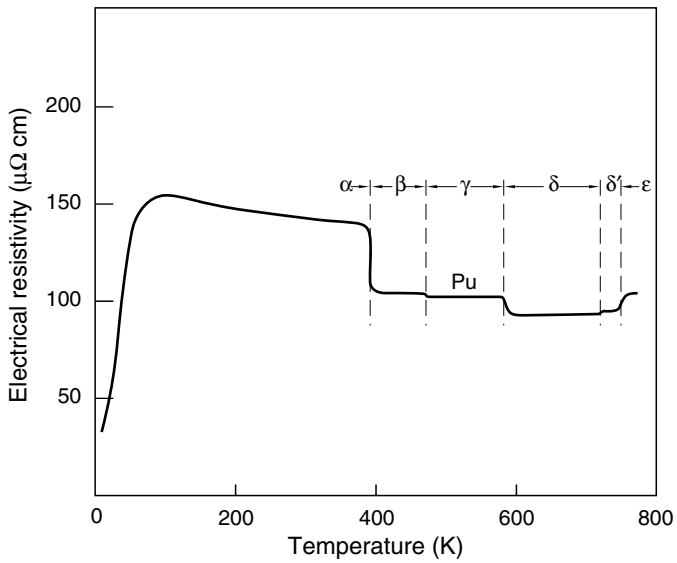

Fig. 7.54 *Electrical resistivity of unalloyed plutonium* (*from Sandenaw and Gibney,* 1958).

simple metal can exhibit; it is called the unitary limit. We also note that Lee *et al.* (1961) and Smith (1980) showed that plutonium does not become superconducting down to 0.75 K. Boivineau (2001) has extended resistivity measurements into the liquid phase using very high heating rates. He found the resistivity to remain nearly constant over the whole liquid range at a value of approximately 108 μΩ cm.

The resistivity of the δ-phase alloys has been measured by a number of investigators. The room-temperature values typically fall between 105 and 125 μΩ cm, depending on the alloying element and concentration. Extensive measurements have been reported on Pu–Ce alloys (Elliott *et al.*, 1962), Pu–Al alloys (Sandenaw, 1960a; Lee *et al.*, 1961; Elliott *et al.*, 1962), and Pu–Ga alloys (Joel *et al.*, 1971). The low-temperature results of Joel *et al.* (1971) for Pu–Ga alloys with gallium concentrations from 3 to 10 at.% are shown in Fig. 7.55. The results of Elliott *et al.* for Pu–Al alloys are very similar. We do not show the results for Pu–Ga alloys with gallium concentrations <3 at.% because they transform to the α′ phase upon cooling. The resistivities of all alloys are lower than that for unalloyed plutonium shown in Fig. 7.54. They also increase with decreasing temperature and exhibit a broad maximum. Increasing gallium concentration moves the maximum to lower temperatures and leads to higher

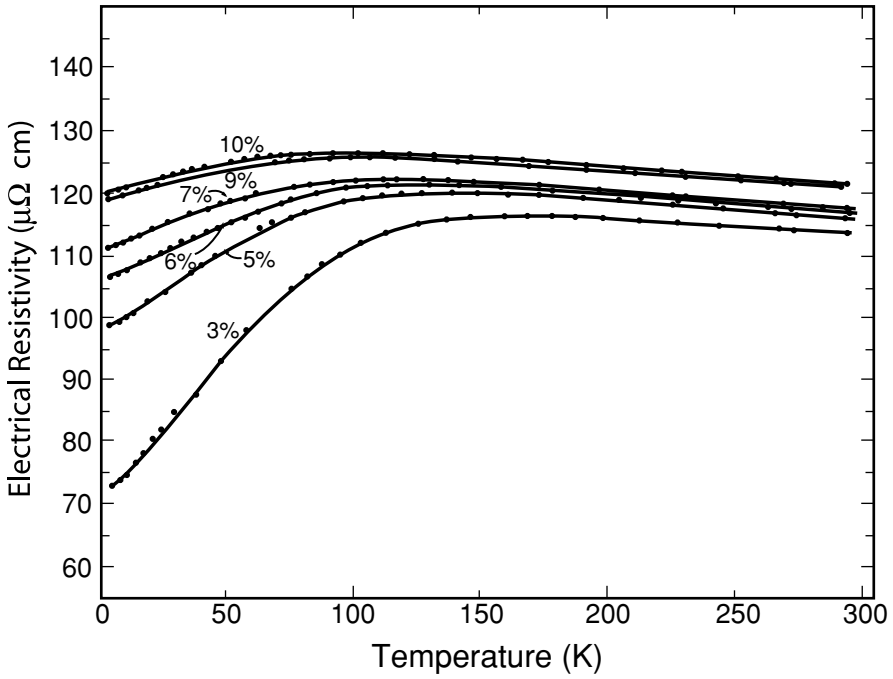

Fig. 7.55 *Electrical resistivity of various δ-phase Pu–Ga alloys* (*after Joel* et al., 1971).

resistivity. However, the increase with alloy concentration is less than what is typically observed for other metals. The low- and high-temperature regimes are shown together in Fig. 7.56 (taken from Blank (1977) and based on the work of Gibney and Sandenaw (1954)).

Gomez Marin (1997) and Dormeval (2001) recently measured resistivities of Pu–Am alloys across the entire range of δ-phase solubility at low temperatures. The resistivities for the entire range of alloys were considerably higher than any other plutonium alloy system. For example, the values for a Pu–15 at.% Am alloy was reported by Dormeval to be 370 μΩ cm at 293 K and 170 μΩ cm at 4 K. This alloy exhibited a slight maximum at 200 K. Alloys with higher americium contents were shown by Gomez Marin to decrease monotonically although not as rapidly as pure americium. Dormeval also reported resistivities of Pu–Ce alloys and of a number of ternary Pu–Ce–Ga and Pu–Am–Ga alloys. Blank (1977) reported the results of Mortimer and Adamson on Pu_3Al and Pu_6Fe. The resistivities at room temperature were 150 and 140 μΩ cm, respectively, and showed a maximum at lower temperatures. The resistivity for Pu_3Al remained unusually high (142 μΩ cm) at 4 K.

The literature shows large variations in low-temperature electrical resistivities measured in unalloyed plutonium. Much of this problem was a result of impurities. In addition, low-temperature measurements in plutonium are plagued by self-irradiation damage (see Section 7.7.9), which increases the resistivity

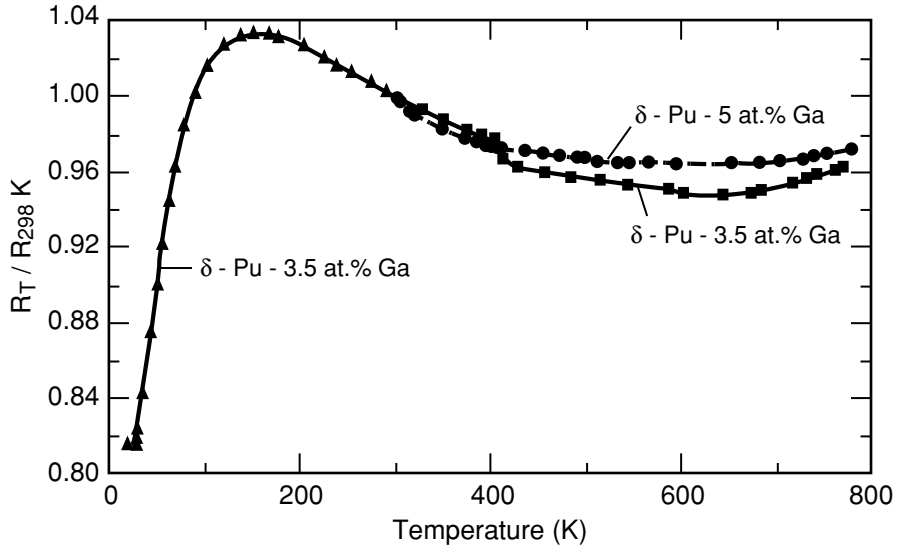

Fig. 7.56 *Electrical resistivity of a δ-phase Pu-*3.5 at. *% Ga alloy between* 25 *and* 750 K *and a δ-phase Pu-*5 at. *% Ga alloy between* 298 *and* 750 K. *The curves were normalized at* 298 K (*taken from Blank,* 1977 *with reference to Gibney and Sandenaw,* 1954).

because there is insufficient mobility of the defects generated to move and heal the lattice (Hecker and Martz, 2001). Olsen and Elliott (1962) reported some of the earliest measurements on the effects of impurities and self-irradiation on the resistivity of α-phase plutonium at low temperatures.

Thermal conductivity measurements on unalloyed plutonium were reported by Sandenaw and Gibney (1958), Lee and Mardon (1961), and Powell (1960). Andrew (1967) measured thermal conductivity of high-purity (99.98%) plutonium, chill-cast to minimize microcracking (density of 19.77 g cm^{-3}), and of preferentially oriented α-phase plutonium (by cooling from the β phase under pressure). The thermal conductivity decreases smoothly from a value of 0.0155 cal s^{-1} cm^{-1} K^{-1} at 300 K to 0.0075 cal s^{-1} cm^{-1} K^{-1} at 80 K for the chill-cast sample. Hence, the mechanisms that cause the increase in electrical resistivity and resistivity maximum at ~100 K do not seem to play a role in the thermal conductivity. Andrew found the thermal conductivity perpendicular to the [020] planes to be about 3 mW cm^{-1} K^{-1} higher than the thermal conductivity parallel to the [020] planes. He also reported a Lorenz number of 3.11×10^{-8} WΩ K^{-2} at 300 K and 5.95×10^{-8} WΩ K^{-2} at 80 K.

Andrew (1969) also reported thermal conductivities for high-purity, well-homogenized δ-phase Pu alloys. The conductivity of the Pu–3.35 at.% Ga alloy varied smoothly from 0.022 cal s^{-1} cm^{-1} K^{-1} at 300 K to 0.0098 cal s^{-1} cm^{-1} K^{-1} at 80 K. The conductivities of a Pu–7 at.% Ga alloy was approximately 10% lower and that of a Pu–10 at.% Ce alloy, approximately 20% higher. As was the case for the unalloyed plutonium, the thermal conductivities do not exhibit the anomalous low-temperature behavior found in resistivity measurements. Lewis *et al.* (1976) reported thermal conductivities calculated from thermal diffusivity measurements on high-purity Pu–3.35 at.% Ga alloys at high temperatures. Their calculated room-temperature value of 0.0205 cal s^{-1} cm^{-1} K^{-1} at 300 K increased to 0.04 cal s^{-1} cm^{-1} K^{-1} at 673 K.

Lewis *et al*. (1976) reported that the thermal diffusivity of high-purity plutonium (<200 ppm impurities) increased approximately linearly from about 0.011 cm^2 s^{-1} at 293 K (α phase) to 0.057 cm^2 s^{-1} at 843 K (ϵ phase). The thermal diffusivities of the δ-phase Pu–3.35 at.% Ga alloy increased smoothly from 0.04 cm^2 s^{-1} at 293 K to 0.065 cm^2 s^{-1} at 673 K.

The thermoelectric power of plutonium at room temperature is large and positive, and it decreases after each allotropic transformation as the temperature is increased, except for the δ′ to ϵ transformation, which shows an increase. The average value and ranges measured are shown in Table 7.22, taken from Wick (1980) and based on the work of Lee and Hall (1959), Costa (1960), Meadon and Lee (1962), and Lallement (1963). The thermoelectric power decreases rapidly at low temperatures with a slight rise at 80 K before falling very rapidly to 4 K. Blank (1977) reviewed thermoelectric power measurements for plutonium alloys. Lee *et al.* (1961) and Brodsky (1961) showed that the thermoelectric power in Pu–Al alloys exhibited an increase with decreasing temperature with a maximum at ~80 K for a δ-phase Pu–6 at.% Al alloy.

Table 7.22 *Thermoelectric power of plutonium* (*Wick*, 1980).

Phase	*Temperature* (K)	*Thermoelectric power, averaged values* ($\mu V\ K^{-1}$)	$\mu V\ K^{-1}$, *range*
α	~20	1.75	~1.5–~2
	~80	10.1	8.6–11.6
	~100	9.8	8.2–11.5
	~293	~13	11.2–15.6
	300	11.5	7–15.5
β	400	9.1	7–10.7
γ	500	8.4	7.4–9.4
δ	600	3.0	2.3–3.7
δ'	725	2.32	–
ϵ	800	3.5	3.2–3.8

The value of the thermoelectric power at room temperature was approximately 4 $\mu V\ K^{-1}$, about one third the value of unalloyed plutonium in the α phase.

(g) Diffusion

Diffusion rates in solids depend principally on crystal structure and homologous temperature (T/T_m), that is, how close the temperature is to the melting point (Sherby and Simnad, 1961). Plutonium, of course, has multiple allotropes and a very low melting point. Sherby and Simnad (1961) showed that the Arrhenius-like rate equation for self-diffusion, $D = D_0 \exp(-Q/k_B T)$, where D_0 is a constant and Q is the activation energy for self-diffusion (vacancy formation and migration), fits the diffusion data for most solids. The activation energy, Q, was found to depend primarily on the homologous temperature and the crystal structure. Experimental data for plutonium are summarized by Lesser and Peterson (1976), Blank (1977), and Deloffre (1997). The diffusion data presented in Table 7.23 are based on Deloffre's summary (1997) of the work of Tate and coworkers (Tate and Cramer, 1964; Tate and Edwards, 1966), Johnson (1964), Edwards *et al.* (1968), Rafalski and coworkers (Rafalski *et al.*, 1967; Harvey *et al.*, 1971), Dupuy and Calais (1968), Wade (1971), and Wade *et al.* (1978).

The data presented in Table 7.23 contrast self-diffusion rates in the various phases of plutonium. There are no data available for α-phase plutonium because it is stable only below 395 K where diffusion rates are extremely slow. Wade *et al.* (1978) showed that the large variations in diffusion rates in the β and γ phases were a result of short-circuit diffusion along paths such as dislocations or grain boundaries. The diffusion rates in ϵ plutonium are anomalously high even for the open bcc crystal structure. In fact, Cornet (1971) showed that the rate of self-diffusion decreased under pressure, similar to what was previously found for white phosphorus (Nachtrieb and Lawson, 1955). He calculated the

Table 7.23 *Diffusion constants in plutonium and Pu–Ga alloys.*

Pu phase method	*Temperature range* (K)	*Diffusion mechanism*	*Frequency factor* D_0 ($cm^2\ s^{-1}$)	*Activation energy* Q ($J\ mol^{-1}$)	*References*
(a) Self-diffusion in unalloyed plutonium					
ϵ Pu diffusion couple ^{238}Pu tracer	773–893	lattice	2×10^{-2} $3 \times 10^{-3} < D_0 < 9 \times 10^{-2}$	$77\,400 \pm 10\,500$	Dupuy and Calais (1968)
ϵ Pu thin film ^{238}Pu tracer	765–886	lattice	$(4.5 \pm 1) \times 10^{-3}$	$66\,940 \pm 1\,675$	Wade (1971)
δ Pu diffusion couple ^{238}Pu tracer	623–713	lattice	4.5×10^{-3}	99 600	Tate and Cramer (1964)
δ Pu thin film ^{238}Pu tracer	594–715	lattice	$(5.17 \pm 0.7) \times 10^{-1}$	$126\,370 \pm 800$	Wade *et al.* (1978)
γ Pu diffusion couple ^{238}Pu tracer	488–580	lattice	2.1×10^{-5}	69 870	Tate and Edwards (1966)
γ Pu thin film ^{238}Pu tracer	484–544	lattice	$(3.8 \pm 10) \times 10^{-1}$	$118\,410 \pm 7\,500$	Wade *et al.* (1978)
	504–564	short circuit	$(1.76 \pm 0.7) \times 10^{-5}$	$69\,040 \pm 1\,670$	
β Pu thin film ^{238}Pu tracer	409–454	lattice	$(1.69 \pm 0.5) \times 10^{-2}$	$108\,000 \pm 1\,200$	Wade *et al.* (1978)
		short circuit	$(3.9 \pm 0.05) \times 10^{-7}$	$56\,070 \pm 60$	
(b) Self- and interdiffusion in Pu–Ga alloys					
δ phase, thin film ^{238}Pu tracer, self-diffusion	613–781	lattice	76.0	152 000	Wade (1971)
	513–613	grain boundary	1.6×10^{-2}	110 000	
ϵ phase, thin film ^{238}Pu tracer, self-diffusion	847–917	lattice	7×10^{-4}	56 070	Wade (1971)
ϵ phase, diffusion couple, interdiffusion	833–909	lattice	5.3×10^{-4}	55 230	Harvey *et al.* (1971)
δ phase, homogenization interdiffusion	698–798	lattice	65	168 000	Johnson (1964)
δ phase, diffusion couple, interdiffusion	673–807	lattice	9.8×10^{-2}	139 300	Rafalski *et al.* (1967)
δ phase, diffusion couple, interdiffusion	688–790	lattice	1.3×10^{-2}	156 000	Edwards *et al.* (1968)

activation volume to be –4.9 cm^3, which is one-third of the molar volume of plutonium. He suggested an interstitial diffusion mechanism instead of the vacancy mechanism typically associated with lattice diffusion. Hill and Kmetko (1976) agreed with the proposed interstitial mechanism and suggested that the high self-diffusivity in the ϵ phase results from the nature of the 5f electron bonding in plutonium.

As shown in Table 7.23, the frequency factor, D_0, in plutonium is higher for self-diffusion than for interdiffusion. This behavior is shown graphically by the work of Edwards *et al.* (1968) in Fig. 7.57. It also agrees with the general observation that diffusion rates decrease with the addition of elements that raise the melting point of the host metal (Shewmon, 1963). Hilliard *et al.* (1959) showed that diffusion rates decrease significantly with increasing solute concentrations in typical alloy systems. Dupuy and Calais (1968) and Wade (1971) reported decreases in D_0 with additional solute additions. However, as reported by Mitchell *et al.* (2001), Edwards *et al.* (1968), and Rafalski *et al.* (1967) all concluded that the interdiffusion of gallium in plutonium did not vary with concentration over the range studied. Likewise, Tate and Edwards (1966) found no concentration dependence of diffusion rates in a series of δ-phase Pu–Al alloys. They reported values of $D_0 = 2.25 \times 10^{-4}$ and $Q = 106{,}690$ J mol^{-1} in the range of 623 to 790 K.

The large differences in interdiffusion rates of gallium between the δ and ϵ phases are particularly important because they lead to microsegregation of gallium in δ-phase plutonium alloys, as discussed in Section 7.7.4. The diffusion data for such alloys were recently summarized by Mitchell *et al.* (2001). Hecker *et al.* (2004) showed that interdiffusion of gallium in the α' phase of plutonium (an expanded α phase resulting from the entrapment of gallium atoms in a martensitically transformed δ-phase plutonium alloy) appears to be quite rapid even at room temperature.

Irradiation enhances both self-diffusion and interdiffusion rates in solids and can lead to phase instability or radiation-enhanced segregation. Such effects are particularly important in plutonium since the radiation is self-induced. Smirnov and Shmakov (1999) provide experimental and theoretical results for the actinides including plutonium and also present a rich Russian literature on this topic.

(h) Liquid plutonium, surface tension, viscosity, and vapor pressure

Liquid plutonium is highly corrosive and easily oxidized. Early measurements of its properties, including compatibility with container materials, were made as part of the LAMPRE program. Comstock (1952) reported some of the first direct measurements on liquid plutonium. There is general agreement today that the melting point of plutonium is (913 ± 2) K. The low melting point (with respect to its position in the periodic table) has many consequences on the practical properties of plutonium. In addition to restricting the temperature

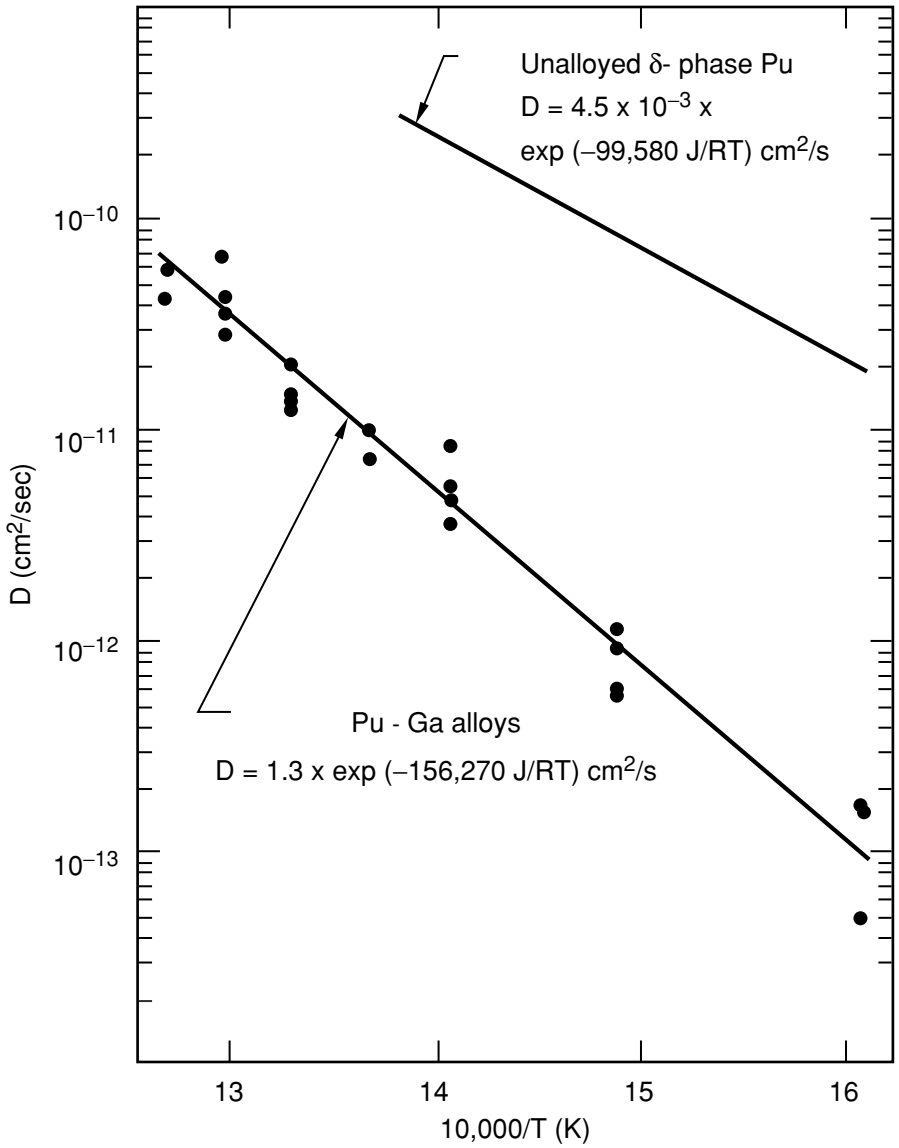

Fig. 7.57 *Diffusion coefficient, D, as a function of temperature for unalloyed plutonium and a δ-phase Pu*-3 at. *% Ga alloy plotted on a customary Arrhenius plot* (*Edwards* et al., 1968).

range of applications, it also affects all thermally activated processes, which scale with the melting point (Hecker, 2000). For example, room temperature represents a homologous temperature of 0.33, a temperature at which many defects become quite mobile. In addition, as pointed out by Nelson *et al.* (1965),

the effective melting point of the α phase is significantly lower than that of the ϵ phase, increasing the homologous temperature at room temperature to 0.53 for the α phase (see Hecker *et al.* (2004) for a discussion of the metallurgical consequences).

Liquid plutonium has many peculiarities, including a density greater than the last three solid allotropes, and its heat of fusion (~2800 J mol^{-1} as shown in Table 7.16) is unusually small. The stability of liquid plutonium has been attributed to the nature of 5f electron bonding in plutonium by Hill and Kmetko (1976) and Brewer (1983). Its melting point decreases with increasing pressure up to 3 GPa (Liptai and Friddle, 1967; Morgan, 1970) consistent with the volume contraction on melting. Other materials such as gallium, bismuth, antimony, germanium, silicon, tellurium, and water show similar behavior. Merz *et al.* (1974) and Boivineau (2001) also reported an increase in sound speed in liquid plutonium with increasing temperature, with a slope of 0.08 to 0.1 m s^{-1} K^{-1}. Using a rapid heating technique, Boivineau showed that the sound speed increases to 2000 K before undergoing a rapid change in slope to a negative value from 2000 to 3600 K. Similar results have been reported for cerium (McAlister and Crozier, 1981), in which 4f electrons also play a role in bonding under pressure. Lawson *et al.* (2000) and Lawson (2001) modified Lindemann's rule for melting to include the temperature dependence of the elastic properties. Lawson *et al.* explain the anomalously low melting point of plutonium and the trend across the light actinides by temperature-induced elastic softening.

The viscosity of liquid plutonium was measured by Wittenberg and coworkers at the Mound Laboratory (Eichelsberger, 1961; Jones *et al.*, 1962; Wittenberg, 1963; Ofte and Rohr, 1965; Ofte *et al.*, 1966). Jones *et al.* (1962) reported the viscosity of liquid plutonium to follow the relation:

$$\log \eta = 672/T + 0.037 \text{ (in centipoise)} \tag{7.26}$$

which yields a viscosity of 6 cP at the melting point. This is one of the highest viscosities measured for metals and is similar to the melting point viscosity of 6.53 cP for uranium (Wittenberg, 1975) and 5.8 cP for iron (Ofte *et al.*, 1966). Ofte *et al.* pointed out that the viscosity of plutonium and its fluid flow properties place it in a class of metals whose melting points are substantially higher than that of plutonium. However, if one accounts for its high mass and low Debye temperature, then plutonium falls only somewhat above the correlation established by Iida *et al.* (1988) for most liquid metals.

Blank (1977) reviewed the measurements of viscosity on liquid Pu–Fe alloys by Ofte and coworkers (Wittenberg *et al.*, 1960; Ofte and Wittenberg, 1964; Wittenberg *et al.*, 1968). The Pu–Fe system is of practical importance because it forms the low-melting eutectic compound, Pu_6Fe. The viscosities of Pu–Fe alloys were uniformly high. That of a Pu–9.5 at.% Fe eutectic alloy (near the compound Pu_6Fe) was a remarkable 25.2 cP at 684 K (and decreased to 6.14 cP at 1081 K). Blank (1977) provides great detail in his summary of the Pu–Fe

system. Wittenberg *et al.* (1960) found the activation energy for viscous flow for the eutectic alloy to be 21.9 kJ mol^{-1}. Ofte *et al.* (1966) reported viscosities for Pu–Ce and Pu–Ce–Co alloys in excess of that for plutonium. The viscosity of Pu–28.4 at.% Ce–23.7 at.% Co was reported as 23 cP at its melting point, nearly matching the viscosity of the Pu–Fe eutectic alloy. The Debye temperatures for these alloys are not available, so it is not possible to check if the viscosities fit the correlation established by Iida *et al.* (1988).

The accepted value for the surface tension of unalloyed liquid plutonium is that reported by Spriet (1963), namely 0.55 N m^{-1}. Wittenberg (1975) also reported 0.55 N m^{-1} for plutonium and 1.5 N m^{-1} for uranium. The value for plutonium fits the correlation of surface tension with melting point and molar volume proposed by Iida *et al.* (1988) for most elements in the periodic table. That of uranium appears to be anomalously high.

The optical properties and normal spectral emissivity of liquid Pu–3.4 at.% Ga at 632.8 nm were measured over the temperature range of 2016 to 2189 K using rotating analyzer ellipsometry by Sheldon *et al.* (2001). The temperature dependence of three optical properties ϵ_λ (emissivity), n_λ (index of refraction), and k_λ (extinction coefficient) were reported as:

$$\varepsilon_\lambda = 5.38 \times 10^{-5} + 0.250$$

$$n_\lambda = -1.29 \times 10^{-4}\ \mathrm{T} + 3.82$$

$$k_\lambda = -7.04 \times 10^{-4} + 5.77$$

The value for ϵ_λ is almost a third higher than that measured for uranium by Krishnan *et al.* (1993), demonstrating that the light actinides exhibit significant variations in emissivity.

Phipps *et al.* (1955) reported the vapor pressure of liquid plutonium. Subsequently, Mulford (1965), Kent and Leary (1968), and Kent (1969) added to these measurements, and reported the vapor pressure to be described by the following equation with T in K and P in atmospheres:

$$\log P = (4.924 \pm 0.120) - (17,420 \pm 184)/T \qquad (7.27)$$

This relationship extrapolates to a boiling point of (3573 ± 100) K. Hence, the boiling point is quite high, in keeping with the position of plutonium in the periodic table. The combination of a high boiling point and a low melting point results in a wide range of liquid stability. Kent and Leary (1968) also reported the standard enthalpy of vaporization (H°_{298}) as (347.7 ± 2.1) kJ mol^{-1} and the standard entropy of vaporization (S°_{298}) as 123.2 J mol^{-1} K^{-1}. Oetting *et al.* (1976) reviewed the available data and recommended the best average for the enthalpy of vaporization as (345.2 ± 0.4) kJ mol^{-1}. A detailed listing of the thermodynamic properties of plutonium gas is given in Oetting *et al.* The data for the Pu_6Fe intermetallic reported by Sandenaw and Harbur (1973) were summarized by Blank (1977).

(i) New tools, new measurements of physical properties

Arko *et al.* (2006) reviewed the properties of actinides in the metallic state in Chapter 21 of this work. Their emphasis is on those properties that are unique or predominantly found in the metallic solid state. Such properties include magnetism, superconductivity, enhanced mass, spin, and charge density waves as well as quantum critical points. We refer the reader to this chapter for discussion of how plutonium fits into the trends across the actinides. They also provide detailed results of photoemission spectroscopy measurements on plutonium and its alloys.

There has been a revival of experimental work (along with a great increase in theoretical activity) in plutonium over the past 5 years. Some of the modern tools of materials science developed during the past couple of decades are being used to make measurements on plutonium and its alloys. We summarize a few salient ones in this section. One of the key barriers to many of the techniques remains the difficulty in synthesizing single crystals of the various phases of plutonium. No single crystals of α plutonium have been fabricated since the pioneering work in the 1960s by Liptai *et al.* (1967), who grew very large grains by a high-pressure technique. However, Lashley *et al.* (2000, 2001) have refined the strain-anneal technique developed in the 1960s by Moment (1968) to grow large grains of δ-phase plutonium alloys, which are suitable for many of the single-crystal measurements. These large-grained, very high-purity plutonium samples have been used for many recent physics experiments.

Zocco and Schwartz (2003) provide a history of the development of TEM techniques and their application to plutonium and its alloys. This technique is an essential tool for metallurgical studies, first demonstrated for plutonium around 1980 and revived in 2000. Zocco and Schwartz show examples of how TEM has helped answer key questions about phase transformations in plutonium alloys, as well as study the effects of self-irradiation damage. Boehlert *et al.* (2001) demonstrated how electron backscattered diffraction can be used to examine the grain structures in Pu–Ga alloys.

Ledbetter and Moment (1976) raised interest in the phonon spectrum of plutonium with their results nearly 30 years ago on the unusual elastic anisotropy of δ-phase plutonium. In a pioneering paper, Wong *et al.* (2003b) recently reported the first complete phonon dispersion curves of plutonium using inelastic X-ray scattering from a third-generation synchrotron facility (the European Synchrotron Radiation Facility in Grenoble, France). Their results are shown in Fig. 7.58 for a Pu–2 at.% Ga δ-phase alloy large-grained polycrystal grown by the techniques developed by Lashley *et al.* (2001). Wong *et al.* confirmed the large elastic anisotropy found by Ledbetter and Moment. They also found a small shear elastic modulus, C', a Kohn-like anomaly in the T_1 [011] branch, and a pronounced softening of the [111] transverse modes. They relate these findings to a strong coupling between the lattice structure and the 5f valence instabilities in plutonium. Dai *et al.* (2003) predicted the phonon dispersion

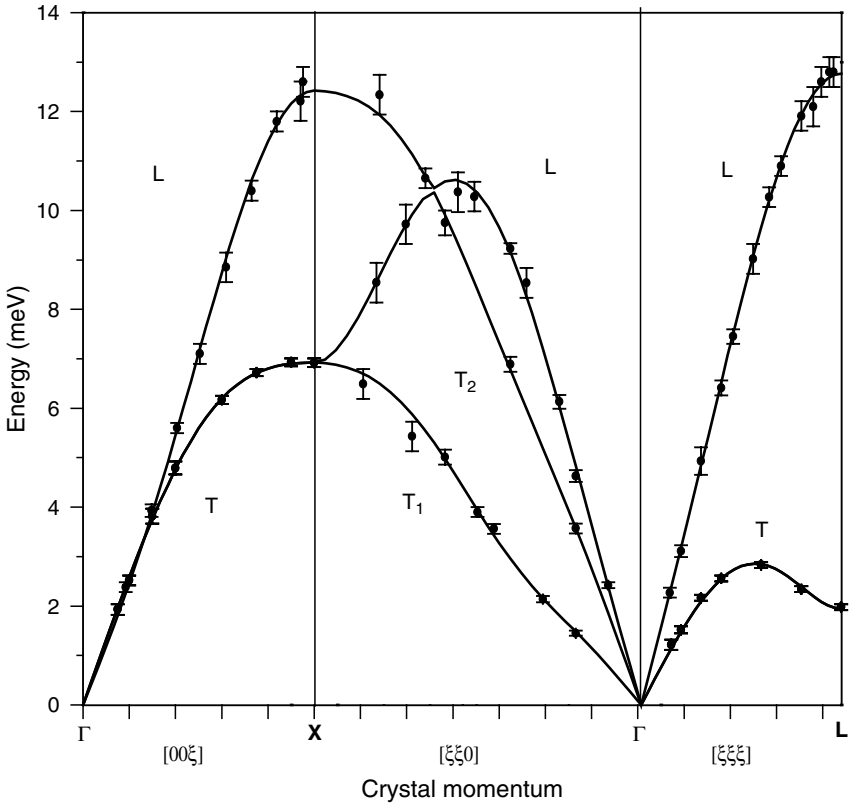

Fig. 7.58 *Phonon dispersion along high-symmetry directions in δ-phase Pu*-2 at. *% Ga alloy. The longitudinal and transverse modes are denoted L and T, respectively. The experimental data are shown with error bars. Along the* [0ξξ] *direction, there are two transverse branches,* [011]<011>(T_1) *and* [011]<100>(T_2). *The softening of the TA* (*transverse acoustic*) [111] *branch toward the L point is apparent. The curves represent the fourth-nearest neighbor Born–von Kármán model fit* (*Wong* et al., 2003*b*).

curves using dynamical mean-field theory (DMFT), which includes electron correlations that are so important in plutonium. Wong *et al.* point out that although the qualitative agreement between theory and experiment is quite good, there are important quantitative differences. Wong *et al.* (2003a) also developed a thermal diffuse scattering technique to complement their inelastic scattering technique.

McQueeney *et al.* (2004) reported the temperature dependence of the phonon spectrum, as observed from measurements of the phonon DOS and sound velocities as shown in Fig. 7.59. The DOS was measured with inelastic neutron scattering on a polycrystalline ^{242}Pu–5 at.% Al δ-phase alloy. The ^{242}Pu isotope was used because the absorption of thermal neutrons is low compared to the

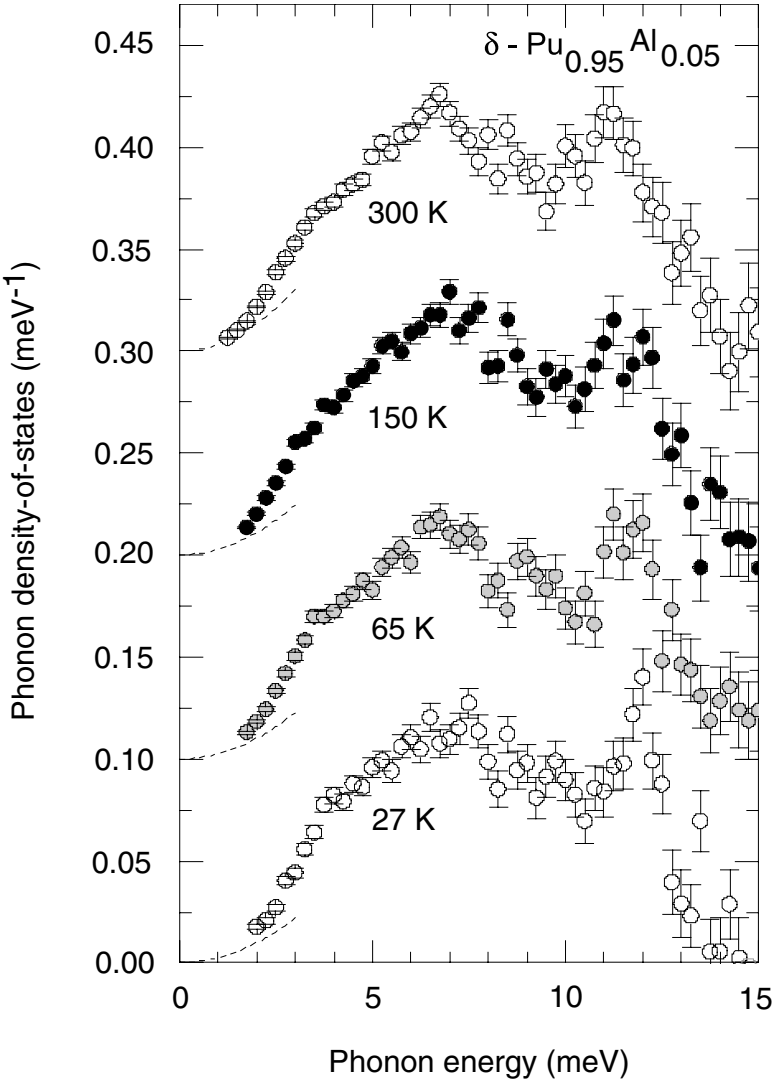

Fig. 7.59 *Phonon density of states of δ-phase Pu*-5 at. *% Al at four temperatures. The dashed line represents the quadratic part of the DOS at each temperature, as estimated by the average sound velocity obtained from resonant ultrasound measurements* (*from McQueeney* et al., 2004).

standard ^{239}Pu isotope. The phonon frequencies and sound velocities soften considerably with increasing temperature in spite of nearly zero thermal expansion over this temperature range. The frequency softening of the transverse branch along the [111] direction is anomalously large (~30%) and sensitive to

alloy composition. Based on a comparison to the results of Wong *et al.*, McQueeney *et al.* concluded that the interatomic potential is extremely sensitive to alloy composition, pressure, and temperature, unlike any other metal. They suggest that this behavior may arise from an unusual temperature dependence of the electronic structure.

We referred to local structure measurements at the modern synchrotron sources earlier using EXAFS along with conventional XRD in Section 7.7.5. Allen *et al.* (2002) reported temperature-dependent EXAFS measurements over the temperature range of 20–300 K of the vibrational properties of a Pu–3.3 at. % Ga δ-phase alloy as a means of discerning differences in the vibrational character of the gallium and plutonium sites. They obtained pair-specific, correlated Debye temperatures, θ_{cD}, of (110.7 ± 1.7) K for the Pu–Pu pairs and (202.6 ± 3.7) K for the Pu–Ga pairs. Allen *et al.* concluded that these results indicate that Ga–Pu bonds are significantly stronger than the Pu–Pu bonds. Lynn *et al.* (1998) previously reported a Pu-specific value of $\theta_D = 127$ K and a Ga-specific $\theta_D = 255$ K using neutron-resonance Doppler spectroscopy on a Pu–3.6 at.% Ga alloy. Nelson *et al.* (2003a,b) reported EXAFS measurements on the vibrational properties of both the δ phase and the α′ phase of a Pu–1.9 at. % Ga alloy (in the δ-phase and mixed, α′ + δ, phase conditions). They found a bond-length contraction for the Pu–Ga bond of 0.11 Å in the δ phase, but only 0.03 Å in the α′ phase. They reported correlated Debye temperatures of θ_{cD} (δ) = (120.4 ± 2.6) K and θ_{cD} (α′) = 159.1 ± 12.5 K.

Moore *et al.* (2003) used high-energy electron energy loss spectroscopy (HE-EELS) in a TEM and synchrotron-radiation-based X-ray absorption spectroscopy to determine phase-specific electronic structure information on plutonium. The sample was a dilute Pu–Ga alloy treated to produce a mixture of the α + δ phases. The TEM examination allowed individual grains of each phase to be examined. Moore *et al.* conclude that Russell–Saunders coupling fails for the 5f states of plutonium, and that only the use of JJ or intermediate coupling is appropriate. In addition, they conclude that their results confirm calculations that there is considerable spin–orbit splitting of the occupied and unoccupied 5f states of plutonium, indicating that spin–orbit splitting cannot be neglected in the Hamiltonian for the 5f states of plutonium.

Superconductivity has recently been discovered above 18 K in a plutonium-based nearly magnetic compound, $PuCoGa_5$ by Sarrao *et al.* (2002, 2003a,b). At the same temperature, this compound exhibits a step-like transition in heat capacity, from which they inferred the electronic specific heat, γ, to be 77 mJ mol^{-1} K^{-2}, which points to strong electron–electron correlations. In addition, field-dependent resistivity data gave an upper critical field of 74 T, a surprisingly large value. Other actinide-based superconductors have transition temperatures below a few K. The cerium-based isostructural compounds $CeCoIn_5$ and $CeIrIn_5$ are also superconducting but only in the 1-K range, and for $CeRhIn_5$ only under pressure. The T_c of $PuCoGa_5$ can be further enhanced to about 22 K by applying pressure (Griveau *et al.*, 2004). $PuRhGa_5$ is superconducting, as

well, with $T_c = 8.6$ K (Bauer *et al.*, 2004). The properties of these plutonium-based superconductors are indicative of an unconventional, most likely magnetically mediated, superconductivity (Sarrao *et al.*, 2003b).

7.7.7 Mechanical properties of plutonium metal and alloys

Mechanical properties of metals and alloys depend to first order on their crystal structure and melting point, which indirectly affects all thermally activated processes. The multiple allotropes of plutonium lead to a rich spectrum of mechanical properties as reviewed recently by Hecker and Stevens (2000). The low melting point allows for relatively easy mobility of defects near and above room temperature. Consequently, the mechanical properties of plutonium are especially sensitive to temperature and strain rate. They are also sensitive to chemistry (both intentional alloying and unintentional impurities) and processing, which, in turn, control the microstructure (phases present, their structure and distribution, and the nature and number of defects). Therefore, it is necessary to know the chemistry and the processing history to compare the properties of plutonium.

Gardner (1980) presented the most comprehensive review of the mechanical properties of plutonium and its alloys. His results for the yield and ultimate tensile strengths of unalloyed plutonium (for a range of purities and processing histories) are summarized in Fig. 7.60. These data demonstrate the dramatic temperature and crystal-structure dependence of the strength properties of plutonium. As reported by Gardner, the monoclinic crystal structure of plutonium (the only element in the periodic table with this low-symmetry structure) precludes the necessary conditions for plastic slip (by dislocation glide) in polycrystalline material for extended plastic flow. Consequently, the α phase of plutonium is brittle at and near room temperature. As shown in Fig. 7.60, it is quite strong. However, the tendency for α plutonium to microcrack during typical processing causes significant scatter in the properties. Moreover, certain impurities lead to the retention of second phases (typically the δ or β phases) or the presence of inclusions (such as oxides, nitrides, carbides, or the eutectic intermetallic, Pu_6Fe), which can have a significant effect on the mechanical properties.

Another important variable in determining the mechanical behavior of α plutonium is the grain size. Merz (1970, 1971) demonstrated that in α plutonium with decreasing grain size the mechanism for plastic flow changes. He fabricated very fine-grained α plutonium (1–3 μm) by extrusion and concurrent recrystallization of electrorefined, high-purity plutonium. He demonstrated that the strength decreased substantially with grain size and the ductility increased. At room temperature, he found surprising plastic elongation of 8% at low strain rates. On the high-temperature end of α-phase stability, he found extended plasticity, that is, elongations in excess of 100% (Merz and Allen, 1973;

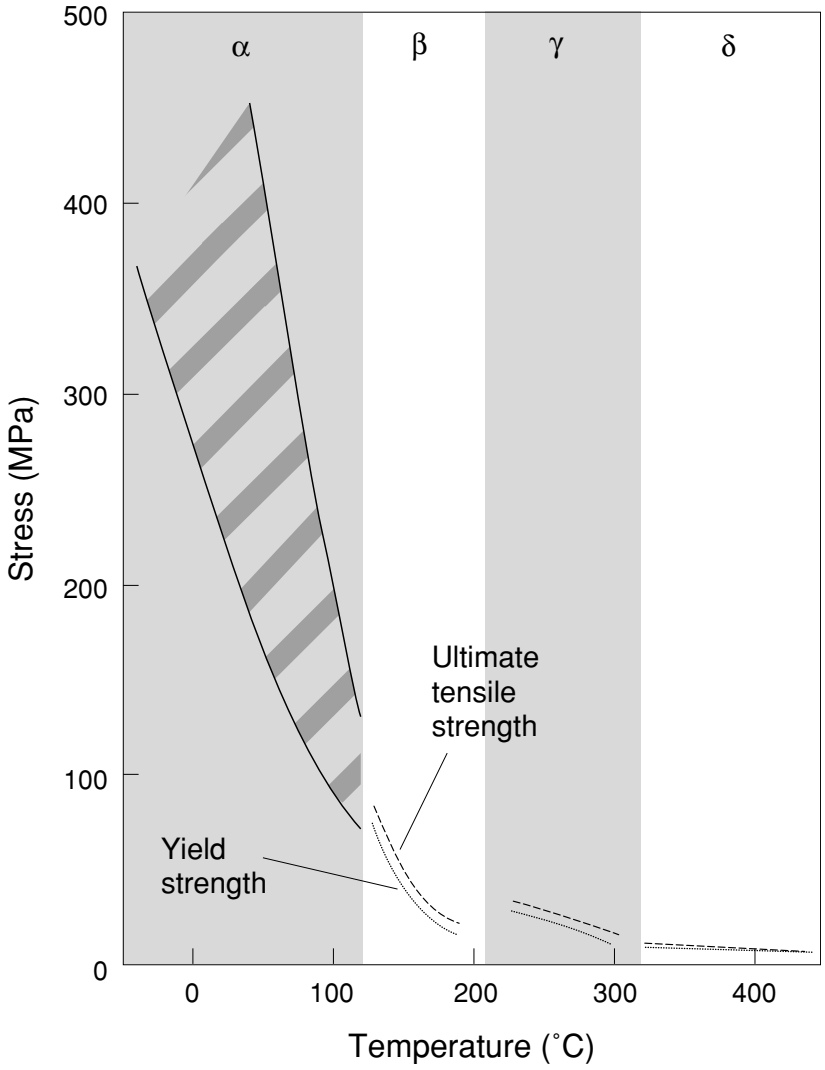

Fig. 7.60 *Strength as a function of temperature for unalloyed plutonium tested in uniaxial tension at nominal strain rates of* 10^{-3} s^{-1} (*after Gardner,* 1980).

Merz, 1974). In the β phase, he found the fine-grained plutonium to exhibit classical superplasticity with several 100% elongation. He explained that the deformation mechanism changed from dislocation glide to grain boundary sliding because of the small grain size and the high homologous temperature

of 0.53 at room temperature for the α phase of plutonium. Fig. 7.61 shows the change in Vickers Microhardness with temperature for several grain sizes in α plutonium (Merz and Nelson, 1970). Hecker and Morgan (1976) found that the strength of coarse-grained α plutonium increased moderately at intermediate strain rates. Hecker and Stevens (2000) pointed out several other interesting features about the mechanical behavior of α plutonium in their review.

As shown in Fig. 7.60, the other phases of unalloyed plutonium are relatively weak compared to the α phase. Gardner shows no data for the ϵ phase. Cornet and Bouchet (1968) showed that the elastic moduli of the ϵ phase is approximately two-thirds that of the δ phase, and we also expect its strength properties to be lower. The other phases of plutonium are also considerably more ductile than the α phase. As pointed out earlier, a few atom percent of alloying

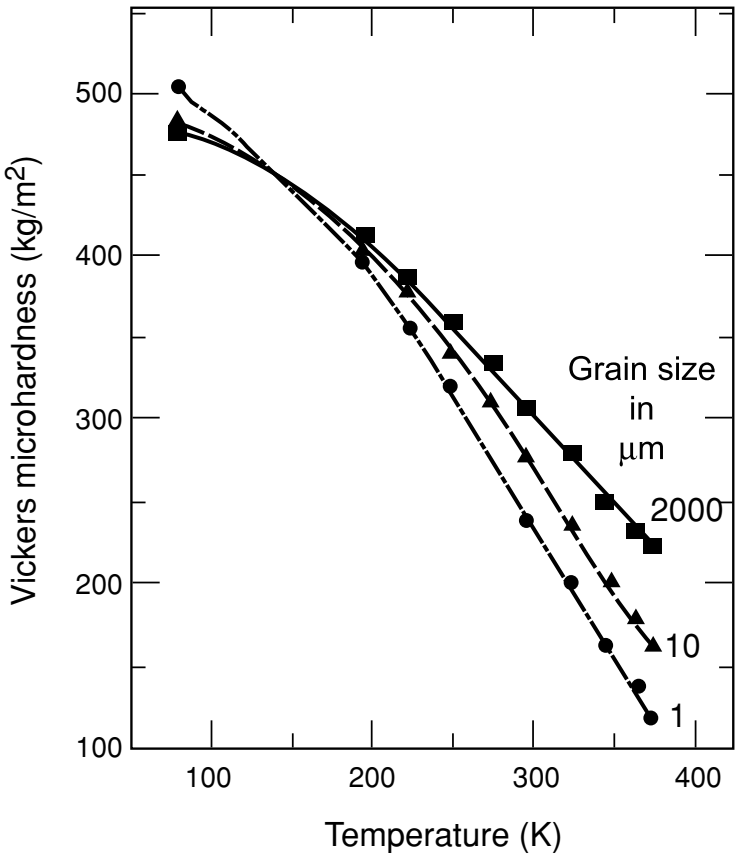

Fig. 7.61 *Vickers microhardness as a function of temperature for unalloyed α plutonium at various grain sizes* (*after Merz and Nelson,* 1970).

additions of elements such as gallium or aluminum retain the fcc δ phase to room temperature. As expected the δ phase alloys are considerably more ductile than the monoclinic α phase. A comparison of room temperature mechanical behavior is shown in Fig. 7.62 (Hecker and Stevens, 2000). The α phase is shown to be strong and brittle (like cast iron), whereas the δ-phase Pu–Ga alloy is weak and ductile (like commercially pure aluminum). Processing of the δ-phase alloys strongly influences the mechanical properties. Particularly important are gallium segregation, which can be minimized by elevated-temperature annealing treatments and thermo-mechanical treatments (see Fig. 7.33). Robbins (2004) recently reported an extensive compilation of the mechanical properties of Pu–3.4 at.% Ga δ-phase alloys. The compression behavior of a typical, well-homogenized alloy is shown in Fig. 7.63 (from the work of Barmore and Uribe (1970)). We should note that the mechanical properties of δ-phase Pu–Al alloys are similar to Pu–Ga alloys with similar atomic concentrations of the alloying element.

Detailed mechanical properties of plutonium and various alloys, including strength, hardness, ductility, creep, impact strength, and fatigue strength are presented by Gardner (1980), by Lesser and Peterson (1976) for unalloyed

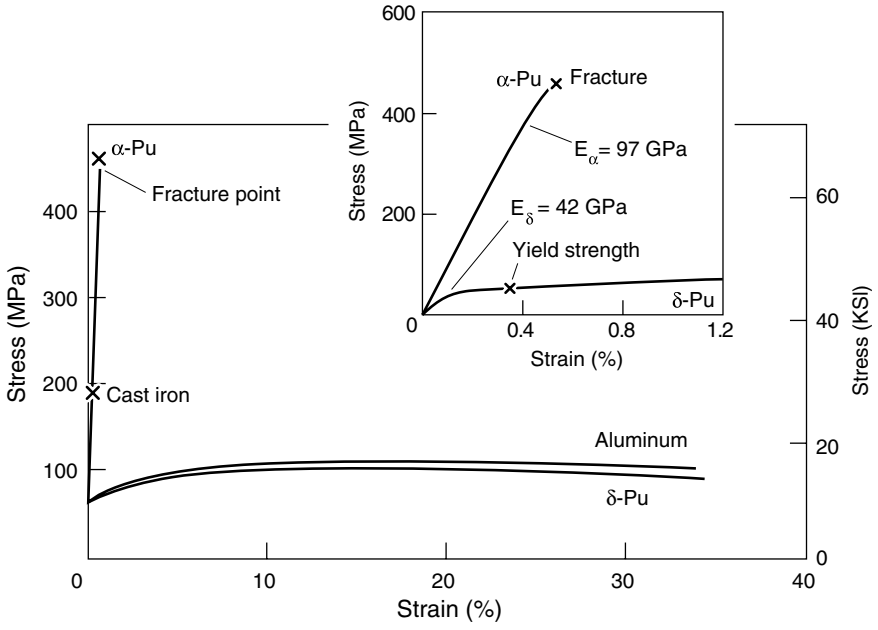

Fig. 7.62 *Typical uniaxial tensile stress–strain curves for unalloyed α plutonium compared to a δ-phase Pu–Ga alloy at a nominal strain rate of* 10^{-3} s^{-1}. *The insert shows the initial stress–strain curve at higher resolution* (*after Hecker and Stevens,* 2000).

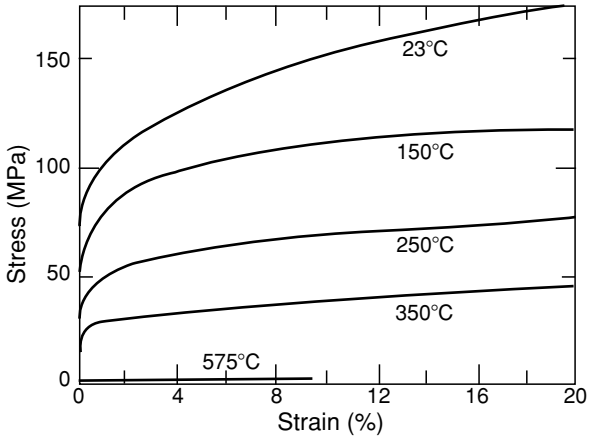

Fig. 7.63 *Uniaxial stress–strain curves in compression for a δ-phase Pu*-3.4 at. *% Ga alloy at different temperatures and a nominal strain rate of* 10^{-2} s^{-1} (*after Barmore and Uribe,* 1970).

plutonium (on pp. 29–33 of their review), and by Blank (1977) for Pu–Al alloys (pp. 180–183) and for Pu–Ga alloys (pp. 221–232). Blank (1976, 1977) also provides mechanical properties for additional alloy systems, with a particularly extensive discussion of the Pu–Fe system (Blank, 1976). Care must be taken during low-temperature experiments on δ-phase alloys to avoid transformation of the retained δ phase to the α′ phase. Since the α′ phase is so much harder than the δ phase, even small amounts of α′ result in significant strengthening.

There are few theoretical treatments of mechanical behavior of plutonium in the literature. The principal problem stems from the fact that the mechanical properties are controlled by microstructure and defects, which are still beyond the reach of *ab initio* calculations for all practical metals. Stout *et al.* (2002) developed a physically based constitutive model to predict the mechanical behavior of fcc δ-phase plutonium alloys. The input to the model was based on previous work with other fcc metals and the published test results on Pu–Ga alloys referenced above. The model is able to predict the temperature and strain-rate effects on the yield and ultimate strengths of Pu–Ga alloys. It also allowed the authors to isolate the effects of microstructural variables such as grain size, alloy content, and impurity content. The effect of gallium solutes has the largest strengthening effect. The yield strength increases by 50% with an increase in gallium from 1 to 6 atomic percent. The grain size effect follows the classical Hall–Petch relationship:

$$\sigma_y = \sigma_0 + \kappa/\sqrt{d} \tag{7.28}$$

where σ_y is the yield strength for a grain diameter d in μm, and σ_0 and κ are measured constants. Hence, decreasing grain size leads to increased strength in

the deformation regime controlled by dislocation glide. (We note that in the deformation regime dominated by grain boundary sliding, the relationship is inverted – small grain size leads to lower strength.) The parameters for Pu–Ga alloys are given by Stout *et al.* (2002). The model allowed them to demonstrate that the typical impurities (such as C, O, N, and Fe form hard inclusions of μm to tens of μm in diameter) in these alloys have little effect on strength values at ambient temperature. However, the fracture behavior will be affected negatively by higher impurity contents. In addition, Beitscher (1970) showed that iron impurities at the level >300 ppm lead to dramatic high-temperature embrittlement (at 683 K and low strain rates) because the Pu_6Fe intermetallic inclusions melt and lead to brittle behavior known as 'hot shortness.'

7.7.8 Oxidation and corrosion in plutonium metal and alloys

Degradation of plutonium surfaces under various atmospheric conditions is of concern during handling and for all considerations that require storage of plutonium, its alloys, or its compounds. Although plutonium is a reactive metal as suggested by a standard reduction potential of –2.02 V for the Pu^{3+}/Pu^0 couple (see Fig. 7.116a), its oxidation rate in very dry air (<0.5 ppm H_2O) is a minuscule 20 pm h^{-1} (Haschke *et al.*, 1996). Clean plutonium surfaces have a silvery, metallic sheen, similar to clean iron or nickel. Plutonium loses its metallic sheen quite rapidly in most atmospheres. It takes on a darker appearance and exhibits interference colors before it begins to develop a loose, olive-green powder of PuO_2 'rust' (see Section 7.8.5.a). Although this process occurs quite slowly in most of the protective atmospheres in which plutonium is handled, experience over the years has yielded many surprises, including pyrophoric behavior and anomalous corrosion rates catalyzed under complex atmospheric conditions of hydrogen or moist air that can increase surface corrosion rates by a staggering 13 orders of magnitude. The enhanced oxidation rates in the presence of moisture were already discovered at Los Alamos during the Manhattan Project by Covert and Kolodney (1945). Uncontrolled surface reactions are one of the greatest risks during storage or use of plutonium metal. Not only do these reactions change the geometry of the material, they typically result in finely powdered forms that are more readily dispersed, and hence, increase the health risk of inadvertent release and uptake of plutonium, a safety hazard of paramount importance for long-term plutonium storage (Haschke *et al.*, 1998).

Waber (1980) summarized the available knowledge on corrosion and oxidation of plutonium up to 1964. Subsequent results to 1976 were summarized by Lesser and Peterson (1976). More recently, Haschke *et al.* (2000a) presented a current understanding of corrosion and oxidation, and Hecker and Martz (2001) summarized current understanding and presented practical examples of plutonium corrosion problems. Much of the discussion here is based on the

report of Hecker and Martz. We refer the reader to Lesser and Peterson (1976) for a description of the reaction of plutonium with other gases such as nitrogen and ammonia at higher temperatures as well as surface reactions of plutonium with acids and other solvents.

(a) Oxidation in air

Corrosion rates depend greatly on plutonium surface chemistry. Hence, it is crucial to understand the specific surface chemistry for different plutonium substrates and for different atmospheric conditions. In dry air, the reactive plutonium metal surface is passivated by a layer of protective $PuO_{2\pm x}$ that forms rapidly over the entire surface. In the Pu–O system, Pu(IV) is a stable oxidation state and forms a classic fluorite-type crystal structure, with four plutonium cations per unit cell arranged in an fcc lattice, and eight oxygen anions at the tetrahedral interstices in a simple cubic packing (as discussed in Section 7.8.5.a, and shown in Fig. 7.90).

The oxidation rate is controlled by the diffusion of oxygen through the oxide surface to the oxide–metal interface, yielding classic parabolic growth rates. Significant stresses build up at the interface because the density of the oxide is 11.46 g cm^{-3} compared to pure α plutonium at 19.86 g cm^{-3}. The oxide layer reaches a steady-state thickness of 4 to 5 μm because at this thickness the oxide begins to spall, leading to a balance between spalling of the oxide and re-oxidation of the surface (Martz *et al.*, 1994). A constant isothermal oxidation rate is maintained by diffusion of oxygen through an oxide layer of constant average thickness. Fig. 7.64 also shows that corrosion rates depend strongly on temperature and atmospheric conditions. The details of this behavior are presented by Haschke *et al.* (1998) and discussed by Hecker and Martz (2001). Activation energies of oxidation in unalloyed plutonium are reported by Blank (1977), based on the work of Thompson (1965), to be 96.2 kJ mol^{-1} for the α phase, 50.2 kJ mol^{-1} for the β phase, and 58.6 kJ mol^{-1} for the γ phase, each in their temperature range of phase stability. However, Blank points out that significantly different results have been cited by other authors because of the substantial influence of microcracks, impurities, and crystallographic textures. The reader is referred to Haschke *et al.* (1998) for a more detailed discussion of the thermodynamics and kinetics of the oxidation process.

(b) Moisture-enhanced oxidation

Corrosion of plutonium metal in moist air occurs at a rate 200 times greater than in dry air at room temperature and five orders of magnitude greater at 100°C. The mechanisms of water-catalyzed corrosion of plutonium have only recently been elucidated (Haschke *et al.*, 1996). It had been generally accepted that the greatest oxygen concentration possible in plutonium oxide was in the

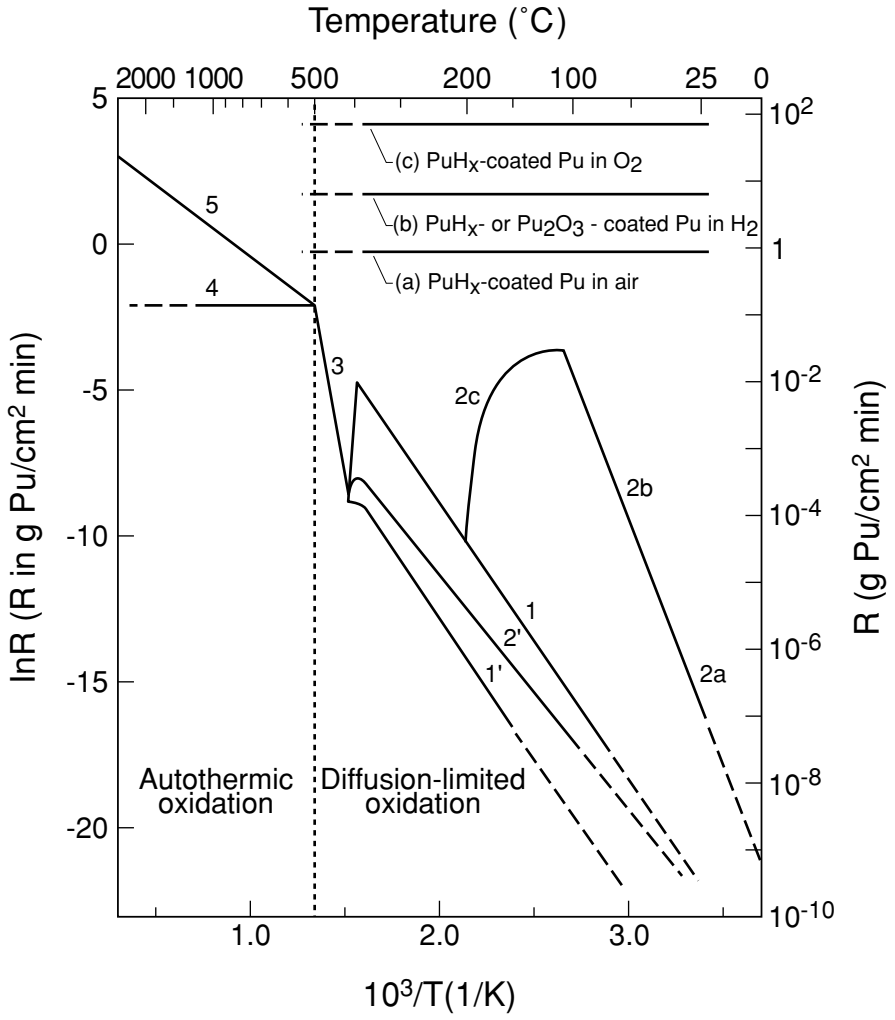

Fig. 7.64 *Oxidation rates of plutonium vs temperature. Curve* 1 *shows the oxidation rate for pure plutonium exposed to dry air or oxygen at an* O_2 *pressure of* 21.3 kPa. *Curve* 2*a presents the oxidation rate when the same, dry Pu samples are exposed to water vapor at the same pressure* (21.3 kPa). *Note the increase of four orders of magnitude in oxidation rate. Curves* 2*b and* 2*c extend the water-exposed oxidation rate to the temperature ranges of* 61–110°C *and* 110–200°C, *respectively. The drop in oxidation rate at higher temperatures is not fully understood, but may be related to the lack of spallation of product oxide at higher temperatures. Curves* 1′ *and* 2′ *present oxidation data for Ga-stabilized δ Pu in dry and moist air, respectively. Distinctions in oxidation rates for various alloys and conditions disappear at high temperatures as shown by curve* 3. *Curve* 4 *shows the constant oxidation rate observed under static conditions, while curve* 5 *shows recent data extrapolated from ignited Pu droplets oxidizing during free-fall in air. The reactions of hydride-coated Pu are shown in curves a–c. Curve a shows the constant reaction rate for hydride-coated Pu exposed to dry air. This represents an increase in reaction rate of over* 10^9 *compared to pure Pu. Curve c shows the same material exposed to pure oxygen. This reaction is* 10^{13} *times faster than pure Pu exposed to* O_2. *Finally, curve b shows the constant reaction rate of either hydride- or cubic sesquioxide-coated Pu to hydrogen* (*at* 101 kPa) (*Martz and Haschke,* 1998*; Haschke* et al., 2000*a*).

dioxide, namely $PuO_{2.0}$. However, Stakebake *et al.* (1993) and Haschke *et al.* (2000a, 2001) demonstrated that hyperstoichiometric plutonium oxide, PuO_{2+x}, forms in the presence of either gaseous or liquid water. The largest value they measured for x was 0.26. Rapid oxidation by adsorbed water produces hydrogen at the gas–solid interface and forms a higher oxide as Pu(IV) cations in PuO_2 are replaced by Pu(V) and an equal number of O^{2-} or OH^- ions in interstitial defect sites (see Section 7.8.5). In moist air, product hydrogen combines with disassociatively adsorbed oxygen to reform water on the surface. A water-catalyzed cycle is propagated as Pu and O_2 are transformed into oxide at the rapid rate characteristic of the metal–water reaction. This change in the composition of the oxide is also accompanied by a dull yellow to a khaki-to-green color change.

(c) Oxidation behavior of plutonium alloys

The overall rate of oxidation is less for alloyed plutonium in the fcc δ phase than it is for unalloyed plutonium (shown in Fig. 7.64) because the lowered stresses upon oxide formation (the δ-phase density is 15.8 g cm^{-3} compared to 19.86 g cm^{-3} for the α phase). Haschke (1999) has also speculated that gallium is not incorporated in the PuO_2 lattice and resides in octahedral sites of the fluorite structure. Consequently, since oxygen diffusion occurs via these sites, he suggested transport of oxygen through the oxide layer may be inhibited. Blank (1977) summarized the work of Raynor and Sakman (1965) and Waber (1980) on oxidation of plutonium δ-phase alloys. Pu–Ga alloys were found to oxidize at a lower rate than unalloyed plutonium at all temperatures in moist air. The oxidation rates were found to be greater in moist argon. However, the protection afforded by alloying was less for the case of moist argon than for moist air. Blank (1977) also summarized oxidation results for Pu–Al alloys. A partial summary, presented in Table 7.24, shows that the addition of aluminum lowers the oxidation rate, but that the behavior depends strongly on temperature and relative humidity. As examples of actual weight gain through oxidation, Blank cites the results of Waber *et al.* (1961): 0.1 mg cm^{-2} for Pu–9 to 12 at.% Al alloys after 500 h at 75°C and 50% relative humidity and 0.5 mg cm^{-2} for Pu–8 at.% Al after 8700 h at 35°C and 20% relative humidity. Blank (1977) also provided a summary of the oxidation behavior of Pu–Fe and other alloys.

(d) Pyrophoricity of plutonium metal in air

Fig. 7.64 also shows that at elevated temperatures, plutonium exhibits an autothermic reaction, igniting spontaneously in air when the temperature reaches 500°C. Studies of pyrophoricity of plutonium by Martz *et al.* (1994) helped to elucidate the role of another oxide of plutonium, namely the cubic (bcc) sesquioxide, Pu_2O_3. The revised view of the plutonium–oxygen interface is shown in Fig. 7.65. Although the dioxide is the one observed when plutonium

Table 7.24 *The relative merit given by the merit ratio (MR) as defined by weight increase of unalloyed α-phase plutonium divided by the weight increase of a δ-phase Pu–Al alloy after the oxidation of the samples by water vapor as compiled by Blank* (1977).

Al content at.%	*T* (°C)	*Relative humidity* (%)	*Time* 12 h	*Time* 50 h	*Time* 1000 h	*Time* 4300 h	*Time* 8700 h	*References*
3.5	30	95			8			Sackman (1960)
3.5	90	95	130					Sackman (1960)
3.5	90	55	50	100	120			Sackman (1960)
3.5	100	0			6			Sackman (1960)
3.0	55	50					~17	Waber (1958)
9	75	50			666			Waber *et al.* (1961)
8	35	20			~19	42.5	51	Waber (1958)

metal is exposed to oxygen or air, there is always a layer of the cubic sesquioxide present at the metal-oxide interface. However, at room temperature, its thickness is small compared to that of the dioxide. The cubic sesquioxide acts as a layer that separates the oxide-rich surface from the plutonium-rich substrate, being simultaneously consumed and formed by competing reactions. The thickness of these various oxides depends upon a variety of factors including temperature and oxygen concentration. At temperatures exceeding 150°C and in oxygen-poor environments, the cubic sesquioxide becomes the predominant phase, appearing as a surface product under oxygen-free environments.

Martz *et al.* (1994) explained the apparent paradox that plutonium metal with low specific surface areas ignites at temperatures above 500°C, whereas metal with large specific surface areas (turnings, chips, and powder) spontaneously ignites in air at temperatures between 150 and 200°C. In such cases, Martz *et al.* concluded that heating metal to 150–200°C in air transforms a large fraction of the surface oxide to cubic sesquioxide. Rapid oxidation of the sesquioxide back to dioxide produces a thermal spike sufficient to heat high-surface-area chips and turnings to the autothermic reaction temperature of 500°C.

(e) Hydrogen- and hydride-catalyzed corrosion

Plutonium reacts readily with hydrogen at rates unprecedented for other metals. It forms an fcc solid solution of PuH_x hydrides with a fluorite structure similar to plutonium oxides (Haschke, 1991; Bartscher, 1996) as discussed in Section 7.8.1 and shown in Fig. 7.72. The hydrogen mole ratio, x, varies from 1.9 to 3.0. As the hydrogen content increases, the hydride exhibits a transition from metallic material near $x = 2$ to a semiconductor near $x = 3$. The electronic structure of the hydride is complex, with electrons apparently being removed from the conduction band and bound as H^- on octahedral sites as the hydrogen concentration is increased in the hydride.

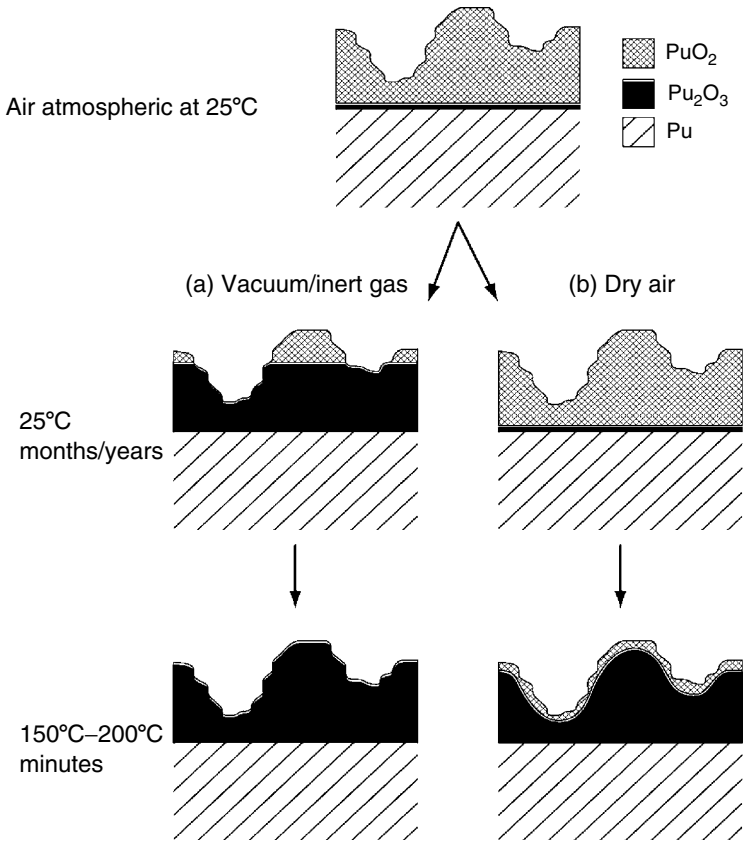

Fig. 7.65 *Evolution of the oxide layer on metallic plutonium. These simplified sketches present the structure of the oxide on Pu. In air, a constant thickness of PuO_2 is present on a thin layer of cubic Pu_2O_3. If this surface is exposed to inert conditions (vacuum or inert gas), the PuO_2 autoreduces to a thicker layer of Pu_2O_3. At elevated temperatures, the rate of the autoreduction reaction increases, increasing the thickness of the internal Pu_2O_3 layer under all conditions. Oxidation of this layer and its subsequent heat evolution is the attributed cause for the pyrophoric behavior of thin films and small particles (Martz* et al., 1994). *In addition, the growth of Pu_2O_3 under inert conditions at elevated temperatures will activate the surface to the hydride reaction, a fact exploited in the hydride–dehydride recovery process for metallic plutonium.*

Reactions of hydrogen on metallic plutonium are complicated by the ever-present layer of plutonium dioxide. Hydrogen gains access to the metal surface only after the dioxide layer is penetrated at cracks or spallation sites, making the nucleation of the hydride reaction heterogeneous. The hydriding rate increases exponentially as nucleation sites grow. Once the entire metal surface is covered with hydride, the reaction occurs very rapidly at rates of 20 cm h^{-1} linear

penetration for H_2 at 1 bar compared to the rate of the oxidation reaction of 20 pm h^{-1} in dry air (10^{11} times faster). Haschke (1991) has suggested that this catastrophic enhancement occurs by one of two mechanisms. First, if PuH_x forms, it catalyzes the dissociation of adsorbed H_2 and promotes transport of atomic hydrogen to the hydride–metal interface. Or alternatively, if cubic Pu_2O_3 is exposed to H_2, then the hydride reaction begins instantaneously because Pu_2O_3 also catalyzes the dissociation of H_2 and becomes the medium for hydrogen transport. In either case, rapid dissociation of adsorbed H_2 results in a dramatic enhancement of the reaction rate. Further, the transport of anions in the fluorite structures of PuH_x or cubic Pu_2O_3 is potentially very rapid because in these anion-deficient fluorite structures both tetrahedral and octahedral sites may be vacant and able to participate in the transport of anions such as hydrogen and oxygen (see Sections 7.8.1 and 7.8.5). Another factor is the high self-diffusivity of oxygen in nonstoichiometric PuO_{2-x}, which increases dramatically from PuO_2 to Pu_2O_3.

If a hydride-coated plutonium surface is exposed to oxygen, it has been proposed that PuH_x will promote a dramatic catalytic enhancement of the corrosion rate (Haschke and Martz, 1998a). In this proposed mechanism, oxygen reacts with the pyrophoric plutonium hydride to produce heat and an oxide layer. The temperature is raised sufficiently that the cubic sesquioxide is preferentially formed. The hydrogen produced at the oxide–hydride interface moves through the PuH_x layer increasing the stoichiometry of the hydride. Excess hydrogen is continuously produced at the oxide–hydride interface and consumed at the hydride–metal interface. Thus, hydrogen is involved in a classic catalytic cycle to enhance the oxidation rate. This hydride-catalyzed reaction continues until all the metal is consumed. The rate for reaction of hydride-coated metal with pure oxygen (Fig. 7.64) is 10^{13} times greater than oxidation rates in dry air. Hydride-coated plutonium also reacts rapidly in air. However, the rate is 100 times slower than that in oxygen, apparently due to additional steps involving reaction or transport of nitrogen in air (Haschke, 1991). These fast reactions generate large amounts of heat (approximately 836.8 kJ mol^{-1} of plutonium), which can produce thermal hazards as well. Of additional concern is the possibility of plutonium nitride formation when the temperature exceeds 200–250°C and hydride is exposed to the nitrogen in air. This reaction results in a consumption of all of the major gases in air, preventing the formation of an inert nitrogen 'blanket' and allowing the reaction to proceed to completion within many storage environments. Hecker and Martz (2001) describe some of the practical consequences of enhanced corrosion problems in the storage of plutonium.

7.7.9 Aging and self-irradiation damage in plutonium

The aging of plutonium and its alloys has received increased attention during the past decade because of interest in extending the lifetimes of plutonium components and in the long-term storage of excess weapons-grade plutonium.

Several reviews of the salient aging issues have been reported by Hecker and Martz (2000, 2001), Wolfer (2000), Martz and Schwartz (2003), and Wirth *et al.* (2001). The complexities of plutonium materials are compounded by changes that occur with age. Phase stability is of concern because the various allotropic phases of plutonium are very close in energy and, hence, sensitive to any changes, including kinetic changes, that can occur with time at temperatures close to ambient. The differences in U.S. and Russian phase diagrams for Pu–Ga (Fig. 7.29) demonstrate that we lack definitive information on some basic characteristics of plutonium alloys such as thermodynamic steady-state phase stability. In addition, the very reactive nature of plutonium just described makes it especially susceptible to surface-induced modifications resulting from different atmospheric environments. If that were not sufficient, the most perplexing change is caused by the radioactive decay of the plutonium nucleus in its various isotopic forms. Moreover, in most practical applications the effects of these three types of aging-induced changes occur simultaneously and in synergy causing significant changes in plutonium and its alloys over time. The phase stability and surface behavior were described in some detail above. We will provide additional details of the salient consequences of self-irradiation damage and transmutation resulting from radioactive decay in plutonium and its alloys.

The two primary consequences of plutonium radioactive decay are the displacement damage in the lattice induced by the self-irradiation, and the transmutation of plutonium into its decay products. Displacement damage can cause changes in lattice parameters, the accumulation of defects and, potentially, void swelling. Transmutation may upset the delicate balance of phase stability and lead to phase changes. One of the decay products, helium, is of particular concern because it can form helium bubbles if self-irradiation occurs at temperatures at which helium is mobile. Schwartz *et al.* (2005) provided an excellent overview of the effects of self-irradiation in plutonium. They identified three self-irradiation-related effects that could cause dimensional changes: lattice damage resulting in an initial transient, helium accumulation, and void swelling.

The unstable plutonium nucleus decays principally by α-particle decay. Two primary energetic nuclear particles are produced by α decay – an α particle and a recoil nucleus. These primary particles are created in much less than a femtosecond (10^{-15} s). The range of the 5 MeV α particle is approximately 10 μm within the crystal lattice. The α particle captures two electrons from the plutonium metal and comes to rest in the lattice as a helium atom. The light α particle loses nearly 99.9% of its energy to electrons, heating the plutonium lattice. Some atomic displacements occur near the end of range, producing ~265 Frenkel pairs (vacancies and self-interstitial atoms). Wolfer (2000) calculated the helium generation to be ~41 atomic ppm per year.

The 86 keV ^{235}U recoil nucleus has a range of ~12 nm and creates roughly 2300 Frenkel pairs. Calculations by Wolfer (2000) showed that there are 3×10^9 α events g^{-1} s^{-1} for a typical ^{239}Pu isotopic mix, resulting in a lattice

displacement rate of roughly 0.1 displacements per atom (dpa) per year. Wolfer (2000) and Wirth *et al.* (2001) used molecular-dynamics simulations showing that in the first 200 ns, 90% of the Frenkel pairs return to their original lattice sites, whereas the other 10% remain as free interstitials and vacancies or interstitial/vacancy clusters. In reactor applications, it was shown that these types of microstructural changes ultimately result in property changes that include void swelling, mechanical hardening, and embrittlement. Wirth *et al.* pointed out that although the damage produced by the α particle and the uranium recoil atom are different, it is the eventual interaction and evolution of these spatially uncorrelated primary defects that may, over time, drive materials evolution and the aging process, thus producing microstructural changes over time scales as long as many decades.

(a) Self-irradiation lattice damage

Studies of self-irradiation lattice damage in plutonium at low temperatures (at which little or no annealing of nonequilibrium defect structures is expected) were reported as early as 1962 by American researchers (Olsen and Elliott, 1962) and British researchers (Lee *et al.*, 1962; Wigley, 1964, 1965), and in 1965 by French researchers (Lallement and Solente, 1967). However, more than 40 years later, we still understand little about the mechanisms of defect migration and agglomeration in plutonium. Few measurements and direct observations of the defect structures in plutonium have been made compared to the vast body of literature that exists for irradiation-induced defect structures in other metals and alloys; see Ehrhart *et al.* (1991) for an excellent review. The early work showed that plutonium undergoes substantial lattice damage as determined by increases in electrical resistivity and by length changes. As shown in Fig. 7.66, the α phase in unalloyed plutonium expands during self-irradiation at 4.2 K. Retained β-phase and retained δ-phase plutonium alloys contract. As discussed below, self-irradiation damage of δ-phase plutonium at room temperature results in a volume expansion. All three phases exhibit increases in electrical resistivity with self-irradiation at this temperature; see Hecker and Martz (2001) for more detailed discussions.

Marples and Hall found that if low-temperature irradiation was allowed to proceed sufficiently long, lattice expansion in the α phase saturated at approximately 10.5 vol %. In the δ-phase alloy, lattice contraction saturated at –15 vol %. Their results on all three phases examined are summarized in Table 7.25. Interestingly, all three phases appear to converge to the same density, 18.4 g cm^{-3}. These results may indicate that all three phases are becoming increasingly disordered, approaching an amorphous state. It would not be surprising to create local amorphous regions as a result of the collision cascades following α-decay events. At sufficiently low temperatures, in the absence of significant defect rearrangement, these regions could eventually consume the entire sample. However, the XRD work done at low temperatures showed that

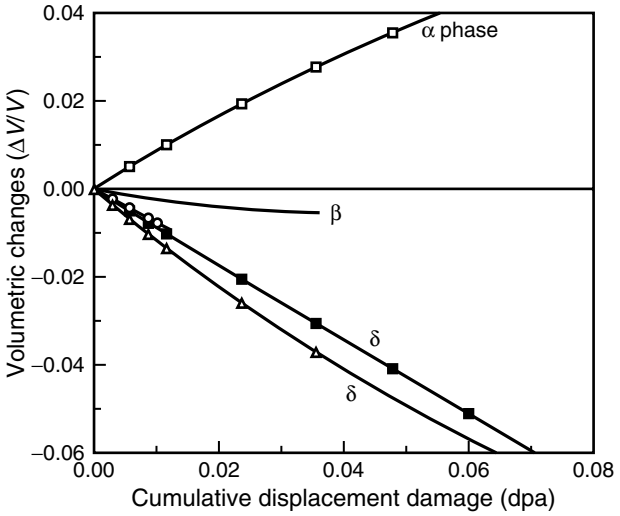

Fig. 7.66 *Volume change vs damage in* dpa (*displacements per atom*) *during self-irradiation of plutonium at* 4.2 K. *The α-Pu data is from Marples* et al. (1970), *as are the data for the δ-phase Pu-*6 at. *% Al alloy* (*solid squares*). *The triangles represent data from Jacquemin and Lallement* (1970) *on a δ-phase Pu-*6 at. *% Al alloy. The β phase was retained by the addition of* 4 at. *% Ti as reported also by Jacquemin and Lallement. Marples* et al. *reported a calculated saturation in volume change of* 10.5% *for the α phase and* –15% *for the δ phase.*

Table 7.25 *Initial and final densities for plutonium self-irradiated at* 4 K (*Marples and Hall,* 1972).

Phase	*Initial density* (g cm^{-3})	*Final density* (g cm^{-3})
α	20.3	18.4
β	18.2	18.4
δ	15.6	17.4
		18.3 after correction for presence of 6 at.% Al

the initial crystal structures were retained, although significant line broadening was observed.

At ambient temperature, damage from self-irradiation of plutonium is partially annealed out by thermally activated recovery. Lattice damage created at low temperatures is also annealed out as the temperature is raised. Some of the early experiments of Wigley (1964, 1965) are summarized by Hecker and Martz (2001). Typical damage recovery (based on electrical resistivity measurements)

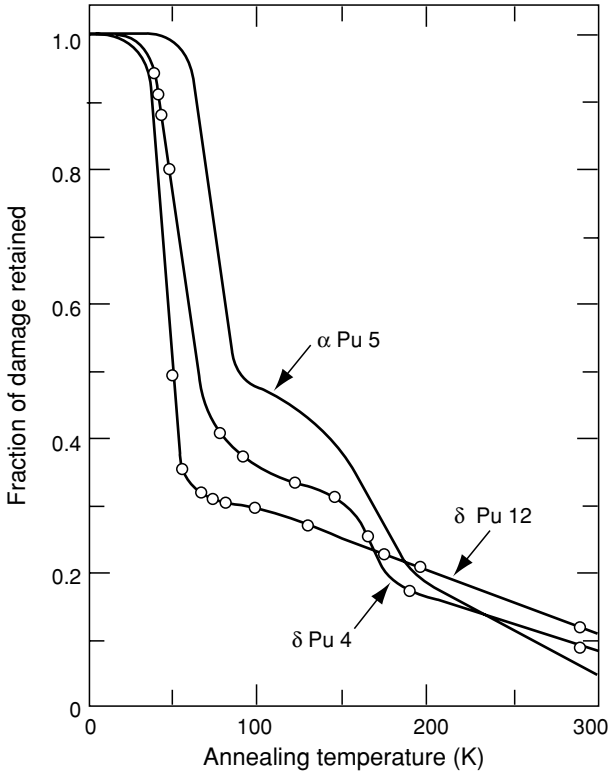

Fig. 7.67 *Damage recovery during isochronal annealing after self-irradiation at* 4.5 K. *δPu*4 *is for an alloy of Pu-*4 at. *% Al with* 920 h *at* 4.5 K. *δPu*12 *is for an alloy of* Pu-12 at. *% Al with* 665 h *at* 4.5 K. *The α-Pu sample, αPu*5, *was self-irradiated for* 640 h *at* 4.5 K (*from Hecker and Martz,* 2001 *based on original data from Wigley,* 1965*; King* et al., 1965).

during isochronal annealing of self-irradiated unalloyed plutonium and δ-phase Pu–Al alloys is shown in Fig. 7.67, based on the work of Wigley (1965) and King *et al.* (1965). Based on comparison to a vast literature of irradiation damage in metals (Ehrhart *et al.*, 1991), Hecker and Martz estimated the following temperatures for the key recovery stages in plutonium alloys: ~18 K for Stage I (recombination and migration of self-interstitials); ~180 K for Stage III (vacancy migration and annihilation); and 410 K for Stage V (thermal dissociation of vacancy and/or interstitial clusters). Unfortunately, the data on plutonium are limited and difficult to interpret quantitatively because of incomplete information about precise isotopic contents, purity levels, prior age, and processing conditions. Wirth *et al.* (2001) reported on recent self-irradiation and isochronal annealing experiments. They found the onset of Stage I to be diffuse and difficult to determine. Their best estimates for the temperatures for the onset

of Stage III and Stage V were 190 K and slightly above 320 K. Hence, the defect mobility in plutonium alloys at ambient temperature is substantial. Although much of the damage is healed at room temperature, some of it remains.

For self-irradiation at ambient temperature, we would then expect lattice damage to compete with recovery resulting from the defect mobility. Chebotarev and Utkina (1975) reported a lattice expansion in δ-phase plutonium alloys. Wolfer (2000) showed that the initial transient results in the formation of dislocation loops that lead to expanded lattice parameters, which tend to saturate within approximately 2 years. Unlike at low temperatures, both the unalloyed α-phase plutonium and alloyed δ-phase plutonium exhibit lattice expansion with age. Ellinger *et al.* (1962a) reported that X-ray samples of typical plutonium in the δ phase (alloyed with 12.8 at.% Al) retained their fcc crystal structure with a 0.1% expansion of the lattice constant (0.3% volume change) after 10 years at ambient temperature. Chebotarev and Utkina (1975) also reported slight lattice expansion in δ-phase Pu–Al alloys, with the expansion increasing with increasing aluminum content. For aluminum contents slightly below 10 at.%, they found an expansion of the lattice parameter of 0.25% after 2.5 years at ambient temperature. They also reported that all changes were recovered after a long-term anneal at 423 K.

Morales *et al.* (2003) confirmed that δ-phase alloys expand at ambient temperature and possibly undergo an orthorhombic distortion at long aging times. In recent TEM studies of aged δ-phase plutonium alloys, Schwartz and coworkers observed nanometer-size helium bubbles (see Wirth *et al.*, 2001; Martz and Schwartz, 2003; Schwartz *et al.*, 2005). These will be discussed in greater detail below.

We report one additional important aspect of self-irradiation damage in plutonium described in recent presentations and abstracts by Russian researchers Gorbunov and Seleznev (2001). They studied unalloyed plutonium consisting mostly of ^{238}Pu, which increased the α-decay damage rate by a factor of 240 over the typical ^{239}Pu. They used thin films to keep the temperature close to room temperature. Starting with a sample of α-phase plutonium, their XRD measurements demonstrated that the sample experienced numerous crystallographic transformations over the period of 1 year (equivalent to 240 years of aging for the typical mix of isotopes in plutonium). Specifically, they claim to find evidence that all six phases of plutonium coexisted at 40 to 50 days of age, and that after roughly 1 year, the sample consisted mostly of the α and δ phases. They suggest that the vacancies and vacancy clusters resulting from the intense self-irradiation affect the delicate balance between bonding and localized 5f electrons and, hence, affect phase stability.

(b) Actinide transmutation products and radiogenic helium

In addition to the lattice damage described above, α decay also results in transmutation products. The decay products for plutonium isotopes and

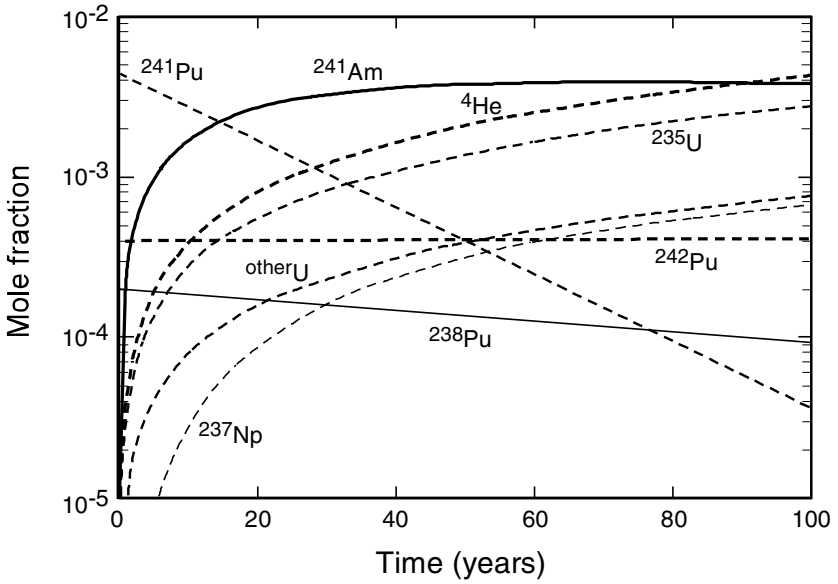

Fig. 7.68 *Transmutation products in typical* ^{239}*Pu metal* (*from Hecker and Martz,* 2001) *as a function of time. For typical* ^{239}*Pu,* 10 years *results in* 1 dpa.

its transmutation products are shown in Fig. 7.68. Helium grows in at the rate of 41.1 atomic ppm per year (based on the assumption made by Wolfer (2000) for typical plutonium). Hence, after 50 years of storage, approximately 2000 ppm helium, 3700 ppm americium, 1700 ppm uranium, and 300 ppm neptunium have grown into plutonium metal. After that length of time, a 1 kg piece of plutonium will contain nearly two-tenths of a liter of helium (measured at standard conditions). Several thousand ppm of americium should help to further stabilize δ-phase alloys. For pure plutonium it is conceivable that the in-growth of americium could stabilize microscopic regions of higher-temperature phases in the monoclinic α phase. However, in both cases, the nonequilibrium conditions that exist immediately following the decay event may further complicate the effects of the transmutation products. Under equilibrium conditions, uranium and neptunium reduce δ-phase stability. As in the case of americium, however, the effect of their presence associated with decay products under the nonequilibrium conditions is not well understood. Our best estimate is that the in-growth of actinides, other than americium, over a time frame of decades should have no major macroscopic effects, but their presence as atomic impurities may influence some microscopic processes. In addition, one must take account of the heat generated during the decay process. For the typical isotopic mixtures discussed above,

the heat is a rather modest 2 W kg^{-1}, making kilogram quantities of plutonium warm to the touch. On the other hand, ^{238}Pu used in radioisotope heat sources is roughly 250 times more radioactive.

The accumulation of radiogenic helium, on the other hand, could potentially affect the properties of plutonium significantly. It is well known that less than 100 ppm of helium in fcc stainless steel can cause swelling or dramatic embrittlement. Once helium atoms are generated in the plutonium lattice, they quickly fill nearby vacancies and diffuse through the lattice as helium-filled vacancies (Howell *et al.*, 1999). Wirth *et al.* (2001) calculated that at relatively high helium generation rates, a critical helium bubble nucleus consists of just two helium atoms and one or two vacancies. Russian researchers (Filin *et al.*, 1989) used angle-resolved positron annihilation to study self-irradiation-induced defects in aged δ-phase Pu–3.6 at.% Ga with 800 ppm helium. They concluded that elementary complexes of helium and vacancies are energetically favorable. Their results showed that pores with radii of 0.4–0.8 nm and 17–23 nm formed at temperatures above 200°C. They concluded that the small pores are probably simple helium-vacancy complexes and the larger pores are complex helium-vacancy clusters, possibly also associated with solute atoms. They observed groups of small bubbles with diameters <1 μm by optical metallography after heating the aged plutonium alloy above 425°C. Using TEM, Zocco and Rohr (1988) observed helium bubbles of 3–7 nm and 10–15 nm in diameter in a 10-year-old δ-phase Pu–Ga alloy after annealing at 400°C. Decades-old plutonium will not only swell substantially after heating to such temperatures, but may also suffer major microstructural void damage under these conditions.

Schwartz and coworkers recently observed nanometer-sized helium bubbles using a Fresnel fringe imaging technique in TEM. Schwartz *et al.* (2005) examined Pu–Ga δ-phase alloys ranging in age from 6 months to 42 years. Their observations revealed that the dominant defects attributable to self-irradiation damage at ambient temperature are nanometer-sized, homogeneously distributed helium bubbles as shown in Fig. 7.69. They found no bubbles in the 6-month-old sample above their resolution limit of 0.7 nm. For samples 16–42 years old, they reported a number density of bubbles in the range of $0.6–2.0 \times 10^{17}$ cm^{-3}, which increases at a steady rate with time. The average diameter of the bubbles in this age range varies from 1.3 to 1.6 nm and is observed to change little with age beyond 16 years. The volume fraction of bubbles increased from roughly 0.01 to 0.03% within the age range of 16–42 years. Based on positron annihilation spectroscopy by Howell and Sterne (personal communications to Schwartz) (Howell and Sterne, 2002), Schwartz *et al.* concluded that helium bubbles containing two to three helium atoms per vacant site must already be present in 6-month old plutonium. Moreover, the characteristic positron lifetime of 180–190 ps remains remarkably constant for

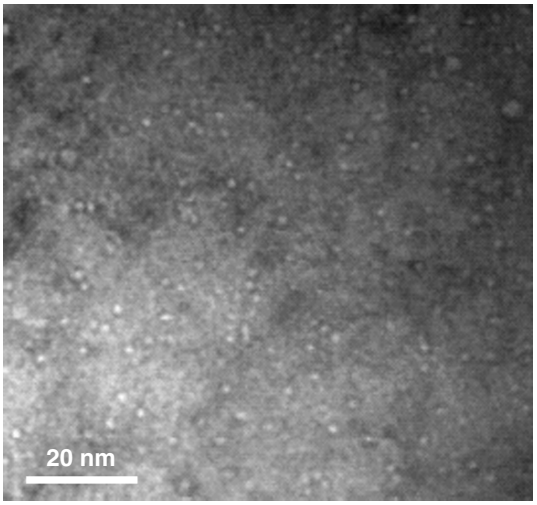

Fig. 7.69 *Transmission electron micrograph of nanometer-scale helium bubbles in a* 30+-year-*old δ-phase Pu*-3.4 at.% *Ga alloy* (*from Martz and Schwartz,* 2003; *Zocco and Schwartz,* 2003; *Schwartz* et al., 2005).

all aged material, implying a constant helium density within the bubbles of 2 to 3 helium atoms per vacant site.

The combination of irradiation-induced lattice damage and the presence of helium can cause void growth and bulk swelling at much lower temperatures without the presence of helium bubbles. Void growth is an obvious potential consequence of vacancy migration and clustering. Sustained void growth requires both the presence of biased defect sinks and the presence of neutral sinks. Wolfer (2000) estimated that for δ-phase plutonium alloys this may vary from 1 to 10 dpa (lifetimes from 10 to 100 years for typical ^{239}Pu). No experimental evidence for void swelling in plutonium has been found to date. In addition, our experience at Los Alamos shows that δ-phase plutonium aged at ambient temperature for 30–40 years retains structural integrity and exhibits no discernable microstructural changes. The influence of aging on the full range of plutonium properties remains to be assessed.

7.8 COMPOUNDS OF PLUTONIUM

From an historical perspective, the early study of plutonium compounds was plagued with difficulties. In addition to the fact that only very small amounts of

plutonium were available for early experimentation, there were also special problems associated with the handling and manipulation due to radioactivity.

The problem of handling very small amounts of plutonium was overcome through the introduction of ultramicroscale experimental methods (Cunningham, 1949; Cefola, 1958; Fried *et al.*, 1958), and characterization of small quantities of compounds was masterfully performed by X-ray crystallography by Zachariasen (1954b), who made a major contributions to the structural chemistry of plutonium, almost entirely with Debye–Scherrer X-ray films of polycrystalline samples.

In more modern times, the available quantities of plutonium are large enough that the study of plutonium compounds can be conducted on the milligram and gram scale, and occasionally even on the multigram or kilogram scale. In the latter case, however, special safeguards to prevent criticality have to be taken (cf. Table 7.2) (Clayton, 1965; Thomas, 1969; Hunt and Boss, 1971; Hunt and Rothe, 1974; Paxton and Pruvost, 1987).

The evolution of modern techniques for handling plutonium has taken advantage of specialized high-efficiency particulate air (HEPA) filtered hoods, gloved boxes, and inert atmosphere dry boxes (Maraman *et al.*, 1975; Louwrier and Richter, 1976; Oi, 1995) that make it possible to work with plutonium with confidence, and the health and safety records of laboratories engaged in research with plutonium are very good. It cannot be denied, however, that laboratory work with plutonium and other actinide elements requires more than ordinary foresight and laboratory experience for the investigator. Laboratory safety guides (Peddicord *et al.*, 1998; *Health Physics Manual of Good Practices for Plutonium Facilities*, 1988) have been published that describe handling techniques and operational procedures in plutonium laboratories.

A considerable body of information on the compounds of plutonium has been amassed over the past 65 years, and the sheer volume of data is a testimony to the intense interest in the chemistry of plutonium. Several thorough monographs, conference proceedings, and reviews of the chemistry of plutonium before 1970 are available, and provide fascinating and often personal accounts of the many individual achievements that defined much of our current understanding in this field (Katzin, 1944; Thomas, 1944; Harvey *et al.*, 1947; Seaborg *et al.*, 1949b; Connick, 1954; Cunningham, 1954; Hindman, 1954; Seaborg, 1958; Grison *et al.*, 1960; Taube, 1964; Kay and Waldron, 1967; Miner, 1970; Blank and Lindner, 1976). Since 1970 there have been a number of comprehensive reviews (Keller, 1971; Cleveland, 1979; Wick, 1980; Carnall and Choppin, 1983; Hoffman, 2000) and finally, there are a series of modern reviews concerning a wide range of more specific topics such as chemistry in marine environments (Choppin and Wong, 1998), colloids in groundwater (Kim, 1991, 1994), bioinorganic chemistry in blood (Taylor, 1998), environmental behavior (Guillaumont and Adloff, 1992; Graf, 1994; Silva and Nitsche, 1995), behavior in carbonate media (Clark *et al.*, 1995), behavior in alkaline media (Shilov, 1998; Shilov and Yusov, 2002), actinide–lanthanide separations (Nash, 1993),

synthetic methodologies for compounds (Meyer and Morss, 1991; Morss and Fuger, 1992), and a comprehensive compendium of XRD data for plutonium compounds (Roof, 1989).

7.8.1 Plutonium hydrides and deuterides

Plutonium hydrides were first observed in 1944 (Johns, 1944) when Johns found that elemental plutonium would react rapidly with H_2 to form a continuous solid solution of varying stoichiometry, PuH_x, with $1.9 \leq x \leq 3$ according to the equation:

$$Pu(s) + x/2H_2(g) \rightarrow PuH_x(s) \tag{7.29}$$

The reaction proceeds at a range of H_2 pressures. Heating is often required to initiate and sustain the process (Haschke, 1991). The chemical reaction is facile and reversible, making hydride–dehydride cycles a convenient route for preparing powdered plutonium metal samples. It is important to emphasize that stoichiometric compounds such as PuH_2 or PuH_3 do not exist as distinct phases apart from the PuH_x solid solution, though many authors describe reactions in terms of the stoichiometry PuH_2 or PuH_3 to facilitate the balancing of equations (Haschke, 1991).

Recent interest in plutonium hydrides has emerged due to considerations of long-term storage and safe handling of plutonium metal and compounds (Haschke and Allen, 2001) and the application of the plutonium–hydrogen reaction for pyrochemical processing of excess weapons plutonium (Flamm *et al.*, 1998; Mashirev *et al.*, 2001). Several excellent reviews have appeared on the synthesis and kinetics (Haschke, 1991), the thermodynamics (Flotow *et al.*, 1984; Lemire *et al.*, 2001), and the physicochemical characteristics of plutonium and other actinide hydrides (Flotow *et al.*, 1984; Ward, 1985; Ward *et al.*, 1992; Ward and Haschke, 1994; Bartscher, 1996; Haschke and Haire, 2000).

(a) Preparation and reactivity

The only practical method for preparing plutonium hydrides is the direct reaction of plutonium metal with gaseous H_2. In general, there are no good procedures for purification of PuH_x once it is formed, so purity is generally controlled through the use of high-purity metal and gaseous reagents. Plutonium metal must be cleaned to remove surface oxide and other impurities, and this is most conveniently conducted inside a secondary positive pressure chamber within an inert atmosphere gloved box to maintain proper H_2 partial pressures and temperatures. A Sieverts apparatus, and pressure–volume–temperature (PVT) relationships are commonly employed to determine the exact Pu–H stoichiometry, which is crucial because of the stoichiometric variability in the PuH_x product ($1.9 \leq x \leq 3$). Even when the stoichiometry is carefully controlled, differences in preparation or storage can result in differences in homogeneity,

morphology, and even crystal structure (see below). Desorption of H_2 is a common problem encountered in working with plutonium hydrides, even under ambient conditions.

Plutonium hydrides are hard, typically black metallic-appearing materials that show different behaviors based on particle size and composition. The color ranges from silver near $x = 2$ to black at higher values of x. Small particles can be extremely reactive towards O_2 and H_2O, and powders near composition PuH_2 can be pyrophoric or ignite spontaneously in air (Flotow *et al.*, 1984; Haschke *et al.*, 1987; Haschke, 1991; Haschke and Allen, 2001). The hydrides can also react with N_2 and CO_2, although these reactions are quite slow. Hence all manipulations and storage should be carried out under inert atmospheres. An excellent and thorough discussion of the practical considerations necessary for preparing plutonium hydrides has appeared (Haschke, 1991).

The kinetics of the Pu–H_2 reaction have been well studied, and the highly complex reaction proceeds through induction, acceleration, parabolic, linear, and terminal stages. Detailed discussions of reaction rates and the role of catalysis are available (Haschke, 1991; Haschke and Allen, 2001). Moreover, hydride stoichiometry and composition changes induced by the addition or removal of H_2 from PuH_x are important in determining plutonium hydride reactivity.

(b) Stoichiometry and phase relationships

The PuH_x phase relationships are remarkably complex. A broad range of nonstoichiometric phases is exhibited that extends from $PuH_{1.9}$ to near stoichiometric PuH_3. Equilibrium data indicate that the hydride composition near the gas–surface interface may also vary from $PuH_{2.3}$ to $PuH_{2.7}$ while the composition at the plutonium metal–plutonium hydride interface remains close to $PuH_{1.95}$ (Ward and Haschke, 1994). The resulting stoichiometry and phase can differ between studies conducted at low temperatures and low pressures, or at high temperatures and high pressures. As a result, two notional phase diagrams, one for slow reaction at low pressure and one for rapid reaction at high pressure, have been proposed and discussed in detail by Haschke and coworkers (Haschke *et al.*, 1987) and by Bartscher (1996). These complex stoichiometry and phase relationships are best understood from consideration of the solid-state structures of the PuH_x system.

The phase relationships in the plutonium–hydrogen system are shown in the phase diagrams of Fig. 7.70 (slow reaction at low pressure) and Fig. 7.71 (rapid reaction at high pressure) (Flotow *et al.*, 1984). Hydrogen dissolves in solid and liquid plutonium (melting point 640°C) to form plutonium metal that is essentially saturated in hydrogen. This is denoted as PuH_s in the figures. Hydrogen-saturated plutonium (PuH_s) coexists with the cubic PuH_x solid solution up to composition $x \approx 1.9$. Between composition $PuH_{1.9}$ and PuH_3, a continuous solid solution forms. The exact value of x is highly dependent upon the

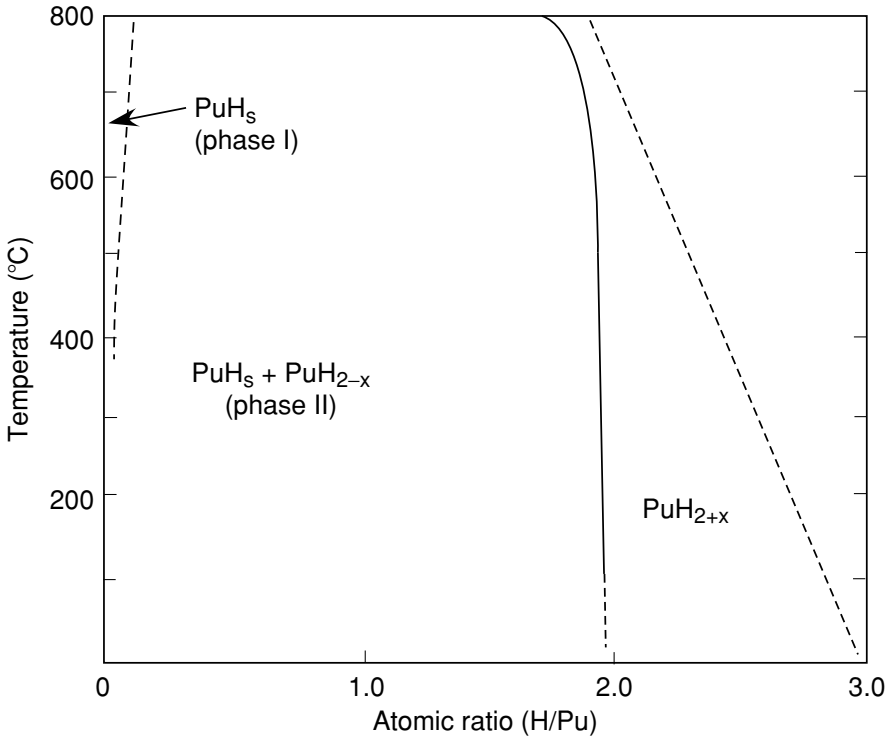

Fig. 7.70 *A plutonium–hydrogen phase diagram depicting equilibrium relationships based on Wick* (1980) *and Flotow* et al. (1984).

conditions of formation (Haschke *et al.*, 1987). The variable composition arises because the hydride reacts reversibly with H_2 between 25 and 500°C and pressures less than 1 bar (Johns, 1944; Haschke *et al.*, 1987). Extrapolation of 25°C data suggests that at 1 bar H_2 pressure, a composition $PuH_{2.93}$ is attained, while at 25 bar H_2, composition PuH_3 is attained. These observations are consistent with the phase diagram for slow reaction at low pressure shown in Fig. 7.70. An alternative phase diagram based on data generated at high pressures and rapid reaction is shown in Fig. 7.71 (Haschke *et al.*, 1987). This diagram is based on measurement of partial molar free energy isotherms that suggest the existence of five hydride phases (indicated as II–VI in Fig. 7.71) in addition to PuH_s (phase I). These data suggest the coexistence of a cubic $PuH_{2.70}$ and a hexagonal $PuH_{2.88}$ in the III + IV two-phase region. Hexagonal phase IV is thought to have a structure similar to that of disordered tysonite (LaF_3), while phase V is thought to be similar to that of orthorhombic YF_3 with a composition near $PuH_{2.95}$. The properties of phase VI are unknown. For a detailed discussion of the plutonium–hydrogen phase equilibria, the reader is

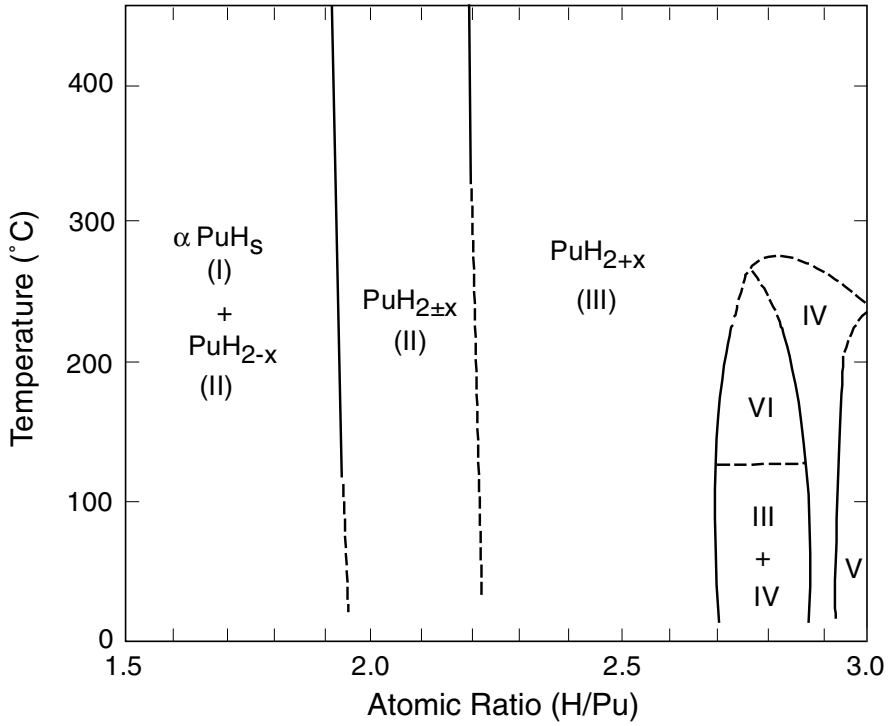

Fig. 7.71 *A plutonium–hydrogen phase diagram for rapid high-pressure reaction conditions, based on Haschke* et al. (1987).

referred to reviews by Flotow *et al.* (1984), Bartscher (1996), and Haschke and Haire (2000).

(c) Solid-state structures

The solid-state crystal structures of plutonium hydrides possess many similarities to those of the lanthanide hydrides, and Haschke and coworkers have suggested a similarity and analogy to the lanthanide trifluoride system (Haschke *et al.*, 1987). A summary of crystallographic data for plutonium hydrides is given in Table 7.26. Plutonium hydride forms a cubic fluorite-type phase over the composition range of PuH_x, where $1.9 < x < 2.7$, and a lanthanum trifluoride-related hexagonal phase beyond $x = 2.9$. The cubic fluorite-type structure based upon CaF_2 is illustrated in Fig. 7.72. As the composition of the fcc PuH_x varies between $1.9 < x < 2.7$, the lattice parameter decreases from 5.360(1) Å at $x = 1.9$ to 5.34(1) Å at $x = 2.7$. Within this fcc arrangement of plutonium metal cations are tetrahedral (t) and octahedral (o) interstices that may be occupied by the H^- ion. For an idealized PuH_2 structure with lattice

Table 7.26 *Crystal structure data for plutonium hydrides.*

Formula	*Symmetry*	*Space group*	*Lattice parameter* a_0 (Å)	c_0 (Å)	*Formula units per cell*	*Calculated density* (g cm^{-3})	*References*
$PuH_{2.0}$	fcc	F*m*3*m*	5.359(1)		4	10.40	Ellinger (1961)
$PuH_{2.51}$[a]	fcc	F*m*3*m*	5.342(4)		4		Muromura *et al.* (1972)
PuH_3	hexagonal	$P6_3/mmc$ or $P\bar{3}c1$	3.78(1)[b] 6.55(1)	6.76(1)	2	9.608	Ellinger (1961)

[a] The values of x between 2.15 and 2.70 are represented by the equation a_0 (Å) = 5.4337 – 0.003575 (H/Pu) (Bartscher, 1996).
[b] Hexagonal LaF_3 (tysonite) has space group $P\bar{3}c1$, which is the same as observed in hexagonal lanthanide hydrides, and is the likely space group for PuH_3. To transform from $P6_3/mmc$ to $P\bar{3}c1$, one would use $a_0 = a'\sqrt{3}$, or $a_0 = 6.55$ (Å) for PuH_3.

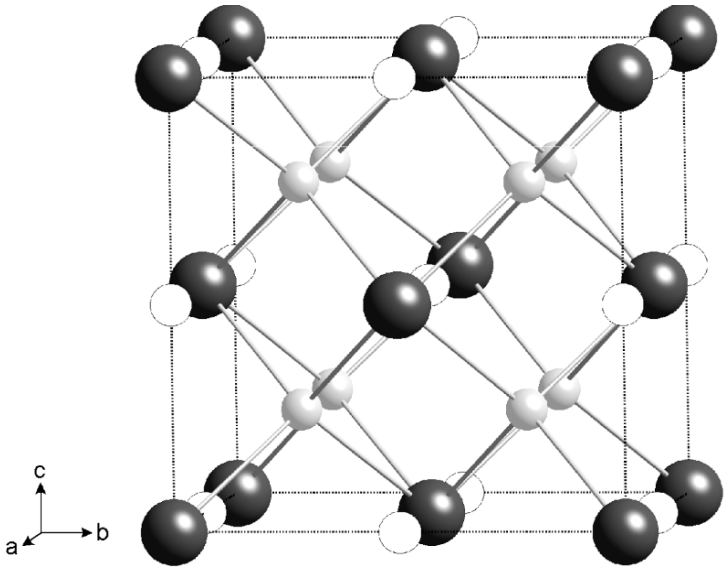

Fig. 7.72 *The cubic* (*Fm*3*m*) *fluorite-like solid-state structure of* PuH_x *showing the fcc arrangement of Pu atoms* (*black*) *with tetrahedral H atoms* (*gray*). *Octahedral vacancies are indicated with white circles, and the unit cell is indicated as a dashed line. For lattice parameter,* $a = 5.336$ Å, *Pu–H* = 2.31 Å, *Pu–Pu* = 3.77 Å, *and Pu-vacancy* = 2.67 Å (*Ellinger,* 1961).

parameter $a = 5.34$ Å, there is eight-fold (cubic) coordination of each plutonium atom by 8 hydrogen atoms, and four-fold tetrahedral (t) coordination of hydrogen atoms by 4 plutonium atoms with a Pu–H distance of 2.31 Å. The six-fold octahedral (o) sites in this model are vacant. Compositions of PuH_x, where $x < 2$, are likely formed by the creation of hydrogen atom vacancies in the normal t sites. At low temperatures, low pressures, and slow reaction times, an extended metastable cubic solid solution can exist all the way up to the PuH_3 phase boundary, and a simplistic model (see discussion below) would have additional hydrogen atoms randomly filling the o sites, with a concomitant decrease in lattice parameter.

The simple model of random occupancy of o sites in the fluorite lattice by additional hydrogen atoms when H–Pu is greater than two is overly simplistic. Since hydrogen mobility can occur at fairly low temperatures, the hydrogen atom can be disordered between t and o sites in the lattice (Muromura *et al.*, 1972; Flotow *et al.*, 1984; Haschke *et al.*, 1987; Ward and Haschke, 1994). Bartscher and coworkers employed elastic neutron scattering on deuterated samples of composition $PuD_{2.25}$, $PuD_{2.33}$, and $PuD_{2.65}$ and demonstrated a progressive depletion of t sites and occupation of o sites relative to PuD_2 (Bartscher *et al.*, 1985). Deuterium atoms in the o sites are displaced by 0.4 Å in the [111] direction (body diagonal) toward the t sites, in analogy with that observed in lanthanide systems (Ward and Haschke, 1994). In lanthanides, this low-temperature ordering of octahedral hydrogen atoms appears with a concomitant doubling of the c-axis of the unit cell. The 'freezing in' of the hydrogen atoms in this structure can be observed by NMR and by heat-capacity measurements (see below) (Cinader *et al.*, 1976; Flotow *et al.*, 1984). Haschke has proposed a conceptual model based on vacancy clusters for interpreting the relative t- and o-site occupancy factors in this structural model (Haschke *et al.*, 1987).

The structural behavior of the Pu–H system near the PuH_3 phase boundary is complex, and this region remains to be fully characterized. At low temperatures and for compositions above $PuH_{2.7}$, a cubic (fcc) form has been identified (Fig. 7.72). Under the appropriate conditions of rapid (high-temperature and high-pressure) reaction, both hexagonal and orthorhombic phases can also be formed near the PuH_3 boundary. In the range $PuH_{2.9}$–$PuH_{3.0}$, there is a hexagonal, nonstoichiometric phase in which the proposed structure is based on a disordered LaF_3 (tysonite) hexagonal structure ($P\bar{3}c1$), and an orthorhombic phase thought to be based on the YF_3 structure (Haschke *et al.*, 1987). The hexagonal phase was originally reported by Ellinger and assigned space group $P6_3/mmc$ (Ellinger, 1961), but more recent studies of the related lanthanide hydrides and fluorides reveal that trigonal space group $P\bar{3}c1$ is more likely the correct choice (Cheetham *et al.*, 1976). According to Haschke, the two-phase regions separating cubic (fcc) and hexagonal hydrides close in on themselves at 200–400°C, and only the cubic phases exist at higher temperatures (Haschke *et al.*, 1987). For more detailed discussion of these phase relationships, the reader is referred to the recent review by Haschke and Haire (2000).

(d) Physical properties and electronic structure

Trends in electronic properties as a function of x in PuH_x systems are crucial for understanding the nature of chemical bonding in plutonium hydrides. All data are consistent with the general description of cubic plutonium hydrides consisting of a localized 5f shell with a trivalent Pu(III) ion, best formulated as $Pu^{3+}(H^-)_x(e^-)_{3-x}$. Plutonium is trivalent for all compositions and exhibits 'rare-earth like' behavior. For nominal composition PuH_2, XPS shows a 4f intensity at the same 4f binding energy as a Pu(III) standard (Willis *et al.*, 1985). Neutron scattering data display an ordered magnetic moment of $0.71\mu_B$ per plutonium atom, which is the same as the trivalent free ion value (Bartscher *et al.*, 1985). Electrical conductivity decreases with increasing x, indicating that electrons are progressively removed from the conduction band and bound as H^- as the value of x increases (Willis *et al.*, 1985). Moreover, as the conductivity decreases, the hydride color changes from silver to black. Valence band XPS recorded on a (nominal composition) PuH_2 film reveal a large 5f peak consistent with a localized 5f shell, while core-level XPS on the same sample shows $4f^{5/2}$ and $4f^{7/2}$ peaks characteristic of Pu(III) (Ward *et al.*, 1992). Recent XPS data on a thin film of nominal composition PuH_3 shows the disappearance of the 5f peak (Gouder, 2005). Cinader and coworkers studied ^1H NMR spectroscopy on cubic PuH_x (where $x = 1.78$, 2.35, 2.65, and 2.78) between 77 and 300°C (Cinader *et al.*, 1976). Evaluation of line shapes, Knight shifts, and relaxation times are consistent with paramagnetic phases with localized 5f moments. Different line shapes and shifts were observed for t and o sites, and they were able to observe the 'freeze in' of the hydrogen atoms at low temperature. Enthalpies and entropies of formation for the extended cubic phase composition are given in Table 7.27.

(e) Applications

The hydriding reaction may be used to prepare plutonium metal powder. Compact pieces of plutonium metal can be converted to one of the hydrides and then powdered under an H_2 atmosphere by a magnet hammer. Subsequent

Table 7.27 *Enthalpies and entropies of formation for cubic plutonium hydrides at* 550 K[a].

Product	$\Delta_f H$ (kJ mol^{-1})	$\Delta_f S$ (J K^{-1} mol^{-1})
$PuH_{1.90}$	-155.6 ± 10.9	-138.5 ± 10.9
$PuH_{2.50}$	-190.4 ± 5.0	-175.7 ± 8.4
$PuH_{3.00}$[b]	-205.9 ± 4.6	-211.7 ± 11.7
$PuD_{1.90}$	-141.8 ± 1.7	-125.1 ± 3.8
$PuD_{2.50}$	-174.5 ± 4.2	-160.2 ± 7.5
$PuD_{3.00}$[b]	-189.1 ± 11.7	-188.3 ± 8.4

[a] Data from (Ward and Haschke, 1994).
[b] Based on extrapolated partial molar Gibbs energy data.

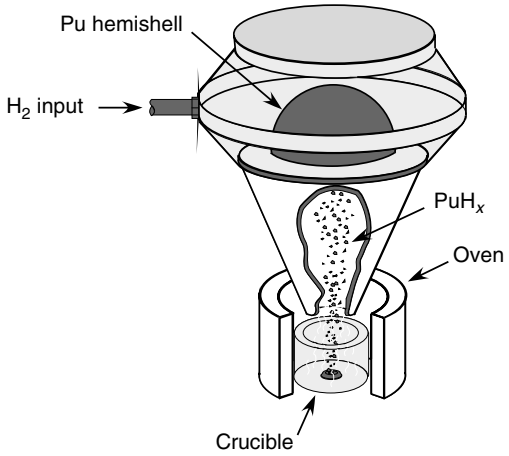

Fig. 7.73 *A schematic representation of the hydride–dehydride or hydride-oxidation chamber for conversion of surplus weapons plutonium. A weapon hemishell sits in the upper chamber, PuH_x spalls off and falls into the lower crucible, where it can be converted to the metal, a nitride or oxide* (*Toevs,* 1997).

decomposition *in vacuo* at more than 400°C leaves finely divided, highly reactive plutonium powder (Stiffler and Curtis, 1960). Both the U.S. and Russian technology for disassembly and conversion of excess plutonium from nuclear weapons employs a hydride–dehydride, or hydride–oxidation process for conversion into an unclassified form that can be examined by inspectors from other nations (Cremers *et al.*, 1995; Toevs, 1997; Nelson, 1998; Mashirev *et al.*, 2001). The U.S. process uses continuous H_2 recycle where the hydride falls into a crucible that is heated, driving off H_2 gas, leaving molten plutonium in the crucible. The H_2 refluxes to the top of the chamber, where it removes additional plutonium from the component. A schematic representation of the reaction chamber employed in this process is shown in Fig. 7.73. For conversion to an oxide, the crucible is not heated, and either O_2 is admitted and the hydride burned to release H_2 and leave an oxide powder, or N_2 is used and burned to a nitride powder. The nitride can then be converted to the oxide by burning with O_2. The three-step process of converting the hydride to the nitride and then the oxide avoids having an H_2–O_2 atmosphere in a glove box (Toevs, 1997). The hydride–dehydride approach to weapons conversion avoids the generation of large volumes of liquid waste from wet chemical methods.

7.8.2 Plutonium borides

Plutonium borides form at stoichiometric compositions PuB_2, PuB_4, PuB_6, PuB_{12}, and PuB_{66}, and at a very restricted solid solution of less than 0.5 at.% Pu in β-rhombohedral boron. These five compounds have high melting points,

and with the exception of the preparation and identification of the compounds, very little experimental work is available. Recent detailed reviews describing the plutonium–boron system have appeared (Potter, 1991; Rogl and Potter, 1997).

Plutonium borides were first reported in 1960 (McDonald and Stuart, 1960), when the crystal structures of 'PuB,' PuB_2, PuB_4, and PuB_6 were described. Additional studies of the plutonium boron phase relationships were reported shortly thereafter (Skavdahl, 1963; Skavdahl and Chikalla, 1964; Skavdahl *et al.*, 1964; Weber *et al.*, 1964). Careful structural investigations employing XRD and metallography demonstrated that cubic samples of 'PuB' were contaminated with cubic PuN, and that 'PuB' was not actually a real phase in the Pu–B system (Eick, 1965; Chipaux *et al.*, 1989). Two additional compounds, plutonium dodecaboride, PuB_{12}, and the hectoboride, PuB_{66} were also discovered (Eick, 1965). The hectoboride was originally reported as having composition PuB_{100} (Eick, 1965), but based on analogy with rare-earth elements, which show a YB_{66}-type structure (Kasper, 1976), Rogl and Potter (1997) suggest that PuB_{66} represents a more-likely composition. Using the similarities between rare-earth and actinide boride systems, Rogl and Potter have provided a cautious assessment of the plutonium–boron phase diagram, shown in Fig. 7.74 (Rogl and Potter, 1997).

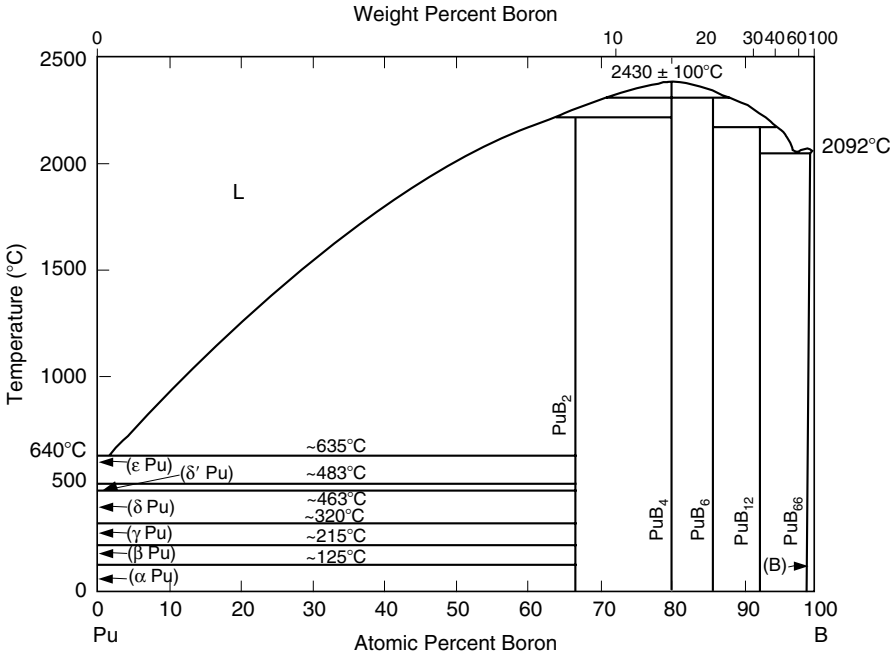

Fig. 7.74 *The plutonium–boron phase diagram* (*redrawn from Rogl and Potter,* 1997).

(a) Preparation

Plutonium borides can be prepared by a variety of methods: heating mixtures of pressed powders of elemental plutonium and boron under vacuum between 900 and 1200°C (McDonald and Stuart, 1960; Weber *et al.*, 1964), arc-melting pure plutonium with crystalline boron under a purified argon atmosphere followed by heat treatment (Eick, 1965), reaction of plutonium hydride with elemental boron at 900°C (Chipaux *et al.*, 1988, 1990), or reduction of PuO_2 by elemental boron and carbon (Skavdahl, 1963; Skavdahl and Chikalla, 1964; Skavdahl *et al.*, 1964; Larroque *et al.*, 1986). All of these reactions are carried out at high temperature (800–1500°C) under Ar or *in vacuo*. A comprehensive listing of preparative methods has been reported (Rogl and Potter, 1997). In view of the recent advances in the low-temperature synthesis of highly refractory materials (Rice, 1983; Wynne and Rice, 1984), and a possible application of actinide borides as an alternative storage form for actinide elements (Lupinetti *et al.*, 2002), it seems likely that this area will grow in interest and importance over the coming decades.

(b) Solid-state structures

The solid-state structures of plutonium borides (as in most metal borides) are dominated by B–B bonding, and the structures are made up of three-dimensional boron atom networks or clusters in which the plutonium atoms occupy otherwise vacant sites (Greenwood and Earnshaw, 1997). The B–B distances in all the plutonium borides are within the same range as those found in elemental boron and other boride complexes, and span 1.73–1.92 Å. The basic structural units in actinide borides, as in all metal borides, are readily described in terms of the B–B bonding configuration, followed by the actinide atom coordination (Potter, 1991; Greenwood and Earnshaw, 1997). Boron bonding units can be conveniently described as belonging to B_2-sp^2, B_6-octahedral, or B_{12}-cubeoctahedral boron atom cluster configurations as shown schematically in **1**, **2**, and **3** below (Potter, 1991; Greenwood and Earnshaw, 1997). To date, the structural characterization of plutonium borides has been performed exclusively by X-ray powder diffraction techniques, and a summary of crystallographic parameters of plutonium borides is given in Table 7.28. No single crystal diffraction studies have been reported.

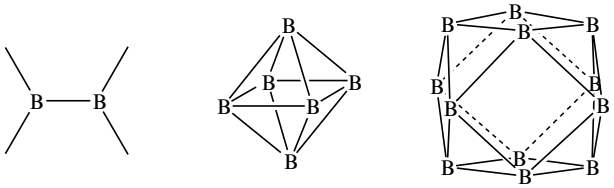

B_2-sp^2 **B_6** **B_{12}**

1 **2** **3**

Table 7.28 *X-ray crystallographic data for plutonium borides.*

Compound	*Structure type*	*Symmetry*	*Space group*	*Unit cell dimensions* (Å)	*Formula units per cell*	*X-ray density* ($g\ cm^{-3}$)[a]	*References*
PuB_2	AlB_2	hexagonal	P6/*mmm*	$a = 3.1857(2)$ $c = 3.9485(4)$	1	12.470	Eick (1965)
PuB_4	ThB_4	tetragonal	P4/*mbm*	$a = 7.1018(3)$ $c = 4.0028(1)$	4	9.285	Eick (1965)
PuB_6	CaB_6	cubic	P$m\bar{3}m$	$a = 4.1134(3)$	1	7.249	Eick (1965)
PuB_{12}	UB_{12}	cubic	F$m\bar{3}m$	$a = 7.4843(3)$	4	5.842	Eick (1965)
PuB_{66} ('PuB_{100}')	YB_{66}	cubic	P$n\bar{3}n$	$a = 23.43(4)3$	24	2.485	Eick (1965)

[a] Calculated for ^{239}Pu.

Plutonium diboride (PuB_2) exhibits the hexagonal AlB_2 structure in space group *P6/mmm* containing one formula unit per unit cell (McDonald and Stuart, 1960; Eick, 1965). The AlB_2 structure is by far the most common phase displayed by metal borides (Spear, 1976). The solid-state structure (Fig. 7.75) consists of graphite-like hexagonal layers of catenated boron atoms with a close B–B contact of 1.84 Å. These hexagonal boron layers are separated by a hexagonal close packed (hcp) layer of plutonium atoms, positioned so that the centroid of a hexagonal ring of boron atoms lies directly above and below each plutonium atom. The closest Pu–B contact in this structure is 2.70 Å, with a closest Pu–Pu separation of 3.19 Å.

Plutonium tetraboride (PuB_4) has a tetragonal lattice (space group *P4/mbm*) formed by chains of B_6 octahedra along the *c*-axis and linked in the lateral direction by pairs of B_2 units in the *ab* plane (McDonald and Stuart, 1960;

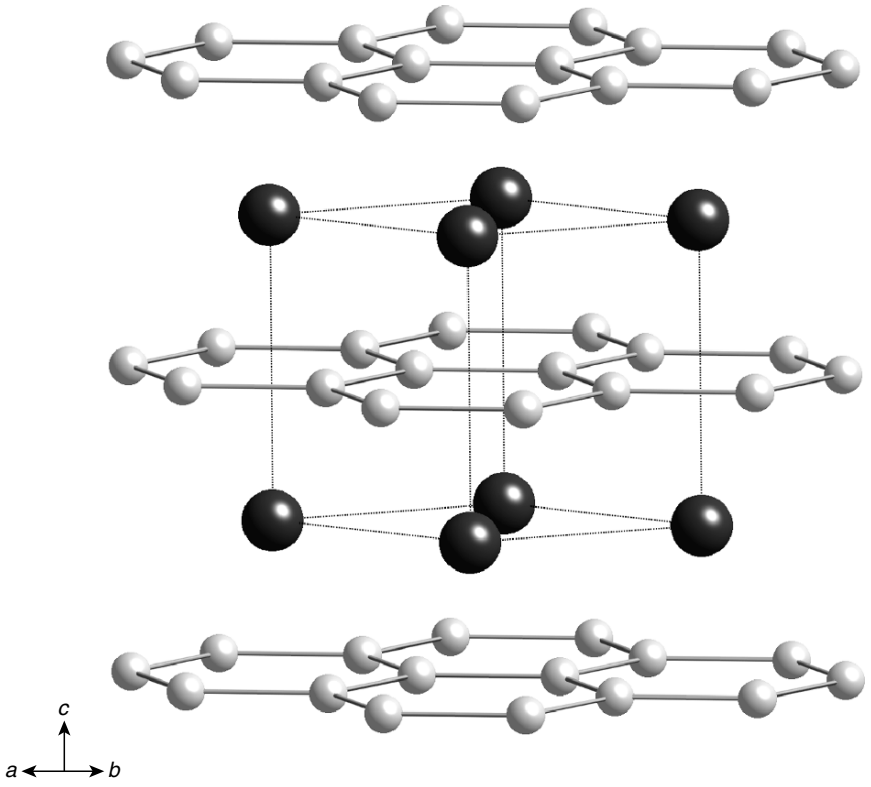

Fig. 7.75 *The solid-state structure of PuB_2 shown perpendicular to the c-axis, and emphasizing the hexagonal graphite-like layers of boron atoms (gray) separated by layers of plutonium atoms (black). The unit cell is indicated as dashed lines.*

Eick, 1965). This forms a three-dimensional network with channels along the *c*-axis that are filled by plutonium atoms. B–B contacts span a narrow range between 1.70 and 1.76 Å, with the shortest Pu–Pu contact of 3.66 Å between chains, and a longer contact of 4.00 Å along the chains. The closest Pu–B contact is 2.72 Å between Pu atoms and B_6 units. This structure type is shown in Fig. 7.76.

Plutonium hexaboride (PuB_6) has a cubic CsCl-type lattice (*Pm3m*) in which the plutonium atom and B_6 octahedra occupy the metal and halogen sites, respectively, as shown in Fig. 7.77(a) (McDonald and Stuart, 1960; Eick, 1965). In this structure, the B_6 octahedra are linked together in all six orthogonal directions. Within this framework, plutonium atoms occupy the corner

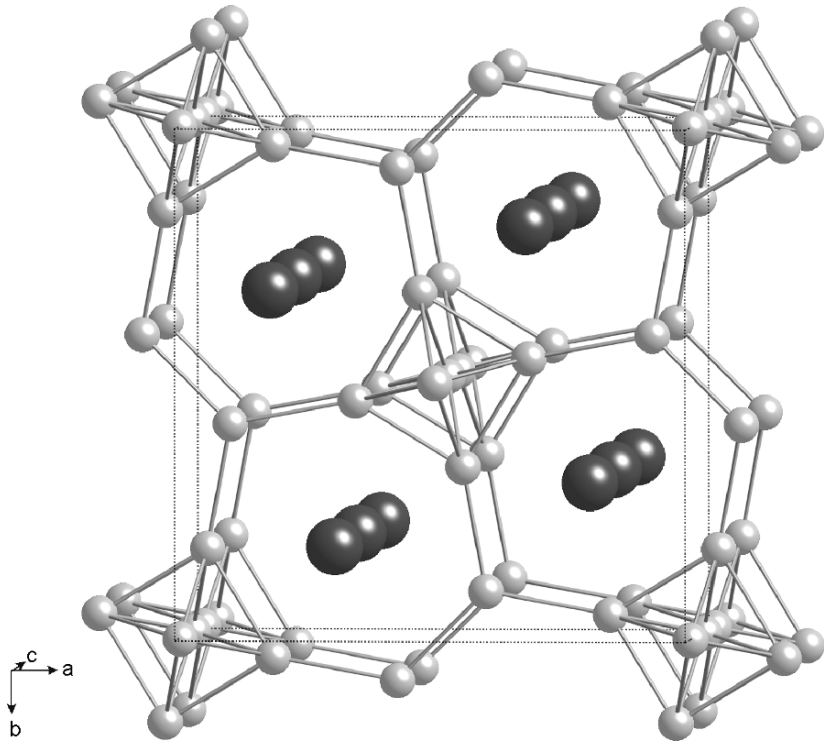

Fig. 7.76 *The solid-state structure of PuB_4 shown looking down the c-axis and emphasizing the open channels filled with plutonium ions* (*black*). *Boron atoms* (*gray*) *comprise octahedral B_6 units linked by bridging B_2 units within the ab plane. The unit cell is indicated as dashed lines.*

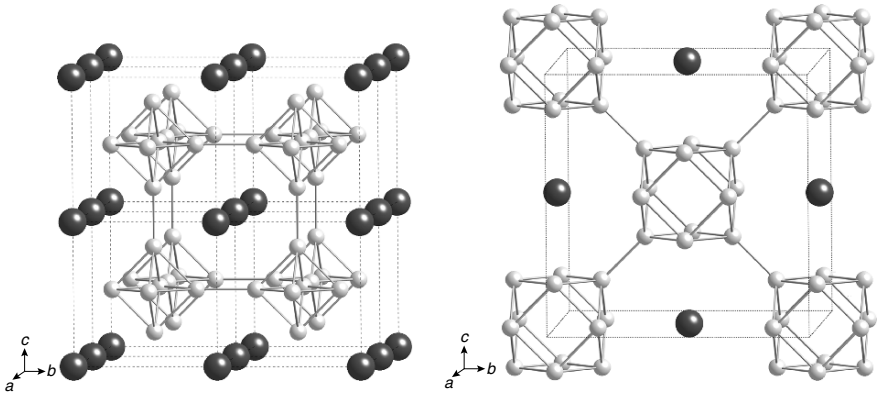

Fig. 7.77 *The solid-state structure of PuB_6 (a), and PuB_{12} (b). PuB_6 has alternating plutonium (black) and B_6 octahedra (gray) in a 'CsCl-type' lattice. PuB_{12} has alternating plutonium (black) and B_{12} cubeoctahedra (gray) in a 'NaCl-type' lattice.*

positions of an interpenetrating cubic sublattice. B–B contacts within the B_6 unit, and linking adjoining B_6 units, are 1.70 Å, Pu–B contacts are 3.03 Å, and the Pu–Pu nonbonding contact is 4.11Å. Plutonium dodecaboride (PuB_{12}) has a cubic NaCl-type fcc lattice (*Fm3m*) in which the plutonium atoms and B_{12} cubeoctahedral clusters occupy the metal and halogen sites, respectively, as shown in Fig. 7.77(b) (Eick, 1965). B–B distances within the B_{12} unit are 1.76 Å, Pu–B distances between plutonium and B_{12} units are 2.79 Å, and the Pu–Pu nonbonding contact is 5.29 Å.

Plutonium hectoboride was originally formulated as 'PuB_{100}' (Eick, 1965), but this phase is most likely of composition PuB_{66}, belonging to a family of metal hectoborides based on the structure of YB_{66} (Potter, 1991; Rogl and Potter, 1997). This structure is exceedingly complicated, and the reader is referred to Richards and Kasper for a detailed description (Richards and Kasper, 1969). A simplified description is that of a well-known 13-icosahedron unit (156 boron atoms) found in β-rhombohedral boron, comprised of 12 B_{12} icosahedra grouped around a 13th central B_{12} unit. The yttrium atoms in YB_{66} are distributed in channels and coordinate to the cage boron atoms.

(c) Properties

Very little is known about the physicochemical properties of plutonium borides. It seems well established that PuB_4 and PuB_{66} are the only congruently melting plutonium borides (Rogl and Potter, 1997). Magnetic susceptibility measurements of PuB_2 and magnetic susceptibility and Mössbauer measurements on solid solutions of $Np_{1-x}Pu_xB_2$ and NpB_2 suggest a tetravalent oxidation state

for neptunium, and presumably plutonium in the diborides. PuB_2 was found to be a weak paramagnet, and the data were fit by a modified Curie–Weiss law with and effective paramagnetic moment of $\mu^*_{eff} = 0.32\mu_B$ and $\theta_p = -30$ K. Renormalization led to $\mu_{eff} = 0.75\mu_B$ (Chipaux *et al.*, 1990). Smith and Fisk (1982) reported little temperature dependence in magnetic susceptibility of PuB_6.

7.8.3 Plutonium carbides and silicides

(a) The plutonium–carbon system

Four compounds are known in the plutonium–carbon system: Pu_3C_2, PuC_{1-x}, Pu_2C_3, and PuC_2. All these compounds undergo peritectic decomposition at high temperatures. The Pu–C phase diagram according to Green and Leary (1970), and assessed by Kassner and Peterson (1995), is shown in Fig. 7.78. Pu_3C_2 decomposes between 558 (Rosen *et al.*, 1963) and 575°C (Mulford *et al.*, 1960) to ϵ-Pu + PuC_{1-x} and may be unstable at lower temperatures

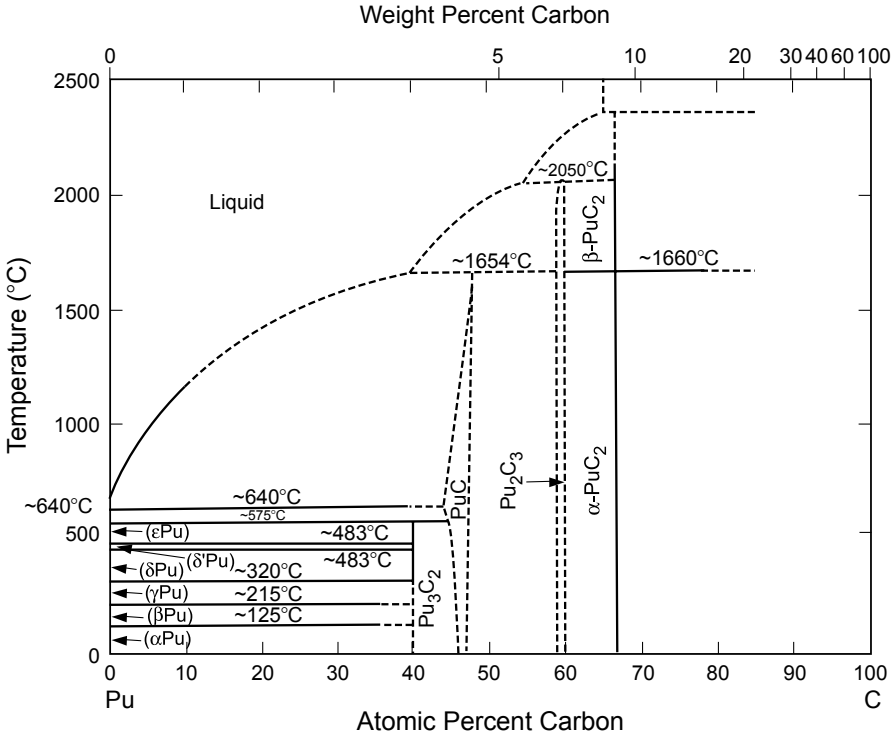

Fig. 7.78 *The plutonium–carbon phase diagram (redrawn from Green and Leary,* 1970*; Kassner and Peterson,* 1995*). See text for discussion of stability of PuC_2 below* 1660°C.

(Pascard, 1962). Plutonium monocarbide 'PuC' exists only as substoichiometric PuC_{1-x}, with a stoichiometry ranging from $PuC_{0.6}$ to $PuC_{0.92}$. At 1654°C, PuC_{1-x} decomposes into Pu_2C_3 plus liquid. Plutonium sesquicarbide Pu_2C_3 occurs in a rather narrow phase region around 60 at.% C. It decomposes at 2050°C into the high-temperature cubic phase PuC_2 and liquid (Mulford *et al.*, 1960). Plutonium dicarbide PuC_2 is only stable between 1660 ± 10 and 2230 ± 20°C (Reavis and Leary, 1970). The polymorphic transformation of PuC_2 below 1660°C to give the metastable tetragonal phase was added to the phase diagram in Fig. 7.78 by Kassner and Peterson (1995).

An extensive literature on plutonium carbides exists because actinide carbides have been considered as advanced nuclear fuels. Topical reviews can be found on general behavior (Storms, 1964, 1967; Ogard and Leary, 1970; Potter, 1975), thermodynamics (Holley, 1974; Holley *et al.*, 1984), thermal expansion and density (Andrew and Latimer, 1975), defect and transport properties (Matzke, 1984), and use as nuclear fuel (Russell, 1964; Andrew and Latimer, 1975; Herbst and Matthews, 1982; Handa and Suzuki, 1984).

(*i*) *Preparation*

Quite a few different preparation methods have been used to synthesize plutonium carbides. Carbides of plutonium can be formed by reaction between plutonium metal, plutonium hydrides, or plutonium oxides with elemental carbon at high temperature using furnace or arc-melting techniques (Drummond *et al.*, 1957; Ogard *et al.*, 1962; Pascard, 1962; Kruger, 1963; Chackraburtty and Jayadevan, 1965; Ogard and Leary, 1970). Plutonium oxide reductions using carbon can leave oxygen impurities in the products, and this is particularly true for the cubic monocarbides PuC_{1-x}. The products depend strongly on the temperature of reaction and reaction time. For example, PuC_{1-x} can be prepared by sintering or arc-melting a plutonium carbon mixture at 1000°C for 5 h, by direct reaction of PuO_2 with elemental carbon between 800 and 1350°C, by sintering $PuH_{2.7}$ with carbon in an inert atmosphere between 880 and 1650°C, or by reaction of PuH_2 with Pu_2C_3 at 650–750°C. The sesquicarbide can be obtained by reaction of PuO_2 with carbon under an argon atmosphere between 1250 and 1450°C at 6 h, 1350°C for 2 h or 1300–1400°C under vacuum. Pu_2C_3 can also be obtained by reaction of plutonium hydride with propane at 650–750°C.

(*ii*) *Crystal structures*

The crystal structures of all plutonium carbides, with the exception of Pu_3C_2 have been determined, and crystallographic data are summarized in Table 7.29. The lattice constants depend on the composition and the history of the individual sample. Plutonium monocarbide 'PuC' exists only as substoichiometric PuC_{1-x}, and adopts the cubic NaCl structure with defects in the carbon

Table 7.29 *X-ray crystallographic data for plutonium carbides.*

Compound	*Symmetry*	*Space group*	*Lattice parameters*			*Formula units per cell*	*Calculated density* (g cm^{-3})	*References*
			a_0 (Å)	b_0 (Å)	c_0 (Å)			
PuC_{1-x}	fcc	F*m*3*m*	4.9582(3) (C-poor)			4	13.6	Mulford *et al.* (1960)
			4.9737(3) (C-rich)					Mulford *et al.* (1960)
Pu_2C_3	bcc	I$\bar{4}$3*d*	8.1258(3) (C-poor)			8	12.70	Mulford *et al.* (1960)
			8.1317(3) (C-rich)					Mulford *et al.* (1960)
PuC_2	tetragonal	I4/*mmm*	3.63	3.63	6.094	2	10.88	Chackraburtty and Jayadevan (1965)

sublattice (Zachariasen, 1949c; Mulford *et al.*, 1960). As the carbon content increases, all the carbide carbon atoms are replaced by acetylide C_2 units adopting a stoichiometry $Pu_4(C_2)_3$ (equivalent to Pu_2C_3) and PuC_2. Pu_2C_3 is cubic with 12 C_2 groups in the unit cell, with each plutonium atom bonded to nine carbon atoms, three at 2.48 Å, three at 2.51 Å, and three at 2.84 Å (Zachariasen, 1952). This structure is illustrated in Fig. 7.79, where only the shortest set of three Pu–C bonds are indicated. Due to the difficulty in accurately locating carbon atoms in the presence of the larger plutonium atoms by XRD, the carbon atoms were placed in assumed locations with a C–C single bond distance of 1.54 Å. Neutron diffraction studies on the isostructural U_2C_3 revealed a much shorter C–C distance of 1.295 Å (Austin, 1959), which is considerably lengthened relative to C_2 unit in acetylene at 1.20 Å.

Plutonium dicarbide, PuC_2 is a high-temperature compound that is not stable below ~1750°C (Mulford *et al.*, 1960) and decomposes to Pu_2C_3 and carbon. High temperature XRD revealed an fcc structure at 1710°C with a lattice parameter $a_0 = 5.70(1)$ Å (Harper *et al.*, 1968) which is consistent with

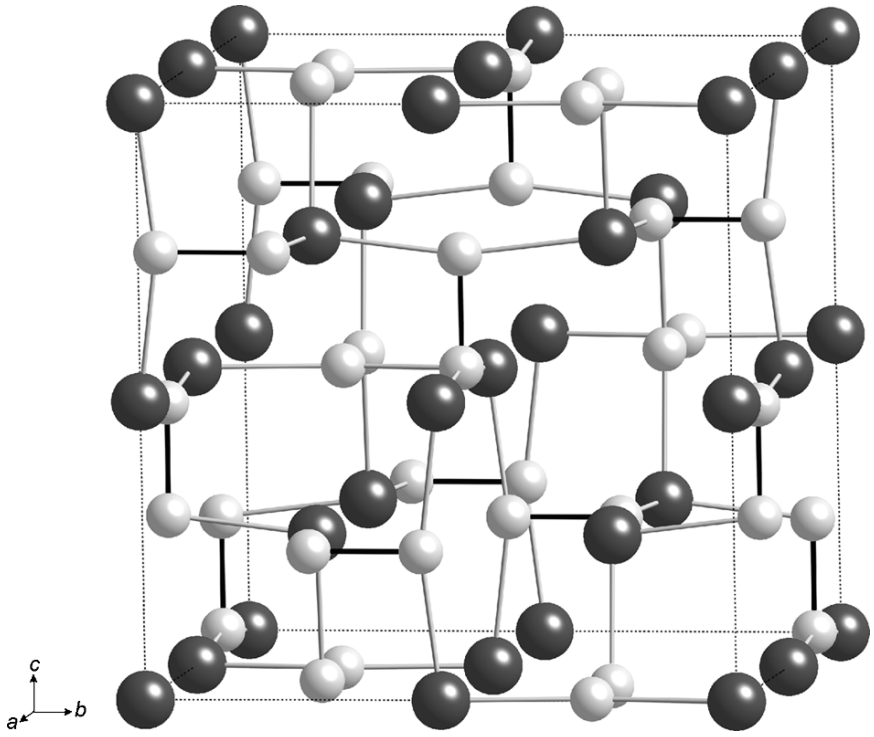

Fig. 7.79 *The solid-state structure of Pu_2C_3 shown looking down the a-axis. Plutonium atoms are black and carbon atoms are gray. The unit cell is indicated as dashed lines. The bold lines between C atoms indicates the* 12 C_2 *groups in the unit cell* (*Zachariasen,* 1952).

the CaC_2 structure that has a NaCl arrangement of Ca atoms and C_2 units (Wells, 1984). A room-temperature structure of what must be considered metastable PuC_2 was found to contain a tetragonal cell, probably due to martensitic transformation on quenching fcc PuC_2 to room temperature (Chackraburtty and Jayadevan, 1965). The tetragonal structure of PuC_2 and its similarity to the NaCl structural unit is shown in Fig. 7.80. For tetragonal PuC_2, the short Pu–C distance is found to be 2.48 Å with Pu–Pu = 3.63 and 3.98 Å (Chackraburtty and Jayadevan, 1965). As in the case of Pu_2C_3, the carbon atom positions are not accurately determined, but a neutron diffraction study on the isostructural tetragonal UC_2 revealed a C–C distance of 1.34 Å (Austin, 1959).

(*iii*) *Chemical properties*

The chemical properties of the plutonium carbides have been studied in some detail (Cleveland, 1979; Wick, 1980). Plutonium monocarbide oxidizes in air at temperatures as low as 200–300°C. It ignites at 400°C in an O_2 atmosphere (Drummond *et al.*, 1957). Compact PuC_{1-x}, kept in air at room temperature, did not show any sign of reaction after 2 months. However, PuC_{1-x} powder was found to be reactive, and sometimes pyrophoric (Ogard *et al.*, 1962). With N_2, PuC_{1-x} reacts more slowly than UC. A PuC_{1-x} sample, kept at 0.5 atm N_2, contains 1 ppm N_2 after 12 h at 200°C and 16 ppm after 12 h at 500°C. If heated

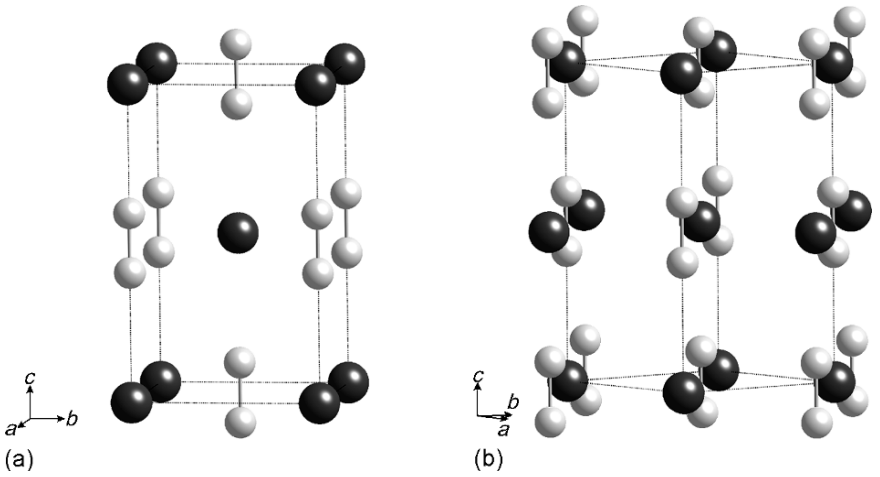

Fig. 7.80 (*a*) *The metastable tetragonal structure of* PuC_2 *shown looking perpendicular to the c-axis, and emphasizing the discrete* C_2 *units within the structure. Plutonium atoms are black and carbon atoms are gray.* (*b*) *The same structure rotated by* 45° *and emphasizing the relationship to the cubic NaCl structure with alternating Pu and* C_2 *units. At high temperature of* 1710°C, $a = b = c = 5.70(1)$ Å.

to 1400°C, the PuC_{1-x} reacts more rapidly to PuN and Pu_2C_3 (Lorenzelli *et al.*, 1966). Plutonium sesquicarbide, Pu_2C_3, shows chemical behavior similar to the monocarbide. It is slightly more stable to oxidation at higher temperatures (Drummond *et al.*, 1957). If heated to 1000°C in H_2, Pu_2C_3 is reduced to $PuC_{0.85}$ (Russell, 1964). PuC_{1-x} reacts with hot water to form $Pu(OH)_3$ and a mixture of H_2 and hydrocarbons. Pu_2C_3 appears to be more stable to hydrolysis in boiling water, but less stable to atmospheric hydrolysis (Drummond *et al.*, 1957).

All the plutonium carbides dissolve in HNO_3–HF mixtures (Storms, 1967). With oxidizing acids, CO_2 is formed. By the dissolution of lower carbides, carbon may be liberated along with hydrocarbons (Storms, 1967) along with organic acids such as mellitic and oxalic acids (Bokelund and Glatz, 1984).

(*iv*) *Thermodynamic properties*

Because of the importance of the plutonium carbides as potential high-temperature reactor fuels, the mechanical, thermal, electrical, magnetic, and thermodynamic properties of these compounds have been determined. For details about these properties and for additional references to the literature, the reader is referred to Holley *et al.* (1984), who reviewed the literature in the 1980s. The 2001 evaluation of plutonium thermodynamic data by the Nuclear Energy Agency (NEA) concludes that little significant thermodynamic information has been published since that time (Lemire *et al.*, 2001) but offers some reassessment of earlier data and provides recommended values for key thermodynamic constants. These are given in Table 7.30.

Monatomic plutonium is the only species that evaporates on heating from Pu–C phases. The equilibria in the solids have been inferred from vapor-pressure measurements (Mulford *et al.*, 1963; Olson and Mulford, 1967; Campbell *et al.*, 1970; Holley *et al.*, 1984). A general survey of the thermal decomposition behavior observed in the plutonium–carbon system has been given by Storms (1967). Specific-heat measurements of plutonium carbides have been reported by numerous authors and reviewed by Holley *et al.* (1984). The NEA review recommends the following temperature dependences (Lemire *et al.*, 2001):

Table 7.30 *Thermodynamic parameters for plutonium carbides.* (*Lemire* et al., 2001).

Compound	$\Delta_f G^\circ_{298}$ (kJ mol^{-1})	$\Delta_f H^\circ_{298}$ (kJ mol^{-1})	S°_{298} (J K^{-1} mol^{-1})	$C^\circ_{p^{298}}$ (J K^{-1} mol^{-1})
$PuC_{0.84}$	-49.8 ± 8.0	-45.2 ± 8.0	74.8 ± 2.1	47.1 ± 1.0
Pu_2C_3	-156.5 ± 16.7	-149.4 ± 16.7	150.0 ± 2.9	114.0 ± 0.4
Pu_3C_2	-123.5 ± 30.0	-113 ± 30	210.0 ± 50	136.8 ± 2.5

$PuC_{0.84}$ ($298.15 \leq T \leq 1875$ K)

$$C_p^o = 71.5910 - 5.95042 \times 10^{-2}T + 4.94346 \times 10^{-5}T^2 - 9.9320 \times 10^5 T^{-2}\text{JK}^{-1}\text{mol}^{-1} \quad (7.30)$$

Pu_2C_3 ($298.15 \leq T \leq 2285$ K)

$$C_p^o = 156.000 - 7.9726 \times 10^{-2}T + 7.04170 \times 10^{-5}T^2 - 2.1757 \times 10^6 T^{-2}\text{JK}^{-1}\text{mol}^{-1} \quad (7.31)$$

Pu_3C_2 ($298.15 \leq T \leq 850$ K)

$$C_p^o = 120.67 + 4.686 \times 10^{-2}T + 1.9456 \times 10^5 T^{-2}\text{JK}^{-1}\text{mol}^{-1} \quad (7.32)$$

(*v*) *Ternary phases*

Several ternary plutonium carbides have been prepared. Of particular importance are the phases formed in the systems Pu–U–C and Pu–Th–C, which may be used in high-temperature reactors and thorium breeders, respectively. The Pu–U–C ternary phase diagram has been reported by Mardon and Potter (1970) and by Rosen *et al.* (1963, 1964). In this system, compounds M_3C_2, MC_{1-x}, M_2C_3, and MC_2 are all observed, where M = (U, Pu), in a wide range of compositions. The Pu–Th–C system has been studied by Reavis and Leary (1970), who reported a partial-phase diagram, and by Dalton *et al.* (1967) and Dalton and Griffin (1964).

A few ternary plutonium carbide phases with transition elements have been prepared by arc melting from the components and have been characterized by their XRD data. These compounds are compiled in Table 7.31. An attempt to estimate ternary phase diagrams for a number of ternary plutonium carbide systems was reported by Holleck (1975). A few mixed carbonitrides, carbide oxides, and carbide hydrides, all of them nonstoichiometric, have been prepared.

(b) The plutonium–silicon system

Five compounds are known in the plutonium–silicon system: Pu_5Si_3, Pu_3Si_2, PuSi, Pu_3Si_5, and $PuSi_2$, melting at 1377, 1441, 1576, 1646, and 1638°C, respectively. The phase diagram determined by Land *et al.* (1965b) and redrawn by Kassner and Peterson (1995) is shown in Fig. 7.81. A recent XRD study by Boulet and coworkers found no new compounds other than the five listed above and confirms the phase diagram (Boulet *et al.*, 2003).

The literature of plutonium silicides is relatively sparse, but there are a few detailed reports on exchange reactions and enthalpies of formation (Krikorian and Hagerty, 1990), physical properties (Taylor, 1966), magnetic properties (Boulet *et al.*, 2003), and the phase diagram (Land *et al.*, 1965b); and an excellent overall review (Potter, 1975).

Table 7.31 *X-ray crystallographic data for selected plutonium ternary carbide phases.*

Compound	*Structure type*	*Space group*	*Lattice parameters*			*Formula units per cell*	*Calculated density* (g cm^{-3})	*References*
			a_0 (Å)	b_0 (Å)	c_0 (Å)			
$PuWC_2$	orthorhombic	P*nma*	5.621(3)	3.245(2)	10.896(7)	4	14.93	Ugajin and Abe (1973)
$PuRh_3C$	cubic	P*m3m*	4.098			1	13.50	Haines and Potter (1975)
$PuRu_3C$	cubic	P*m3m*	4.124			1	13.12	Haines and Potter (1975)

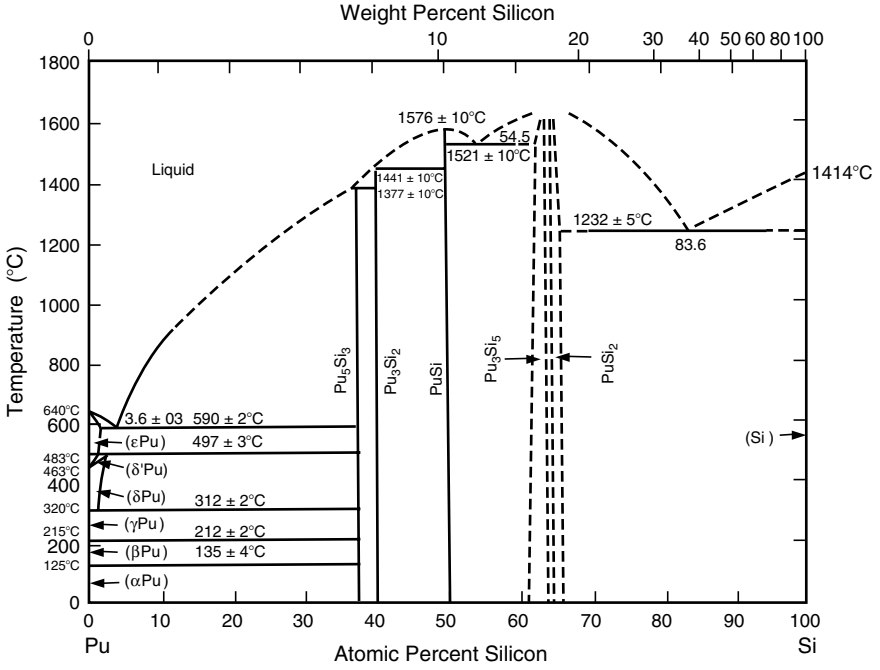

Fig. 7.81 *The plutonium–silicon phase diagram from Land* et al. (1965*b*) *and redrawn from Kassner and Peterson* (1995).

(*i*) *Preparation*

The preparation of plutonium–silicon phases is best carried out by reduction *in vacuo* of plutonium trifluoride with elemental silicon at temperatures above 1200°C in a BeO crucible (Runnalls, 1958):

$$4PuF_3 + (3 + 4x)Si \rightarrow 4PuSi_x + 3SiF_4 \qquad (7.33)$$

Volatile SiF_4 is pumped off, and the plutonium silicide remains. The silicides may also be prepared by arc melting of silicon with plutonium metal or plutonium hydride in an argon atmosphere (Pardue *et al.*, 1964b; Land *et al.*, 1965b; Krikorian and Hagerty, 1990), by reduction of PuO_2 with Si or SiC *in vacuo* at 1400°C (Pardue *et al.*, 1964b), and by fluidized-bed reduction of PuO_2 in the presence of SiO_2 with silane (Fletcher *et al.*, 1967).

(*ii*) *Crystal structures*

The crystal structures of all plutonium silicides have been determined. The basic crystallographic data are listed in Table 7.32. Silicon, like boron, is more electropositive than carbon; thus silicides are more closely related structurally to the borides than the carbides. With increasing silicon content, there is an

Table 7.32 *X-ray crystallographic data for plutonium silicides.*

Compound	*Structure type*	*Space group*	*Lattice parameters*			*Formula units per cell*	*Calculated density* ($g\ cm^{-3}$)	*References*
			a_0 (Å)	b_0 (Å)	c_0 (Å)			
Pu_5Si_3	W_5Si_3	I4/*mcm*	11.409(3)		5.448(2)	2	11.98	Cromer *et al.* (1964)
			11.407(5)		5.444(3)	2		Land *et al.* (1965b)
			11.4035(8)		5.448(3)	2		Boulet *et al.* (2003)
Pu_3Si_2	U_3Si_2	P4/*mbm*	7.483(2)		4.048(2)	2	11.33	Land *et al.* (1965b)
			7.5061(3)		4.0642(3)	2		Boulet *et al.* (2003)
PuSi	FeB	P*nma*	7.933(3)	3.847(1)	5.727(5)	4	10.15	Land *et al.* (1965b)
			7.9360(1)	3.8510(1)	5.7336(1)	4		Boulet *et al.* (2003)
Pu_3Si_5	AlB_2	P6/*mmm*	3.875(4)		4.102(7)	0.5	8.96	Land *et al.* (1965b)
($PuSi_{2-x}$)			3.884(3)		4.082(3)	0.5		Runnalls and Boucher (1955)
			3.8793(6)		4.0860(8)	0.5		Boulet *et al.* (2003)
$PuSi_2$	$ThSi_2$	I4/*amd*	3.967(1)		13.72(3)	4	9.08	Ellinger (1961)
			3.98(1)		13.58(5)	4		Zachariasen (1949b)
			3.9707(3)		13.6809(5)	4		Boulet *et al.* (2003)

increasing tendency to catenate into isolated Si_2 units, or into chains, layers or three-dimensional networks of silicon atoms. Plutonium silicides adopt examples of all these structure types.

The plutonium-rich compound Pu_5Si_3 adopts the tetragonal W_5Si_3 structure, and this structural unit is shown in Fig. 7.82 (Cromer *et al.*, 1964). In this structure, there is a silicon chain composed of columns of alternating $SiPu_8$ square antiprisms with Pu–Si = 3.025 Å. The linear silicon chain runs parallel to the *c*-axis with a Si–Si distance of 2.72 Å. Interspersed between the square antiprisms is another chain of edge-shared $PuSi_4$ tetrahedra that also runs parallel to the *c*-axis, with Pu–Pu = 2.72 Å. In the linear plutonium chain, each plutonium atom in the $PuSi_4$ tetrahedra shows a Pu–Si distance of 2.89 Å. The silicon atoms in the $PuSi_4$ tetrahedra bridge to the plutonium atoms in the $SiPu_8$ antiprisms with a Si–Pu distance of 3.01 Å. These bridges are omitted

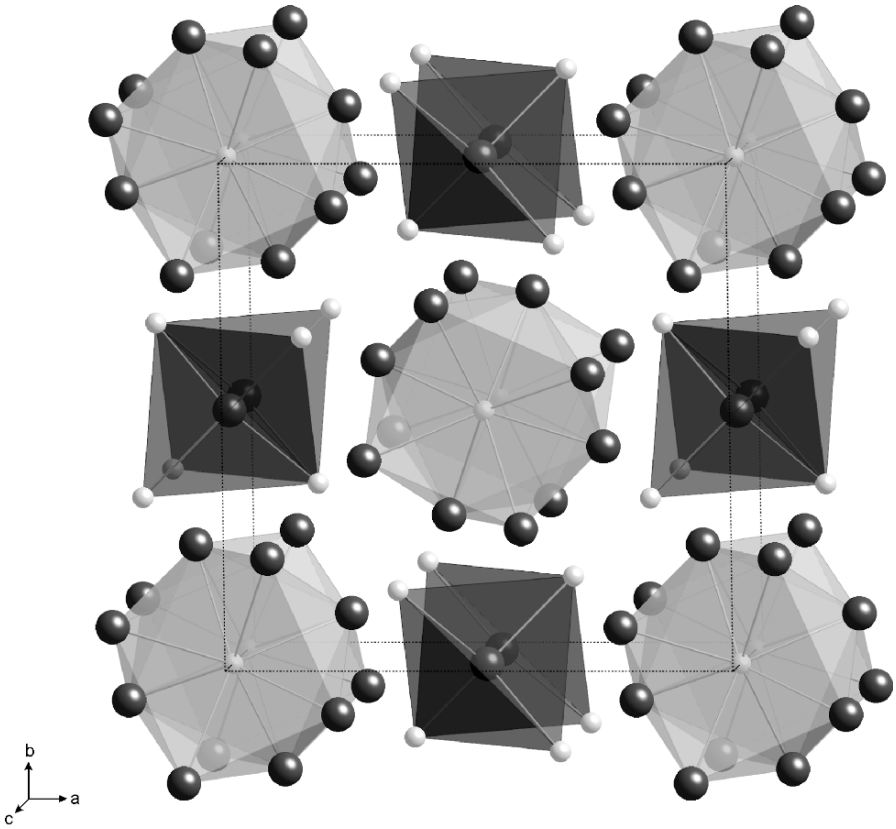

Fig. 7.82 *A polyhedral representation of the solid-state structure of Pu_5Si_3 shown looking down the c-axis, and emphasizing the alternating columns of $SiPu_8$ antiprisms and $PuSi_4$ tetrahedra within the structure. Plutonium atoms are black and silicon atoms are gray.*

from Fig. 7.82 for clarity. Pu_3Si_2 adopts the U_3Si_2 structure, and the basic structural unit is shown in Fig. 7.83. This structure contains a network of Si_2 pairs that are perpendicular to the four-fold axis with Si–Si = 2.35 Å, identical to the Si–Si distance observed in elementary silicon. The plutonium atoms form a puckered cage with Pu–Pu distances of 3.41 Å. The Pu–Si distances range from 2.99 to 3.03 Å.

Plutonium monosilicide is isostructural with ThSi and USi, adopting the FeB structure with infinite one-dimensional zig-zag chains of silicon atoms (Si–Si = 2.35 Å) (Land *et al.*, 1965b). Each silicon atom in the chain is also surrounded by six plutonium atoms at the apices of a trigonal prism with Pu–Si distances spanning the range 2.95–3.03 Å. The PuSi structure is shown in Fig. 7.84. There are four Pu–Pu distances of 3.62 Å, and two Pu–Pu distances of 3.73 Å.

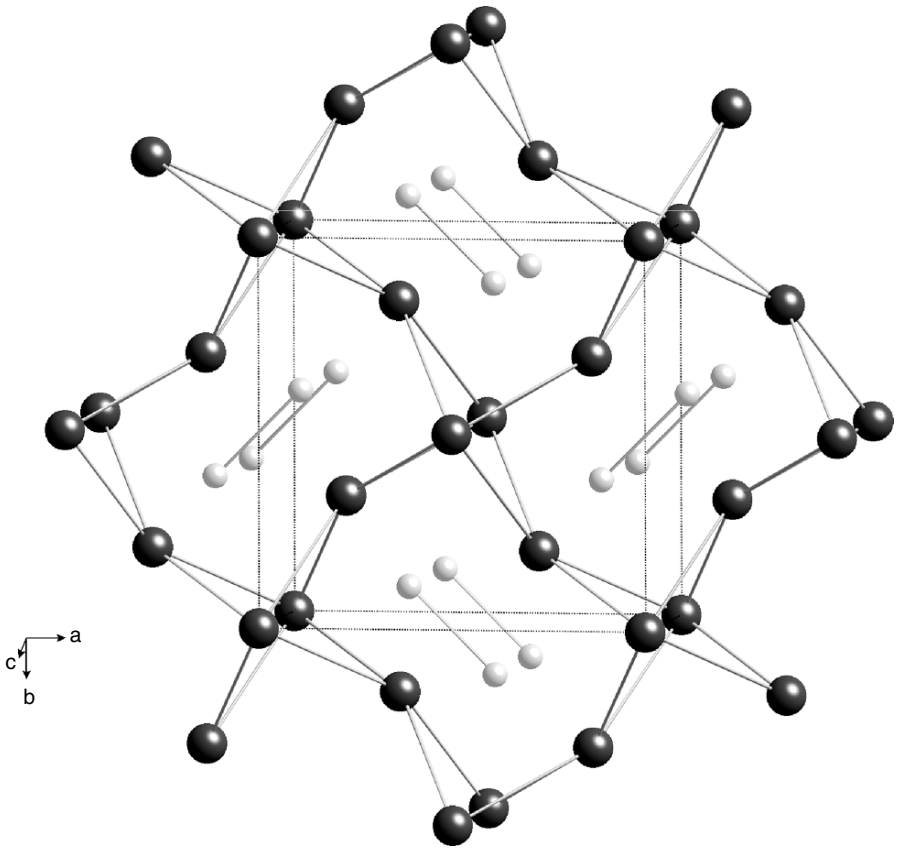

Fig. 7.83 *The solid-state structure of Pu_3Si_2 shown looking down the c-axis, and emphasizing the discrete Si_2 units within the structure. Plutonium atoms are black and silicon atoms are gray.*

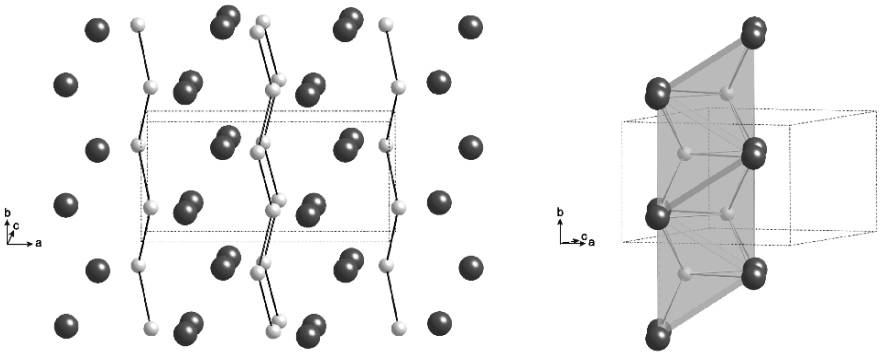

Fig. 7.84 (*left*) *The solid-state structure of PuSi shown looking down the c-axis, and emphasizing the zig-zag chains of Si atoms that run perpendicular to the c-axis. Plutonium atoms are black and silicon atoms are gray.* (*right*) *The same structure rotated by* 45° *and emphasizing the trigonal prismatic* $SiPu_6$ *coordination polyhedra.*

The disilicides form two different structural types that are best considered as defect structures of $PuSi_{2-x}$. There is a hexagonal form of nominal formula Pu_3Si_5 (Runnalls and Boucher, 1955; Ellinger, 1961; Boulet *et al.*, 2003), that adopts the hexagonal AlB_2 structure (discussed for PuB_2, and shown in Fig. 7.75), but the solid is silicon deficient, with vacancies in the silicon sublattice. In this structure there are hexagonal (graphitic) layers of silicon atoms (Si–Si = 2.23 Å) with plutonium atoms interleaved between them (see Fig. 7.75). There is also a tetragonal form that adopts the three-dimensional $ThSi_2$ network structure as shown in Fig. 7.85 (Zachariasen, 1949a,b). In this structure, the silicon atoms form an open, three-coordinated, three-dimensional network. The Si–Si bond lengths are 2.35 and 2.29 Å, which are slightly shorter than that observed in elementary silicon. In the large spaces in this network are the plutonium atoms, each bonded to 12 silicon neighbors with Pu–Si = 3.02 Å. The next nearest neighbors to silicon are six plutonium atoms at this same distance.

(*iii*) *Properties*

The plutonium silicides are hard, brittle, and pyrophoric, with a metallic appearance. They oxidize in air to form PuO_2 (Westrum, 1949b) and are rapidly attacked by water (Pardue and Keller, 1964). Due to their high melting points and high Pu densities, plutonium silicides have been considered as reactor fuels, but the difficulty of preparing them as pure phases has hampered their development for this purpose (Pardue and Keller, 1964; Potter, 1975).

A recent determination of the magnetic properties of PuSi and tetragonal ($ThSi_2$-type) $PuSi_2$ revealed that PuSi orders ferromagnetically around 72 K,

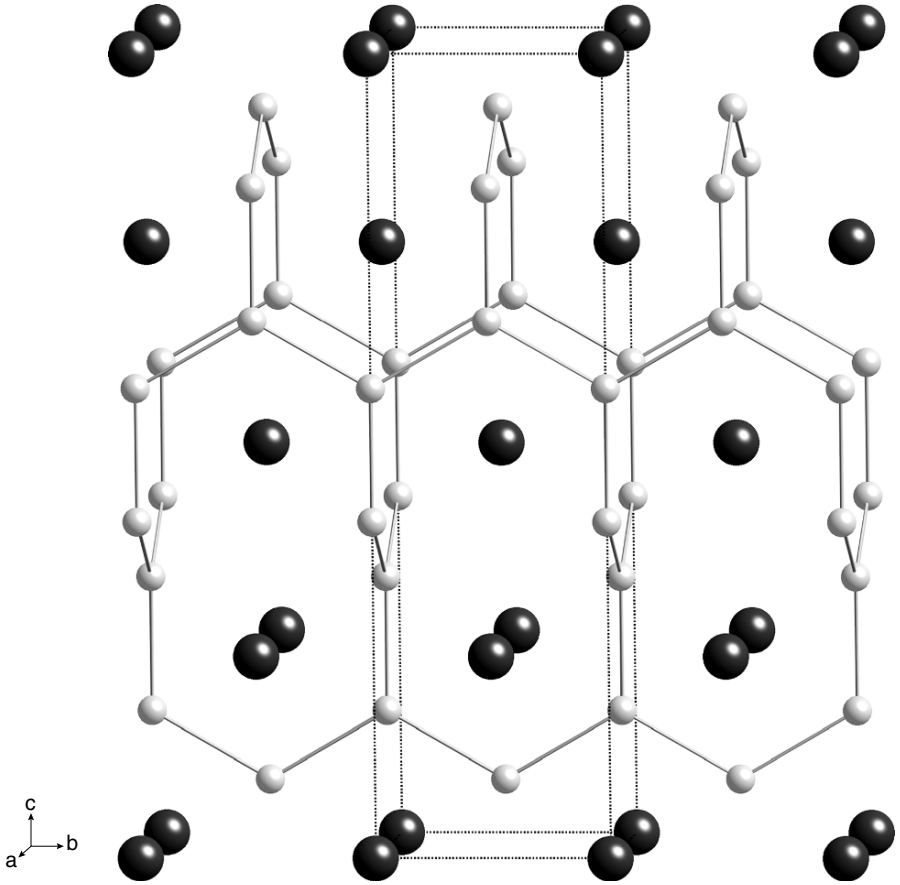

Fig. 7.85 *The solid-state structure of tetragonal $PuSi_2$ shown looking down the a-axis, and emphasizing the three-dimensional network structure of the silicon atoms. Plutonium atoms are black and silicon atoms are gray.*

whereas $PuSi_2$ shows no magnetic ordering (Boulet *et al.*, 2003). The values of the effective moments of PuSi (μ_{eff} ca. $0.72\mu_B$) and $PuSi_2$ (μ_{eff} ca. $0.54\mu_B$) are consistent with a $5f^5$ electronic configuration and a Pu^{3+} oxidation state.

7.8.4 Plutonium pnictides

With pnictogen elements, plutonium forms compounds in three basic families with the highest order composition being PuX_2 that is only found for the heaviest pnictogen elements (X = Sb and Bi). With antimony, thermal dissociation permits the preparation of an intermediate composition Pu_4Sb_3. By far, the most important class of compounds are the monopnictides PuX (N, P,

As, Sb, Bi), which form an isostructural series that has played an important role in understanding the degree of localized versus delocalized bonding with 5f electrons.

Plutonium pnictides are generally prepared by reaction of plutonium metal or hydride with the pnictogen in evacuated sealed quartz tubes that are heated to 400–750°C. The monopnictides can be prepared by thermal dissociation of a higher pnictide. Reviews of synthesis (Spirlet, 1991) and structural properties are available (Damien *et al.*, 1986).

(a) The plutonium–nitrogen system

There is only one compound in the plutonium–nitrogen system that is known with certainty: the cubic mononitride PuN. The Pu–N phase diagram has recently been assessed (Wriedt, 1989; Kassner and Peterson, 1995) and is illustrated in Fig. 7.86. The locations of the boundaries on the Pu-rich and N-rich sides of PuN have not been evaluated in detail, but the composition range of PuN is probably quite narrow. PuN decomposes under 1 bar of N_2 pressure at 2570°C into N_2-saturated liquid plutonium and N_2. Liquid plutonium is formed

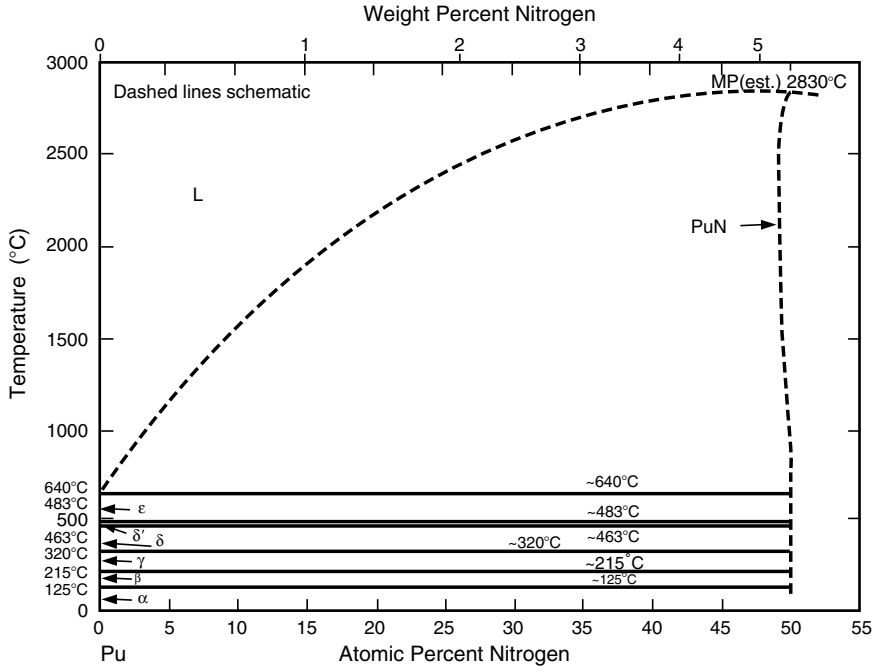

Fig. 7.86 *The plutonium–nitrogen phase diagram* (*Wriedt,* 1989*; Kassner and Peterson,* 1995).

above 1500°C due to incongruent evaporation of PuN. Because of problems associated with sample vaporization, the melting point of PuN has not been observed.

There is a fascinating report by Green and Reedy (1978a) of the observation of matrix isolated PuN_2 containing a molecular N_2 unit and characterized using IR spectroscopy. Theoretical studies discussing the existence, and the nature of chemical bonding in PuN_2 have subsequently appeared (Archibong and Ray, 2000; Tan, 2003).

(*i*) *Preparation*

Cubic PuN can be prepared most conveniently by reaction of metal with H_2 (150–200°C) to produce plutonium hydride, followed by heating the hydride under N_2 at temperatures between 500 and 1000°C (Pardue *et al.*, 1964a, 1967). The preparation can also be accomplished by reaction of plutonium metal with N_2 containing small amounts of H_2 at 250°C (Anselin, 1963a,b; Bridger and Dell, 1967). In view of the facile reactivity of plutonium metal with H_2 (see Section 7.7.1) it is likely that this reaction is catalyzed by surface hydriding of the plutonium metal at 200°C. In the absence of H_2, the direct reaction of pure plutonium metal with N_2, even over a period of 150 h at 1000°C, does not ensure complete conversion to PuN (Brown *et al.*, 1955). The nitride can also be prepared by the carbothermic reduction of PuO_2 under N_2 (Muromura, 1982; Suzuki *et al.*, 1983; Bardelle and Bernard, 1989; Takano *et al.*, 2001), though care must be taken to avoid product contamination with carbon and oxygen impurities. This is a common approach for making nitride fuels as it avoids making large quantities of plutonium hydride in a nuclear facility. The nitride can also be prepared by the reaction of plutonium hydride with ammonia between 600 and 650°C (Abraham *et al.*, 1949c). An interesting low-temperature route to PuN is the reaction of PuI_3 with sodium or potassium metal in liquid ammonia:

$$PuI_3 + NH_{3(l)} + 3M \rightarrow PuN + 3MI + 1.5H_2, \quad M = Na, K \tag{7.34}$$

In this approach, PuI_3 is dissolved in liquid ammonia, followed by reduction with a stoichiometric amount of sodium or potassium metal. The reaction likely proceeds through the *in situ* formation of the active metal amide, MNH_2 (M = Na, K), which undergoes subsequent metathesis with PuI_3. PuN precipitates from liquid ammonia as a black powder, which is washed with liquid ammonia and annealed at 700°C for 24 h (Cleveland *et al.*, 1974, 1975).

Freshly prepared PuN is black, turning brown in moist air due to hydrolysis (Storms, 1964). Formulations of (U, Pu, Zr)N that contain only a few percent of plutonium are golden-yellow. Because of problems with sample vaporization, the melting point of PuN has not been observed, but it has been estimated that congruent melting occurs at 2830 ± 50°C for an N_2 pressure of 50 ± 20 atm (Spear and Leitnaker, 1968).

(*ii*) *Crystal structure*

The crystal structure of PuN was first studied by Zachariasen and shown to exhibit the cubic NaCl structure (Zachariasen, 1949c,d). In cubic PuN, the plutonium and nitrogen atoms alternate in a fcc sphere packing arrangement, with both Pu and N having regular octahedral coordination. Using a lattice parameter of 4.905 Å, the Pu–N and Pu–Pu distances are 2.45 and 3.47 Å, respectively. Many lattice parameter studies of PuN have been reported and recently were summarized (Wriedt, 1989). The rather large variation in lattice parameter is most likely due to the effects of impurities, self-irradiation damage, or nitrogen concentration. A lattice parameter value of 4.918 Å was reported from the results of neutron diffraction on ^{239}PuN at –213°C (Boeuf *et al.*, 1984). Crystallographic properties of PuN and other plutonium pnictides are given in Table 7.33.

(*iii*) *Properties*

Plutonium mononitride is a refractory material with great potential for use as a nuclear reactor fuel (Matzke, 1986; Blank, 1994). It has a high melting point, high density, and high thermal conductivity. Moreover, it is compatible with austenitic steels up to 600°C and with sodium up to its boiling point of 890°C. One drawback is that PuN has a high volatility (due to release of N_2) at the high temperatures possible in a reactor accident. Due to the potential use of PuN in reactor fuels (Sano *et al.*, 1971; Bernard, 1989; Ogawa *et al.*, 1998; Albiol and Arai, 2001), there is an extensive literature on PuN, and topical reviews can be found on the physical and chemical properties (Spear and Leitnaker, 1968; Benedict, 1979), thermodynamic properties (Matsui and Ohse, 1987; Lemire *et al.*, 2001), phase equilibria (Wriedt, 1989), and synthesis (Spirlet, 1991). Selected physical properties of PuN are given in Table 7.34 (Holleck and Kleykamp, 1972; Kleykamp, 1999), and thermodynamic properties of PuN and other plutonium pnictides can be found in Table 7.35.

Powdered PuN reacts with O_2 at 200°C and ignites at 280–300°C to form PuO_2 (Kruger and Moser, 1967a). In moist O_2, the oxidation rate is increased: in the presence of 500 ppm water vapor, the reaction rate at 279°C is three times that without H_2O vapor. In air at room temperature, PuN powder is converted to PuO_2 within 3 days, but compact PuN is oxidized rather slowly (Pardue *et al.*, 1967).

PuN reacts slowly with cold water, but readily with hot water (Bridger *et al.*, 1969). In moist air, PuN decomposes within a few hours at 80–90°C, and within days at room temperature (Storms, 1964). The hydrolysis of PuN was determined in a stream of Ar–H_2O as a function of temperature to give hydrated PuO_2 (Bridger and Dell, 1967). Concentrated mineral acids will decompose PuN with decreasing violence of reaction in the order $HNO_3 > HCl > H_3PO_4 > H_2SO_4 > HF$ (Pardue *et al.*, 1964a).

Table 7.33 *X-ray crystallographic data for plutonium pnictides.*

Compound	*Symmetry*	*Space group*	*Lattice parameter,* a_0 (Å)	*Formula units per cell*	*Calculated density* (g cm^{-3})	*References*
PuN	fcc	F*m*3*m*	4.9055(3)	4	14.22	Ellinger (1961)
			4.9053–4.9056 (N-rich)			Olson and Mulford (1964)
			4.9051 (N-deficient)			Olson and Mulford (1964)
			4.9053 (O-free)			Bridger and Dell (1967)
			4.908 (O-saturated)			Bridger and Dell (1967)
PuP	fcc	F*m*3*m*	5.664(4)	4	9.87	Kruger and Moser (1966a)
			5.6582(1)–5.6613(1)		9.89	Kruger and Moser (1967a)
PuAs	fcc	F*m*3*m*	5.855(4)	4	10.39	Kruger and Moser (1966a)
			5.8586(1)		10.34	Kruger and Moser (1967a)
PuSb	fcc	F*m*3*m*	6.241(1)	4	9.86	Kruger and Moser (1967a)
			6.2396(1)	4		Mitchell and Lam (1971)
Pu_4Sb_3	cubic	I$\bar{4}$3*d*	9.2406[a]	4		Mitchell and Lam (1974)
			9.2370(5)			Charvillat (1978)
$PuSb_2$	orthorhombic	C*mca*	$a = 6.19(1)$	8	9.735	Charvillat *et al.* (1977)
			$b = 6.05(1)$			
			$c = 17.58(4)$			
PuBi	fcc	F*m*3*m*	6.350(1)	4	11.62	Ellinger (1961)

[a] Labeled as Pu_3Sb_4.

Table 7.34 *Selected properties of PuN of relevance to nuclear fuel.*

Property	*Value*	*References*
Decomposition temperature, 1 bar N_2	2570°C	Oetting (1967)
Nitrogen partial pressure at		
1500°C	2×10^{-7} bar	Alexander *et al.* (1969)
2000°C	1×10^{-4} bar	Alexander *et al.* (1969)
Metal partial pressure at		
1500°C	1×10^{-6} bar	Alexander *et al.* (1969)
2000°C	6×10^{-4} bar	Alexander *et al.* (1969)
Thermal conductivity at		
1000°C	13 W K^{-1} m^{-1}	Alexander *et al.* (1976)
1500°C	14 W K^{-1} m^{-1}	Alexander *et al.* (1976)
2000°C	15 W K^{-1} m^{-1}	Alexander *et al.* (1976)

Table 7.35 *Selected thermodynamic properties of plutonium pnictides, PuX (X = N, P, As, Sb, Bi)* (*Lemire* et al., 2001).

Compound	$\Delta_f G^\circ_{298}$ (kJ mol^{-1})	$\Delta_f H^\circ_{298}$ (kJ mol^{-1})	S°_{298} (J K^{-1} mol^{-1})	$C^\circ_{p_{298}}$ (J K^{-1} mol^{-1})
PuN	-273.7 ± 2.6	-299.2 ± 2.5	64.8 ± 1.5	49.6 ± 1.0
PuP	-313.8 ± 21.1	-318 ± 21	81.3 ± 6.0	50.20 ± 4.00
PuAs	-241.4 ± 20.1	-240 ± 20	94.3 ± 7.0	51.6 ± 4.0
PuSb	-152.1 ± 20.1	-150 ± 20	106.9 ± 7.5	52.8 ± 3.5
PuBi	-119.6 ± 20.2	-117 ± 20	120 ± 10	

(b) The plutonium–phosphorus system

Plutonium monophosphide, PuP, is the only well-defined binary plutonium–phosphorus compound known. Cubic PuP can be prepared by reaction of metal with H_2 (150–200°C) to produce plutonium hydride, followed by heating the hydride with PH_3 (Kruger *et al.*, 1966; Kruger and Moser, 1966b). By employing a stepwise reaction consisting of alternate hydride decomposition and reaction of the decomposition product with PH_3, one can obtain very pure PuP product. At least two cycles of alternate hydride decomposition and reaction with phosphine are required. The conversion cycles are followed by 4 h annealing at 1400°C. The preparation can also be accomplished by reaction of powdered plutonium hydride with excess (100–150%) red phosphorus in tantalum-lined pressure vessels at 600–800°C in an argon atmosphere (Moser and Kruger, 1966). After completion of the reaction, excess phosphorus is removed by distillation at 300°C. Alternatively, the phosphide can be prepared by induction melting of plutonium chips with elemental phosphorus *in vacuo* or under pressure of 1 atm of helium. The exothermal reaction goes to completion

at 1400°C (Gorum, 1957). Another method involves the reaction of sol–gel prepared PuO_2 with a stream of PH_3 at temperatures of 1000°C or greater (Cogliati *et al.*, 1969).

PuP has a dark-gray color and melts with decomposition at 2600°C under argon. It exhibits the NaCl structure (see Table 7.33) (Gorum, 1957; Kruger *et al.*, 1966), with lattice constants that depend on sample history. Below 125 K, a tetragonal distortion is observed (Mueller *et al.*, 1979). A number of physical properties (microhardness, thermal expansion, thermoelectric power, temperature conductivity, and heat capacity) have been measured (Hall *et al.*, 1985).

PuP is ferromagnetic below a Curie temperature of $T_c = 126 \pm 1$ K. Above this temperature, the magnetic susceptibility has a temperature dependence given by $\chi_m = 190 \times 10^{-6} + N_L\mu^2/[3k(T–126)]$ cm^3 mol^{-1} where $\mu = 1.06\mu_B$ (Lam *et al.*, 1969). The ferromagnetic moment obtained by extrapolation to 0 K was found to be $0.42/\mu_B$ (Lam *et al.*, 1969). The Landé *g*-factor obtained by a correlation between Knight shift and χ_m is $g = 2/7$ (Fradin, 1970). Thermodynamic and magnetic properties have been discussed (Arai and Ohmichi, 1995).

(c) The plutonium–arsenic system

Plutonium arsenide, PuAs, may be prepared by reaction of plutonium metal with excess arsenic under 1 atm of helium or *in vacuo* at 500–1200 K (Gorum, 1957; Pardue *et al.*, 1964b; Mitchell and Lam, 1974) for a period of 3–7 h. It can also be prepared by reaction of PuH_3 with As *in vacuo* (0.02 Torr, 2.6×10^{-5} atm) at temperatures above 400°C, which are slowly increased to 700°C. The product is homogenized *in vacuo* at a still higher temperature (Kruger and Moser, 1967b; Fradin, 1970; Handwerk and Kruger, 1971; Charvillat and Damien, 1973). Finally, it can be prepared by reaction of plutonium partially converted to the hydride with AsH_3 at 250°C and subsequent recycling at 400, 500, 600, and 700°C in a similar manner as just described for PuP in Section 7.8.4(b) (Anselin, 1963b; Lam *et al.*, 1969). Because of the low decomposition temperature of AsH_3 (300°C), the primary reaction is done at 250°C, and only the annealing cycles are carried out at the higher temperatures mentioned above. Plutonium arsenide is a gray, metallic-looking material, black in finely divided form. Its crystallographic properties are listed in Table 7.33.

(d) The plutonium–antimony system

Arc melting of mixtures of plutonium and antimony yields PuSb (Kruger and Moser, 1966a). In addition to the monopnictide, plutonium also forms a dipnictide $PuSb_2$ (Charvillat *et al.*, 1977), and an intermediate composition, Pu_4Sb_3 (Damien *et al.*, 1986). Cubic PuSb melts at 1980 ± 30°C under 3 atm of argon (Mitchell and Lam, 1974).

The diantimonide exhibits an unusual orthorhombic structure formed by ten layers of atoms, and this structure is shown in Fig. 7.87. Each plutonium atom has four nearest antimony atoms ranging 3.15–3.30 Å away forming a distorted Sb_4 square just below, and another just above but rotated by 45 degrees. The local coordination polyhedron about plutonium is that of a distorted square antiprism. The Sb–Sb distances within the square are 3.095 Å, and the Sb–Sb distances linking the two groups of antiprisms are 2.755 Å. The structure is described in more detail for AB_2 rare-earth compounds by Wang and Steinfink (1967).

(e) Valency and electronic structure in PuX compounds

Plutonium monopnictides show moderately delocalized 5f electrons. The degree of localization increases with atomic number of the pnictogen, with delocalization being largely dominated by plutonium–pnictogen interactions. The lattice parameter is affected by this partial delocalization, making it hard to deduce plutonium valence from the crystal structure or lattice parameter value.

Magnetic susceptibility measurements of plutonium monopnictides show high-temperature Curie–Weiss-like behavior that gives effective moments close to the value of $1.24\mu_B$, consistent with an f^5 ion, and trivalent plutonium (Vogt and Mattenberger, 1993, 1995). The ordered magnetic moments are significantly smaller, and the experimental data suggest partial f-electron localization. For example, X-ray photoemission studies of PuSb clearly indicate localized f-electrons (Gouder *et al.*, 2000), while resistivity measurements show a semimetallic Kondo-like behavior (Blaise *et al.*, 1985). Magnetism experiments show a very strong anisotropy in all PuX compounds, with magnetic moments oriented along the [100] direction (Mattenberger *et al.*, 1986). Neutron scattering experiments (Lander *et al.*, 1984, 1985) support Cooper's interpretation of moderate f-electron delocalization being responsible for the reduction in the ordered moment and strong anisotropy in plutonium monopnictides (Cooper *et al.*, 1983). Recent electronic structure calculations of PuX compounds based upon a self-interaction correlated local spin density (SIC-LSD) approach support the interpretation that the plutonium 5f-electron manifold is best described in a mixed picture of localized and delocalized states (Petit *et al.*, 2002).

7.8.5 Plutonium chalcogenides

(a) The plutonium–oxygen system

Binary plutonium oxides, especially PuO_2, are of tremendous technological importance. They find widespread application as nuclear fuels, as long-term storage forms for both spent nuclear fuels and surplus weapons materials, and

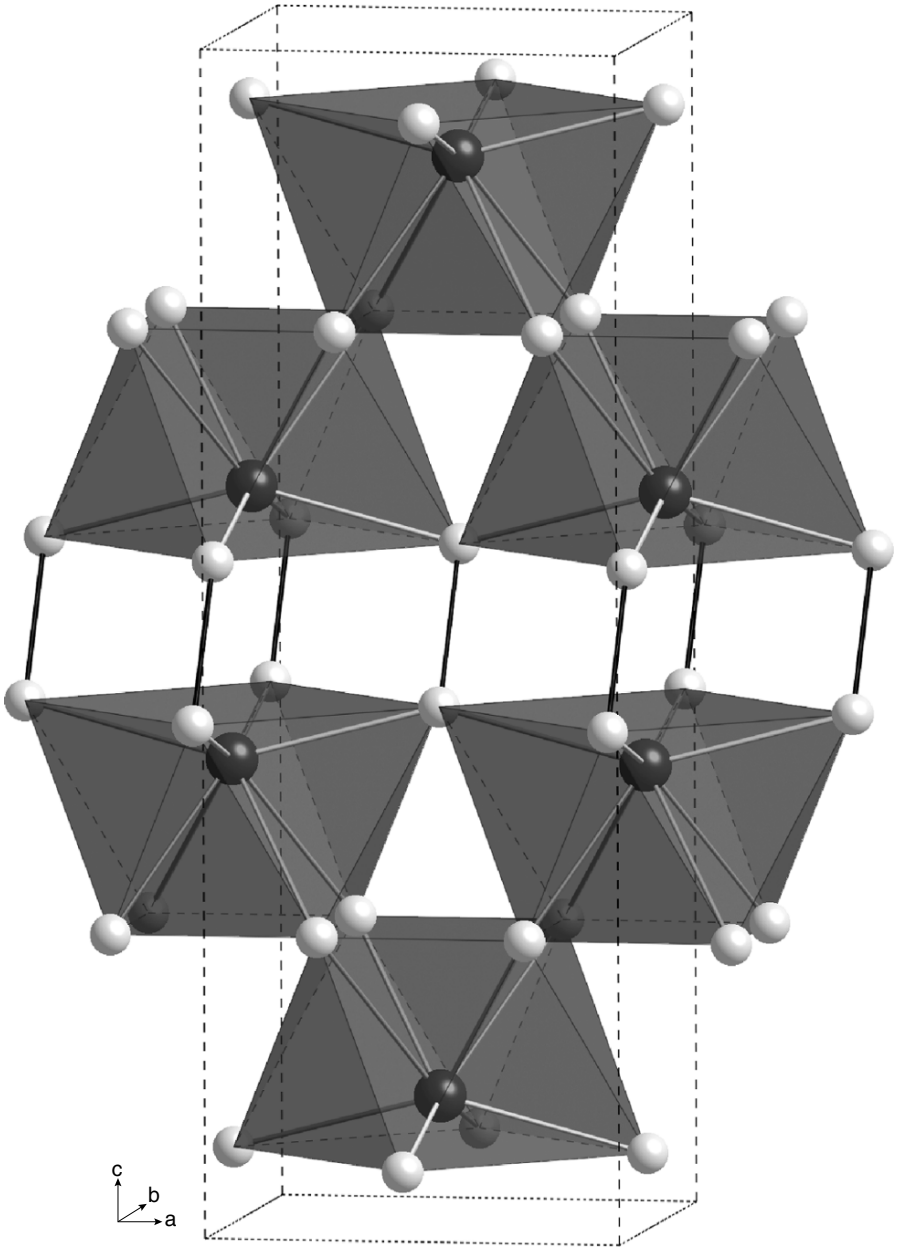

Fig. 7.87 *The solid-state structure of $PuSb_2$ shown looking perpendicular to the c-axis, and emphasizing the antiprismatic $PuSb_8$ polyhedral layers. Plutonium atoms are black and antimony atoms are gray.*

as heat and power generators (^{238}Pu) for interplanetary exploration. Their properties are also important because oxide particulates contribute to environmental actinide migration, participate in corrosion reactions in nuclear weapons, and exist as chemical intermediates in the purification and preparation of other actinide compounds. This same family of oxides is also of fundamental scientific interest. Even though plutonium oxides were among the first compounds of plutonium to be studied, it is astonishing to consider how much remains unknown about plutonium oxides. A number of reviews on the plutonium–oxygen system have appeared (Chikalla *et al.*, 1962; IAEA, 1967; Wriedt, 1990; Naito *et al.*, 1992).

(*i*) *Phase equilibria*

A good deal of discussion has appeared in the literature regarding the phase diagram for the plutonium–oxygen system, and there are conflicting sets of data for some phases (IAEA, 1967; Wriedt, 1990; Naito *et al.*, 1992; Haschke *et al.*, 2000a). The system is complex, and additional study is still needed to resolve certain issues surrounding the phase diagram. To adequately describe the issues associated with the plutonium–oxygen system, Haschke and Haire (2000) chose to present two diagrams, one based on the most recent assessment with modifications, and another, more pedagogical diagram based upon analogy with the more well-studied and better understood lanthanide oxide systems. There is great utility in this approach, and we have adopted it for our discussion. The proposed phase diagram based on the most recent assessments is shown in Fig. 7.88, and a table of crystallographic data for plutonium oxides is given in Table 7.36.

There are four fundamental equilibrium solid phases in the plutonium–oxygen system. The first of these is the stoichiometric hexagonal sesquioxide of formula Pu_2O_3 with a very small composition range near 60 at.% oxygen and with an ideal stoichiometry of $PuO_{1.5}$. This phase is also commonly known in the literature as hexagonal A-Pu_2O_3, or β-Pu_2O_3, and other designations have also been used (Wriedt, 1990; Haschke and Haire, 2000). We will use the designation A-Pu_2O_3. There is a bcc sesquioxide of composition $PuO_{1.52}$, reported to have only a small composition range near 60.3 at.% oxygen, but this narrow stoichiometry range is not supported by all the available data (Haschke and Haire, 2000). This phase has been commonly referred to as cubic C-Pu_2O_3, α-Pu_2O_3, and α-$Pu_2O_{3+\delta}$, but again, other designations have also appeared in the literature. We will use the designation C-Pu_2O_3.

There is a bcc oxide of intermediate composition $PuO_{1.61}$ with a composition range between 61.7 and 63.0 at.% oxygen that is commonly referred to as C′-Pu_2O_3, α′-Pu_2O_3, $PuO_{1.6+\delta}$, and others. This cubic phase is not stable at room temperature but exists above 335°C. Due to its broad composition range, Haschke and Haire referred to this phase as $PuO_{1.6+\delta}$ to help distinguish this bcc phase from the oxygen-deficient fcc PuO_{2-x}. We will use the designation

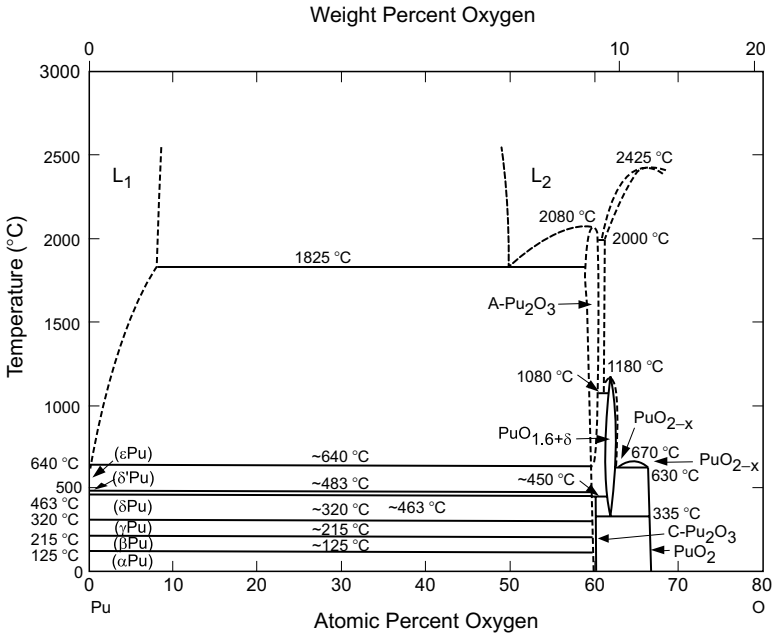

Fig. 7.88 *The plutonium–oxygen phase diagram* (*Wriedt,* 1990*; Naito* et al., 1992*; Haschke* et al., 2000*a*).

$PuO_{1.6+\delta}$. There is a fcc dioxide PuO_2 with a wide composition range that runs from $PuO_{1.6}$ to PuO_2, and sometimes referred to as substoichiometric PuO_2 or PuO_{2-x}. At room temperature, PuO_{2-x} has a fairly narrow composition range between $PuO_{1.98}$ and $PuO_{2.03}$, while at higher temperatures the homogeneity range widens to $PuO_{1.6}$ and PuO_2 as indicated in the phase diagram. Note that the oxygen-deficient fcc $PuO_{1.6}$ (PuO_{2-x}) is not the same as the bcc $PuO_{1.61}$ described above; this is why we prefer the nomenclature $PuO_{1.6+\delta}$ for the bcc phase. On the plutonium-rich side, cubic $PuO_{1.6+\delta}$ coexists with cubic C-Pu_2O_3 until it undergoes a peritectoid decomposition into hexagonal A-Pu_2O_3 and cubic $PuO_{1.6+\delta}$ above 450°C. On the oxygen-rich side of this composition range, C-Pu_2O_3 coexists with PuO_{2-x} below 630°C, and with metal-rich PuO_{2-x} at higher temperatures until it congruently transforms into PuO_{2-x} at 1180°C. Hexagonal A-Pu_2O_3 coexists with oxygen-saturated metal and displays an increasing extent of nonstoichiometry until the congruent melting point of 2080°C is reached. PuO_2 undergoes congruent melting at 2425°C. Only recently has there been enough new data to suggest the addition of a hyperstoichiometric fcc oxide, PuO_{2+x} with composition that runs from stoichiometric PuO_2 to $PuO_{2.27}$ between room temperature and 350°C (Haschke *et al.*, 2000b). This is not shown in Fig. 7.88, but is included in the notional phase diagram shown in Fig. 7.92.

Table 7.36 *X-ray crystallographic data for plutonium oxides.*

Compound or phase	*Structure type*	*Symmetry*	*Space group*	*Unit cell dimensions* (Å)	*Formula units per cell*	*X-ray density* ($g\ cm^{-3}$)	*References*
PuO	NaCl	fcc	F*m*3*m*	$a = 4.96(1)$	4	13.88	Ellinger (1961)
$PuO_{1.5}$ ($A\text{-}Pu_2O_3$, $\beta\text{-}Pu_2O_3$)	La_2O_3	hexagonal	P$\bar{3}$*m*1	$a = 3.841(6)$ $c = 5.958(5)$	1	11.47	Ellinger (1961)
$PuO_{1.51}$ ($C\text{-}Pu_2O_3$, $\alpha\text{-}Pu_2O_3$)	Mn_2O_3	bcc	I*a*3	$a = 11.02(2)$	16	10.44	Ellinger (1961)
$PuO_{1.61}$ ($PuO_{1.6+\delta}$, $C'\text{-}Pu_2O_3$, $\alpha'\text{-}Pu_2O_3$)	Mn_2O_3	bcc	I*a*3	$a = 10.95 - 11.01$			Gardner *et al.* (1965)
PuO_2	CaF_2	fcc	F*m*3*m*	$a = 5.3960(3)$ for stoichiometric composition	4	11.46	Ellinger (1961)
$^{238}PuO_2$	CaF_2	fcc	F*m*3*m*	$a = 5.4141(1)$	4		Roof (1973)
$PuO_{2.26}$	CaF_2	fcc	F*m*3*m*	$a = 5.404$	4		Haschke *et al.* (2000b)

(*ii*) *Preparation*

Plutonium monoxide, PuO

While it has been reported on numerous occasions, the existence of a *stable* condensed oxide of formula PuO is still uncertain and is therefore not indicated in the phase diagram of Fig. 7.88. The material that has been described by many authors is most likely a disordered oxide–carbide $Pu(O_x,C_{1-x})$. Mooney and coworkers (Mooney and Zachariasen, 1949; Zachariasen, 1949d) described powder patterns that could be attributed to cubic PuO, and Holley *et al.* reported a NaCl-type fcc phase with $a_0 = 4.96(1)$ Å as a surface film formed on plutonium metal. Westrum (1949a) describes the material as a semimetallic substance with an almost metallic luster. This surface material has also been observed upon heating oxide-coated plutonium metal *in vacuo* at 250–500°C (Terada *et al.*, 1969). Other reports on the preparation of PuO include the reaction of molten plutonium (microgram quantities) with stoichiometric oxygen generated by thermal decomposition of Ag_2O (Akimoto, 1960), by reduction of PuO_2 with carbon at 1500–1800°C (Skavdahl, 1964), or by reduction of PuOCl or PuO_2 with Ba vapor at 1250°C (Westrum, 1949a). Reshetnikov (2003) has recently claimed to prepare pure PuO by heating PuOCl with calcium at 1200°C, but no characterization data are provided to substantiate the claim. Haschke and Haire (2000) point out that plutonium oxide that results from metal oxidation may be covered with a layer of unbound carbon formed as a result of interaction of the oxide with hydrocarbons or CO_2, and that experiments by Forbes *et al.* (1966) indicate that all products thus obtained contain carbon. The observed lattice parameter is nearly identical to that found for oxide–carbide solid solutions (Mulford *et al.*, 1965; Oetting, 1967). Work on the Pu–O–C phase diagram has shown conclusively that the oxygen-rich limit of the $Pu(O_x,C_{1-x})$ phase lies at a composition of approximately $PuC_{0.3}O_{0.7}$ (Forbes *et al.*, 1966; Taylor *et al.*, 1967; Larson, 1980; Larson and Haschke, 1981). Larson and Haschke (1981) used XPS data to demonstrate that a material believed to be PuO was in fact $PuO_{0.65\pm0.15}C_{0.45\pm0.15}$.

Although the above paragraph argues that most materials that were thought to be PuO were likely contaminated with carbon, and therefore likely to be $Pu(O_xC_{1-x})$ there are several intriguing reports about an unstable, metallic-gray, pyrophoric product that deserve additional study. Reshetnikov (2003) describes an explosion that occurred in 1949 upon grinding a sample thought to be plutonium with a glass rod. Similarly, Haschke described a steel-gray product formed upon the thermal decomposition of PuOH (Haschke *et al.*, 1983; Haschke, 1992). This material underwent a violent exothermic reaction with oxygen, destroying a quartz microbalance container. Such behavior would not be expected for PuO_xC_{1-x}. Thus there may be some instances where a metastable form of solid PuO has indeed been prepared. The full characterization of the material produced by Haschke was not undertaken due its pyrophoric nature (Haschke, 1992), and characterization of the material prepared by Reshetinikov

was not provided. We will need to wait for additional characterization data to resolve this issue.

While the existence of solid-phase PuO is unresolved, there is little doubt that gaseous PuO is one of the major species of plutonium oxides in the vaporization process (Green and Reedy, 1978b; Capone *et al.*, 1999; Ronchi *et al.*, 2000). PuO is observed in both the mass spectrum of effusing vapors over PuO_2 (Capone *et al.*, 1999; Ronchi *et al.*, 2000), and in the IR absorption spectra of vapors trapped in argon and krypton matrixes. $Pu^{16}O$ trapped in an argon matrix displays an infrared vibrational frequency of 822.28 cm^{-1} (Green and Reedy, 1978b).

Plutonium sesquioxide phases, Pu_2O_3

There is a good deal of confusion about both the preparative methods and the phase relationships between hexagonal (A-Pu_2O_3) and cubic (C-Pu_2O_3) forms of plutonium sesquioxide. The methods of preparation of hexagonal and cubic forms are very similar, yet these oxides are described as separate and distinct phases at low temperature. As outlined in recent reviews (Wriedt, 1990; Haschke and Haire, 2000), these compounds are thought to be distinct phases because (i) both cubic and hexagonal phases have been observed to coexist; (ii) the transformation between hexagonal and cubic forms has not been observed; and (iii) their regions of composition do not overlap. It has been suggested that kinetic factors may favor the formation of the cubic sesquioxide at low temperature in the presence of plutonium metal (Haschke and Haire, 2000). For example, cubic C-Pu_2O_3 readily forms as a surface layer when PuO_2-coated δ-stabilized plutonium metal is heated to 150–200°C under vacuum (Terada *et al.*, 1969). This observation is highly suggestive that the preexisting fcc lattice of metal atoms in either the underlying metal, the fcc dioxide, or both, imparts some control over the nature of the product in the reaction, and that once the cubic sesquioxide is formed, this phase cannot transform into the hexagonal form unless the temperature exceeds 450°C. The hexagonal form apparently does not transform back into the cubic form at this temperature, suggesting perhaps that more kinetic energy is necessary to rearrange the metal atoms in the lattice. This behavior is not consistent with the known behavior of the isomorphic lanthanide oxides, where hexagonal Nd_2O_3 will transform reversibly to cubic Nd_2O_3 near 600°C (Haire and Eyring, 1994). Thus cubic C-Pu_2O_3 may be only metastable at low temperatures.

Several methods of preparation have been reported for the hexagonal A-Pu_2O_3 sesquioxide. Plutonium dioxide can be reduced with plutonium metal (Holley *et al.*, 1958), dry hydrogen (Flotow and Tetenbaum, 1981), or carbon (Skavdahl, 1964) to form A-Pu_2O_3. Pure hexagonal A-Pu_2O_3 has been prepared by reducing pure PuO_2 with a 20% excess of plutonium turnings or chips in a closed tantalum crucible at 1500°C according to the stoichiometry (Holley *et al.*, 1958):

$$3PuO_2 + Pu \rightarrow 2Pu_2O_3 \qquad (7.35)$$

After a reaction period of 3 h, the excess plutonium metal was removed by sublimation from the open crucible at 1800–1900°C *in vacuo* (Holley *et al.*, 1958; Chikalla *et al.*, 1962, 1964). At higher reaction temperatures, large, flat crystals of hexagonal A-Pu_2O_3 were obtained. In another procedure, Gardner *et al.* (1965) reduced pure PuO_2 powder with a 20% excess of hydride-powdered plutonium metal in a ThO_2 crucible at 1500°C for 3 h in a stream of purified dry hydrogen.

Hydrogen reduction of PuO_2 to produce hexagonal A-Pu_2O_3 can be accomplished at 1550°C in very dry hydrogen purified over titanium turnings (Gardner *et al.*, 1965). Complete reduction of PuO_2 by hydrogen has also been reported to occur in the temperature range 1700–2000°C (Dayton and Tipton, 1961; Flotow and Tetenbaum, 1981). Pure hexagonal A-Pu_2O_3 may be prepared by the stoichiometric reduction of PuO_2 with carbon at (1800 ± 50)°C for 5.5 h in a pure helium atmosphere (Skavdahl, 1964; Forbes *et al.*, 1966) according to the reaction:

$$2PuO_2 + C \rightarrow Pu_2O_3 + CO \tag{7.36}$$

Chikalla and coworkers reported a large-scale preparation (ca. 110 g Pu) of hexagonal A-Pu_2O_3 by sintering pressed compacts of PuO_2 and carbon *in vacuo*, followed by melting under an inert atmosphere (Chikalla *et al.*, 1962, 1964; Skavdahl, 1964). Reaction of PuO_2 with a slight excess of carbon at 1650°C *in vacuo* produced a mixture of hexagonal A-Pu_2O_3 and a small amount of $Pu(O_x,C_{1-x})$. The latter, being more volatile than the Pu_2O_3, could be removed by heating *in vacuo*. Final arc melting resulted in hexagonal A-Pu_2O_3 with an O:Pu ratio of (1.500 ± 0.015), with 175 ppm carbon impurity and 93% theoretical density.

The cubic C-Pu_2O_3 sesquioxide is a silvery, metallic, lustrous solid, which is difficult to prepare by high-temperature methods. Haschke and Haire point out that reports of its preparation by simply heating PuO_2 *in vacuo* to temperatures between 1650 and 1800°C (Westrum, 1949a; Dayton and Tipton, 1961) are suspect because the O:Pu ratio of congruently vaporizing PuO_{2-x} is 1.85–1.90 in this temperature range (Ackermann *et al.*, 1966). The best means of preparation seems to be the heating of PuO_2 coated δ-stabilized plutonium metal to 150–200°C under vacuum (Terada *et al.*, 1969).

Hyperstoichiometric sesquioxide, $PuO_{1.6+\delta}$ (C'-Pu_2O_3, α'-Pu_2O_3, $PuO_{1.61}$)

When PuO_2 is melted, there is an evolution of oxygen resulting in a melt composition of $PuO_{1.62}$, which is the approximate composition of cubic C-Pu_2O_3 (Chikalla *et al.*, 1964). This phase can only be retained with extremely fast quenching. Since it is a high-temperature form of C-Pu_2O_3, it has been given the designation C'-Pu_2O_3 (or α'-Pu_2O_3, $PuO_{1.61}$, $PuO_{1.6+\delta}$). It is likely bcc. Slow cooling of the melt yields a mixture of C-Pu_2O_3 and PuO_{2-x} even in the absence of oxygen. Sari *et al.* (1968) reported that this compound has a composition range from $PuO_{1.62}$ to $PuO_{1.63}$ at 350°C, which extends to a range of $PuO_{1.62}$ to

$PuO_{1.69}$ at 600°C. Because of this broad composition range, we prefer the designation $PuO_{1.6+\delta}$.

Substoichiometric plutonium dioxide, PuO_{2-x}

The oxides between compositions $PuO_{1.61}$ to $PuO_{1.98}$ are mainly single-phase materials at temperatures above about 650°C. They may be prepared by heating PuO_2 at high temperature with carbon, hydrogen, or *in vacuo* (IAEA, 1967). The crystal lattice expands with decreasing oxygen composition (Gardner *et al.*, 1965; IAEA, 1967). Some annealing may be required, but prolonged heating *in vacuo* will cause a change in composition due to incongruent vaporization. This olive-green phase exists in the stoichiometry range $PuO_{1.61}$ to $PuO_{1.98}$ and is closely related to the stoichiometric oxide $PuO_{2.00}$. Its exact composition depends on the temperature and the oxygen partial pressure over the plutonium oxide solid (Drummond and Welch, 1957). Atlas and coworkers performed density measurements at 750°C that are consistent with the formation of oxygen vacancies in the crystal lattice (Atlas *et al.*, 1966). Atlas and Schlehman (1967) conducted a detailed study of the variation in oxygen content, x, with oxygen pressure. The composition–pressure–temperature relationship is shown in Fig. 7.89.

Stoichiometric plutonium dioxide, $PuO_{2.00}$

Plutonium dioxide is formed when metallic plutonium is ignited in air or by calcination of a number of plutonium compounds (except phosphates). Plutonium dioxide often forms when oxygen-containing compounds are heated *in vacuo* or in an inert atmosphere to 1000°C. The most widely used approach to prepare pure, crystalline PuO_2 is by heating Pu(III) or Pu(IV) oxalate to

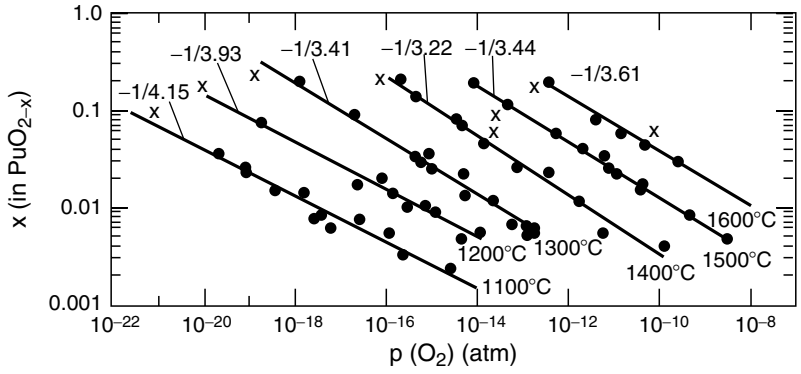

Fig. 7.89 *Variation of x in PuO_{2-x} with temperature and oxygen pressure (Atlas and Schlehman,* 1967). *Slopes (i.e.* –1/4.15, *etc.) of the log–log plots are shown above the lines. Experimental data points marked in x represent values derived from weight change measurements, whereas the circles represent gas-analysis results.*

1000°C in air. The Pu(III) oxalate is often preferred because it forms a powder that is easy to manipulate, while the Pu(IV) oxalate forms a tacky solid (see Section 7.9.1(e)i). The heating rate must be kept slow up to about 700°C to avoid rapid decomposition and gas evolution, followed by heating to 1000°C to remove any residual carbon. Drummond and Welch (1957) studied the stoichiometry of PuO_2 as a function of preparative history, and found that many materials need to be heated to 1250°C to produce reproducible stoichiometric PuO_2.

The method of preparation and process details have a significant influence on the PuO_2 product characteristics, which affect all subsequent uses of the material, such as fabrication and sintering properties of fuel materials containing PuO_2 or its behavior in long-term storage. PuO_2 is normally olive green, but it's observed color is a function of purity, particle size, method of preparation, stoichiometry, and possible reactions with water. The observed colors range from dull yellow, to green, khaki, buff, slate or black. Many of these samples are most likely hyperstoichiometric PuO_{2+x} (see section PuO_{2+x}). All samples turned to a darker, khaki color upon ignition to 1200°C. The qualitative characteristics of various PuO_{2+x} preparations obtained from different starting materials are summarized in Table 7.37 (Drummond and Welch, 1957).

Special preparations of PuO_2

Plutonium dioxide may be pressed and sintered to form pellets or compacts, which may be used in reactor technology or (in the case of $^{238}PuO_2$) in heat- and power-source technology for space exploration. For detailed descriptions, the reader is referred to the *Plutonium Handbook* (Wick, 1980). As an illustrative example of the general pellet-forming process, $^{238}PuO_2$ used to fabricate GPHS and LWRHU fuel pellets (see Section 7.3) for the Cassini mission was subjected to ^{16}O isotope exchange (to reduce neutron emission), ball milling, granulation and seasoning at 1100 and 1600°C to produce $^{238}PuO_2$ granules with <210 μm sized particles. The granules were then blended using those seasoned at

Table 7.37 *Qualitative characteristics of PuO_{2+x} from decomposition of selected materials at* 870°C (*Drummond and Welch,* 1957).

Material	*Color*	*Appearance*
metal	dull yellow	powder
sulfate	yellow-green to green	bulky powder
nitrate	dull yellow	bulky solid
chloride	dull yellow	powder
fluoride	khaki with black traces	granular solid
oxalate	yellow-buff	bulky powder
iodate	buff	very bulky
hydroxide	black with yellow traces	dense, shiny particles

1100°C (60 wt %) with those seasoned at 1600°C (40 wt %) by rolling the granules in a ball-mill jar without balls. After blending, the fuel charges were loaded into a hot press graphite die, placed under vacuum, and heated to 1530°C under a force of 11.8 kN. During hot pressing, the PuO_2 is reduced by the graphite die. After the pellets sat overnight, the PuO_{2-x} stoichiometry was about $PuO_{1.93}$. To oxidize the pellets back to a stoichiometry of PuO_2 and increase their density to meet mission specifications, the pellets were sintered in flowing Ar–$H_2{}^{16}O$ for 6 h at 1000°C, followed by 6 h at 1527°C (Rinehart, 1992, 2001).

Two other forms of PuO_2 also deserve a more detailed description: PuO_2 microspheres and single crystals. Plutonium dioxide microspheres with 10–250 μm diameter may be prepared by the sol-gel process for ^{239}Pu (Wymer and Coobs, 1967; Lloyd and Haire, 1968; Louwrier *et al.*, 1968; Wymer, 1968), ^{238}Pu (Grove *et al.*, 1965; Hass *et al.*, 1966; Hincks and McKinley, 1966), or MOX (U, Pu)O_2 (Vaidya *et al.*, 1983; Smolders and Gilissen, 1987; Stratton *et al.*, 1987). In this process, a stable Pu(IV) hydroxide sol is prepared by extraction or evaporation of HNO_3 from HNO_3–$Pu(NO_3)_4$ solution, injection of the resulting sol into a dehydrating organic solvent (for instance, 2-ethylcyclohexanol), and firing the resulting gel to form PuO_2 microspheres (Hass *et al.*, 1966; Lloyd and Haire, 1968; Wymer, 1968).

Very dense microspheres, which have a remarkable freedom from loose α-particle contamination, may be prepared by plasma spheroidization (Jones *et al.*, 1964). In this method, plutonium oxide is first compacted into pellets, which are fired at 1500°C for 1 h in an oxygen-enriched plasma to inhibit loss of oxygen during melting. The resulting compacts are ground to the desired mesh size, and are then fed into an induction-coupled plasma torch, which uses argon, oxygen, or Ar–O_2 mixtures as feed gas. In the high temperature of the plasma torch (up to 20,000°C), each plutonium oxide particle immediately melts to a small spherical droplet, which, upon leaving the plasma zone, immediately solidifies into a small sphere with a smooth surface. Depending on the particle size of the feed particles, microspheres from 10 to 250 μm may be obtained (Jones *et al.*, 1964).

Spheres with less than 50 μm diameter are amber-colored and have a clear, vitreous appearance. Those of more than 50 μm diameter do not transmit light and appear opaque black (Jones *et al.*, 1964). If prepared in an O_2 plasma, they have the lattice constants of stoichiometric PuO_2. Each individual sphere usually consists of a single crystal (Jones *et al.*, 1964).

Plutonium dioxide single crystals of considerable size have been prepared by several authors (Phipps and Sullenger, 1964; Schlechter, 1970; Finch and Clark, 1972; Rebizant *et al.*, 2000). Finch and Clark (1972) obtained PuO_2 single crystals from Li_2O–$2MoO_3$ melt in a temperature gradient ranging from 1270 to 1300°C in a tightly closed platinum vessel over a 2 week period. Crystals of $2 \times 3 \times 3$ mm have been obtained in this fashion. Schlechter (1970) grew single crystals of approximately the same size by slow thermal decomposition of

$Pu(SO_4)_2$ either in LiCl–KCl eutectic or in $PbCl_2$–KCl melt at 600–800°C and subsequent cooling at a rate of 2.2°C h^{-1} from 715°C to room temperature. Phipps and Sullenger (1964) obtained PuO_2 single crystals with well-defined faces and edges up to 60 μm long when they prepared plutonium-bearing glass fibers by drawing the molten glass (90% SiO_2–30% Na_2O) from a platinum–rhodium bushing at 1300°C. $(U,Pu)O_2$ single crystals have been grown through a chemical transport reaction (Rebizant *et al.*, 2000).

Higher oxides, PuO_{2+x}, PuO_3, and PuO_4

While plutonium is capable of forming molecular compounds of oxidation state VI and VII, most practitioners have been of the opinion that in the plutonium–oxygen system, the stoichiometric tetravalent oxide $PuO_{2.0}$ represents the highest obtainable binary oxide. The historical basis for this opinion began in 1944, when Moulton (1944) observed that during ignition of plutonyl nitrate, only PuO_2 was formed, but no PuO_3 or any other higher oxide was produced. Moulton took this as evidence for the nonexistence of any oxide of composition higher than PuO_2. In 1953, Brewer (1953) predicted from thermodynamic calculations that any solid anhydrous oxide of plutonium higher than PuO_2 would probably not be stable. This view seemed to be confirmed by the work of Westrum (1949a), who used strongly oxidizing conditions (O_2 at 400°C and 70 atm pressure; ozone at 600–1000°C; atomic oxygen) but failed to oxidize PuO_2. Katz and Gruen (1949) also reported that PuO_2 is not oxidized to a higher oxide with NO_2 or atomic oxygen at 500°C. Moreover, Weigel and coworkers (Marquart *et al.*, 1983) attempted to prepare anhydrous PuO_3 by careful decomposition of PuO_2CO_3, $(NH_4)_2PuO_2(CO_3)_2$, and $PuO_3 \cdot 0.8H_2O$, but did not succeed in preparing any higher oxide. Gouder has attempted to prepare thin films of PuO_3 by reacting PuO_2 with oxygen atoms, and found no evidence for its formation (Gouder, 2005).

A number of recent reports on higher-valent oxides such as $PuO_{2.26}$ in the solid state, and PuO_3 and PuO_4 in the gas phase have challenged these traditional views. While not all of the data are consistent, and there are still disagreements among practitioners, these recent reports strongly suggest that the established views on the oxidation behavior of plutonium are worth reconsideration, and that additional detailed study is appropriate.

PuO_{2+x} As early as 1957, Drummond and Welch (1957) had prepared compositions of PuO_2–$PuO_{2.09}$, and concluded that compounds with O:Pu ratios higher than 2.0 were the result of low temperature ignition of plutonium compounds. Oxygen-rich PuO_2 can also be prepared by heating cubic C-Pu_2O_3 in oxygen at 1000°C, and the material formed in this manner displayed a slightly reduced lattice constant (a_0) of 5.382 Å as compared to 5.396 Å for stoichiometric PuO_2. It was possible that the higher O:Pu ratio in these preparations was attributed to excess oxygen dissolved in the crystal lattice. In other studies, mass changes indicating the formation of $PuO_{2.1}$ during

atmospheric corrosion of plutonium metal had been attributed to adsorption of water (Sackman, 1960).

These views remained widely held until Stakebake and coworkers found evidence for a new fluorite-related phase of composition $PuO_{2.17}$ formed as a surface layer by plutonium metal reaction with water vapor at 200–350°C (Stakebake *et al.*, 1993). XPS data were consistent with the presence of Pu(VI). Confirmatory evidence for the formation of a higher oxide was reported by Haschke *et al.* (2000a,b), who studied the reaction of PuO_2 with water vapor between 25 and 350°C. Mass spectroscopic analysis of the gases produced in this reaction showed that H_2 and H_2O were the only gaseous products and indicated that the reaction proceeds according to the reaction:

$$PuO_2(s) + xH_2O(g) \rightarrow PuO_{2+x}(s) + xH_2(g) \qquad (7.37)$$

The final product approached a composition of $PuO_{2.3}$. XRD analyses of the reaction products revealed a single fcc phase with a fluorite-related structure and a slightly expanded lattice. The lattice expansion was accompanied by a linear increase in the O:Pu ratio, consistent with the formation of a solid-solution of PuO_{2+x} in analogy with UO_{2+x} (Allen and Tempest, 1986). Isothermal measurements showed that hydrogen is generated at linear, temperature-dependent rates from which the authors derived an activation energy (E_a) for the reaction of (39 ± 3) kJ mol^{-1}. This was interpreted as being consistent with a chemical reaction, and not with radiolysis, which is expected to be temperature-independent. It should be noted, however, that the rates observed for hydrogen evolution in the reaction of PuO_2 with water vapor at 25°C are in close agreement to the rate of hydrogen evolution observed during exposure of PuO_2 to aqueous salt solutions (Haschke *et al.*, 1983). The report of H_2 being the only gaseous product is not consistent with the observations of Vladimirova and Kulikov (2002), who reported the observation of both H_2 and O_2 in the gas phase during their study of the reaction of PuO_2 with sorbed water using high- and low-burnup plutonium, and therefore different radiolytic dose rates. Their data are consistent with the rates of formation of H_2 and O_2 being in direct proportion to the dose rate. They followed their reactions for 600 days, but did not report on the characterization of the oxide at the end of the experiment.

There is good agreement that water vapor reacts with PuO_2 to generate hydrogen. The generation of hydrogen in storage containers represents a significant safety concern (Haschke and Martz, 1998b), and has led to use of strict standards for stabilization, packaging, and storage of plutonium residue materials that require thermal stabilization using calcinations in air, followed by sealing the materials in nested welded stainless steel containers before storage or transport (Paffett *et al.*, 2003b).

Haschke and coworkers have suggested that the formation of explosive H_2–O_2 mixtures by reaction of water vapor with PuO_2 in air-filled containers is not possible because moisture-enhanced corrosion proceeds via a water-catalyzed cycle (Haschke *et al.*, 2001). In their proposed mechanism, water

absorbs strongly on the oxide below 120°C and desorbs as the temperature is increased to 200°C. Dissociative adsorption of water forms surface OH^-, promotes the formation of PuO_{2+x}, and releases H_2. When O_2 is present, they propose a surface catalyzed H_2–O_2 recombination to form surface adsorbed water that then reacts to form PuO_{2+x}, and atomic H on the surface. In the absence of O_2, H atoms associate as H_2 as indicated in equation 7.37 above. Association of H atoms with dissociatively adsorbed oxygen reforms H_2O and prevents the accumulation of H_2 whenever O_2 is present. H_2 appears only after O_2 is depleted.

While this proposed mechanism is plausible, it remains speculative until more data are produced to confirm the proposed mechanisms or to establish an alternative mechanism. What is clear from the above discussion is that our understanding of plutonium oxide chemistry, particularly the associated surface reactions is clearly inadequate.

Gas phase PuO_3 and PuO_4 By analyzing data on transpiration experiments of plutonium oxide, Krikorian and coworkers found that the observed oxygen pressure could only be explained by the presence of a PuO_3 molecule in the gas phase (Krikorian *et al.*, 1997). The presence of gas-phase PuO_3 was confirmed by Ronchi and coworkers a few years later (Ronchi *et al.*, 2000). Knudsen-effusion experiments in combination with mass spectrometry were used to show that PuO_2(s) exposure to oxygen above 1800–1900°C produces gas-phase molecules of PuO_3, along with the expected PuO and PuO_2 gas-phase molecules. These workers concluded that formation of PuO_3(g) was not formed from a gas-phase reaction of PuO_2(g) with oxygen or carbon dioxide gases, but rather the product of a reaction of gaseous oxygen with the surface of the solid PuO_2. In another recent report, Domanov *et al.* (2002) heated PuO_2 in a stream of helium–oxygen and employed a thermogradient tube furnace to separate and condense the volatile components that were subsequently analyzed by α-detection. The data were interpreted as producing volatile or gas-phase PuO_3 and PuO_4. The latter species was expected to have an abnormally high volatility, close to that of OsO_4. As the partial pressure of oxygen was decreased, the yield of the proposed PuO_4 species decreased. These data, while indirect, are quite intriguing. The relationship between the volatile species observed by Domanov *et al.* to those reported by Krikorian *et al.* and Ronchi *et al.* is uncertain. Further study using mass spectrometry as a function of oxygen partial pressure would help to clarify whether gas phase PuO_4 really exists. The clear finding from these studies, however, is that plutonium oxides can exist in oxidation states higher than IV, at least in the gas phase. These findings clearly challenge the traditional view that PuO_2 is the terminal species.

(*iii*) *Solid-state structures*

A summary of crystallographic data for plutonium oxides is given in Table 7.36. The majority of solid-state structures of plutonium oxides are structurally

related to the fluorite structure displayed by PuO_2. As a result of these structural similarities, we discuss the fluorite structure first to make the comparison with other oxide structures more understandable.

Cubic PuO_{2-x}

Plutonium dioxide forms a cubic fluorite phase over the composition range of PuO_{2-x}, where $0.4 < x < 0$. The cubic fluorite-type unit cell based upon CaF_2 is illustrated in Fig. 7.72. The lattice consists of an fcc arrangement of plutonium metal cations with O anions occupying most or all the four-fold tetrahedral sites, while the six-fold octahedral sites are vacant. In this structure, when $x = 0$, each plutonium atom is surrounded by eight oxygen atoms at the corners of a cube. Each cubic PuO_8 coordination polyhedron shares an edge with each of 12 neighboring PuO_8 polyhedra as shown in Fig. 7.90a. In this high-symmetry environment, all the Pu–O distances are the same. For a lattice parameter $a_0 = 5.396$ Å, this corresponds to a Pu–O distance of 2.337 Å, and a Pu–Pu distance of 3.816 Å. When $x > 0$, there are disordered oxygen vacancies.

Cubic C-Pu_2O_3

The C-Pu_2O_3 form of the sesquioxide displays the bcc Mn_2O_3 structure that is related to the fluorite structure with a doubled unit cell. The unit cell of the C-type sesquioxide can be considered as consisting of eight fluorite unit cells [a_0(bcc) = $2a_0$(fcc)] from which one-fourth of the oxygen atoms have been removed in an ordered way, and with the metal positions remaining almost unchanged from their fcc positions. The local coordination of the plutonium atom decreases from eight to six, and the PuO_8 cubes become PuO_6 octahedra but now with two types of plutonium atom. For one-fourth of the plutonium atoms, these missing oxygen atoms are at the ends of a body diagonal of the original PuO_8 cube, and for the other three-fourths they are at the ends of a face diagonal. Both PuO_6 coordination groups may be described as distorted octahedral, and each oxygen atom is four-coordinate and approximately tetrahedral. For cubic Pu_2O_3 with $a = 11.02$ Å, one plutonium atom has six equidistant Pu–O distances of 2.367 Å, and another plutonium atom has three pairs of Pu–O distances of 2.342, 2.360, and 2.383 Å. A comparison of the cubic PuO_2 and Pu_2O_3 structures is shown in Fig. 7.90.

Hexagonal A-Pu_2O_3

The A-type hexagonal sesquioxide formed at elevated temperatures displays the A-La_2O_3 crystal structure, typical of light lanthanide sesquioxides (Haire and Eyring, 1994). A striking feature of the hexagonal A-Pu_2O_3 structure is the highly unusual seven-coordination of the plutonium atoms. This gives three different Pu–O distances, three at 2.359, one at 2.353, and three at 2.623 Å. The local PuO_7 geometry is that of a mono-capped octahedron. Actually, there is also an eighth oxygen atom below the opposite face, but a much greater distance of 3.605 Å. This last oxygen atom, together with the seven in the PuO_7

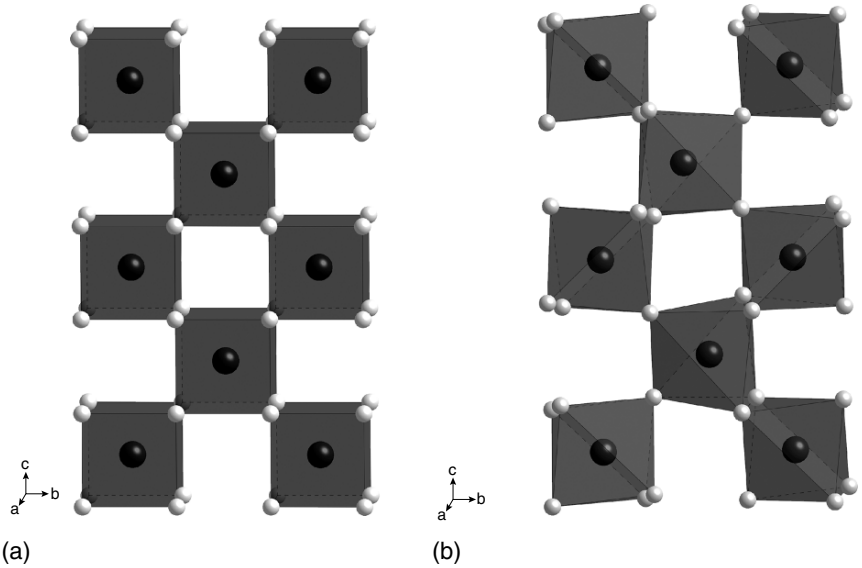

Fig. 7.90 (*a*) *A polyhedral representation of a layer of the fluorite-type structure of stoichiometric* PuO_2*, emphasizing the alternating cubic* PuO_8 *coordination polyhedra and vacancy sites within the structure, and illustrating the overall face-centered cubic arrangement of Pu metal atoms.* (*b*) *A polyhedral representation of a layer of the cubic C-type* Pu_2O_3 *structure drawn on the same scale and orientation, emphasizing the similarity in the fcc arrangement of Pu metal atoms between the cubic structures of* PuO_2 *and C-*Pu_2O_3*. The local coordination environment around Pu is now reduced to six near neighbors, with alternating* PuO_6 *distorted octahedra. Plutonium atoms are black and oxygen atoms are gray.*

polyhedron forms a distorted cube. These distorted cubes form the basis of the representation given for the A-type lattice given in Fig. 7.91.

Intermediate oxide structures, PuO_{2-x}

Intermediate oxides that display O:Pu stoichiometries between 1.5 and 2.0 (or those with stoichiometry between Pu_2O_3 and PuO_2) are not well characterized for plutonium. In general, intermediate oxides are common to both lanthanides and actinides, although their properties are much better established for the lanthanides. Since both sesquioxides and dioxides are known for plutonium, it is reasonable to assume that plutonium can form a homologous series of intermediate mixed-valent oxide phases Pu_nO_{2n-2} in analogy with the lanthanides. Unfortunately, very few data exist in this stoichiometry region for plutonium, though it is known that heavier actinides, americium, curium, berkelium, and californium form some members of an intermediate An_nO_{2n-2} series

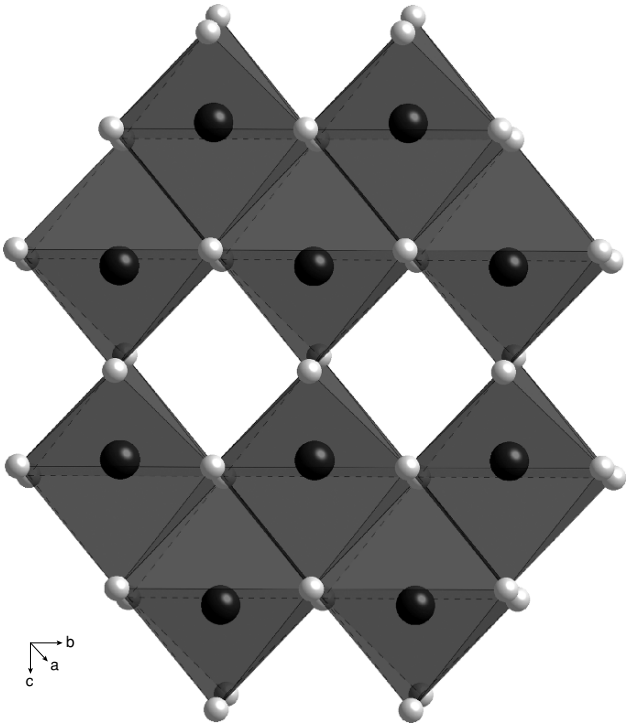

Fig. 7.91 *A polyhedral representation of a layer of the hexagonal A-type Pu_2O_3 emphasizing the hexagonal arrangement of Pu atoms. The local coordination environment around Pu has eight near neighbors, giving a highly distorted PuO_8 cube. Plutonium atoms are black and oxygen atoms are gray.*

(Haire and Eyring, 1994). Since Pu_2O_3 will take up oxygen to yield a hyperstoichiometric sesquioxide, and PuO_2 will lose oxygen to give a substoichiometric dioxide, the potential for such a series is most intriguing. Upon comparison of the ionic radii and relative free energies of the trivalent and tetravalent oxidation states of plutonium with those of cerium and praseodymium, Haschke concluded that such a mixed-valence series should be stable, and reported data from oxygen titration experiments in which the existence of a series Pu_nO_{2n-2} with $n = 5$, 7, 9, 10, and 12 was inferred (Haschke, 1992). Since the solid phases were not identified, the existence of the Pu_nO_{2n-2} series is not definitive, but clearly this is another area in which more detailed study is warranted.

The possibility of the existence of an intermediate oxide series of formula Pu_nO_{2n-2} is strongly suggested by structural principles established for the more well-studied cerium and praseodymium systems, and forms the basis of the

pedagogical phase diagram introduced by Hashke and coworkers (Haschke *et al.*, 2000a), shown in Fig. 7.92. In the structural model upon which this phase diagram is based, there is an fcc array of plutonium atoms in which all (and only) the tetrahedral interstices are occupied with oxygen atoms to form the end-member PuO_2. The intermediate phase compositions and structures are realized by omission of oxygen atoms in a regular way. Except for small shifts away from the vacant oxygen sites, the metal atoms maintain their fcc positions, and this leads to a homologous series Pu_nO_{2n-2} where Pu_2O_3 is the other end-member. Since Pu_2O_3 has a bcc structure, this end-member corresponds to $n = 4$ (Pu_4O_6). With this understanding, it is easy to rationalize the phase diagram of Fig. 7.92. There is a stoichiometric hexagonal sesquioxide (O:Pu = 1.5); a cubic sesquioxide with some vacancies occupied by oxygen (O:Pu = 1.5–1.7), showing variable lattice parameters; an oxide phase corresponding to the Pu_nO_{2n-2} homologous series (rhombohedral, narrow stoichiometry range); a substoichiometric fcc dioxide (O:Pu = 1.8–2.0) with variable and larger lattice parameter than the stoichiometric dioxide; and the stoichiometric and hyperstoichiometric dioxide. Like in the lanthanide systems, the intermediate oxides merge into a continuous PuO_{2-x} solid solution above 700°C. Whether the plutonium oxide system actually contains all of these

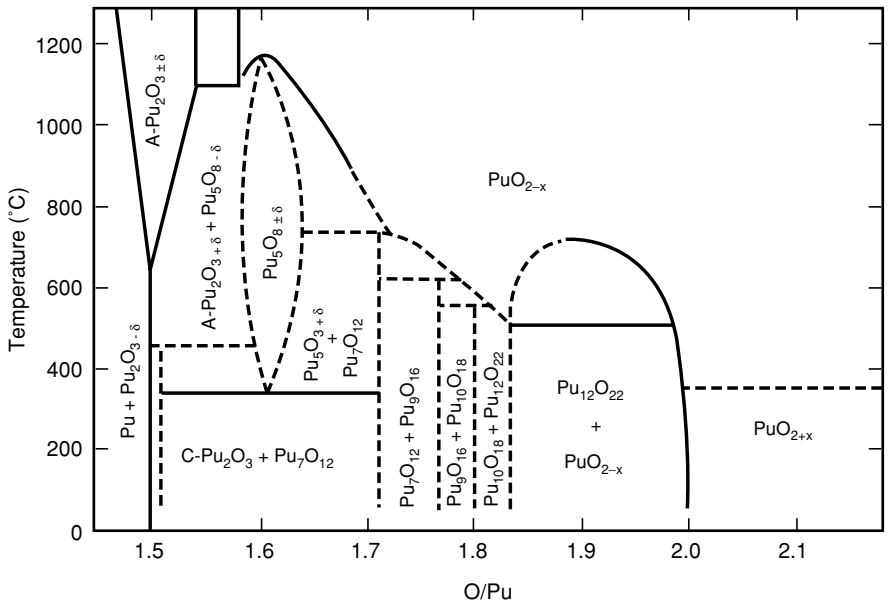

Fig. 7.92 *A pedagogical plutonium–oxygen phase diagram introduced by Hashke and Haire* (2000), *and based upon structural principles established for the more well-studied Ce and Pr oxide systems* (*Haschke* et al., 2000*a*).

features and closely resembles the lanthanide system will require more extensive study.

PuO_{2+x} structural studies

XRD analysis of the products of reaction between PuO_2 and water vapor show a single fcc phase with a fluorite-related structure with an expanded lattice. After reaching a minimum of 5.3975 Å at $PuO_{2.00}$, the lattice parameter increases over a narrow stoichiometry range, consistent with an initial stepwise expansion of the lattice and then a gradual increase with increasing oxygen composition. Results for O:Pu in the 2.016–2.169 range follow Vegard's law, implying that the oxide is a continuous PuO_{2+x} solid solution with a lattice constant given by:

$$a_0 = 5.3643 + 0.01764\ \mathrm{O:Pu} \tag{7.38}$$

Once the PuO_2 stoichiometry is reached, the lattice parameter is not very sensitive to composition, as shown in Fig. 7.93. Haschke and coworkers proposed that the additional oxygen atoms are accommodated in the vacant octahedral sites in the fluorite lattice, and that charge balance is maintained by replacing Pu(IV) with a higher oxidation state plutonium cation. Initial XPS data were interpreted as being consistent with Pu(VI), but more recent XANES spectroscopy has been interpreted as indicating the presence of Pu(V) (Conradson *et al.*, 2003). Recent EXAFS studies indicate that the original proposal of oxygen atoms in octahedral sites is far too simplistic (Conradson *et al.*, 2004b), and warrants further discussion.

Conradson and coworkers investigated 24 PuO_{2+x} samples prepared by a variety of methods including heterogeneous oxidation of plutonium metal and PuO_2 with gaseous H_2O and/or O_2, and by the hydrolysis and precipitation of the aqueous Pu(IV) ion (Conradson *et al.*, 2003, 2004b). Fourier transforms (FT) of the EXAFS data for selected plutonium oxide compounds are shown in Fig. 7.94. For stoichiometric, ordered $PuO_{2.0}$ the first peak in the Fourier transform is the contribution of the eight nearest neighbor oxygen atoms at 2.33 Å, well separated from the more distant second nearest neighbor peak of 12 plutonium atoms at 3.80 Å (the peaks in Fig. 7.94 are all phase-shifted to lower R). Regular features from the well-ordered extended structure subsequently continue to a very high distance from the central absorbing atom. This spectrum is therefore consistent with the crystal structure of stoichiometric PuO_2 shown in Fig. 7.90a.

However, as x increases from $PuO_{2.00}$ to $PuO_{2.26}$, the amplitudes of all of the peaks in the Fourier transform decrease monotonically, indicative of diminished order via displacements of the plutonium and oxygen atoms from their lattice sites coupled to the incorporation of the nonstoichiometric oxygen atoms into interstitial, essentially defect sites. What contradicts the current models in this process is the splitting of the first oxygen shell in the EXAFS (clearly evident

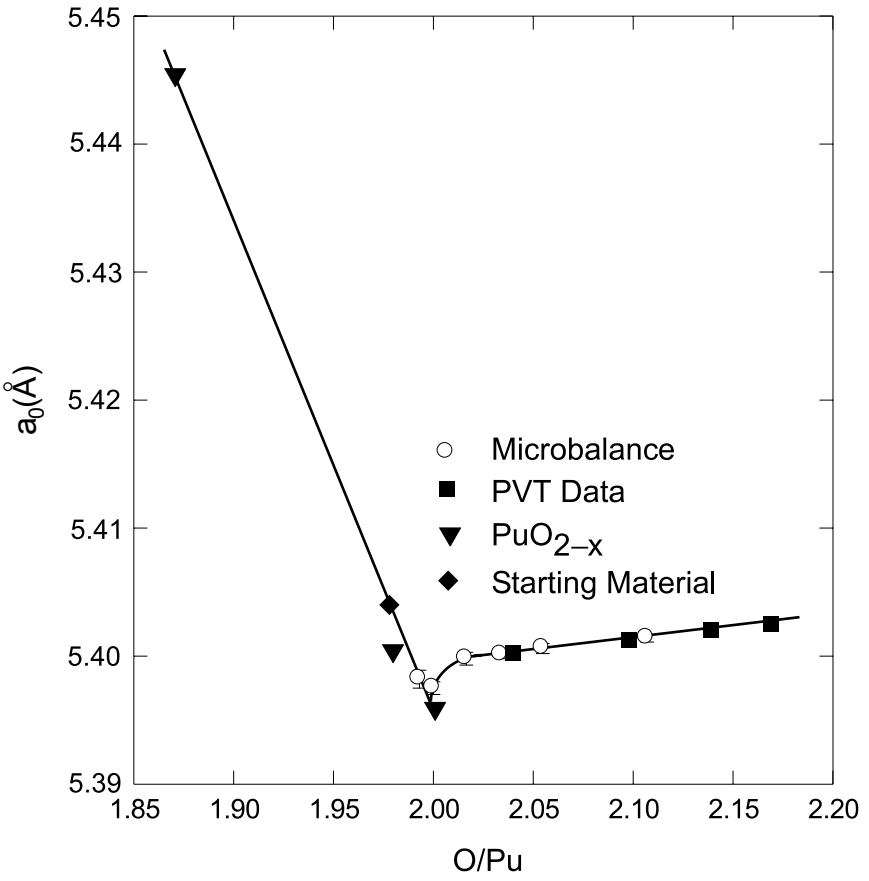

Fig. 7.93 *Variation of the cubic lattice parameter* (a_0) *of* $PuO_{2\pm x}$ *with O*:*Pu ratio at* 25°C. *Data for* PuO_{2-x} *are shown by gray triangles, microbalance data by open circles, and PVT data by solid squares* (*Haschke* et al., 2000*b*).

in Fig. 7.94) and the appearance of a short Pu–O bond distance of 1.84 Å. Traditional diffraction techniques that probe long-range order have never observed this phenomenon, but the bond distance is similar to the 1.85 Å distance found in axial Pu=O bonds in molecular Pu(V) compounds. Indeed, XANES results were interpreted as being consistent with a mixture of Pu(IV) and Pu(V). Combined, these data suggest that as the plutonium center becomes partially oxidized in PuO_{2+x}, there is a strong driving force to form short, strong, covalent Pu=O bonds.

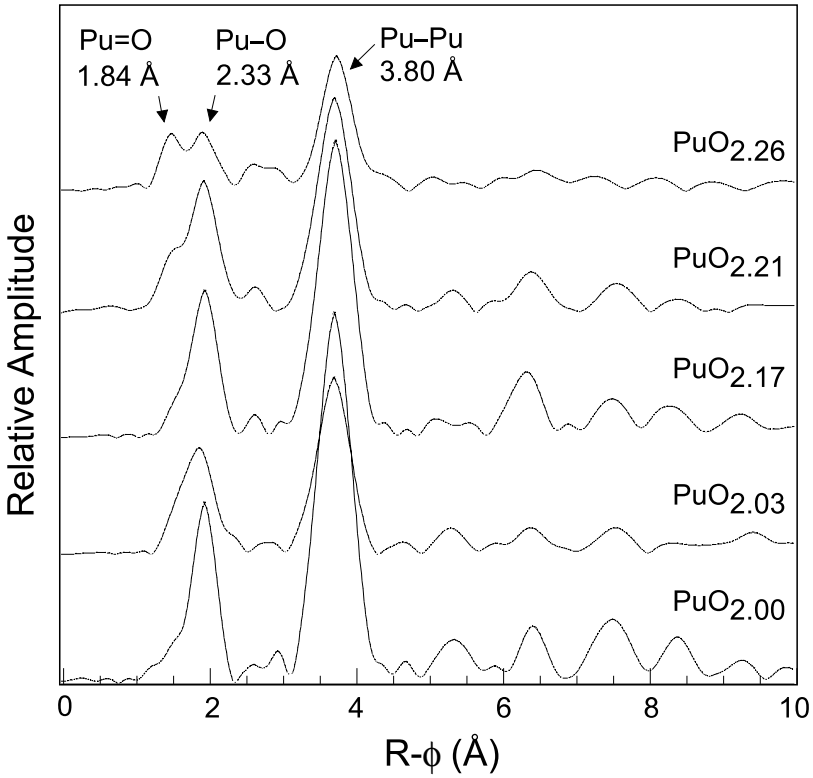

Fig. 7.94 *A comparison of k^3-weighted EXAFS moduli of PuO_{2+x} samples as indicated, and all data are taken from Conradson* et al. (2004*b*). *The peak positions are phase-shifted to lower distance from the actual Pu–O or Pu–Pu distances.*

These data also show that the plutonium atoms retain their essentially fcc positions, and while the plutonium sublattice retains its order through the progression of $PuO_{2.00}$ to $PuO_{2.26}$, the nearest-neighbor oxygen atoms are found in a multisite distribution. In addition to Pu–O distances of 2.33 Å, the additional oxygen atom in PuO_{2+x} generates new bonds both shorter and longer than the 2.33 Å value. These new Pu–O distances were tentatively assigned to bridging O^{2-}/OH^- (2.13, 2.28 Å) and possibly H_2O (2.41 Å) ligands. Based on these observations, Conradson *et al.* suggest that the oxidation produces linear PuO_2^+ moieties that are aperiodically distributed through the lattice, and suggest several structural models that would be consistent with all the observations (Conradson *et al.*, 2004b). Finally, recent XPS results indicate a hydroxylated surface in PuO_{2+x} samples whose thickness depends on exposure conditions (temperature, partial pressure of H_2O) (Paffett *et al.*, 2003a). Much more study in this area is expected in the coming years.

The original report of PuO_{2+x} and its relevance to long-term storage of plutonium through H_2 gas generation has prompted several theoretical studies of this material. To study the electronic structure of PuO_{2+x} with $x = 0.25$, a periodic supercell consisting of four PuO_2 formula units has been used, constituting the conventional fluorite cubic cell of Pu_4O_8 (as shown in Fig. 7.71 for PuH_2). The additional oxygen atom was placed on the octahedral interstitial site, giving rise to a hypothetical Pu_4O_9 compound. Employing a self-interaction correction local spin density method, Petit *et al*. (2003) concluded that stoichiometric PuO_2 displays Pu(IV) with a localized f^4 shell. When oxygen is introduced into the octahedral interstitial site, the nearby plutonium atoms turn into Pu(V) (f^3) by transferring electrons to the oxygen. Oxygen vacancies cause Pu(III) (f^5) to form by taking up electrons released by oxygen (Petit *et al.*, 2003). In another DFT study, Korzhavyi *et al.* (2004) find a similar result, and calculate the thermodynamics for reactions of PuO_2 with either O_2 or H_2O to form PuO_{2+x}. In both cases the reactions are endothermic, i.e. to occur they require a supply of energy. However, the calculations also show that PuO_{2+x} can be formed as an intermediate product by reaction with H_2O radiolysis products such as H_2O_2. While the placement of the interstitial oxygen atom in the octahedral hole of a hypothetical Pu_4O_9 system is not consistent with the experimental findings for PuO_{2+x}, they are consistent with the formation of Pu(V), and offer insights to guide further experimental study.

Penneman and Paffet applied Zachariasen's classic bond strength–bond length relationships (Zachariasen, 1954a,b) to the Pu_4O_9 ($PuO_{2.25}$) entity to suggest that a better description is Pu_4O_8OH containing Pu(V) ions (Penneman and Paffett, 2004, 2005). Bond strength–bond length arguments justify the location of a hydroxide ion, rather than a central oxide ion, in a plutonium dioxide structure, providing an alternative interpretation for the experimental data on plutonium dioxide oxidation by water.

(*iv*) *Properties of plutonium oxides*

Oxygen diffusion

Fluorite-related lanthanide oxides exhibit unusual diffusional properties in that the oxygen substructure (excess interstitial oxygen ions and oxygen vacancies) is mobile below 300°C, which places them in the category of fast-ion conductors (Haire and Eyring, 1994). In actinide oxides of the fluorite structure, interstitial excess oxygen ions and oxygen vacancies are extremely mobile with diffusion rates similar to those of other fluorite-type superionic conductors (Matzke, 1982). Chemical diffusion measurements on PuO_{2-x} reveal relatively high values for diffusion coefficients (Bayoglu and Lorenzelli, 1984), and activation energies in the vicinity of 46 kJ mol^{-1}, which is very close to the migration energy of anion vacancies in UO_{2-x} (49 kJ mol^{-1}) (Chereau and Wadier, 1973; Bayoglu and Lorenzelli, 1979).

For stoichiometric PuO_2, oxygen diffusion has been studied by gas-phase isotope exchange by Bayoglu and coworkers, and by Deaton and Wiedenheft who obtained activation energies of 177 and 187 kJ mol^{-1}, respectively (Deaton and Wiedenheft, 1973; Bayoglu *et al.*, 1983). Murch and Catlow (1987) have suggested that since oxygen interstitials in PuO_2 are almost certainly less mobile than oxygen vacancies, one can assume that the activation energy for oxygen diffusion in stoichiometric PuO_2 can be partitioned into two parts, given by

$$Q = H_F/2 + H_v^m \tag{7.39}$$

where H_v^m is the anion vacancy migration enthalpy and H_F is the enthalpy for anion Frenkel defect formation. With H_v^m given by 46 kJ mol^{-1}, the Frenkel energy is given by 262–282 kJ mol^{-1}.

Melting behavior

The melting behavior of the individual plutonium oxides has been studied by many authors (Holley *et al.*, 1958; Pijanowski and DeLucas, 1960; Chikalla *et al.*, 1962, 1964; Lyon and Baily, 1965, 1967; Chikalla, 1968; Riley, 1970), and has been thoroughly reviewed (IAEA, 1967; Wriedt, 1990; Lemire *et al.*, 2001).

Stoichiometric hexagonal A-Pu_2O_3 ($PuO_{1.50}$) was found to have a melting point of 2085 ± 25°C (Chikalla *et al.*, 1962, 1964), which agrees well with the value of 2075°C reported by Riley (1970). The value of 2080°C was adopted by the IAEA review panel (IAEA, 1967), and by Wriedt (1990) in their reviews.

No melting point can be reported for cubic C-Pu_2O_3 ($PuO_{1.52}$), since this compound undergoes a solid-state peritectoid decomposition to A-Pu_2O_3 ($PuO_{1.5}$) and C′-Pu_2O_3 ($PuO_{1.6+\delta}$) at 450°C (Wriedt, 1990). No melting point for C′-Pu_2O_3 ($PuO_{1.6+\delta}$) can be reported as it transforms congruently to PuO_{2-x} above a temperature of about 1180°C (Wriedt, 1990).

The melting point of PuO_{2-x} depends on the O:Pu ratio. For stoichiometric $PuO_{2.00}$, a number of values have been reported; however, the best values are thought to be those reported by Lyon and Baily (1965, 1967), who found 2390 ± 20°C, or Aitken and Evans (1968) who found a value of 2445°C. These experiments were performed on specimens sealed in tungsten capsules to prevent loss of oxygen. Wriedt (1990) proposed a value of 2445°C, and Adamson *et al.* (1985) recommend the intermediate value of 2428°C.

Vaporization behavior

The plutonium oxide vaporization process is extremely complicated because the solid undergoing vaporization changes its composition during the process. The majority of vapor pressure measurements of plutonium oxides have been carried out by the Knudsen-effusion method (Phipps *et al.*, 1950b; Mulford and Lamar, 1961; Paprocki *et al.*, 1962a; Pardue and Keller, 1964; Ackermann *et al.*, 1966; IAEA, 1967; Capone *et al.*, 1999), with the notable exception of a few

mass spectrometry reports (Battles *et al.*, 1968, 1969; Battles and Blackburn, 1969; Kent, 1973). All these data have been reviewed (Wriedt, 1990). The results of these measurements are often conflicting because the condensed oxide phase PuO_{2-x} is at its congruent vaporizing composition, which varies with temperature. When inert containers are used, solid PuO_2 that has a higher O:Pu ratio than the congruent composition will produce vapor with relatively high concentrations of $PuO_2(g)$, $O_2(g)$, and O(g). In contrast, compositions with a lower O:Pu ratio than the congruent composition will produce relatively high concentrations of PuO(g) (Wriedt, 1990). Thus, the early Knudsen measurements yield insufficient information to explain the vaporization behavior of PuO_2 and PuO_{2-x} in detail.

Battles and coworkers (Battles *et al.*, 1968, 1969; Battles and Blackburn, 1969) have determined the species that occur in the vapor of PuO_{2-x} and in the vapor over the binary condensed phase mixture of Pu_2O_3 and $PuO_{1.61}$ over a period of 20 hours. A typical set of data is shown in Fig. 7.95.

In the case of single-phase material, it was found that initially stoichiometric $PuO_{2.00}$ slowly turns into $PuO_{1.831}$ and retains the latter composition. In the vapor, the species PuO_2^+ (g) and PuO^+(g) were observed. At 2219 K the partial pressures of Pu(g) and of O(g) were calculated to be 2.6×10^{-9} and 2.6×10^{-7} atm, respectively. The mass spectrometry results (Battles *et al.*, 1968, 1969; Battles and Blackburn, 1969; Kent, 1973) are in good agreement with those measured by effusion in open containers by Ackermann and coworkers (Ackermann *et al.*, 1966). Partial pressures of O(g), $O_2(g)$, Pu(g), PuO(g) and $PuO_2(g)$ have been tabulated for various PuO_{2-x} compositions and temperatures (Kent and Zocher, 1976; Green *et al.*, 1983).

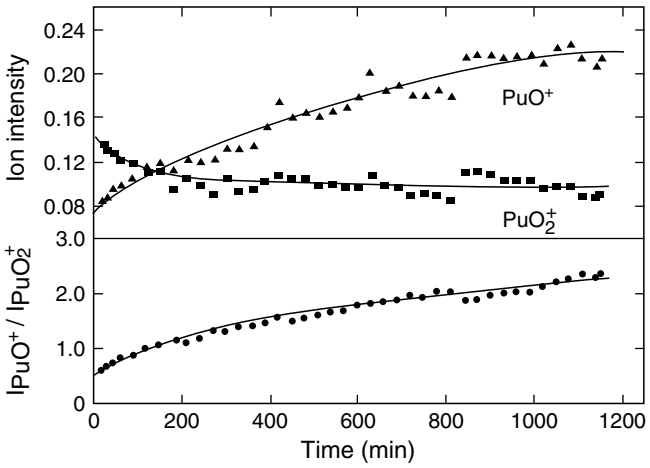

Fig. 7.95 *Mass spectroscopic intensities of gaseous* PuO_2^+ *and* PuO^+, *and the ratio of intensities* $I_{PuO^+}/I_{PuO_2^+}$ *as a function of time at* 2225 K (*Battles* et al., 1968, 1969).

More recently, Krikorian and coworkers suggested that heating PuO_2 in the presence of oxygen produced the PuO_3 molecule in the gas phase (Krikorian *et al.*, 1997), and this was definitively proven by Ronchi and coworkers who used Knudsen-effusion experiments in combination with mass spectrometry to show that PuO_2 exposure to oxygen above 1800–1900°C produces a gas phase molecule PuO_3, along with the expected PuO and PuO_2 gas phase molecules (Ronchi *et al.*, 2000).

Thermodynamic properties of plutonium oxides

The thermodynamic properties of the plutonium oxides have been studied and assessed by numerous authors, and the reader is directed to extensive compilations by Rand (1966), IAEA (1967), Wriedt (1990), and the recent OECD-NEA review of plutonium and neptunium thermodynamics (Lemire et al., 2001). A summary of the most recent OECD-NEA selected thermodynamic data for plutonium oxides is given in Table 7.38.

Stoichiometric Pu_2O_3 ($PuO_{1.5}$) Flotow and Tetenbaum (1981) measured the low-temperature heat capacity from –265 to 77°C on a sample of $^{242}Pu_2O_3$. The heat capacity (C_p°) and entropy (S°) at standard conditions derived from their data were selected by the OECD-NEA reviewers, and are given in Table 7.38 (Lemire *et al.*, 2001). Estimates of the heat capacity of Pu_2O_3 at higher temperatures have been given by IAEA (1967), Glushko (1982), and Besmann and Lindemer (1983). The NEA reviewers recommended the following expressions for heat capacity of Pu_2O_3 over two separate temperature ranges.

$$(298.15 - 350\text{K})$$
$$C_p^\circ = 169.466 - 79.98 \times 10^{-3}T - 25.459 \times 10^5 T^{-2}\ \text{J K}^{-1}\text{mol}^{-1} \qquad (7.40)$$

$$(350 - 2358\text{K})$$
$$C_p^\circ = 122.953 + 28.548 \times 10^{-3}T - 15.012 \times 10^5 T^{-2}\ \text{J K}^{-1}\text{mol}^{-1} \qquad (7.41)$$

There are no direct measurements of the enthalpy of formation of Pu_2O_3. The value has been derived indirectly from the partial molar Gibbs energies and enthalpies of oxygen in the single-phase oxides Pu_2O_3 and PuO_2, and the two-phase fields between these phases. A thorough discussion of the data and measurement techniques is available in the most recent reviews (IAEA, 1967;

Table 7.38 *Thermodynamic parameters for plutonium oxides* (*Lemire* et al., 2001).

Compound	$\Delta_f G^\circ_{298}$ (kJ mol^{-1})	$\Delta_f H^\circ_{298}$ (kJ mol^{-1})	S°_{298} (J K^{-1} mol^{-1})	C°_{p298} (J K^{-1} mol^{-1})
Pu_2O_3	−1580.4 ± 10.1	−1656.0 ± 10.0	163.0 ± 0.6	117.0 ± 0.5
$PuO_{1.61}$	−834.8 ± 10.1	−875.5 ± 10.0	83.0 ± 5.0	61.2 ± 5.0
PuO_2	−998.1 ± 1.0	−1055.8 ± 1.0	66.13 ± 0.26	66.25 ± 0.26

Wriedt, 1990; Lemire *et al.*, 2001). The recommended values for the enthalpy and Gibbs energy of formation are listed in Table 7.38.

Hyperstoichiometric $PuO_{1.52}$ (C-Pu_2O_3) The only thermodynamic data for this phase are the enthalpies of combustion reported by Chereau *et al.* (1977). Their values correspond to an enthalpy of formation of –845 kJ mol^{-1} (Lemire *et al.*, 2001).

Hyperstoichiometric $PuO_{1.6+\delta}$ No experimental data are available. Thermodynamic functions were estimated by NEA reviewers (Lemire *et al.*, 2001).

Stoichiometric $PuO_{2.00}$ The thermodynamic properties of stoichiometric $PuO_{2.00}$ have been the subject of a large number of studies (Sandenaw, 1963; Pardue and Keller, 1964; Ackermann *et al.*, 1966; Rand, 1966; Kruger and Savage, 1968; Engel, 1969; Ogard, 1970; Flotow *et al.*, 1976), and have been extensively reviewed (IAEA, 1967; Cordfunke *et al.*, 1990; Wriedt, 1990; Carbajo *et al.*, 2001; Lemire *et al.*, 2001).

To overcome difficulties performing low-temperature heat capacity measurements on $^{239}PuO_2$, Flotow *et al.* (1976) performed studies with the less radio active isotopes $^{242}PuO_2$ and $^{244}PuO_2$ to avoid problems associated with radiation damage of the solid for low temperatures up to 350 K. These measurements are thought to provide the most reliable values for standard heat capacity (C_p°) and entropy (S°). Their values were selected by the NEA review, and are listed in Table 7.38. High-temperature measurements of enthalpy were measured by Kruger and Savage (1968), Engel (1969), Ogard (1970), and Oetting (1982). Fink (1982) used these data to derive a complex expression for heat capacity, and these were refit to polynomials by Cordfunke *et al.* (1990). The Fink expressions were recently modified by the NEA review to give the following polynomial expression over the temperature range 298.15–2500 K (Lemire *et al.*, 2001):

$$C_p^\circ = 84.495 + 10.639 \times 10^{-3} T - 6.1136 \times 10^5 T^2 - 19.00564 \times 10^5 T^{-2} \text{ J K}^{-1}\text{mol}^{-1} \quad (7.42)$$

The original polynomial functions derived by Fink are far more complex than the NEA modification, and for more information the reader is referred to the original Fink citation (Fink, 1982) or a recent review by Carbajo *et al.* (2001).

There is good agreement between authors on the values for the enthalpy and Gibbs free energy (Holley *et al.*, 1958; Glushko, 1982). The values accepted by the NEA review are given in Table 7.38 (Lemire *et al.*, 2001).

Chemical properties of plutonium oxides

Dissolution of PuO_2 PuO_2 that has been ignited at high temperatures is difficult to dissolve. Christensen and Maraman (1969), Gilman (1965, 1968),

Ryan and Bray (1980), and Nikitina *et al.* (1997a,b), have reviewed the methods reported. In general, the rate of dissolution for each reagent often depends on the ignition temperature used to prepare the oxide and on the previous history of the sample. The reagent most frequently used is a boiling mixture of 16 M HNO_3 with 1 M HF as a fluoride complexant. Instead of HF, H_2SiF_6, or Na_2SiF_6 may also be used. High-temperature fired PuO_2 is dissolved only slowly. Irradiated PuO_2 dissolves better, the rate of dissolution being higher, the higher the burnup.

The difficulty in dissolving PuO_2 has led to the search for aggressive approaches to achieve dissolution, such as the use of fused salts (Harvey *et al.*, 1947; Feldman, 1960; Crocker, 1961), dioxygen difluoride, O_2F_2 (Malm *et al.*, 1984), or krypton difluoride, KrF_2 (Asprey *et al.*, 1986). Dioxygen difluoride, and krypton difluoride react readily with PuO_2 to form PuF_6 and/or PuO_2F_2, but this approach has not been pursued on a large scale because of the extreme difficulty in handling KrF_2 and O_2F_2. Two major improvements to the dissolution of PuO_2 have recently appeared. They are based on the electrochemical oxidative dissolution in HNO_3 with Ag(II) as a catalyst (Bourges *et al.*, 1986; Sakurai *et al.*, 1989, 1993; Madic *et al.*, 1992), and oxidative dissolution catalyzed by Ce(IV) in the presence of anions of oxygen-containing acids of group IV–VII elements (Horner *et al.*, 1977; Scheitlin and Bond, 1980). The kinetics and mechanism of these processes and their use for dissolving plutonium from recycled products and wastes have been reviewed (Nikitina *et al.*, 1997a).

Compatibility with Container Materials Because of its importance as a nuclear reactor and heat source fuel, the compatibility of PuO_2 with refractory materials (both metals and ceramics) has been extensively studied. Paprocki *et al.* (1962b) studied the chemical reactions of plutonium dioxide with reactor materials.

An extensive study of the compatibility of $^{238}PuO_2$ with container materials has been reported by Selle *et al.* (1970a,b). They studied the reactions of $^{238}PuO_2$ with container materials such as tantalum, molybdenum, tungsten, rhenium, platinum, rhodium, and their alloys in the temperature range 1000–2500°C and for time periods up to 532 days. For the results, the reader is referred to the comprehensive original reports. Such studies have led to the use of iridium–0.3% tungsten alloys for encapsulation of $^{238}PuO_2$ general-purpose heat sources, and Pt–30%Rh alloys for encapsulation of $^{238}PuO_2$ light weight radioisotope heater units (see Section 7.3).

(b) The plutonium–sulfur, -selenium, and -tellurium systems

With heavier chalcogen elements (X = S, Se, and Te), plutonium forms binary compounds in four basic families (Table 7.39) with the highest-order composition being PuX_3 that is only found for tellurium. All the heavy chalcogen

Table 7.39 *Crystallographic properties of binary plutonium chalcogenides.*

Compound	*Symmetry*	*Space group*	*Lattice parameters*			*Density* ($g\ cm^{-3}$)	*References*
			a_0 (Å)	b_0 (Å)	c_0 (Å)		
PuX							
$PuS_{0.95}$	fcc	F*m*3*m*	5.5280(5)				Marcon (1969)
PuS	fcc	F*m*3*m*	5.5400(5)			10.60	Marcon (1969)
PuS	fcc	F*m*3*m*	5.5437(3)				Wastin *et al*. (1995)
PuSe	fcc	F*m*3*m*	5.79334(1)			10.86	Kruger and Moser (1967a)
PuSe	fcc	F*m*3*m*	5.7992(5)				Wastin *et al*. (1995)
PuSe	fcc	F*m*3*m*	5.773(3)				Damien (1976)
PuSe	fcc	F*m*3*m*	5.776(1)				Marcon (1969)
PuTe	fcc	F*m*3*m*	6.183(4)			10.32	Gorum (1957)
PuTe	fcc	F*m*3*m*	6.151(3)				Allbutt *et al*. (1970)
PuTe	fcc	F*m*3*m*	6.1900(6)				Wastin *et al*. (1995)
Pu_2X_3							
Pu_3S_4	bcc	I$\bar{4}$3*d*	8.395			9.41	Damien (1976)
γ-Pu_3S_{4+x}	bcc	I$\bar{4}$3*d*	8.4155(5)			8.53	Marcon (1969)
γ-Pu_3S_{3-x}	bcc	I$\bar{4}$3*d*	8.4590(5)			8.41	Marcon (1969)
α-Pu_2S_3	orthorhombic	P*nmm*	3.97(1)	7.37(2)	15.45(3)	8.31	Marcon (1969)
γ-Pu_2S_3	bcc	I$\bar{4}$3*d*	8.4585				Damien (1976)
γ-Pu_2Se_3	bcc	I$\bar{4}$3*d*	8.7965(5)				Marcon (1969)

γ-Pu_2Se_3	bcc	I$\bar{4}$3*d*	8.802				Damien (1976)
Pu_3Se_4	bcc	I$\bar{4}$3*d*	8.768				Damien (1976)
η-Pu_2Se_3	orthorhombic	P*bnm*	4.10(1)	11.10(2)	11.32(2)		Marcon (1969)
γ-Pu_2Te_3	bcc	I$\bar{4}$3*d*	9.355				Damien (1976)
η-Pu_2Te_3	orthorhombic	P*bnm*	11.94(2)	12.10(2)	4.339(6)		Damien (1976)
***PuX*$_{2-x}$**							
$PuS_{1.76}$	tetragonal	P4/*nmm*	3.936		7.958		Allbutt and Dell (1967) and Damien (1976)
$PuS_{1.9}$	tetragonal	P4/*nmm*	3.943(3)		7.962(5)		Marcon (1969)
$PuS_{2.0}$	monoclinic	P2_1/*a*	7.962(10)	3.981(5)	7.962(10)		Marcon (1969)
$PuS_{2.0}$	tetragonal	P4/*nmm*	3.974		7.947	8.0	Allbutt and Dell (1967)
$PuSe_{1.8}$	tetragonal	P4/*nmm*	4.100(5)		8.364(5)		Marcon (1969)
$PuSe_{1.814}$	tetragonal	P4/*nmm*	4.088		8.539		Allbutt and Dell (1967) and Damien (1976)
$PuSe_{1.9}$	tetragonal	P4/*nmm*	4.165		8.41(1)		Marcon (1969)
$PuSe_{1.987}$	tetragonal	P4/*nmm*	4.132		8.343		Allbutt and Dell (1967) and Damien (1976)
$PuTe_{1.81}$	tetragonal	P4/*nmm*	4.334		8.984		Damien (1976)
$PuTe_{2.02}$	tetragonal	P4/*nmm*	4.391		8.938		Damien (1976)
***PuX*$_3$**							
$PuTe_3$	pseudo-tetragonal	B*mmb*	4.338(5) 6.151(3)	4.338(5)	25.60(9)		Damien (1973) Damien (1976)

elements form the series of substoichiometric complexes PuX_{2-x}. For the sesquichalcogenides of formula Pu_2X_3, sulfur forms an α-phase, all the chalcogenides form a γ-phase, while selenium and tellurium form an η-phase. All the heavier chalcogenides form the simple binary PuX.

(*i*) *Preparation*

All of the heavier chalcogenide compounds of plutonium can be prepared by gas–solid reaction between the appropriate stoichiometry of plutonium hydride (PuH_x) and chalcogen element in quartz tubes sealed under secondary vacuum (Damien, 1973, 1976; Damien and De Novion, 1981; Damien *et al.*, 1986). After a typical reaction time of 1 week at 350–750°C, the dichalcogenide, PuX_{2-x} is formed. Compounds with lower X/Pu ratio can be prepared by thermal decomposition of PuX_{2-x} in a sealed tube where one end is kept outside the furnace to allow for the deposition of the chalcogen element. The monochalcogenide, PuX requires much-higher temperature for formation. Typically the quartz tube is heated to 800°C, and the products are pressed into pellets and sintered at 1200–1600°C. This approach works for all the chalcogenide elements except tellurium. Reaction of plutonium hydride with excess tellurium under high vacuum at 350°C for 1 week produces $PuTe_3$ (Damien, 1973). The plutonium tritelluride undergoes decomposition in a stepwise fashion to produce $PuTe_{2-x}$ at 400°C, η-Pu_2Te_3 at 700°C, and γ-Pu_2Te_3 at 900°C (Allbutt *et al.*, 1970; Damien, 1973).

In addition to preparation using plutonium hydride, all the plutonium chalcogenides (sulfur, selenium, tellurium) may be prepared by direct synthesis from the elements (Gorum, 1957; Marcon and Pascard, 1966a,b; Kruger and Moser, 1967a; Marcon, 1969; Wastin *et al.*, 1995). For volatile compounds, the reactions may be carried out in two- or three-zone vacuum-sealed quartz tubes that are placed in a temperature gradient resistance furnace (Spirlet, 1982; Spirlet and Vogt, 1982). The product stoichiometry and phase is controlled by the reaction temperature and stoichiometry of reactants. For compounds that are not highly volatile, excellent results have been obtained when using levitation melting in an induction coil or in a Hukin magnetic levitation cold crucible, by semilevitation melting on a pedestal, or by arc melting (Wastin *et al.*, 1995).

There are other methods for preparation of a few specific plutonium chalcogenide. In the early work of Abraham *et al.* (1949b), PuS was accidentally obtained when PuF_3 was reduced with Ca vapor in a BaS crucible at 1250°C. High-purity PuS may also be obtained when compact plutonium metal is first reacted to give the hydride, the hydride is ground to powder in an inert-gas atmosphere, and, after decomposition to the metal, is reacted with H_2S. A similar reaction of the plutonium hydride with H_2S may also be used to prepare α-Pu_2S_3. Finally, PuSe can be obtained by reacting a higher selenide with plutonium metal (Marcon, 1969).

(*ii*) *Solid-state structures*

Crystallographic properties of binary plutonium chalcogenides are summarized in Table 7.39.

Plutonium tritelluride crystallizes in the orthorhombic $NdTe_3$ structure type (Norling and Steinfink, 1966; Damien, 1973). In this structure, the unit cell contains 12 planar layers each consisting of a single type of atom. Since the separation between the plutonium and tellurium layers is about 0.9 Å, the two layers can be considered as a single puckered layer. In this way, the structure can be described as consisting of four puckered Pu–Te layers and four densely packed tellurium layers. Each plutonium atom is surrounded by nine near-neighbor tellurium atoms, and the $PuTe_9$ coordination polyhedron approximates a capped square antiprism with a distortion of the plutonium atom out of the center of the tellurium prism, as depicted in Fig. 7.96.

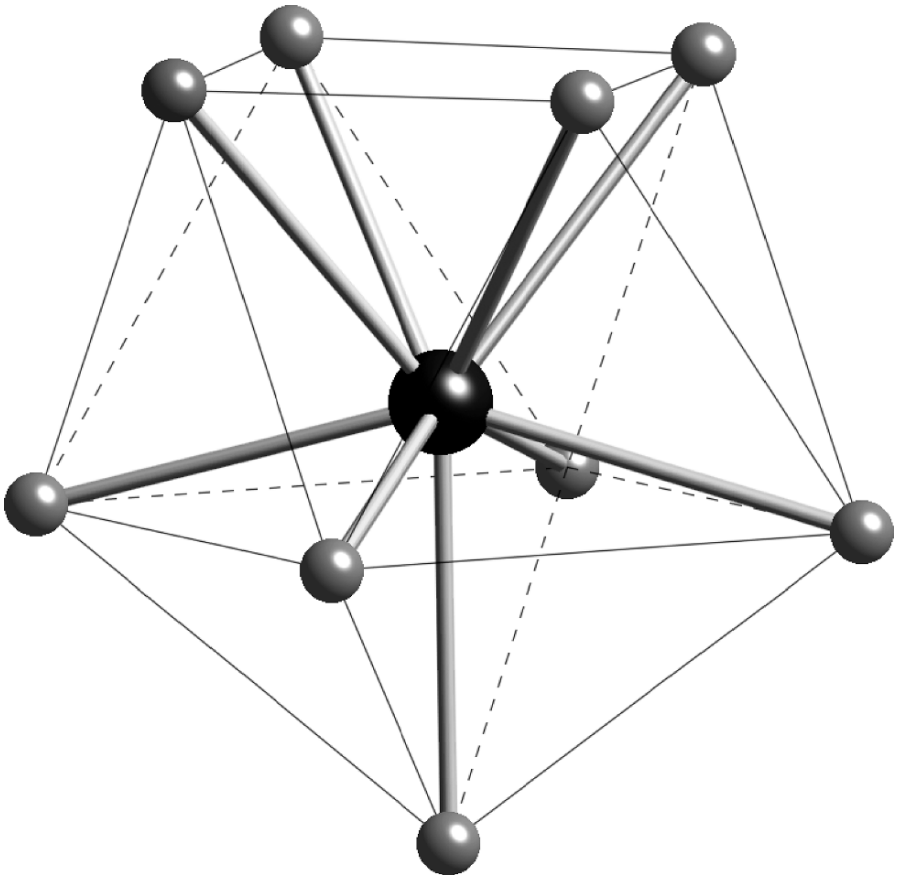

Fig. 7.96 *Local coordination sphere around plutonium in $PuTe_3$ and PuX_2. The plutonium atom is black and tellurium atoms are gray.*

The ideal structure of plutonium dichalcogenides, PuX_2 is the anti-Fe_2As in space group $P4/nmm$ ($Z = 2$) (Damien *et al.*, 1986). In this structure, layers of five chalcogen atoms in the basal face-centered square plane are separated by two slabs of alternating Pu^{3+} (nine-fold coordination) and X^{2-} ions. The local PuX_9 coordination polyhedron is identical to that seen in $PuTe_3$, depicted in Fig. 7.96. All the PuX_{2-x} compounds are distorted from this idealized structure due to the formation of X–X bonding pairs within the basal planes. A typical structure is shown in Fig. 7.97. This distortion gives rise to a number of pseudo-cubic, tetragonal, orthorhombic, and monoclinic ($\beta = 90°$) anti-Fe_2As superstructures (Flahaut, 1979; Rolland *et al.*, 1994). From Table 7.39, it can be seen that all PuX_{2-x} (X = S, Se, and Te) compounds display the pseudo-tetragonal cell of the anti-Fe_2As structure, with the exception of PuS_2, which displays the monoclinic ($\beta = 90°$) $CeSe_2$ variant of the structure (Marcon and Pascard, 1968).

The sesquichalcogenides of plutonium are isostructural with the rare-earth analogs (Damien *et al.*, 1986). The low-temperature stoichiometric phase,

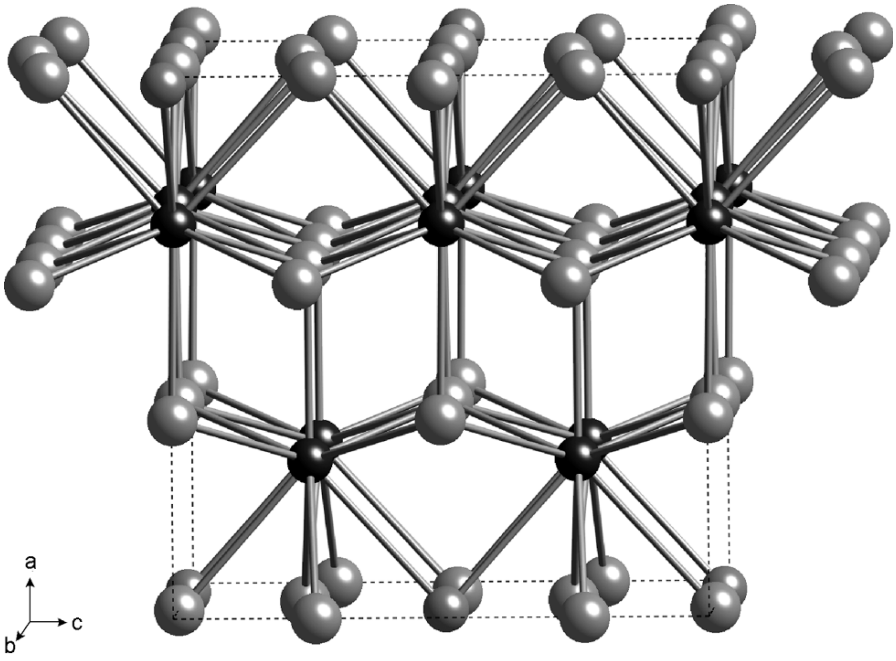

Fig. 7.97 *Solid-state crystal structure of plutonium dichalcogenides, PuX_2, emphasizing the local PuX_9 coordination. The X–X bonding pairs are not indicated for clarity. The distortions in the chalcogen layers due to X–X bonding are clearly evident in this model, based on monoclinic $LaTe_2$ (Stöwe,* 2000). *Plutonium atoms are black and chalcogen atoms are gray.*

referred to as α-Pu_2X_3 only exists for the sulfide, and has the orthorhombic La_2S_3-type structure, with two plutonium sites displaying local PuS_7 and PuS_8 coordination. The high-temperature γ-Pu_2X_3 phase is not a stoichiometric phase, and exists over a range of compositions varying from Pu_2X_3 to Pu_3X_4. This phase displays the cubic Th_3P_4 structure, where the coordination number of the plutonium atom is eight. For selenium and tellurium, there is a η-Pu_2X_3 phase that displays the orthorhombic U_2S_3 structure. The η-Pu_2Se_3 is thermally unstable and transform near 800°C into the cubic γ-Pu_2Se_3 of the Th_3P_4 structure. Early reports of a β-phase for Pu_2S_3 have been shown to be incorrect, as the material is now known to be a ternary oxychalcogenide (Carre *et al.*, 1970). All monochalcogenides of plutonium (PuX) have the cubic NaCl crystal structure.

(*iii*) *Properties*

The monochalcogenides have a metallic luster that can be described as gold, copper, and black for the sulfide, selenide, and telluride, respectively. The monochalcogenides have been the subject of extensive study directed towards understanding valency and the itinerant or localized nature of their 5f electrons. Several excellent overviews are available (Rossat-Mignod *et al.*, 1984; Buyers and Holden, 1985; Dunlap and Kalvius, 1985; Fournier and Troc, 1985; Santini *et al.*, 1999; Wachter, 2003).

Single crystal samples of PuX have been examined by neutron scattering, magnetic susceptibility, and electrical resistivity. All of the PuX compounds (X = S, Se, Te) are nonmagnetic with magnetic susceptibilities that are almost temperature independent for temperatures above 50 K (Lander *et al.*, 1987). Electrical resistivity increases continuously from room temperature with two changes of thermal behavior around 200 and 30 K, confirming the hypothesis that the PuX compounds are semiconductors with small energy gaps. Fournier *et al.* (1990) suggest that the ground state of the monochalcogenides is a weak magnetic nonconducting $6d^1$–$5f^5$ Kondo state with a high Kondo temperature of ca. 400 K.

Wachter and coworkers proposed that these properties of PuX compounds can be consistently explained by the assumption that the plutonium chalcogenides are related to the high-pressure intermediate-valent form of the isoelectronic samarium chalcogenides. Pressure in the divalent SmX serves to enhance f–d hybridization to achieve an intermediate valence state, whereas in PuX, f–d hybridization is achieved without pressure because of the larger radial extension of the 5f wave functions relative to the 4f wave functions. Using PuTe as an example, they conclude that SmTe achieves the same state under a pressure of 58 kbars, and achieves an intermediate valence of 2.75 (Wachter *et al.*, 1991). The intermediate valence model is supported by experimental measurement of elastic constants and observation of a negative value for c_{12} (–39 GPa) (Mendik *et al.*, 1993; Wachter *et al.*, 2001). Photoemission measurements on PuSe films

(Gouder *et al.*, 2000) were interpreted as a 5f localization and not an intermediate valent configuration where 5f and 6d states hybridize. Wachter suggested that the existence of a strong Pauli paramagnetism gives a high DOS near the Fermi level, complicating the interpretation. Recent photoemission studies on PuTe single crystals confirm the presence of a strong three-peak structure near the Fermi level in agreement with of an intermediate valence state in PuTe (Durakiewicz *et al.*, 2004).

(c) Ternary and polynary plutonium chalcogenides

A large number of ternary and polynary plutonium/metal chalcogenides have been described in the literature. The majority of these compounds are ternary and quaternary oxide phases, some of which have gained technological importance. The term 'ternary oxide phases' in this context includes two general classes of material. The first are oxoplutonate compounds with PuO_x^{n-} polyhedral anions and mono-, di-, or trivalent metal cations. A typical example would be Ba_3PuO_6. The second general class are oxometallate compounds with MO_x^{n-} polyhedral anions of main group or transition metal elements in which the plutonium serves as the tri- or tetravalent counter cation. A typical example of this class of compound would be $PuCrO_3$.

Ternary and polynary sulfides, selenides, and tellurides are few, generally not well characterized and will not be discussed.

(*i*) *Preparation of alkali metal oxoplutonates*

When plutonium dioxide and alkali metal oxides, hydroxides, peroxides, or carbonates are intimately mixed and heated in a stream of oxygen, inert gas, or vacuum, they react to form ternary oxide phases in which the plutonium is the central atom of an oxoplutonate anion $\left(PuO_x^{n-}\right)$ and may assume any of the oxidation states from IV to VII. Alkali metal oxoplutonates have been prepared with all the alkali metals with the exception of francium.

Pu(IV). The only alkali oxoplutonate(IV) known at the time of writing is greenish brown Li_8PuO_6, which is obtained by heating a Li_2O–PuO_2 mixture (4.2:1) in a sealed evacuated tube at 600°C (Keller *et al.*, 1965b).

Pu(V). For pentavalent plutonium, Li_7PuO_6, Li_3PuO_4, and Na_3PuO_4 have been reported. These compounds may be obtained by reaction of Li_2O or Na_2O with PuO_2 in an oxidizing atmosphere for 8 h at 700–900°C, respectively. Li_3PuO_4 may be prepared by heating a 3:1 mixture of $LiOH \cdot H_2O$ and PuO_2 in an oxygen stream at 900°C for 24 h (Yamashita *et al.*, 1992). M_3PuO_4 compounds are also reportedly obtained by thermal decomposition of hexavalent M_6PuO_6 for 4 h in an argon atmosphere to give the M_3PuO_4 product and PuO_2 (1100°C, M = Li; 1000°C, M = Na) (Keller, 1964). Brownish-green Li_7PuO_6 was prepared by reacting Li_3PuO_4 with two equivalents of Li_2O at 600°C for 6 h in an evacuated quartz tube (Koch, 1964).

Pu(VI). For hexavalent plutonium, M_6PuO_6, M_4PuO_5, (M = Li, Na), and M_2PuO_4 (M = K, Rb, Cs) compounds have been prepared. These compounds may be either dark green (M_6PuO_6) or brown (M_4PuO_5 and M_2PuO_4). The compounds M_4PuO_5 and M_6PuO_6 dissolve in dilute acids to form yellow-brown or yellow-green aqueous solutions (respectively) and show characteristic Pu(VI) absorption spectra (Koch, 1964).

Li_6PuO_6 is obtained by heating a 3:1 mixture of Li_2O and PuO_2 at 400–500°C in an oxygen atmosphere. If a 2:1 mixture is used, Li_4PuO_5 is formed. When Li_4PuO_5 is heated at 900–1000°C, Li_3PuO_4 is formed. Li_4PuO_5 may also be prepared by heating a 4:1 mixture of $LiOH \cdot H_2O$ and PuO_2 under an oxygen stream at 600°C for 24 h (Yamashita *et al.*, 1992).

Heating a 2:1 mixture of Na_2O and PuO_2 in an oxygen atmosphere at 400°C results in the formation of cubic α-Na_4PuO_5, which may be converted to tetragonal β-Na_4PuO_5 by raising the temperature to 500°C. At 900°C, β-Na_4PuO_5 decomposes to Na_3PuO_4. When a 3:1 mixture of Na_2O and PuO_2 is used, α-Na_4PuO_5 is produced at 400°C; and Na_6PuO_6 is produced at 500°C. Upon heating Na_6PuO_6 to 750°C, it is converted to β-Na_4PuO_5 (Koch, 1964; Keller *et al.*, 1965a).

The M_2PuO_4 class of compounds (M = K, Rb, Cs) may be conveniently prepared by reaction of a 2:1 mixture of MOH with PuO_2 in gold crucibles under an oxygen atmosphere, and heated to at least 450°C (Hoekstra and Gebert, 1977). These compounds decompose in air above 650°C. The rubidium and cesium analogs may also be prepared by heating the corresponding oxoplutonates (VII), M_3PuO_5 to temperatures above 320°C (Pagès *et al.*, 1971a,b).

Pu(VII). For heptavalent plutonium, M_5PuO_6 (M = Li, Na) and M_3PuO_5 (M = Rb, Cs) have been reported. Greenish-black Li_5PuO_6 is formed when a 3:1 mixture of Li_2O and PuO_2 is heated in a stream of oxygen at 430°C (Keller and Seiffert, 1969). The corresponding sodium compound, Na_5PuO_6, has not yet been isolated in the pure state. However, the reaction product of Na_2O_2 and PuO_2 in O_2 atmosphere at 400°C, yields a green aqueous solution upon dissolution in dilute aqueous hydroxide, which shows the characteristic absorption spectrum of Pu(VII) (Keller and Seiffert, 1969).

The black compounds M_3PuO_5 (M = Rb, Cs) have been obtained by heating 3:1 mixtures of the corresponding superoxide MO_2 with PuO_2 at 250°C for more than 6 h. These compounds are reportedly less sensitive to air than the corresponding Np compounds, but have a lower thermal stability. At 320°C, they reportedly decompose to M_2PuO_4 and M_2O_2 (Pagès *et al.*, 1971a,b).

(*ii*) *Preparation of ternary and quaternary alkaline-earth oxoplutonates*

The oxoplutonates of the alkaline-earth elements can be prepared in a manner similar to the alkali-metal oxoplutonates. The alkaline-earth oxides, peroxides

or carbonates react with PuO_2 to form alkaline-earth oxoplutonates, in which the plutonium may occur in oxidation states III, IV, V, VI, and VII.

Pu(III). The only alkaline-earth oxoplutonate(III) that has been reported is $BaPu_2O_4$, which is formed by reacting a 1:3:2 mixture of BaO, elemental Pu and PuO_2 (Keller, 1962). An intimate mixture of Pu, PuO_2, and BaO is first heated in a stream of hydrogen to convert plutonium metal to hydride (PuH_x). The resulting mixture of PuH_x, PuO_2, and BaO is powdered in an inert-gas atmosphere and then heated in a stream of argon at 600°C for 2 h and at 1200°C for 8 h. At 600°C, the plutonium hydride decomposes, and the resulting finely divided metal reacts with PuO_2 to give Pu_2O_3. The Pu_2O_3 in turn reacts with BaO to form $BaPu_2O_4$, which may be isostructural with the lanthanide compounds $BaPr_2O_4$ and $BaNd_2O_4$ (Keller, 1962). No lattice constants of $BaPu_2O_4$ have been reported.

Pu(IV). Discrete alkaline-earth oxoplutonates(IV) can be prepared with the heavy alkaline-earth elements strontium and barium but not for the lighter alkaline-earth elements beryllium and magnesium. Beryllium and magnesium oxides react with PuO_2 to form solid solutions rather than stoichiometric compounds. The mutual solubilities of MO–PuO_2 systems (M = Be, Mg) have been determined by Hough and Marples (1965) and by Carroll (1964). With the heavier alkaline-earth elements, heating stoichiometric mixtures of MO (M = Sr, Ba) with PuO_2 gives $MPuO_3$ (Chackraburtty *et al.*, 1963; Chackraburtty and Jayadevan, 1964). Chackraburtty and coworkers have recommended the use of excess alkaline-earth oxide (3:1 mixtures) to ensure complete conversion of PuO_2 to oxoplutonate. The excess alkaline-earth oxide may be subsequently removed by extraction with methanol (Russell *et al.*, 1960; Keller, 1962, 1964; Chackraburtty and Jayadevan, 1964). $BaPuO_3$ has also been prepared by ball-milling a stoichiometric mixture of $BaCO_3$ and PuO_2, followed by heating under argon at 1197°C for 24 h (Christoph *et al.*, 1988). $SrPuO_3$ and $BaPuO_3$ can also be prepared by reduction of Sr_3PuO_6 or Ba_3PuO_6 in a stream of hydrogen at 1600–1800°C.

Pu(V). Deep black $Ba_3PuO_{5.5}$ is obtained by reacting a mixture of Ba_3PuO_6, PuO_2, and BaO in a stream of argon at 1100–1200°C. It is uncertain whether this compound contains Pu(V) or a mixture of Pu(IV) and Pu(VI) (Keller, 1962, 1964). There are a few quaternary compounds of general formula Ba_2MPuO_6, where M is a trivalent metal ion (M = La, Nd, In). These compounds are prepared by heating a 4:1:1:1 mixture of PuO_2, $PuO_2(NO_3)_2{\cdot}nH_2O$, M_2O_3, and BaO_2 in a platinum crucible at 750–950°C for 8–10 h (Awasthi *et al.*, 1968).

Pu(VI). For hexavalent plutonium, there are ternary alkaline-earth oxoplutonates (VI) of formula $MPuO_4$ and M_3PuO_6 (M = Ca, Sr, Ba) and quaternary compounds of general formula Ba_2MPuO_6, where M is a divalent metal ion (M = Sr, Mn, Pb, Mg, Ca). It is uncertain whether the manganese compound, Ba_2MnPuO_6, contains Mn(II)/Pu(VI) or Mn(III)/Pu(V).

M_3PuO_6 compounds have been prepared by heating 3:1 to 5:1 mixtures of MO (M = Ca, Sr, Ba) with PuO_2 in a stream of oxygen at 950–1050°C

(M = Ca) (Chackraburtty *et al.*, 1963; Awasthi *et al.*, 1968), 900–1200°C (M = Sr), or 800–1300°C (M = Ba) (Keller, 1962, 1964). Sr_3PuO_6 and Ba_3PuO_6 form solid solutions, which range in composition from Ba_3PuO_6 to $Ba_{0.75}Sr_{2.25}PuO_6$.

The reaction of a 1:1 mixture of SrO and PuO_2 in an oxidizing atmosphere at 900–1000°C yields $SrPuO_4$ (Keller, 1962, 1964). $BaPuO_4$ appears to be produced by shaking Ba_3PuO_6 with excess, CO_2-free water for 15–30 min. BaO dissolves and leaves $BaPuO_4$ as the residue (Keller, 1962, 1964).

Pu(VII). Alkaline-earth oxoplutonates(VII) have not yet been prepared by solid-state reactions at elevated temperatures, as has been done with alkali oxoplutonates (VII). However, the compound $Ba_3(PuO_5)_2 \cdot xH_2O$ was obtained by precipitation with $Ba(OH)_2$ from aqueous solutions of Pu(VII) (Komkov *et al.*, 1968).

(*iii*) *Solid-state structures*

Characterization of most alkali and alkaline-earth oxoplutonates are limited to X-ray powder diffraction data. These data have been summarized in Table 7.40. All of the oxoplutonate compounds contain PuO_6^{n-} polyhedra that are octahedral with six equidistant Pu–O bonds, or tetragonally distorted with two short (plutonyl-like) and four long, or four short and two long Pu–O bonds. Representative examples of these structure types will be discussed.

Perovskites – $MPuO_3$

Plutonium (and other light actinides) form an extensive class of complex oxides that are related to the perovskite ($CaTiO_3$) structure in which Pu(IV), Pu(VI), or Pu(VII) ions exist in octahedral PuO_6^{n-} coordination. General structural classifications of perovskites have been discussed (Galasso, 1968; Wells, 1984; Zhou and Goodenough, 2005). The idealized ABO_3 perovskite structure consists of a simple cubic lattice with apex-shared, BO_6 octahedra with large A cations at the center of the unit cell, bonded to 12 oxygen atoms situated at the centers of the cell edges. In this ideal ABO_3 structure, all atomic positions are fixed by symmetry and the packing is very dense. In most perovskites, the actual unit cell symmetry is lower than cubic, which can be accomplished by rotation of the BO_6 octahedra allowing a lengthening of the B–O bonds and lowering the effective A-site coordination number (typically to eight).

Through rotation of a BO_6 unit, the perovskite structure can accommodate a large range of A:B:O radius ratios. Barium plutonate ($BaPuO_3$) is an excellent example of how a 5f element is accommodated into this important structure type. The structure of $BaPuO_3$ had been somewhat controversial, the cell symmetry being reported variously as cubic or orthorhombic (Russell *et al.*, 1960; Keller, 1962; Chackraburtty *et al.*, 1963; Christoph *et al.*, 1988). Christoph and coworkers utilized Zachariasen's bond-length–bond-strength relationships to predict that in the structure of $BaPuO_3$ the PuO_6 octahedra

Table 7.40 *Crystallographic data of alkali and alkaline-earth oxoplutonates.*

Compound	*Symmetry*	*Space group*	*Lattice constants*			*Density* ($g\ cm^{-1}$)	*References*
			a_0 (Å)	b_0 (Å)	c_0 (Å)		
Pu(IV)							
α-$BaPuO_3$	cubic	F*m*3*m*	4.357(7)			8.34	Keller (1962)
α-$BaPuO_3$	cubic	F*m*3*m*	4.373(3)				Chackraburtty *et al.* (1963)
α-$BaPuO_3$	cubic	P*m*3*m*	4.391 (4.385)				Russell *et al.* (1960)
β-$BaPuO_3$	orthorhombic	P*nma*[a]	5.982(4)	5.976(11)	5.847(4)		Chackraburtty *et al.* (1963)
β-$BaPuO_3$	orthorhombic	P*nma*[b]	6.193(1)	8.744(1)	6.219(1)	8.37	Christoph *et al.* (1988)
$SrPuO_3$	cubic	F*m*3*m*	4.28(3)				Keller (1962)
$SrPuO_3$	orthorhombic	A*mm*2[c]	4.273(4)	5.981(5)	6.124	7.94	Chackraburtty and Jayadevan (1964)
Li_8PuO_6	hexagonal		5.64(2)		15.95(5)		Walter (1965)
Ba_2CePuO_6	cubic	F*m*3*m*	8.72(2)				Awasthi *et al.* (1968)
Ba_2TiPuO_6	cubic	F*m*3*m*	8.06(2)				Awasthi *et al.* (1968)
Pu(V)							
Li_3PuO_4	tetragonal	I4/*mmm*	4.464(2)		8.367(5)	6.45	Keller *et al.* (1965b)
$Ba_3PuO_{5.5}$	cubic	F*m*3*m*	8.813(7)				Keller (1962)
Ba_2LaPuO_6	pseudo-cubic	F*m*3*m*	8.63(2)				Awasthi *et al.* (1968)
Ba_2NdPuO_6	cubic	F*m*3*m*	8.66(2)				Awasthi *et al.* (1968)
Ba_2InPuO_6	cubic	F*m*3*m*	8.50(2)				Awasthi *et al.* (1968)
Pu(VI)							
K_2PuO_4	tetragonal	I4/*mmm*	4.298(3)		13.07(1)	5.22	Hoekstra and Gebert (1977)

Rb_2PuO_4	tetragonal	I4/*mmm*	4.323(3)		13.74(1)		Hoekstra and Gebert (1977)
Cs_2PuO_4	tetragonal	I4/*mmm*	4.368(3)		14.71(1)		Hoekstra and Gebert (1977)
$SrPuO_4$	rhombohedral	$R\bar{3}$	6.51(2)			7.72	Keller (1962)
Li_4PuO_5	tetragonal	I4/*m*	6.677(2)		4.421(3)	5.84	Keller *et al*. (1965a)
α-Na_4PuO_5	cubic	F*m*3*m*	4.718(5)			5.20	Keller *et al*. (1965a)
β-Na_4PuO_5	tetragonal	I4/*m*	7.449(5)		4.590(5)	5.36	Keller *et al*. (1965a)
Li_6PuO_6	hexagonal	$R\bar{3}$	5.184(2)		14.59(5)	5.35	Keller *et al*. (1965a)
Na_6PuO_6	hexagonal	$R\bar{3}$	5.76(2)		15.9(1)	5.16	Keller *et al*. (1965a)
Ba_3PuO_6	cubic	F*m*3*m*	8.844(6)			7.17	Keller (1962)
Ba_2SrPuO_6	cubic	F*m*3*m*	8.780(2)				Keller (1962)
Ba_2SrPuO_6	orthorhombic		6.204(42)	6.188(62)	8.822(32)		Gens *et al*. (1985)
$BaSr_2PuO_6$	cubic	F*m*3*m*	8.717(8)				Keller (1962)
Ba_2MnPuO_6	cubic	F*m*3*m*	8.32(2)				Awasthi *et al*. (1968)
Ba_2ZnPuO_6	pseudo-cubic	F*m*3*m*	8.38(2)				Awasthi *et al*. (1968)
Ba_2PbPuO_6	cubic	F*m*3*m*	8.58(2)				Awasthi *et al*. (1968)
Ba_2MgPuO_6	cubic	F*m*3*m*	8.332(6)				Gens *et al*. (1985)
Ba_2CaPuO_6	cubic	F*m*3*m*	8.611(4)				Gens *et al*. (1985)
***Pu*(*VII*)**							
Li_5PuO_6	hexagonal	$R\bar{3}$	5.19(2)		14.48(2)	3.53	Keller and Seiffert (1969a)
Li_5PuO_6	monoclinic[d]	C2/*m*	5.0679(6)	8.7315(8)	5.0293(6)	5.88	Keller *et al*. (1965a)
Na_5PuO_6	monoclinic[d]	C2/*m*	5.6877(8)	8.7314(13)	5.6074(9)	5.75	Keller *et al*. (1965a)

[a] Original space group P*mcm*, recalculated by Roof (1989) in standard setting P*nma*.
[b] Neutron diffraction data; original space group P*bnm*, recalculated by Roof (1989) in standard setting P*nma*.
[c] Original space group B centered, recalculated by Roof (1989) in standard setting A*mm*2.
[d] Keller *et al*. (1965a) reported that Li_5PuO_6 and Na_5PuO_6 are hexagonal and isotypic with rhenium analogs Li_5ReO_6 and Na_5ReO_6. Betz and Hoppe (1984) described the structures of Li_5ReO_6 and Na_5ReO_6 as being monoclinic. Roof (1989) recalculated both Pu structures using the data from Betz and Hoppe, and these are the cell constants reported here with $\beta = 110.24°$ for Li_5PuO_6 and $\beta = 111.01(1)°$ for Na_5PuO_6.

should rotate by about 11 degrees to give the theoretical Pu–O distance predicted by Zachariasen's relationship. This prediction was tested by performing a low-temperature neutron diffraction study on $Ba^{242}PuO_3$ which confirmed the expectations of a distortion away from the cubic perovskite structure (Christoph *et al.*, 1988). The idealized cubic and experimentally confirmed orthorhombic solid-state structures are illustrated in Fig. 7.98. In the low-temperature neutron structure, the PuO_6 octahedra are rotated by about 15 degrees from the idealized position in the cubic perovskite, and this is indicated in Fig. 7.98(b). The PuO_6 rotation gives Pu–O–Pu angles of 157.07 (8) and 160.53(5) degrees. The plutonium atom coordination is only slightly distorted from octahedral with Pu–O distances of 2.2306(5), 2.2295(12), and 2.2230(12) Å. The mean Pu–O distance is 2.228 Å.

Double perovskites M_3PuO_6 and Ba_2MPuO_6

Another important class of plutonium perovskite oxide is the so-called 'double perovskite' typified by M_3PuO_6 (M = Ba, Sr) and Ba_2MPuO_6 (M = Mg, Ca, Sr, Mn, Zn). The double perovskite can be considered as an ideal perovskite with M^{2+} and Pu^{6+} ions occupying alternating octahedral sites in a cubic unit cell with doubled cell edges. The ordered fcc structure (*Fm*3*m*) has the elpasolite (K_2NaAlF_6) structure, and the basic structural unit is shown in Fig. 7.99. This figure maintains the same orientation as Fig. 7.98, and emphasizes the alternating PuO_6 and MO_6 octahedra in the double perovskite structure. As in the ideal

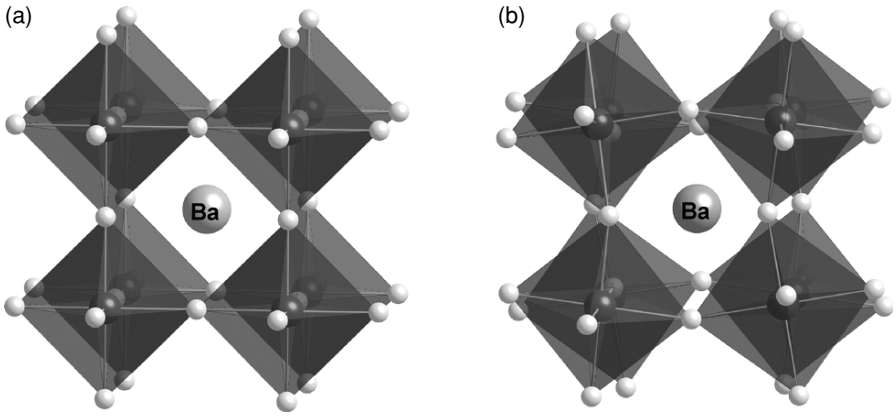

Fig. 7.98 *Idealized cubic* (*a*) *and experimental orthorhombic* (*b*) *crystal structures of $BaPuO_3$, emphasizing the rotation of the local PuO_6 octahedra between cubic and orthorhombic symmetries. The cubic structure is based on the original report by* (*Russell* et al., 1960), *and the orthorhombic structure is based on the low-temperature neutron diffraction study* (*Christoph* et al., 1988). *In this polyhedral representation, the plutonium atoms are dark gray* (*center of octahedra*), *oxygen atoms are white, and the central barium atom is light gray.*

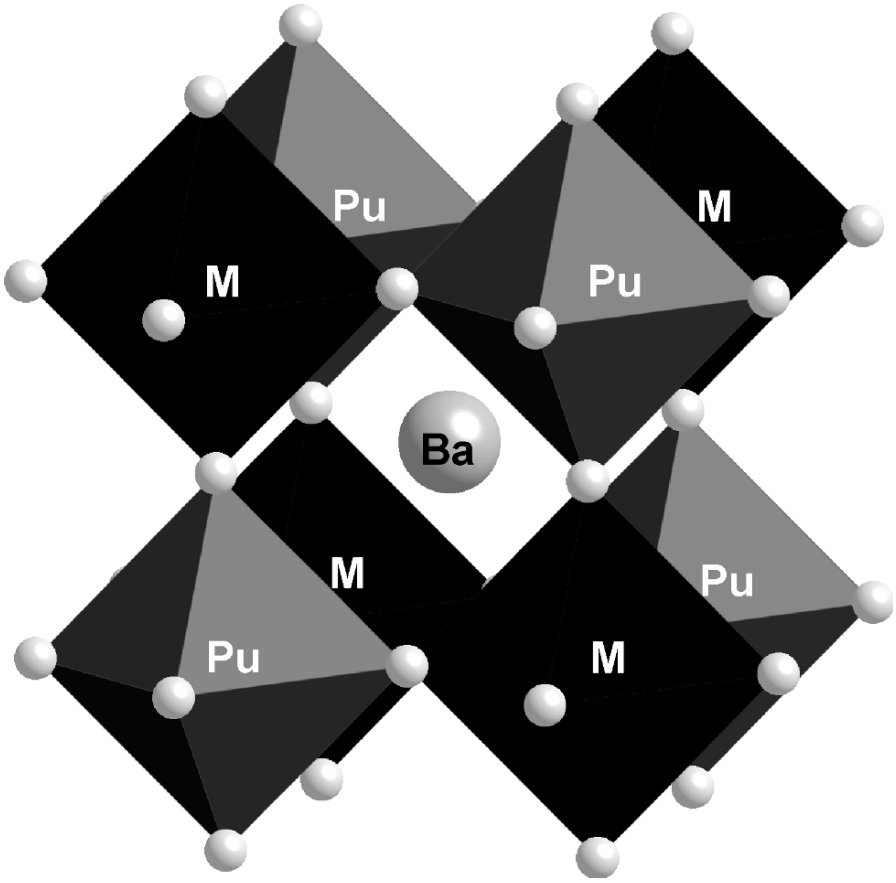

Fig. 7.99 *Polyhedral representation of the idealized double perovskite structure of Ba_2MPuO_6 compounds. This polyhedral representation emphasizes the alternating octahedral PuO_6 (gray) and MO_6 (black) sites in the structure. The central barium ion is light gray.*

perovskite structure, many of these compounds are distorted away from ideal cubic symmetry, and this is often observed as the presence of extra, weak diffraction lines (Gens *et al.*, 1985).

M_4PuO_5

These hexavalent compounds are isostructural with M_4UO_5 (M = Li, Na) and crystallize in tetragonal space group I4/*m*. The solid-state structure of Li_4PuO_5 displays an extended pseudo-octahedral chain of $PuO_4(\mu\text{-}O)_2$ units with a square-planar arrangement of four short equatorial Pu–O bonds of 1.98 Å,

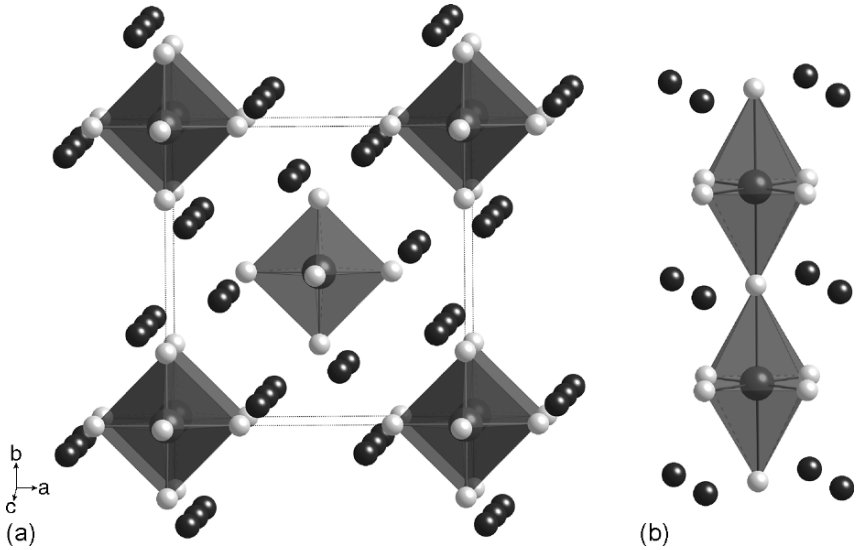

Fig. 7.100 *Polyhedral representation of the solid-state structure of M_4PuO_5 compounds. (a) A view looking down the crystallographic c-axis, and (b) a view perpendicular to the c-axis. The view in (b) emphasizes the distorted PuO_6 polyhedra (gray) surrounded by Li or Na ions (black).*

and two longer axial Pu–O bridging bonds of 2.21 Å that link the planar PuO_4 units together (Keller *et al.*, 1965a). The basic structural unit is shown in Fig. 7.100. This compound is isostructural with β-Na_4PuO_5 that has four short Pu–O bonds of 2.09 Å and two longer Pu–O bonds of 2.29 Å (Keller *et al.*, 1965a). This class of compound is significant in that it demonstrates that hexavalent complex actinide oxides do not necessarily retain actinyl (AnO_2^{2+}) ions with two short metal–oxygen bonds in the solid state.

M_5PuO_6

For heptavalent actinides, Keller reported that M_5PuO_6 (M = Li, Na) compounds were hexagonal and isotypic with rhenium analogs M_5ReO_6 (M = Li, Na) (Keller *et al.*, 1965a). Since Keller's original report, Betz and Hoppe (1984) determined that the structures of M_5ReO_6 were monoclinic and characterized by tetragonally distorted MO_6^{5-} units. In 1994, Morss and coworkers reexamined the structures of both Li_5NpO_6 and Li_5ReO_6 by neutron diffraction and confirmed the monoclinic structure for Li_5ReO_6, but in contrast to the original report, the structure of Li_5NpO_6 was not identifiable (Morss *et al.*, 1994). Thus the actual solid-state structure of M_5PuO_6 compounds remains unresolved.

(*iv*) *Ternary and quaternary oxides of plutonium with main group and transition elements*

A number of ternary oxides of plutonium with the oxides of metallic and semimetallic elements have been prepared. In these compounds plutonium occurs as Pu(III) or Pu(IV), and the tendency for plutonium to assume the role of the cation increases as one proceeds from group III toward group VII elements. A wide variety of compositions are observed, with stoichiometric compounds and nonstoichiometric phases being formed. The crystallographic properties of those compounds having a stoichiometric composition are summarized in Table 7.41. Compounds of the type $PuXO_4$, containing Pu(III) and X = P or As, as well as the phosphates and arsenates of Pu(IV) and Pu(VI) will be discussed in Section 7.8.5.c(i).

Trivalent compounds

Ternary and quaternary oxides containing trivalent plutonium range from simple compounds of the types $PuMO_3$ and $PuMO_4$, to more complex formulae such as $Pu(ReO_4)_3$, or to complicated silicate structures such as $Ba_2Pu_8(SiO_4)_6O_2$ related to apatite.

$PuMO_3$. This class of compound displays the perovskite structure (Fig. 7.98), but with Pu(III) now serving the role of the cation. These compounds have been prepared by Russell *et al.* (1960) for M = Al(III), V(III), Cr(III), and Mn(III), and by Keller *et al.* (1972) for M = Sc(III) by heating mixtures of PuO_2 with the appropriate metal oxide (Al_2O_3, V_2O_5, CrO_3) or carbonate ($MnCO_3$) under argon or hydrogen atmospheres between 1500 and 1600°C for several hours (Russell *et al.*, 1960). Attempts to prepare analogous compounds with M = Fe (III) and Ga(III) were unsuccessful (Chackraburtty and Jayadevan, 1964).

Ba_2PuPaO_6. This is the only known compound in this class, and it shows a double perovskite structure (Fig. 7.99). This compound is prepared as a white powder by heating a 4:1:1 mixture of $BaCO_3$, Pa_2O_5, and Pu_2O_3 at 1350–1400°C *in vacuo* (Keller, 1965b). It is unknown whether this compound contains Pu(III)/Pa(V) or Pu(IV)/Pa(IV).

$PuMO_4$. A few such compounds have been prepared with M = Nb(V) or Ta(V), and contain trivalent plutonium. They are obtained by heating intimate mixtures of Pu_2O_3 and M_2O_3 and M_2O_5 *in vacuo* at 1200°C (Keller and Walter, 1965).

$Pu(ReO_4)_3$. Reaction of plutonium(III) oxalate with Re_2O_7 yields green plutonium(III) perrhenate, $Pu(ReO_4)_3$. This salt-like compound is also obtained by solid-state reaction of PuO_2 with Re_2O_7. $Pu(ReO_4)_3$, is deliquescent in air, and forms hydrates with 1, 2, or $3H_2O$. $Pu(ReO_4)_3$ decomposes at 700°C to PuO_2 and Re_2O_7 (Silvestre *et al.*, 1977). The X-ray powder pattern of anhydrous $Pu(ReO_4)_3$ has not yet been interpreted.

Pu(III) silicates. No simple plutonium(III) silicates are known. However, De Alleluia and coworkers (De Alleluia *et al.*, 1983) have prepared a number of

Table 7.41 *Crystallographic data of ternary oxides of plutonium with main group and transition elements.*

Compound	*Symmetry*	*Space group*	*Lattice constants*			*Density* ($g\ cm^{-1}$)	*References*
			a_0 (Å)	b_0 (Å)	c_0 (Å)		
Pu(III)							
$PuAlO_3$	orthorhombic	A*mm*2	3.750	5.314	5.350	9.78	Runnalls (1965)
$PuScO_3$	orthorhombic	P*bnm*	5.654	5.839	8.104		Keller *et al.* (1972)
$PuVO_3$	orthorhombic[a]	P*nma*	5.61	7.78	5.48	9.38	Russell *et al.* (1960)
$PuCrO_3$	orthorhombic[a]	P*nma*	5.51	7.76	5.46	9.65	Russell *et al.* (1960)
$PuMnO_3$	orthorhombic[b]	P*nma*	5.497(3)	7.730(4)	5.450(3)	9.72	Russell *et al.* (1960)
$PuAsO_4$	monoclinic[c]	$P2_1/n$	6.92(2)	7.09(2)	6.66(2)		Keller and Walter (1965)
$PuNbO_4$	monoclinic[d]	I2/*a*	5.46	11.27	5.17	8.29	Keller and Walter (1965)
$PuTaO_4$	monoclinic[e]	$C2_1/c$	7.618(1)	5.531(1)	7.767(1)	10.0	Keller and Walter (1965)
$Ba(Pu_{0.5}Pa_{0.5})O_3$	cubic		8.748	5.17			Keller (1965b)
$Pu_{9.33}(SiO_4)_6O_2$	hexagonal	$P6_3m$	9.589(5)		7.019(5)		De Alleluia *et al.* (1983)
$Pu_8(SiO_4)_6$	hexagonal	$P6_3m$	9.595(5)		7.037(5)		De Alleluia *et al.* (1983)
$LiPu_9(SiO_4)_6O_2$	hexagonal	$P6_3m$	9.566(5)		6.999(5)		De Alleluia *et al.* (1983)
$NaPu_9(SiO_4)_6O_2$	hexagonal	$P6_3m$	9.594(5)		7.025(5)		De Alleluia *et al.* (1983)
$Mg_2Pu_8(SiO_4)_6O_2$	hexagonal	$P6_3m$	9.559(5)		6.973(5)		De Alleluia *et al.* (1983)
$Ca_2Pu_8(SiO_4)_6O_2$	hexagonal	$P6_3m$	9.570(5)		7.043(5)		De Alleluia *et al.* (1983)
$Sr_2Pu_8(SiO_4)_6O_2$	hexagonal	$P6_3m$	9.604(5)		7.122(5)		De Alleluia *et al.* (1983)
$Ba_2Pu_8(SiO_4)_6O_2$	hexagonal	$P6_3m$	9.701(5)		7.198(5)		De Alleluia *et al.* (1983)
$Sr_3Pu_6(SiO_4)_6$	hexagonal	$P6_3m$	9.619(5)		7.131(5)		De Alleluia *et al.* (1983)
Pu(IV)							
$PuSiO_4$	tetragonal	$I4_1/amd$	6.906(6)		6.221(6)	7.37	Keller (1963)
$PuGeO_4$	tetragonal	$I4_1/a$	5.040(2)		11.11(1)	8.82	Keller (1963)
$Pu(TeO_3)_2$	orthorhombic		5.60	10.46	11.76		Wroblewska *et al.* (1979)
$Pu(NbO_3)_4$	tetragonal[f]	I4/*mmm*	7.67(1)		7.74(1)	5.85	Keller (1965a)

$Pu(TaO_3)_4$	tetragonal[f]	I4/*mmm*	7.654(5)		7.731(5)	Keller (1965a)
$Pu(MoO_4)_2$	orthorhombic[g]	P*mna*	9.422(8)	13.993(10)	10.039(11)	Tabuteau *et al.* (1972)
$Pu(ReO_4)_4{\cdot}4H_2O$	monoclinic[h]		32.4	6.69	16.85	Silvestre *et al.* (1977)
$LiPu_2(VO_4)_3$	tetragonal		7.09		6.35	Pagès and Freundlich (1976)
$NaPu_2(VO_4)_3$	tetragonal		7.14		6.37	Pagès and Freundlich (1976)
$AgPu_2(VO_4)_3$	tetragonal		5.06		11.32	Pagès and Freundlich (1976)
$CdPu(VO_4)_2$	tetragonal		7.04		6.33	Pagès and Freundlich (1976)
$CaPu(VO_4)_2$	tetragonal		7.16		6.33	Pagès and Freundlich (1976)
$SrPu(VO_4)_2$	tetragonal		7.29		6.47	Pagès and Freundlich (1976)
$Na_2Pu(MoO_4)_3$	tetragonal		5.198		11.280	Tabuteau *et al.* (1972)
$Li_4Pu(MoO_4)_4$	tetragonal		11.085		10.600	Tabuteau *et al.* (1972)
$Na_4Pu(MoO_4)_4$	tetragonal		11.20		11.69	Tabuteau *et al.* (1972)
$K_2Pu(MoO_4)_3$	monoclinic[i]	*Cc* or *C*2/*c*	17.538(9)	11.992(6)	5.243(4)	Tabuteau and Pagès, 1980)
$K_8Pu(MoO_4)_6$	monoclinic[j]	*Cc* or *C*2/*c*	10.416(4)	10.416(4)	7.748(4)	Tabuteau and Pagès (1980)
$Rb_2Pu(MoO_4)_3$	monoclinic[k]	*Cc* or *C*2/*c*	17.77(3)	12.068(13)	5.282(7)	Tabuteau and Pagès (1980)
$Rb_8Pu(MoO_4)_6$	monoclinic[l]	*Cc* or *C*2/*c*	10.67(2)	17.71(5)	7.99(12)	Tabuteau and Pagès (1980)
$Cs_2Pu(MoO_4)_3$	orthorhombic		26.516(31)	9.702(25)	5.178(9)	Tabuteau and Pagès (1980)

[a] Original space group P*bnm*, atomic positions transformed to standard setting P*nma* by Roof (1989).
[b] Russell *et al.* indicated that $PuMnO_3$ is orthorhombic and perhaps isomorphic with $PuCrO_3$. The structure was refined by Roof using original d-spacings and transformed into standard space group P*nma* (Roof, 1989).
[c] $\beta = 105.45°$.
[d] $\beta = 94.58°$. Keller and coworkers reported lattice constants and suggested that the structure was of the β-fergusonite type (Keller and Walter, 1965). The latter structure was refined in I2/*a* by Santoro *et al.* (1980).
[e] $\beta = 100.94°$. Keller and coworkers reported the structure to be of the $CeTaO_4$ type, whose structure was refined by Santoro *et al.* (1980). Lattice constants, atomic positions and thermal parameters refined by Roof (1989).
[f] Space group assignment described by Roof (1989).
[g] Lattice constants refined by Roof and transformed into standard space group *Pmna* (Roof, 1989).
[h] $\beta = 110.07°$.
[i] $\beta = 104.80(6)°$.
[j] $\beta = 116.59(4)°$.
[k] $\beta = 107.78(10)°$.
[l] $\beta = 116.3(1)°$.

complex silicates of the types $Pu_8(SiO_4)_6$; $Pu_{9.33}(SiO_4)_6O_2$; $M_2Pu_9(SiO_4)_6O_2$ (M = Li, Na), $M_2Pu_8(SiO_4)_6O_2$ (M = Mg, Ca, Sr, Ba), and $Sr_3Pu_6(SiO_4)_6$. All these compounds have hexagonal apatite-type structures, some with lattice defects. All these compounds, which show the blue color of Pu(III), are prepared by reducing mixtures of PuO_2, SiO_2, and the respective alkali or alkaline-earth oxides in ultrapure H_2 at temperatures between 1100 and 1400°C in alumina or iridium vessels for periods up to 3 days. In these systems, the reduction to Pu(III) is accomplished much more readily than the reduction to Pu(III) in other mixed oxide systems.

Tetravalent compounds

$PuMO_4$. Compounds of this type containing M = Si or Ge can be obtained by hydrothermal synthesis from 1:1 mixtures of PuO_2 and MO_2 at 250°C. They may also be prepared by solid-state reactions at 1200°C from the same components (Keller, 1963). $PuSiO_4$ is green; $PuGeO_4$ is pale brown or olive brown.

$Pu(MO_3)_4$. These compounds contain Pu(IV) and M(V) (M = Nb, Ta) and may be obtained by solid-state reaction of a 2:1 mixture of M_2O_5 and PuO_2 (Keller, 1965a).

$Pu(MO_3)_2$. The only representative of this type of compound is white plutonium(IV) tellurite, $Pu(TeO_3)_2$, which is prepared by heating a 1:2 mixture of PuO_2 and TeO_2 for 24 h at 700°C (Wroblewska *et al.*, 1979).

$Pu(MO_4)_2$. The only compound of this type known now is brown-red plutonium(IV) molybdate, $Pu(MoO_4)_2$. This compound may be prepared by heating a stoichiometric mixture of PuO_2 and MoO_3 for 2 h at 500°C, followed by 4 h at 800°C (Tabuteau *et al.*, 1972).

A number of quaternary plutonium(IV) molybdates have been obtained by reaction of $Pu(MoO_4)_2$ with M_2MoO_4 (M = Li, Na, K, Rb, Cs) compounds at high temperature (Tabuteau *et al.*, 1972). Reaction of Li_2MoO_4 with $Pu(MoO_4)_2$ at 500°C gives $Li_4Pu(MoO_4)_4$. $Li_4Pu(MoO_4)_4$ melts congruently at 630°C and has a reversible solid-state transformation at 510°C. Solid-state reaction of Na_2MoO_4 with $Pu(MoO_4)_2$ at 600°C gives $Na_2Pu(MoO_4)_3$ and $Na_4Pu(MoO_4)_4$. Both compounds show peritectic decomposition, $Na_2Pu(MoO_4)_3$ at 714°C and $Na_4Pu(MoO_4)_4$ at 708°C. Similarly, $M_2Pu(MoO_4)_3$ and $M_8Pu(MoO_4)_6$ have been prepared by solid-state reactions between M_2MoO_4 and $Pu(MoO_4)_2$ (M = K, Rb). With Cs_2MoO_4, only $Cs_2Pu(MoO_4)_3$ has been prepared by solid-state reaction with $Pu(MoO_4)_2$ (Tabuteau *et al.*, 1972).

Pu(IV) perrhenates. Plutonium(IV) perrhenate tetrahydrate, $Pu(ReO_4)_4 \cdot 4H_2O$, is obtained as a red powder by dissolving the oxalate $Pu(C_2O_4)_2 \cdot 6H_2O$ in 0.5 M perrhenic acid solution, evaporating the resulting solution to dryness, and heating the residue to a temperature below 100°C. So far, the anhydrous compound has not been prepared. At 250°C, $Pu(ReO_4)_4 \cdot 4H_2O$ decomposes partially to $Pu(ReO_4)_3$ (Silvestre *et al.*, 1977).

Pu(IV) vanadates. No simple plutonium(IV) vanadate has been prepared. However, Pagès and Freundlich (1976) prepared a number of quaternary plutonium(IV) vanadates of the types $MPu_2(VO_4)_3$ (M = Li, Na, Ag) and $M'Pu(VO_4)_2$, (M′ = Ca, Sr, Cd). Heating a 4:3:1 mixture of PuO_2, V_2O_5, and Ag_2O at 500°C produces $AgPu_2(VO_4)_3$. The corresponding alkali compounds (M = Li, Na) are prepared by heating 1:1:3 mixtures of M_2CO_3, PuO_2, and V_2O_5 at 700–750°C. The alkaline-earth compounds are obtained in the same manner from a mixture of $M'CO_3$, PuO_2, and V_2O_5. The compounds $MPu_2(VO_4)_3$ and $M'Pu(VO_4)_2$ have the zircon structure, while $AgPu_2(VO_4)_2$ has the scheelite structure.

(d) Ternary oxides of plutonium with lanthanide oxides

No stoichiometric compounds of plutonium oxides with lanthanide oxides have been observed. The following systems have been studied in some detail: PuO_2–CeO_2 (Farkas, 1966), PuO_{2+x}–$YO_{1.5}$ (Jackson and Rand, 1963), PuO_2–$EuO_{1.5}$ (Haug, 1963; Haug and Weigel, 1963), PuO_2–$HoO_{1.5}$ (Engerer, 1967), PuO_2–$TmO_{1.5}$ (Leitner, 1967), and PuO_2–$LuO_{1.5}$ (Sriyotha, 1968). Preliminary data are available for the systems PuO_{2+x}–$YO_{1.5}$ (Jackson and Rand, 1963) and PuO_{2+x}–$EuO_{1.5}$ (Haug, 1963; Haug and Weigel, 1963), while pseudo-binary phase diagrams have been established for the systems PuO_{2+x}–$HoO_{1.5}$ (Engerer, 1967), PuO_{2+x}–$TmO_{1.5}$ (Leitner, 1967), and PuO_{2+x}–$LuO_{1.5}$ (Sriyotha, 1968) up to temperatures of 1700°C in oxygen-free atmosphere (argon) and in 1 atm O_2. A detailed discussion of all these systems is beyond the scope of this work.

From these phase diagrams, it may be concluded that $PuO_{2\pm x}$ may dissolve considerable amounts of $LnO_{1.5}$ to form a solid solution. For instance, in the system $PuO_{2\pm x}$–$HoO_{1.5}$, 46.0 mol% $HoO_{1.5}$ at 1250°C, and 72.0 mol% at 1700°C. The anion defects formed by inclusion of $LnO_{1.5}$ into the PuO_2 lattice may be partially compensated by oxidation of Pu(IV) to Pu(>IV). For instance, the average oxidation number $\overline{W}$ of plutonium in the system PuO_{2+x}–$HoO_{1.5}$ at $p(O_2) = 1$ atm for a composition of 50 mol% $HoO_{1.5}$ and 1400°C was found to be $\overline{W} = 4.36$ at an O:(Pu + Ho) ratio of 1.84 (Engerer, 1967). At a composition of 70 mol% $HoO_{1.5}$ and 1100°C, it was found to be $\overline{W} = 4.51$ at an O:(Pu + Ho) ratio of 1.68. In general, the average oxidation number of the plutonium in the fluorite phases containing lanthanide elements is lower than the corresponding oxidation number in the uranium or neptunium systems at approximately the same composition in the fluorite phases.

The solubility of $PuO_{2\pm x}$ in $LnO_{1.5}$ (Ln = Ho, Tm, Lu) is considerably larger than the solubility of uranium or neptunium oxides. In the system PuO_{2+x}–$HoO_{1.5}$ and at $p(O_2) = 1$ atm, it is 18.5 mol% PuO_2 at 1100°C, and 25 mol% at 1550°C (Engerer, 1967).

A different situation exists in the system $PuO_{2(+x)}$–CeO_2. At 1000°C, the compositions PuO_2–CeO_2 form a series of solid solutions throughout the whole range of concentrations. Microspheres of PuO_2–CeO_2 have been prepared by

the sol-gel process (Farkas, 1966). A detailed X-ray study of the lattice constants of various compositions demonstrates that the solid solutions obey Vegard's law (Mulford and Ellinger, 1958).

(e) Ternary oxides of plutonium with actinides

Ternary oxides of plutonium with actinides have been prepared with thorium, protactinium, uranium, and curium.

(*i*) *The plutonium–thorium system*

At 1000°C the PuO_2–ThO_2 system, forms a series of solid solutions throughout the whole composition range (Mulford and Ellinger, 1958) and these follow Vegard's law. Above 1650°C, under an argon atmosphere, a partial phase separation with formation of C-Pu_2O_3 takes place. The melting points of $(Th,Pu)O_2$ solid solutions are practically constant up to 25 wt % Th and show a linear increase at higher Th contents. $(Pu,Th)O_2$ microspheres have been prepared by the sol–gel process and in the induction-coupled plasma torch.

(*ii*) *The plutonium–uranium–oxygen system*

The plutonium–uranium–oxygen system is one of the best-understood plutonium–actinide oxide systems due to its widespread application in nuclear reactor fuel. For this reason, the mixed plutonium–uranium oxide system has been extensively studied. In spite of this great technological importance, only relatively limited data have been reported in the open literature. There is much more information in the proprietary literature of fuel manufacturing organizations. Plutonium–uranium oxides of general formula $(U,Pu)O_2$ are often referred to as 'mixed oxide' or MOX, and can refer to fuels containing 2–30% PuO_2. These fuels behave very differently depending on the percentage of PuO_2. Fuels for light water reactors (LWR) only contain a small percentage of plutonium (2–6%), and will therefore behave like UO_2 with a small amount of impurity, while fuels for fast breeder reactors (FBR) have a higher percentage of plutonium (15–35%), and behave very differently (Schneider and Roepenack, 1986). Four plants currently produce commercial quantities of MOX fuel. Two are in France, one in Belgium, and one in the United Kingdom. In 2000, about 190 metric tons per year of MOX was produced, incorporating 10–12 metric tons of plutonium. MOX production capacity is presently around 300 metric tons per year, using 18–22 metric tons of plutonium. Since 1963 about 400 metric tons of plutonium have been used in MOX. We only cover the fundamental aspects of the plutonium–uranium–oxygen system; for further details, the reader is referred to part C of the *Gmelin Handbook* (Koch, 1972), to the *Plutonium Handbook* (Wick, 1980), and to a number of original papers (Russell *et al.*, 1962; Markin and Street, 1967; Thuemmler *et al.*, 1967; Benedict and Sari, 1969; Dean

et al., 1970; Sari *et al.*, 1970), and reviews (IAEA, 1967; Matzke, 1982; Schneider and Roepenack, 1986; Matthews, 1987; Baily *et al.*, 1989; Bernard, 1989; Bairiot and Deramaix, 1992; Carbajo *et al.*, 2001; Bairiot *et al.*, 2003).

The plutonium–uranium–oxygen phase diagram

The details of the Pu–U–O phase diagram up to 1000°C have been obtained primarily through lattice constant measurements at high temperature and on quenched samples. It is well established that mixed uranium–plutonium oxides with stoichiometric compositions form a continuous solid solution from UO_2 to PuO_2, and the lattice parameters follow Vegard's law (see Fig. 7.101) so long as the stoichiometry is carefully controlled (Markin and Street, 1967; Thuemmler *et al.*, 1967).

The room-temperature phase diagram of the ternary U–Pu–O system is shown in Fig. 7.102 (IAEA, 1967; Markin and Street, 1967; Benedict and Sari, 1969; Koch, 1972). The system is characterized by four single-phase regions: orthorhombic U_3O_8; a cubic fluorite phase, $MO_{2\pm x}$, which occupies the largest area of the single-phase region; a cubic superstructure, M_4O_9; and a fcc C-M_2O_3 phase.

The orthorhombic U_3O_8 phase includes plutonium in its lattice to form $(U,Pu)_3O_{8-x}$ (Benedict, 1970). The maximum amount of plutonium accommodated at 1000°C corresponds to a Pu:(U + Pu) ratio of 0.06, which decreases to 0.02 at 1400°C. It is assumed that the plutonium ions introduced into the lattice occupy the U_{II} positions in U_3O_8.

The fluorite phase $(U,Pu)O_{2\pm x}$ may be hyperstoichiometric, stoichiometric, or substoichiometric with regard to the O:(U + Pu) ratio. The stoichiometric region corresponds to the pseudo-binary system UO_2–PuO_2, in which the lattice constants obey Vegard's law (see Fig. 7.101). Since PuO_2 loses oxygen at high temperature, deviations from Vegard's law can be observed. At room temperature, the range of the single-phase substoichiometric fluorite structure goes up to the ratio Pu:(U + Pu) = 0.17. A large region with two cubic phases extends from Pu:(U + Pu) ~0.20 up to the binary Pu–O system. One of these two cubic phases is an fcc phase with O:(U + Pu) = 1.985. In the range $0.2 \leq$ Pu:(U + Pu) ≤ 0.5, this phase is in equilibrium with a second fcc phase; and for higher plutonium contents, in equilibrium with a bcc phase of the C-Pu_2O_3 type. In the region Pu:(U + Pu) > 0.5 with low O:(U + Pu) ratios, there exists a bcc single-phase region, which extends up to Pu:(U + Pu) = 0.95 and contracts for Pu:(U + Pu) = 0.97 to a single line at O:(U + Pu) ~1.51. In the region Pu:(U + Pu) ≥ 0.97, a hexagonal phase of A-Pu_2O_3 type exists.

Oxidation of $(U,Pu)O_2$ mixtures yields one- or two-phase products, depending on conditions (Brett and Fox, 1966). In the hyperstoichiometric fluorite phase $(U,Pu)O_{2+x}$, only U is oxidized to U (>IV). At room temperature, for a ratio Pu:(U + Pu) ≤ 0.30 and for O:(U + Pu) ≤ 2.20, a two-phase region $M_4O_9 + MO_{2+x}$ is observed. The M_4O_9 phase exists in the range $2.20 \leq$ O:(U + Pu) ≤ 2.27. For O:(U + Pu) > 2.27 and Pu:(U + Pu) < 0.5, a Pu-rich

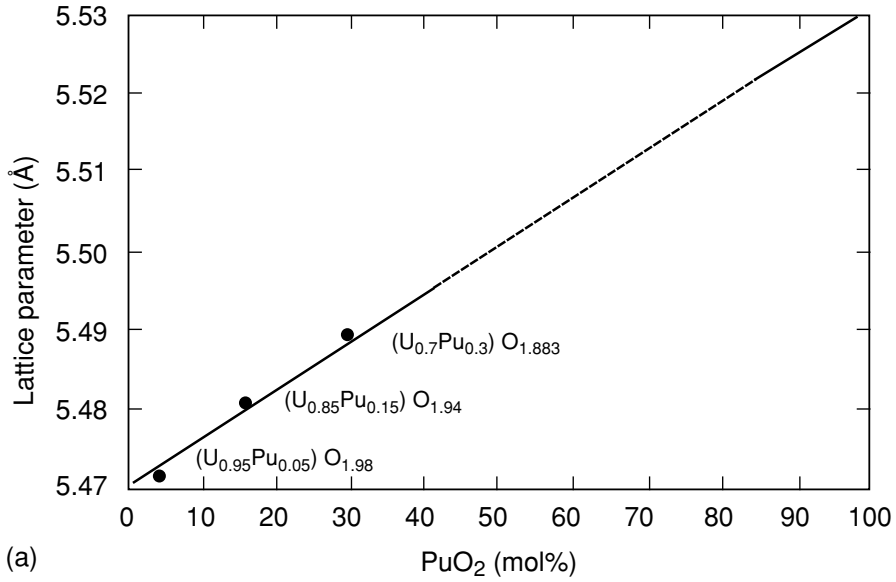

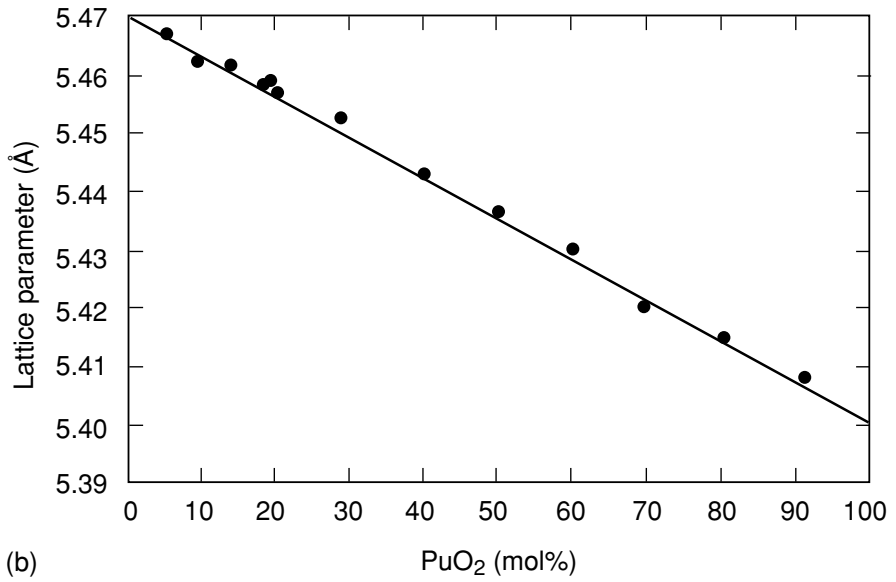

Fig. 7.101 *Lattice parameters of UO_2–PuO_2 mixed oxides that show* (*a*) *the dependence on O*:*M ratio, and* (*b*) *the dependence on PuO_2 concentration* (*Thuemmler* et al., 1967).

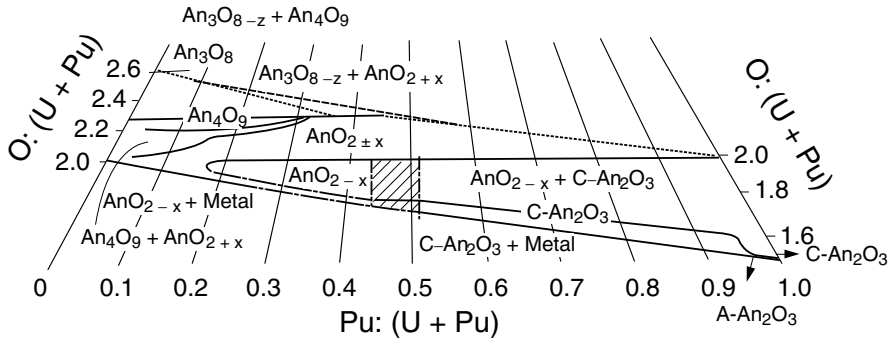

Fig. 7.102 *The phase diagram for the ternary U–Pu–O system in the composition range* $(U,Pu)O_2$–$(U,Pu)O_{2.67}$ *at room temperature* (*Benedict and Sari,* 1969).

fluorite phase is in equilibrium with uranium-rich M_3O_8. The oxidation of $(U,Pu)O_2$ at 600°C yields a metastable U_3O_7 type phase for Pu:(U+Pu) <0.25 and O:(U+Pu) = 2.28. Dean and Boivineau (1970) postulate a rhombohedral phase at composition M_7O_{12} for up to 60 at.% plutonium. According to Nakayama (1971), the phase relationships in the U–O system apply to $0.8 > y > 0.7$ in the MOX system $(U_yPu_{1-y})O_{2+x}$. For $y > 0.7$ there exists the tetragonal phase $(U_yPu_{1-y})O_{2+0.36y}$, which is stable up to 600°C.

Preparation

The preparation of well-defined uranium–plutonium mixed oxides is of particular importance because it is applied to the industrial production of nuclear fuel element materials. The majority of all work reported deals with oxides that contain up to 30% PuO_2, the type commonly encountered in fuel element fabrication. Oxides with more than 30% PuO_2 are much less-frequently studied. A large body of literature has been accumulated on the production of $(U,Pu)O_2$ ceramics for use in nuclear reactors, and a detailed account of all of this work is beyond our scope. The reader is referred to the reviews given in the *Plutonium Handbook* (Wick, 1980), the *Gmelin Handbook* (Koch, 1973c), and the peer-review literature (Schneider and Roepenack, 1986; Baily *et al.*, 1989; Bernard, 1989).

The major technical challenge in preparing $(U,Pu)O_2$ for fuel applications is to produce a product with the maximum degree of homogeneity. There are two main routes to deliver the required properties: comilling of UO_2 and PuO_2 and coprecipitation of UO_2 and PuO_2. Once the $(U,Pu)O_2$ material is formed, both processes entail mixing, pressing, sintering, and grinding operations (Schneider and Roepenack, 1986; Baily *et al.*, 1989; Bernard, 1989; Güldner and Schmidt, 1991). Hundreds of tons of mixed oxide (MOX) fuel have been produced using these processes.

Coprecipitation Processes The main process is the ammonium/uranyl/plutonyl/carbonate process (AUPuC) that produces a powder that is soluble in nitric acid. In this approach, gaseous NH_3 and CO_2 are dissolved into a mixed uranyl/plutonyl nitrate aqueous solution (<40% Pu) to generate an AUPuC of formula $[NH_4]_4[(U,Pu)O_2(CO_3)_3]$. The AUPuC precipitates as a coarse green crystalline product. These crystals are calcined into a $(U,Pu)O_2$ powder by firing at 800°C under a reducing atmosphere of N_2/H_2. The resulting $(U,Pu)O_2$ shows good flowability and sinterability (Schneider and Roepenack, 1986).

Comilling Processes Comilling generally involves mechanical grinding of UO_2 and PuO_2 powders followed by a granulation step before pressing into pellets. This process has been employed extensively at the CEA (Commissariat à l'Energie Atomique) plant in Cadarache, France. An alternate comilling approach designed by Belgonucleaire, and practiced at the French MELOX plant is referred to as the micronized master blend (MIMAS) process. In this process, plutonium and uranium oxides are mixed into a master blend that is 30% PuO_2. The master blend is homogenized and micronized in a dry ball mill, and then blended with free-flowing UO_2 powder to achieve the desired plutonium enrichment, and then pellitized (Schneider and Roepenack, 1986; Baily *et al.*, 1989; Bernard, 1989).

Properties

Due to their technological importance, the thermophysical properties of mixed uranium–plutonium oxide phases have been studied in detail. Unfortunately, most of these data are not available in the open literature. The data that are available have been critically reviewed by Fink (1982) and by Carbajo *et al.* (2001). Much of the discussion that follows has been summarized from those critical reviews.

Vaporization Behavior Vapor pressure measurements on the $(U,Pu)O_2$ system were carried out by Dean *et al.* (1970) with a Knudsen-effusion cell using ^{239}Pu and ^{233}U. Mass spectroscopy studies of vaporization of the $(U,Pu)O_2$ system were carried out by Ohse and Olson (1970), Battles *et al.* (1970), and Raj *et al.* (1999) to evaluate the effect of O:M ratio on the nature of gaseous species. These workers found that the total vapor pressure varies with O:M ratio and goes through a minimum value, suggesting there is no congruently vaporizing composition.

Solidus and Liquidus Temperatures There is an extensive literature on melting behavior. UO_2 melts at a higher temperature (2730–2876°C) than PuO_2 (2238–2445°C), and the $(U,Pu)O_2$ solid solution melts at a temperature between that of pure UO_2 and pure PuO_2. The liquidus and solidus curves of the PuO_2–UO_2 system are shown in Fig. 7.103 for the stoichiometric

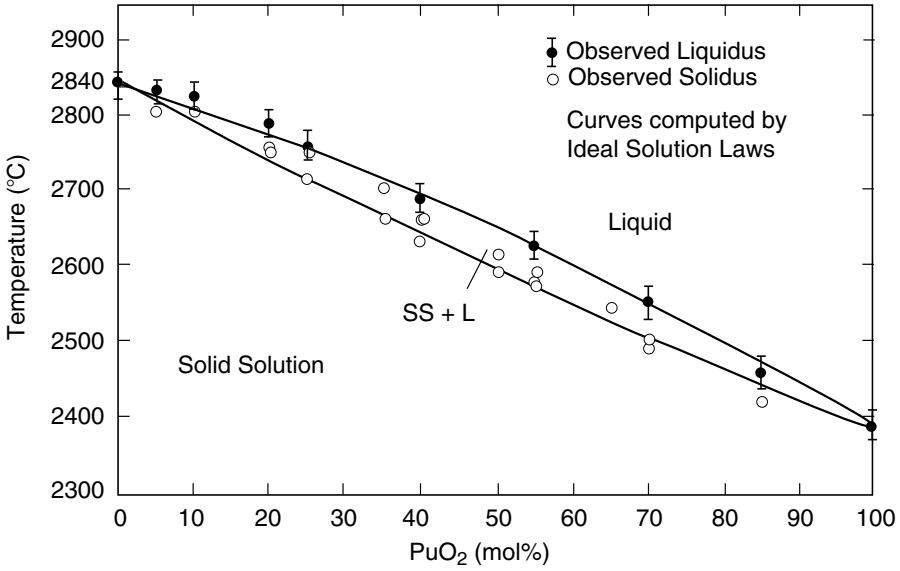

Fig. 7.103 *The solid–liquid phase diagram for the UO_2–PuO_2 system at stoichiometric composition AnO_2 (Lyon and Baily,* 1967).

compositions (Lyon and Baily, 1967). In MOX fuel, the actual melting temperature decreases with increasing PuO_2 content of the fuel as shown in Fig. 7.103 and with burnup (Carbajo *et al.*, 2001). Adamson has developed the following equations that predict the liquidus $[T_L(y)]$ and solidus $[T_S(y)]$ temperatures (in K), where y is the mole fraction of PuO_2 in $(U,Pu)O_2$ (Adamson *et al.*, 1985).

$$T_L(y) = 3120 - 388.1y - 30.4y^2 \tag{7.43}$$

$$T_S(y) = 3120 - 655.3y + 336.4y^2 - 99.9y^3 \tag{7.44}$$

Thermal Expansion and Density MOX fuel density is a function of the fuel composition, temperature, porosity, burnup, and O:M ratio (Carbajo *et al.*, 2001). The $(U,Pu)O_2$ is slightly heavier than UO_2. The density decreases with temperature due to thermal expansion. Fuel burnup changes the porosity and hence the density. At low burnup, the density increases by densification, and at higher burnup the density decreases due to swelling (Carbajo *et al.*, 2001). Martin (1988) developed equations to describe the thermal expansion and density of stoichiometric $(U,Pu)O_2$ compositions. The densities of UO_2 and PuO_2 at 273 K are 10.97 and 11.46 g cm^{-3}, respectively. The density of the solid

solution $(U_{1-y}Pu_y)O_2$ changes according to the linear scaling law below, with y being the mole fraction of PuO_2 (Carbajo *et al.*, 2001).

$$\rho_s(273) = 10970 + 490y(\text{kg m}^{-3}) \tag{7.45}$$

Enthalpy and Heat Capacity Enthalpy and heat capacity are functions of the temperature, fuel composition (fractions of UO_2 and PuO_2), gadolinium content (added as a burnable neutron "poison"), O:M ratio, and burnup. The heat capacity is an important thermodynamic property that is necessary for understanding the various chemical interactions likely to occur during the irradiation of the fuel as well for modeling fuel behavior. Temperature and composition are the main influences on both enthalpy and heat capacity. Both enthalpy and heat capacity increase with temperature. The heat capacity reaches a maximum at the melting point, and then decreases. The heat capacity of UO_2 is lower than that of PuO_2. Carbajo *et al.* (2001) recommended the calculation of enthalpy and heat capacity of solid MOX fuel $U_{1-y}Pu_yO_2$ by using the Neumann–Kopp molar additivity rule, since the $(U,Pu)O_2$ system is an almost ideal solid solution. For example, to calculate the specific heat, one would use:

$$\text{Cp}(\text{T}, \text{MOX}) = (1 - y)\text{Cp}(\text{T}, \text{UO}_2) + y\text{Cp}(\text{T}, \text{PuO}_2) \tag{7.46}$$

where the heat capacity values for UO_2 and PuO_2 are calculated using polynomial expressions developed by Fink (2000) for UO_2, and Cordfunke *et al.* (1990) for PuO_2. Enthalpy polynomials were derived by integrating the Cp equations. For a detailed discussion, listings of the polynomial expressions, and tables of the necessary constants used in these equations, the reader is referred to the original publications (Cordfunke *et al.*, 1990; Fink, 2000; Carbajo *et al.*, 2001). A recent study by Kandan and coworkers experimentally verified that the enthalpies of $(U,Pu)O_2$ solid solutions does obey the Neumann–Kopp molar additivity rule (Kandan *et al.*, 2004).

Enthalpy of Fusion There is only one experimental value for the enthalpy of fusion of a MOX fuel of composition $U_{0.8}Pu_{0.2}O_2$, where Leibowitz *et al.* (1974) obtained a value of 67(3) kJ mol^{-1}.

Thermal Conductivity The thermal conductivity of MOX fuels is a function of the temperature, fuel composition, porosity, burnup, and deviation from stoichiometric composition. Thermal conductivity is a property that does not follow the law of mixtures. The existing data have been reviewed by Carbajo *et al.* (2001). The thermal conductivity decreases with temperature up to approximately 2000 K and then increases with temperature. Addition of PuO_2 to the fuel or increasing porosities reduces the thermal conductivity. Burnup, and/or deviations from stoichiometry significantly decrease the thermal conductivity. For fully dense MOX fuel, Carbajo *et al.* recommended an equation that is a combination of that proposed by Dureiz *et al.* (2000) and

that of Ronchi *et al.* (1999). For full details and discussion, the reader is referred to the review by Carbajo *et al.* (2001).

7.8.6 Plutonium halides and oxyhalides

The decreasing stability of the higher actinide oxidation states in progressing from uranium through neptunium to plutonium is perhaps most clearly revealed in the halogen compounds of plutonium. With the significant and most important exception of fluorine (and, to a minor degree, chlorine), all the halogens form solid binary trihalides of general formula PuX_3 (X = F, Cl, Br, I). For tetrahalides, the only stable solid is the tetrafluoride, PuF_4, while the binary tetrachloride is only marginally stable in the high temperature gas phase as $PuCl_4(g)$. Gas phase data have been interpreted in terms of PuF_5, but there are no known pentahalides, PuX_5, in the solid state (Jouniaux, 1979; Jouniaux *et al.*, 1979; Kleinschmidt, 1988). Fluorine forms the only binary PuX_6, the technologically important hexafluoride, PuF_6. All the halogens form trivalent oxyhalides PuOX (X = F, Cl, Br, I), while fluorine forms a number of oxyfluorides that include pentavalent $PuOF_3$, and hexavalent $PuOF_4$ and PuO_2F_2.

Complex tetrahalide salts of formula M_2PuX_6 are known for X = F, Cl, Br, where M is a monovalent cation. The fluoride ion forms a range of complex salts of general formula $MPuF_5$, $MPuF_6$, M_2PuF_6, M_3PuF_7, M_4PuF_8, and $M_7Pu_6F_{31}$ for the appropriate choice of monovalent cation, M.

Plutonium hexafluoride is by far the most volatile compound of plutonium and is of extraordinary interest in that it makes possible the study of a gaseous binary compound with a rare-earth-like f^2 electron configuration.

A number of reviews have been published in which the properties of the halides have been discussed in detail (Katz and Sheft, 1960; Hodge, 1961; Bagnall, 1967a,b; Brown, 1968; Peterson, 1995).

(a) Plutonium fluorides

(*i*) *Preparation*

Because of their importance in the preparation of plutonium metal (see Sections 7.7.1 and 7.7.2), the binary plutonium fluorides have received a fair amount of attention. Their preparation has been discussed in detail by Johns and Moulton (1944), Reavis *et al.* (1960), Dawson *et al.* (1951), and Dawson and Truswell (1951). The most common procedures involve hydrofluorination of plutonium dioxide or oxalates to generate PuF_3 and PuF_4, while stronger oxidizing conditions such as F_2 will generate PuF_6.

$$2PuO_2 + H_2 + 6HF \xrightarrow{600^\circ C} 2PuF_3 + 4H_2O \tag{7.47}$$

$$Pu_2(C_2O_4)_3 + 6HF \xrightarrow{600^\circ C} 2PuF_3 + 3CO + 3CO_2 + 3H_2O \tag{7.48}$$

$$2Pu(C_2O_4)_2 + 6HF \xrightarrow{600^\circ C} 2PuF_3 + 3CO + 5CO_2 + 3H_2O \tag{7.49}$$

$$PuO_2 + 4HF \xrightarrow[O_2]{550^\circ C} PuF_4 + 2H_2O \tag{7.50}$$

$$PuO_2 + 3F_2 \overset{300^\circ C}{\rightleftharpoons} PuF_6 + O_2 \tag{7.51}$$

$$PuF_4 + F_2 \overset{300^\circ C}{\rightleftharpoons} PuF_6 \tag{7.52}$$

Hydrogen fluoride stored in iron cylinders contains hydrogen, which forms on reaction with the container. Occasionally sulfur dioxide is present. Under reducing conditions like these, PuF_3 results. To secure positive results, either hydrogen may be added, or the absence of reducing agents can be ensured by the addition of oxygen. Between room temperature and 150°C, hydroxyfluorides of the type $Pu(OH)_2F_2$ or $Pu(OH)F_3$ are produced by reaction of PuO_2 with HF. These intermediate compounds are readily converted either to PuF_3 by HF and H_2, or to PuF_4 by HF and O_2 by raising the temperature above 200°C. Instead of plutonium dioxide or one of the oxalates, various other plutonium(III) or plutonium(IV) compounds may also be used as starting materials for fluoride preparations, such as plutonium(IV) nitrate or plutonium peroxide.

Plutonium trifluoride

Plutonium trifluoride is insoluble in water and may therefore be prepared as a hydrate by precipitation from aqueous solution by addition of hydrofluoric acid to an aqueous Pu(III) solution. The preparation of PuF_3 from solution is best accomplished by first reducing Pu(IV) with hydroxylamine (Dawson *et al.*, 1954b) or with SO_2 (Jones, 1953; Weigel, 1965). The purple crystals of the hydrated trifluoride, $PuF_3 \cdot nH_2O$, appear to contain less than one water molecule of hydration. According to Jones (1953), the exact composition of the hydrated compound is $PuF_3 \cdot (0.40 \pm 0.05)H_2O$.

Anhydrous PuF_3 may be obtained by heating $PuF_3 \cdot nH_2O$ in a stream of hydrogen fluoride gas at 200–300°C, or by first heating plutonium(III) oxalate in a stream of hydrogen at 150 to 600°C, followed by hydrogen fluoride at 200 to 300°C (Dawson and Truswell, 1951). The latter method has been used on the 100–350 g scale. PuF_4 may be reduced directly to anhydrous PuF_3 by heating in a stream of hydrogen at 600°C (Garner, 1950).

Plutonium tetrafluoride

Addition of hydrofluoric acid to aqueous plutonium(IV) solutions precipitates pale pink plutonium tetrafluoride hydrate, $PuF_4 \cdot 2.5H_2O$. Attempts to dehydrate this substance by heating *in vacuo* did not yield anhydrous plutonium

tetrafluoride, but rather the trifluoride. According to Dawson *et al.* (1954b), this rather surprising result may be accounted for by the following reaction scheme:

$$PuF_4 + H_2O \rightleftharpoons PuO_2 + 4HF \tag{7.53}$$

$$3PuF_4 + PuO_2 \rightleftharpoons 4PuF_3 + O_2 \tag{7.54}$$

with a net reaction of:

$$4PuF_4 + 2H_2O \rightleftharpoons 4PuF_3 + 4HF + O_2 \tag{7.55}$$

Increasing temperature and high vacuum displaces the equilibrium toward the right and aids in the production of the trivalent fluoride. Both plutonium trifluoride and tetrafluoride hydrates are insoluble in water and will dissolve in acid only sparingly. By contrast, they may be dissolved with comparative ease in aqueous solutions of ions that form stable complexes with fluoride ions, such as Zr(IV), Fe(III), and Al(III), or with BO_3^{3-} which forms BF_4^-. Solutions of 0.1 M HNO_3 saturated with boric acid or aluminum nitrate are therefore especially well suited for the dissolution of PuF_3 or PuF_4. Detailed procedures for the dissolution of PuF_4 with nitric acid have been summarized by Navratil (1969a–c).

Plutonium tetrafluoride hydrate, $PuF_4 \cdot 2.5H_2O$, may be dehydrated in a stream of HF gas to anhydrous PuF_4. According to Khanaev *et al.* (1967), the dehydration of $PuF_4 \cdot 2.5H_2O$ proceeds through the successive formation of $PuF_4 \cdot 2.5H_2O$, and ultimately anhydrous PuF_4.

Both plutonium trifluoride and plutonium tetrafluoride react with oxygen at elevated temperatures. Fried and Davidson (1949) concluded that the reaction of plutonium trifluoride with oxygen proceeds according to the equation:

$$4PuF_3 + O_2 \xrightarrow{600^\circ C} 3PuF_4 + PuO_2 \tag{7.56}$$

This conclusion was confirmed by Dawson and Truswell (1951), who measured the oxygen partial pressure for the reverse reaction of PuF_4 with PuO_2. In the presence of water vapor and oxygen, the reaction product is PuO_2 (Dawson and Elliott, 1953). Plutonium tetrafluoride is stable in oxygen at 600°C and *in vacuo* at 900°C. On heating PuF_4 *in vacuo*, some material sublimes and the residue is found to be PuF_3. Fried and Davidson (1949) interpreted this as a disproportionation of PuF_4 into PuF_3 and PuF_5. Dawson *et al.* (1951) confirmed these conclusions but were able to show that the sublimate is probably not PuF_5. It is possible that the compound formed in this process is an oxyfluoride, as observed by Jouniaux *et al.* (1979) for the reaction of PuO_2 with F_2.

Intermediate fluoride and plutonium pentafluoride

During the preparation of plutonium hexafluoride (see below), a brick-red solid residue has been observed. This solid was identified by X-ray powder diffraction and fluorine analysis by pyrohydrolysis to be the mixed-valent compound

Pu_4F_{17} (Mandleberg *et al.*, 1956). Hawkins (1956) and Gendre (1962) have also reported evidence for the existence of this compound, but it has not been isolated in the pure state. Jouniaux and coworkers proposed the formation of gas-phase PuF_5 in their thermochromatographic study (Jouniaux *et al.*, 1979), and Kleinschmidt (1988) also interpreted his mass spectroscopy results on PuF_6 in the presence of alumina in terms of formation of this gas-phase species.

Plutonium hexafluoride

It is well known that fluorine oxidizes transition metals to their highest oxidation states. This general characteristic also holds true for plutonium. The high volatility of PuF_6 has made this compound of great technological importance, and therefore a considerable amount of information about PuF_6 is available.

Plutonium hexafluoride was first prepared at Los Alamos by Florin and coworkers (Florin, 1950a,b, 1953; Florin and Tannenbaum, 1952; Florin *et al.*, 1956). The preparation and determination of some fundamental properties was carried out at Harwell by Mandleberg and colleagues (Hurst *et al.*, 1953; Mandleberg *et al.*, 1953, 1956), while Malm and coworkers (Malm and Weinstock, 1954; Weinstock and Malm, 1956a,b) performed extensive research on the basic properties of PuF_6 at Argonne National Laboratory. Scientists at Argonne (Chemical Engineering Division) performed extensive research on PuF_6 in connection with the development of the fluoride volatility process (Adams *et al.*, 1957; Steindler *et al.*, 1958, 1959; Steindler, 1963). The review by Steindler (1963) gives an excellent summary on the preparation and properties of plutonium hexafluoride.

Plutonium hexafluoride is most easily prepared by using elemental fluorine as an oxidizing–fluorinating agent with PuF_4 or PuO_2, typically at 600°C according to the following reactions:

$$PuO_2 + 3F_2 \rightleftharpoons PuF_6 + O_2 \tag{7.57}$$

$$PuF_4 + F_2 \rightleftharpoons PuF_6 \tag{7.58}$$

The fluorination of plutonium dioxide produces oxygen, which accumulates in any apparatus in which the gases are recirculated over the unreacted solid, and periodic removal of oxygen is required to avoid dilution of fluorine. Since plutonium tetrafluoride is always formed in the fluorination of plutonium dioxide, the preferred method of preparing PuF_6 is the fluorination of PuF_4.

The preparation of PuF_6 from PuF_4 and F_2 proceeds at a reasonable rate only at fairly high temperatures, typically at 300°C. Passage of fluorine over PuF_4, in a conventional tube furnace is possible, but is not very efficient. In order to prevent thermal decomposition of the PuF_6 product, special reaction vessels are employed to permit rapid condensation of the volatile products close to the point of their preparation. Fluorination reactor vessels of this type were first used by Florin and coworkers (Florin, 1950a,b, 1953; Florin and Tannenbaum, 1952; Florin *et al.*, 1956), and by Weinstock and coworkers (Malm and

Weinstock, 1954; Weinstock and Malm, 1956b). Two of these reactor designs are shown in Fig. 7.104. The starting charge of PuF_4 is placed in a nickel dish, which is heated in a fluorine atmosphere by an induction coil. The induction coil consists of copper tubing, through which liquid nitrogen is circulated, such that the coil serves as both the heating element and the product condenser. Once formed, the PuF_6 product collects on the surface of the coil in crystalline form. This type of reactor works very well for gram-quantity preparations. For larger quantities, fluidized-bed fluorination is the preferred method. Quantities up to 500 g of Pu have been volatilized in the fluidized-bed fluorination of PuF_4. For details of the technique, see Levitz *et al.* (1968).

The use of elemental fluorine at elevated temperature is the only known method of economically producing PuF_6. Los Alamos researchers evaluated

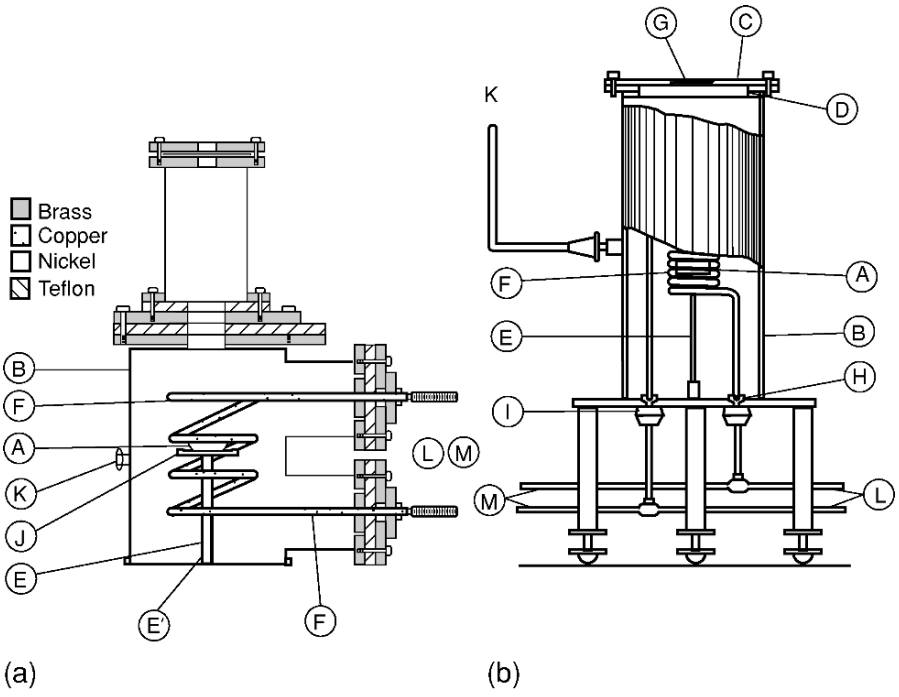

Fig. 7.104 *Two fluorination reactors for the preparation of plutonium hexafluoride. (a) The reactor used by Florin, Tannenbaum and Lemons, and (b) the reactor used by Weinstock and Malm. The legend for both reactors is as follows: A, nickel dish filled with PuF_4; B, brass reactor can; C, removable cover for loading the reactor; D, tongue and groove Teflon gasket for closure; E, nickel supporting rod for nickel dish; E', nickel supporting tube; F, copper tubing induction coil that also serves as cooling coil; G, Fluorothene window; H, Teflon seal and insulator; I, Micalox insulator; J, support for nickel dish; K, connecting line to fluorine source, storage vessels and pumping systems; L, RF connection; M, liquid nitrogen circulation.*

the use of alternative oxidation fluorinating agents that proved capable of producing PuF_6 at or below room temperature (Eller *et al.*, 1992). Plutonium tetrafluoride, oxide, and oxyfluorides are all readily converted to PuF_6 by reaction with gaseous dioxygen difluoride O_2F_2 or O_2F_2/HF solutions at or below room temperature (Malm *et al.*, 1984; Erilov *et al.*, 2002). In a similar fashion, gaseous krypton difluoride, KrF_2 will also produce PuF_6 at ambient or low temperatures (Asprey *et al.*, 1986). The ability of both O_2F_2 and KrF_2 to volatilize plutonium at ambient temperature at moderate rates could have practical applications for recovery of plutonium as volatile PuF_6 from solid wastes.

Plutonium hexafluoride, when rigorously freed from traces of hydrogen fluoride, can be handled in glass equipment. Samples of PuF_6 can be purified by trap-to-trap distillation at cryogenic temperatures to remove HF, F_2, and other impurities. The handling and manipulation of PuF_6 is a very hazardous operation. A broken container means the spreading of hazardous plutonium through the air by the volatile and hydrolytically reactive hexafluoride. An actual multigram release of plutonium from a ruptured container has occurred and has been described by Trevorrow *et al.* (1965). Kessie and Ramaswami (1965) have described methods to prevent the spread of PuF_6 vapor through the ventilation system by operating the vacuum line containing the compound in a moist atmosphere. This hydrolyzes any escaped PuF_6 and converts it to PuO_2F_2, which is a filterable solid.

The rate of formation of plutonium hexafluoride by fluorination of the dioxide and the tetrafluoride was studied by Steindler (1963), who derived activation energies between 43.5 and 52.3 kJ mol^{-1}. These activation energies were found to be greater, the smaller the specific surface area. In the case of a PuF_4 sample having a bulk density of 1.3 g cm^{-3}, the rate of reaction with fluorine was found to follow the relationship

$$\log_{10}(\text{rate/mg PuF}_4\ \text{cm}^{-2}\text{h}^{-1}) = 5.917 - 2719/T \qquad (7.59)$$

The dependence of the reaction rate on the F_2 partial pressure is shown in Fig. 7.105 (Steindler, 1963).

(*ii*) *Solid-state structures*

Crystallographic data for plutonium halide and oxyhalide compounds are given in Table 7.42.

PuF_3. Plutonium trifluoride crystallizes in hexagonal (trigonal) symmetry and adopts the LaF_3 (tysonite) structure. Zachariasen (1949d) indexed the powder pattern based on hexagonal symmetry in space group $P6_3/mmc$. Subsequent work has shown that the tysonite structure has the larger trigonal cell ($P\bar{3}c1$), where $a_0 = a_0'/\sqrt{3}$ (Cheetham *et al.*, 1976). The polymeric structure is complicated, but the simple description is that each plutonium atom is surrounded by nine fluorine atoms, and the plutonium atoms lie on a two-fold axis of symmetry.

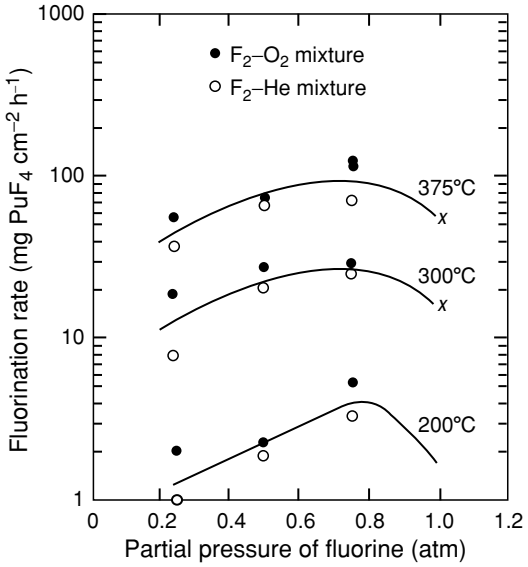

Fig. 7.105 *Fluorination of PuF_4 by fluorine diluted with He/O_2 mixtures to produce PuF_6* (*Steindler,* 1963).

PuF_4. Plutonium tetrafluoride has the ZrF_4 structure and is isostructural with all the lanthanide and actinide tetrafluorides (Wells, 1984). It possesses monoclinic symmetry, space group C2/*c*, with 12 molecules per unit cell (Zachariasen, 1949d). The basic repeating unit contains five plutonium atoms arranged in a distorted pyramid with four plutonium atoms forming a distorted base, and the fifth occupying the apex of the pyramid. Both types of nonequivalent plutonium atom are surrounded by eight fluorine atoms forming a slightly distorted square antiprism that shares vertices with eight other antiprisms. The local PuF_8 pseudo-antiprismatic coordination geometry in PuF_4 is illustrated in Fig. 7.106.

PuF_6. The solid-state structure of PuF_6 was determined by XRD by Florin and coworkers (Florin *et al.*, 1956). Crystalline PuF_6 possesses orthorhombic symmetry with four molecules per unit cell, with Pu–F distances spanning a range from 2.01 to 2.13 Å. The individual PuF_6 molecules in the crystal do not exhibit perfect octahedral symmetry, but spectroscopic studies clearly show that the compound retains octahedral symmetry in the gas phase (see below).

(*iii*) *Properties*

The plutonium trihalides have a small but finite volatility at elevated temperatures. Phipps *et al.* (1949, 1950a) were the first to measure the vapor pressures of the trihalides PuX_3, where X = F, Cl, and Br. In the case of PuF_3, the results are

Table 7.42 *Some physical constants and X-ray crystal structure data for plutonium halides and oxyhalides.*

Compound	*Color*	*Symmetry*	*Space group*	*Lattice parameters*			*Density* (g cm^{-3})	*References*
				a_0 (Å)	b_0 (Å)	c_0 (Å)		
PuF_3	violet-blue	trigonal	$P\bar{3}c1$[a]	7.092		7.254(1)	9.32	Zachariasen (1949d)
PuF_4	pale brown	monoclinic	$C2/c$[b]	12.59(3)	10.69(2)	8.29(4)	7.04	Keenan and Asprey (1969)
$PuF_4{\cdot}2.5H_2O$	pink	orthorhombic	*Pnam*	12.66(3)	11.03(5)	6.99(5)	4.89	Dawson *et al.* (1954a)
PuF_6	reddish brown	orthorhombic	*Pnma*[c]	9.888(9)	8.961(8)	5.203(5)	5.085	Florin *et al.* (1956)
$PuCl_3$	emerald green	hexagonal	$P6_3/m$	7.394(1)		4.243(1)	5.708	Burns *et al.* (1975)
$PuBr_3$	green	orthorhombic	*Cmcm*[d]	4.097(8)	12.617(10)	9.147(10)	6.71	Brown and Edwards (1972)
$PuBr_3{\cdot}6H_2O$	blue	monoclinic	$P2/n$[e]	10.022(5)	6.798(3)	8.181(4)		Brown *et al.* (1968)
PuI_3	bright green	orthorhombic	*Cmcm*[d]	4.326(6)	13.962(20)	9.974(20)	6.92	Brown and Edwards (1972)
PuOF	metallic	tetragonal	*P4/nmm*	4.05(1)		5.71(1)	8.20	Zachariasen (1951)
PuOCl	blue-green	tetragonal	*P4/nmm*	4.012(2)		6.792(10)	8.82	Zachariasen (1949d)
PuOBr	dark green	tetragonal	*P4/nmm*	4.022(4)		7.571(11)	9.08	Zachariasen (1949d)
PuOI	green	tetragonal	*P4/nmm*	4.042(2)		9.169(15)	8.47	Zachariasen (1949d)
PuO_2F_2	white	rhombohedral	$R\bar{3}m$	4.154		15.84	6.50	Wyckoff (1963)
$PuOF_4$	chocolate brown	trigonal	*R3m*	12.90(2)		5.56(2)		Burns and O'Donnell (1977)

[a] Originally reported by Zachariasen in hexagonal space group $P6_3/mmc$. The hexagonal LaF_3 (tysonite) has trigonal space group $P\bar{3}c1$, which is the likely space group for PuF_3. To transform from $P6_3/mmc$ to $P\bar{3}c1$, one would use $a_0 = a'\sqrt{3}$ to derive $a_0 = 7.092$ (Å), which is the value reported above.
[b] $\beta = 126.0(2)$.
[c] Lattice constants refined from original data by Roof (1989).
[d] Original space group *Ccmm*, changed to standard setting *Cmcm* by Roof (1989).
[e] $\beta = 92.97(3)$.

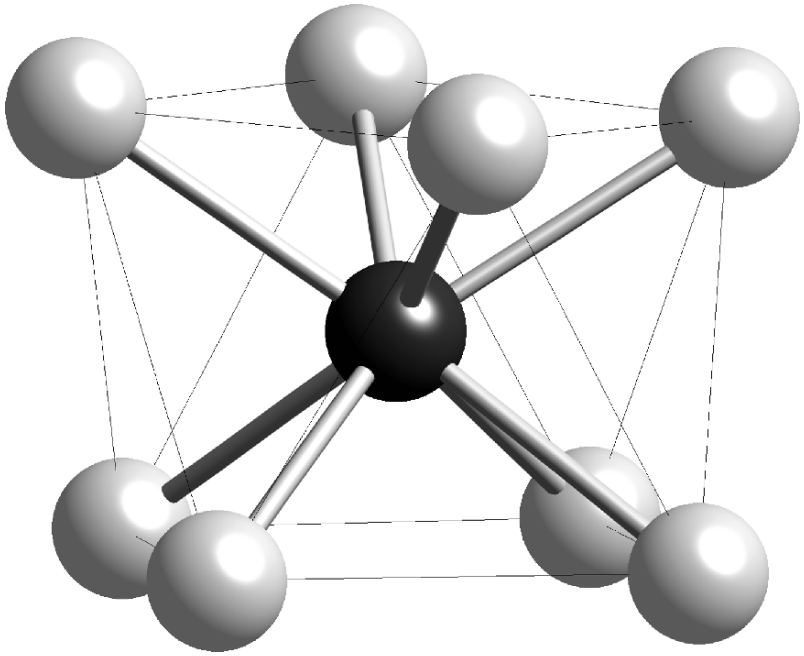

Fig. 7.106 *A view of the local coordination geometry of PuF_4 that emphasizes the local PuF_8 pseudo-antiprismatic coordination environment. The plutonium atoms are black and fluorine atoms gray.*

somewhat conflicting. In the work of Phipps *et al.* (1949, 1950a), an apparent inflection in the vapor–pressure curve implied an improbably low value for the melting point of 1447 K. A direct measurement by Westrum and Wallmann (1951) yielded values of (1698 ± 2) K for the melting point and (1699 ± 2) K for the solidification point, leading these authors to a different interpretation of the data and thus to a vapor–pressure equation that was different from the equation(s) given by Phipps *et al.* (1949, 1950a). Carniglia and coworkers (Carniglia, 1953; Carniglia and Cunningham, 1955) also measured the PuF_3 vapor pressure. Their data, agreed in general with the results of Phipps *et al.* (1949, 1950a), but the calculated enthalpies and entropies are both somewhat smaller. Kent (1968) reinvestigated the PuF_3 vapor pressure in the range 1243–1475 K by evaporating a mixture of PuF_3 and plutonium metal from a tantalum Knudsen cell attached to a mass spectrometer. He observed the species PuF_2^+, PuF^+, and Pu^+, but very little PuF_3^+. Kent used these data to obtain several important thermodynamic quantities, and have been reviewed by Lemire *et al.* (see Table 7.43).

The vapor pressure of PuF_4 has been measured by Mandleberg and Davies (1954, 1961), Chudinov and Choporov (1970), and Berger and Gäumann

(1961). Rand (1966) and Lemire *et al.* (2001) critically assessed these data. They prefer the results of Chudinov and Choporov to the data reported by the two other groups of authors. Chudinov and Choporov used a modified Knudsen method employing a nickel effusion cell, which is not attacked by fluorides. Rand discounts the measurements reported by Mandleberg and Davies because the tantalum effusion cell used by these authors would have reduced PuF_4 to PuF_3. On the basis of the known instability of PuF_5, there is also reason to believe that the disproportionation of PuF_4 into PuF_3 and PuF_5 postulated by Mandleberg and Davies is unlikely to occur, because the calculated pressure of PuF_6 in equilibrium with PuF_4 at 1200 K is 10^{-11} Torr, and because PuF_5 is less stable than PuF_6. The data of Berger and Gäumann (1961) yield too small an entropy change for a sublimation process, suggesting some reduction in their platinum effusion vessel. Another serious objection to these results is the implication that PuF_4 appears to be less volatile than UF_4, something that is not consistent with general trends in vapor pressures of other actinide halides.

In the case of $PuCl_3$ and $PuBr_3$, the only measurements reported are those by Phipps *et al.* (1949, 1950a) and, for $PuCl_3$, those by Weinstock (1944). No other recent measurements are reported. The vapor–pressure equations for PuI_3 were reported by Katz and Sheft (1960).

A detailed assessment and review of the important thermodynamic quantities such as the enthalpy of formation, standard entropy, heat capacity, and fusion data have been given by Lemire *et al.* (2001). Selected thermodynamic constants are given in Table 7.43.

Plutonium hexafluoride is a low-melting, highly volatile solid, whose vapor has the brown color of nitrogen dioxide, and which melts to a deep brown, transparent liquid. The following melting points have been reported: 325 K (52°C), 327 K (54°C), 323.7 K (50.5°C), and 324.74 K (51.59°C), the most-accurate value being the last, measured at $p = 533$ Torr. The boiling point was reported as 335.3 K (62.15°C).

The vapor pressure of PuF_6 has been measured by several authors (Hurst *et al.*, 1953; Mandleberg *et al.*, 1953, 1956; Florin *et al.*, 1956 Adams *et al.*, 1957). The most careful determination and description is that of Weinstock *et al.* (1959), who fit their data to a three-term function of temperature to derive a number of important thermochemical properties. A refit of their data by Lemire *et al.* (2001) gives $\Delta_{\text{subl}}H^\circ = (48.65 \pm 1.00)$ kJ mol^{-1} and $\Delta_f H^\circ = -(1861.35 \pm 20.17)$ kJ mol^{-1}.

Additional thermodynamic data for PuF_6 have been assessed and compiled by Rand (1966), Fuger *et al.* (1983), and Lemire *et al.* (2001). Thermodynamic data calculated from spectroscopic measurements were reported by Sundaram (1962), Nagarajan (1962), and Hawkins *et al.* (1954).

The PuF_6 molecule has 15 fundamental modes of vibration. These vibrations fall into two groups according to their predominant Pu–F stretching (ν_1, ν_2, ν_3) or bending (ν_4, ν_5, ν_6) modes. The symmetries of these modes indicate that ν_3, ν_4, ν_5, and ν_6 are all triply degenerate, ν_2 doubly degenerate, and ν_1 nondegenerate.

Table 7.43 *Thermodynamic parameters for plutonium halides* (*Lemire* et al., 2001).

Compound	$\Delta_f G^\circ_{298}$ (kJ mol^{-1})	$\Delta_f H^\circ_{298}$ (kJ mol^{-1})	S°_{298} (J K^{-1} mol^{-1})	C°_{p298} (J K^{-1} mol^{-1})[a]
Solids				
PuF_3 (cr)	−1517.4 ± 3.7	−1586.7 ± 3.7	126.1 ± 0.4	92.6 ± 0.3
PuF_4 (cr)	−1756.7 ± 20.0	−1850 ± 20	147.3 ± 0.4	116.2 ± 0.3
PuF_6 (cr)	−1729.9 ± 20.2	−1861.3 ± 20.2	221.8 ± 1.1	168.1 ± 2.0
PuOF (cr)	−1091.6 ± 20.2	−1140 ± 20	96 ± 10	69.4 ± 10
$PuCl_3$ (cr)	−891.8 ± 2.0	−959.6 ± 1.8	161.7 ± 3.0	101.2 ± 4.0
$PuCl_4$ (cr)	−879.4 ± 5.8	−968.7 ± 5.0	201 ± 10	121.4 ± 4.0
$PuBr_3$ (cr)	−767.3 ± 2.7	−792.6 ± 2.0	198 ± 6	101.8 ± 6.0
PuOBr (cr)	−838.4 ± 8.5	−870 ± 8	127 ± 10	73 ± 8
PuI_3 (cr)	−579 ± 4.5	−579.2 ± 2.8	228 ± 12	110 ± 8
PuOI (cr)	−776.6 ± 20.5	−802 ± 20	130 ± 15	75.6 ± 10.0
Cs_2PuCl_6 (cr)	−1838.2 ± 6.7	−1982 ± 5	412 ± 15	
Cs_3PuCl_6 (cr)	−2208.0 ± 9.5	−2364.4 ± 9.0	545.9 ± 11.0	258.6 ± 10.0
$CsPu_2Cl_7$ (cr)	−2235.1 ± 5.3	−2399.4 ± 5.7	424 ± 7.3	254.9 ± 10.0
Cs_2PuBr_6 (cr)	−1636.3 ± 6.1	−1697.4 ± 4.2	470 ± 15	
$Cs_2NaPuCl_6$ (cr)	−2143.5 ± 5.2	−2294.2 ± 2.6	440 ± 15	
Gases				
PuF (g)	−141 ± 10.1	−112.6 ± 10.0	251 ± 5	33.5 ± 3.0
PuF_2 (g)	−626.1 ± 6.7	−614.3 ± 6.0	297 ± 10	51.5 ± 5.0
PuF_3 (g)	−1161.1 ± 4.8	−1167.8 ± 3.7	336.1 ± 10.0	72.2 ± 5.0
PuF_4 (g)	−1517.9 ± 22.2	−1548 ± 22	359 ± 10	92.4 ± 5.0
PuF_6 (g)	−1725.1 ± 20.1	−1812.7 ± 20.1	368.9 ± 1.0	129.3 ± 1.0
$PuCl_3$ (g)	−641.3 ± 3.6	−647.4 ± 2.0	368.6 ± 10.0	78.5 ± 5.0
$PuCl_4$ (g)	−764.7 ± 10.4	−792 ± 10	409 ± 10	103.4 ± 5.0
$PuBr_3$ (g)	−529.8 ± 15.7	−488 ± 15	423 ± 15	81.6 ± 10.0
PuI_3 (g)	−366.5 ± 15.7	−305 ± 15	435 ± 15	82 ± 5

[a] Temperature coefficients of this function are tabulated by Lemire *et al.* (2001) in their Table 4.3.

Only ν_3 (stretching) and ν_4 (bending) are infrared active. The first comprehensive gas-phase absorption spectrum covering 4,000–20,000 cm^{-1} was reported by Steindler and Gunther in 1964 (Steindler and Gunther, 1964a,b). The observed spectrum is shown in Fig. 7.107. These measurements were refined in the wavelength region between 3000 and 9000 cm^{-1} by Walters and Briesmeister (1984) using a very long pathlength cell. In both of these early studies, the spectrometers gave spectral resolutions of several wavenumbers so that vibrational components of the spectra were not resolved. Kugel *et al.* (1976) studied PuF_6 at much higher resolution using an intracavity laser quenching technique. Analysis of the room-temperature absorption spectrum is rendered difficult by the clustering of electronic transitions as well as number of hot bands that result from the low-energy bending vibrations (ν_4, ν_5, ν_6). In a low-temperature matrix, the elimination of rotations and hot bands greatly simplifies the spectral analysis. Dewey *et al.* (1986) studied the absorption and emission of matrix-isolated PuF_6 at 8 K and were able to assign transitions below 17,000 cm^{-1}. From these data, all the vibrational frequencies have been determined from the fundamental or combination bands, and they are compiled in Table 7.44 (Dewey *et al.*, 1986).

Kim and coworkers studied the fine structure in the vibronic band near 800 nm, resolving Coriolis fine structure at the Doppler-limited resolution (Kim *et al.*, 1987). Finally, David and Kim (1988) reported the entire absorption spectrum of PuF_6 in the near IR and visible regions at high sensitivity and high resolution. They measured isotope shifts between $^{239}PuF_6$ and $^{242}PuF_6$ to identify the specific vibrational modes. The Raman spectrum of PuF_6 has not yet been observed, because of the rapid photochemical decomposition at 5641 Å (Hawkins *et al.*, 1954).

The magnetic susceptibility of plutonium hexafluoride was measured at several temperatures by Gruen *et al.* (1956). Molar susceptibilities of 131×10^{-6} cgs units at 81 K and of 173×10^{-6} cgs units at 131 K were observed. Gruen *et al.* indicated that, based on the small susceptibilities observed compared with the susceptibility of isoelectronic compounds of U(IV), Np(V), and PuO_2^{2+}, which show larger, strongly temperature-dependent values, the ground electronic state of plutonium hexafluoride is nondegenerate (see Section 7.9.3). Furthermore, the first excited state of plutonium hexafluoride must be at least 1000 cm^{-1} (0.12 eV) above the ground state, which means that there is a much greater splitting than required for the isoelectronic U(IV) compounds.

Florin *et al.* (1956) studied the equilibrium system

$$PuF_6(g) \rightleftharpoons PuF_4(s) + F_2(g) \tag{7.60}$$

and obtained the equilibrium constant in the range 160–600°C. Their data showed a significant break at 308°C, suggesting a phase change. Weinstock and coworkers (Malm and Weinstock, 1954; Weinstock and Malm, 1956a) reported a measurement of the equilibrium constant at 220°C. Trevorrow and coworkers (Trevorrow and Shinn, 1960; Trevorrow *et al.*, 1961) reexamined this system and made a careful determination of the equilibrium constant in the

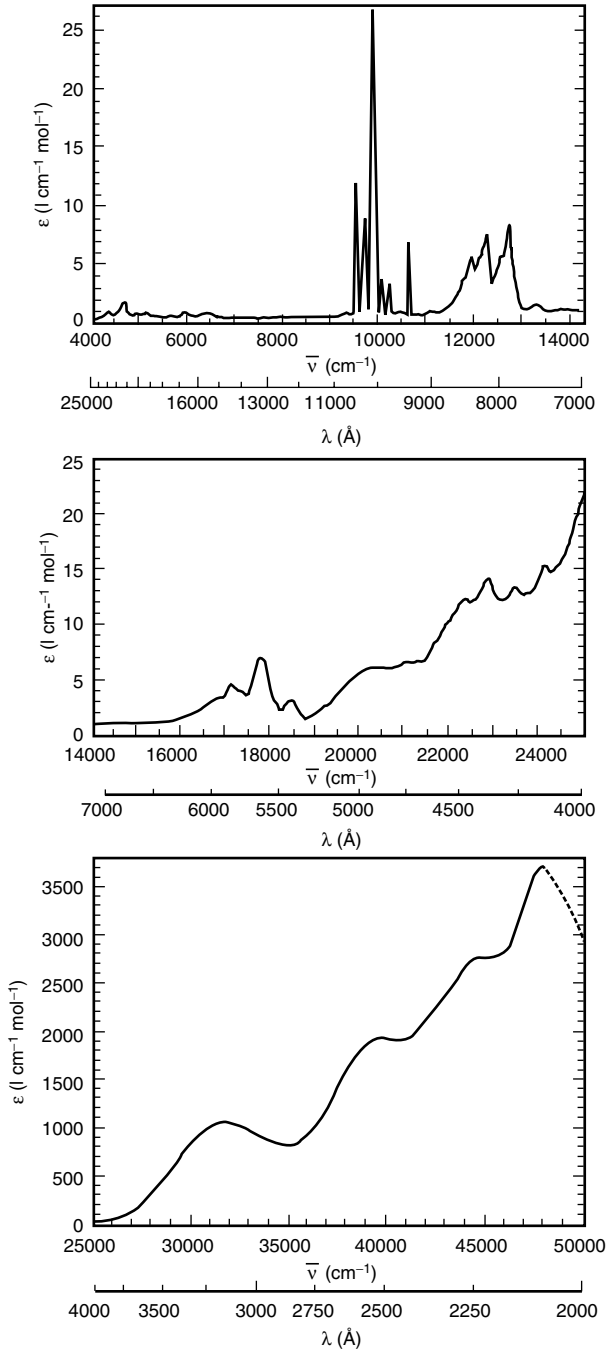

Fig. 7.107 *The absorption spectrum of gaseous PuF_6 from Steindler and Gunther* (1964*a*).

Table 7.44 *Vibrational frequencies of the PuF_6 molecule.*

Mode	*Matrix frequency* (cm^{-1})[a]	*Gas phase frequency* (cm^{-1})[b]
ν_1	(625)	(628)
ν_2	(519)	(523)
ν_3	612	616
ν_4	200[b]	(203)
ν_5	(209)	(211)
ν_6	(177)	(173)
$\nu_1 + \nu_3$	1236	1244
$\nu_2 + \nu_3$	1130	1139
$\nu_3 + \nu_5$	821	827
$\nu_1 + \nu_4$	–	831
$\nu_2 + \nu_4$	–	726
$\nu_4 + \nu_5$	–	414
$\nu_2 + \nu_6$	696	696

[a] From matrix isolation experiments by Dewey *et al.* (1986).
[b] From fluorescence measurements by Weinstock and Goodman (1965).

temperature range 150–400°C. Fig. 7.108 shows a plot of the log of the equilibrium constant K_p versus inverse temperature using the data of various authors (Florin *et al.*, 1956; Trevorrow and Shinn, 1960; Trevorrow *et al.*, 1961). Trevorrow and Shinn (1960) measured the equilibrium constant of the reverse reaction in the temperature range 170–395 K. This equilibrium has been measured at high pressures of fluorine (up to 825 bar) (Steindler *et al.*, 1958) and found to be pressure-independent. The free energy of the reaction

$$PuF_4(s) + F_2(g) \rightarrow PuF_6(g) \tag{7.61}$$

can be calculated from the equation

$$\Delta G^\circ = -RT\ \ln K = 2.55 \times 10^4 + 5.27T(\mathrm{K})\mathrm{J\ mol^{-1}} \tag{7.62}$$

The calculated value of ΔG° at 275°C is (28.36 ± 0.38) kJ mol^{-1}. The mean value of ΔH° for the reaction is (25.48 ± 0.59) kJ mol^{-1} and the mean value of ΔS° for the reaction is $-(5.44 \pm 0.84)$ J K^{-1} mol^{-1}.

Radiation decomposition

The α radioactivity of ^{239}Pu (Table 7.l) causes a continuous decomposition of PuF_6 (Steindler *et al.*, 1963; Wagner *et al.*, 1965). As the emitted α particle travels through the crystal lattice, bonds are ruptured and decomposition of PuF_6 to F_2 and lower plutonium fluorides occurs. The observed rate of decomposition (Gruen *et al.*, 1956) of gaseous PuF_6 is not a linear function of time but decreases with time from 1.78 to 0.064% of the initial PuF_6 (100 Torr) per day in the range from 0.5 to 571 days at 26°C. The initial high decomposition rate of 1.78% per day may be partly attributed to the reaction of the PuF_6 with the

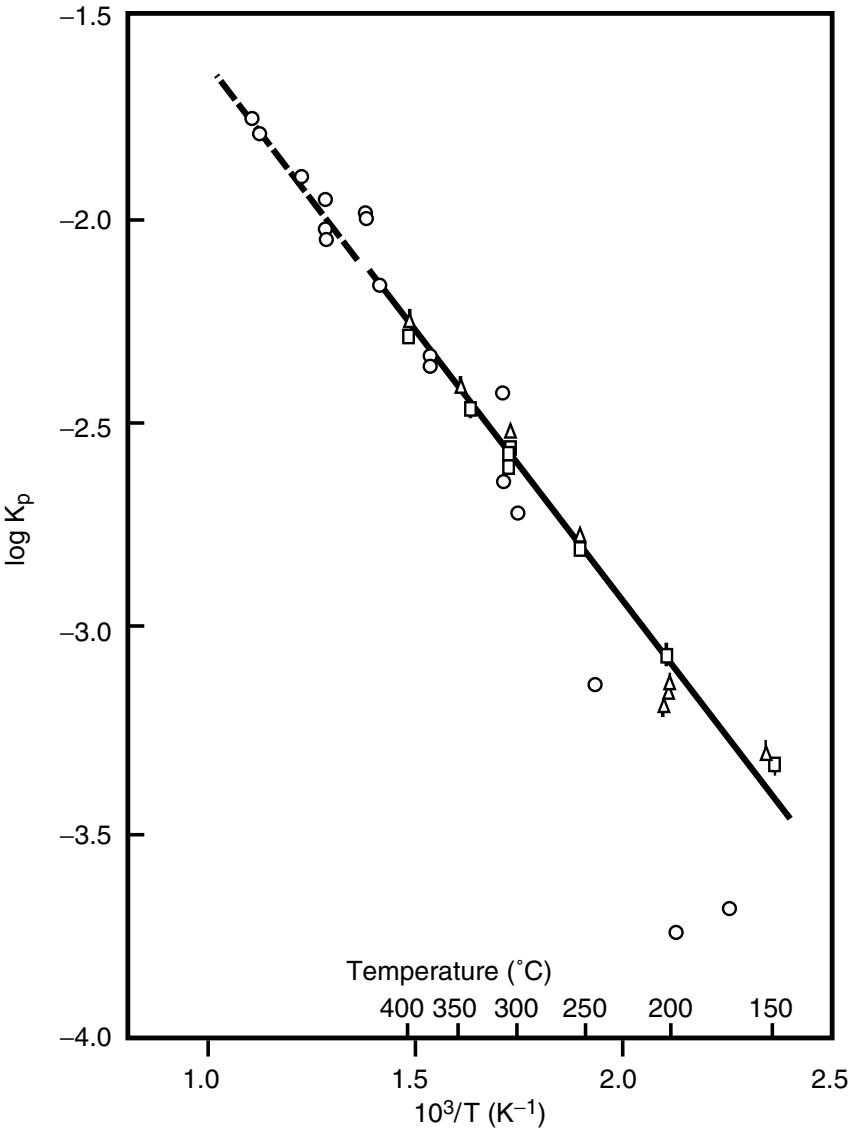

Fig. 7.108 *The relationship between the equilibrium constant and temperature for reaction* 7.60 (*Trevorrow and Shinn,* 1960). *Open circles are data from Florin* et al. (1956), *triangles are from Trevorrow* et al. *with heating to equilibrium, and squares are from Trevorrow* et al. *with cooling to equilibrium* (*Trevorrow* et al., 1961).

container material. If the pressure of the PuF_6 is lowered from 100 to 50 Torr, a lower decomposition rate is observed. Malm measured surprisingly low gas pressure in decades-old, sealed PuF_6 cylinders at ANL, and it was believed to be the result of recombination, probably involving F atoms (Morss, 2005).

Increase of the temperature introduces some thermal decomposition besides radiation decomposition. Observed rates after 77 days were $(0.64 \pm 0.66)\%$ per day at 82°C, but only $(0.18 \pm 0.03)\%$ per day at 26°C. Other factors influencing the decomposition of PuF_6 include the initial pressure and presence or absence of PuF_4, and presence or absence and partial pressure of He, Kr, O_2, N_2, or F_2. The exact mechanism of PuF_6 decomposition is still not completely known.

Steindler *et al.* (1963) studied the decomposition of PuF_6 under the influence of γ radiation. This is important because of the possible use of PuF_6 in the fluoride volatility process (see Section 7.5.7(c)). It was observed that PuF_6, if exposed to fission-product radiation, decomposes to form PuF_4 and F_2 with a *G*-value of (7.5 ± 1.7). Addition of 1 atm of He does not significantly change the *G*-value (number of molecules decomposed per 100 eV of radiation absorbed). Krypton, on the other hand, causes a marked enhancement of PuF_6 decomposition by γ radiation. The *G*-value observed in the presence of F_2 or O_2 is less than that observed with pure PuF_6. On the other hand, irradiation of mixtures of $PuF_4 + F_2$ produced larger quantities of PuF_6 than those calculated from the thermodynamic equilibrium constant at the temperature of the irradiation.

Because of the decomposition of PuF_6 by its own α radiation, the compound is best stored in the gaseous state under reduced pressure.

Chemical properties

Because plutonium hexafluoride tends to decompose into PuF_4 and F_2, it is a highly reactive fluorinating agent. The majority of its chemical properties are due to this reactivity.

(b) Plutonium chlorides, bromides, and iodides

In the plutonium–chlorine system, the only stable solid compound is $PuCl_3$, which has been prepared and characterized in large quantities. The only stable higher valent chloride is $PuCl_4$, which is not stable as a solid, and only known as a gaseous species that decomposes upon condensation. For the plutonium–bromine and plutonium–iodine systems, the only stable binary compounds are the trihalides, $PuBr_3$ and PuI_3.

(*i*) *Preparation*

Plutonium trichloride

This was one of the first plutonium compounds to have been prepared and characterized in detail following the initial discovery of the element (Abraham *et al.*, 1949a). Abraham *et al.* (1949a) and Garner (1950) have provided detailed

discussions on the fundamental methods for its preparation. Of the various preparative methods, the hydrochlorination of plutonium(III) oxalate hydrate was found to work best on medium-scale reactions (1–10 g) according to the general reaction:

$$Pu_2(C_2O_4)_3 \cdot 10H_2O + 6HCl \rightarrow 2PuCl_3 + 3CO_2 + 3CO + 13H_2O \qquad (7.63)$$

The direct chlorination of plutonium metal at 303–500°C and subsequent sublimation at 600–800°C yields emerald green crystals of $PuCl_3$ on the 500 mg scale (Baumgärtner *et al.*, 1965). If metallic plutonium in 100 g quantities is available, this may be converted to the hydride, which is then reacted with HCl gas at 450°C in a fluid-bed reaction. The resulting $PuCl_3$ is fused at 800°C and sparged with HCl for 45 min to remove oxychlorides. The molten $PuCl_3$ may be purified by filtering through a fritted silica disk (Bjorklund *et al.*, 1959; Reavis *et al.*, 1960).

Chlorination of PuO_2 with either phosgene or carbon tetrachloride at temperatures above 500°C can produce analytically pure samples of $PuCl_3$ (Tolley, 1953; Boreham *et al.*, 1960). This process has been used at Los Alamos to convert large quantities of PuO_2 to anhydrous $PuCl_3$ (West *et al.*, 1988).

Christensen and Mullens (1952) developed a very straightforward procedure that is applicable in most transuranium chemistry laboratories, in which plutonium(III) oxalate is reacted with hexachloropropene at 180–190°C:

$$Pu_2(C_2O_4)_3 \cdot 10H_2O + 3C_3Cl_6 \rightarrow 2PuCl_3 + 3C_3Cl_4O + 3CO_2 + 3CO + 10H_2O \qquad (7.64)$$

The oxalate is refluxed with excess hexachloropropene for 18 h, yielding $PuCl_3$ of 96–98% purity, which is separated by filtration and further purified by sublimation. The method has been applied for preparations on the 100 g scale.

A method for continuous production of 98% $PuCl_3$ at a rate of 250 g h^{-1} was reported by Rasmussen and Hopkins (1961). In this process, $Pu(C_2O_4)_2 \cdot 6H_2O$ is first precipitated from Pu(IV) solution, dried on a filter drum, and calcined to reactive PuO_2. The PuO_2 is chlorinated to $PuCl_3$ with phosgene in a vibrating Hastelloy tube furnace at 500°C.

Plutonium(III) chloride, which is obtained by evaporation of a plutonium(III) solution in HCl, followed by dehydration of the $PuCl_3 \cdot 6H_2O$ residue in a stream of HCl, is a slate-blue solid. $PuCl_3$ prepared by one of the anhydrous methods is a blue-green solid or an emerald green, fine crystalline powder. Emerald green single crystals are obtained by condensation from the vapor phase (Burns *et al.*, 1975). As for other lanthanide and actinide trihalides, sublimation in evacuated, sealed quartz tubes is advisable for purification of $PuCl_3$ (Fuger and Cunningham, 1963).

Plutonium tetrachloride

As early as 1945, Brewer *et al.* (1949) predicted that no solid binary plutonium(IV) chloride should exist. However, from their calculations, the possible existence of

gaseous $PuCl_4$ in an atmosphere of Cl_2 over $PuCl_3$ was inferred. Abraham *et al.* (1949a) were the first to observe an enhanced volatility of $PuCl_3$ in a stream of chlorine. This increase in volatility was ascribed to the formation of $PuCl_4$ by the equilibrium

$$PuCl_3 + 0.5\,Cl_2 \rightleftharpoons PuCl_4 \tag{7.65}$$

The $PuCl_4$ gas, on condensation, decomposes again to form solid $PuCl_3$ and Cl_2 gas. Abraham *et al.* (1949a) made the first calculations of the $PuCl_4$ partial pressure over $PuCl_3$ in an atmosphere of Cl_2 and predicted values in the range 10^{-5} mmHg at 500°C to 0.3 mmHg at 800°C. Benz (1962) employed a transpiration technique to determine the equilibrium constant and free energy for the above reaction.

Gruen and deKock (1967) measured the absorption spectrum of the gas phase over solid $PuCl_3$ in 1 atm of Cl_2. The absorption spectrum observed at 928°C is shown in Fig. 7.109, and shows unequivocally the presence of a new species, which is different from Cl_2 and $PuCl_3$. This spectrum is regarded as proof of the existence of gaseous $PuCl_4$.

Even though solid $PuCl_4$ has never been prepared, a number of tetravalent chloro complexes derived from $PuCl_4$, such as Cs_2PuCl_6, have been obtained, and are stable.

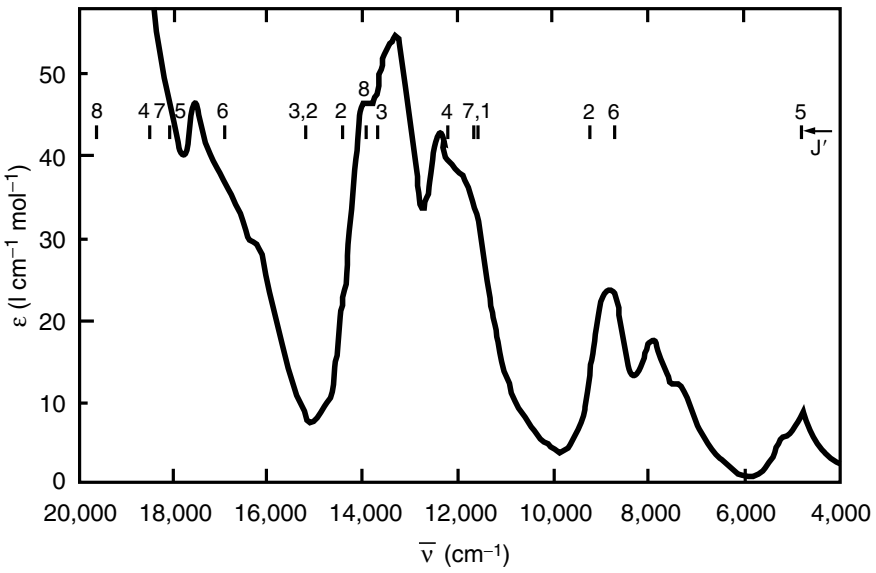

Fig. 7.109 *The absorption spectrum of gaseous $PuCl_4$ at* 928°C (*Gruen and deKock*, 1967).

Plutonium tribromide

This compound was first prepared by Hyde *et al.* (1944), and is a light-green solid. The methods for the preparation of $PuBr_3$ have been summarized by Bluestein and Garner (1944) and by Davidson *et al.* (1949). The two best methods for the preparation of $PuBr_3$ are the direct synthesis from the elements (Davidson *et al.*, 1949; Gruen and deKock, 1967), and the hydrobromination of the hydride at 600°C in a stream of HBr (Reavis *et al.*, 1960).

$$2Pu + 3Br_2 \rightarrow 2PuBr_3 \tag{7.66}$$

$$PuH_x + xHBr \xrightarrow{600°C} PuBr_3 + xH_2 \tag{7.67}$$

Other satisfactory methods for the preparation of $PuBr_3$ include the dehydration of $PuBr_3 \cdot 6H_2O$ by controlled vacuum thermal decomposition (Brown *et al.*, 1968) and the hydrobromination of plutonium(III) oxalate at 400–600°C (Bluestein and Garner, 1944; Davidson *et al.*, 1949; Weigel *et al.*, 1982), either with pure HBr (Bluestein and Garner, 1944; Davidson *et al.*, 1949) or an HBr/H_2 mixture (Weigel *et al.*, 1982). These methods have the advantage that they do not require plutonium metal as the starting material, but make use of starting materials such as $Pu_2(C_2O_4)_3 \cdot 10H_2O$, which can be prepared from aqueous solutions (see Section 7.9.1.e.(i)).

Another method involves bromination of $Pu(OH)_4$ (dried at 70°C). This reaction proceeds satisfactorily above 600°C with HBr gas (Davidson *et al.*, 1949; Fomin *et al.*, 1958), and at 800°C with bromine and sulfur dibromide (Davidson *et al.*, 1949; Davidson and Katz, 1958). Plutonium(IV) oxalate or the tribromide hexahydrate react with HBr at 500°C and at 30–300°C, respectively, but the product of the latter reaction is usually contaminated with PuOBr. NH_4Br addition minimizes the PuOBr formation. Finally, one may convert $PuCl_3$ with HBr at 750°C (Davidson *et al.*, 1949; Bonnelle, 1976) and react PuO_2 mixed with carbon, sulfur, or phosphorus with Br_2 at elevated temperatures. Plutonium tribromide is a light green solid.

Plutonium triodide

The first attempts to prepare this compound were made by Hagemann *et al.* (1949). After initial failures, in which the oxyiodide was the reaction product, they finally succeeded in preparing PuI_3 by reacting plutonium metal with HI at 400°C. A more straightforward approach is the redox transmetallation reaction between plutonium metal and mercuric iodide, according to the reaction:

$$2Pu + 3HgI_2 \rightarrow 2PuI_3 + 3Hg \tag{7.68}$$

The plutonium metal and HgI_2 are sealed in a silica tube, and heated for 2 hours at 500°C (Asprey *et al.*, 1964). The mercury byproduct is conveniently separated by distillation away from the product. PuI_3 is extremely sensitive to moisture. Its properties have not been well characterized.

(*ii*) *Solid-state structures*

Crystallographic data on plutonium halides are summarized in Table 7.42.

$PuCl_3$. The crystal structure of $PuCl_3$ was first determined by Zachariasen (1948a) and later refined by Burns *et al.* (1975). Plutonium(III) chloride crystallizes in the hexagonal UCl_3 structure with two formula units per cell. Each plutonium atom has nine-fold coordination with a local tricapped trigonal prismatic coordination environment. Six chlorine atoms form a trigonal prism with Pu–Cl bonds of 2.886(1) Å, and the other three chlorine atoms cap the rectangular faces with Pu–Cl distances of 2.919 (1) Å (Burns *et al.*, 1975). The trigonal prisms share their triangular bases to form infinite chains along the crystallographic *c*-axis. These basic structural features are shown in Fig. 7.110.

$PuBr_3$ and PuI_3. Plutonium tribromide and triiodide are isostructural and display an orthorhombic structure known as the $PuBr_3$ structure. The structures

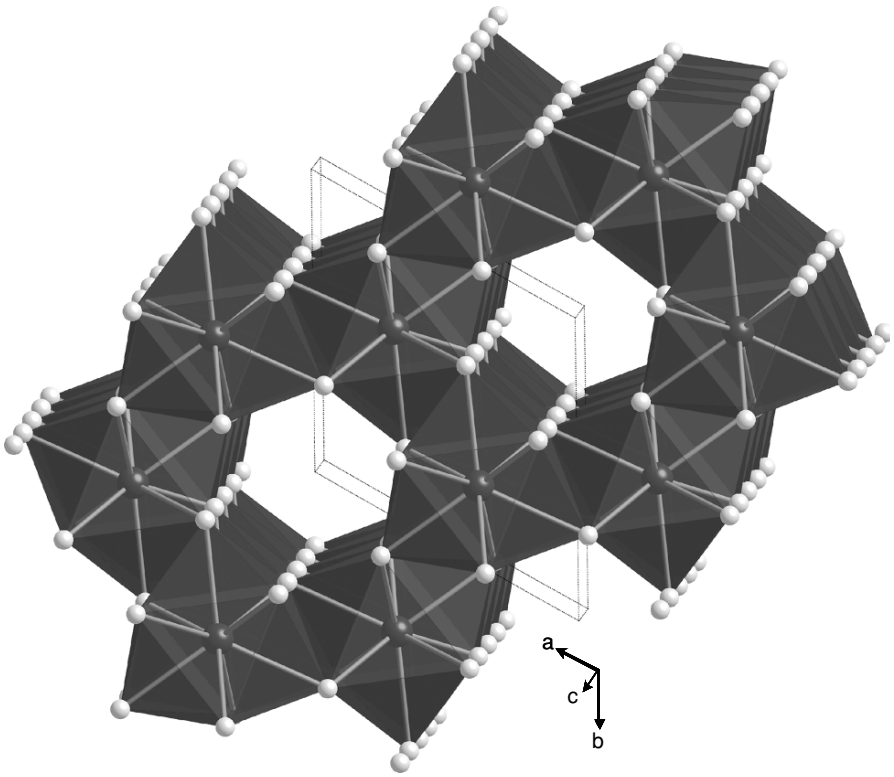

Fig. 7.110 *The solid-state crystal structure of $PuCl_3$ viewed down the c-axis and emphasizing both the hexagonal cell, and the infinite chains of tricapped trigonal prisms. Plutonium atoms are black, and chlorine atoms are light gray.*

of both $PuBr_3$ and PuI_3 were originally determined by Zachariasen (1948a), with subsequent refinements of the iodide reported by Asprey and coworkers (Asprey *et al.*, 1964). For $PuBr_3$, there are six Pu–Br bonds of 3.08 Å that form a trigonal prismatic geometry. There are two additional Pu–Br bonds that cap two of the three rectangular faces with Pu–Br distances of 3.06 Å. As in the $PuCl_3$ structure, these capped trigonal prisms stack in an infinite chain (this time along the *a*-axis) by sharing triangular bases as illustrated in Fig. 7.111. The infinite columns are now separated from each other such that the ninth bromine atom that would complete the tricapped trigonal prism is 4.03 Å away, and outside the bonding radius.

The main difference between the $PuCl_3$ and $PuBr_3$ structures is that in the $PuCl_3$ structure, each plutonium atom is nine-coordinate, while in the $PuBr_3$ structure, each plutonium atom is eight coordinate. This is surprising because the ninth bromine atom in the $PuBr_3$ structure is essentially in the correct position. The change in structure is thought to be due to the larger size of bromine and iodine (Brown, 1968), and the associated electron–electron repulsion between halogen atoms. A comparison of the column stacking between $PuBr_3$ and $PuCl_3$ structures is shown in Fig. 7.112.

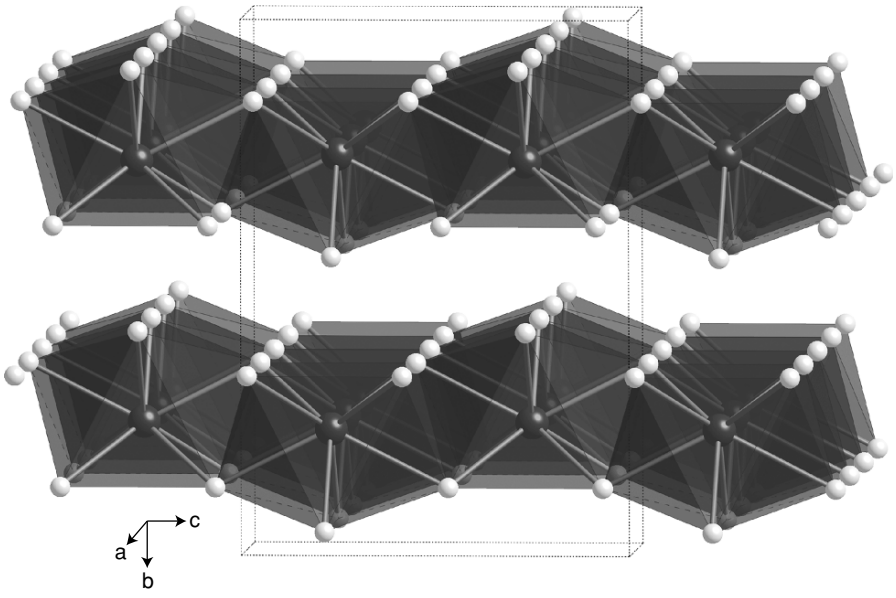

Fig. 7.111 *The solid-state crystal structure of $PuBr_3$ viewed down the a-axis and emphasizing the infinite chains of bicapped trigonal prisms. Plutonium atoms are black, and bromine atoms are light gray.*

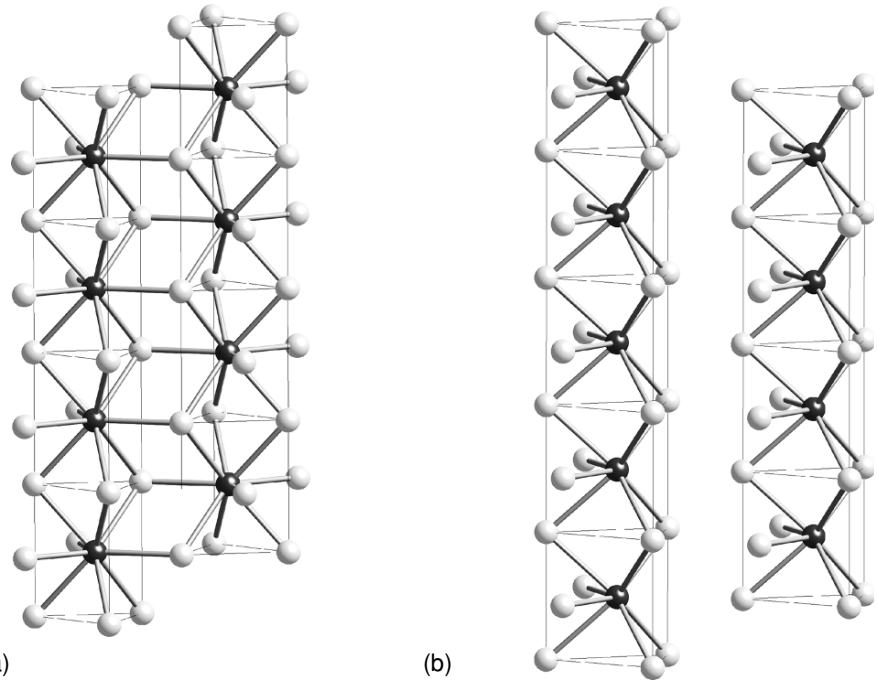

Fig. 7.112 *A comparison of the column stacking of $PuCl_3$ and $PuBr_3$ units.* (*a*) *The column arrangement of $PuCl_3$ units showing how tricapped trigonal prisms are formed by linking adjacent trigonal prismatic columns.* (*b*) *The column arrangement of trigonal prismatic units in the $PuBr_3$ structure, illustrating the vacant coordination site.*

(*iii*) *Properties*

The more important physical properties of plutonium(III) chloride are well known. Thermodynamic data are given in Table 7.43. The enthalpy of formation was first measured by Westrum and Robinson (1949a), then by Fuger and Cunningham (1963) and has been assessed by Fuger *et al*. (1983), and by Lemire *et al.* (2001). The standard free energy of formation as a function of T(K) was determined by Benz (1961), who found the following temperature dependence (958–1014 K):

$$\Delta G = -924.7 + 0.222\ 92T(\text{kJ mol}^{-1}) \tag{7.69}$$

By electromotive force (EMF) measurements in fused PuCl–NaCl, Benz and Leary (1961) found the standard free energy and entropy of formation of pure solid $PuCl_3$ at 700°C to be 711 kJ mol^{-1} and 215.9 J K^{-1} mol^{-1}, respectively. From potentiometric measurements based on the $Pu/PuCl_3$ electrode, the free

energy of formation of solid $PuCl_3$ in the 755–916 K temperature range was found to fit the expression

$$\Delta G = -909.6 + 0.175T(\text{kJ mol}^{-1}) \tag{7.70}$$

The optical properties of solid and gaseous $PuCl_3$ have been studied. Lipis and Pozharskii (1960) measured the absorption spectrum of $PuCl_3$ in the range 340–1000 nm. This spectrum is altered by water of crystallization, but not by absorbed or occluded water.

Conway and coworkers (Lammermann and Conway, 1963; Conway and Rajnak, 1966) measured the absorption spectrum of Pu^{3+} in an anhydrous $LaCl_3$ matrix and calculated the electrostatic, spin–orbit, and configuration-interaction parameters from these data.

The absorption spectrum of gaseous $PuCl_3$ was measured by Gruen and deKock (1967). Its energies and intensities are summarized in Table 7.45.

The magnetic susceptibility of $PuCl_3$ was measured in the range 90–600 K by Dawson *et al.* (1951). The temperature dependence of χ suggested a $5f^5$ electronic configuration for the Pu^{3+} ion.

The chemical properties of plutonium trichloride have been studied in great detail because of its application in molten-salt chemistry and metal production. $PuCl_3$ may be readily reduced to the metal by Ca, Mg, or La. The phase diagram

Table 7.45 *Energies and intensities of $PuBr_3(g)$ and $PuCl_3(g)$ transitions* (*Gruen and deKock,* 1967).

	$\bar{\nu}$ (cm^{-1})	ϵ (L cm^{-1} mol^{-1})	$\bar{\nu}$ (cm^{-1})	ϵ (L cm^{-1} mol^{-1})
$PuBr_3(g)$	5 810	2.2	17 390	20
	6 290	3.3	17 600	17 sh
	7 720	2.2 sh	17 860	19
	7 870	7	18 660	25 sh
	8 060	4.8	22 220	170 sh
	8 400	7.5 sh	22 730	210
	8 500	14	23 040	220
	8 930	4.0	23 360	230
	9 520	3.3 sh	23 580	230
	9 710	3.7	23 810	215
	10 870	4.0	24 510	180 sh
	14 490	3.7 sh	24 750	175 sh
	15 380	6 sh	25 000	165 sh
	16 390	9.5 sh	27 500	290 sh
	16 830	16	29 500	420 sh
	17 140	16	31 500	800
$PuCl_3(g)$	22 990	310	24 450	200
	23 360	330	24 940	160
	23 750	290	31 750	1 900

of the system $PuCl_3$–Pu has been studied by Johnson and Leary (1964). The metal solubility at the monotectic (740°C) was found to be 7%, but there was no indication of the formation of divalent plutonium. For the reaction of $PuCl_3$ melts with Am metal, see Mullins *et al.* (1966).

With water, $PuCl_3$ reacts to form several hydrates with 1, 2, or 6 H_2O, depending on the H_2O partial pressure (Abraham *et al.*, 1949a).

Sheft and Davidson (1949b) and Weigel *et al.* (1977) have measured the vapor-phase hydrolysis of $PuCl_3$ by determining the equilibrium constant of the reaction

$$PuCl_3(s) + H_2O(g) \rightleftharpoons PuOCl(s) + 2HCl(g) \tag{7.71}$$

as a function of temperature. The two groups obtained nearly identical results with regard to the thermodynamic parameters of the above reaction.

With alkaline or alkaline-earth chlorides, a number of ternary chloro complexes are formed. For the individual compounds, see Section 7.8.6(d).

The optical properties of gaseous $PuBr_3$ have been studied by Gruen and deKock (1967). The energies and intensities are summarized in Table 7.45. The absorption spectrum of solid $PuBr_3$ was determined by Lipis and Pozharskii (1960) in the 340–1000 nm range. It was found to be similar to that of aqueous $PuBr_3$, but differed considerably from that of solid $PuCl_3$. This difference, together with the structural difference between $PuCl_3$ and $PuBr_3$, has been interpreted by Fomin *et al.* (1958) to indicate a change in the nature of bonding from predominantly ionic in $PuCl_3$ to predominantly covalent in $PuBr_3$.

The enthalpy of formation of $PuBr_3$ was first determined by Westrum (1949c) from its enthalpy of solution in 6 M HCl. The enthalpy of solution in O_2-free 0.1 and 1.0 M HCl, was also measured by Brown *et al.* (1977).

Sheft and Davidson (1949a) and Weigel *et al.* (1982) have measured the vapor-phase hydrolysis of plutonium(III) bromide by determining the equilibrium constant of the reaction

$$PuBr_3 + H_2O \rightleftharpoons PuOBr + 2HBr \tag{7.72}$$

as a function of temperature. The results of both groups are in close agreement. The enthalpies of formation derived from these measurements, and reviewed by Lemire *et al.* (2001), are listed in Table 7.43.

$PuBr_3$ reacts with moisture to form the hexahydrate $PuBr_3 \cdot 6H_2O$ (Mullins *et al.*, 1966). The structural data of $PuBr_3 \cdot 6H_2O$ are listed in Table 7.42.

The enthalpy of formation of PuI_3 is reported by Brown *et al.* (1977).

(c) Oxyhalides of plutonium

Plutonium forms a number of oxyhalides in the valence states III and VI. So far, no oxyhalides of Pu(IV) or Pu(V) have been prepared. With Pu(III), the oxyhalides, PuOF, PuOCl, PuOBr, and PuOI are known.

(*i*) *Preparation and properties*

For plutonium(III) oxyfluoride, no direct method of preparation has been reported. Rather, PuOF was accidentally obtained in the attempted reduction of PuF_3 by hydrogen (Cunningham, 1954), and in an attempt to measure the melting point of plutonium metal.

Plutonium(III) oxychloride, PuOCl, was first prepared by Abraham *et al.* (1949a) by heating $PuCl_3 \cdot 6H_2O$ in a sealed tube at 400°C. The resulting preparation contained 60% PuOCl and 40% $PuCl_3$. In another similar preparation, a product containing 60–65% PuOCl and 40–35% $PuCl_3$ was obtained, which could be converted to pure PuOCl by heating in a sealed tube with 95 Torr H_2 and 55 Torr HCl at 675°C.

A preparation method yielding pure PuOCl in a one-step reaction was reported by Westrum and Robinson (1949b). They also made the first determination of the enthalpy of formation using the reaction of $PuCl_3$ with a stream of H_2, HCl and water vapor at 675°C.

The formation of PuOCl in the vapor-phase hydrolysis of $PuCl_3$ (see Section 7.8.6.b.(iii)) has been studied by several authors (Abraham and Davidson, 1949; Sheft and Davidson, 1949b; Weigel *et al.*, 1977), who have also determined the enthalpy of formation. The best values at the time of writing are given in Table 7.43.

Plutonium(III) oxybromide, PuOBr, was first observed by Davidson *et al.* (1949) as a residue from the sublimation of small amounts of $PuBr_3$ in a silica tube. It can be obtained in a pure state by treating gently heated Pu(IV) hydroxide (70°C) with moist hydrogen bromide at 750°C (Davidson *et al.*, 1949; Sheft and Davidson, 1949a), or by vapor-phase hydrolysis (Weigel *et al.*, 1982).

The enthalpy of formation of PuOBr was determined by Weigel *et al.* (1982) by measurement of the equilibrium constant of the vapor-phase hydrolysis of $PuBr_3$. Rand (1966), Fuger *et al.* (1983), and Lemire *et al.* (2001) have assessed previous values of the enthalpy of formation and the recommendations of the latter are listed in Table 7.43.

Plutonium(III) oxyiodide, PuOI, was observed to form in attempts to prepare PuI_3 (Hagemann *et al.*, 1949). In all reactions in which even traces of water are present, or are being formed in the course of the reaction, the bright-green PuOI is formed.

So far, no oxyhalides of tetravalent or pentavalent plutonium have been prepared. However, there is thermochromatographic evidence for the existence of $PuOF_3$ (Jouniaux, 1979; Jouniaux *et al.*, 1979), but this compound has not yet been isolated.

The only oxyhalides of hexavalent plutonium that have been isolated and prepared in substantial quantities are plutonyl fluoride, PuO_2F_2 (Alenchikova *et al.*, 1961a), plutonium(VI) oxytetrafluoride, $PuOF_4$ (Burns and O'Donnell, 1977), and plutonyl chloride, $PuO_2Cl_2 \cdot 6H_2O$ (Alenchikova *et al.*, 1959). $PuOF_4$ is formed when an excess of PuF_6 is condensed on a 0.23% solution of

deionized water in HF, and the mixture is warmed to room temperature. After evaporation of unreacted HF and PuF_6, the $PuOF_4$ separates as a chocolate-brown solid. PuO_2F_2 is prepared by slow, low-temperature hydrolysis of PuF_6:

$$PuF_6 + 2H_2O \rightarrow PuO_2F_2 + 4HF \tag{7.73}$$

Alenchikova *et al.* (1961a) studied the system PuO_2F_2–HF–H_2O and observed $PuO_2F_2 \cdot H_2O$, $PuO_2F_2 \cdot HF \cdot 4H_2O$, and anhydrous PuO_2F_2 solids in equilibrium with the solution for 0–1.3% HF, 1.9–0.85% HF, and 87–100% HF, respectively.

Plutonyl chloride hexahydrate, $PuO_2Cl_2 \cdot 6H_2O$, has been prepared by vacuum evaporation at room temperature of Pu(VI) chloride solutions (Alenchikova *et al.*, 1959) formed by oxidation of Pu(IV) chloride solutions with chlorine. The greenish-yellow $PuO_2Cl_2 \cdot 6H_2O$ was identified by chemical and spectrophotometric analysis. $PuO_2Cl_2 \cdot 6H_2O$ is not stable, and gradually decomposes to a Pu(IV) compound.

(*ii*) *Solid-state structures*

All the PuOX compounds with heavier halides (Cl, Br, I) have the well-known PbClF structure type, and were first characterized by Zachariasen (1949d). This basic structure is built up of layers of different atom types. Each complex layer in the PuOX structure consists of a central sheet of coplanar oxygen atoms with a sheet of halogen atoms on each side, and plutonium atoms sandwiched in between. The basic layer structure is shown in Fig. 7.113(a). Within one of these complex layers, the plutonium atoms are coordinated by four oxygen and four chlorine atoms, making a local square antiprismatic coordination geometry. A view of the structure that emphasizes the square antiprismatic geometry is shown in Fig. 7.113(a).

The crystal structure of PuOF was originally reported to be cubic by Zachariasen (1949d), but a subsequent study of powder diffraction data showed that the compound was actually tetragonal (Zachariasen, 1951). In the tetragonal form, the structure fits into a class of MOF structures that display a superstructure that is related to the fluorite structure. In the tetragonal superstructure, the oxygen and fluorine atoms arrange themselves in sheets separated by a layer of plutonium atoms. The local coordination around plutonium is that of cube, with four fluorine atoms on one side, and four oxygen atoms on the opposite side. This cubic PuF_4O_4 coordination environment is compared with the square antiprismatic coordination environment found in PuOX (X = Cl, Br, I) in Fig. 7.113(b).

(d) Ternary halogenoplutonates

With ammonium, alkali, and alkaline-earth halides, and, in a few cases, with transition-metal halides, plutonium(III), (IV), (V), and (VI) halides form a large number of ternary halogenoplutonates.

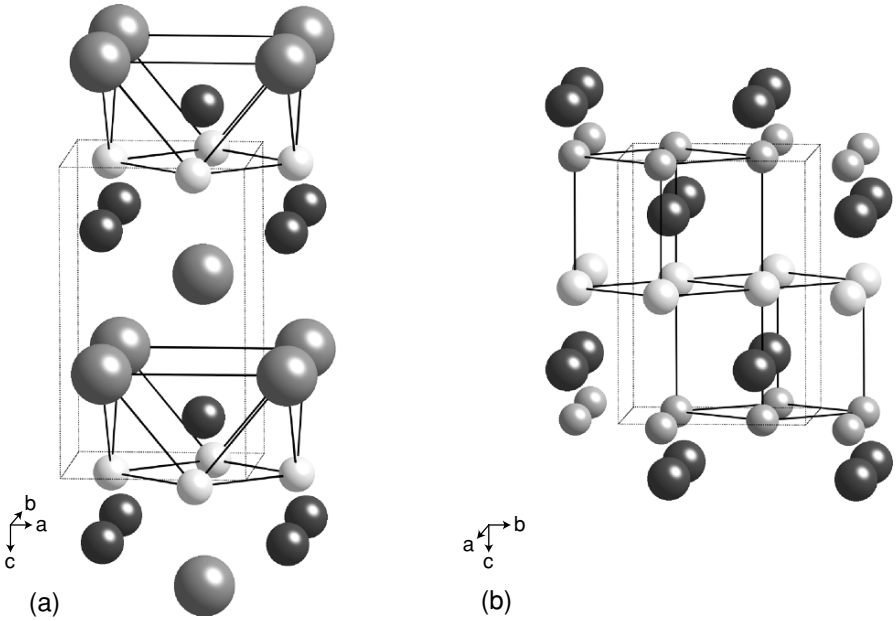

Fig. 7.113 *Comparison of PuOX solid-state structures.* (*a*) *The basic structural unit for PuOX* ($X = Cl, Br, I$) *illustrating the layered nature of the repeat units, and the local* PuO_4X_4 *square antiprismatic local coordination geometry.* (*b*) *The basic structural unit for tetragonal PuOF showing the layered nature of repeat units, and the local cubic* PuO_4F_4 *coordination geometry.*

The fluoroplutonates and pseudo-binary systems containing plutonium fluorides are of major interest as potential materials for molten-salt fuels in high-temperature reactors. Therefore, much work has been devoted to the individual compounds and, in some cases, to pseudo-binary phase diagrams. Leary (1962) has summarized the phase diagram work done up to 1962.

The preparation of individual fluoroplutonates depends on the nature of the compound to be prepared. The following methods are the ones usually employed.

1. A compound is precipitated from aqueous solution, and dried below 100°C.
2. Stoichiometric amounts of alkali halide and plutonium(III) or plutonium(IV) halide in HCl or HF solution(s) are evaporated to dryness. The residue is heated in a platinum boat or a sapphire dish at 300°C in a stream of HF.
3. Stoichiometric amounts of PuF_4 or PuO_2 and alkali or alkaline-earth fluoride are intimately mixed and heated at 300–600°C in a stream of HF, $HF + O_2$, or $HF + H_2$ (the latter for preparation of Pu(III) complexes).
4. Stoichiometric amounts of PuF_4 or PuO_2 and NH_4F are heated together in a closed vessel at 70–100°C. The product is pulverized and heated again in

the same manner. This procedure is repeated until a homogeneous product has been obtained.

5. Thermal decomposition of a higher complex, or treatment of another plutonium fluoro complex with elemental fluorine.
6. PuF_6 and alkali or alkaline-earth fluoride are reacted.
7. Alkali carbonate is added to plutonium nitrate solution, the solution evaporated with HF and treated with F_2.
8. PuF_4 is fused with the stoichiometric amount of the corresponding alkali fluoride.
9. PuF_4 is fused with the stoichiometric amount of alkali or metal fluoride.
10. Cooled solution of Pu(v) in dilute acid is added to ice-cold saturated RbF solution.

The known fluoroplutonate complexes have been compiled in Table 7.46. The phase diagrams of the systems LiF–PuF_3 and NaF–PuF_3 have been reported by Barton *et al.* (1961). These two systems are the only ones based on PuF_3 for which phase diagrams have been determined. No other systems, neither based on PuF_3 nor based on PuF_4, have been reported.

With the chloride systems, a different situation exists. Even though only very few compounds have been characterized as individual entities, several phase diagrams have been determined. Most of the compounds occurring in these phase diagrams have never been studied in great detail. Phase diagrams have been reported for solid–liquid equilibria in the binary systems $PuCl_3$–MCl, where M = Li (Bjorklund *et al.*, 1959), Na (Bjorklund *et al.*, 1959), K (Benz *et al.*, 1959), Rb (Benz and Douglass, 1961b), Cs (Benz and Douglass, 1961b), and $PuCl_3$–$M'Cl_2$, where M′ = Mg, Ca, Sr, and Ba (Johnson *et al.*, 1961). An excellent summary of these phase diagrams was reported by Leary (1962). Some of the systems based on $PuCl_3$ have become of practical importance in fused-salt ER of plutonium, and in the DOR and pyroredox processes (see Section 7.7.2). As a representative phase diagram of such a system, the diagram of the system KCl–$PuCl_3$ is shown in Fig. 7.114 (Benz *et al.*, 1959). In these systems based on $PuCl_3$, compounds such as $RbPu_2Cl_7$ (light blue), $CsPu_2Cl_7$ (greenish blue to deep green), $RbPuCl_5$ (brownish to greenish yellow), Cs_3PuCl_6 (green), or M_3PuCl_9 (M = Sr, Ba) (no color given) have been observed, but none of these compounds have been studied in detail.

The hexachloroplutonates M_2PuCl_6, where M = Na, Rb, Cs, $(CH_3)_4N^+$, or $(C_2H_5)_4N^+$, are obtained as pale greenish yellow (alkali compounds) or orange-yellow (alkylammonium compounds) crystals by precipitation from concentrated HCl solution. Except for Cs_2PuCl_6, the properties of these compounds are not known in detail. Cs_2PuCl_6 is sufficiently stable to be useful as a primary plutonium standard (Miner *et al.*, 1963). No bromo or iodo complexes of plutonium(IV) are known, with the sole exception of the red bromo complex, $[(C_2H_5)_4N]_2PuBr_6$, which was prepared by Ryan and Joergensen (1964) by precipitation from ethanolic HBr solution on the addition of acetone.

Table 7.46 *X-ray crystal structure data for plutonium double fluorides.*

Plutonium valence	*Compound*	*Color*	*Symmetry*	*Space group*	*Lattice parameters*			*Angle* (deg)	*Density* ($g\ cm^{-3}$)	*References*
					a_0 (Å)	b_0 (Å)	c_0 (Å)			
Pu(III)	$NaPuF_4$	blue	hexagonal	P321	6.129(6)		3.753(4)			Zachariasen (1948a)
					6.13(2)		3.76(1)		6.87	Keller and Schmutz (1964)
	$KPuF_4$		orthorhombic	P*nma*	6.23	3.75	15.42		6.53	Jove and Pagès (1977)
	$RbPuF_4$		orthorhombic	P*nma*	6.39	3.80	15.86		6.91	Jove and Pagès (1977)
	KPu_2F_7	blue	cubic	F*m*3*m*	5.880				5.31	Schmutz (1966)
Pu(IV)	$LiPu_4F_{17}$		tetragonal		8.84(1)		11.31(2)		7.25	Jove and Cousson (1977)
	KPu_2F_9	red-brown	orthorhombic[a]	P*nma*	8.58(4)	11.35(6)	6.96(4)		6.74	Zachariasen (1948b)
	$LiPuF_5$	brown	tetragonal	$I4_1/a$	14.67(2)		6.479(5)			Keenan (1966)
			tetragonal	$I4_1/a$	14.65(1)		6.486(5)		6.51	Keller and Schmutz (1966)
	$NaPuF_5$	green	rhombohedral	$R\bar{3}$	8.93(3)			$\alpha = 107.48(16)$	6.03	Zachariasen (1948b)
	$KPuF_5$	green	rhombohedral	$R\bar{3}$	9.27(3)			$\alpha = 107.03(08)$	5.66	Zachariasen (1948b)
	$RbPuF_5$	green	rhombohedral	$R\bar{3}$	9.46(3)			$\alpha = 106.93(16)$	5.88	Zachariasen (1948b)
	α-NH_4PuF_5	light brown	rhombohedral	$R\bar{3}$	9.42					Benz *et al.* (1963)
	β-NH_4PuF_5	yellow-green	orthorhombic		9.83	6.98	6.27			Benz *et al.* (1963)
	$Li_7Pu_6F_{31}$	brown	tetragonal		14.650(1)		6.468(5)		4.96	Schmutz (1966)
	$Na_7Pu_6F_{31}$	brown/green	rhombohedral	$R\bar{3}$	9.006			$\alpha = 107.75$	6.14	Schmutz (1966)
			(hexagonal)		14.52(2)		9.704(3)		6.14	Keller and Schmutz (1966)
	$K_7Pu_6F_{31}$	green/brown	rhombohedral	$R\bar{3}$	9.275(5)			$\alpha = 107.17$	5.77	Schmutz (1966)
			(hexagonal)		14.93(2)		10.28(1)		5.76	Keller and Schmutz (1966)
	$Rb_7Pu_6F_{31}$	green/brown	rhombohedral	$R\bar{3}$	9.466(5)			$\alpha = 106.90(1)$	6.14	Schmutz (1966)
			(hexagonal)		15.21(2)		10.61(1)			Keller and Schmutz (1966)

Table 7.46 (*Contd.*)

Plutonium valence	*Compound*	*Color*	*Symmetry*	*Space group*	*Lattice parameters* a_0 (Å)	b_0 (Å)	c_0 (Å)	*Angle* (deg)	*Density* (g cm^{-3})	*References*
	$(NH_4)_7Pu_6F_{31}$	orange	rhombohedral	$R\bar{3}$	9.42			$\alpha = 107.33$		Benz *et al.* (1963)
	$Tl_7Pu_6F_{31}$		(hexagonal)		15.08		10.40			Jove *et al.* (1976)
	Na_2PuF_6	pink	hexagonal	P321	6.059(5)	7.130(5)			5.84	Keller and Schmutz (1966)
		pink-brown	hexagonal	P321	6.055(3)		3.571(5)			Alenchikova *et al.* (1958)
	Rb_2PuF_6		orthorhombic	*Cmcm*	6.971(18)	12.033(16)	7.602(10)			Keenan (1967)
	Cs_2PuF_6		orthorhombic		12.145	7.156	4.056			Riha and Trevorrow (1965)
	$(NH_4)_2PuF_6$	pink								Benz *et al.* (1963)
	Tl_2PuF_6		orthorhombic	*Pmma*[b]	11.35(2)	6.89(1)	4.05(1)			Jove *et al.* (1974)
	$CaPuF_6$	red-brown	hexagonal	$P\bar{3}c1$[c]	3.997		7.097		6.65	Keller and Salzer (1967)
	$SrPuF_6$	red-brown	hexagonal	$P\bar{3}c1$[c]	7.091		7.255		6.95	Keller and Salzer (1967)
	Na_3PuF_7		tetragonal	I4/*mmm*	5.460		10.920		3.98	Riha and Trevorrow (1965)

	Tl_3PuF_7		cubic	F$m3m$[d]	9.30				8.13	Jove *et al.* (1974)
	$(NH_4)_4PuF_8$	pink-red								Benz *et al.* (1963)
Pu(v)	Rb_2PuF_7	green	monoclinic	P$2_1/c$	6.270(8)	13.416(8)	8.844(8)	$\beta = 90$		Penneman *et al.* (1965)
	$CsPuF_6$	green	rhombohedral	R$\bar{3}$	8.036(3)		8.388(4)		5.16	Penneman *et al.* (1965)
	$RbPuO_2F_2$	lavender	rhombohedral	R$\bar{3}m$	6.796(8)			$\alpha = 36.28$		Keenan (1965)
	$(NH_4)PuO_2F_2$	lavender	rhombohedral	R$\bar{3}m$	6.817(6)			$\alpha = 36.27$		Keenan (1965)
Pu(vi)	$KPuO_2F_3{\cdot}H_2O$		cubic		8.126					Alenchikova *et al.* (1961b)
	$RbPuO_2F_3{\cdot}H_2O$		cubic		8.458					Alenchikova *et al.* (1961b)
	$CsPuO_2F_3{\cdot}H_2O$		cubic		8.916					Alenchikova *et al.* (1961b)

[a] Space group reported as P*nam*, changed to standard setting P*nma* by Roof (1989).
[b] Original lattice constant reported in space group P*mcm*. Changed to standard setting P*mma* by Roof (1989).
[c] Roof (1989) suggests that the original space group P$6_3/mmc$ is likely the trigonal space group P$\bar{3}c1$, hence the *a*-axis lattice constant has been divided by $\sqrt{3}$ to derive the value reported above.
[d] Jove reports the lattice constants, Avignant describes that the structure is isotypic of $(NH_4)_3ZrF_7$ (Avignant and Cousseins, 1971), and this structure is described by Hurst (Hurst and Taylor, 1970).

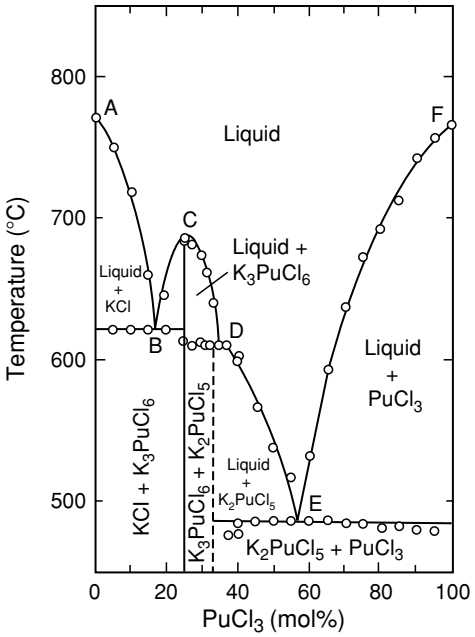

Fig. 7.114 *The phase diagram of the KCl–$PuCl_3$ system* (*Benz* et al., 1959). *Key points in the diagram include A, the KCl melting point at* 771°C*; B, eutectic point at* 621°C *corresponding to* 17% *$PuCl_3$; C, K_3PuCl_6 melting point at* 685°C*; D, peritectic point at* 611°C *and* 35% *$PuCl_3$; E, eutectic point at* 486°C *and* 57% *$PuCl_3$;and F, $PuCl_3$ melting point at* 769°C.

A number of derivatives of plutonyl chloride, PuO_2Cl_2, which is known as the hexahydrate $PuO_2Cl_2 \cdot 6H_2O$ (Alenchikova *et al.*, 1959), have been prepared. These compounds contain the anion $[PuO_2Cl_4]^{2-}$. Probably the best-known compounds of this type are the rubidium salt, $Rb_2PuO_2Cl_4$, and the cesium salt, $Cs_2PuO_2Cl_4$, which form orange-yellow crystals. The lattice constants of both compounds have been determined by Werner (1982) and are listed in Table 7.47. The lattice constants and other crystallographic properties determined for halo complexes of plutonium are listed in Table. 7.47.

7.9 SOLUTION CHEMISTRY

Descriptive solution and coordination chemistry played a key role in the discovery of plutonium and in the formulation of the actinide series concept (Seaborg and Loveland, 1990). The need to separate and purify plutonium from nuclear fuel during the Manhattan Project drove much of the early solution chemistry and included the extraction of plutonium coordinated by organic ligands, pyrochemical processing in molten salts, and the distillation or

Table 7.47 *X-ray crystal structure data for plutonium double chlorides*[a].

Compound	*Color*	*Symmetry*	*Space group*	*Lattice parameters*			*Density* ($g\ cm^{-3}$)	*References*
				a_0 (Å)	b_0 (Å)	c_0 (Å)		
Pu(III)								
K_2PuCl_5		orthorhombic	P*nma*	12.626(12)	8.674(7)	7.953(5)		Axler *et al.* (1992)
K_2PuCl_5		orthorhombic	P*nma*	12.674(3)	8.727(2)	7.969(2)	3.73	Morss and Fujino (1988b)
Rb_2PuCl_5		orthorhombic	P*nma*	13.093(8)	8.909(5)	8.178(5)	4.09	Morss and Fujino (1988b)
Pu(IV)								
K_2PuCl_6		monoclinic[b]	P2/*m*	7.218(5)	7.611(6)	10.208(7)	3.14	Morss and Fujino (1988a)
Rb_2PuCl_6		hexagonal	$P6_3mc$	7.377(2)		11.880(7)	3.69	Morss and Fujino (1988a)
Cs_2PuCl_6	pale yellow	trigonal	$P\bar{3}m$	7.44(1)		6.04(1)	4.10	Zachariasen (1948c)
$[(CH_3)_4N]_2PuCl_6$	orange-yellow	fcc	F*m*3*m*	12.96(5)			1.330	Staritzky and Singer (1952)
$[(C_2H_5)_4N]_2PuCl_6$	yellow	orthorhombic	F*mmm*	14.23(1)	14.53(3)	13.53(5)	1.691	Staritzky and Singer (1952)
Pu(VI)								
$Rb_2PuO_2Cl_4$	orange	monoclinic[c]	I2/*c*	11.60(3)	7.42(5)	5.50(3)		Werner (1982)
$Cs_2PuO_2Cl_4$	orange	monoclinic[d]	I2/*c*	11.879(6)	7.693(6)	11.533(7)		Werner (1982)
$[(CH_3)_4N]_2PuO_2Cl_4$	yellow	tetragonal	I4/*m*	10.00(5)		12.90(5)		Staritzky and Singer (1952)
$[(C_2H_5)_4N]_2PuO_2Cl_4$	yellow	tetragonal	I4/*m*	9.20(5)		11.90(5)		Staritzky and Singer (1952)

[a] All oxidation states Pu(III) through Pu(VI) have been observed in molten salts of the alkali chlorides (Gruen *et al.*, 1960; Benz and Douglass, 1961a; Swanson, 1964).
[b] $\beta = 91.59(4)°$.
[c] $\beta = 100.1(6)°$.
[d] $\beta = 96.99(5)°$.

centrifugation of volatile halide, alkoxide, and borohydride complexes (Koch, 1972, 1973a–c, 1976a,b). Solution and coordination chemistry continues to play a role in modern plutonium processing and separations, and for recycle of plutonium in closed nuclear fuel cycles. More recently, interest has grown in the chemistry of plutonium under biologically and environmentally relevant conditions, as attention has turned to understanding the long-term fate and transport of plutonium stored in geological repositories (Clark *et al.*, 1995; Neu *et al.*, 2002; Silva and Nitsche, 2002). Selected aspects of plutonium coordination chemistry have been reviewed by Cleveland (1979) and Carnall and Choppin (1983), and within broader reviews on actinide elements (Lemire *et al.*, 2001; Burns *et al.*, 2004). In this section we describe the preparation, stability, structure, and spectroscopy, of aqueous and nonaqueous molecular complexes of plutonium.

7.9.1 Aqueous solution chemistry

The chemistry of plutonium in aqueous solution is unique and rich. It is also complicated, primarily due to the small energy separations between the various oxidation states and the extreme oxophilicity of plutonium cations. Five oxidation states, Pu(III), Pu(IV), Pu(V), Pu(VI), and Pu(VII), can be readily prepared and stabilized in aqueous solution under the appropriate conditions. The lower oxidation states, Pu(III) and Pu(IV), are generally more stable in acid solution while the higher oxidation states, Pu(VI) and Pu(VII), are favored under alkaline conditions. Tetravalent plutonium is the most stable and consequently the most studied, followed by plutonium in the trivalent and hexavalent states. In the decades following the discovery of plutonium, its solution chemistry was motivated by the need to separate plutonium from mixtures of actinides and fission products in multiple oxidation states under highly acidic conditions. Processes that used oxidation and/or reduction steps in solution and condensed phases bolstered the study and understanding of aqueous Pu(III) and Pu(VI). In contrast, pentavalent plutonium is most stable in near-neutral pH solutions that are dilute in both plutonium and other ions. Although Pu(V) was identified along with the other common oxidation states, research on the solution complexes of this oxidation state was not widely pursued until the 1990s when the behavior of plutonium in environmental matrices gained importance. Heptavalent plutonium was the last oxidation state to be discovered, and it was first reported in 1967 (Krot and Gel'man, 1967). Plutonium in this oxidation state is stable only in highly alkaline solution and in the presence of strong oxidizing agents, and is therefore the least well studied. There are very recent spectroscopic studies that suggest the possibility of the existence of Pu(VIII) in alkaline solution (Nikonov *et al.*, 2004, 2005). The existence of this oxidation state is equivocal, and we look forward to future research in this area.

Under noncomplexing strongly acidic conditions, such as in perchloric or triflic acid solutions, both Pu(III) and Pu(IV) exist as the simple hydrated (or

aquo) ions, $Pu^{3+}_{(aq)}$ or $Pu^{4+}_{(aq)}$, retaining their overall formal charge. In the sections that follow, we refer to the $Pu^{3+}_{(aq)}$ or $Pu^{4+}_{(aq)}$ species as simply Pu^{3+} and Pu^{4+}, or Pu(III) and Pu(IV), respectively. Pentavalent and hexavalent plutonium cations have such large positive charges that in aqueous solution they immediately hydrolyze to form a unique class of trans dioxo cations, $PuO^{+}_{2(aq)}$ and $PuO^{2+}_{2\,(aq)}$, which are commonly referred to as plutonyl ions. Under noncomplexing acid conditions (such as perchloric or triflic acid), both ions exist as the simple hydrated (or aquo) ions, $PuO^{+}_{2(aq)}$ and $PuO^{2+}_{2(aq)}$, and we refer to these as simply PuO^{+}_{2} and PuO^{2+}_{2}, or Pu(V) and Pu(VI), respectively. These plutonyl cations have estimated effective charges of 2.2 and 3.3, respectively (Choppin, 1983). Heptavalent plutonium is not stable in acid solution, and can only be prepared under highly alkaline solution conditions. Under alkaline conditions, the heptavalent ion forms a tetra-oxo species PuO^{-}_{4}, which is always coordinated with hydroxide ions to give $PuO_4(OH)^{3-}_{2}$. We will refer to this species as Pu(VII). The OECD-NEA has evaluated thermodynamic properties for plutonium ions in aqueous solution, and a selected set of their recommended values is given in Table 7.48 (Lemire *et al.*, 2001).

(a) Stoichiometry and structure of plutonium ions

From an historical perspective, the charge and composition of plutonium ions in acid solution were inferred from solvent extraction studies. For example, plutonium(III) and plutonium(IV) are written as Pu^{3+} and Pu^{4+} in part from an interpretation of charge balances in solvent extraction studies with thenoyltrifluoroacetone (Poskanzer and Foreman, 1961), and also from the lack of hydrogen-ion dependence of the reversible Pu(IV)/Pu(III) redox couple (Rabideau, 1956). The Pu(V)/Pu(IV) redox couple on the other hand, is not rapidly reversible, nor independent of hydrogen-ion concentration, indicating that the two ions differ in degree of oxygenation. The existence of the trans dioxo ions in Pu(V) and Pu(VI) (PuO^{+}_{2} and PuO^{2+}_{2}, respectively) was originally based on crystallographic data on solid compounds. For Pu(VI), XRD data for $NaPuO_2(O_2CCH_3)_3$ and $Cs_2PuO_2Cl_4$ confirmed that the compounds were isostructural with the corresponding uranium, neptunium, and americium analogs, and contained the linear PuO^{2+}_{2} unit (Werner, 1982). Similar structural

Table 7.48 *Selected chemical thermodynamic values for plutonium aquo ions* (*Lemire* et al., 2001).

Formula	$\Delta_f G^\circ$ (kJ mol^{-1})	$\Delta_f H^\circ$ (kJ mol^{-1})	S° (J K^{-1} mol^{-1})
Pu^{3+}	-579.0 ± 2.7	-591.8 ± 2.0	-184.5 ± 6.2
Pu^{4+}	-478.0 ± 2.7	-539.9 ± 3.1	-414.5 ± 10.2
PuO^{+}_{2}	-852.6 ± 2.9	-910.1 ± 8.9	$+1 \pm 30$
PuO^{2+}_{2}	-762.4 ± 2.8	-822.0 ± 6.6	-71 ± 22

comparisons were found for other Pu(VI) compounds, and helped to assign the basic formula PuO_2^{2+} to Pu(VI) in solution. Plutonium(V), likewise, was assigned the formula PuO_2^{+} because of the existence of the PuO_2^{+} unit in the solid-state structure of $KPuO_2CO_3$ (Ellinger and Zachariasen, 1954), and in part because the oxidation–reduction couple Pu(VI)/Pu(V) is reversible and independent of the hydrogen-ion concentration (except for the shift in potential due to hydrolysis). This argued that there was no structural rearrangement during redox, and therefore that the oxygen content was identical in both ions.

Recent X-ray absorption and vibrational spectroscopic studies provide more direct characterization of the solution forms of the ions in all oxidation states. Under noncomplexing acid conditions, Pu(III), Pu(IV), Pu(V), and Pu(VI) are coordinated by water molecules, resulting in hydrated cations of general formula $Pu(OH_2)_n^{3+}$, $Pu(OH_2)_n^{4+}$, $PuO_2(OH_2)_n^{+}$, and $PuO_2(OH_2)_n^{2+}$, respectively. Structural analysis in solution using EXAFS spectroscopy has been recently employed to determine the number of coordinated water molecules (n) and the Pu–O distances in the aquo ions (Allen *et al.*, 1997; Conradson *et al.*, 2004a). For the Pu(III) aquo ion, $Pu(OH_2)_n^{3+}$, EXAFS studies report coordination numbers of 9 (Conradson *et al.*, 2004a) and 10 (Allen *et al.*, 1997), with Pu–O distances of 2.48(1) and 2.51(1) Å, respectively. These coordination number estimates are consistent with previous estimates of 9 that were based upon comparison with Cm(III) from luminescence lifetime measurements (Kimura and Choppin, 1994), and Am(III) determined from optical absorption spectroscopy (Carnall, 1989). Relativistic DFT calculations suggest eight or possibly nine water molecules for the Pu(III) aquo ion, $Pu(OH_2)_9^{3+}$ (Blaudeau and Bursten, 2000). A recent single crystal XRD study of a salt containing the $Pu(OH_2)_9^{3+}$ unit substantiates the coordination number of 9 for the Pu(III) aquo ion (Matonic *et al.*, 2001) in the solid state. In this compound, the $Pu(OH_2)_9^{3+}$ ion adopts a tricapped trigonal prismatic coordination environment, where all nine coordinated water molecules show a similar Pu–O distance that averages 2.51 Å (Matonic *et al.*, 2001) comparable to the values observed by EXAFS. For Pu(IV), EXAFS analysis indicates the presence of eight water molecules at a shorter Pu–O distance of 2.39(1) Å (Conradson *et al.*, 2004a). For Pu(V) and Pu(VI) aquo ions, EXAFS data reveal two short plutonyl Pu=O bonds at 1.81(1) and 1.75(1) Å (respectively) consistent with expectations for trans dioxo ions. Each plutonyl unit is coordinated by four or five water molecules with Pu–O bond distances of 2.47(1) and 2.41(1) Å, respectively (Conradson *et al.*, 2004a). Similar analyses on the aquo ions of UO_2^{2+}, NpO_2^{2+}, and NpO_2^{+} indicate that a coordination number of 5 is the most common, but that this value will be affected by changes in the ionic strength of solution (Antonio *et al.*, 2001). Theoretical analysis of XANES, coupled with experimental measurements, have provided new insights on the electronic structure of these ions, especially the nature of the bonding interactions between plutonium and axial oxygen atoms in the PuO_2^{+}, and PuO_2^{2+} aquo ions (Ankudinov *et al.*, 1998).

Ions of Pu(VII) also contain Pu=O multiple bonds, and the preponderance of evidence indicates the presence of polyoxo ions with four or more oxo groups depending on solution conditions. The reversibility of the Pu(VII/VI) reduction, similar to the Pu(VI/V) reversible reduction supports the formulation of a polyoxo ion. A series of anionic polyoxo species that form between 0.5 and 18 molar hydroxide has been proposed and includes $PuO_4(OH_2)_2^-$, $PuO_4(OH)(OH_2)^{2-}$, $PuO_4(OH)_2^{3-}$, $PuO_5(OH)^{4-}$, or PuO_6^{5-}, depending on hydroxide concentrations (Spitsyn *et al.*, 1969; Krot, 1975; Tananaev *et al.*, 1992). Of the proposed species, only $PuO_4(OH)_2^{3-}$ has a known analog in neptunium chemistry (Grigor'ev *et al.*, 1986). The neptunium analog, $NpO_4(OH)_2^{3-}$, has a highly unusual geometry with four short Np=O bonds in a square plane, with two axial OH^- ligands (Grigor'ev *et al.*, 1986; Bolvin *et al.*, 2001; Williams *et al.*, 2001). Current research is aimed at defining conditions that favor the various forms, and at identifying their exact structure and reactivity.

Structural representations of the simple aquo ions of plutonium are given in **4**, **5**, **6,** and **7** below.

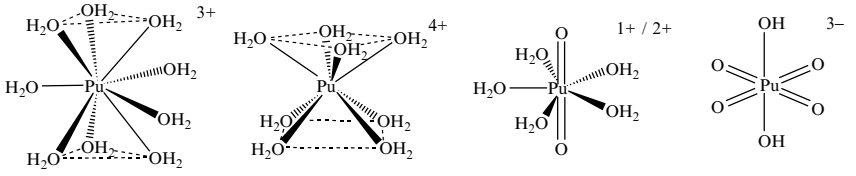

4 **5** **6** **7**

(b) Spectroscopic properties of plutonium ions

The electronic absorption spectra of plutonium ions, like those of most other actinide elements, are characterized by the presence of a few very sharp bands with relatively low molar absorptivities compared to those of d-block metal ions. The very sharp bands are strongly reminiscent of spectra of the rare-earth ions, which are attributed to electronic transitions within the shielded 4f–4f manifold of states (Edelstein, 1991). In the actinide elements, similar but relatively less shielded transitions are attributed to the 5f shell (Carnall *et al.*, 1991; Carnall, 1992; Denning, 1992, 1999). The 5f–5f transitions are more intense than the 4f–4f transitions of the lanthanides, due in part to relativistic effects that generate larger spin–orbit coupling. Energy levels for trivalent actinide ions calculated using 5f transitions compare well with experimental spectra, supporting this representation of electronic structure in plutonium (Mikheev *et al.*, 1983; Carnall, 1992). Since these transitions are forbidden by the selection rules, the absorption bands are narrow, but still not very intense.

Internal 5f–5f transitions of the plutonium ions give absorption bands in the visible and near-IR region of the electronic absorption spectrum. These

absorption features are characteristic for each oxidation state and therefore frequently used for identification and quantitative analysis of plutonium ions in solution (Cohen, 1961a). Representative electronic absorption spectra of plutonium ions of common oxidation states are given in Fig. 7.115 and molar absorptivities for distinctive bands are given in Table 7.49. Plutonium ions of all oxidation states have strong absorbance in the UV region of the optical spectrum (Stewart, 1956; Cohen, 1961b). In addition to conventional electronic absorption spectroscopy, two-photon optical absorption spectroscopy has also been used to probe the electronic structure of plutonium ions isolated in host matrices and these data have provided useful extrapolations for interpreting the spectra of the solvated ions (Denning, 1991).

Photothermal spectroscopic techniques have been applied to increase the sensitivity and selectivity of the optical absorption method of plutonium analysis. For example, photoacoustic spectroscopy, in which the pressure pulse generated from absorbed light heating the solution is transduced to an electronic signal, generally has 10 to 100 times greater sensitivity (depending on the spectral region) than conventional spectrophotometry (Stumpe *et al*., 1984; Neu *et al*., 1994). Thermal-lensing spectroscopy has sensitivities similar to photoacoustic spectroscopy and also uses the heating of the solution due to the absorption of small amounts of energy to detect and quantify analytes. This method optically probes the gradient in the refractive index, which is generated from solution heating, as a 'thermal lens' (Moulin *et al*., 1988). The use of fiber optics and pulsed laser diode excitation sources with either of these techniques allows for remote or in-process detection and quantification of plutonium ions (Neu *et al*., 1994; Wruck *et al*., 1994) in micromolar concentrations or lower. Both methods have been used in solution thermodynamic studies aimed at quantitatively evaluating complexation of plutonyl ions by chelating ligands and even by the oxo ligands of other actinyl ions (Bennett *et al*., 1992; Stoyer *et al*., 2000).

Vibrational spectroscopy, both infrared absorption and Raman scattering, are useful for 'fingerprint' comparisons, for structure determination, for analyzing intramolecular bond strength, and for understanding the electronic structure of plutonium ions. Comparison of infrared and Raman spectra of actinyl ions across the actinide series were used to establish that higher valent plutonium (V, VI) species in aqueous solution exist as linear trans dioxo ions with strong covalent Pu=O bonds. The hexavalent actinide ions all show an asymmetric O=An=O stretching frequency (ν_3) in the energy region 930–970 cm^{-1}, with the Pu(VI) aquo ion in noncomplexing perchlorate solution observed at 962 cm^{-1} (Jones and Penneman, 1953). These studies confirmed the symmetric and linear, or nearly linear, structures of both PuO_2^+, and PuO_2^{2+} in a more compelling way than do arguments based on similarities in the fine structure of the visible absorption spectrum. Infrared spectroscopic studies of plutonyl species in condensed phases, using very long pathlengths, powerful excitation sources, and sensitive detectors also contributed to vibrational band assignments for

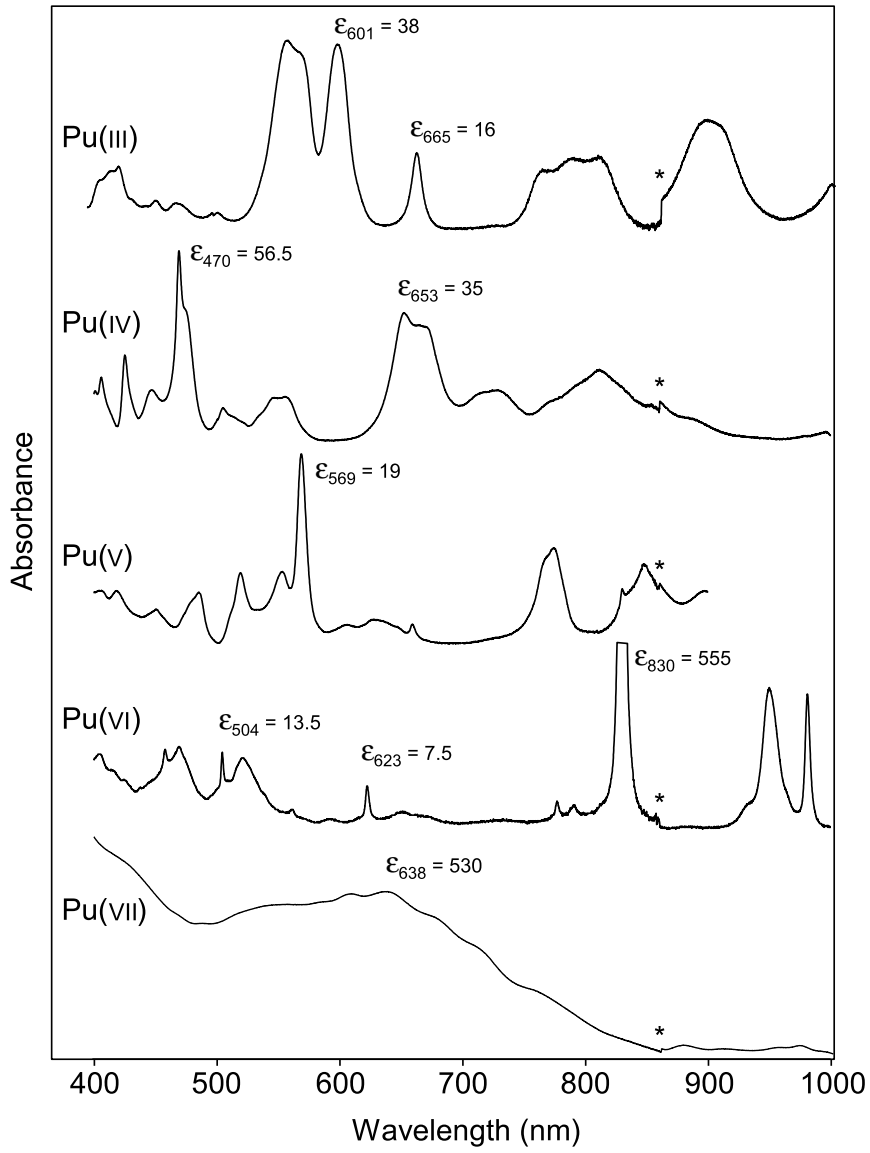

Fig. 7.115 *Electronic absorption spectra of major plutonium aqua ions recorded at* 25°C. *The asterisk marks a spectrophotometer grating change. Plutonium*(III) *recorded on* 1.89 mM *solution in* 1 M $HClO_4$ *using* 1 cm *cell. Plutonium*(IV) *recorded on* 2.91 mM *solution in* 1 M $HClO_4$ *using* 1 cm *cell. Plutonium*(V) *recorded on* 10.2 mM *solution in* 1 M $(Na,H)ClO_4$ *solution at pH* 3.14 *using* 1 cm *cell. Plutonium*(VI) *recorded on* 0.89 mM *solution in* 1 M $HClO_4$ *using* 1 cm *cell. Plutonium*(VII) *recorded on* 20 mM *solution in* 2.5 M *NaOH using* 1 cm *cell* (*spectra courtesy of Phillip D. Palmer of Los Alamos National Laboratory*).

Table 7.49 *Characteristic optical absorption bands of plutonium aquo ions in* 1 M (*H,Na*) ClO_4 *at* 25°C *unless noted otherwise* (*Cohen*, 1961*b*).

Species	*Peak max.* (nm)	*Full width at half height* (nm)[a]	*Molar absorption,* ϵ (L mol^{-1} cm^{-1})
Pu^{3+}	244	broad	1500
	561	broad	38
	601	21.7	38
	665	10.9	16
Pu^{4+}	470	13.6 (shoulder)	56.5
	653	42.7 (shoulder)	35
PuO_2^{+}[b]	569	8.6	19
	1131	32	22
PuO_2^{2+}	504	3.0	13.5
	623	3.8	7.5
	830	2.5	555
$PuO_4(OH)_4^{3-}$[c]	638	broad	530

[a] FWHM estimated from Cohen (1961b).
[b] 10°C, 0.2 M $HClO_4$.
[c] Pu(VII) spectrum from Krot and Gel'man (1967).

ions in solution (Bovey and Steers, 1960; Vdovenko *et al.*, 1973; Kim and Campbell, 1985). Complementary Raman studies assigned the symmetric O=Pu=O stretching frequency (ν_1) for PuO_2^{2+} in 1.0 M (H,Na)ClO_4 at (834 ± 3) cm^{-1}, which compares well with ν_1 for the analogous NpO_2^{2+} and UO_2^{2+} ions at (855 ± 2) cm^{-1} and (865 ± 5) cm^{-1}, respectively. These ν_1 frequencies were assigned to ground state vibrations from both fluorescence spectra intervals and Raman shifts (Madic *et al.*, 1984; Tait *et al.*, 2004). This Raman shift also agrees with the prediction of 830 cm^{-1} based on the visible spectrum of plutonium(VI) in HCl that contains a 708 cm^{-1} frequency interval in the fine structure within the wavelength region 390–430 nm. The Raman shift of PuO_2^{+} in 1.0 M ClO_4^{-} was observed at 748 cm^{-1}. Disproportionation of PuO_2^{+} was evidenced by the decrease of the intensity of the 748 cm^{-1} PuO_2^{+} band and the increase of bands located at 833 and 817 cm^{-1} assigned to PuO_2^{2+} and $(PuO_2)_2(OH)_2^{2+}$, respectively (Madic *et al.*, 1984).

Correlations of vibrational frequencies to bond strength and molecular structure of the linear O=An=O moiety have been made. Recent X-ray absorption spectroscopy studies of solution and polycrystalline actinide samples allow for correlation of the energy of the symmetric ν_1 Raman frequency with measured An=O bond lengths. Clear trends can be seen within a particular oxidation state of an actinide and a general trend of heavier actinyl ions having weaker bonds has emerged. The Raman frequency for Pu(VI) is sensitive to complexation environment, showing shifts in ν_1 greater than 40 cm^{-1} between solution species for which the measured changes in the Pu=O bond length are only minimal.

Comparisons of Pu(V) with Np(V), and Pu(VI) with U(VI) and Np(VI) aquo complexes show that as nuclear charge increases across the series uranium to plutonium, the stretching frequencies actually decrease with decreasing An=O bond length. The bond shortening is clearly a result of the actinide contraction, and the weaker bonding is an indication of 5f orbital contraction across the actinide series (Tait *et al.*, 2004). The nature of chemical bonding in the plutonyl ions is discussed in Section 7.9.3 and in Chapter 17.

(c) Oxidation and reduction reactions

(*i*) *Oxidation–reduction equilibria between plutonium ions*

The oxidation–reduction (redox) relationships of the plutonium ions present one of the most complex and fascinating aspects of the aqueous solution chemistry of plutonium. The redox potentials that couple the four common oxidation states (III, IV, V, VI) of plutonium in acid solution are all of comparable magnitude and very close to 1 V. Moreover, the kinetics of the reactions among oxidation states creates a unique situation where finite amounts of multiple oxidation states can coexist in solution under the appropriate conditions. This situation is unique for plutonium among all the elements in the periodic table. The complications arising from this unusual behavior are responsible for a considerable amount of research devoted to understanding the kinetics and mechanisms of these important reactions. We will discuss these reactions independently, and then discuss several examples to illustrate the complexity of the system. Much of this discussion follows from the excellent reviews by Cleveland (1979) and by Newton (1975, 2002).

The equilibrium concentrations of species involved in these reactions are usually determined from the potentials and the pertinent complex formation constants. Calculating standard potential values for the various couples is challenging since nearly all the data were acquired at high ionic strength, requiring extrapolation to infinite dilution. It is particularly difficult to study tetravalent plutonium independently of its hydrolysis and disproportionation. Redox reactions and corresponding electrochemical potentials that are useful for making predictions of plutonium chemistry in solution are given in Table 7.50. The constants listed for reactions in acid and some of those in base are from direct measurements, while those at pH 8 were estimated from hydrolysis data and standard potentials in acid for Pu(III), Pu(IV), and Pu(VI) and related ions (Allard *et al.*, 1980). Electrochemical studies and reported potentials have been reviewed in recent publications (Mikheev and Myasoedov, 1985; Capdevila and Vitorge, 1995; Peretrukhin *et al.*, 1995; Lemire *et al.*, 2001) and in Chapter 19 of this work. Formal redox potential schemes for selected plutonium couples at 25°C have been derived for 1 M $HClO_4$ (Lemire *et al.*, 2001), 1 M HCl (Rabideau and Cowan, 1955; Rabideau *et al.*, 1959), and 1 M HNO_3 (Artyukhin *et al.*, 1958), and are shown in Fig. 7.116.

Table 7.50 *Formal electrochemical potentials for redox couples relating the plutonium ions in acidic, neutral, and basic aqueous solution versus the standard hydrogen electrode (SHE).*

Couple	*Acidic*[a]	*Neutral*[b]	*Basic*[c]
Pu(IV)/Pu(III)	+0.982	−0.39	−0.96
Pu(V)/Pu(IV)	+1.170	+0.70	−0.67; +0.52[d]
Pu(VI)/Pu(V)	+0.913	+0.60	+0.12
Pu(VI)/Pu(IV)	+1.043	+0.65	+0.34
Pu(V)/Pu(III)		+1.076	
Pu(VII)/Pu(VI)			+0.85
Pu(V)/Pu(IV)	+1.17		

[a] Formal potential in 1 M $HClO_4$ solution (Lemire *et al.*, 2001).
[b] pH 8 (Allard *et al.*, 1980).
[c] Determined in 1 M NaOH solution (Peretrukhin *et al.*, 1995).
[d] Formal oxidation potential (Allard *et al.*, 1980).

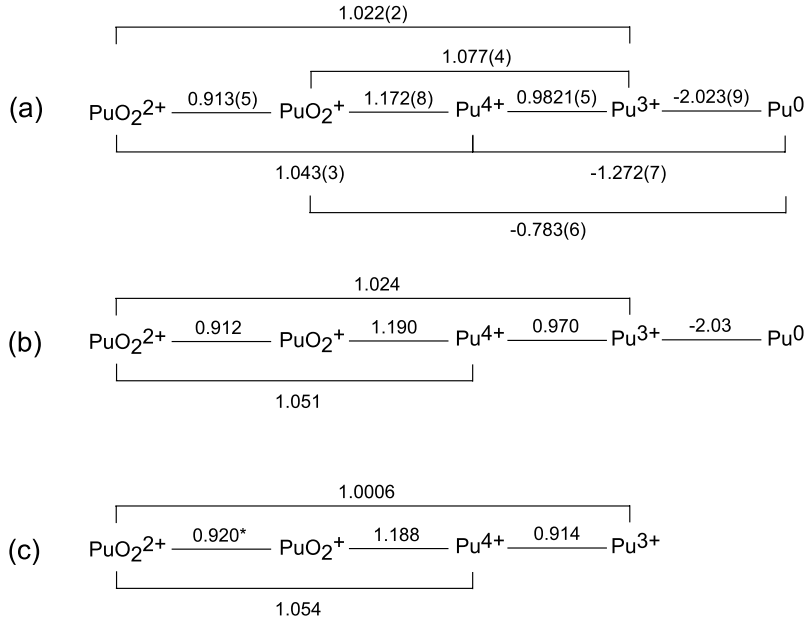

Fig. 7.116 *Formal redox potentials for selected plutonium couples at* 25°C *in V vs SHE* (*a*) *in* 1 M $HClO_4$ (*Lemire* et al., 2001), (*b*) *in* 1 M *HCl* (*Rabideau and Cowan*, 1955*; Rabideau* et al., 1959), *and* (*c*) 1 M HNO_3 (*Artyukhin* et al., 1958).

The formal potential of the Pu(VII)/Pu(VI) couple depends upon the square of the hydroxide ion concentration, and is about 0.85 V in 1 M NaOH, corresponding to the reaction (Spitsyn *et al.*, 1969; Musante and Ganivet, 1974; Krot, 1975):

$$PuO_4(OH)_2^{3-} + 2H_2O \rightleftarrows PuO_2(OH)_4^{2-} + 2OH^- + e^- \qquad (7.74)$$

In voltammetric studies performed at lower hydroxide concentration (with a different proposed reaction), the Pu(VII/VI) reduction in 0.01 M hydroxide ion was observed at +1.20 V vs standard hydrogen electrode (Musante and Ganivet, 1974). Due to the instability of Pu(VII) at low hydroxide concentration (and therefore low ionic strength) it is not possible to extrapolate the potential to estimate a standard potential and other standard thermodynamic values.

The redox couples between Pu(V)/Pu(III), Pu(VI)/Pu(III), Pu(V)/Pu(IV), and Pu(VI)/Pu(IV), are quasireversible or irreversible because they involve the breaking or forming of Pu=O multiple bonds. In contrast, the redox couples between species where no Pu=O bond forming or breaking occurs, such as Pu(IV)/Pu(III), Pu(VI)/Pu(V), and Pu(VII)/Pu(VI) couples are reversible. Experimental, standard, and predicted reduction and oxidation potentials have been reported under a wide range of conditions, with the exception of those for Pu(VII). Standard redox potentials in acidic solution are described in greater detail in Chapter 19. Since the redox couples that connect the four main oxidation states (III, IV, V, VI) are relatively similar, it is possible for all four oxidation states to coexist under the appropriate solution conditions. The ability to have multiple oxidation states in solution at the same time will depend upon several key factors. The most important of these are the tendency of Pu(IV) and Pu(V) to disproportionate, and the relatively slow kinetics of reactions that involve the making or breaking of Pu=O bonds in plutonyl ions (PuO_2^+ and PuO_2^{2+}). Other factors are plutonium ion concentration, ionic strength, pH, temperature, and presence or absence of complexing ligands. Thermodynamic and activation data for redox reactions between plutonium ions are summarized in Table 7.51.

(*ii*) *Disproportionation of Pu(IV)*

In acid solution in the absence of complexing ligands, the disproportionation of Pu(IV) proceeds according to the following equation:

$$3Pu^{4+} + 2H_2O \rightleftharpoons 2Pu^{3+} + PuO_2^{2+} + 4H^+ \qquad (7.75)$$

From this equation one can derive the equilibrium constant expression as:

$$K = \frac{[Pu^{3+}]^2[PuO_2^{2+}][H^+]^4}{[Pu^{4+}]^3} \qquad (7.76)$$

Rabideau carefully determined the equilibrium constant for this reaction in $HClO_4/NaClO_4$ solution under a constant ionic strength of 1.0 M (Rabideau, 1953). Rabideau's work on this system is seminal in that it takes into account the plutonium self-reduction by α particle radiolysis, and the hydrolysis of Pu(IV) at low pH. The concentration of Pu(IV) in the equilibrium constant expression above has been corrected for both effects. The equilibrium constant, K, was determined to have a weighted average value of 0.0089 for 1.0 M ionic

Table. 7.51 *Thermodynamics and activation data for plutonium redox reactions* (*Newton,* 2002).

Process	I (M)	ΔG (kJ mol^{-1})	ΔH (kJ mol^{-1})	ΔS (J K^{-1} mol^{-1})	*S* complex* (J K^{-1} mol^{-1})	*References*
$Pu^{3+} + {}^*Pu^{4+} = Pu^{4+} + {}^*Pu^{3+}$		0.0	0.0	0.0	0.0	
$Pu^{3+} + Pu^{4+} + H_2O = [Pu(Pu)OH^*]^{6+} + H^+$	2	56.1	31.0	-84.2 ± 17	-485	Keenan (1957)
$Pu^{3+} + PuO_2^+ + 4H^+ = 2Pu^{4+} + 2H_2O$		-18.2	-120.9	-344		
$Pu^{3+} + PuO_2^+ + H^+ = [Pu(PuO_2)H^*]^{5+}$	1	82.5	33.5	-164 ± 2	-332	Lavallee and Newton (1972)
	2	78.3	43.1	-117 ± 3	-289	Koltunov *et al.* (1980b)
$Pu^{3+} + PuO_2^{2+} = Pu^{4+} + PuO_2^+$		6.3	-35.6	-140		
$Pu^{3+} + PuO_2^{2+} = [Pu(PuO_2)^*]^{5+}$	1	70.7	20.1	-169 ± 1	-416	Rabideau and Kline (1958)

strength. Rabideau and Cowan (1955) subsequently studied this same disproportion reaction in HCl solution and found the same fourth order dependence on hydrogen ion concentration. It was concluded that the mechanism of Pu(IV) disproportion was identical in both media. The fourth order dependence on hydrogen ion concentration is consistent with experimental observations of essentially no disproportionation of Pu(IV) in strongly acidic solutions. The study in HCl solution is somewhat more straightforward in that α particle reduction was essentially absent. In addition, the value of the equilibrium constant is somewhat smaller ($K = 0.00192$ in 1 M HCl) than observed in perchloric acid ($K = 0.0084$ in 1 M $HClO_4$) and this difference is attributed to stabilization of Pu(IV) ions by complexation with chloride ions in HCl solution. Rabideau and Cowan (1955) also examined the temperature dependence of the equilibria in HCl, and found that raising the temperature from 25 to 45°C increased the value of the equilibrium constant by a factor of 70 ($K = 0.00142$ at 25°C; $K = 0.0967$ at 45.16°C).

Connick studied the kinetics of the disproportionation reaction and found that the overall reaction takes place in two separate steps with a transient Pu(V) intermediate (Connick, 1949). In the first slow step (equation (7.77)), two equivalents of Pu(IV) combine to generate Pu(III) and Pu(V). This reaction is slow because it involves the formation of a Pu=O bond in forming Pu(V). In the second step (equation (7.78)), the Pu(V) produced in the first step reacts with Pu(IV) in a rapid equilibrium.

$$2Pu^{4+} + 2H_2O \rightleftharpoons Pu^{3+} + PuO_2^+ + 4H^+ \text{ (slow)} \tag{7.77}$$

$$PuO_2^+ + Pu^{4+} \rightleftharpoons Pu^{3+} + PuO_2^{2+} \text{ (fast)} \tag{7.78}$$

Thus, the disproportionation is complete when both reactions (7.77) and (7.78) have reached equilibrium. The addition of equations (7.77) and (7.78) yields the common representation of the Pu(IV) disproportionation reaction that was given in equation (7.75). Equation (7.75) represents a reaction that comes to equilibrium in any plutonium solution, but equation (7.75) does not adequately represent the disproportionation of tetravalent plutonium because it fails to include Pu(V), even as an infinitesimally small intermediate. Silver (1971, 2003) has shown that a linear combination of equations (7.77) and (7.78) produces a new equation for the dissociation of Pu(IV) and is shown in equation (7.79), where the parameter M represents the equilibrium ratio for $[PuO_2^{2+}]/[PuO_2^+]$.

$$\begin{aligned}(2 + 3M)[Pu^{4+}] + (2M + 2)[H_2O] \rightleftharpoons (1 + 2M)[Pu^{3+}] \\ + [PuO_2^+] + M[PuO_2^{2+}] + (4M + 4)[H^+]\end{aligned} \tag{7.79}$$

The value of M was found as the root of the cubic equation (7.80) where $K_{(7.77)}$ and $K_{(7.78)}$ are the equilibrium constants for equations (7.77) and (7.78), respectively.

$$K^2_{(7.78)}[H^+]^4 - K_{(7.77)}(M^2 + 2M^3) = 0 \tag{7.80}$$

As the value of the ratio M increases, the coefficient of Pu(v) decreases and the stoichiometry of equation (7.79) approaches the stoichiometry of equation (7.75). In 1 M perchloric acid, the value of M is about 50.

(*iii*) *Disproportionation of Pu*(*v*)

In moderately acidic solutions Pu(v) is unstable towards disproportionation reactions. The disproportionation of Pu(v) into Pu(vi) and Pu(iv) or Pu(iii) is expected to proceed by either of two possible mechanisms. From a study of the rate of the disproportionation of Pu(v) in 0.5 M HCl, Connick (1949) has shown that the actual mechanism consists of the slow reaction (7.81) coupled with the rapid equilibrium (7.78).

$$PuO_2^+ + Pu^{3+} + 4H^+ \rightleftharpoons 2Pu^{4+} + 2H_2O \text{ (slow)} \tag{7.81}$$

$$PuO_2^+ + Pu^{4+} \rightleftharpoons Pu^{3+} + PuO_2^{2+} \text{ (fast)} \tag{7.78}$$

with an overall reaction

$$3PuO_2^+ + 4H^+ \rightleftharpoons Pu^{3+} + 2PuO_2^{2+} + 2H_2O \tag{7.82}$$

Connick (1949) pointed out that the disproportionation of Pu(v) proceeded by the mechanism of equation (7.82) under the conditions of his experiment, but that this mechanism cannot be true under all circumstances. At very low concentrations of Pu(iii) the mechanism must necessarily change to that represented by equation (7.83).

$$2PuO_2^+ + 4H^+ \rightleftharpoons Pu^{4+} + PuO_2^{2+} + 2H_2O \tag{7.83}$$

Thus equations (7.82) and (7.83) are limiting cases for Pu(v) disproportionation, and the actual reaction path depends on the plutonium species present in solution (Connick, 1949). The use of equations (7.82) or (7.83) have been widely cited in the literature, but Connick's original caveats on their intimate connection to solution conditions has not always been kept in mind. Without this understanding, equations (7.82) and (7.83) would appear to be contradictory because they do not predict the same reaction products (Pu^{3+} in (7.82), and Pu^{4+} in (7.83)). Under many solution conditions encountered in the laboratory, Pu(v) disproportionation may follow both mechanisms, in which case neither equation 7.82 or 7.83 by itself adequately describes Pu(v) disproportionation. This apparent discrepancy has been discussed in detail by Silver (1971, 1997, 2002, 2004) who has shown that the disproportionation reaction under any particular solution condition can be expressed as a linear combination of these two limiting cases. In this manner Pu(v) disproportionates in accordance with

the stoichiometry of equation (7.84), where the parameter M represents the equilibrium ratio for $[PuO_2^{2+}]/[PuO_2^{+}]$.

$$\begin{aligned}(3 + 2M/K_{(7.78)})[PuO_2^{+}] + (4 + 4M/K_{(7.78)})[H^{+}] \rightleftharpoons \\ [Pu^{3+}] + (M/K_{(7.78)})[Pu^{4+}] + (2 + M/K_{(7.78)})[PuO_2^{2+}] \\ + (2 + 2M/K_{(7.78)})[H_2O]\end{aligned} \tag{7.84}$$

The value of M was found as the positive, real root of equation (7.85) where $K_{(7.78)}$ and $K_{(7.77)}$ are the equilibrium constants for equations (7.78) and (7.77), respectively.

$$2K_{(7.78)}^2[H^{+}]^4 + (K_{(7.78)}[H^{+}]^4 M - K_{(7.77)}M^3) = 0 \tag{7.85}$$

The mathematical details are beyond the scope of this discussion, and the interested reader should see the works of Silver (1971, 1997, 2002, 2004) for more detail.

It is noteworthy that both reactions 7.82 and 7.83 for the disproportionation of Pu(v) have equilibrium constants with a fourth order dependence on the hydrogen ion concentration. This illustrates why Pu(v) solutions are only stable at near-neutral pH where the hydrogen ion concentration is low. Many workers have used this observation to prepare solutions of Pu(v) in the absence of other oxidation states (Gevantman and Kraus, 1949; Markin and McKay, 1958; Gel'man and Zaitseva, 1965a,b; Newton, Hobart *et al.*, 1986a).

Rabideau studied the kinetics and mechanism of the Pu(v)-Pu(v) reaction in the absence of Pu(iii) (Rabideau, 1957).

(*iv*) *Equilibrium between Pu*(*iii*), (*iv*), (*v*), *and* (*vi*)

The reaction that describes the equilibrium between all four oxidation states has been used in the discussion of the disproportionation of Pu(iv) and Pu(v). The equilibrium constant for this reaction is given by:

$$K = \frac{[\text{Pu(III)}][\text{Pu(VI)}]}{[\text{Pu(IV)}][\text{Pu(V)}]} \tag{7.84}$$

This equilibrium constant has been determined in various media, but not all studies have corrected for the hydrolysis of Pu(iv). Rabideau and Kline (1958) determined this equilibrium constant in unit ionic strength $HClO_4/NaClO_4$ solution for various hydrogen ion concentrations. They obtained a value of $K = (13.1 \pm 0.08)$ at 25°C that is corrected for hydrolysis and is independent of H^+ concentration over the range $0.1 \leq H^+ \leq 1.0$ M. In D_2O solution, the corresponding hydrolysis-corrected value was determined to be (40.6 ± 1.0). Rabideau and Kline studied the kinetics of the reaction in both H_2O and D_2O solution, and determined that a hydrogen atom transfer process is not

involved in the reaction. In complexing acids such as HCl and HNO_3, the equilibrium was found to shift to favor higher concentrations of Pu^{4+}.

Because this system is rather complicated, it is instructive to examine a series of figures that describe the system under various conditions. Equilibrium oxidation state distribution diagrams are useful for predicting the behavior of various plutonium stock solutions made up in the laboratory. Equilibrium diagrams showing the predominant oxidation state as a function of pH and average oxidation state for 1.0 M ionic strength are given in Fig. 7.117.

Fig. 7.117(a) shows the distribution for a solution with average oxidation state IV. It is seen that a solution which is initially pure Pu(IV) will contain significant concentrations of Pu(III) and Pu(VI) at equilibrium in 1 M acid. At pH 1 Pu(III) predominates and at pH 2 the solution is primarily a mixture of Pu(III) and Pu(V). The calculations that produced these plots took the first hydrolysis constant for Pu(IV) into account. It should be pointed out that the distribution in the region between pH 1 and 2 is less certain as the second hydrolysis constant was not taken into account. A small amount of irreversible hydrolysis to give colloidal Pu(IV) hydroxide is also expected at very low concentrations. Fig. 7.117(b) shows a distribution for a solution with average oxidation state V, for example an equimolar mixture of Pu(IV) and Pu(VI). Here, Pu(VI) predominates until a pH of about 1.2 is reached. At higher values, Pu(V) becomes predominant.

It is also important to know how rapidly redox equilibria will be reached in plutonium solutions. The rate constants and hydrogen ion dependences for the reactions above are known for solutions at 25°C and unit ionic strength. The kinetics of the system are somewhat complicated in that the forward and reverse

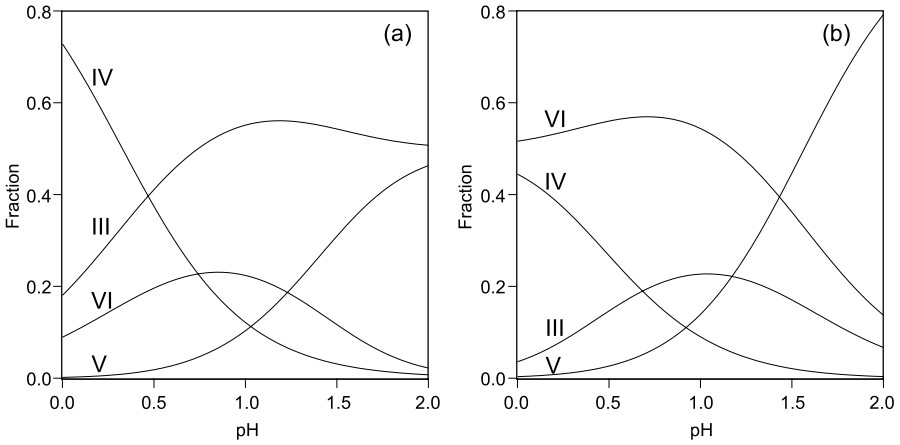

Fig. 7.117 *Oxidation state distribution diagram showing the predominant oxidation state of plutonium in* 1 M *(H,Na)*ClO_4 *solution as a function of pH and* (*a*) *average oxidation state Pu(IV), and* (*b*) *average oxidation state Pu(V)* (*calculations courtesy of T. W. Newton*).

rates of all three of the reactions listed above must be considered. The disproportionation of Pu(IV) in 0.1 M acid has been calculated and the results for 1.0 M ionic strength at pH 1.0 are shown in Fig. 7.118(a). Appreciable concentrations of the other oxidation states appear after relatively short periods of time. The rates depend on the total plutonium concentration, so the time scale is given in units of M s (molar second). The time required to reach any particular distribution is found by dividing the total concentration. For example, Fig. 7.118(a) indicates that if the concentration of Pu(IV) is 0.002 M, then half of the Pu(IV) will be gone in about 3 hours. In a similar fashion, Pu(V) is quite stable at pH 3 and can be formed, for example, by mixing Pu(III) and Pu(VI). The course of this reaction at unit ionic strength is shown in Fig. 7.118(b). For a concentration of 0.001 M, equilibrium is reached in about a day and within about 10% of equilibrium within about 5 hours. Reducing the ionic strength decreases the rate. Selected oxidation and reduction rate data for different plutonium oxidation states are given in Table 7.52.

(*v*) *Preparation and stability of pure oxidation states*

Newton and coworkers have provided excellent experimental procedures for the preparation of oxidation state pure plutonium solutions. The following discussion comes essentially from Newton *et al.* (1986a).

Pu(III). Acidic solutions of Pu(III) are conveniently prepared by dissolving weighed samples of pure α-phase metal in 6 M HCl or $HClO_4$, with cooling, followed by dilution to the desired concentration. Corrosion products on the

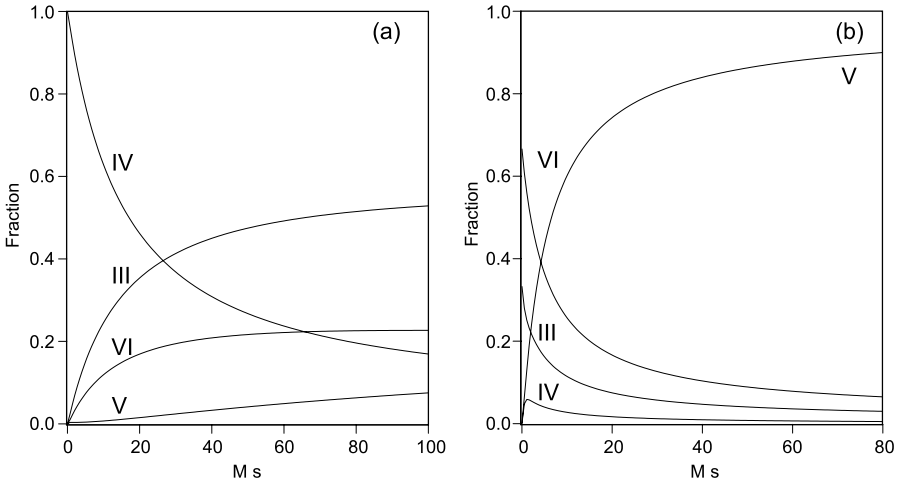

Fig. 7.118 *Kinetics for disproportionation of plutonium in* 1 M $(H,Na)ClO_4$ *solution at* (*a*) *pH 1 and average oxidation state Pu*(IV), *and* (*b*) *pH 3 and average oxidation state Pu*(V) (*calculations courtesy of T. W. Newton of Los Alamos*).

Table 7.52 *Selected plutonium oxidation and reduction rate as compiled by data Newton* (2002).

Agent	*Concentration* (M)	*Solution*	*Temperature* (°C)	*Results*	*References*
Pu(III) oxidation					
NO_3^-	0.2 ($NaNO_3$)	0.5 M HCl	room	$t_{1/2} \approx 600$ h; autocatalytic; rapid in 16 M HNO_3	Connick (1954)
HNO_2	~0.05	2 M HNO_3	16	$k'' = (0.88 \pm 0.03)$ $[HNO_2]^{0.5}[H^+]^{0.5}[NO_3^-]^{0.4}$ M^{-1} min^{-1} E_a (16–32°) = (55.8 ± 3.4) kJ mol^{-1} net reaction is the HNO_2 catalyzed oxidation of Pu(III) by HNO_3	Koltunov and Marchenko (1973) and Newton (2002)
Pu(IV)	3×10^{-6}	2 M (H,Li)ClO_4	25	$k'' = 6.4 \times 10^4$ $[H^+]^{-1}$ M^{-1} s^{-1} $E_a = (31 \pm 5)$ kJ mol^{-1} also studied in Cl^- and SO_4^{2-} solutions	Keenan (1957) Nikitenko and Ponomareva (1989)
Pu(V)	1.3×10^{-3}	2 M (H,Na)NO_3	38	$k'' = (k + k_1[NO_3^-][H^+])$ M^{-1} s^{-1} $k_o = (0.21 \pm 0.09)$ M^{-2} s^{-1} $k_1 = (0.59 \pm 0.07)$ M^{-3} s^{-1}	Koltunov and Mikhailova (1977) and Newton (2002)
Pu(VI)	10^{-4}	1 M $HClO_4$	25	$k'' = 2.68[H^+]^0$ M^{-1} s^{-1} $\Delta H^* = (20.2 \pm 0.4)$ kJ mol^{-1}	Rabideau and Kline (1958) Alei *et al.* (1967)
Pu(IV) oxidation					
HNO_3	1–5	HNO_3	90	steady-state Pu(IV)–Pu(VI) concentrations reached in about 1 d. Fraction Pu(VI) at the steady state is given by $0.11([Pu(IV)]_0)^{-0.61}$ $([HNO_3])^{-0.74}$	Glazyrin *et al.* (1989)

O_3		1 M $(H,Na)NO_3$	20	$k = (1.32 \pm 0.13) \times 10^{-2}\ [O_3]^0[H^+]^{-1}\ min^{-1}$ $[Pu(IV)] = 10^{-6}$–10^{-5} M $E_a = (19 \pm 5)$ kJ mol^{-1}	Vyatkin *et al.* (1972)
Pu(V) oxidation					
Ce(IV)	6×10^{-5}	2 M $HClO_4$	23	very rapid; $k'' > 7 \times 10^5\ M^{-1}\ s^{-1}$	Newton and Burkhart (1971)
O_2	1 atm	4 M NaOH	25 ± 2	$k = 4.5 \times 10^{-4}\ min^{-1}$	Budantseva *et al.* (1998)
Pu(IV) reduction					
Fe(II)	2×10^{-3}	2 M $(H,Li)ClO_4$	20	$k'' = 27[H^+]^{-1}\ M^{-1}\ s^{-1}$ $E_a = (82 \pm 2.5)$ kJ mol^{-1}	Newton and Cowan (1960)
$H_2C_2O_4$ oxalic acid	0.04 excess Pu(IV)	5 M $(H,Na)NO_3$	98	$k'' = \dfrac{0.215}{[Pu(IV)] + [H^+]^2/K}\ M^{-1}\ min^{-1}$ $K = 86.8$ M $= [PuC_2O_4^{2+}][H^+]^2/[Pu^{4+}][H_2C_2O_4]$ (recalculated from the original data)	Newton (2002)
H_2O_2	~0.01	2 M $(H,Na)NO_3$	25	$k'' = (11.9 \pm 1.0)[H^+]^{-1}[NO_3^-]^{-1}$ E_a (15–45°) $= (95.5 \pm 3.8)$ kJ mol^{-1}	Koltunov *et al.* (1981a)
H_2O_2	7.9×10^{-4}	0.5 M HCl	25	$t_{1/2} = 64$ min (excess H_2O_2) complicated by rapid formation of Pu(IV)–H_2O_2	Mazumdar *et al.* (1970)
NH_3OH^+	~0.1	2.5 M $(H,Na)(NO_3,ClO_4)$	25	$k'' = 13.7/[[H^+]^2\ (1 + [NO_3^-]/0.35)]\ M^{-1}\ s^{-1}$ E_a (25–45°) $= (120 \pm 8)$ kJ mol^{-1} for approach to equilibrium in the reaction: $Pu(IV) + NH_3OH^+ = Pu(III) + NHOH\bullet + 2H^+$	Barney (1976)

Table 7.52 (*Contd.*)

Agent	*Concentration* (M)	*Solution*	*Temperature* (°C)	*Results*	*References*
			30	$-d[Pu(IV)]/dt = (0.27 \pm 0.07)\left(\frac{[Pu(IV)][NH_3OH^+]}{[Pu(III)][H^+]^2(1+[NO_3^-]/0.33)}\right)^2$ M min^{-1} E_a (30–45°) = (186 ± 8) kJ mol^{-1} after equilibrium established	
NH_3OH^+ oxidized to N_2	0.2	3 M HNO_3	30	$-d[Pu(IV)]/dt = (0.195 \pm 0.013)\left(\frac{[Pu(IV)][NH_3OH^+]}{[Pu(III)][H^+]^2(1+[NO_3^-]/0.33)}\right)^2$ M min^{-1} E_a (30–45°) = (205 ± 3) kJ mol^{-1} after equilibrium established	Koltunov and Zhuravleva (1978)
Pu(IV) (disproportionation)	1×10^{-2}	1 M (H,Na)ClO_4	25	$-d[Pu(IV)]/3dt = [Pu^{4+}]^2(2.56 \times 10^{-5}\,[H^+]^{-3} + 3.9 \times 10^{-6}\,[H^+]^{-4})$ M s^{-1} also studied in HNO_3 solutions	Rabideau (1953) Artyukhin *et al.* (1959)
Pu(V) reduction					
ascorbic acid $C_6H_8O_6$	0.02	2 M (H,Na)ClO_4	25	$k' = (4.2 \pm 0.4)10^{-2}[H^+]^{1.2}$ M^{-1} min^{-1} E_a (25.1–44.9°) = (57.3 ± 6.3) kJ mol^{-1}	Koltunov *et al.* (1980a)
		4 M (H,Na)ClO_4	25	$k' = (7.4 \pm 0.5)10^{-2}[H^+]^{2.2}$ M^{-1} min^{-1} *note*: the reaction studied occurs in parallel with the reduction of Pu(V) by Pu(III). Pu(III) is the final product	

Pu(V)	$\sim 10^{-3}$	1 M $(H,Na)ClO_4$	25	$k'' = 3.6 \times 10^{-3}\ [H^+]\ M^{-1}\ s^{-1}$ $\Delta H^* = (79 \pm 4)$ kJ mol^{-1}	Rabideau (1957)
	5.3×10^{-4}	3.3 M NaOH	22	$k'' = 0.024\ M^{-1}\ s^{-1}$ E_a (10–30°) = 88 kJ mol^{-1}	Shilov (1997)
Pu(VI) reduction					
EDTA	2×10^{-3}	1 M $NaClO_4$ pH 3–5	room	$k'' = 4.3 \pm 1.6\ M^{-1}\ s^{-1}$	Kabanova *et al.* (1960)
Fe(II)	4×10^{-5}	2 M $(H,Li)ClO_4$	25	$k'' = 1000 + (2 \times 10^{-4} + 1.3 \times 10^{-3}\ [H^+])^{-1}\ M^{-1}\ s^{-1}$ evidence for a binuclear intermediate $E_a = (22.6 \pm 0.8)$ kJ mol^{-1} for first rate constant	Newton and Baker (1963) and Beitz *et al.* (1986)
HNO_2	0.027	0.55 M $(H,Na)NO_3$	20	$k'' = (2.4 \pm 0.2)/[H^+]\ M^{-1}\ min^{-1}$	Koltunov and Zhuravleva (1968)
	0.02	2 M $(H,Na)NO_3$	22	(a) forward reaction $k'' = (10.55 \pm 0.86)/[H^+]\ M^{-1}\ min^{-1}$ E_a (8–30°) = (111 ± 2) kJ mol^{-1} (b) reverse reaction $k'' = (9.63 \pm 0.42)\ \dfrac{[NO_3^-]^{0.4}[H^+]^{0.6}}{[HNO_2]^{0.5}}\ M^{-1}\ min^{-1}$ E_a (8–30°) = (92 ± 3) kJ mol^{-1}	Koltunov and Ryabova (1980)
NH_3OH^+	0.016	3 M $(H,Na)ClO_4$	60	$k'' = (4.22 \pm 0.12)/[H^+]\ M^{-1}\ min^{-1}$ $E_a = (78 \pm 2)$ kJ mol^{-1}	Koltunov *et al.* (1981b)

Table 7.52 (*Contd.*)

Agent	*Concentration* (M)	*Solution*	*Temperature* (°C)	*Results*	*References*
$N_2H_5^+$	0.02	2 M (H,Na) (NO_3,ClO_4)	40	$k'' = (0.314 \pm 0.042)$ $[H^+]^{-1}[NO_3^-]^0$ M^{-1} min^{-1} $-d[Pu(VI)]/dt = k_a[Pu(VI)]\left(\frac{[N_2H_5^+]}{[H^+]}\right)^{0.85}$ $k_a = (0.243 + 0.024)$ min^{-1} $E_a = (67.4 \pm 0.8)$ kJ mol^{-1} for either rate law	Koltunov and Zhuravleva (1973) and Newton (2002)
EDTA	2×10^{-3}	1 M $NaClO_4$; pH 3–5	room	$k'' = 4.3 \pm 1.6$ M^{-1} s^{-1}	Kabanova *et al.* (1960)

surface of the metal may be removed electrochemically (Bergstresser, 1950) or mechanically. The standard potential for the three-electron oxidation of α-Pu metal is –(2.000 ± 0.009) V (Lemire *et al.*, 2001). Alternatively, plutonium in higher oxidation states in acid solutions may be reduced electrolytically using either a mercury or platinum cathode. The potential should be about 0.75 V (vs NHE) or less (Cohen, 1961a). Chemical reductants such as hydroxylamine or hydrazine may also be used, but these are generally less satisfactory because the oxidized form of the reducing agent is often left in the solution. The Pu(III) aquo ion imparts a blue or blue-violet color to aqueous acidic solutions and exhibits hydrolysis, complexation, and solubility properties similar to the rare-earth ion neodymium(III).

In solutions of noncomplexing acids, Pu(III) is stable with respect to reaction with the oxygen in air. However, in dilute sulfuric acid, for example, the reaction occurs at a conveniently measurable rate (Newton and Baker, 1956). At a pH of 4, Pu(III) is slowly oxidized but at pH values greater than about 4 or 5, or in 0.4 M $NaHCO_3$, Pu(III) is rapidly oxidized by atmospheric oxygen (Newton *et al.*, 1986a). For ^{239}Pu, α-particle induced oxidation occurs in $HClO_4$ solutions at a rate of about 1.5% per day, approaching a steady state containing about 10% Pu(IV) and 90% Pu(III) (Rabideau *et al.*, 1958). In HCl solutions the α-particle induced oxidation proceeds to nearly pure Pu(IV) (Newton *et al.*, 1986a).

Pu(IV). Solutions of Pu(IV) are conveniently prepared by the electrolytic oxidation of Pu(III) at about 1.2 V. At this potential Pu(VI) is thermodynamically stable, but its rate of formation is insignificant due to the slow kinetics of forming the Pu=O bond (Cohen, 1961a). Alternatively, Pu(IV) may be prepared by reacting Pu(III) with Pu(VI) according to the equation:

$$2Pu^{3+} + PuO_2^{2+} + 4H^+ \rightleftharpoons 3Pu^{4+} + 2H_2O \qquad (7.86)$$

This reaction is the reverse of the Pu(IV) disproportionation reaction (equation 7.75), and the equilibrium constant is approximately 112 in 1 M $HClO_4$ solution at 25°C (Rabideau, 1953), so at equilibrium under these conditions as much as 28% of the plutonium will be in other oxidation states. Higher acid concentrations or the presence of complexing anions such as chloride will give larger fractions of Pu(IV). This is why it is a common practice to prepare and store Pu(IV) solutions in 3 M HCl (Newton *et al.*, 1986a). Acidic solutions of Pu^{4+} that are free of complexing agents are orange-brown or tan in color.

In acid solutions Pu(IV) is thermodynamically unstable with respect to reaction with oxygen, but the rate of this reaction is negligible. In $HClO_4$, α-particle induced reduction occurs to give the same steady state as described for Pu(III). In HCl solutions, however, Pu(IV) is significantly stabilized (Rabideau *et al.*, 1958). Newton *et al.* (1986a) found that stock solutions of Pu(IV) in about 3 M HCl are stable for many months. Even in 1 M acid, Pu(IV) hydrolyzes appreciably, and, at pH values greater than about 1, significant formation of green colloidal Pu(IV) hydroxide occurs. The rate of colloid formation depends on the plutonium concentration as well as the pH. Rates under specific conditions

have been described (Costanzo *et al.*, 1973; Toth *et al.*, 1981; Newton and Rundberg, 1984). Complexation constants for tetravalent plutonium are among the highest for any cation of any element, being most similar to those of Th(IV), U(IV), and Np(IV).

Pu(V). Solutions of Pu(V) are conveniently prepared by the electrolytic reduction of 0.02 M Pu(VI) in $HClO_4$ solution at pH near 3. A potential close to 0.54 V (vs SCE) is suitable (Cohen, 1961a). In most preparations it is necessary to readjust the pH during electrolysis because hydrogen ions are transported from the counter electrode compartment (Newton *et al.*, 1986a). The use of a photochemically produced reducing agent in a two-phase system has also been described (Choppin and Saito, 1984). The PuO_2^+ ion imparts a pink or light purple color to aqueous solutions, has a low effective charge and undergoes hydrolysis only at higher pH (approximately pH = 9 for millimolar plutonium).

In acid solution Pu(V) disproportionates with the reaction rate proportional to the fourth power of the hydrogen ion concentration and the square of the Pu(V) concentration (Rabideau, 1957). Thus both the thermodynamics and the kinetics favor Pu(V) at low acidities. However, α-radiolysis effects, even at pH values greater than 3, cause fairly rapid formation of colloidal Pu(IV) and Pu(VI) (Newton *et al.*, 1986b). These effects are more pronounced at higher Pu(V) concentrations, and less pronounced at low concentrations. Pu(V) can persist in near-neutral pH solutions when the total plutonium concentration is very low ($<10^{-6}$ M), as may be the case in slightly-contaminated natural waters and some waste solutions.

Pu(VI). Solutions of Pu(VI) are conveniently prepared by oxidation with hot, concentrated $HClO_4$ (Newton *et al.*, 1986a). Plutonium ions in lower oxidation states, in the absence of coordinating anions are oxidized to Pu(VI) by fuming strongly with $HClO_4$. The remaining free acid may be estimated gravimetrically and traces of chlorine oxides can be removed by boiling the diluted solutions. Acidic solutions of PuO_2^{2+} in the absence of complexing agents are yellow or orange in color. Hexavalent plutonium nitrate can also be generated by heating nitric acid solutions of plutonium almost to dryness at about 170°C. A glassy solid results after cooling the nitrate melt that is a very stable storage form for Pu(VI) and is readily soluble in aqueous solutions (Stoll *et al.*, 1982).

In $HClO_4$ solutions Pu(VI) is unstable with respect to α-particle induced reduction. With millimolar or greater plutonium concentrations, at pH values between about 0 and 2, the rate of reduction is about 1.2 to 2% of the total plutonium per day (Rabideau *et al.*, 1958; Newton *et al.*, 1986b). At very low plutonium concentrations (2.2×10^{-5} M) the rates are much slower. It has also been reported that chloride ions inhibit the α-reduction of Pu(VI) in analogy with Pu(IV) (Rabideau *et al.*, 1958).

Pu(VII). Blue-black heptavalent plutonium is the least stable oxidation state, prepared by vigorous oxidation of highly alkaline solutions of hexavalent plutonium. In alkali solutions, ozonization, anodic oxidation or treatment with peroxydisulfate, or other strong oxidants can produce the heptavalent form (Komkov

et al., 1969; Krot *et al.*, 1976; Tananaev *et al.*, 1992). The high formal potential of Pu(VII) puts it outside the region of thermodynamic stability of water for hydroxide concentrations less than about 7 M, and heptavalent plutonium is instantly reduced in acid solutions. This plutonium ion is less stable than the heptavalent neptunium analog (Varlashkin *et al.*, 1984; Tananaev *et al.*, 1992).

(*vi*) *Pu(VI) oxygen exchange with solvent water*

Masters and Rabideau (1963) measured the rate of exchange between PuO_2^{2+} and ^{18}O-enriched water in dilute $HClO_4$ solution. The studies were conducted under chlorine atmosphere to ensure that Pu(VI) was the only oxidation state present. This was done because the rate of exchange was found to be accelerated by the presence of lower oxidation states of plutonium in the solutions (Rabideau and Masters, 1963). Like the exchange for the uranyl ion (Gordon and Taube, 1961), the exchange rate was found to be extremely slow with a half-time of 4.55×10^4 h at 23°C. The exchange rate was found to be the sum of the rates of two separate reaction paths that include the intrinsic $PuO_2^{2+} - H_2^{18}O$ exchange reaction and the exchange induced by the breaking of Pu=O bonds by α-particle reduction. Studies employing ^{238}Pu demonstrated that the exchange rate was much faster than with ^{239}Pu, and extrapolation of the rates to the flux conditions of ^{239}Pu solutions suggested a half-time for radiation-induced exchange of about the same order of magnitude (approximately 10^4 h). This was interpreted as indicating that in 0.15 M Pu(VI) solution, the major contribution to the exchange is from radiation-induced reaction, and that the rate of the intrinsic exchange reaction is even slower.

(*vii*) *Oxidation and reduction by actinide ions*

These reactions have been studied primarily in acidic solutions because hydrolysis and precipitation of these high-valent metal ions limit their solubility at higher pH values. Most of the actinide separations and processing technology has been developed in acid solutions motivating much of the quantitative study of plutonium redox reactions. An important subset of these reactions has been described by Newton (2002) and is given in Table 7.53. The use of catalysts to enhance the rate of reactions has also been studied for plutonium both to accomplish process steps more rapidly on an industrial scale and to determine rate constants that are otherwise difficult to determine because of back reactions, competing reactions, or other complications (Newton, 1975).

The redox reactions between plutonium and other actinides are important because they are applicable to many aqueous solutions used in separation processes and waste operations. These reactions are also useful because the reactions involving ions with similar structures but different reduction potentials can be compared. For example, the rates of reactions (reaction 3 through

Table 7.53 *Thermodynamic constants for plutonium-actinide redox reactions at* 25°C (*Newton,* 2002).

	ΔG (kJ mol^{-1})	ΔH (kJ mol^{-1})	ΔS (J K^{-1} mol^{-1})	k'' (M^{-1} s^{-1})	I (M)	ΔG^* (kJ mol^{-1})	ΔH^* (kJ mol^{-1})	ΔS^* (J K^{-1} mol^{-1})	*References*
1. $Pu^{3+} + NpO_2^{2+} \rightleftarrows Pu^{4+} + NpO_2^+$									
	−15.1	−60.7	−153	$35.5 + 3.1\ [H^+]^{-1}$	1.0	64.2	14.6	−166	Fulton and Newton (1970)
2. $Pu^{3+} + PuO_2^{2+} \rightleftarrows Pu^{4+} + PuO_2^+$									
	6.3	−35.6	−140	2.7	1.0	70.5	20.2	−169	Rabideau and Kline (1958)
3. $2Pu^{4+} + 2H_2O \rightleftarrows Pu^{3+} + PuO_2^+ + 4H^+$									
	18.2	121	344	$2.9 \times 10^{-5}\ [H^+]^{-3}$	1.0	101.0	154.5 ± 0.5	180 ± 2	Lavallee and Newton (1972)
				$4.4 \times 10^{-2}\ [H^+]$[a]	1.0	80.8	33.5 ± 0.5	-158 ± 2	
4. $Np^{4+} + Pu^{4+} + 2H_2O \rightleftarrows NpO_2^+ + Pu^{3+} + 4H^+$									
	−23.4	92	387	$0.253\ [H^+]^{-3}$	2.0	76.6	142 ± 6	218 ± 21	Rykov *et al.* (1969)[b]
				$2.2 \times 10^{-5}[H^+]$	1.0	99.6	50	-167 ± 21	
5. $U^{4+} + Pu^{4+} + 2H_2O \rightleftarrows UO_2^+ + Pu^{3+} + 4H^+$									
	−36.4	68.5	352	$34.4\ [H^+]^{-2}$	2.0	64.3	102 ± 2.5	126 ± 8	Newton (1959)
				$1.9 \times 10^{-5}\ [H^+]^2$	1.0	100	33.1	-216 ± 8	

6. $U^{4+} + PuO_2^{2+} + 2H_2O = UO_2^{+} + PuO_2^{+} + 4H^{+}$								
	−30.0	33	213	$[(4.35[H^+]^{-1})^{-1} + (11.25[H^+]^{-2})^{-1}]^{-1}$	2	69.5	73.6 ± 0.4	15 ± 2	Newton (1958)
						66.9	88.8 ± 1.2	74 ± 5	
6a. $PuO_2^{2+} + U^{4+} + H_2O = [PuO_2(UOH)^{*}]^{5+} + H^{+}$									
	69.5	73.6	14 ± 2		2			−368	Newton (1958)
6b. $PuO_2^{2+} + U^{4+} + H_2O = [PuO_2(UO)^{*}]^{4+} + 2H^{+}$									
	66.9	89.1	75 ± 5		2			−303	Newton (1958)
7. $Np^{4+} + PuO_2^{2+} + 2H_2O \rightleftarrows NpO_2^{+} + PuO_2^{+} + 4H^{+}$									
	−17.1	56.5	247	$3.5 \times 10^{-4}\,[H^+]^{-2}$	1.0	92.76	130 ± 4	126 ± 13	Newton and Montag (1976)
				$8.8 \times 10^{-6}\,[H^+]^{-3}$	1.0	102	168 ± 8	222 ± 25	
8. $Pu^{4+} + PuO_2^{2+} + 2H_2O \rightleftarrows PuO_2^{+} + 4H^{+}$									
	24.5	85.3	204	$1.2 \times 10^{-7}\,[H^+]^{-3}$	2	112.5	164	172	Rabideau (1957)[c]
				$3.6 \times 10^{-3}\,[H^+]$[a]		87.0	79 ± 11	25 ± 38	

[a] The reaction was measured in the opposite direction, with the result given here.
[b] An estimate for the reverse reaction.
[c] Calculated from the reverse reaction.

8 in Table 7.53) that involve the making of An=O bonds as An^{4+} is oxidized to AnO_2^+ differ by orders of magnitude for the different elements. Four hydrogen ions are produced in the overall reaction, but only two or three are given up in the activation processes. The rate laws for oxidation of U^{4+} and Np^{4+} by PuO_2^{2+} show consecutive rate-determining steps of which only one or two can be redox reactions. This reaction is described below for U^{4+}, as an illustration of the importance of considering multiple intermediates and pathways.

The reaction between U^{4+} and PuO_2^{2+} proceeds through AnO_2^+ intermediates, and in acid solution leads eventually to Pu^{3+} (Newton, 1958, 1975). In dilute solutions (1.8×10^{-4} M Pu(VI) and 0.62×10^{-4} M U(IV) in 1 M $HClO_4$), approximately 96% of the U(IV) reacts according to the following equation:

$$2\text{Pu(VI)} + \text{U(IV)} \rightarrow 2\text{Pu(V)} + \text{U(VI)} \tag{7.87}$$

The remaining U(IV) reacts according to

$$\frac{2}{3}\text{Pu(VI)} + \text{U(IV)} \rightarrow \frac{2}{3}\text{Pu(III)} + \text{U(VI)} \tag{7.88}$$

Equations 7.87 and 7.88 only represent the change in oxidation states of the actinides but do not account for the overall stoichiometry. The reaction rates, as studied by spectrophotometric monitoring of the concentration of Pu(VI), are consistent with the rate law:

$$-\frac{\text{d[Pu(VI)]}}{\text{d}t} = 2k''[\text{Pu(VI)}][\text{U(IV)}] \tag{7.89}$$

This requires that the activated complexes be formed from one Pu(VI) and one U(IV), probably according to the reaction

$$\text{Pu(VI)} + \text{U(IV)} \rightarrow \text{Pu(V)} + \text{U(V)} \tag{7.90}$$

followed by the rapid reaction

$$\text{Pu(VI)} + \text{U(V)} \rightarrow \text{Pu(V)} + \text{U(VI)} \tag{7.91}$$

Steady-state calculations show that U(V) disproportionation into U(VI) and U(IV)

$$2\text{U(V)} \rightarrow \text{U(IV)} + \text{U(VI)} \tag{7.92}$$

is too slow to account for the disappearance of U(V) and is unimportant with respect to reaction (7.91). Under these conditions (1 M $HClO_4$) the U(IV) undergoes hydrolysis, while Pu(VI) does not. Thus

$$[\text{U(IV)}] = [U^{4+}](1 + K/[H^+]) \tag{7.93}$$

and

$$[\text{Pu(VI)}] = [PuO_2^{2+}] \tag{7.94}$$

where K is the first hydrolysis constant for U(IV). In terms of the species present, the rate law (7.89) becomes

$$-\frac{\mathrm{d}[\mathrm{Pu(VI)}]}{\mathrm{d}t} = 2k''\left(1+\frac{K}{[\mathrm{H^+}]}\right)[\mathrm{PuO_2^{2+}}][\mathrm{U^{4+}}] \tag{7.95}$$

The hydrogen-ion dependence as a function of temperature suggests that the most important activated complex is that formed by the prior loss of H^+, and that a second activated complex resulting from the loss of two H^+ ions may also be involved. The decrease in the apparent H^+ dependence with decreasing $[H^+]$ is not consistent with parallel rate-determining steps, but suggests consecutive reactions (6a and 6b in Table 7.53) instead.

From the linearity of $\{k''([H^+] + K)\}^{-1}$ vs $[H^+]$ for the data at each temperature (k_1 and k_2 are rate constants distinct from k' or k''). Newton arrived at the following rate law:

$$-\frac{\mathrm{d}[\mathrm{Pu(VI)}]}{\mathrm{d}t} = \frac{2[\mathrm{Pu(VI)}][\mathrm{U(IV)}]}{1+K/[\mathrm{H^+}]}\left(\frac{1}{k_1[\mathrm{H^+}]^{-1}}+\frac{1}{k_2[\mathrm{H^+}]^{-2}}\right)^{-1} \tag{7.96}$$

The rate law (7.96) governs many detailed mechanisms, all of which require a binuclear intermediate that can react to give products or dissociate to give reactants at rates that depend on $[H^+]$. A simple mechanism consistent with the rate law is:

$$\mathrm{U^{4+}} + \mathrm{H_2O} \rightarrow \mathrm{UOH^{3+}} + \mathrm{H^+} \quad \text{(rapid equilibrium)} \tag{7.97}$$

$$\mathrm{UOH^{3+}} + \mathrm{PuO_2^{2+}} \rightleftarrows \mathrm{PuO_2(UOH)^{5+}} \quad \text{(rate-determining, reversible)} \tag{7.98}$$

$$\mathrm{PuO_2(UOH)^{5+}} \rightarrow \mathrm{PuO_2(UO)^{4+}} + \mathrm{H^+} \quad \text{(rapid equilibrium)} \tag{7.99}$$

$$\mathrm{PuO_2(UO)^{4+}} + \mathrm{H_2O} \rightarrow \mathrm{UO_2^+} + \mathrm{PuO_2^+} + 2\mathrm{H^+} \quad \text{(rate-determining)} \tag{7.100}$$

The two net activation processes required by the rate law do not depend on the details of the mechanism. The activation parameters ΔG^*, ΔH^*, and ΔS^* for these processes as determined from simultaneous treatment of the hydrogen ion and temperature data are listed in Table 7.53 under reactions 6a and 6b. For a more detailed discussion of redox reactions between plutonium and other actinide ions, the reader is referred to Newton (2002).

(*viii*) *Oxidation and reduction by nonactinide species*

Plutonium ions are well known to undergo redox reactions with ions of almost every element in the periodic table and many inorganic and organic redox reagents. Almost all of the redox reactions of aqueous plutonium ions are first order in the oxidizing or reducing agent, but some are either inhibited or catalyzed by the reaction products. The rates are often strongly influenced by

the concentration of H^+ and of complexing ligands. For example, reductions using synthetic and natural organic acids, such as oxalic, ascorbic, hydroxamic, and humic acids are pH dependent with rates that generally increase with increasing [H^+] (Cleveland, 1979; Choppin *et al.*, 1986; Nikitenko, 1988; Czerwinski and Kim, 1997; Ruggiero *et al.*, 2000; Moulin and Moulin, 2001; Taylor *et al.*, 2002). Common strong oxidizing agents that are relatively poor ligands for the actinides, such as dichromate, bromate, and iodate, have comparatively rapid plutonium oxidation rates (Newton, 1975). A large body of empirical observations has been accumulated on the oxidation–reduction behavior of plutonium with various reagents, while quantitative data are available for a relatively small subset. Since among plutonium ions, Pu(IV) forms the strongest complexes, redox reactions of the other ions can be interpreted using similar but simplified reactions and rate laws.

There is a broad qualitative relation between the rates of redox processes and the particular plutonium ions involved. Generally, the reactions of Pu^{4+} with single-electron reductants, such as Fe^{2+}, are rapid. The oxidation of Pu^{3+} or the reduction of Pu^{4+} with two-electron reagents is expected to be slower, although the variation in rate for different reagents varies from slow to a rate too fast to measure. A similar situation exists for one-electron reduction of PuO_2^{2+} to PuO_2^{+}. In contrast, reactions that make or break Pu=O multiple bonds are inherently slower. Multielectron processes, such as Pu^{4+} oxidation to PuO_2^{2+}, can proceed in one two-electron step or two one-electron steps. Oxidation of Pu^{4+} or reduction of PuO_2^{+} can generally proceed by direct reaction with the oxidizing or reducing agent, or by oxidation or reduction through the disproportionation reaction. Reactions of plutonium ions are further complicated in that slight changes in solution conditions can profoundly affect the rate and even the direction of the reaction, particularly for Pu^{4+}, owing to its tendency to form multiple stable molecular complexes. For example, reactions in sulfuric acid or carbonate media may take a different course or proceed at a different rate compared to those in perchlorate solutions. Early observations on the redox behavior of plutonium that were made on tracer level concentrations before all of the oxidation states had been well established cannot be applied directly to higher concentrations without reservations. Many of those experiments were qualitative, designed to determine whether reactions were complete or not, and will not be discussed here. A few important systems that relate to plutonium processing and also illustrate particular details of plutonium chemistry will be described here, including reactions with ferrous ion, nitrate, nitrite, hydroxylamine, and hydrogen peroxide. For additional detailed information or lists of reactions and rates, the reader is directed to reviews by Newton (2002) and Cleveland (1979), and general references that contain oxidation and reduction potentials (Wick, 1980).

The multistep reduction of Pu(VI) by Fe(II) is important in fuel reprocessing and has complicated mechanisms and rate laws that were described by Newton (1958, 2002).

When Fe(II) is added to an excess of Pu(VI), the predominant reaction is

$$PuO_2^{2+} + Fe^{2+} \rightarrow PuO_2^{+} + Fe^{3+} \tag{7.101}$$

Using a 60% excess of Pu(VI), Newton (1958) found that for each mole of Fe(II) oxidized approximately one mole of Pu(VI) was reduced as the acid concentration was varied from 2.0 to 0.05 M. Although Fe(II) is capable of reducing Pu(VI) all the way to Pu(III), appreciable amounts of Pu(IV) are observed, even if an excess of Fe(II) is used.

In addition to Pu^{4+} disproportionation, the following reactions were found to be important:

$$PuO_2^{+} + Fe^{2+} + 4H^{+} \rightarrow Pu^{4+} + Fe^{3+} + 2H_2O \tag{7.102}$$

$$Pu^{4+} + Fe^{2+} \rightarrow Pu^{3+} + Fe^{3+} \tag{7.103}$$

From sets of individual reactions in which the pH, then ionic strength, then metal ion concentrations were varied, Newton and Baker (1963) found the following rate law:

$$-\frac{d[PuO_2^{2+}]}{dt} = \{A + (B + C[H^{+}])^{-1}\}[PuO_2^{2+}][Fe^{2+}] \tag{7.104}$$

The necessity of three parameters in the rate law equation indicates three rate-determining steps and three important activated complexes. The above three-parameter equation may be rearranged to give

$$-\frac{d[PuO_2^{2+}]}{dt} = A[PuO_2^{2+}][Fe^{2+}] + \left(\frac{1}{B^{-1}[PuO_2^{2+}][Fe^{2+}]} + \frac{1}{C^{-1}[PuO_2^{2+}][Fe^{2+}]/[H^{+}]}\right)^{-1} \tag{7.105}$$

In this equation, parameter A is associated with the path that leads directly to products, and the B and C terms involve consecutive reactions that parallel the direct reaction. Newton and Baker found several mechanisms that were consistent with the data. All involve the same three activated complexes formed in both consecutive and parallel paths, as well as PuO_2^{2+} hydrolysis.

Plutonium reduction and oxidation reactions in nitric acid solutions have been extensively studied. Descriptions of Pu(IV) oxidation and reduction in nitrate solutions benefited from recent spectroscopic studies that measured the formation constants for two Pu(IV) nitrate species, $Pu(NO_3)_n^{4-n} (n = 1, 2)$ (Berg *et al.*, 2000). Complexation of Pu(IV) by nitrate can decrease the concentration of aquo Pu^{4+}, and thereby slow down the rates of some reactions, or it can provide additional reaction pathways for other reactions. For example,

reactions involving Pu(IV) either as a reactant or product with pentavalent metal ions are much faster in nitrate solutions than in perchlorate solutions. Conversely, oxidation of Pu(IV) by Ce(IV) or Np(VI) are both slower in HNO_3. Reductions of Pu(IV) are also generally slower in HNO_3 than in $HClO_4$ (Newton, 2002).

A great deal of information is available for Pu(IV) redox involving nitrous acid, hydroxylamine, and hydrazine in HNO_3, systems that are important for processing applications. Nitrous acid is commonly used to adjust the oxidation state of plutonium, both as a pure reagent and inadvertently as a contaminant in nitric acid. The key to understanding plutonium redox reactions in nitric and nitrous acid is that small equilibrium concentrations of NO_2 are present in HNO_2–HNO_3 mixtures. For example, although Pu(III) is quite stable in dilute nitric acid solutions, in the presence of HNO_2 it is readily oxidized to Pu(IV) by the following reaction:

$$2Pu^{3+} + 3H^+ + NO_3^- \rightleftarrows 2Pu^{4+} + HNO_2 + H_2O \qquad (7.106)$$

An empirical rate law and a plausible mechanism for the reaction were derived by Koltunov and Marchenko (1973). The oxidation may be retarded by the addition of a "holding reductant" to react with the HNO_2 as soon as it is formed. Effective reductants include sulfamic acid, ferrous sulfamate or hydrazine (Cleveland, 1979).

Plutonium(V) is reduced very slowly by nitrous acid (Koltunov *et al.*, 1982b). These studies consistently show that NO_2, formed by reaction of HNO_2 with HNO_3, is the important oxidant in the Pu(III) or Pu(V) oxidation by HNO_3. The rate of the following equilibrium reaction involving Pu(V) and Pu(VI) has been measured in both directions (Koltunov and Ryabova, 1980).

$$2PuO_2^{2+} + HNO_2 + H_2O \rightleftarrows 2PuO_2^+ + NO_3^- + 3H^+ \qquad (7.107)$$

Hydroxylamine and hydrazine are very useful reducing agents for all of plutonium's higher oxidation states, because they are nonmetallic, yield volatile oxidation products, and tend to react rapidly. These reactants are two-electron reducing agents, so one-electron oxidation leads to radical intermediates that can either decompose to stable products or be oxidized by plutonium and therefore influence the overall stoichiometry and the rate law. If the two one-electron oxidations occur at approximately the same rates, the stoichiometry will change during the course of the overall reaction and the rate laws will be very complicated. Additional redox agents and mechanistic complexity are added when the reduction of plutonium by these reagents is conducted in nitric acid solutions.

When hydroxylamine is oxidized by plutonium(IV), the two limiting overall reactions are (Barney, 1976):

$$2Pu^{4+} + 2NH_3OH^+ \rightleftarrows 2Pu^{3+} + N_2 + 4H^+ + 2H_2O \qquad (7.108)$$

and

$$2Pu^{4+} + NH_3OH^+ \rightleftarrows 2Pu^{3+} + 3H^+ + 0.5N_2O + 0.5H_2O \qquad (7.109)$$

The empirical rate law for the plutonium reduction by hydroxylamine in 2.5 M [(H, Na) (NO_3, ClO_4)] was found to be

$$-\mathrm{d}[\mathrm{Pu(IV)}]/\mathrm{d}t = [\mathrm{Pu}^{4+}]^2[\mathrm{NH_3OH}^+]^2/[\mathrm{Pu}^{3+}]^2[\mathrm{H}^+]^4(1+\beta_1[\mathrm{NO_3^-}])^2 \quad (7.110)$$

The factor $(1+\beta_1[\mathrm{NO_3^-}])$ is consistent with the formation of a nitrate complex. An independent investigation using 3 M (H,Na)NO_3 and large excess amounts of NH_3OH^+ gave results at 30°C that agreed reasonably well with the rate law and stoichiometries (Koltunov and Zhuravleva, 1978), yet the rate law does not account for higher nitrate complexes that are known to form when the $[NO_3^-]$ is greater than ~2–3 M (Berg *et al.*, 1998).

Yarbro *et al.* (1998) recently summarized past studies of Pu(IV) reduction by hydroxylamine and reported results with hydroxylamine nitrate (HAN) in the presence of excess plutonium. Rather than define the kinetic expression in terms of concentrations (although plausible mechanisms and complex stoichiometries were discussed), the following fractional conversion was defined:

$$X = 1 - (N_\mathrm{A}/N_{\mathrm{A}^0}) \quad (7.111)$$

where X is the fraction of compound reacted, N_{A^0} is the initial number of moles of the reactant A and N_A is the number of moles of reactant A at some time t. If acid and nitrate concentrations are constant, then the fractional conversion of HAN can be described as follows:

$$\begin{aligned} -\mathrm{d}X/\mathrm{d}t = {} & (kk_\mathrm{H}^{0.44}/C_{\mathrm{Pu}^0}[\mathrm{H}^+]^{0.56})([\mathrm{H}^+]^{0.65} \\ & + k_\mathrm{a}[\mathrm{NO_3^-}])[(1-X)/X]^2([\mathrm{HAN}_0] - C_{\mathrm{Pu}^0}X)^{0.44} \end{aligned} \quad (7.112)$$

where k is the kinetic constant; k_H is the dissociation constant for HAN; k_a is the dissociation constant for HNO_3; C_{Pu^0} is the initial plutonium molar concentration and $[\mathrm{HAN}_0]$ is the initial HAN molar concentration. This expression is useful at low HAN to plutonium molar ratios.

An improved understanding of this system and more broadly applicable rate law requires additional research, including quantitative evaluation of multiple plutonium nitrate complexes (beyond the 1:1 complex), the oxidation of HAN by nitric acid, the reoxidation of Pu(III) by nitrous acid, the disproportionation of Pu(IV), and, for solutions concentrated in Pu, radiolytic oxidation of Pu(III) and reduction of Pu(IV). The Pu(IV) hydroxylamine reaction has also been studied in perchlorate solutions using relatively high $[\mathrm{Pu(IV)}]_o/[\mathrm{NH_3OH}^+]_o$ ratios (Koltunov and Zhuravleva, 1978). These conditions favor the path in which the radical intermediate is oxidized to N_2O. Kinetic studies of Pu(IV) reduction by a derivatized hydroxylamine, where the reducing agent was present in molar excess of plutonium, showed similar dependencies on hydrogen ion and hydroxylamine concentrations (Anyun *et al.*, 2002).

The reduction of Pu(VI) by NH_3OH^+ has been studied in 3 M perchlorate solutions at temperatures near 60°C (Koltunov *et al.*, 1981b). When $[H^+]$ is

<0.55 M, the disproportionation of Pu(V) is relatively slow and the net reaction is probably as follows:

$$2PuO_2^{2+} + NH_3OH^+ \rightleftarrows 2PuO_2^+ + 3H^+ + 1/2N_2O + 1/2H_2O \qquad (7.113)$$

This reaction requires that a radical intermediate be oxidized by Pu(VI). The rate law was found to be

$$-d[Pu(VI)]/dt = 2k_0[PuO_2^{2+}][NH_3OH^+]/[H^+] \qquad (7.114)$$

This rate law is much simpler than the one for the reduction of Pu(IV), and shows that the rate-determining step is the initial formation of the radical intermediate. At higher $[H^+]$, the disproportionation of Pu(V) becomes important. The Pu(IV) formed is rapidly reduced by NH_3OH^+ to Pu(III), which in turn reacts rapidly with Pu(VI). These steps lead to the catalytic reduction of Pu(VI) by Pu(III). Thus, during the course of the reaction, the concentration of Pu(V) will increase to a maximum, then decrease as the concentration of Pu(III) increases. The complex rate laws for this system have been integrated numerically and give concentrations that are in good agreement with the experimental results (Koltunov *et al.*, 1981b).

The reduction of Pu(IV) by hydrazine has been studied in 2 M $(H,Na)NO_3$ (Koltunov and Zhuravleva, 1974). The limiting overall reactions are probably the following:

$$Pu^{4+} + N_2H_5^+ \rightleftarrows Pu^{3+} + NH_4^+ + H^+ + 1/2N_2 \qquad (7.115)$$

and

$$4Pu^{4+} + N_2H_5^+ \rightleftarrows 4Pu^{3+} + N_2 + 5H^+ \qquad (7.116)$$

The stoichiometric ratio was found to depend on the initial reactant concentrations, just as with hydroxylamine. At 50°C with a $[H^+]$ range between 0.5 and 1.9 M, the rate law for the Pu(IV)–hydrazine reaction was found to be

$$-d[Pu(IV)]/dt = k[Pu^{4+}][N_2H_5^+]/(K_h + [H^+]) \qquad (7.117)$$

This rate law shows that the rate-determining step is the formation of the radical intermediate ($N_2H_4\cdot$), not its subsequent reaction. The parameter K_h was interpreted as the hydrolysis constant for Pu(IV), but the 1:1 Pu(IV)–nitrate complex should be included in the rate law. An alternative explanation involves the formation of low steady-state concentrations of a plutonium–hydrazine intermediate (Newton, 2002). Additional kinetic studies of the reduction of Pu(IV) have been reported for substituted hydrazines, with similar overall reactions and small changes in reaction rates (Koltunov *et al.*, 1989).

The reduction of Pu(VI) by $N_2H_5^+$ was shown to have features similar to the reduction of Pu(IV) (Koltunov and Zhuravleva, 1973). The initial reaction is most probably

$$PuO_2^{2+} + N_2H_5^+ \rightleftarrows PuO_2^+ + NH_4^+ + 1/2N_2 + H^+ \qquad (7.118)$$

The final reaction product is Pu(III), which arises from the reduction of Pu(IV) described above. The reduction of Pu(V) to Pu(IV) occurs by two parallel pathways: direct reaction of Pu(V) with hydrazine, and comproportionation of Pu(VI) with Pu(III) to give Pu(IV). The kinetics of the reduction of Pu(V) by hydrazine as well as the use of the overall reductions in the nuclear fuel cycle have been described (Koltunov and Baranov, 1993). The rate law in 2 M Na (NO_3,ClO_4) was found to be approximately

$$-\mathrm{d}[\mathrm{Pu(VI)}]/\mathrm{d}t = k[\mathrm{PuO_2^{2+}}][\mathrm{N_2H_5^+}]/[\mathrm{H^+}] \tag{7.119}$$

The nitrate dependence was found to be zero in the range from 0.15 to 2 M at constant ionic strength. The reduction of Pu(VI) by substituted hydrazines has been shown to proceed with similar overall reactions, some differences in the exponents of the reactants in the rate equation, and small changes in reaction rates (Koltunov *et al.*, 2004).

Both fundamental research and process application of plutonium redox reactions with hydrogen peroxide are complicated by the incomplete characterization of molecular Pu(IV) and Pu(VI) complexes that form with peroxide, and the chemical and radiolytic complexities of plutonium–hydrogen peroxide mixtures. Recent studies indicate the utility of hydrogen peroxide reduction of Pu(VI) and mixtures of Pu(VI) and Pu(IV) on the mM scale by 0.3% H_2O_2 in the presence of extraction resins (Morgenstern *et al.*, 2002). Hydrogen peroxide is more commonly used to reduce Pu(VI) in nitrate solutions. Maillard and Adnet (2001) studied effects of acidity and plutonium and H_2O_2 concentrations on the kinetics of Pu(VI) reduction. The kinetics results generally showed an induction period where the [Pu(VI)] does not change, followed by a linear decrease of [Pu(VI)]. The length of the induction period depends on temperature, [HNO_3], and [H_2O_2], but not on the H_2O_2/Pu(VI) ratio. Total reduction time decreases with increasing [Pu(VI)] and [HNO_3] from 0.5 to 6 M [HNO_3], but increases when [HNO_3] varies from 6 to 8 M. Red-brown peroxo complexes were observed and PuO_2^+ was an intermediate in these reductions.

The kinetics of the reduction of ~1 mM PuO_2^+ by [H_2O_2] has been studied in 1.0 M NaCl solutions at near-neutral pH. The reduction was found to be first order with respect to [H_2O_2] and inverse first order with respect to [H^+] and described by the rate equation (7.119) with $k = 3.59$ to 1.79×10^{-9} $\mathrm{min^{-1}}$ (Morgenstern and Choppin, 1999).

$$\mathrm{d}[\mathrm{Pu(V)}]/\mathrm{d}t = k\,[\mathrm{PuO_2^+}][\mathrm{H_2O_2}]/[\mathrm{H^+}] \tag{7.120}$$

(*ix*) *Autoradiolysis*

When plutonium isotopes undergo radioactive decay in aqueous solution they deposit a great deal of energy (approximately 5 MeV per α particle) in α particle tracks that both heat the solution and produce ions, radicals, and solvated electrons. The predominant products generated by water radiolysis in the bulk

solution are H, OH, HO_2, and H_2O_2 (Spinks and Woods, 1990; Vladimirova and Kulikov, 2002). Under plutonium process conditions α radiation generates concentrations of these reactive species that can significantly affect individual stages of reactions as well as the final products. If solute concentrations (most commonly plutonium and nitrate) are less than approximately 1 M, then there will be little direct reaction between the α particles or the transient species and the solute within the tracks.

Reactive species that diffuse out of the alpha-tracks can act as either oxidizing or reducing agents for plutonium and other solutes. For example, in 0.4 M H_2SO_4, 0.53 μmol of Fe(II) is oxidized to Fe(III) per joule of deposited energy (Spinks and Woods, 1990), expressed as $G[\text{Fe(III)}] = 0.53$ μmol J^{-1}; whereas Ce(IV) is reduced with $G[\text{Ce(III)}] = 0.33$ μmol J^{-1} (Spinks and Woods, 1990). The G-values for the reduction of Pu(IV) or Pu(VI) in 1 M $HClO_4$, 0.36 – 0.03 μmol J^{-1}, are similar (for either oxidation state) to those for Fe(II) or Ce(IV) (Kasha, 1949; Newton, 2002). The reduction of Pu(IV) reaches a steady state in which its rate equals the rate of oxidation of Pu(III). At 4°C, the mean oxidation number was found to depend slightly on the total plutonium concentration and/or the dose rate, e.g. 3.05 in 0.022 M Pu, which corresponds to an energy deposition rate of 0.01 Sv L^{-1} (Rabideau *et al.*, 1958).

Plutonium radiolysis in nitrate solution was reviewed by Miner and Seed (1967). Recent research has emphasized the behavior of plutonium in HNO_3 solutions that have much higher dose rates. The results are complicated due to the formation of HNO_2, volatile NO_x, and H_2O_2. Andreichuk *et al.* (1990) studied the oxidation of Pu(III) to Pu(IV) in HNO_3 solutions by using radiation from *in situ* ^{244}Cm. This group first studied the formation of HNO_2 from HNO_3 by ^{244}Cm irradiation in the absence of plutonium (Andreichuk *et al.*, 1984b). These studies, where nitric acid concentrations and dose rates ranged up to 8.6 M and 11.5 W L^{-1}, respectively, showed initial rates of HNO_2 formation to be closely proportional to dose rate, with a yield of 0.21 μmol J^{-1} in 1.89 M HNO_3. A steady-state concentration of 6 mM HNO_2 was reached after 30 h with a dose rate of 3.2 W L^{-1}. In subsequent measurements of Pu(III) oxidation from a dose rate of 3.2 Gy s^{-1}, where $[\text{Pu(III)}]_0 = 10$ mM, and $[HNO_3] < 0.5$ M, steady state was reached within 1 h and approximately 15% of the plutonium had been oxidized. Small concentrations of a $\text{Pu(IV)} \cdot H_2O_2$ complex were observed. At higher acid concentrations, the peroxide complex was not detected and oxidation to Pu(IV) was complete. The reaction was observed to be autocatalytic; that is, initial rates were low but increased to a maximum when approximately one-half the Pu(III) had been oxidized. The corresponding radiation yields of Pu(IV) ranged up to approximately 5 μmol J^{-1} in 2.9 M acid. These yields were relatively high because Pu(III) is readily oxidized in the presence of HNO_2. Plutonium was oxidized further to Pu(VI), but only after no Pu(III) remained. The initial rates for the alpha-radiolytic oxidation of Pu(IV) were similarly found to be proportional to the concentration of the Pu(IV) multiplied by the dose rate

(Andreichuk *et al.*, 1979). For example, for 0.01 M $[Pu(IV)]_0$, the yield in 6 M HNO_3 is 0.00044 μmol W^{-1}.

The alpha-radiolytic reduction of Pu(VI) is much more complicated. Small steady-state concentrations of Pu(V) are formed initially, followed by the formation of HNO_2. Further reaction is autocatalytic because the Pu(V) disproportionation is catalyzed by both HNO_2 and Pu(IV) (Vladimirova, 1982). The Pu(VI)/Pu(IV) steady-state ratios were found to vary widely, depending on total plutonium concentration, HNO_3 concentration, and dose rate (Andreichuk *et al.*, 1979, 1984a,b). For example, a dose rate of 3.46 W L^{-1} in 1 M HNO_3 for plutonium concentrations of 2.1 and 14.8 mM yielded Pu(VI)/Pu(IV) ratios of 5.1 and 0.047, respectively. For 10 mM Pu in 6 M HNO_3, the dose rates of 1.4 and 13.8 W L^{-1} yielded Pu(VI)/Pu(IV) ratios of 0.76 and 3.15, respectively. Kinetic models for the rates of the radiolytic oxidation of Pu(IV) and the reduction of Pu(VI) have been presented by Vladimirova (1990, 1998) and Frolov *et al.* (1990). In a study designed to mimic conditions of dissolved nuclear fuel in nitric acid, Rance and Zilberman (2002) found that the addition of U and fission products to Pu(VI) solutions eliminates the induction periods for reduction. This study reported *G*-values of 0.6–1.1 for 3 g L^{-1} ^{239}Pu solutions that contained from 0.12 to 9.2% ^{238}Pu.

Haschke and Oversby have proposed an alternate disproportion reaction to explain the instability of Pu(VI) in aqueous solution that does not require water radiolysis (Haschke and Oversby, 2002; Haschke, 2005):

$$PuO_2^{2+} + 1/2H_2O \rightleftarrows PuO_2^{+} + H^{+} + 1/4O_2 \qquad (7.121)$$

Their proposed mechanism invokes the disproportionation of PuO_2^{2+} to produce PuO_2^{+} and heptavalent PuO_2^{3+}, followed by the water oxidation by PuO_2^{3+} to produce oxygen. The fact that PuO_2^{3+} has never been observed makes this mechanism doubtful. In a subsequent report, Newton and Hobart (2004) reiterate that below pH 6 the instability of Pu(VI) clearly results from reactions with reducing species produced by alpha radiolysis of water.

Chlorine is formed by radiolysis of HCl solutions, counteracting the processes that reduce plutonium, such that neither Pu(IV) nor Pu(VI) appear to be reduced in 1 M HCl (see discussion in Section 7.9.1.c(ii)). However, at lower chloride concentrations, alpha-reduction of $^{239}Pu(IV)$ does take place. Rabideau and Kline (1958) showed that *G*[Pu(III)] decreases from 0.36 in 1 M $HClO_4$ μmol J^{-1} to approximately 0.077 in 0.5 M HCl–0.5 M $HClO_4$. More recent experiments by Büppelmann *et al.* (1988) using higher chloride concentrations, more nearly neutral acid concentrations, and ^{238}Pu to give higher dose rates, show that Pu(IV) can be oxidized to Pu(V) or Pu(VI). With NaCl concentrations less than 3 M and dose rates of 0.15 W L^{-1}, the product is primarily Pu(V). Higher concentrations of NaCl and/or higher dose rates give Pu(VI). These reactions involve the oxidation of Pu(IV) hydroxide by HClO or ClO^{-}. The effect of dose rate on the reduction of Pu(VI) in $HClO_4$ is illustrated by the

Table 7.54 *Alpha-induced reduction of Pu(VI)* (*Newton,* 2002).

Pu(VI) (mM)	*Dose rate* (W L^{-1})	*Yield* (μeq J^{-1})	*Radiation source*	*References*
<2	<0.002	0.33–0.38	^{239}Pu	Rabideau *et al.* (1958)
1.1	0.15	0.04	^{238}Pu	Büppelmann *et al.* (1988)
1.4	4.16	0.0024	^{244}Cm and ^{239}Pu	Frolov *et al.* (1990)

results of experiments using ^{239}Pu, ^{238}Pu, and ^{239}Pu–^{244}Cm mixtures as summarized in Table 7.54. From the Table it is clear that the yield decreases as the dose rate increases.

(d) Hydrolytic stability of plutonium ions

The hydrolytic behavior of the plutonium ions has been the subject of many studies. This interest has been intensified by the practical importance of hydrolysis in the manipulation of plutonium solutions. This class of solution phenomena is as important in the chemistry of plutonium as it is for the actinide elements generally because of the existence of highly charged positive ions in aqueous solution. Hydrolysis leads to the formation of ionic species or precipitates by the action of water as illustrated in equation (7.122) for trivalent plutonium. While hydrolysis reactions are often written as in equation (7.122), hydrolysis is actually a complexation reaction with the hydroxide ion. Therefore, it is also common to express hydrolysis as a complex formation as indicated in equation (7.123). The hydrolysis constant $^*\beta$ (corresponding to equation (7.122)) is related to the formation constant β (equation (7.123)) by the ion product of water, K_w (Grenthe *et al.*, 1997).

$$Pu^{3+} + H_2O \rightleftharpoons Pu(OH)^{2+} + H^+ \tag{7.122}$$

$$Pu^{3+} + OH^- \rightleftharpoons Pu(OH)^{2+} \tag{7.123}$$

Characterization of the hydrolysis behavior of plutonium is the cornerstone of understanding its aqueous coordination chemistry, particularly the thermodynamic stability of complexes. The tendency to undergo hydrolysis increases with the charge/size ratio of the ion. Therefore hydrolysis is most pronounced for Pu^{4+}, and the least pronounced for PuO_2^+. The tendency for hydrolysis follows the general order

$$Pu^{4+} > PuO_2^{2+} \approx Pu^{3+} > PuO_2^+$$

Plutonium ions hydrolyze readily and thereby limit both the stability fields of individual aquo ions and the overall solubility of plutonium ions in aqueous

solution. At the extreme end of the spectrum, Pu(IV) hydrolyzes even in pH 1 solutions and can form complicated polymeric (or colloidal) hydroxides and precipitates (Lemire *et al.*, 2001; Neck and Kim, 2001; Rothe *et al.*, 2004), making even the first hydrolysis product of Pu(IV) difficult to characterize. Each of the other common oxidation states forms more soluble and discrete hydroxide species, although Pu(VI) also forms both monomeric and polymeric hydroxide species. The coordination numbers and structures of all of the pure hydroxides can be inferred from the hydration numbers, the stoichiometry of the hydroxo species, and X-ray structures of corresponding solids. X-ray absorption spectroscopy has been used to determine the bond lengths and coordination numbers more directly. Selected hydrolysis constants for plutonium ions are given in Table 7.55 and follow the usual hydrolysis equilibrium expression and associated hydrolysis constant, $^*\beta_n$ (Lemire *et al.*, 2001).

$$Pu^{x+} + nH_2O \rightleftharpoons Pu(OH)_n^{(x-n)+} + nH^+ \tag{7.124}$$

$$^*\beta_n = \frac{[Pu(OH)_n^{(x-n)+}][H^+]^n}{[Pu^{x+}]} \tag{7.125}$$

A complete review of hydrolysis products and the solubility of plutonium hydroxides is available in the NEA compilation of the chemical thermodynamics of neptunium and plutonium (Lemire *et al.*, 2001) and its most recent update (Guillaumont *et al.*, 2003). Hydration and hydrolysis of plutonium are compared with that of the other actinide elements in Chapter 23.

Pu(III) The tendency of an ion to displace a proton from water increases with charge and, for a given charge, with decreasing ionic radius. The acidity of the tripositive actinide ions, then, should follow the order

$$Pu^{3+} > Np^{3+} > U^{3+}$$

with Pu^{3+} being the strongest acid and therefore the trivalent actinide ion of this triad that undergoes the most extensive hydrolysis. On the basis of its ionic radius, Pu^{3+} should have an acidity similar to the lanthanide ions, and should have a first hydrolysis constant lying between those of Ce^{3+} and Pr^{3+}.

The hydrolysis of Pu^{3+} can be studied only with careful control of the plutonium solubility and maintenance of an inert or reducing atmosphere to avoid oxidation to Pu^{4+}, which is increasingly favored as the solution pH is raised. The first hydrolysis product, $Pu(OH)^{2+}$, has been inferred from solvent extraction, potentiometric and spectrophotometric titration studies in acid solutions up to pH ~3 (where it accounts for ca. 70% of plutonium present). Kraus and Dam (1949) have studied the hydrolysis of trivalent plutonium according to equation (7.122). From titration curves of plutonium(III) chloride and perchlorate solutions with alkali, Kraus and Dam (1949) identified the first hydrolysis species $Pu(OH)^{2+}$ and reported the first hydrolysis constant $^*\beta_1$.

Table 7.55 *Hydrolysis constants for plutonium ions.*

Reaction stoichiometry	I (M)	$\log_{10}{}^{*}\beta_{mn}$	$\log_{10}{}^{*}\beta^{\circ}_{mn}$	*References*
$Pu^{3+} + H_2O \rightleftarrows Pu(OH)^{2+} + H^+$	0.1	−6.9	−6.9 ± 0.3	Baes and Mesmer (1976) and Lemire *et al.* (2001)
$Pu^{3+} + 2H_2O \rightleftarrows Pu(OH)_2^+ + 2H^+$	–	−15.0	–	Fuger (1992)
$Pu^{4+} + H_2O \rightleftarrows Pu(OH)^{3+} + H^+$	1.0	−0.45	0.6 ± 0.2	Metivier and Guillaumont (1972) and Guillaumont *et al.* (2003)
$Pu^{4+} + 2H_2O \rightleftarrows Pu(OH)_2^{2+} + 2H^+$	1.0	−0.75	0.6 ± 0.3	Metivier and Guillaumont (1972) and Guillaumont *et al.* (2003)
$Pu^{4+} + 3H_2O \rightleftarrows Pu(OH)_3^+ + 3H^+$	1.0	−0.33	−2.3 ± 0.4	Metivier and Guillaumont (1972) and Guillaumont *et al.* (2003)
$Pu^{4+} + 4H_2O \rightleftarrows Pu(OH)_{4(aq)} + 4H^+$	1.0	−0.63	−8.5 ± 0.5	Metivier and Guillaumont (1972) and Guillaumont *et al.* (2003)
$PuO_2^+ + H_2O \rightleftarrows PuO_2(OH)_{(aq)} + H^+$	0.1	−9.73	≤−11.3 ± 1.5	Bennett *et al.* (1992) and Lemire *et al.* (2001)
$PuO_2^{2+} + H_2O \rightleftarrows PuO_2(OH)^+ + H^+$	0		−5.5 ± 0.5[a]	Guillaumont *et al.* (2003)
$PuO_2^{2+} + 2H_2O \rightleftarrows PuO_2(OH)_{2(aq)} + 2H^+$	0		−13.2 ± 0.5[a]	Guillaumont *et al.* (2003)
$2PuO_2^{2+} + 2H_2O \rightleftarrows (PuO_2)_2(OH)_2^{2+} + 2H^+$	0.1	−7.8	−7.5 ± 0.5[a]	Okajima and Reed (1993), Guillaumont *et al.* (2003), Reilly *et al.* (2000), and Madic *et al.* (1984)
$2PuO_2^{2+} + 4H_2O \rightleftarrows (PuO_2)_2(OH)_4 + 4H^+$	0.1	−19.3	–	Okajima and Reed (1993) and Reilly *et al.* (2000)

[a] Asymmetric uncertainties (+0.5, −1.5).

Later studies reported the same species stoichiometry and contributed to the recommended hydrolysis constant of $\log_{10} {}^*\beta_1 = -7.0$ (Baes and Mesmer, 1976; Lemire *et al.*, 2001). The overall formula for $Pu(OH)^{2+}$ is likely to be $Pu(OH)(OH_2)_8^{2+}$ based upon the coordination number 9 observed for the Pu^{3+} aquo ion (see Section 7.9.1(a)) (Matonic *et al.*, 2001). Quantitative evaluation of the formation of higher hydrolysis products is inhibited by oxidation and precipitation of Pu(III/IV) hydroxides. Based on the hydrolysis of other trivalent actinides the second hydrolysis constant for formation of $Pu(OH)_2^+$ via equation (7.122) is approximately $\log_{10} {}^*\beta_2 = -15.0$ (Baes and Mesmer, 1976; Fuger, 1992).

The solid trivalent plutonium hydroxide that precipitates from aqueous solutions is presumed to be $Pu(OH)_3 \cdot nH_2O$, by analogy with the known Am^{3+} hydroxide. Solubility studies that were performed as a function of ionic strength provide a solubility product of $\log_{10} K_{sp} = -(15.8 \pm 1.5)$ under standard conditions (Felmy *et al.*, 1989).

Pu(IV). On the basis of size and charge, the plutonium(IV) ion should undergo much more extensive hydrolysis than does plutonium(III). For the same reasons as in the case of the III state, the tendency to undergo hydrolysis should be greater in plutonium than for its predecessors in the actinide series:

$$Pu^{4+} > Np^{4+} > U^{4+} > Pa^{4+} > Th^{4+}$$

In the early stages of hydrolysis, only monomeric species such as $Pu(OH)^{3+}$ are important. It is likely that Pu^{4+} hydrolyzes in a stepwise manner to yield monomeric $Pu(OH)_n^{4-n}$ ($n = 1, 2, 3, 4$); however, the intermediate hydrolysis products ($2 \leq n \leq 4$) undergo irreversible polymerization with the formation of large colloidal aggregates (see below).

The first hydrolysis product for the formation of $Pu(OH)^{3+}$, has been determined from solution complex formation studies.

$$Pu^{4+} + H_2O \rightleftharpoons Pu(OH)^{3+} + H^+ \qquad (7.126)$$

Reported hydrolysis constants for this reaction vary widely, with limited correlation between the experimental technique used and the resulting value of the hydrolysis constant (Baes and Mesmer, 1976; Lemire *et al.*, 2001; Guillaumont *et al.*, 2003). From the many reported values, several are considered the most accurate. Rabideau (1957) carefully measured the pH dependence of the Pu^{4+}/Pu^{3+} redox couple and calculated a hydrolysis constant of $\log_{10} {}^*\beta_1 = -1.41$ at $I = 0.1$ M using the Nernst equation. Compared with directly measuring the formation of the hydrolysis product, for example, by quantifying the shift in the optical absorption bands for Pu^{4+} as the hydroxide forms, or calculating a constant to best model the solubility of (oxy)hydroxide solids, this approach explicitly considers the formation and subsequent hydrolysis of Pu^{3+} at low pH. The 2003 NEA review recommended the value of $\log_{10} {}^*\beta_1 = (0.60 \pm 0.20)$ under standard conditions ($I = 0$) (Guillaumont *et al.*, 2003), which is based on

values proposed in recent studies by Knopp *et al.* (1999) and Neck and Kim (2001). The constant for the second hydrolysis product was originally estimated to be $\log_{10} {}^*\beta_2 = -3.7$ at $I = 0.1$ M (Kraus and Nelson, 1950). The 2003 NEA review recommended $\log_{10} {}^*\beta_2 = (0.60 \pm 0.30)$ for $I = 0$ based on the most recent studies (Guillaumont *et al.*, 2003). The overall formulae for $Pu(OH)^{3+}$ and $Pu(OH)_2^{2+}$ are likely to be $Pu(OH)(OH_2)_7^{3+}$ and $Pu(OH)_2(OH_2)_6^{2+}$ based upon the coordination number 8 observed for the Pu^{4+} aquo ion (see Section 7.9.1(a)).

$$Pu^{4+} + 2H_2O \rightleftharpoons Pu(OH)_2^{2+} + 2H^+ \tag{7.127}$$

Characterization of subsequent third and fourth hydrolysis species [$Pu(OH)_3^+$ and $Pu(OH)_4$] is frustrated by the propensity of these hydroxides to polymerize, as discussed below. The direct observation of the solution species and definitive determination of the constants are prevented by the detection limits of current techniques coupled with the sparing solubility of the (hydr)oxide phases. Attempts to accurately determine these constants from solubility data are focused on the following: identifying discrete solution ion and colloidal species, improving the quantification of the Pu^{4+} ion, refining the operational definitions of the solid/solution phase (commonly delineated by the phase separation method), and better characterizing and controlling the solid phase [crystalline PuO_2, hydrated PuO_2, crystalline or amorphous $Pu(OH)_4$]. Based on the most recent work by Knopp *et al.* (1999), and by Neck and Kim (2001), the 2003 NEA review proposed the value of $\log_{10} {}^*\beta_3 = -(2.3 \pm 0.4)$, and $\log_{10} {}^*\beta_4 = -(8.5 \pm 0.5)$ for the third and fourth hydrolysis constants at $I = 0$, respectively (Guillaumont *et al.*, 2003).

The published solubility product of amorphous Pu(IV) hydroxide, $Pu(OH)_4(s)$, is $\log_{10} K_{sp} = -(58 \pm 1)$ (Capdevila and Vitorge, 1998; Lemire *et al.*, 2001; Neck and Kim, 2001). This value gives a calculated Pu(IV) solution concentration near pH 7 of 10^{-11} M, while observed solubilities span a range of 10^{-8}–10^{-13} M due to interactions with other simple ligands, formation of other hydroxide species, redox instability, and the formation of colloidal species (Neck and Kim, 2001; Rothe *et al.*, 2004).

Pu(IV) polymerization. It has been known for half a century that aqueous solutions of Pu(IV) will form colloidal polymers under the appropriate solution conditions (Kraus and Nelson, 1950; Kraus, 1956). Early emphasis focused on avoiding Pu(IV) polymer because of its intractability and potential for interference in plutonium process chemistry. Newer concerns involve retention of plutonium in nuclear waste repositories where radioactive heating and low acidity of ground waters favor Pu(IV) colloid formation and thus could provide a potential transport pathway for migration of plutonium away from the repository. Radiocolloids are very fine, well-dispersed, intrinsic particles of radioactive compounds, whose formation in the case of the actinides is intimately connected to their hydrolysis chemistry.

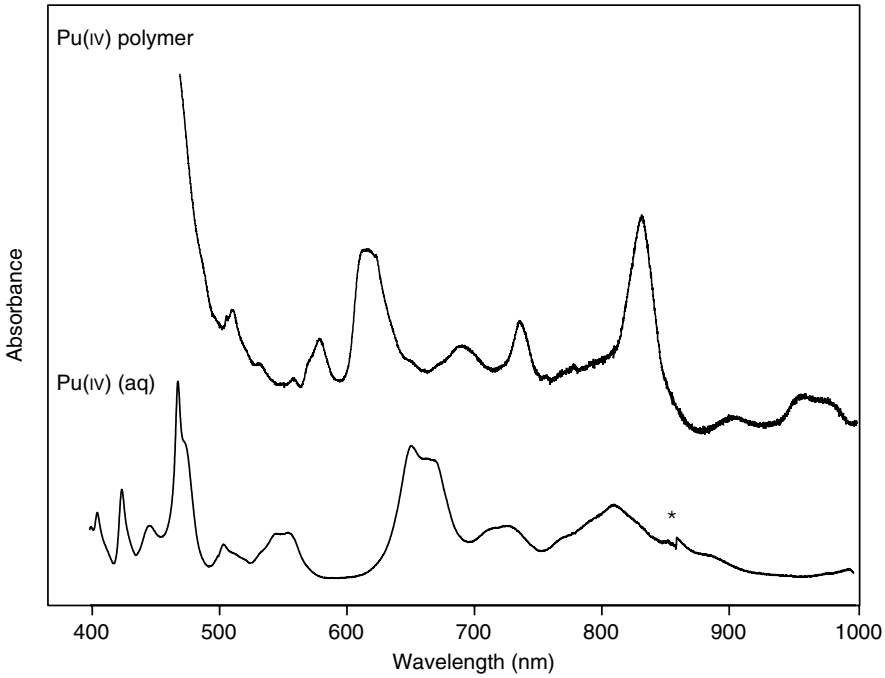

Fig. 7.119 *Electronic absorption spectra of Pu(IV) polymer compared to the Pu(IV) aquo ion. Plutonium(IV) polymer recorded on* 9.0 mM *solution; plutonium(IV) aquo ion recorded on* 2.91 mM *solution in* 1 M $HClO_4$ *using* 1 cm *cell. The asterisk indicated a spectrometer grating change* (*spectra courtesy of P. D. Palmer of Los Alamos*).

For plutonium (IV) the colloid can form green solution-like sols that are optically clear, display a characteristic absorption spectrum (Fig. 7.119), and do not settle on long-standing (Ockenden and Welch, 1956; Lloyd and Haire, 1978). Under the appropriate conditions, these colloids may decompose or disaggregate into soluble ionic species, or age into relatively insoluble materials (Newton *et al.*, 1986b).

The formation of colloidal Pu(IV) polymer was first reported by Kraus, and much of the early information on it is based on the work of Kraus and his coworkers (Kraus and Nelson, 1950; Kraus, 1956). Pu(IV) polymer can be prepared by a number of methods (Hobart *et al.*, 1989). Precipitation methods include the partial neutralization of Pu(IV) solutions, addition of water to 'dried' acid samples, or precipitation with alkali followed by peptization in dilute acid (90°C). Redox methods include slow oxidation of Pu(III) by oxygen and/or alpha irradiation products, or the reduction of Pu(V). The polymer formation depends on acidity, Pu(IV) concentration, presence of other ions, and temperature (Rainey, 1959). Solutions of Pu(IV) polymer can be very readily obtained when plutonium(IV) hydroxide is treated with less than four equivalents of

hydrogen ion per mole of plutonium; when plutonium(IV) hydroxide is dissolved in dilute acid, plutonium polymer forms. Likewise, if a solution of plutonium(IV) in moderately concentrated acid is poured slowly into boiling water, polymeric plutonium is obtained. It is also formed when a plutonium nitrate solution is depleted of nitric acid by extraction with *n*-hexanol. The colloid polymer is ideally formed in nitrate solution in about 0.8 mole per mole of plutonium(IV) (Lloyd and Haire, 1978). This colloidal polymer may be isolated as a solid, which shows the electron diffraction pattern typical of an amorphous substance and has a practical size of up to 20 Å. This colloid can easily be redissolved. On standing or artificial aging, the particle size increases, and the solid becomes finely crystalline and exhibits the XRD pattern of PuO_2. The colloidal character of plutonium(IV) polymer is manifested by the strong absorption of the polymer on glass and on substances such as paper, cotton, and silica, which acquire a negative surface charge when immersed in water.

Until recently, the characterization of plutonium(IV) colloid has met with only limited success. Thiyagarajan *et al.* (1990) measured the structures of Pu(IV) hydrous polymers by small-angle neutron scattering (SANS) in aqueous media and after solvent extraction into an organic phase. The SANS data indicate long, thin, rod-like particles that measured (4.7 ± 0.2) by (190.0 ± 20.0) nm. XRD was consistent with a fcc crystal system similar to that found in crystalline PuO_2 (see Section 7.8.5.a(iii)).

Light scattering methods have also be used to characterize macromolecular Pu(IV) hydroxide solutions. Rundberg *et al.* (1988) and Triay *et al.* (1991) employed autocorrelation photon spectroscopy (APS) to determine the size distribution of Pu(IV) colloidal suspensions that were prepared by dilution, peptization, and autoxidation of Pu(III). The plutonium(IV) colloids measured by APS were assumed to be spherical particles in order to utilize the Stokes–Einstein relationship to calculate a particle diameter. In the initial study by Rundberg *et al.* (1988) the average size of the colloid diameter was measured to be (2.9 ± 0.2) nm. The diameter of a plutonium colloid sample measured over a period of 2 years resulted in reproducible diameters of 180 nm. Subsequently, Triay *et al.* (1991) examined colloid diameters as a function of preparation method, and found that the size of the colloids varied from 1 to 370 nm depending on method of preparation. Small colloid diameters on the order of 1.5 nm were found when the colloid was prepared by the method of Savage and Kyffin (1986) by heating a plutonium nitrate solution with hydrogen peroxide, neutralizing most of the free acid with sodium hydroxide, and diluting to known volume to give 2.5 g L^{-1} solutions. Dilution of a well-characterized Pu(IV) stock solution using distilled water yields colloids in the range of 2–6 nm in diameter (Triay *et al.*, 1991). Peptization gave a mixture of two different sizes (14 and 370 nm). Autoxidation of Pu(III) yielded the largest single-sized colloid.

More recently, Rothe *et al.* (2004) investigated Pu(IV) colloid growth using a combination of laser-induced breakdown detection (LIBD) and X-ray absorption fine structure (XAFS) spectroscopy. LIBD measurements gave colloid sizes ranging from 12 to 25 nm depending on solution conditions.

Rothe *et al.* proposed a model for colloid formation that is consistent with their XAFS, LIBD, and UV-Vis spectroscopic data, based on the stepwise buildup of polynuclear species and loss of water, in analogy to a mechanism proposed by Fujiwara and coworkers (Fujiwara *et al.*, 2001). In this model, they propose hydrolysis of aquo Pu^{4+} to form an eight coordinate monomer $Pu(OH)_2(OH_2)_6^{2+}$ followed by condensation of two monomers to form a dimer of cubic units connected at their edges. The condensation of $Pu(OH)_2^{2+}$ units as reactants satisfies a –2 slope dependency on LIBD data, and the eight coordinate monomer $Pu(OH)_2(OH_2)_6^{2+}$ satisfies the coordination environment from XAFS data. This basic condensation model is described in equation (7.128), and the structural model for the resulting dimer is illustrated in **8**.

$$2Pu(OH)_2(H_2O)_6^{2+} + xH_2O \rightleftharpoons Pu_2O_p(OH)_{8-2p}(OH_2)_{6+p} + 4H^+ + (2+x)H_2O \quad (7.128)$$

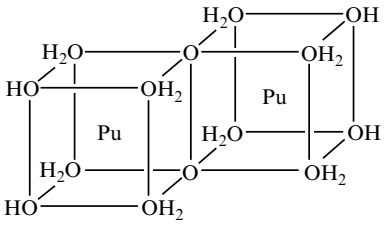

8

In rationalizing the formation of higher order polymers, a trimeric species could be envisioned as forming through the subsequent condensation of monomeric $Pu(OH)_2(OH_2)_6^{2+}$ with the dimer **8**. To be consistent with XAFS data, the new trimer must retain an essentially fcc Pu sublattice with an approximately 3.87 Å distance between Pu centers. This is possible through condensation of the third monomeric $Pu(OH)_2(OH_2)_6^{2+}$ unit along cube edges to form a chain, or by condensing a third monomeric unit along two edges of neighboring cubes of the dimer to form a trimer of cubes sharing one common corner. Examples of these proposed trimeric units are shown in **9** and **10**.

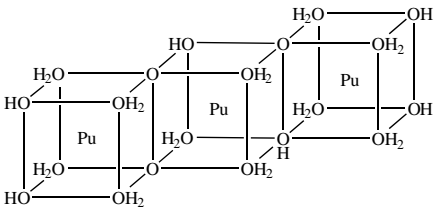

9

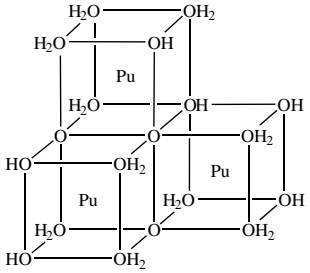

10

The fundamental components of this polymerization mechanism are to grow oligomeric units that maintain a Pu–Pu separation near 3.87 Å, maintain a Pu:OH ratio of 2, and keep the overall cluster size small enough to be consistent with UV-Vis results. Polymerization to larger units can proceed by subsequent condensation of dimers or trimers with each other, or with monomeric units.

The XAFS data from Rothe *et al.* reveal the presence of several different Pu–O distances between 2.20 and 2.42 Å consistent with different coordinating oxygen atoms (–O, –OH, and OH_2). Similarly, the XAFS data show a Pu–Pu distance between 3.86 and 3.89 Å. The fcc cubic environment and the 3.8 Å Pu–Pu separation gives a basic structural unit that is similar to that observed in fcc PuO_2 (see Section 7.8.5(a)). These workers also observed a small feature in their XAFS data near 1.9 Å, and they argued that this feature was too short to be reconcilable with a Pu(IV)–O bond. As this feature had also been observed in ThO_2 XAFS spectra (Rothe *et al.*, 2002), and in XAFS reported by other workers, it was concluded that this feature was most consistent with multiple electron excitation. Essentially identical structural features were observed in XAFS data of Pu(IV) colloid samples reported by Conradson and coworkers (Conradson *et al.*, 2004b). The primary focus of the Conradson study was to examine the structural features of solid PuO_{2+x} materials (see Section 7.8.5(a)). The XAFS data from PuO_{2+x} solids show many remarkable structural similarities to the Pu(IV) colloid samples studied by Rothe *et al.* (2004) and Conradson *et al.* (2004b). Both studies show a range of Pu–O distances consistent with different coordinating oxygen atoms (–O, –OH, and OH_2). In the oxide of stoichiometry of $PuO_{2.26}$, the short interatomic distance near 1.9 Å is no longer a small feature, but has become a dominant spectroscopic feature (see Fig. 7.94). Conradson also reported XAFS data on a number of Pu(IV) colloid samples whose XAFS spectra vary as a function of preparation and aging. Conradson's data show that both Pu(IV) polymers and solid PuO_{2+x} compounds share structural features, and are consistent with an fcc arrangement of plutonium atoms with a 3.8 Å separation. The difference between the two studies is that in solid PuO_{2+x} compounds, the XANES data were consistent with a mixture of Pu(IV) and Pu(V). Conradson *et al.* suggested that the short internuclear distance that averaged 1.86 Å was consistent with the presence of Pu(V), where solution measurements show a distance of 1.85 Å for PuO_2^+. In the freshly prepared samples studied by Rothe *et al.* (2004) this feature was quite small. In the aged samples studied by Conradson *et al.* (2004b) this feature was quite pronounced. These two XAFS studies remind us of the complex nature of the Pu(IV) polymer, and suggest that the elegant polymerization mechanism proposed by Rothe *et al.* may need to be expanded. We look forward to future advances in this area.

Pu(V). Of the common oxidation states of plutonium only Pu(V) is not hydrolyzed until the solution pH becomes basic. Because of the tendency of pentavalent plutonium to disproportionate or be reduced by even weak agents there are very few studies on the hydrolysis of this plutonium ion. Similarly, the

presence of inorganic and organic ligands will generally favor the formation of Pu(IV)–ligand complexes in accordance with their relative formation constants. Early conventional spectrophotometric studies showed that Pu(V) hydrolyses above pH 9 to form stepwise products, $PuO_2(OH)$ and $PuO_2(OH)_2^-$ (Baes and Mesmer, 1976; Madic *et al.*, 1984; Fuger, 1992). By analogy with Np(V) hydroxides, which have been studied in detail by optical absorption and Raman spectroscopy (Madic *et al.*, 1984; Sullivan *et al.*, 1991), Pu(V) hydroxide complexes $PuO_2(OH)$ and $PuO_2(OH)_2^+$ likely have two or three inner-sphere water molecules in the equatorial plane and pentagonal bipyramidal coordination geometry. The monohydroxide hydrate solid is amorphous and has not been structurally characterized. Attempts to increase the crystallinity of the $NpO_2(OH)$ analog have produced Np_2O_5 (Runde *et al.*, 2002). Bennett and coworkers used photoacoustic spectroscopy to perform spectrophotometric titrations of millimolar and submillimolar PuO_2^+, which provided a formation constant for the first hydrolysis product of $\log_{10} {}^*\beta_1 = -(9.73 \pm 0.10)$ (Bennett *et al.*, 1992). Mixed hydroxo carbonato complexes, such as $PuO_2(OH)(CO_3)_2^{4-}$ or $PuO_2(OH)_2(CO_3)^{3-}$ may form (by analogy with Np(V) chemistry) but they have not been characterized. In addition, there is some evidence that the super-stoichiometric Pu(IV) oxide (PuO_{2+x}) contains Pu(V) (Conradson *et al.*, 2003, 2004b). Thus, Pu(V) hydroxides may be much more important in plutonium chemistry and material science than was previously thought.

Pu(VI). Plutonium(VI) hydrolysis is intermediate between that of Pu(III) and Pu(IV), corresponding to its effective charge of ~3.2. Similar to Pu(IV), low solubility and polymerization challenge the characterization of products above neutral pH. The first hydrolysis products, $PuO_2(OH)^+$ and $PuO_2(OH)_2$ have hydrolysis constants of $\log_{10} {}^*\beta_1 = -(5.5 \pm 0.5)$ and $\log_{10} {}^*\beta_2 = -(13.2 \pm 1.5)$ at $I = 0$, respectively (Lemire *et al.*, 2001), comparable to the analogous U(VI) species (Grenthe *et al.*, 1992). Structurally, these monomeric species likely have three or four water molecules in addition to hydroxide in the equatorial plane and a pentagonal bipyramidal geometry with respect to inner-sphere oxygen atoms as indicated in **11**. There is substantial data from potentiometric, optical absorption, and Raman studies that indicates that at higher plutonium concentrations (estimated to be $\sim 5 \times 10^{-4}$ M) the first hydrolysis product is the dimer, $(PuO_2)_2(OH)_2^{2+}$, with two bridging hydroxides and pseudo-pentagonal bipyramidal coordination as shown in **12** (Madic *et al.*, 1984; Okajima and Reed, 1993; Reilly *et al.*, 2000). The hydrolysis constant for the dimer is estimated to be $\log_{10} {}^*\beta_{22} = -(7.5 \pm 1.5)$ at $I = 0$ (Lemire *et al.*, 2001). Polymerization is less pronounced for Pu(VI) than for U(VI) and there is no evidence for the trimeric hydroxide complexes that have been well characterized for uranyl, e.g. $(UO_2)_3(OH)_5^+$, (Grenthe *et al.*, 1992; Palmer and Nguyen-Trung, 1995). Solids precipitated from these systems have been formulated based on stoichiometry as $PuO_2(OH)_2$ or various hydrated phases, but neither their structures nor solubility products have been determined.

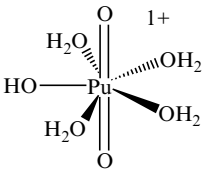

11

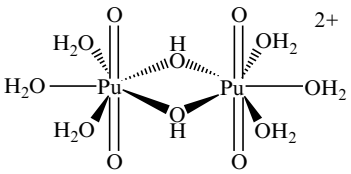

12

Under alkaline solution conditions of 1 M LiOH, Tananaev (1989) presented data to suggest the formation of $PuO_2(OH)_4^{2-}$ that converts to $PuO_2(OH)_3^-$ upon lowering the hydroxide concentration. The single crystal XRD structures (Clark *et al.*, 1999a) and solution XAFS data (Wahlgren *et al.*, 1999; Clark *et al.*, 1999a; Moll *et al.*, 2000; Bolvin *et al.*, 2001) have been reported on the $UO_2(OH)_4^{2-}$ and $NpO_2(OH)_4^{2-}$ analogs.

Pu(VII). Heptavalent plutonium has only been studied in strongly alkaline solutions, given its immediate reduction to Pu(VI) under all other conditions. Interest in the coordination environment of Pu(VII) in solution has been renewed because highly alkaline conditions could be technologically useful in nuclear waste processing, and because Pu(VII) hydroxides provide an opportunity to examine structure/bonding relationships in actinide systems with an unusual number of Pu–O multiple bonds. Pu(VII) appears to be analogous to Np(VII) for which many more studies have been reported. A series of anionic polyoxo species that form between 0.5 and 18 M hydroxide has been proposed and includes the following, $PuO_4(OH_2)_2^-$, $PuO_4(OH)(OH_2)^{2-}$, $PuO_4(OH)_2^{3-}$, $PuO_5(OH)^{4-}$, or PuO_6^{5-}, depending on hydroxide concentrations (Spitsyn *et al.*, 1969; Krot, 1975; Tananaev *et al.*, 1992). Of the proposed species, only $PuO_4(OH)_2^{3-}$ has a proven analog in neptunium chemistry, and its likely structure is shown in **7** (see Section 7.9.1.a) (Grigor'ev *et al.*, 1986). No hydrolysis constants are known. Crystalline samples of analogous Pu(VII) compounds have been prepared (Zakharova *et al.*, 1972).

(e) Complex ions

In this section we describe the preparation, stability, structure, and in selected cases the spectroscopy and solid-state forms, of molecular complexes of plutonium in aqueous solution. The little information that is available on the non-aqueous coordination and organometallic chemistry of plutonium will be described in Section 7.9.2. The stoichiometry and stability of aqueous plutonium complexes has generally been determined indirectly from proton, ligand, and metal titrations, including the following approaches: measured plutonium extraction efficiencies as a function of extractant ligand concentrations, pH titrations of protic ligands in the absence and presence of plutonium, pH/ligand/plutonium titrations monitored by optical spectroscopy, and less

frequently from multinuclear NMR and vibrational spectroscopic analysis. The structures of solution species have also been inferred from the characterization of corresponding solids. More direct methods, including electrospray mass spectroscopy and X-ray absorption spectroscopy, are increasingly being applied to characterize molecular plutonium complexes. Fluorescence spectroscopy has the potential to be used to characterize plutonium species, similar to its application in uranyl chemistry, as emission from plutonium ions has been observed, albeit under very special conditions.

The coordination chemistry of plutonium ions is generally characteristic of exceptionally 'hard' Lewis acids, those that show preference for complexation by hard (i.e. first row donor atom) ligands. Weak Lewis bases, such as HS^- form weak complexes with plutonium and strong Lewis bases, such as CO_3^{2-}, F^-, and PO_4^{3-} form very stable complexes. Plutonium ions have relatively large ionic radii and therefore form complexes with high coordination numbers (8–14). For a given ligand the strength of complexation (the stability of the Pu–ligand complex) and the tendency of ions to hydrolyze decrease following the effective charges:

$$Pu^{4+} > PuO_2^{2+} \approx Pu^{3+} > PuO_2^{+}$$

Overall, the bonding in plutonium complexes can generally be described as ionic, where the geometry of coordination complexes is primarily governed by steric considerations (ligand–ligand repulsions). Plutonium–ligand orbital overlap is considered to be important in some types of complexes, and comparatively more important than in corresponding complexes of lanthanides and lighter actinides with similar ionic radii. Ligand exchange in plutonium complexes is facile, and reaction rates are generally fast.

Complexation in this chapter generally refers to inner-sphere coordination, where the ligand is directly bonded to plutonium and displaces more weakly bound ligands and/or solvent water. Outer sphere complexation and ion pairing are also important interactions, particularly in high ionic strength and otherwise complicated solutions. Equilibrium constants for the reactions of plutonium ions with ligands reflect the competition between protons and plutonium for ligand atom bonding and are experimentally determined. Formation constants are pH independent values calculated from equilibrium constants, ligand pK_as, and plutonium hydrolysis constants and therefore more directly reflect the strength of interaction between the plutonium ion and the deprotonated ligand. For weaker ligands it is important to note that this interaction may be on the order of plutonium–solvent interactions, a factor not easily separated out to provide a quantitative pure plutonium–ligand interaction constant. In the text that follows, we will use K for the consecutive or stepwise formation constants, and β for the cumulative or overall formation constants (Lemire *et al.*, 2001). In cases where complex formation involves a deprotonation of a ligand, the equilibrium constant (K) or formation constant (β) will be denoted by an asterisk as indicated below.

$$PuL_{n-1} + L \rightleftharpoons PuL_n, \quad K_n = \frac{[PuL_n]}{[PuL_{n-1}][L]} \tag{7.129}$$

$$PuL_{n-1} + HL \rightleftharpoons PuL_n + H^+, \quad {}^*K_n = \frac{[PuL_n][H^+]}{[PuL_{n-1}][HL]} \tag{7.130}$$

$$Pu + nL \rightleftharpoons PuL_n, \quad \beta_n = \frac{[PuL_n]}{[Pu][L]^n} \tag{7.131}$$

$$Pu + nHL \rightleftharpoons PuL_n + nH^+, \quad {}^*\beta_n = \frac{[PuL_n][H^+]^n}{[Pu][HL]^n} \tag{7.132}$$

Selected formation constants and equilibrium constants will be defined and conditions specified in summary tables. The emphasis is on describing the types of molecular plutonium complexes that form and highlighting specific chemical, structural, and physical properties. For a more comprehensive discussion of stability constant determinations and analysis done to compute thermodynamic constants under standard conditions the reader is referred to specialized critical reviews (Grenthe *et al.*, 1997; Lemire *et al.*, 2001; Guillaumont *et al.*, 2003). Comparisons across the actinide series and a fine description of the details of plutonium complexation in solution are given in Chapter 23. Selected formation and equilibrium constants for plutonium complexes are given in Table 7.56.

(*i*) *Oxoanions*

Plutonium ions are oxophilic and therefore readily form complexes with oxo ligands, as exemplified by high hydration numbers and extreme hydrolysis described in Section 7.9.1(d). Anionic inorganic oxo ligands effectively complex plutonium to form complexes whose stability depends on the charge and basicity of the ligand. For a given plutonium ion the order of complexation strength for common oxoanions is: $ClO_4^- < IO_3^- < NO_3^- < SO_4^{2-} << CO_3^{2-} < PO_4^{3-}$. Perchlorate is often referred to as a noninteracting counter ion, but does coordinate to plutonium at very high concentrations. Nitrate complexes are much more stable than analogous perchlorate species and slightly more stable than chloride complexes of the same stoichiometry. Phosphate is an exceptionally strong ligand for plutonium. These ions usually chelate plutonium ions in a bidentate fashion. The stability of plutonium oxoanionic complexes follow the general trends of Pu(IV) being the strongest and Pu(V) being the weakest.

The coordination numbers of plutonium oxoanion complexes ranges from 7 for PuO_2^+ to up to 12 for Pu^{4+}, where water is successively displaced from the inner coordination sphere by chelating ligands. Water that remains bonded to the Pu center can hydrolyze to form mixed-ligand complexes that contain one or more bidentate oxoanion and one or more hydroxide ligand. These species are favored at near-neutral pH and lower oxoanion concentrations. Solution

complex formation constants and solid-state structures are known for relatively few of these species, such as Pu(IV) hydroxo oxalates. It is difficult to distinguish mixed-ligand complexes from the coexistence of individual complexes, which explains the uncertainty in, for example, plutonium(IV) carbonate speciation and thermodynamic stability.

Carbonate

Plutonium carbonates are of interest because of their fundamental chemistry and environmental behavior, including aspects of actinide mineralogy and nuclear waste isolation. Separation schemes based on carbonate that utilize the pH-dependent complexing properties of this ligand have been proposed as alternatives to acid-based or organic extraction processes for used nuclear fuels (Asanuma *et al.*, 2001). Some features are common to the carbonate complexation of plutonium ions. Carbonate binds plutonium in a bidentate fashion and has a small bite angle so that coordination numbers of resulting complexes are generally quite high, 7–10. The actinyl ions, PuO_2^+ and PuO_2^{2+} have pentagonal and hexagonal bipyramidal structures in which the linear triatomic O=An=O unit forms the axis of a pentagonal or hexagonal bipyramidal coordination polyhedron with respect to carbonato and aquo oxygen atoms bound to the metal center. In addition to chelating the plutonium ion, carbonate ligands often hydrogen bond to outer sphere waters or counter ions to produce chains and layers and other less regular hydrogen bond networks in the solid-state structures. For all of the oxidation states the stability constant for the initial monocarbonato complex is known with the greatest accuracy and precision because they can be determined spectrophotometrically from the reduction/shift in the characteristic absorption band for the aquo ion. Thermodynamic constants of the limiting carbonato complexes are better known from the solubility and carbonate titration studies than are those corresponding to intermediate species because the former usually have large stability fields. And the limiting molecular complexes are usually isostructural with the solution species from which they are precipitated. Intermediate carbonate complexes are not well characterized for any of the oxidation states. Several reviews on actinide carbonate and environmental chemistry describe plutonium carbonato complexes in detail (Grenthe *et al.*, 1986b; Newton and Sullivan, 1986; Fuger, 1992; Clark *et al.*, 1995; Choppin and Wong, 1998).

Trivalent plutonium carbonato complexes generally oxidize rapidly to tetravalent species. In aqueous Pu(III) solutions there is evidence for the stepwise formation of the carbonato complexes, $Pu(CO_3)^+$ and $Pu(CO_3)_2^-$. Additional carbonato and hydroxocarbonato complexes may form, but are immediately oxidized to Pu(IV) species. Formation constants of $\log_{10}\beta_1 = 7.5$ and $\log_{10}\beta_2 = 12.4$ have been estimated at low ionic strength (0.1–0.5 M) (Cantrell, 1988). These values have not been verified, but are consistent with well-known constants of Am(III) carbonato complexes (Silva *et al.*, 1995).

Table 7.56 *Formation constants for plutonium oxo anions.*

Reaction stoichiometry	*I* (M)	$\log_{10}\beta_n$	$\log_{10}\beta_n^\circ$	*References*
carbonate				
$Pu^{3+} + CO_3^{2-} \rightleftarrows PuCO_3^+$	0.1–0.5	7.5		Cantrell (1988)
$Pu^{3+} + 2CO_3^{2-} \rightleftarrows Pu(CO_3)_2^-$	0.1–0.5	12.4		Cantrell (1988)
$Pu^{4+} + CO_3^{2-} \rightleftarrows PuCO_3^{2+}$	0.3	17.0 ± 0.7		Nitsche and Silva (1996) and Rai *et al.* (1999)
$Pu^{4+} + 4CO_3^{2-} \rightleftarrows Pu(CO_3)_4^{4-}$	1.5	44.5	37.0 ± 1.1[a]	Capdevila *et al.* (1996) and Guillaumont *et al.* (2003)
$Pu^{4+} + 5CO_3^{2-} \rightleftarrows Pu(CO_3)_5^{6-}$	0		36.65 ± 1.13[a]	Guillaumont *et al.* (2003)
$Pu(CO_3)_4^{4-} + CO_3^{2-} \rightleftarrows Pu(CO_3)_5^{6-}$	3.0	-1.36 ± 0.09	–	Capdevila *et al.* (1996)
$Pu^{4+} + 2CO_3^{2-} + 4OH^- \rightleftarrows Pu(CO_3)_2(OH)_4^{4-}$	~ 0.1	46.4 ± 0.7[b]		Yamaguchi *et al.* (1994)
$Pu^{4+} + 2CO_3^{2-} + 2OH^- \rightleftarrows Pu(CO_3)_2(OH)_4^{2-}$		44.8[b]		Rai *et al.* (1999)
$PuO_2^+ + CO_3^{2-} \rightleftarrows PuO_2CO_3^-$	0.5	4.60 ± 0.04	5.12 ± 0.14[a]	Bennett *et al.* (1992) and Guillaumont *et al.* (2003)
$PuO_2^+ + 3CO_3^{2-} \rightleftarrows PuO_2(CO_3)_3^{5-}$		7.5	5.025 ± 0.92[a]	Wester and Sullivan (1983), Capdevila *et al.* (1992), and Guillaumont *et al.* (2003)
$PuO_2^{2+} + CO_3^{2-} \rightleftarrows PuO_2CO_3$	3.5	8.6 ± 0.3	9.5 ± 0.5[a]	Robouch and Vitorge (1987) and Guillaumont *et al.* (2003)
	0.1	8.7 ± 0.3		Pashalidis *et al.* (1997)
$PuO_2^{2+} + 2CO_3^{2-} \rightleftarrows PuO_2(CO_3)_2^{2-}$	0.1	13.1 ± 0.1	14.7 ± 0.5[a]	Sullivan *et al.* (1982)
	3.5	13.6 ± 0.7		Robouch and Vitorge (1987) and Guillaumont *et al.* (2003)

$PuO_2^{2+} + 3CO_3^{2-} \rightleftarrows PuO_2(CO_3)_3^{4-}$	0.1	18.2 ± 0.4	18.0 ± 0.5[a]	Ullman and Schreiner (1988), Robouch and Vitorge (1987), and Guillaumont *et al.* (2003)
$3PuO_2(CO_3)_3^{4-} \rightleftarrows (PuO_2)_3(CO_3)_6^{6-} + 3CO_3^{2-}$	3.0	-7.4 ± 0.2		Grenthe *et al.* (1986a)
nitrate				
$Pu^{4+} + NO_3^- \rightleftarrows PuNO_3^{3+}$	2	0.51 ± 0.05	1.95 ± 0.15[a]	Berg *et al.* (2000) and Guillaumont *et al.* (2003)
$Pu^{4+} + 2NO_3^- \rightleftarrows Pu(NO_3)_2^{2+}$	2	1.05 ± 0.08		Berg *et al.* (2000)
phosphate				
$Pu^{4+} + H_3PO_4 \rightleftarrows PuH_3PO_4^{4+}$	2	2.3	2.4 ± 0.3[a]	Denotkina *et al.* (1960) and Guillaumont *et al.* (2003)
$PuO_2^+ + HPO_4^{2-} \rightleftarrows PuO_2HPO_4^-$	1	2.39 ± 0.04		Moskvin and Poznyakov (1979)
sulfate				
$Pu^{3+} + HSO_4^- \rightleftarrows PuSO_4^+ + H^+$			1.93 ± 0.614[a]	Guillaumont *et al.* (2003)
$Pu^{3+} + 2HSO_4^- \rightleftarrows Pu(SO_4)_2^- + 2H^+$			1.74 ± 0.76[a]	Guillaumont *et al.* (2003)
$Pu^{4+} + HSO_4^- \rightleftarrows PuSO_4^{2+} + H^+$			4.91 ± 0.22[a]	Guillaumont *et al.* (2003)
$Pu^{4+} + 2HSO_4^- \rightleftarrows Pu(SO_4)_4 + 2H^+$			7.18 ± 0.32[a]	Guillaumont *et al.* (2003)
$PuO_2^{2+} + SO_4^{2-} \rightleftarrows PuO_2SO_4$			3.38 ± 0.20[a]	Guillaumont *et al.* (2003)
$PuO_2^{2+} + 2SO_4^{2-} \rightleftarrows PuO_2(SO_4)_2^{2-}$			4.4 ± 0.2[a]	Guillaumont *et al.* (2003)

[a] NEA Update Vol 5 (Guillaumont *et al.*, 2003).
[b] Species may not exist, based on later studies of Pu(IV) carbonates (Capdevila *et al.*, 1996).

Tetravalent plutonium probably forms stepwise complexes, $Pu(CO_3)_n^{4-2n}$, $n = 1$–5, with increasing solution pH and carbonate concentration (Newton and Sullivan, 1986; Clark *et al.*, 1995). The end members of this series and the tetracarbonato complex have been characterized, while the bis- and tris-species are inferred from studies of other actinide(IV) carbonates. Monocarbonato Pu(IV) of formula $Pu(CO_3)^{2+}$ is prepared by addition of carbonate to acidic solutions of the ion or from carbonate-mediated dissolution of hydroxide or oxide solids. The formation constant for $Pu(CO_3)^{2+}$ is reported to be $\log_{10} \beta_1 = (17.0 \pm 0.7)$ (Nitsche and Silva, 1996; Rai *et al.*, 1999). Given the generally accepted hydration number of eight for Pu(IV), this complex likely has six additional water molecules in the inner coordination sphere. In concentrated carbonate solutions, $Pu(CO_3)_4^{4-}$ is in equilibrium with $Pu(CO_3)_5^{6-}$. The formation constants for these individual species are highly correlated with each other and with the lower carbonate species.

Capdevila *et al.* (1996) studied the formation of the limiting carbonato complex of formula $Pu(CO_3)_5^{6-}$ by electronic absorption spectroscopy with varying ionic strength. From the study of the equilibrium in equation (7.133), they were able to determine an equilibrium constant for the reaction of $\log_{10} K_5 = -(1.36 \pm 0.09)$, and the formation constant for the limiting complex of $\log_{10} \beta_5 = (35.8 \pm 1.3)$ in 3 M $NaClO_4$ solution. The NEA review recommended a zero ionic strength value of $\log_{10} \beta_5 = (36.65 \pm 1.13)$ (Lemire *et al.*, 2001). By combining the value for β_5 with the equilibrium constant K_5 for equation (7.133), the formation constant for $Pu(CO_3)_4^{4-}$ at zero ionic strength was recommended to be $\log_{10} \beta_4 = (37.0 \pm 1.1)$ (Lemire *et al.*, 2001).

$$Pu(CO_3)_4^{4-} + CO_3^{2-} \rightleftarrows Pu(CO_3)_5^{6-} \tag{7.133}$$

Recent conventional spectrophotometric and electrochemical studies have focused on refining the thermodynamic constants for the carbonato species and determining the stability field and stoichiometry of mixed hydroxo/carbonato Pu(IV) complexes (Capdevila and Vitorge, 1999). The NEA critical review of thermodynamic data suggests that spectroscopic signatures and solubility characteristics that have been attributed to mixed hydroxo/carbonato complexes are in fact explained by the simultaneous and independent formation of hydrolysis products and carbonato complexes (Lemire *et al.*, 2001). Counter arguments are that colloidal Pu(IV) polymer formation is suppressed by carbonate complexation, and that absorption spectra of Pu(IV) in carbonate solutions over the entire pH range are wholly reproduced by linear combinations of known individual hydroxide and carbonate spectra.

Plutonium(IV) carbonato solids of general formula $M_xAn(CO_3)_y \cdot nH_2O$ have been prepared with a variety of cations ($M = Na^+, K^+, NH_4^+, C(NH_2)_3^+$; $y = 4$, 5, 6, 8) by precipitating or crystallizing the solution species. For example, $[Na_6Pu(CO_3)_5]_2 \cdot Na_2CO_3 \cdot 33H_2O$ was crystallized from 2.5 M Na_2CO_3 solution and characterized by single-crystal XRD (Clark *et al.*, 1998). The structure

contains the discrete $Pu(CO_3)_5^{6-}$ ion, which can be viewed as a pseudo-hexagonal bipyramid with three CO_3^{2-} ligands in an equatorial plane and two in axial positions as shown in **13**. Solution XAFS data for Pu(IV) in 2.5 M Na_2CO_3 solution gave bond distances and coordination numbers that corresponded extremely well with the average Pu–O, nonbonding Pu– –C, and distal Pu– –O distances of 2.42(1), 2.87(1), and 4.12(1) Å, respectively, found in the solid-state structure for the $Pu(CO_3)_5^{6-}$ ion. A peak-by-peak correspondence of the optical absorption spectra of the solution and diffuse reflectance spectrum of the ground crystalline solid, together with the solution XAFS data provide conclusive evidence that the $Pu(CO_3)_5^{6-}$ ion is the limiting species in high carbonate solutions. Depending on reaction conditions, green amorphous powders of compositions $K_4Pu(CO_3)_4{\cdot}nH_2O$, $K_6Pu(CO_3)_5{\cdot}nH_2O$, $K_8Pu(CO_3)_6{\cdot}nH_2O$, and $K_{12}Pu(CO_3)_8{\cdot}nH_2O$ have all been reported (Gel'man and Zaitsev, 1958). Since Clark *et al.* identified the $Pu(CO_3)_5^{6-}$ ion as the limiting species, it is reasonable to assume that the latter two solids are more realistically formulated as $[K_6Pu(CO_3)_5][K_2CO_3]{\cdot}nH_2O$ and $[K_6Pu(CO_3)_5][K_2CO_3]_3{\cdot}nH_2O$. Sodium salts of formula $Na_4Pu(CO_3)_4{\cdot}3H_2O$, $Na_6Pu(CO_3)_5{\cdot}2H_2O$, and $Na_6Pu(CO_3)_5{\cdot}4H_2O$ have also been claimed as light green crystalline compounds that appear to dehydrate in air (Gel'man and Zaitsev, 1958). Similarly, the $(NH_4)_4Pu(CO_3)_4{\cdot}4H_2O$ and $[Co(NH_3)_6]_2Pu(CO_3)_5{\cdot}5H_2O$ salts have been reported (Ueno and Hoshi, 1970).

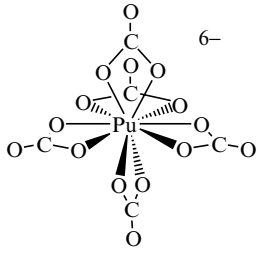

13

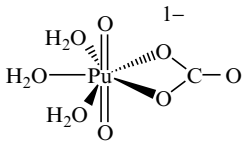

14

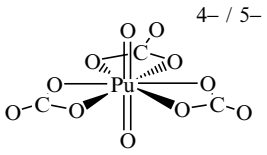

15

Pentavalent plutonium carbonato complexes are prepared by addition of alkali metal carbonate solutions to mildly acidic solutions of PuO_2^+, or by the one-electron reduction of Pu(VI) carbonato complexes. The mono- and triscarbonato complexes, $PuO_2(CO_3)^-$ and $PuO_2(CO_3)_3^{5-}$, have been observed directly by optical absorption spectroscopy, and their formation constants have been determined. In contrast, the biscarbonato complex $PuO_2(CO_3)_2^{3-}$ has not been observed directly, and is only inferred. Sensitive laser photoacoustic spectroscopy was used to determine the formation constant of $\log_{10}\beta_1 = (4.6 \pm 0.04)$ for $PuO_2(CO_3)^-$ (Bennett *et al.*, 1992). Using the Nernst equation, the measured reversible reduction of hexavalent $PuO_2(CO_3)_3^{4-}$ at 339 mV vs SHE in 1 M Na_2CO_3 and comparisons with Np(V) carbonato formation constants, the formation constant for $PuO_2(CO_3)_3^{5-}$ can be estimated to be $\log_{10}\beta_3 = 7.5$

(Wester and Sullivan, 1983; Capdevila *et al.*, 1992). These solution species are likely isostructural with the corresponding $NpO_2(CO_3)(OH_2)_3^-$, and $NpO_2(CO_3)_3^{5-}$ complexes which have been characterized by EXAFS spectroscopy, and illustrated in **14** and **15** (Clark *et al.*, 1996). These complexes have the general actinyl carbonate structure with axial O=An=O units at a bond distance of 1.85 Å and bidentate carbonato and water oxygen atoms arrayed about the equatorial plane to form a pentagonal or hexagonal bipyramidal coordination polyhedron at average bond distances of 2.45 and 2.42 Å, respectively. Optical absorption spectra do not suggest that the biscarbonato complex $PuO_2(CO_3)_2^{3-}$ is ever a predominant solution species, consistent with the small difference between the stability constants for the mono- and tris-species that suggest a very small stability field for this intermediate species. Mixed hydroxo carbonato complexes have been proposed for Np(v) (Sullivan *et al.*, 1991), but the identification and existence of analogous Pu(v) species is questionable.

Solids corresponding to the Pu(v) carbonate solution species have been prepared as microcrystalline powders via precipitation and the orthorhombic solid-state structure of $KPuO_2CO_3$ has been determined (Ellinger and Zachariasen, 1954). Much more data is available for analogous salts of Np(v) carbonates, $MNpO_2CO_3$, and $M_3NpO_2(CO_3)_2$, where M is an alkali metal or ammonium ion (Simakin *et al.*, 1974; Volkov *et al.*, 1974a,b, 1981). These structure types have been reviewed by Clark *et al.* (1995). These compounds show interesting structural changes due to the size similarity of hydrated ions such as K^+ and NpO_2^+, and the extent of hydration. For example, for $MNpO_2CO_3$ where M = Cs^+, Rb^+, NH_4^+, K^+, Na^+, and Li^+, a hexagonal-to-orthorhombic phase change is observed within the NpO_2CO_3 layer at the potassium–sodium boundary. The solids both contain actinyl carbonate layers and the hexagonal and orthorhombic sheets are related by displacement of the chains of actinyl units through half a translation along the crystallographic *a*-axis. These basic layers are illustrated qualitatively in **16** and **17**. The orthorhombic structure **17** is more open than the hexagonal structure **16**, which appears to allow for the closer contacts necessary for the smaller sodium and lithium cations.

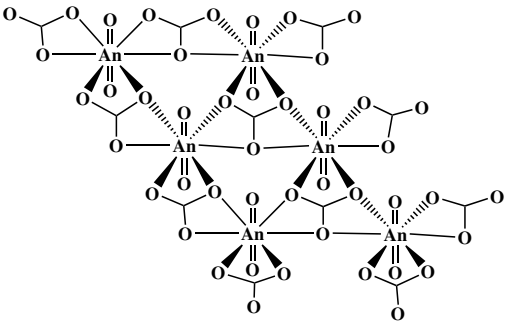

16

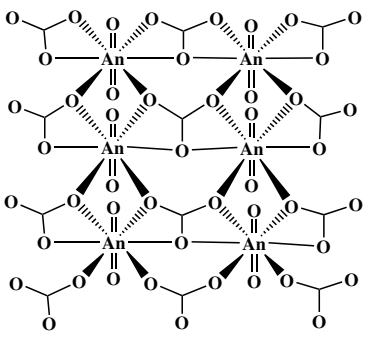

17

The biscarbonato solid $M_3NpO_2(CO_3)_2$ displays an overall orthorhombic structure, but exhibits a pseudo-hexagonal layer similar to **16**, except that one half of the AnO_2^+ ions in the anionic carbonate layer have been replaced by alkali metal cations. One can envision that M^+ and AnO_2^+ cations form alternating chains within the hexagonal sheet and give rise to the approximate composition $[M_{0.5}(AnO_2)_{0.5}(CO_3)]$ within the layer. This arrangement is illustrated qualitatively in **18**. The cation and anion layers are oriented such that an alkali metal cation, M^+, lies directly above and below the linear AnO_2^+ ion of adjacent sheets. The anionic carbonate layer and the cationic potassium layers line up such that they are parallel to the crystallographic *c*-axis, and this allows for an M–O=An interaction between layers and yields a maximally ordered structure (Clark *et al.*, 1995).

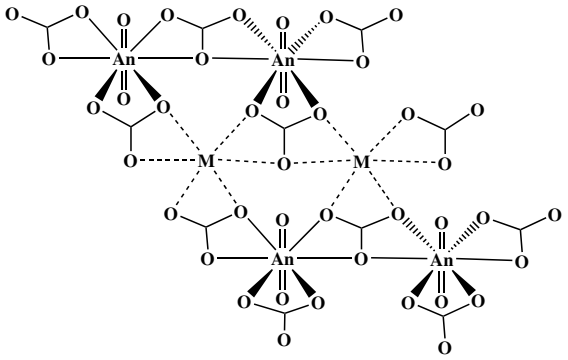

18

Hexavalent plutonium carbonato complexes have been studied primarily as an extension of uranyl carbonate chemistry. Uranyl carbonato complexes are very important in uranium geochemistry actinide contaminant environmental transport, uranium mining, and nuclear fuel production and reprocessing, owing to their high solubility and stability in aqueous solution. Substitution of the plutonyl ion in uranyl phases has the potential to form solid solutions.

Carbonate complexation of Pu(VI) increases with pH and carbonate concentration. Pashalidis *et al.* (1997) studied the solubility of both UO_2CO_3 and PuO_2CO_3 in aqueous carbonate solutions and determined equilibrium constants for the formation of $PuO_2(CO_3)$, $PuO_2(CO_3)_2^{2-}$, and $PuO_2(CO_3)_3^{4-}$. These results are in good agreement with earlier studies on $AnO_2(CO_3)$ solids of uranium, neptunium, and plutonium by Ullman and Schreiner (1988), and $PuO_2(CO_3)$ solids by Robouch and Vitorge (1987). The most recent NEA review recommends $\log_{10}\beta_1 = (9.5 \pm 0.5)$, $\log_{10}\beta_2 = (14.7 \pm 0.5)$, and $\log_{10}\beta_3 = (18.0 \pm 0.5)$ for the corresponding formation constants (Guillaumont *et al.*, 2003).

Both $PuO_2(CO_3)_{(aq)}$ and $PuO_2(CO_3)_3^{4-}$ have been spectroscopically observed. In contrast, while the $AnO_2(CO_3)_2^{2-}$ species has been spectroscopically observed for U(VI) and Np(VI), the stability field of the corresponding $PuO_2(CO_3)_2^{2-}$ analog appears to be so small that it has not been directly observed. Spectrophotometric and calorimetric studies of the formation of the monocarbonato complex from the Pu(VI) hydroxide illustrated that carbonate can outcompete hydroxide to coordinate to plutonium, and provided the first formation constants (Sullivan *et al.*, 1982). Subsequent solubility studies and additional spectrophotometric data provide a formation constant of $\log_{10}\beta_1 = (8.7 \pm 0.3)$ for $PuO_2(CO_3)$ in 0.1 M $NaClO_4$ (Pashalidis *et al.*, 1997). X-ray powder diffraction and XAFS studies of the corresponding $PuO_2(CO_3)$ solid show that it is isostructural with rutherfordine, $UO_2(CO_3)$ (Reilly *et al.*, 2000). This solid has a layered structure where the local coordination environment of the plutonyl ion is a hexagonal bipyramidal arrangement of oxygen atoms with the plutonyl units perpendicular to the orthorhombic plane (Clark *et al.*, 1995). Each plutonium atom forms six equatorial bonds with the oxygen atoms of four carbonate ligands, two in a bidentate manner and two in a monodentate manner. The orthorhombic plane is identical to that shown in **17**. The orthorhombic plane of hexagonal bipyramidal plutonyl units forms infinite, two-dimensional layers.

Solution EXAFS and single crystal XRD studies show the limiting $PuO_2(CO_3)_3^{4-}$ is isostructural with the uranyl analog, which has pseudo-hexagonal pyramidal coordination geometry as illustrated in **15**. The Pu=O distance was found to be 1.74 Å with an average Pu–O distance to carbonate ligands of 2.45 Å (Clark *et al.*, 1999b; Neu *et al.*, 2000; Conradson *et al.*, 2004a). The stability constant for $PuO_2(CO_3)_3^{4-}$ has been determined from solubility, calorimetry, and spectrophotometric studies to be $\log_{10}\beta_3 = (18.2 \pm 0.4)$ in 0.1 M electrolytes (Robouch and Vitorge, 1987; Ullman and Schreiner, 1988). Pashalidis *et al.* determined a value of (17.8 ± 0.2) in 0.1 M $NaClO_4$ solution, and the recent NEA assessment recalculated their value to correct for a systematic error and obtained (18.4 ± 0.2) (Guillaumont *et al.*, 2003). This species can be readily precipitated to form salts with monovalent cations.

In contrast with uranyl carbonate chemistry where the bis carbonato $UO_2(CO_3)_2^{2-}$ and its trimeric oligomer $(UO_2)_3(CO_3)_6^{6-}$ are major species (Allen *et al.*, 1995; Banyai *et al.*, 1995), the bis carbonato plutonyl complex, $PuO_2(CO_3)_2^{2-}$, has a small stability field and neither it nor the trimer $(PuO_2)_3(CO_3)_6^{6-}$ have been characterized. Similar to the hexavalent hydroxides, oligomerization reactions appear to decrease dramatically across the series from uranium to plutonium. Mixed actinyl trimers, $(UO_2)_2(PuO_2)(CO_3)_6^{6-}$ and $(UO_2)(PuO_2)_2(CO_3)_6^{6-}$ have been proposed based on optical absorption and emf studies (Grenthe *et al.*, 1986b). Similarly, additional polymeric species known for uranyl $(UO_2)_2(CO_3)(OH)_3^-$, $(UO_2)_3O(OH)_2(HCO_3)^+$, and $(UO_2)_{11}(CO_3)_6(OH)_{12}^{2-}$ under conditions of high metal ion concentration or high ionic strength (Grenthe *et al.*, 1992) have not been observed for plutonyl.

Nitrate

Nitrates were among the first complexes studied for plutonium and are very important in plutonium processing (Cleveland, 1979). The effectiveness of solvent extraction and ion-exchange processes in nitric acid, for example, depends strongly on the stoichiometry, stability, molecular geometry and molecular charge of nitrate complexes. Nitrate tends to bind plutonium in a bidentate fashion and to retain its planar molecular geometry, similar to carbonate. But it is a much weaker ligand. Because nitric acid solutions of plutonium and nitrate solids of Pu(IV) and Pu(VI) are both prevalent forms in process and synthetic chemistry, a tremendous number of mixed-ligand complexes are known that contain one or more mono- or bidentate nitrates in the inner coordination sphere.

Trivalent nitrate species have been prepared in nitric acid solution, but they are unstable with respect to oxidation.

Aqueous Pu(IV) nitrate complexes are very well studied because of their use in solvent extraction methods and ion-exchange chromatography. The solution species, $Pu(NO_3)_n^{4-n}$ ($n = 1$–6), have been studied in detail. There is evidence from numerous ion exchange and extraction studies and more recent NMR and EXAFS experiments that the mono-, bis-, tetra, and the hexanitrato complexes are significant, but the tris- and pentanitrato complexes are not (Veirs *et al.*, 1994). X-ray absorption data for the system suggest aquo ligation decreases in the inner sphere even before sequential bidentate nitrates bind the metal center. Solution EXAFS data gives coordination numbers of 11–12 for the first coordination sphere, with average Pu–O bond distances of 2.49 and 2.38 Å for nitrate and water ligands, respectively (Allen *et al.*, 1996b). Formation constants measured for the mononitrato complex, $Pu(NO_3)^{3+}$, were critically evaluated by the NEA reviewers, who recommend the constant $\log_{10}\beta_1 = (1.95 \pm 0.15)$ at $I = 0$ (Lemire *et al.*, 2001). A recent spectrophotometric study in 2 molal $HClO_4$ and extensive analysis by Monte Carlo methods sheds new light on the relative importance of the $Pu(NO_3)^{3+}$ and $Pu(NO_3)_2^{2+}$ complexes, and reported the constants $\log_{10}\beta_1 = (0.51 \pm 0.05)$ and $\log_{10}\beta_2 = (1.05 \pm 0.08)$ (Berg *et al.*, 2000).

Cation exchange resins have a strong affinity for the hexanitrato species, $Pu(NO_3)_6^{6-}$. This nitrate-based purification method is used to separate plutonium from most of the elements in the periodic table, and is used on an industrial scale (Section 7.5.5). There has been some discussion over whether the limiting Pu(IV) nitrate in solution is the penta- or hexanitrato species and some experiments suggest that the hexanitrate is only a major species in the presence of resins or in concentrated salt solutions that favor ion pairing (Veirs *et al.*, 1994; Clark and Delegard, 2002).

Plutonium(IV) nitrate solids are readily formed in nitric acid by dissolution of hydroxides or carbonates followed by precipitation or crystallization. Crystalline orthorhombic $Pu(NO_3)_4{\cdot}5H_2O$ can be obtained in this way and

also by heating a Pu(VI) nitrate salt (Staritzky, 1956). Hexanitrato complexes, $M_2Pu(NO_3)_6{\cdot}2H_2O$, where M = Rb, Cs, NH_4, and pyridinium, are obtained from moderately concentrated (8 to 14 M) nitric acid. A single crystal XRD study was performed on $(NH_4)_2Pu(NO_3)_6$ by Spirlet *et al.* (1992). In the solid state the icosohedral $Pu(NO_3)_6^{2-}$ unit is characterized by three mutually perpendicular planes formed by the trans NO_3^- ligands giving virtual T_h symmetry as illustrated in **19**. The 12 Pu–O bond distances average 2.487(6) Å.

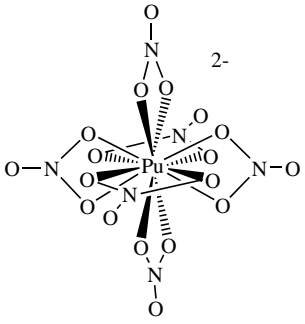

19

Numerous additional solution studies on Pu(IV) mixed ligand-nitrate complexes have been performed in the development and performance testing of extractants. Most notably these include TBP and phosphine oxides. As other examples, a variety of mixed amide-nitrate complexes have been proposed based upon NMR, IR, and extraction behavior (Berthon and Chachaty, 1995; Preston and du Preez, 1995; Romanovski *et al.*, 1999).

No inner-sphere Pu(V) nitrate complexes have been characterized. The existence of the solid nitrates of Np(V) and Pa(V), $NpO_2(NO_3){\cdot}xH_2O$ (x = 1, 5), $RbNpO_2(NO_3)_2{\cdot}H_2O$, and $PaO(NO_3)_3{\cdot}xH_2O$ (x = 1–4) suggests that it might be possible to isolate solid Pu(V) nitrates if the oxidation state could be stabilized in nitrate solution. Pu(VI) nitrates are weak complexes and only the mononitrate, $PuO_2(NO_3)^+$, species is significant in solution. Mixed TBP-nitrate complexes have been widely studied, including a recent EXAFS study of the structural changes as the actinyl species are reduced to An(IV) (Den Auwer *et al.*, 1999). The hydrated solid, $PuO_2(NO_3)_2{\cdot}xH_2O$, x = 3,6, has been characterized.

Sulfate

Trivalent plutonium forms at least two stepwise complexes, $PuSO_4^+$ and $Pu(SO_4)_2^-$ in acid solutions according to equations below (Fardy and Buchanan, 1976; Rao *et al.*, 1978; Nash and Cleveland, 1983).

$$Pu^{3+} + HSO_4^- \rightleftharpoons PuSO_4^+ + H^+ \quad (7.134)$$

$$Pu^{3+} + 2HSO_4^- \rightleftharpoons Pu(SO_4)_2^- + 2H^+ \quad (7.135)$$

The NEA reviewers recalculated the formation constants for these species according to the reactions above, extrapolated to zero ionic strength and recommended $\log_{10} {}^*\beta_1 = (1.93 \pm 0.61)$ and $\log_{10} {}^*\beta_2 = (1.74 \pm 0.76)$ (Lemire *et al.*, 2001). The fact that higher order anions such as $Pu(SO_4)_4^{5-}$ are found in solids such as $K_5Pu(SO_4)_4{\cdot}4H_2O$ suggests that higher order ions of formula $Pu(SO_4)_n^{3-2n}$ must form to a small extent in solution (Mudher *et al.*, 1995). There is some evidence for the formation of solid $Pu_2(SO_4)_3{\cdot}xH_2O$. The Pu(III) solid is likely isostructural with $Am_2(SO_4)_3{\cdot}8H_2O$, which is comprised of eight coordinate Am(III) (Bullock *et al.*, 1980). The ternary salts of $MPu(SO_4)_2{\cdot}H_2O$, where M is an alkali metal, are isostructural with the Nd(III) analog (Iyer and Natarajan, 1989, 1990). Similarly, the $(NH_4)Pu(SO_4)_2{\cdot}4H_2O$ is isomorphous with the corresponding Sm(III) compounds; and all of these structures contain nine coordinate metal centers containing water and bidentate sulfate ligands. Salts of other complex anions, such as $K_5Pu(SO_4)_4$, which is isostructural with $K_5La(SO_4)_4$, are also known (Mudher *et al.*, 1995).

Sulfate has high affinity for plutonium(IV). The stability of the complexes has been studied both to understand the properties of the complexes themselves and to evaluate how sulfate competes with extractants (Laxminarayanan *et al.*, 1964; Sokhina *et al.*, 1978; Solovkin and Rubisov, 1983). As for Pu(III), formation constants for Pu(IV) sulfato complexes are accurately expressed as solution reaction constants from bisulfate addition to Pu^{4+} according to reactions (7.136) and (7.137).

$$Pu^{4+} + HSO_4^- \rightleftharpoons PuSO_4^{2+} + H^+ \quad (7.136)$$

$$Pu^{4+} + 2HSO_4^- \rightleftharpoons Pu(SO_4)_{2\,(aq)} + 2H^+ \quad (7.137)$$

The data are most consistent with the formation of two complexes, $PuSO_4^{2+}$ and $Pu(SO_4)_2$, but higher order species $Pu(SO_4)_n^{4-2n}$ are implied by the existence of salts such as $K_4Pu(SO_4)_4{\cdot}2H_2O$. The NEA review recommends the constants $\log_{10} {}^*\beta_1 = (2.75 \pm 0.01)$ and $\log_{10} {}^*\beta_2 = (4.43 \pm 0.01)$ in 2.2 molal $(H, Na)_2SO_4$ solutions (Lemire *et al.*, 2001). Extrapolation to zero ionic strength gives $\log_{10} {}^*\beta_1 = (4.91 \pm 0.22)$ and $\log_{10} {}^*\beta_2 = (7.18 \pm 0.32)$ (Lemire *et al.*, 2001). Based upon the crystal structure of $Pu_2(OH)_2(SO_4)_3(H_2O)_4$, mixed hydroxo sulfato complexes are also thought to form in solution at higher pH (Wester, 1983).

The neutral hydrates can be precipitated as $Pu(SO_4)_2{\cdot}nH_2O$ ($n = 9, 8, 6, 4$), and subsequently dehydrated up to 400°C. The red tetrahydrate Pu(IV) phase is noteworthy because of its high purity (Cleveland, 1979). The common bicapped square antiprismatic geometry of four sulfates and four waters is adopted by the

Pu(IV) centers in the tetra- and octahydrates. Each sulfate group is shared by two Pu(IV) ions, and sulfates not bonded to plutonium are hydrogen bonded to water molecules (Kierkegaard, 1956; Jayadevan *et al.*, 1982). Two orthorhombic polymorphs of the tetrahydrate differ only by hydrogen bonding in the structures (Jayadevan *et al.*, 1982). The octahydrate loses four water molecules at relatively low temperature, and can be fully dehydrated. Ternary salts have also been characterized, such as the green Pu(IV) compounds $M_4Pu(SO_4)_4{\cdot}xH_2O$ and $M_6Pu(SO_4)_5{\cdot}xH_2O$ (M = K, NH_4) (Sood *et al.*, 1992). The structure of the anion in $K_4Pu(SO_4)_4{\cdot}2H_2O$ consists of chains of plutonium atoms linked by pairs of bridging sulfate groups, and the plutonium atom exhibits a tricapped trigonal prismatic coordination geometry. The structure of the Pu(IV) mixed hydroxo-sulfato complex, $Pu_2(OH)_2(SO_4)_3(H_2O)_4$, has been determined and is isomorphous with the hydroxosulfates of Zr, Hf, and Ce (Wester, 1983).

Sulfate complexes of Pu(V) have not been characterized, but they may be important environmental species since sulfate can be a major component of natural waters and minerals. Therefore research on these types of complexes is merited.

Mono- and bis-sulfato complexes of plutonyl(VI), $PuO_2(SO_4)$ and $PuO_2(SO_4)_2^{2-}$, are generally prepared from acidic solutions. Solution equilibrium constants derived in terms of formation constants for the reactions listed below have been measured (Patil and Ramakrishna, 1976; Ullman and Schreiner, 1986).

$$PuO_2^{2+} + SO_4^{2-} \rightleftharpoons PuO_2SO_4(aq) \tag{7.138}$$

$$PuO_2^{2+} + 2SO_4^{2-} \rightleftharpoons PuO_2(SO_4)_2^{2-} \tag{7.139}$$

The NEA reviewers evaluated these results and recommended the zero ionic strength formation constants of $\log_{10}\beta_1 = (3.38 \pm 0.20)$ and $\log_{10}\beta_2 = (4.4 \pm 0.2)$ (Lemire *et al.*, 2001). Changes in the electronic structure of hexavalent plutonium and neptunium as a function of sulfate, selenate, and chromate complexation have been studied by optical and IR spectroscopy and attributed to covalence variation in An=O bonding or distortions in the ligand arrangement (Budantseva *et al.*, 2000).

Plutonyl sulfate solids of formula $M_2PuO_2(SO_4)_2$ have been prepared and are likely isostructural with the neptunyl analogs. The solid state layered structure of $Cs_2NpO_2(SO_4)_2$ is built up by anionic layers $[NpO_2(SO_4)_2]_n^{2n-}$, linked together by Cs^+ ions. Each NpO_2^{2+} ion in the anionic layer is linked via the sulfate ions to three other atoms to form an hexagonal net similar to the actinyl(V) carbonate structures (Fedosseev *et al.*, 1999).

Phosphate

Because of their very low solubility as exemplified by stable minerals and ore bodies, actinide phosphates have been proposed as potential radioactive waste

forms (Boatner and Sales, 1988). Phosphate has multiple protonation states, PO_4^{3-}, HPO_4^{2-} and $H_2PO_4^-$, and related condensed phosphate anions such as $P_2O_7^{4-}$ and $(PO_3)_n^{n-}$ with many coordination modes that can lead to intricate three-dimensional structures in the solid state, making the plutonium phosphate compounds particularly challenging to characterize. The limited information that is available for plutonium phosphate solution species comes from solubility studies and X-ray and optical absorption spectroscopic studies. In the solid state, the major classes of actinide phosphate are phosphates, hydrogenphosphates, dihydrogen phosphates, diphosphates (pyrophosphates), and polytrioxophosphates (metaphosphates). In addition there are numerous ternary compounds, mixed valent uranium phosphates, halophosphates, organophosphates, and more recently, open framework and templated phases.

Plutonium(III) phosphate solution species are proposed to have the formula $Pu(H_2PO_4)_n^{3-n}$ ($n = 1$–4), but they have not been spectroscopically or structurally characterized (Moskvin, 1971a). For Pu(III), the blue, hexagonal $PuPO_4{\cdot}0.5H_2O$ has been prepared by precipitation from relatively dilute HNO_3/H_3PO_4 solution, then heated to yield the anhydrous compound (Bamberger, 1985). Anhydrous plutonium pyrophosphate PuP_2O_7 has been prepared by the thermal decomposition of plutonium oxolatophosphates (Bjorklund, 1957; Bamberger, 1985).

By considering the protonation behavior of phosphoric acid (Grenthe *et al.*, 1992) the following plutonium(IV) complexes may form: $Pu(H_3PO_4)_x(H_2PO_4)_y^{(4-y)+}$ ($x = 0$, 1; $y = 0$, 1, 2) under acidic conditions; $Pu(HPO_4)_3(H_2PO_4)_x^{(2+x)-}$ ($x = 1$, 2) at neutral pH; and $Pu(HPO_4)_x^{4-2x}$ ($x = 1$–3) under basic conditions. All of the known Pu(IV) solids have such low solubilities that only experiments with $Pu(HPO_4)_2{\cdot}xH_2O$ have yielded solution speciation information. The solution complex in equilibrium with the solids, $Pu(H_3PO_4)^{4+}$, has a formation constant of $\log_{10}\beta_1 = 2.3$ in 2 M (H,Na)NO_3 (Denotkina *et al.*, 1960), and the NEA reviewers recommended the value $\log_{10}\beta_1 = (2.4 \pm 0.3)$ at zero ionic strength (Lemire *et al.*, 2001).

The chemistry of tetravalent actinide phosphates has been recently reviewed and a new classification system proposed for these compounds (Brandel and Dacheux, 2004a,b). New characterization data indicates that a number of previously reported actinide phosphate phases appear to be polyphase mixtures, particularly the "$M_3(PO_4)_4$" group of compounds. Solid Pu(IV) phosphates can be considered a subset of known Th(IV) and U(IV) compounds. Plutonium(IV) polytrioxophosphate, $Pu(PO_3)_4$, can be crystallized by dissolving PuO_2 in polyphosphoric acid (Douglass, 1962). The hydrogenphosphate, $Pu(HPO_4)_2{\bullet}xH_2O$, is reported to precipitate as a gelatinous solid upon addition of phosphoric acid to nitric acid solutions of Pu(IV) and can be used as precursor for other phosphate phases. Anhydrous plutonium diphosphate PuP_2O_7, has been prepared by the thermal decomposition of plutonium oxolatophosphates or by heating a mixture of PuO_2 and BPO_4 (Bjorklund, 1957; Bamberger, 1985). Additonal Pu(IV) phosphates and diphosphates are likely

based on the growing list of thorium and uranium phosphate phases reported. For example, Bénard *et al.* reported two distinct thorium types in $Th_4(PO_4)_4(P_2O_7)$, one eight-coordinate with oxygen from five phosphate and one diphosphate group and around the thorium atom (Bénard, Brandel *et al.*, 1996). Thorium(IV) can be replaced by Pu(IV) up to a maximum value of x = 1.67 for $Th_{4-x}M_x(PO_4)_4(P_2O_7)$ (Dacheux, Brandel *et al.*, 1998). Ternary compounds of the general formula $M(I)Th_2(PO_4)_3$ and $M(II)Th(PO_4)_2$ with M(I) = alkali cation, Tl, Ag, Cu, (Louer, Brochu *et al.*, 1995; Bénard, Brandel *et al.*, 1996) and M(II) = Ca, Sr, Cd, Pb, (Merigou, Genet *et al.*, 1995) are also known for U(IV).

Plutonium(V) phosphate, $NH_4PuO_2HPO_4{\cdot}4H_2O$, was precipitated from solutions of PuO_2^+ in nitric acid with the addition of $(NH_4)_2HPO_4$ (Gel'man and Zaitseva, 1964). There is evidence for $PuO_2HPO_4^-$ from adsorption studies of PuO_2^+ on iron oxides in phosphoric acid, but it has not been fully characterized (Moskvin and Poznyakov, 1979; Morgenstern and Kim, 1996). Its formation constant has been reported to be $\log_{10}\beta_1 = (2.39 \pm 0.04)$ in 1 M NH_4Cl (Moskvin and Poznyakov, 1979). It is likely that additional complexes are formed, but their stoichiometries are not certain.

Denotkina *et al.* reported the first studies of Pu(VI) phosphates (Denotkina, Shevchenko *et al.*, 1965; Denotkina and Shevchenko, 1967). This work was later revised and augmented by Fischer *et al.* who prepared a series of compounds of Pu(VI) with phosphates and arsenates with the general formulas, $MPuO_2XO_4{\bullet}yH_2O$ and $M'(PuO_2XO_4)_2{\bullet}zH_2O$ (X = P, As; M = H^+, K^+, Rb^+, NH_4^+; M′ = Ca^{2+}, Sr^{2+}), and compared the characterization data with analogous uranium and neptunium compounds (Fischer, Werner *et al.*, 1981). The hydrogenphosphate compounds, $PuO_2(HXO_4){\bullet}yH_2O$ (X = P, As), were prepared by reacting Pu(VI) hydroxide with aqueous solutions of H_3PO_4 and H_3AsO_4. The compounds $MPuO_2(PO_4){\bullet}yH_2O$ (M = K^+, NH_4^+) precipitated from aqueous solutions of Pu(VI) in dilute nitric acid upon addition of K_2PO_4 and $(NH_4)_2PO_4$. The acidic proton in the solid arsenate hydrogenarsenate complex was partially exchanged by mixing the solid with a solution of the Group 1 or 2 metal chloride. Weger *et al.* reported preliminary data on the solubility and speciation of Pu(VI) in phosphate solutions and observed evidence for colloid formation from filtration data and for three complexes between pH 2.7 to 12 in the visible–near infrared absorption spectra (Weger, Okajima *et al.*, 1993). Further work is needed to determine if the absorption features are due to soluble or colloidal species.

Iodate

The precipitate of Pu(IV) iodate, $Pu(IO_3)_4$, was one of the first forms of ^{239}Pu isolated and is a common end product in low pH actinide/lanthanide separations (Cleveland, 1979). This useful solid has not been characterized, but likely has the same stoichiometry as the thorium perchlorate analog that forms upon reaction of thorium hydroxide with perchloric acid, $Th(ClO_4)_4{\cdot}4H_2O$. Attempts

to prepare Pu(IV) iodates by hydrothermal methods have produced Pu(VI) phases (described below).

Similarly, most conditions that would be used to attempt to prepare Pu(V) iodates have yielded Pu(VI) or Pu(IV) solids. The solid-state structure of $NpO_2(IO_3)$ was recently determined by single crystal XRD (Albrecht-Schmitt *et al.*, 2003). Its structure consists of neptunyl(V) cations linked to one another by $O_2Np{-}O{=}Np{=}O$ bonds and bridging iodate anions, creating a pentagonal bipyramidal NpO_7 unit.

The binary plutonyl(VI) iodate, $PuO_2(IO_3)_2{\cdot}H_2O$, has been prepared under hydrothermal conditions and has a layered structure with PuO_7 pentagonal bipyramids linked by iodate anions. By contrast, $UO_2(IO_3)_2$ is one-dimensional, and contains chains of edge-sharing UO_8 hexagonal pyramids. A second actinyl (VI) compound with water in the inner coordination sphere, $AnO_2(IO_3)_2(H_2O)$, has been characterized for uranyl and neptunyl, but not for the slightly smaller plutonyl ion (Bean *et al.*, 2001; Runde *et al.*, 2003b). The addition of cations to the starting solution for these hydrothermal preparations produces ternary phases where the cations are located between chains and layers in the three-dimensional structure (Shvareva *et al.*, 2005). A dimeric plutonyl hydoxo iodate $(PuO_2)_2(IO_3)(\mu\text{-}OH)_3$ was isolated from a hydrothermal reaction of Pu(IV) in a mixed hydroxide, H_5IO_6 solution. In this structure hydroxide bridges are the primary structural element and seven-coordinate plutonium atoms are bridged by iodate and hydroxide (Bean *et al.*, 2005).

Perchlorate

Because perchlorates and perchloric acid solutions (similar to nitrates) are very common starting materials in actinide chemistry there are numerous examples of perchlorate containing plutonium compounds. However, pure binary plutonium perchlorates have not been characterized in the solution or solid state. Perchlorate is such a weak ligand that it most likely does not form inner-sphere complexes in aqueous solution, but acts as a simple counter ion. For comparison, crystals of uranyl perchlorate, $UO_2(ClO_4)_2{\cdot}nH_2O$ have been obtained with 6 and 7 hydration water molecules. The uranyl is coordinated with 5 water molecules in the equatorial plane with a distance of U–O(aquo) of 2.45 Å. The complex is best formulated as $[UO_2(H_2O)_5][ClO_4]_2{\cdot}nH_2O$ (Alcock and Esperas, 1977).

Oxalate

Oxalates have been widely used in plutonium separations and processing (Cleveland, 1979; Wick, 1980). The rapid formation of microcrystalline phases that are easily filtered from solution is the basis for the large-scale recovery of plutonium from concentrated solutions. In addition, the low solubility of the oxalates makes them useful in 'polishing' or 'finishing' steps where minor amounts of material are recovered. Plutonium oxalates may also be important in environmental chemistry since oxalate is a major byproduct of plant

metabolism and can be concentrated in some soils. The stoichiometry for the oxalate complexes has been determined from a combination of thermogravimetric analyses and XRD on solid compounds. The oxalate ligand $\left(C_2O_4^{2-}\right)$ generally binds actinide ions in a mono- or bidentate fashion, and can also bridge metal centers to produce a variety of chains, layers, and intricate three-dimensional structures with high coordination numbers. Solution species are only poorly studied, as expected given their low solubilities.

The solid trivalent plutonium oxalate system is dominated by two hydrates of formula $Pu_2(C_2O_4)_3{\cdot}10H_2O$ and $Pu_2(C_2O_4)_3{\cdot}6H_2O$ that are readily precipitated from solution in the presence of reducing agents, such as hydroxylamine. The blue, monoclinic decahydrate $Pu_2(C_2O_4)_3{\cdot}10H_2O$ forms in concentrated solutions and can be dehydrated or fired to produce highly pure finely divided PuO_2 (Rao *et al.*, 1963). This stoichiometric oxalate is isostructural with lanthanide (III) oxalate decahydrate, which includes nine-coordinate metal centers (Jenkins *et al.*, 1965). A single crystal XRD structure of a nonahydrate $Pu_2(C_2O_4)_3{\cdot}9H_2O$ has been recently reported (Runde *et al.*, 2005a). This two-dimensional solid consists of tricapped trigonal prismatic PuO_9 units that are linked by $C_2O_4^{2-}$ groups and a network of interstitial water molecules. The plutonium atom is coordinated to six oxygen atoms from three bidentate oxalate ligands and three oxygen atoms from coordinated water. The Pu–O distances range from 2.47 to 2.56 Å (Runde *et al.*, 2003a). Complex plutonium(III) oxalates of general formula $MPu(C_2O_4)_2{\cdot}xH_2O$ (M = Na, K, Cs, NH_4) have also been prepared (Runde *et al.*, 2005a).

Solution oxalate complexes are mainly of the form, $Pu(C_2O_4)_n^{3-2n}$, $n = 2$–4. The bis-oxalate species is the most important, while the latter complexes have very narrow ranges of stability (Cleveland, 1979; Hasilkar *et al.*, 1994). Numerous mixed-ligand Pu(III) oxalate complexes have been postulated to form but have not been studied in detail.

Tetravalent plutonium oxalates have been prepared with 2, 4, and 5 oxalate ligands bound to plutonium. The binary oxalate hydrates, $Pu(C_2O_4)_2{\cdot}xH_2O$ ($x = 0$, 1, 2, or 6), can be prepared from Pu(III) solutions in the presence of peroxide or other mild oxidizing agents, or precipitated directly from Pu(IV) solutions. Detailed structural analyses of these solids have not been reported. They are likely isostructural with the related binary Th(IV) and U(IV) oxalates, which generally have a coordination number of eight, comprised of bidentate and bridging oxalate and water molecules in the inner sphere arranged in irregular cubic and square antiprismatic coordination geometries. Complex salts of the tetra- and pentaoxalates, including $Na_4[Pu(C_2O_4)_4]{\cdot}5H_2O$, $(NH_4)_6[Pu(C_2O_4)_5]{\cdot}5H_2O$, and $K_6[Pu(C_2O_4)_5]{\cdot}5H_2O$ have been prepared. Uranium and thorium analogs of the tetraoxalate contain a ten-coordinate actinide (IV) atom in an irregular bicapped square antiprism linked to other metal centers by oxalato or aquo bridges (Favas *et al.*, 1983; Harrowfield *et al.*, 1983). Hydrothermal synthesis produced single crystals of $KPu(C_2O_4)_2(OH){\cdot}2H_2O$ (Runde, 2005a). The single-crystal structure of $KPu(C_2O_4)_2(OH){\cdot}2H_2O$ shows

a three-dimensional framework built up from oxalate-linked PuO_9 polyhedra. Each PuO_9 polyhedron consists of eight oxygen atoms from four chelating oxalate ligands and one hydroxide ligand. This finding is suggestive that $Pu(C_2O_4)_4(OH)^{5-}$ may be the limiting Pu(IV) solution complex under high oxalate concentrations (Runde, 2005a).

Plutonium(V) in the presence of oxalate disproportionates to a mixture of oxidation states under most conditions (Nikitenko, 1988). Plutonium(V) oxalates (such as $NH_4PuO_2(C_2O_4) \cdot xH_2O$) can be isolated by rapid precipitation from neutral pH solutions and have been identified by optical absorption spectroscopy and chemical analyses (Zaitseva *et al.*, 1973). Plutonium(VI) oxalates that are isostructural with uranyl oxalates have been prepared (Jenkins *et al.*, 1965; Bessonov *et al.*, 1996). The simple binary, $PuO_2(C_2O_4) \cdot 3H_2O$, is the most studied and was recently employed in an EPR study to show the evidence for the participation of 5f electrons in plutonium chemical bonding (Bhide *et al.*, 2000).

Peroxide

Hydrogen peroxide is commonly used to reduce Pu(V) or Pu(VI) to Pu(IV) and to precipitate Pu(IV) from acidic solution, often in the presence of other anions (Balakrishnan and Ghosh Mazumdar, 1964; Hagan and Miner, 1980). Efficient separation and purification processes have been developed from this chemistry (see Section 7.5.3(b)) even though the exact nature of species in solution is not definitively known (Cleveland, 1979; Wick, 1980). Plutonium(IV) can also be reduced by hydrogen peroxide to form Pu(III) or Pu(III)/Pu(IV) mixtures, depending upon the acidity, presence of sulfate, and total plutonium concentration (Balakrishnan and Ghosh Mazumdar, 1964; Koltunov, 1982a).

Connick and McVey (1949) spectroscopically identified two Pu(IV) peroxide complexes in acidic solution. Small amounts of peroxide produced a brown complex with absorption bands at 495 ($\epsilon = 266$ L mol^{-1}cm^{-1}) and 540 nm, with a suggested peroxo-bridged formula of $[Pu(O_2)(OH)Pu]^{5+}$ and corresponding formation constant of 8.8×10^6 in 0.5 M HCl. As more peroxide is added, the brown complex converts to a red complex with an absorption maximum at 513 nm. The equilibrium between these two solution complexes (equilibrium constant of 145 in 0.5 M HCl) suggests intermediates of general composition $[Pu(\mu\text{-}O_2)_2Pu]^{4+}$. While there is no structural information to confirm the proposed solution complex stoichiometries, Runde (2005b) has recently isolated single crystals containing the $Pu_2(\mu\text{-}O_2)_2(CO_3)_6^{8-}$ ion, that confirms the presence of a doubly bridged $Pu_2(\mu\text{-}O_2)_2$ core as illustrated in **20**. When the peroxide concentration is increased, two green precipitates form with different oxygen to plutonium ratios that also incorporate other anions present in the solution, e.g. sulfate, nitrate, and chloride (Leary *et al.*, 1959). The hexagonal form ($a = 4.00$ Å) precipitates preferentially at high acidity and high ionic strength and has an oxygen to plutonium ratio of 3.0–3.4 depending on whether the solid is dry or wet, respectively. At less than 2 M acidity a fcc

form ($a = 16.5$ Å) of higher purity and with an oxygen to plutonium ratio of 3.0 is obtained (Hagan and Miner, 1980) regardless of whether the solid is wet or dry.

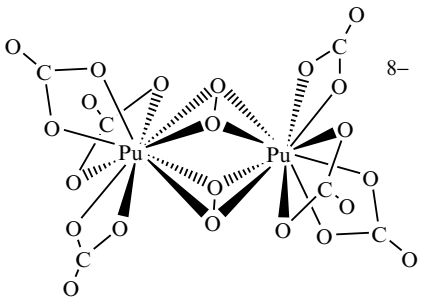

20

Less is known about the complexation of plutonyl ions by peroxide in alkaline media. Nash *et al.* (1980) reported that Pu(VI) in a 3 mM H_2O_2/0.05 M $NaHCO_3$ solution is reduced to Pu(V) via an intermediate reddish-brown colored complex, which was assumed to be a 1:1 Pu(VI) peroxo complex. The rate of formation of this complex was determined to be $(6.9 \pm 0.8) \times 10^3$ M^{-1} s^{-1} in 0.05 M $NaHCO_3$ (Nash *et al.*, 1980).

(*ii*) *Carboxylate and polyaminocarboxylate complexes*

Plutonium complexes with carboxylates and polyaminocarboxylic acids are important in separations, decontamination, and environmental migration. They have also been studied to achieve a better understanding of fundamental aqueous actinide chemistry. Owing to their multiple anionic chelating oxygen donor atoms, these ligands form highly stable and soluble complexes with plutonium ions. Solution complex formation constants for the plutonium species follow the usual trend where Pu(IV) complexes are the most stable and Pu(V) complexes the least stable. These ligands and other multidentate chelating organic acids stabilize Pu(IV) complexes to such a great extent, that under most conditions plutonium ions of the other oxidation states are rapidly oxidized/reduced to the tetravalent state.

Many studies have been reported for plutonium complexes with citrate, tartrate, malonate, glycine, and other carboxylates and amino acids, most recently by researchers at the Russian Academy of Sciences. Among these the acetate complexes are arguably the most comprehensively studied. The solution chemistry of plutonium complexes of other similar ligands can be inferred by considering the acetate complexes and the comparative basicity of the ligands; hence, only the acetate complexes will be discussed in this section. Among plutonium complexes of the amino polyacetates, iminodiacetate (IDA), nitrilotriacetate (NTA), ethylenediaminetetraacetate (EDTA), diethylenetriamine pentaacetate (DTPA), and derivatives, the EDTA complexes have been studied

most extensively and used most broadly in applications. The pentaacetate analog, DTPA, has special application for treatment of internal human plutonium contamination through chelation therapy. The stoichiometry and stability of plutonium polyacetate solution complexes are generally known from spectrophotometric and potentiometric titration experiments. Solution and solid-state structures have been proposed by inference. The chemistry of the lower valent ions, Pu^{3+} and Pu^{4+} is comparative and will be described first, followed by that of the higher oxidation state ions, PuO_2^+ and PuO_2^{2+}. Formation constants for selected carboxylate and aminocarboxylate ligands are given in Table 7.57.

Pu(III) and (IV). Acetate complexes of Pu(III) have been studied primarily for stabilization with respect to oxidation to Pu(IV). Each of the stepwise complexation species from the mono- to pentaacetate has been reported. The formation constants for the first two species are $\log_{10}\beta_1 = 2.02$ and $\log_{10}\beta_2 = 3.34$ in 0.3 M $NaClO_4$ (Moskvin, 1969; Nair and Joshi, 1981). These constants have been reported from independent studies and compare well with values reported for acetate complexes of trivalent lanthanides. The limiting pentaacetate complex has an estimated formation constant of $\log_{10}\beta_5 = 16.7$ (Cleveland, 1979), which is high relative to the formation constants for the mono- and bis complexes and may therefore be considered an upper limit. Similarly, stepwise constants for Pu(IV) have been reported. Values for the first and limiting (penta) species are known with the greatest certainty, $\log_{10}\beta_1 = 5.31$ and $\log_{10}\beta_5 = 22.6$ (Cleveland, 1979). Solid-state structures of the lower valent plutonium acetate complexes are not known.

Plutonium(III) complexes of NTA^{3-} and $EDTA^{4-}$ have been studied directly by optical spectroscopy, voltammetry, and cation exchange, as well as indirectly in the study of Pu(IV) EDTA complexes at very low pH. Multiple species have been identified from pH and ligand titration experiments. In solutions with pH > 5, Pu(III) complexes are rapidly oxidized to Pu(IV). Studies at low pH have yielded the formation constant for the Pu(NTA) complex of $\log_{10}\beta_1 = 10.26$ (Merciny *et al.*, 1978; Anderegg, 1982). The protonated species Pu(EDTA)H forms in strong acid solutions and is deprotonated to $Pu(EDTA)^-$ above pH 3, and then to the mixed EDTA hydroxo complex, $Pu(EDTA)(OH)^{2-}$. Solution formation constants for the first complex and protonated forms have been reported from multiple independent studies (Cauchetier and Guichard, 1973; Merciny *et al.*, 1978). A value for the stability constant of the binary, deprotonated species, $Pu(EDTA)^-$, $\log_{10}\beta_1 = 16.1$ is reported in a critical review of EDTA thermodynamic data (Anderegg, 1977). $DTPA^{5-}$, with an additional bidentate acetate group, forms a more stable 1:1 complex with Pu^{3+}, $\log_{10}\beta_1 = 21.5$ (Merciny *et al.*, 1978).

Tetravalent plutonium–EDTA complexes are important because EDTA stabilizes Pu^{4+} over all other oxidation states sufficient for use in chemical processing, and because the complexes may promote the transport of plutonium contamination in the environment. Studies of Pu–EDTA complexation are challenging because of the extreme hydrolysis of Pu^{4+} and low solubility of

Table 7.57 *Formation constants for selected organic acids and aminopolycarboxylates.*

Ligand	*Complex*	Pu^{+3}	Pu^{+4}	PuO_2^+	PuO_2^{2+}	*References*
acetate, Ac^-	[ML]/[M][L]	2.02	5.31		2.2	Moskvin (1969), Nair and Joshi (1981), Cleveland (1979), Magon *et al.* (1968), and Eberle and Wade (1970)
	$[ML_2]/[M][L]^2$	3.34			3.6	Moskvin (1969) and Nair and Joshi (1981)
	$[ML_5]/[M][L]^5$	16.7	22.6			Cleveland (1979)
IDA^{2-}	[ML]/[M][L]			6.2	8.5	Eberle and Wade (1970) and Cassol *et al.* (1973)
NTA^{3-}	[ML]/[M][L]	10.3	12.9	6.8		Merciny *et al.* (1978), Anderegg (1982), and AlMahamid *et al.* (1996)
$EDTA^{4-}$	[ML]/[M][L]	16.1	26.4	12.3	14.6	Anderegg (1977), Boukhalfa *et al.* (2004), and Cauchetier and Guichard (1975)
	$[ML_2]/[M][L]^2$		35.39			Boukhalfa *et al.* (2004)
$DTPA^{5-}$	[ML]/[M][L]	21.5	29.5			Merciny *et al.* (1978), Anderegg (1982), Moskvin (1969), and Nair and Joshi (1981)
$citrate^{2-}$	[ML]/[M][L]	8.9	15.6			Martell and Smith (2001)
	$[ML_2]/[M][L]^2$		29.8			
$lactate^-$	$[ML_4]/[M][L]^4$		16.2			Martell and Smith (2001)
$oxalate^{2-}$	[ML]/[M][L]		8.30		6.6	Martell and Smith (2001) and Rogozina *et al.* (1973)
	$[ML_2]/[M][L]^2$	9.3	14.9		9.4	
	$[ML_3]/[M][L]^3$	9.4	23.4			
	$[ML_4]/[M][L]^4$	9.9	27.5			
$malonate^{2-}$	[ML]/[M][L]				4.8	Martell and Smith (2001) and Rogozina *et al.* (1973)
$succinate^{2-}$	[ML]/[M][L]				3.4	Martell and Smith (2001)
$glutamate^{2-}$	[ML]/[M][L]	4.7				Martell and Smith (2001) and Rogozina *et al.* (1973)
$aspartate^{2-}$	[ML]/[M][L]	4.8				Martell and Smith (2001) and Rogozina *et al.* (1973)
$glycinate^-$	[ML]/[M][L]	3.2				Martell and Smith (2001) and Rogozina *et al.* (1973)

plutonium hydroxides, inherent limits of analytical and spectrophotometric techniques, large number of potential species, precipitation of EDTA in strong acid solution, and uncertainties in experimental proton concentrations. Despite these limitations, solubility, potentiometric, spectrophotometric, and electrochemical studies provide species formulations that are consistent between techniques (Cauchetier and Guichard, 1973; Rai *et al.*, 2001; Boukhalfa *et al.*, 2004).

In acidic solution (pH < 4) and at 1:1 ligand to metal ratio, Pu(EDTA) is the predominant species, with an overall formation constant of $\log_{10}\beta_1 = 26.44$ in 1 M (Na,H)ClO_4. The absorption maximum of the binary complex is at 496 nm. At higher pH the hydrolysis species Pu(EDTA)$(OH)^-$ and Pu(EDTA)$(OH)_2^{2-}$ form with the corresponding overall stability constants of $\log_{10}\beta = 21.95$ and 15.29, respectively. The reduction potential of the complex Pu(EDTA) at pH = 2.3 is reported to be $E_{1/2} = 342$ mV (vs SHE). It was recently determined that under conditions of neutral pH and excess EDTA relative to Pu^{4+}, a second ligand coordinates to the ion. The formation of such species, as well as mixed-ligand EDTA complexes, can be anticipated knowing that the Pu^{4+} ions may accommodate up to 12 ligand donor atoms in their inner coordination sphere as in the hexanitrato structure, **19**. The bis chelate complex, Pu$(EDTA)_2^{4-}$, forms with an overall formation constant of $\log_{10}\beta = 35.39$ (Boukhalfa *et al.*, 2004). In the presence of ancillary ligands, mixed-ligand complexes form, as exemplified by the citrate and carbonate complexes Pu(EDTA)$(citrate)^{3-}$ and Pu$(EDTA)(CO_3)^{2-}$ (Boukhalfa *et al.*, 2004).

Dissolution of Pu(IV) hydrous oxides, PuO_2, $PuO_2{\cdot}xH_2O$, and '$Pu(OH)_4$' in the presence of EDTA has been studied both to understand how EDTA may promote plutonium solubility in waste and the environment and as a method to determine the thermodynamic stability of the resulting Pu–EDTA solution complexes. Dissolution rates of 0.0074 and 0.42 μmol g^{-1} day^{-1} Pu in the presence of 10 mM EDTA were measured for the oxide and hydroxide, respectively, in a study that measured the solubility over months (Ruggiero *et al.*, 2002). A faster dissolution rate for the oxide has been reported in a study of shorter duration (Rai *et al.*, 2001).

DTPA solution complexes have been studied in pure solutions using the same methods as those employed for the EDTA and NTA complexes. The formation constants are less accurately known because they have been studied by fewer researchers, but mostly because they form in highly acidic solutions where there is uncertainty in the proton concentration and the protonation state of DTPA. The constant, $\log_{10}\beta_1 = 29.5$, can be considered a best estimate (Moskvin, 1971b). Given the high stability constant and positive results from plutonium complexation in aqueous solution, DTPA has been studied as a plutonium decontamination agent (Stradling *et al.*, 1989). It is highly effective in chelating plutonium in complex media that mimic physiological environments, and is the standard against which other potential therapeutic agents are measured. The efficacy of plutonium solubilization and complexation by DTPA has been studied in blood, urine, and cells (Rosenthal *et al.*, 1975). Most mammalian studies are

done with Zn and Ca salts ($CaNa_3DTPA$ or $ZnNa_3DTPA$) since early chelation therapy studies indicated that these essential metals were scavenged and depleted in the body. For a more detailed account of *in vivo* actinide chelation, the reader is referred to chapter 31 of this work.

Pu(V) and (VI). Plutonium(VI) acetate complexes have been well studied in solution, and characterized in detail in the solid state. Plutonium(V) acetate complexes are not stable with respect to oxidation or reduction, depending on the solution conditions. Spectrophotometric and potentiometric studies have yielded the following average formation constants for plutonium(VI) acetates $\log_{10}\beta_1 = 2.2$, $\log_{10}\beta_2 = 3.6$, and $\log_{10}\beta_3 = 5.0$, in 1.0 M $(Na,H)ClO_4$ (Magon *et al.*, 1968; Moskvin, 1969; Eberle and Wade, 1970; Cleveland, 1979). In the presence of alkali ions, triacetate complexes of the form $MAnO_2(CH_3COO)_3$ precipitate from solutions containing Pu(VI). The cubic pink sodium plutonyl acetate and the analogous cesium salt are the most studied (Jones, 1955).

Plutonium(V) and plutonium(VI) aminocarboxylate complexes have been identified in electrochemical and pH titration studies (Cauchetier and Guichard, 1975). A stability constant for the complex of Pu(V) with NTA^{3-} was reported to be $\log_{10}\beta_1 = 6.8$ in 0.1 M $(Na,H)ClO_4$ (AlMahamid *et al.*, 1996) consistent with a number of previous studies (Eberle and Wade, 1970). The related iminodiacetate (IDA^{2-}) complex has a reported formation constant $\log_{10}\beta_1 = 6.2$ (Eberle and Wade, 1970), which as expected is somewhat lower than the constant for the Pu(V) complex with NTA^{3-}. A stability constant for a Pu(V) complex with $EDTA^{4-}$ has been estimated to be $\log_{10}\beta_1 = 12.3$ from spectrophotometric titrations (Cauchetier and Guichard, 1975). The reduction to Pu(IV) proceeds at a rate that depends on pH, plutonium concentration, and the ligand to metal ratio. At neutral pH and submicromolar plutonium

Table 7.58 *Formation constants and Gibbs energies for selected aqueous plutonium halides.*[a]

Species	*Reaction*	$\log_{10}\beta_n^\circ$	$\Delta_r G_m^\circ$ (kJ mol^{-1})
PuF^{3+}	$F^- + Pu^{4+} \rightleftarrows PuF^{3+}$	8.84 ± 0.10	-50.46 ± 0.57
PuF_2^{2+}	$2F^- + Pu^{4+} \rightleftarrows PuF_2^{2+}$	15.7 ± 0.2	-89.62 ± 1.14
PuO_2F^+	$F^- + PuO_2^{2+} \rightleftarrows PuO_2F^+$	4.56 ± 0.20	-26.03 ± 1.14
PuO_2F_2 (aq)	$2F^- + PuO_2^{2+} \rightleftarrows PuO_2F_2(aq)$	7.25 ± 0.45	-41.38 ± 2.57
$PuCl^{2+}$	$Cl^- + Pu^{3+} \rightleftarrows PuCl^{2+}$	1.2 ± 0.2	-6.85 ± 1.14
$PuCl^{3+}$	$Cl^- + Pu^{4+} \rightleftarrows PuCl^{3+}$	1.8 ± 0.3	-10.27 ± 1.71
PuO_2Cl^+	$Cl^- + PuO_2^{2+} \rightleftarrows PuO_2Cl^+$	0.23 ± 0.03	-1.31 ± 0.17
PuO_2Cl_2 (aq)	$2Cl^- + PuO_2^{2+} \rightleftarrows PuO_2Cl_2(aq)$	-1.15 ± 0.30	6.56 ± 1.71
$PuBr^{3+}$	$Br^- + Pu^{4+} \rightleftarrows PuBr^{3+}$	1.6 ± 0.3	-9.13 ± 1.71
PuI^{2+}	$I^- + Pu^{3+} \rightleftarrows PuI^{2+}$	1.1 ± 0.4	-6.28 ± 2.28

[a] Data from Lemire *et al.* (2001).

concentrations, the higher oxidation states can persist in the presence of excess NTA and EDTA for weeks (AlMahamid *et al.*, 1996). For Pu(VI), stability constants have been reported for the complexes with IDA^{2-} and $EDTA^{4-}$, $\log_{10}\beta_1 = 8.5$ (Cassol *et al.*, 1973), $\log_{10}\beta_1 = 14.6$ (Cauchetier and Guichard, 1975), respectively. Comparable constants reported for uranyl aminocarboxylates and for other ligand complexes of Pu(VI), suggest that these constants, while not yet confirmed by multiple independent studies, accurately describe the stability of the solution species.

(*iii*) *Halides*

Halide complexes were among the first complexes studied for plutonium and the fluorides and chlorides are of particular importance in plutonium purification and metal production as discussed in Sections 7.5 and 7.7.1. The formation constants for aqueous halide complexes of plutonium(III, IV, and VI) that have been critically evaluated by the NEA reviewers are listed in Table 7.58 (Lemire *et al.*, 2001; Guillaumont *et al.*, 2003). Only the addition of one or two halide ligands to any plutonium aqueous species is considered reliably established by these reviewers.

Many double salts of plutonium(III–VI) fluorides and chlorides have been reported (see Tables 7.46 and 7.47) and these salts have been prepared by aqueous or high temperature methods or combinations of these methods as described in Section 7.8.6(d). Where XRD data are available, the plutonium salts are usually observed to be isostructural with analogous compounds for thorium, uranium, neptunium, or the early lanthanides. For example, K_2PuCl_5 is isostructural with K_2PrCl_5 (Axler *et al.*, 1992) and $[K(18\text{-Crown-6})]_2PuO_2Cl_4$ is isostructural with $[K(18\text{-Crown-6})]_2UO_2Cl_4$ (Danis *et al.*, 2001; Clark, in preparation).

(*iv*) *Cation–cation complexes*

Owing to the linear structure and primary ionic bonding in the equatorial plane of actinyl ions AnO_2^{2+} and AnO_2^{+} (see Section 7.9.3), the oxygen atoms within these ions have a negative charge and can form bonds with a second metal center to produce 'cation–cation' complexes. This type of interaction was first characterized for UO_2^{2+} and NpO_2^{+} (Sullivan *et al.*, 1961), and is most well known for NpO_2^{+} (Stout *et al.*, 1993). For example, the structure of $NpO_2(ClO_4)\cdot 4H_2O$ consists of layers of NpO_2^{+} cations where axial O=Np=O units link to the equatorial plane of adjacent NpO_2^{+} units (Grigor'ev *et al.*, 1995). Interactions of this type have also been observed for the plutonyl ions. Newton and Burkhart (1971) oxidized Pu(IV) with Cr(VI) in dilute $HClO_4$ solution to form a $CrOPuO^{4+}$ cation, and recovered the complex by ion exchange. Photoacoustic spectroscopy was used to estimate an equilibrium

constant of $K = (2.2 \pm 1.5)$ L mol^{-1} for the interaction between UO_2^{2+} and PuO_2^+ in a 6.0 M perchlorate solution (Stoyer *et al.*, 2000).

7.9.2 Nonaqueous and organometallic chemistry

There is an extensive literature on the nonaqueous and organometallic coordination chemistry of the light actinide elements thorium and uranium. A good deal of this chemistry should, in principle, be accessible to plutonium. Extending this chemistry to plutonium and other transuranium elements would be of great value in elucidating trends in structure and bonding across the actinide series. Unfortunately, the corresponding plutonium chemistry is virtually unexplored, clearly due to the extreme difficulty associated with handling plutonium isotopes, the paucity of synthetic laboratories equipped to conduct this kind of chemical research, and the scarcity of suitable starting materials. The known chemistry has been summarized in several excellent reviews by Ephritikhine (1992), Burns and Sattelberger (2002), Burns *et al.* (2005), and Burns and Eisen in Chapter 25 of this work.

(a) Sigma-bonded ligands

(*i*) *Organic-solvent soluble halides*

As discussed in Section 7.8.6(b), the binary trihalides, PuX_3 (X = F, Cl, Br, I) are polymeric solids that are insoluble in polar organic solvents. Therefore, the PuX_3 compounds have not been particularly useful starting materials for the nonaqueous preparation of other inorganic or organometallic complexes. Over the last two decades, there has been considerable effort to develop organic-solvent soluble forms of plutonium trihalides. Karraker (1987) reported the reaction between alpha plutonium metal and 1,2-diiodoethane in tetrahydrofuran (THF) solvent to give the solvated triiodide complex $PuI_3(THF)_x$, and suggested that such complexes would be useful synthetic starting materials for preparation of nonaqueous inorganic and organometallic compounds. Zwick, Avens and coworkers subsequently reported that stoichiometric amounts of elemental iodine would oxidize plutonium metal in aprotic, coordinating solvents such as THF, pyridine (Py), or dimethylsulfoxide (DMSO) to give hydrocarbon soluble Lewis base adducts of formula PuI_3L_4 in extremely high yields (Zwick *et al.*, 1992; Avens *et al.*, 1994). Unlike the corresponding reaction between uranium metal and iodine, there is no need to rigorously remove any oxide coating from the surface of plutonium metal. The reaction is exothermic, however, and will cause the solvent to boil if the rate of iodine addition is too rapid.

$$2Pu + 3ICH_2CH_2I \xrightarrow[THF]{} 2PuI_3(THF)_x + 3C_2H_4 \qquad (7.140)$$

$$2Pu + 3I_2 \xrightarrow[L]{} 2PuI_3L_4, \quad (L = THF, Py, DMSO) \tag{7.141}$$

Infrared spectra of PuI_3L_4 compounds are virtually identical to their UI_3L_4 counterparts, and show vibrational bands characteristic of coordinated ligands. Thermogravimetric analysis demonstrated that upon heating PuI_3L_4, all four coordinated solvent molecules are displaced between 56 and 180°C to give anhydrous PuI_3. Room temperature ^{1}H NMR spectra of $PuI_3(THF)_4$ in $CDCl_3$ solution shows a single THF ligand environment, consistent with the spectra of the $NpI_3(THF)_4$ and $UI_3(THF)_4$ analogs (Avens *et al.*, 1994). Unlike the uranium and neptunium analog spectra, $PuI_3(THF)_4$ shows reasonably sharp ^{1}H NMR resonances ($\Delta\nu_{1/2} = 11.4$ Hz). Subsequent variable temperature ^{1}H NMR experiments in CD_2Cl_2 solution revealed a dynamic solution process that generates equivalent THF ligand resonances at room temperature, but freezes out a static structure at –90°C with two types of coordinated THF ligand consistent with the solid-state structure of $UI_3(THF)_4$ (**21**). The NMR data were interpreted in terms of the dynamic equilibrium between **21** and **22** shown below. Therefore, while no crystallographic data have been presented for $PuI_3(THF)_4$, the detailed characterization of the series of $AnI_3(THF)_4$ complexes (An = U, Np, Pu) leaves little doubt that in the solid state, the molecule displays the pentagonal bipyramidal coordination geometry, with two trans iodide ligands occupying apical coordination sites, and the third iodide and four THF ligands lying in the equatorial plane as shown in **21** below.

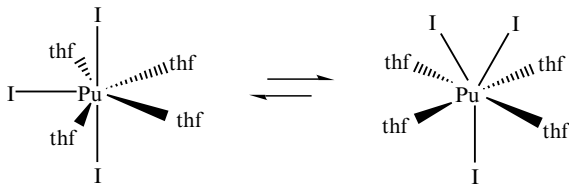

21 **22**

In a variation of the oxidative dissolution of plutonium metal, Enriquez *et al.* (2003) found that plutonium metal will also dissolve in acetonitrile solvent in the presence of three equivalents of thallium or silver hexafluorophosphate as the oxidant to give a blue solution containing $Pu(NCMe)_9^{3+}$. Filtration and cooling gives crystals of $[Pu(NCMe)_9][PF_6]_3 \cdot MeCN$.

$$Pu \xrightarrow[MeCN]{3MPF_6} [Pu(NCMe)_9][PF_6]_3 \cdot MeCN, \quad (M = Ag, T1) \tag{7.142}$$

The solid-state crystal structure reveals a $Pu(NCMe)_9^{3+}$ cation surrounded by three noncoordinating PF_6^- anions. The $Pu(NCMe)_9^{3+}$ ion displays a nine-coordinate tricapped trigonal prismatic coordination environment as

shown in **23**. There is little variation in the Pu–N bond distances between apical and capping ligands, which span the narrow range between 2.554(4) and 2.579(5) Å.

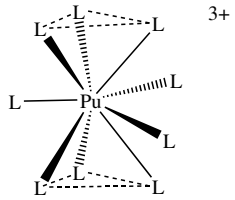

23

While binary $PuCl_4$ is unstable in the solid state (see Section 7.8.6(b)), it can be stabilized by formation of Lewis base adducts. Bagnall and coworkers showed that the reaction of Cs_2PuCl_6 with amide ($RCONR'_2$) or phosphine oxide (R_3PO) ligands in dichloromethane or acetonitrile solvent gives the Lewis base adducts $PuCl_4L_2$ or $PuCl_4L_3$, depending on the steric demands of the Lewis base (Bagnall *et al.*, 1961, 1985a). These adducts were characterized by IR, diffuse reflectance, and X-ray powder diffraction. In many cases, the solids were reported to be isostructural with thorium or uranium counterparts. The $PuCl_4L_2$ complexes were presumed to contain a pseudo-octahedral plutonium center, with trans Lewis base ligands. These Lewis base adducts have the potential to serve as good synthetic starting materials, though their general utility has yet to be explored.

(*ii*) *Amides*

The Lewis base adducts of plutonium triiodide have proven to be useful starting materials for the preparation of a number of trivalent organometallic and nonaqueous coordination compounds. A THF slurry of $PuI_3(THF)_4$ reacts smoothly at room temperature with three equivalents of $NaN(SiMe_3)_2$ to give an air-sensitive yellow-orange $Pu[N(SiMe_3)_2]_3$ in 93–95% yield (Zwick *et al.*, 1992; Avens *et al.*, 1994).

$$PuI_3(THF)_4 + 3NaN(SiMe_3)_2 \xrightarrow{THF} Pu[N(SiMe_3)_2]_3 + 3NaI \qquad (7.143)$$

The tris silylamide complex sublimes at 60°C under reduced pressure, gives an elemental analysis consistent with the formulation of $Pu[N(SiMe_3)_2]_3$, and shows a single ^1H NMR resonance at $\delta = 0.7$ ppm. The infrared spectra display vibrational features nearly identical to the uranium counterpart, and reveal the asymmetric $\nu(PuNSi_2)$ stretch at 986 cm^{-1}. Based on the similarity in spectroscopic properties, it is presumed that this compound will display the

well-established pyramidal structure that is shared by the uranium and lanthanide analogs as indicated in **24**.

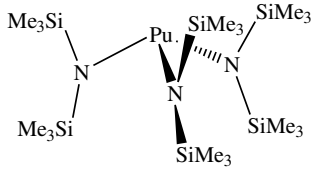

24

(*iii*) *Alkoxides*

Zwick and coworkers reported that the alcoholysis of $Pu[N(SiMe_3)_2]_3$ with the sterically demanding 2,6-$Bu^t_2C_6H_3(OH)$ gives the tan, air-sensitive tris aryloxide derivative $Pu(O\text{-}2,6\text{-}Bu^t_2C_6H_3)_3$ in 70% yield (Zwick *et al.*, 1992). The structural formulation as a monomeric compound is based on the similarity of spectroscopic data (^1H NMR and IR) to the well-characterized uranium analog which shows a monomeric structure in the solid state (Van der Sluys *et al.*, 1988).

$$Pu[N(SiMe_3)_2]_3 + 3HO\text{-}2,6\text{-}Bu^t_2C_6H_3 \xrightarrow{\text{hexane}} Pu(O\text{-}2,6\text{-}Bu^t_2C_6H_3)_3 + 3HN(SiMe_3)_2 \quad (7.144)$$

The tris aryloxide complex will coordinate Lewis bases to form $LPu(O\text{-}2,6\text{-}Bu^t_2C_6H_3)_3$ complexes (shown in **25**), where L is triphenylphosphine oxide, 4,4′-dimethoxybenzophenone, or *N*,*N*-di-isopropyl-benzamide (Oldham *et al.*, 2000). The relative binding affinities were found to correspond with that observed in process extraction chemistry (see Section 7.5.4), with the phosphine oxide and benzamide showing similar binding affinities, which were much larger than that of the benzophenone. Kinetic investigations of the self-exchange process probed by ^{31}P NMR spectroscopy yielded activation parameters indicative of an associative process, with a five-coordinate $L_2Pu(O\text{-}2,6\text{-}Bu^t_2C_6H_3)_3$ intermediate (**26**).

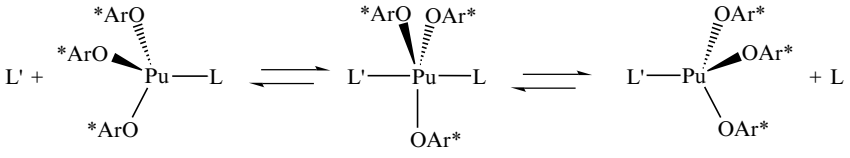

25 **26** **25**

Bradley and coworkers prepared aliphatic alkoxide complexes of general formula $Pu(OR)_4$ using $(Hpy)_2PuCl_6$ and benzene/alcohol solutions containing ammonia (Bradley *et al.*, 1957). With excess isopropanol, the reaction mixture was stirred with NH_3 at room temperature, and then the NH_4Cl and C_5H_6NCl salts removed by filtration. Solvent removal produced a mixture of grass-green $Pu(OPr^i)_4$ and $(Py)Pu(OPr^i)_4$. Recrystallization from isopropanol gives emerald green $Pu(OPr^i)_4(Pr^iOH)$. The base-free, homoleptic $Pu(OPr^i)_4$ compound sublimes at 220°C (0.05 mmHg). A similar reaction employing a large excess of *t*-butanol/benzene gave pale green $Pu(OBu^t)_4$, which sublimes at 112°C (0.05 mmHg). These aliphatic alkoxides were extremely sensitive to moisture, but appeared to be unaffected by dry air. No other characterization data have been reported.

$$(Hpy)_2PuCl_6 + xsPr^iOH \xrightarrow[NH_3/C_6H_6]{} Pu(OPr^i)_4(HOPr^i) + 4(NH_4)Cl + 2HpyCl \quad (7.145)$$

Very little is known about the trivalent isopropoxide, $Pu(OPr^i)_3$, although its use in catalytic reduction of ketones by isopropanol has been reported. Warner and coworkers examined the ability of trivalent and tetravalent lanthanide and actinide isopropoxides to facilitate the Meerwein–Ponndorf–Verley reduction of ketones (Warner *et al.*, 2000). Tetravalent $Pu(OPr^i)_4$ was found to be inactive in ketone reduction, but *in situ* production of $Pu(OPr^i)_3$ by dissolution of $Pu[N(SiMe_3)_2]_3$ in neat isopropanol generated an effective catalyst for the reduction of a range of substituted aryl-alkyl ketones, with yields that were equal or higher than similar reactions employing lanthanides.

(*iv*) *Alkyls*

There is only one example in the literature of an alkyl complex of plutonium, but its characterization data is limited to IR spectroscopy. Zwick and coworkers reported that the reaction of $Pu(O\text{-}2,6\text{-}Bu^t_2C_6H_3)_3$ with three equivalents of $LiCH(SiMe_3)_2$ in hexane solution yields yellow-brown $Pu[CH(SiMe_3)_2]_3$ as an oily solid (Zwick *et al.*, 1992). The IR spectrum was virtually identical to the well-characterized $U[CH(SiMe_3)_2]_3$ analog (Van der Sluys *et al.*, 1989). Other chemical characteristics, such as extreme sensitivity to air, rapid decomposition in solution, and thermal instability are consistent with this formulation. If the formulation is correct, then this complex would be an extremely rare example of a true organometallic complex of plutonium containing metal–carbon sigma bonds.

(*v*) *Borohydrides*

The first attempt to prepare plutonium borohydride was made by Schlesinger and Brown at the University of Chicago Metallurgical Laboratory in 1942 (Schlesinger and Brown, 1943). These authors tried to prepare plutonium borohydride in tracer quantities by reaction of uranium tetrafluoride containing trace amounts of plutonium with aluminum borohydride. Excess aluminum borohydride was removed and the reaction products that were volatile at 60°C were condensed at 20, 0, –23, –80, and –190°C. Only a few percent of the plutonium was recovered from the volatile fractions, the bulk of the plutonium remaining in the nonvolatile residue in the reaction vessel. It was therefore concluded that plutonium borohydride was either not formed or was not volatile at 60°C.

The first unequivocal preparation of plutonium(IV) borohydride was accomplished by Banks, Edelstein and coworkers (Banks *et al.*, 1978; Banks, 1979; Banks and Edelstein, 1980) at the Lawrence Berkeley Laboratory. Treatment of anhydrous PuF_4 with $Al(BH_4)_3$ at 0°C for 4 h in a solvent-free sealed tube reaction gives $Pu(BH_4)_4$ according to the reaction below.

$$PuF_4 + 2Al(BH_4)_3 \rightarrow Pu(BH_4)_4 + 2Al(BH_4)F_2 \qquad (7.146)$$

The unreacted $Al(BH_4)_3$ passes through a dry-ice trap and is collected in a liquid nitrogen trap. The $Pu(BH_4)_4$ is not as volatile and can be collected in the dry-ice trap. By intermolecular exchange in the gas phase with D_2, the deuterated compound $Pu(BD_4)_4$ may also be prepared. $Pu(BH_4)_4$ is a pyrophoric bluish-black liquid that melts at approximately 14°C. Infrared spectroscopy indicates that the compound adopts a monomeric pseudo-tetrahedral coordination geometry similar to $Zr(BH_4)_4$ and $Hf(BH_4)_4$ in the gas phase. Low temperature X-ray powder diffraction was consistent with this assessment, and suggests that the monomeric compound consists of a tetrahedral arrangement of four BH_4^- units coordinated by three B–H bridges per borohydride, giving the 12-coordinate structure shown in **27** below.

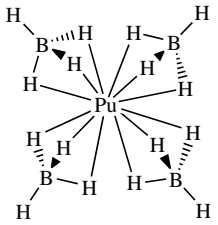

27

(b) Pi-bonded ligands

(*i*) *Cyclooctatetraene complexes*

The synthesis and characterization of the uranium(IV) sandwich complex, U(η-$C_8H_8)_2$, uranocene, was an important milestone in the history of organometallic chemistry, as it represented the logical extension of the bonding concepts that were developing for organotransition metal complexes (Seyferth, 2004). It was only a few years later when the plutonium analog was reported.

Bis(cyclooctatetraenyl)plutonium, or 'plutonocene' has been prepared by metathesis of $[NEt_4]_2[PuCl_6]$ with two equivalents of $K_2(C_8H_8)$ in THF solution to give a bright red product (Karraker *et al.*, 1970). Alternatively, $Pu(C_8H_8)_2$ may be prepared by reaction of degassed cyclooctatetraene, C_8H_8, with finely divided plutonium metal (prepared through hydride–dehydride cycles) in a sealed glass tube. The reaction mixture was heated at 160°C for 15 min, producing a red sublimate of $Pu(C_8H_8)_2$ (Starks and Streitwieser, 1973). Plutonocene reacts rapidly with air, and is only sparingly soluble in aromatic and chlorinated hydrocarbon solvents.

$$(NEt_4)_2PuCl_6 + 2K_2C_8H_8 \rightarrow Pu(\eta\text{-}C_8H_8)_2 + 2(NEt_4)Cl + 4KCl \quad (7.147)$$

$$Pu + 2C_8H_8 \rightarrow Pu(\eta\text{-}C_8H_8)_2 \quad (7.148)$$

The hydrocarbon solution solubility of plutonocene is enhanced by adding alkyl groups to the C_8H_8 rings. A number of alkyl substituted derivatives have been prepared, including $Pu(EtC_8H_7)_2$, $Pu(Bu^nC_8H_7)_2$, and $Pu(Bu^tC_8H_7)_2$ using the metathesis route employing $[NEt_4]_2[PuCl_6]$ and the potassium salt of the annulene dianion (Karraker, 1973; Eisenberg *et al.*, 1990). The tetramethyl-substituted complex Pu(1,3,5,7-$Me_4C_8H_4)_2$ was originally claimed (Solar *et al.*, 1980), but subsequent studies on other alkyl substituted complexes led Streitwieser to conclude that this compound was almost certainly the trivalent complex $[K(THF)_2][Pu(1,3,5,7\text{-}Me_4C_8H_4)_2]$ (Eisenberg *et al.*, 1990).

Single crystal XRD studies on $U(C_8H_8)_2$ shows that this molecule adopts a sandwich-type structure with the uranium center sandwiched between two planar C_8H_8 rings in rigorous D_{8h} symmetry (Zalkin and Raymond, 1969; Avdeef *et al.*, 1972). X-ray powder diffraction, infrared, electronic absorption, solution NMR, and Mössbauer spectroscopy reveal that the neptunium and plutonium analogs maintain the identical D_{8h} structure as shown in **28** (Karraker *et al.*, 1970; Karraker, 1973; Eisenberg *et al.*, 1990). Plutonocene is unique in that it has a $J = 0$ ground state with temperature-independent paramagnetism. Optical spectroscopy shows electronic transitions with intensities approaching 1000 (L mol^{-1} cm^{-1}), which argued against the assignment as 5f–5f transitions, and suggested an unusual 5f–6d orbital mixing with appreciable covalency in the bonding (Karraker *et al.*, 1970; Hayes and Edelstein, 1972).

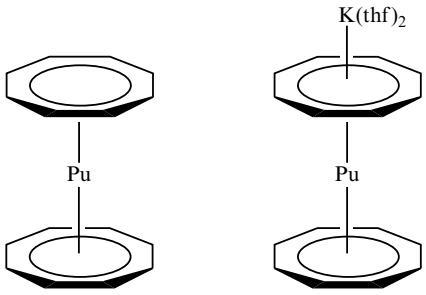

28 **29**

A number of trivalent plutonocene complexes of the type $[K(THF)_2][Pu(RC_8H_7)_2]$ have been prepared, where R = an alkyl group or H. These are prepared by reaction of $PuBr_3$ or PuI_3 with $K_2(RC_8H_7)$ in THF solution at –10 to –20°C (Karraker and Stone, 1974). These complexes may also be prepared by the direct reaction of potassium metal with $Pu(RC_8H_7)_2$ in THF solution (Eisenberg *et al.*, 1990).

$$PuX_3 + 2K_2C_8H_8 \xrightarrow[THF]{} [K(THF)_2][Pu(\eta\text{-}C_8H_8)_2] + 3KX \ (X = Br, I) \quad (7.149)$$

$$Pu(\eta\text{-}C_8H_8)_2 + K \xrightarrow[THF]{} [K(THF)_2][Pu(\eta\text{-}C_8H_8)_2] \quad (7.150)$$

The trivalent $[K(THF)_2][Pu(C_8H_8)_2]$ complex was described as turquoise-green, and it has been characterized by elemental analysis, X-ray powder diffraction, and magnetic susceptibility measurements (Karraker and Stone, 1974). The lime green $[K(THF)_2][Pu(Bu^tC_8H_7)_2]$ was not isolated, but was produced *in situ* in deuterated THF solvent, and characterized by ^1H NMR (Eisenberg *et al.*, 1990). The change in chemical shifts in the NMR spectrum with temperature was indicative of paramagnetic behavior expected for Pu(III). The solid-state structure of the uranium analog, $[K(diglyme)][U(C_8H_8)_2]$ has been determined by single crystal XRD revealing that the potassium ion is also involved in a multihapto interaction with a C_8H_8 ring. The X-ray powder diffraction data on the plutonium analogs indicate similar structures, as shown in **29** (Karraker and Stone, 1974).

(*ii*) *Cyclopentadienyl complexes*

Cylcopentadienyl ligands (C_5H_5, Cp) have played a central role in the development of the field of organometallic chemistry. The same is true in the field of organoactinide chemistry that was inaugurated with Reynolds and Wilkinson's seminal report on the preparation of $(C_5H_5)_3UCl$ in 1956 (Reynolds and Wilkinson, 1956). The first plutonium compounds containing cyclopentadienyl

ligands were reported by Baumgärtner and coworkers in 1965 (Baumgärtner *et al.*, 1965).

The microscale reaction between anhydrous $PuCl_3$ and molten $(C_5H_5)_2Be$ at around 70°C produces tris(cyclopentadienyl)plutonium, $(C_5H_5)_3Pu$, (or Cp_3Pu) (Baumgärtner *et al.*, 1965). Fractional sublimation first removes unreacted $(C_5H_5)_2Be$, and allows the moss green $(C_5H_5)_3Pu$ product to be isolated at a sublimation temperature of approximately 170°C. The transmetallation using $(C_5H_5)_2Be$ has been very useful for preparing transplutonium tris(cyclopentadienyl) complexes, but the nuisance of α-n reactions between the plutonium and beryllium nuclei limit the scale of the reaction. To prepare larger quantities of $(C_5H_5)_3Pu$, Crisler and Eggerman (1974) turned to the reaction between plutonium chloride starting materials with sodium or magnesium metathesis reagents. Both $PuCl_3$ and Cs_2PuCl_6 react with $(C_5H_5)_2Mg$ in THF solution to yield an emerald green product. In THF solution the first product is most likely $(C_5H_5)_3Pu(THF)$, which loses the THF ligand during sublimation to yield $(C_5H_5)_3Pu$ at 140°C under reduced pressure. The reaction is over within minutes when Cs_2PuCl_6 is employed as compared to hours for the reaction with $PuCl_3$. This is most likely because Cs_2PuCl_6 contains discrete $PuCl_6^{2-}$ ions, while $PuCl_3$ displays an extended three-dimensional structure (see Section 7.8.6(b)). Tris (cyclopentadienyl)plutonium can also be prepared from the reaction of $PuCl_3$ with $(C_5H_5)Na$ in THF solution, but the reaction requires 10 days. Zwick and coworkers found that a very convenient way to circumvent this solubility problem is to react $PuI_3(THF)_4$ with three equivalents of $(C_5H_5)Li$ in THF solution (Zwick *et al.*, 1992).

$$2PuCl_3 + 3Be(C_5H_5)_2 \xrightarrow[\text{melt}]{70^\circ} 2(\eta\text{-}C_5H_5)_3Pu + 3BeCl_2 \tag{7.151}$$

$$PuCl_3 + 3Na(C_5H_5) \xrightarrow[\text{THF}]{} (\eta\text{-}C_5H_5)_3Pu(THF) + 3NaCl \tag{7.152}$$

$$2PuCl_3 + 3Mg(C_5H_5)_2 \xrightarrow[\text{THF}]{} 2(\eta\text{-}C_5H_5)_3Pu(THF) + 3MgCl_2 \tag{7.153}$$

$$PuI_3(THF)_4 + 3Li(C_5H_5) \xrightarrow[\text{THF}]{} (\eta\text{-}C_5H_5)_3Pu(THF) + 3LiI \tag{7.154}$$

X-ray powder diffraction data suggest that $(C_5H_5)_3Pu$ is isostructural with $(C_5H_5)_3Ln$ compounds. The lanthanide analogs have been shown to contain polymeric zigzag chains of distinct $(C_5H_5)_2Ln(\mu\text{-}\eta^2\text{-}\eta^5\text{-}C_5H_5)$ units (Hinrichs *et al.*, 1983).

Bagnall and coworkers reported that the reaction between $(C_5H_5)Tl$ and Cs_2PuCl_6 in acetonitrile solution does not give an overall reduction to trivalent plutonium as discussed above, but produces tetravalent $(C_5H_5)_3PuCl$ (Bagnall *et al.*, 1982a). The chloride can be replaced with thiocyanate via a simple metathesis reaction with stirring in a THF solution of K(NCS) for 16 h (Bagnall *et al.*, 1982a). Both the chloride and thiocyanate complexes are dark brown and

moisture sensitive, and both are soluble in THF and acetonitrile solution. The anionic analog, $(C_5H_5)_3Pu(NCS)_2^-$, is also reported as a tetraphenylarsonium salt, but little characterization data have been reported (Bagnall *et al.*, 1982b).

$$Cs_2PuCl_6 + 3Tl(C_5H_5) \xrightarrow[CH_3CN]{} (\eta\text{-}C_5H_5)_3PuCl + 2CsCl \tag{7.155}$$

$$(\eta\text{-}C_5H_5)_3PuCl + K(NCS) \xrightarrow[THF]{} (\eta\text{-}C_5H_5)_3Pu(NCS) + KCl \tag{7.156}$$

The chloride compound, $(C_5H_5)_3PuCl$, was found to be isostructural with its uranium counterpart (Bagnall *et al.*, 1982a), which contains a pseudo-tetrahedral unit in which the centroids of the Cp rings occupy three vertices, and the chloride takes up the fourth as illustrated in **30**.

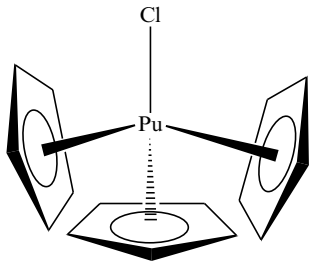

30

Bagnall and coworkers have prepared several examples of mono(cyclopentadienyl) plutonium complexes (Bagnall *et al.*, 1985b). Room temperature reaction of $(C_5H_5)Tl$ with $PuCl_4L_2$ or Cs_2PuCl_6 in dry acetonitrile for 48 h gave $(C_5H_5)PuCl_3L_2$ in 50–85% yield depending on the nature of the Lewis base, L. Neutral Lewis base ligands (L) included a number of phosphine oxide (R_3PO) and amide ($RCONR'_2$) derivatives. Similar reactions employing $(C_5H_5)Tl$ and $Pu(NCS)_4L_2$ produced the analogous $(C_5H_5)Pu(NCS)_3L_2$ complexes (Bagnall *et al.*, 1986). All of these materials have been characterized by infrared and Vis-NIR spectroscopy. It is assumed that these complexes adopt a structure similar to their uranium analogs.

7.9.3 Electronic structure and bonding

(a) Ionic and covalent bonding models

The nature of metal–ligand bonding in light actinide compounds and complexes is quite complicated. In general, the actinides are best viewed as being intermediate between the strongly ionic bonding observed in lanthanide elements, and the more covalent bonding observed in d-block transition elements. There are clearly cases that show ionic behavior, and there are just as clearly cases that show considerable covalency.

Many plutonium–ligand bonds are nondirectional, and determined largely by electrostatic attraction to the metal, electrostatic repulsion between ligands, and steric demands around the metal center. These metal–ligand bonds are relatively weak, and kinetically labile in solution. There are also examples of metal–ligand bonds that are incredibly strong, show a stereochemical orientation, and are kinetically inert. The former situation is often taken as evidence for ionic behavior, while the latter is clearly consistent with covalent interactions. The view that plutonium complexes are generally ionic is supported by the premise that the 5f orbitals are core-like in that they are so contracted they cannot interact in bonding with the ligands. This is generally what is observed, especially for the heavier actinide elements. However, the 5f orbitals of the lighter actinides are much less contracted, and there are certain classes of compounds where the 5f orbitals have been shown to play a significant role in covalent metal–ligand bonding. By consideration of the behavior of the 5f orbitals alone, it is difficult to reconcile these stark differences in chemical behavior.

This is an area where electronic structure calculations have taught us a great deal about how to think about the nature of chemical bonding in molecular plutonium complexes. Electronic structure calculations have demonstrated that for metal–ligand bonding in plutonium (and all light actinides) one cannot consider the 5f orbitals alone, but must consider the relative roles of both the virtual 5f and 6d orbitals as well as the 'semicore' 6s and 6p orbitals. The radial distributions of the plutonium 6s and 6p semicore orbitals lie in the valence region, and they must be considered as active in chemical bonding. In addition, the virtual 6d orbitals are relatively low-lying, and have far larger radial extent than the 5f orbitals. This is illustrated in the radial distribution function for a Pu^{3+} ion shown in Fig. 7.120 (Schreckenbach *et al.*, 1999). Most modern quantum chemical calculations find evidence of mixing of the 6p semicore orbital into metal–ligand bonding combinations. Moreover, there is now a general consensus that the dominant metal–ligand bonding takes place through ligand interactions with the 6d orbitals. The 6d orbitals are strongly split by the presence of a ligand field (as in transition element complexes), but the more contracted 5f orbitals show only weak splitting. The ground state electron configurations are therefore generally governed by the occupation of these closely spaced 5f orbitals, which leads to many open shell states. Spin–orbit coupling and electron correlation effects are extremely important, particularly for understanding spectroscopic properties. In addition to Chapter 17, several excellent reviews exist that describe trends and views on the electronic structure of actinide molecular complexes (Bursten and Strittmatter, 1991; Pepper and Bursten, 1991; Denning, 1992; Schreckenbach *et al.*, 1999; Matsika *et al.*, 2001).

(b) Specific examples

There are a number of specific examples in plutonium chemistry where covalency in metal–ligand bonding plays an important role in the observed chemical

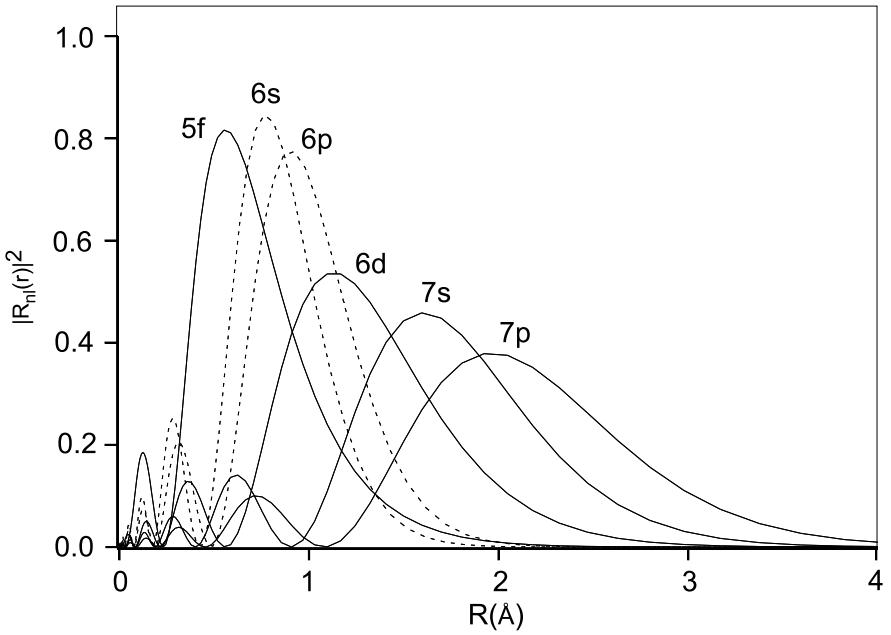

Fig. 7.120 *Radial probability densities of* Pu^{3+} *valence orbitals from relativistic Hartree–Fock orbitals* $\Phi_{nl}(r)$ (*Schreckenbach* et al., 1999). *The authors are grateful to P.J. Hay of Los Alamos for providing the raw data used to prepare this figure.*

behavior. These are plutonium hexafluoride, PuF_6, the linear plutonyl cation, PuO_2^{2+}, and the organoplutonium sandwich compound plutonocene, $Pu(\eta\text{-}C_8H_8)_2$. We provide a qualitative discussion of the bonding in these systems, illustrate the main 6d and 5f orbital interactions, and highlight the 'strong field-weak field' differences in 6d and 5f interactions that make spin–orbit splitting important for understanding spectroscopic properties. Before discussing the examples, we remind the reader that unlike p- or d-orbitals, there is no unique way of representing the angular dependence functions of all seven f-orbitals. In high symmetry cubic point groups, a cubic set of orbitals is used, while in systems containing a high order axis of symmetry, a general set can be used. These two common sets of f-orbital depictions are simply linear combinations of each other, and they are illustrated qualitatively in Fig. 7.121. We will use both the general and cubic orbital sets in describing the bonding in our examples.

(*i*) *PuF_6*

As discussed in Section 7.8.6(a), plutonium hexafluoride is a stable molecule in the gas-phase. In view of the electronegativity difference between hexavalent plutonium and the fluoride anion, this observation might seem somewhat surprising in that one might expect Pu–F bonds to show the greatest ionic

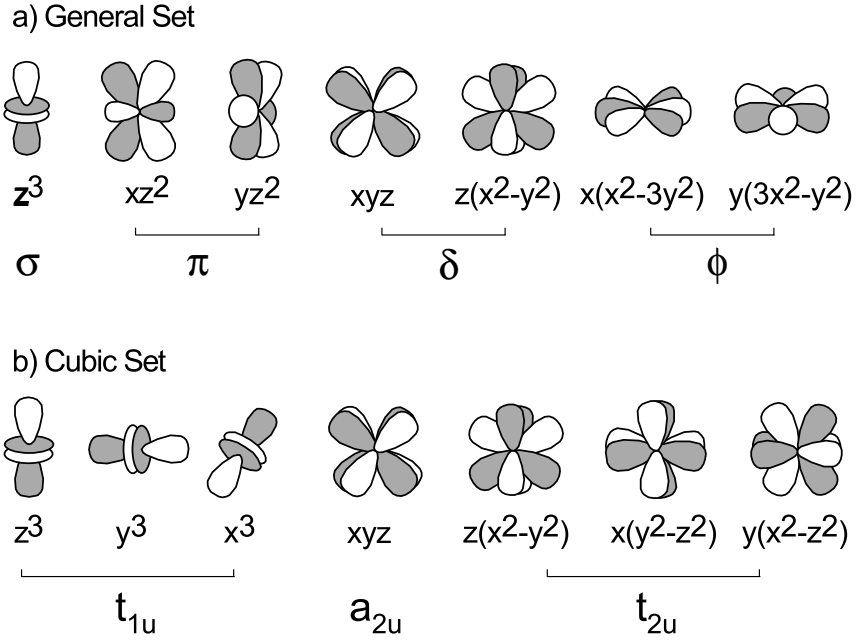

Fig. 7.121 *Qualitative representations of the general (a) and cubic (b) sets of valence f orbitals.*

behavior. Spectroscopic properties show that this is clearly not the case. Electronic structure calculations have provided some valuable insights into the nature of Pu–F bonding in this system.

A number of high-level electronic structure calculations have been performed on AnF_6 systems, with the majority of calculations performed on uranium. Calculations on PuF_6 have been reported by Kugel *et al.* (1976), Koelling *et al.* (1976), Boring and Hecht (1978), Wadt (1987), Hay and Martin (1998), Schreckenbach *et al.* (1999), and Onoe (1997). It is clear from all the theoretical calculations that the purely ionic bonding model is an inadequate description of PuF_6. A qualitative molecular orbital diagram for PuF_6 based on an octahedral ligand field that contains the basic features of these calculations is shown in Fig. 7.122. The octahedral point group is relatively straightforward as the 5f and 6d orbitals cannot mix by symmetry. The set of σ lone pairs on the six F atoms transform as $a_{1g} + e_g + t_{1u}$ symmetry under O_h symmetry. The 12 π lone pairs transform as $t_{1u} + t_{1g} + t_{2u} + t_{2g}$ under O_h symmetry. As expected, the set of σ lone pairs interacts most strongly with the Pu atom, resulting in molecular orbitals of a_{1g}, e_g, and t_{1u} symmetry which are lower-lying that the π symmetry orbitals. Of the four triply degenerate sets of F ligand π orbitals, the t_{2g} is of appropriate symmetry to interact with the 6d orbitals of the plutonium atom,

the t_{2u} can interact with the 5f orbitals, and the t_{1g} orbital cannot interact with any low-lying metal orbitals, and should remain as an noninteracting set of lone pairs. The t_{1u} orbital can interact with the 5f orbitals of the plutonium atom, but it can also mix with the t_{1u} set of σ orbitals derived from mixing between the semicore 6p and valence 7p orbitals. From simple overlap considerations, one would expect the F lone pair t_{2u} and t_{2g} orbitals to be the most stabilized by donation to the metal, the t_{1g} will be entirely nonbonding, and the t_{1u} will stabilized by π bonding from above, but destabilized by mixing with the σ interaction from below. In all the calculations, appreciable covalency with both 5f and 6d orbitals is present. The covalent interactions are found in Pu–F σ- and π-bonding that takes place through t_{2g} and e_g interactions with Pu 6d orbitals, and σ bonding that takes place through t_{1u} interactions with the 5f and 6p/7p orbitals. These metal–ligand bonding interactions are illustrated qualitatively in the molecular orbital diagram of Fig. 7.122. Wadt employed a Mulliken population analysis to determine the relative amount of plutonium 5f and 6d contribution to bonding (Wadt, 1987). The σ and π components of the t_{1u} interactions are mixed, but the virtual $5t_{1u}$ orbital (the $3t_{1u}$ orbital in Fig. 7.122) was calculated to comprise 71% Pu f, 3% Pu p, and 26% F p character

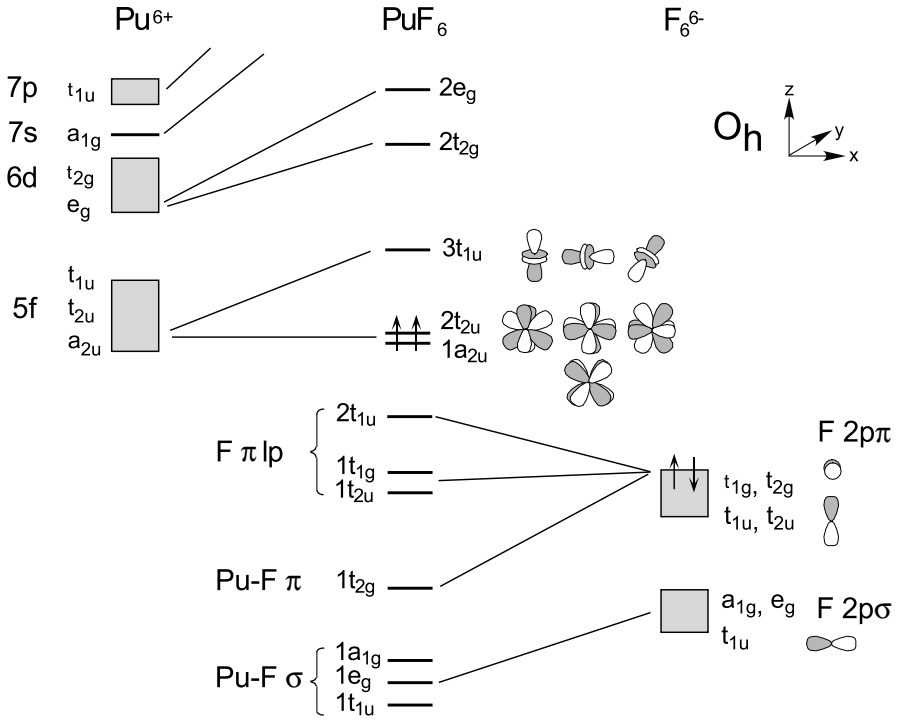

Fig. 7.122 *A qualitative molecular orbital interaction diagram for PuF_6.*

indicating a significant amount of covalency involving Pu 5f orbital interaction with the F ligands. It also shows the importance of mixing 'semicore' 6p character into a f–p σ hybrid orbital that enhances σ bonding. The total population of the Pu 5f orbitals was calculated to be 4.24. Since this system is nominally $5f^2$, the extra 2.24 electrons in 5f orbitals come from σ and π donation from occupied F ligand orbitals into Pu 5f orbitals.

For octahedral PuF_6, a simple filling of this qualitative MO scheme with the 16 valence electrons would give a valence electronic configuration $(1a_{2u})^2$ or $(1a_{2u})^1(2t_{2u})^1$ corresponding to $^1A_{1g}$ or $^3T_{1g}$ ground states, respectively. The 5f ordering in an octahedral ligand field is $a_{2u} < t_{2u} < t_{1u}$, and the calculations indicate that the $1a_{2u}$ and $2t_{2u}$ 5f orbitals are nearly degenerate, suggesting that the $^3T_{1g}$ state would be the likely ground state. This one-electron picture is oversimplistic, because the ligand field splitting of the 5f orbitals is so weak that spin–orbit effects must also be considered. Spin–orbit coupling splits the 5f manifold and gives a $^1\Gamma_{1g}$ (in O_h double group symmetry) ground state. The inclusion of spin–orbit coupling is necessary to understand the stabilization of a singlet ground state, and is in agreement with experiment that shows an absence of temperature-dependent contributions to the magnetic susceptibility, and indicates a nondegenerate ground state. Sophisticated electronic structure calculations are needed to quantify these spin–orbit effects. Wadt employed spin–orbit configuration interaction (CI) calculations that examined all possible arrangements of two electrons in seven 5f levels (Wadt, 1987). Wadt found that the ground $^1\Gamma_{1g}$ state in the octahedral double group representation was comprised of 78% $^3T_{1g}$ and 18% $^1A_{1g}$. More recently, Hay and Martin (1998) performed hybrid DFT calculations on both the $^1A_{1g}$ and $^3T_{1g}$ states and found the $^3T_{1g}$ state to lie lower in energy, consistent with Wadt's study, but did not include the spin–orbit coupling.

(*ii*) PuO_2^{n+}

The linear trans dioxo cations of light actinide elements are among the most well-studied actinide molecular systems. Electronic structure calculations on actinyl ions have revealed a great deal about covalency in metal–oxygen bonds and the relative roles of the valence 5f, 6d, and semicore 6p orbitals. The majority of theoretical studies have been devoted to UO_2^{2+}, but the smaller subset of calculations on PuO_2^{2+} reveals that much of the basic bonding description is essentially the same. The most thorough review on the subject is Denning's 1992 examination of experimental and theoretical work performed up to that time (Denning, 1992). Subsequent reviews build upon that work, and the reader is referred to discussions by Pepper and Bursten (1991), Dyall (1999), Denning *et al.* (2002), and Chapter 17 of this work for additional information.

The trans dioxo cations, AnO_2^{n+}, are invariably linear, regardless of the number of valence 5f electrons. The metal–oxygen bonds are unusually short, strong, and chemically inert. Based on all the experimental and theoretical

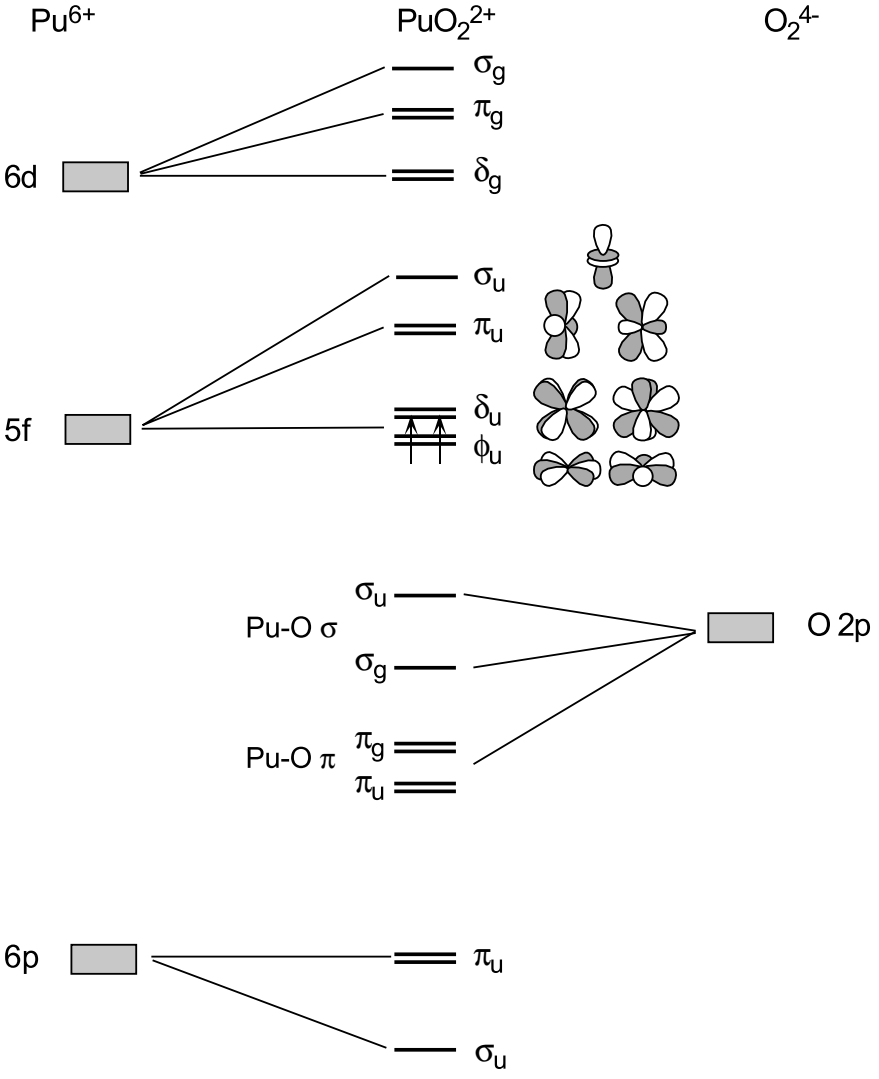

Fig. 7.123 *A qualitative molecular orbital interaction diagram for a linear triatomic* PuO_2^{2+} *ion.*

studies, there is uniform agreement on the molecular orbital description of bonding in these systems. A qualitative molecular orbital diagram for the linear triatomic PuO_2^{2+} ion that contains the basic features of the calculations is given in Fig. 7.123. In centrosymmetric $D_{\infty h}$ symmetry, the molecular orbitals are

conveniently labeled according to their axial symmetry, and the 5f and 6d orbitals cannot mix. The in-phase and out-of-phase combinations of the two O 2p σ orbitals span σ_u and σ_g symmetry, while the corresponding O 2p π orbitals span π_u and π_g symmetry. The metal 6d orbitals span σ_g, π_g, and δ_g symmetry, while the 5f orbitals span σ_u, π_u, δ_u, and φ_u symmetry. Metal–oxygen σ bonds are formed by interaction of the O 2p σ orbitals with metal $6d_{z^2}$ (σ_g) and a hybrid metal orbital formed by mixing $5f_{z^3}$ with the semicore $6p_z$ (σ_u). Metal–oxygen π bonds are formed by interaction of O 2pπ orbitals with metal $6d_\pi$ (π_g) and $5f_\pi$ (π_u) orbitals. The 5f δ_u and φ_u orbitals have no symmetry match with the ligands, and they remain as unperturbed, essentially degenerate, nonbonding 5f orbitals as indicated in Fig. 7.123.

In this qualitative diagram, the 14 valence electrons occupy the molecular orbitals to give a ground state electron configuration of $(\sigma_g^2\pi_g^4\sigma_u^2\pi_u^4)(\delta_u^2)$. Since the δ_u orbital is a nonbonding 5f orbital on the metal, this gives rise to formal Pu–O triple bonds in the linear PuO_2^{2+} unit. These four metal–ligand bonding orbitals are shown qualitatively in **31–34** below.

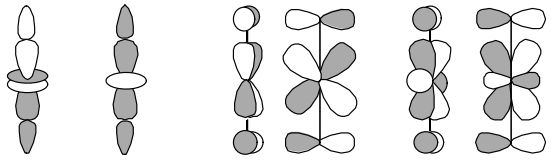

σ_u σ_g π_g π_u

31 **32** **33** **34**

Much discussion and debate has centered around the ordering of the four occupied metal–oxygen bonding orbitals σ_g, π_g, σ_u, and π_u. It is now generally accepted that a filled–filled interaction takes place between the σ_u Pu–O bonding orbital and the lower-lying (semicore) metal $6p_z$ orbital that also has σ_u symmetry. This repulsive interaction keeps the metal–oxygen bonding σ_u at high energy, and this now classical picture has been verified experimentally by Denning and coworkers using polarized oxygen Kα X-ray absorption and emission spectroscopy on a uranyl sample (Denning *et al.*, 2002). The linear trans dioxo cations were the first systems where theoretical calculations revealed that the closed shell (semicore) 6p orbitals were active in chemical bonding. Several studies have focused on the role of semicore 6p involvement, and have shown that $5f_{z^3}$–$6p_z$ hybridization forms an unusually strong metal–oxygen σ bond, and stabilizes the linear geometry (Dyall, 1999; Kaltsoyannis, 2000).

This basic bonding picture holds for all the trans dioxo cations from uranium through plutonium (Hay *et al.*, 2000) and americium. For the 5f orbitals, the overall ordering of levels is $\delta_u \sim \varphi_u < \pi_u << \sigma_u$ because the π_u and σ_u orbitals are destabilized by bonding interactions at lower energy. This basic orbital ordering scheme makes it easy to understand why the AnO_2^{n+} ions remain linear regardless of the number of 5f electrons. As the 5f electron count increases from UO_2^{2+} (f^0) to AmO_2^{2+} (f^3), each successive 5f electron is added to the nonbonding

5f orbitals of δ_u or φ_u symmetry. This is in contrast to transition element complexes where d^0 dioxo complexes are invariably cis, while d^2 dioxo complexes are invariably trans in order to maximize metal–oxygen π bonding. For the actinyl ions, the trans geometry maximizes σ bonding, and the formal metal–oxygen triple bond is retained regardless of the metal 5f electron count.

From this basic molecular orbital description, it is also easy to understand why most equatorial ligands show only a weak interaction with the highly covalent linear AnO_2^{2+} core. Let us consider the D_{4h} symmetry case of four equatorial ligands that only interact via σ bonding to form $PuO_2L_4^{2+}$. The four lone-pair orbitals of the equatorial ligands span a_{1g}, b_{1g}, and e_u symmetry, and these correspond to the $D_{\infty h}$ σ_g, δ_g, and π_u orbitals of the linear PuO_2^{2+} ion. The σ_g orbital has already been significantly destabilized by formation of the axial PuO_2^{2+} σ bonds, and the π_u orbital has very little overlap with incoming ligands in the equatorial plane. This leaves only one component of the degenerate δ_g orbital $\left(d_{x^2-y^2}, d_{xy}\right)$ that is directed towards the incoming ligands. In D_{4h} symmetry, the δ_g orbital $\left(d_{x^2-y^2}, d_{xy}\right)$ transforms as $b_{1g} + b_{2g}$, and only the b_{1g} orbital has the appropriate symmetry to interact. Overall, this gives only one molecular orbital (b_{1g}) that is bonding to all four equatorial bonds with a formal bond order of one quarter. The $PuO_2L_4^{2+}$ molecule therefore has two strong covalent Pu–O triple bonds in the axial direction, and four weak, relatively ionic bonds in the equatorial plane. This qualitative molecular orbital interaction diagram is illustrated in Fig. 7.124.

As in the PuF_6 example, the weak ligand field splitting of the 5f manifold, particularly the δ_u and φ_u orbitals mandates that electron repulsion and spin–orbit interactions be taken into account in order to understand the complexity of molecular electronic spectra. In the actinyl ions, Matsika and coworkers concluded that after consideration of the axial ligand field, electron repulsion was generally larger than spin–orbit coupling, leading them to the use of a Russell–Saunders-like Λ-S coupling scheme to calculate electronic states and optical transitions (Matsika *et al.*, 2001). For the $5f^2$ PuO_2^{2+} system, the $(\delta_u,\varphi_u)^2$ configuration gives two $^3\sum_g^-$ states, $^3\Pi_g$, ^3H_g and several higher energy singlets when only considering electron repulsion. When spin–orbit interaction is taken into account, the ^3H_g is lowered considerably, giving a ground state of $^3H_{4g}$ in agreement with spectroscopic data (Bleaney, 1955; Denning, 1992). Hay *et al.* (2000) obtain the same $^3H_{4g}$ ground state using spin–orbit configuration interaction (CI) calculations.

(*iii*) *Pu*(C_8H_8)$_2$

Following the discovery of the transition metal sandwich complex ferrocene, Fe(η-C_5H_5)$_2$, R. D. Fischer predicted the existence of the U(η-C_8H_8)$_2$ sandwich complex based on the recognition that the nodal properties of f-orbitals would require an expanded C_8H_8 ring (Fischer, 1963). Five years later uranocene, U(η-C_8H_8)$_2$, was synthesized and only shortly thereafter the plutonium

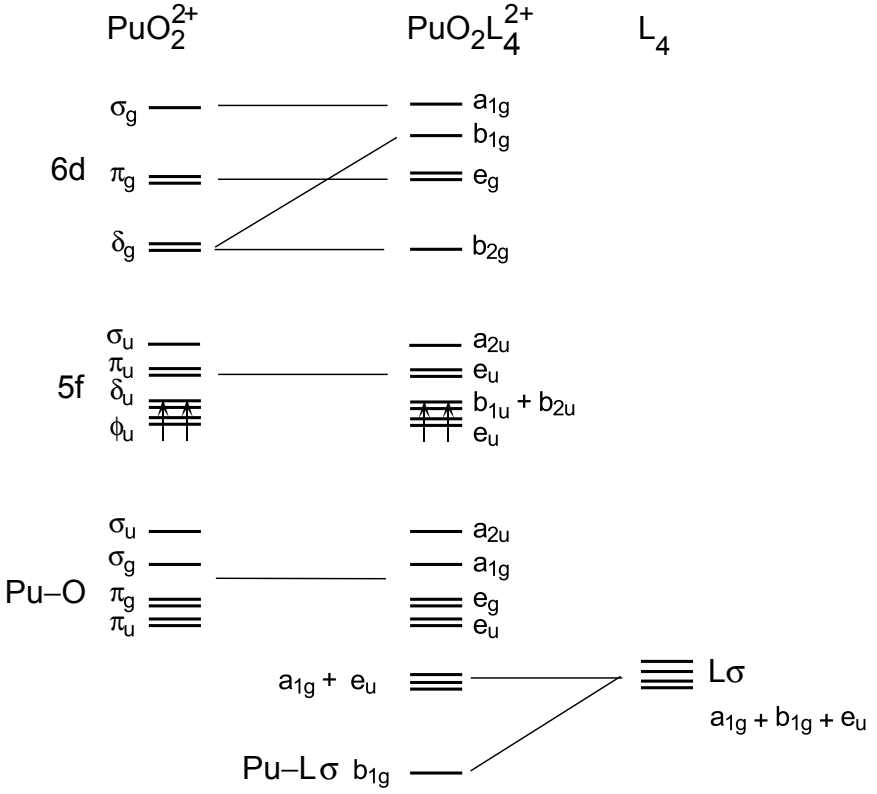

Fig. 7.124 *A qualitative molecular orbital interaction diagram for a linear triatomic PuO_2^{2+} ion interacting with four equatorial ligands, L, to form $PuO_2L_4^{2+}$.*

analog was prepared. As one of the first organometallic actinide complexes, the actinocene system has been the topic of much study aimed at understanding the relative roles of 5f and 6d orbitals in bonding (Boerrigter *et al.*, 1988; Brennan *et al.*, 1989; Kaltsoyannis and Bursten, 1997; Li and Bursten, 1998). A qualitative molecular orbital interaction diagram for Pu(η-C_8H_8)$_2$ under D_{8h} symmetry that contains the basic features of the electronic structure calculations is given in Fig. 7.125. The eight carbon $2p_\pi$ orbitals of the planar $C_8H_8^{2-}$ ring transform as a_{2u}, e_{1g}, e_{2u}, e_{3g}, and b_{1u} symmetry in D_{8h}, and these are often referred to as π_0, π_1, π_2, π_3, and π_4. This π_n nomenclature is convenient for visualization because the value of n refers to the number of nodes in the Hückel p_π orbitals of the $C_8H_8^{2-}$ ring. When two $C_8H_8^{2-}$ rings are brought together in D_{8h} symmetry, the in-phase and out-of-phase combinations of these π_n orbitals give rise to 16 orbitals as indicated in Fig. 7.125. These orbitals retain their π_n parentage as π_0 ($a_{1g} + a_{2u}$), π_1 ($e_{1g} + e_{1u}$), π_2 ($e_{2g} + e_{2u}$), π_3 ($e_{3g} + e_{3u}$), and π_4 ($b_{1u} + b_{2g}$). Interaction of these 16 π orbital combinations with Pu 6d atomic

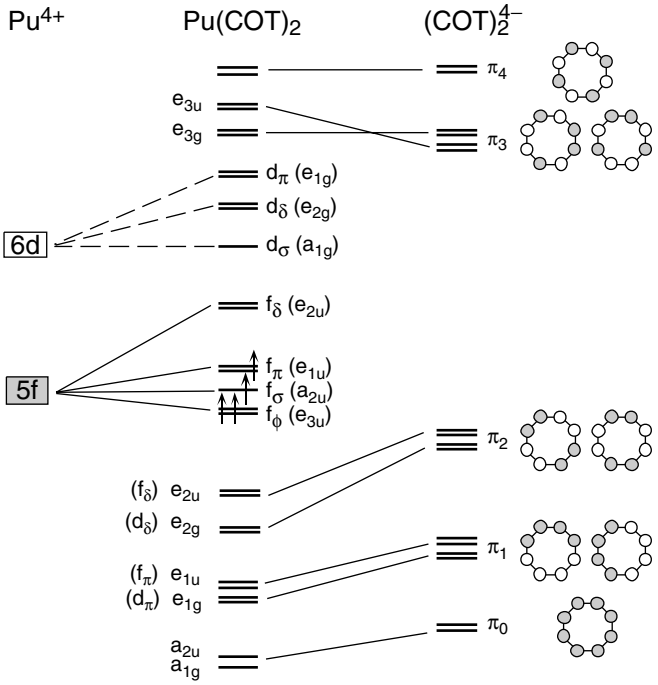

Fig. 7.125 *A qualitative molecular orbital interaction diagram for plutonocene, Pu(η-C_8H_8)$_2$.*

orbitals of d_σ, d_π, and d_δ symmetry gives rise to metal–ligand bonding molecular orbitals of a_{1g}, e_{1g}, and e_{2g} symmetry, respectively. Both the d_π (e_{1g}) and d_δ (e_{2g}) molecular orbitals are significantly destabilized due to strong interactions that occur with ligand orbitals at lower energy. The Pu 5f orbitals are split into the f_σ, f_π, f_δ, and f_φ molecular orbitals of a_{2u}, e_{1u}, e_{2u}, and e_{3u} symmetry, respectively. The lobes of the f_δ orbital are directed towards the $C_8H_8^{2-}$ rings, and interaction with the ligands strongly destabilizes this orbital and moves it significantly higher in energy than the remaining f_σ, f_π, and f_φ orbitals. Ligand interactions with the remaining f_σ, f_π, and f_φ orbitals are significantly weaker, giving rise to an f-orbital splitting pattern where one degenerate set is removed from the 5f manifold, leaving the other five orbitals clustered at lower energy (Boerrigter *et al.*, 1988). These general interactions are illustrated in Fig. 7.125.

As seen in the other examples, the 6d orbital interactions with the ligands are significantly stronger than the 5f interactions. The δ-type interactions have significant metal–ligand overlap and give rise to appreciable covalency through both 6d and 5f orbital interactions. A Mulliken population analysis for nonrelativistic orbitals showed that the $6d_\delta$ orbital is approximately 88% ligand and

11% 6d in character, while the $5f_\delta$ orbital is 48% ligand and 49% 5f in character (Boerrigter *et al.*, 1988). The latter represents significant 5f covalency. In addition, these calculations reveal that the semicore 6p orbitals also have a considerable amplitude at the position of the rings, and that this permits a strong interaction with deeper lying ring orbitals of the appropriate symmetry (Boerrigter *et al.*, 1988). These $6d_\delta$ (e_{2g}) and $5f_\delta$ (e_{2u}) metal–ligand bonding orbitals are illustrated qualitatively in **35** and **36**.

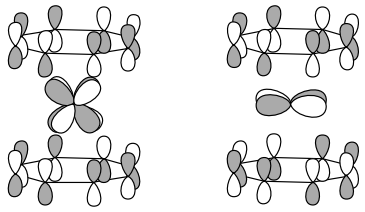

f_δ **d_δ**

35 **36**

This general bonding scheme has been experimentally confirmed by Brennan and coworkers who performed variable energy photoelectron spectroscopy on $U(\eta\text{-}C_8H_8)_2$ over a photon energy range of 24–125 eV (Brennan *et al.*, 1989). A mapping of the intensity changes in the ionization from the $5f_\delta$ (e_{2u}) orbital

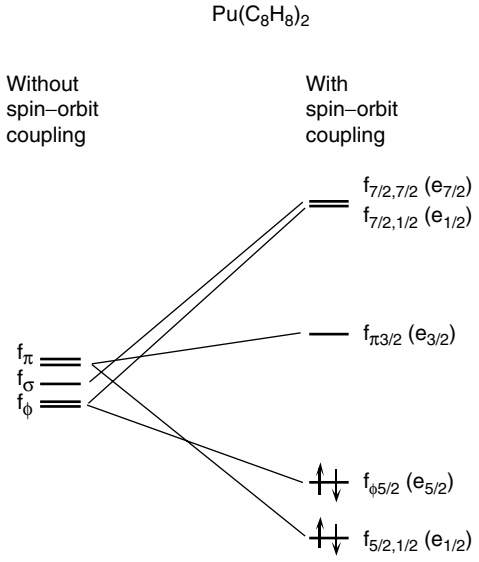

Fig. 7.126 *The effect of spin–orbit coupling on the 5f orbitals of Pu(η-C_8H_8)$_2$ adapted from Boerrigter* et al. (1988). *For consistency with Chapter* 17, *the D_{8h}* double group notation is given in parentheses.*

provided conclusive spectroscopic evidence for substantial 5f orbital covalency in $U(\eta\text{-}C_8H_8)_2$.

Relativistic calculations employing the HFS LCAO method conclude that the f_σ, f_π, and f_φ orbitals are nearly degenerate, and that they are equally populated with the four valence electrons in $Pu(\eta\text{-}C_8H_8)_2$ (Boerrigter *et al.*, 1988). This is not consistent with the experimental observation of a $M_j = 0$ ground state. As in our other examples, spin–orbit coupling must be taken into account in order to understand spectroscopic data. Boerrigter and coworkers have shown that strong ligand field splitting effectively removes the $5f_\delta$ orbital from the 5f orbital manifold, and this simplifies the discussion of spin–orbit coupling. The spin–orbit interaction on a degenerate set of f_σ, f_π, and f_φ orbitals gives a four-level pattern with two low-lying orbitals, the $f_{5/2,1/2}$ and $f_{\varphi 5/2}$, and three high-lying orbitals, the $f_{\pi 3/2}$, and the degenerate $f_{7/2,7/2}$ and $f_{7/2,1/2}$, as shown in Fig. 7.126. After inclusion of spin–orbit coupling, it is easy to see that $Pu(\eta\text{-}C_8H_8)_2$ is closed shell as both the low-lying $f_{5/2,1/2}$ and $f_{\varphi 5/2}$ are fully occupied leading to a $M_j = 0$ ground state in agreement with the measured magnetic properties.

ACKNOWLEDGMENTS

The authors acknowledge expert assistance from Karen Kippen, Leonard Martinez, Meredith Coonley, Ed Lorusso, and Susan Ramsay in preparing the manuscript. The authors are grateful to Thomas W. Newton and Phillip D. Palmer for electronic absorption spectra and calculations. DLC and MPN acknowledge the Division of Chemical Sciences, Geosciences, and Biosciences, Office of Basic Energy Research, U.S. Department of Energy for their support of actinide chemistry research at Los Alamos National Laboratory.

REFERENCES

(1963) *Plutonium Chemistry Symposium*, Report TID-7683, Argonne National Laboratory, 44 pp.

Abraham, B. M. and Davidson, N. R. (1949) High-temperature Hydrolysis of Plutonium Oxychloride, in *Natl. Nucl. Energy Ser.,* Div IV **14B**(Transuranium Elements, Pt. I) (eds. G. T. Seaborg, J. J. Katz, and W. M. Manning), McGraw-Hill, New York, pp. 779–83.

Abraham, B. M., Brody, B. B., Davidson, N. R., Hagemann, F., Karle, I., Katz, J. J., and Wolf, M. J. (1949a) Preparation and Properties of Plutonium Chlorides and Oxychlorides, in *Natl. Nucl. Energy Ser.,* Div IV **14B**(Transuranium Elements, Pt. I) (eds. G. T. Seaborg, J. J. Katz, and W. M. Manning), McGraw-Hill, New York, pp. 740–58.

Abraham, B. M., Davidson, N. R., and Westrum, E. F., Jr (1949b) Preparation and Properties of Some Plutonium Sulfides and Oxysulfides, in *Natl. Nucl. Energy Ser.,*

Div IV **14B**(Transuranium Elements, Pt. I) (eds. G. T. Seaborg, J. J. Katz, and W. M. Manning), McGraw-Hill, New York, pp. 814–17.

Abraham, B. M., Davidson, N. R., and Westrum, E. F., Jr (1949c) Preparation of Plutonium Nitride, in *Natl. Nucl. Energy Ser.,* Div IV **14B**(Transuranium Elements, Pt. I) (eds. G. T. Seaborg, J. J. Katz, and W. M. Manning), McGraw-Hill, New York, pp. 945–8.

Abrikosov, I. A., Ruban, A. V., Johansson, B., and Skriver, H. L. (1998) *Comput. Mater. Sci.,* **10**(1–4), 302–5.

Ackermann, R. J., Faircloth, R. L., and Rand, M. H. (1966) *J. Phys. Chem.,* **70**(11), 3698–706.

Adams, M. D., Steunenberg, R. K., and Vogel, R. C. (1957) *The Transfer of Plutonium Hexafluoride in the Vapor Phase*, Report ANL-5796, Argonne National Laboratory, 14 pp.

Adamson, M. G., Aitken, E. A., and Caputi, R. W. (1985) *J. Nucl. Mater.,* **130**, 349–65.

Adler, P. H. (1991) *Metall. Trans. A,* **22A**(10), 2237–46.

Adler, P. H., Olson, G. B., and Margolies, D. S. (1986) *Acta Metall.,* **34**(10), 2053–64.

Aitken, E. A. and Evans, S. K. (1968) *A Thermodynamic Data Program Involving Plutonium and Urania at High Temperatures*, Report GEAP-5672, General Electric Company, Vallecitos Nucleonics Laboratory, 10 pp.

Akatsu, J. (1982) *Sep. Sci. Technol.,* **17**(12), 1433–42.

Akatsu, J., Moriyama, N., Dojiri, S., Matsuzuru, H., and Kobayashi, Y. (1983) *Sep. Sci. Technol.,* **18**(2), 177–86.

Akhachinskii, V. V. and Bashlykov, S. N. (1970) *Atomnaya Energiya,* **29**(6), 439–47.

Akimoto, Y. (1960) *Chemistry Division Semi-annual Report - June through November 1959*, USAEC Report UCRL-9093, Lawrence Radiation Laboratory.

Albiol, T. and Arai, Y. (2001) *Review of Actinide Nitride Properties with Focus on Safety Aspects*, Report JAERI-Review, Department of Nuclear Energy System, Tokai Research Establishment, Japan Atomic Energy Research Institute, i–vi, pp. 1–50.

Albrecht, E. D. (1964) *J. Nucl. Mater,* **12**(2), 125–130.

Albrecht-Schmitt, T. E., Almond, P. M., and Sykora, R. E. (2003) *Inorg. Chem.,* **42**(12), 3788–95.

Albright, D. and Kramer, K. (2004) *B. Atom. Sci.,* **60**(6), 14–16.

Alcock, N. W. and Esperas, S. (1977) *J. Chem. Soc. Dalton Trans.,* **9**, 893–6.

Alei, M., Johnson, Q. C., Cowan, H. D., and Lemons, J. F. (1967) *J. Inorg. Nucl. Chem.,* **29**, 2327.

Alenchikova, I. F., Zaitseva, L. L., Lipis, L. V., Fomin, V. V., and Chebotarev, N. T. (1958) *Proc. Second UN Int. Conf. Peaceful Uses Atomic Energy*, vol. 28, Geneva, 1958, pp. 309–15.

Alenchikova, I. F., Zaitseva, L. L., Lipis, L. V., and Fomin, V. V. (1959) *Zh. Neorg. Khim.,* **4**, 961–2.

Alenchikova, I. F., Lipis, L. V., and Nikolaev, N. S. (1961a) *Atomnaya Energiya,* **10**, 592–6.

Alenchikova, I. F., Zaitseva, L. L., Lipis, L. V., Nikolaev, N. S., Fomin, V. V., and Chebotarev, N. T. (1961b) *Zh. Neorg. Khim.,* **6**, 1513–19.

Alexander, C. A., Ogden, J. S., and Pardue, W. M. (1969) Report BMI-1862, A7, Batelle Memorial Institute, Columbus, OH.

Alexander, E. C., Jr., Lewis, R. S., Reynolds, J. H., and Michel, M. C. (1971) *Science* **172**(3985), 837–40.

Alexander, C. A., Clark, R. B., Kruger, O. L., and Robbins, J. L. (1976) Fabrication and High-temperature Thermodynamic and Transport Properties of Plutonium Mononitride. *Plutonium 1975 and Other Actinides*, *Proc. Conf. in Baden-Baden,* Sept. 10–13, 1975/*Proc. Fifth Int. Conf. on Plutonium and Other Actinides*, 1975 (eds. H. R. Blank and R. Lindner), pp. 277–86.

Allard, B., Kipatsi, H., and Lilijenzin, J. O. (1980) *J. Inorg. Nucl. Chem.,* **42**(7), 1015–27.

Allbutt, M. and Dell, R. M. (1967) *J. Nucl. Mater.,* **24**(1), 1–20.

Allbutt, M., Dell, R. M., and Junkison, A. R. (1970) Plutonium Chalcogenides, in *Chem. Extended Defects Non-Metal. Solids,* (eds. L. Eyring and M. O'Keefe), Proc. Inst. Advan. Study. Scottsdale, AZ, pp. 124–47.

Allen, G. C. and Tempest, P. A. (1986) *Proc. R. Soc. Lon. Ser. A,* **406**(1831), 325–44.

Allen, P. G., Bucher, J. J., Clark, D. L., Edelstein, N. M., Ekberg, S. A., Gohdes, J. W., Hudson, E. A., Kaltsoyannis, N., Lukens, W. W., Neu, M. P., Palmer, P.D., Reich, T., Shuh, D. K., Tait, C. D., and Zwick, B. D. (1995) *Inorg. Chem.,* **34**(19), 4797–807.

Allen, J. W., Zhang, Y. X., Tjeng, L. H., Cox, L. E., Maple, M. B., and Chen, C. T. (1996a) *J. Electron Spectro. Rel. Phenom.,* **78**, 57–62.

Allen, P. G., Veirs, D. K., Conradson, S. D., Smith, C. A., and Marsh, S. F. (1996b) *Inorg. Chem.,* **35**(10), 2841–5.

Allen, P. G., Bucher, J. J., Shuh, D. K., Edelstein, N. M., and Reich, T. (1997) *Inorg. Chem.,* **36**(21), 4676–83.

Allen, P. G., Henderson, A. L., Sylwester, E. R., Turchi, P. E. A., Shen, T. H., Gallegos, G. F., and Booth, C. H. (2002) *Phys. Rev. B.,* **65**(21), 214107/1–214107/7.

Al Mahamid, I., Becraft, K. A., Hakem, N. L., Gatti, R. C., and Nitsche, H. (1996) *Radiochim. Acta,* **74**, 129–34.

Amano, O., Sasahira, A., Kani, Y., Hoshino, K., Aoi, M., and Kawamura, F. (2004) *J. Nucl. Sci. Technol.,* **41**(1), 55–60.

Anderegg, G. (1977) *Critical Survey of Stability Constants of EDTA Complexes,* Pergamon Press, Oxford.

Anderegg, G. (1982) *Pure Appl. Chem.,* **54**, 2693.

Anderson, H. H. and Asprey, L. B. (1960) *Solvent-extraction Process for Plutonium*. US Patent no. 2924 506. (U.S. Atomic Energy Commission).

Anderson, J. W. and Maraman, W. J. (1962) *Trans. Am. Foundrymen's Soc.,* **70**, 1057–72.

Anderson, J. W., Leary, J. A., and McNeese, W. D. (1960) *Preparation and Fabrication of Plutonium Fuel Alloy for Los Alamos Molten Plutonium Reactor Experiment No. 1*, Report LA-2439, Los Alamos Scientific Laboratory, 30 pp.

Andreichuk, N. N., Vasil'ev, V. Y., Rykova, A. G., Osipov, S. V., Kalashnikov, V. M., and Vysokoostrovskaya, N. B. (1979) *Sov. Radiochem.,* **21**(6), 727–36.

Andreichuk, N. N., Rotmanov, K. V., Frolov, A. A., and Vasil'ev, V. Y. (1984a) *Sov. Radiochem.,* **26**(1), 90–4.

Andreichuk, N. N., Rotmanov, K. V., Frolov, A. A., and Vasil'ev, V. Y. (1984b) *Sov. Radiochem.,* **26**(6), 701–6.

Andreichuk, N. N., Frolov, A. A., Rotmanov, K. V., and Vasil'ev, V. Y. (1990) *J. Radioanal. Nucl. Chem. Lett.,* **143**(2), 427–32.

Andrew, J. F. (1967) *J. Phys. Chem. Solids,* **28**(4), 577–80.

Andrew, J. F. (1969) *J. Nucl. Mater.,* **30**(3), 343–5.
Andrew, J. F. and Latimer, T. W. (1975) *Review of Thermal Expansion and Density of Uranium and Plutonium Carbides*, Report LA-6037-MS, Los Alamos Science Laboratory, Los Alamos, NM, 17 pp.
Angelo, J. A., Jr, and Buden, D. (1985) *Space Nuclear Power,* Orbit Book Company, Malabar, FL, 286 pp.
Ankudinov, A. L., Conradson, S. D., Mustre de Leon, J., and Rehr, J. J. (1998) *Phys. Rev. B,* **57**(13), 7518–25.
Anselin, F. (1963a) *J. Nucl. Mater.,* **10**(4), 301–220.
Anselin, F. (1963b) *Compt. Rend.,* **256**, 2616–19.
Antonio, M. R., Soderholm, L., Williams, C. W., Blaudeau, J.-P., and Bursten, B. E. (2001) *Radiochim. Acta,* **89**(1), 17–25.
Antonio, M. R., Chiang, M.-H., Williams, C. W., and Soderholm, L. (2004) *Mater. Res. Soc. Symp. Proc*., **802**, 157–68.
Anyun, Z., Jingxin, H., Xianye, Z., and Fangding, W. (2002) *J. Radioanal. Nucl. Chem.,* **252**(3), 565–71.
Arai, Y. and Ohmichi, T. (1995) *J. Solid State Chem.,* **115**(1), 66–70.
Archibong, E. F. and Ray, A. K. (2000) *Theochem,* **530**(1,2), 165–70.
Arko, A. J., Joyce, J. J., and Havela, L. (2006) *The Chemistry of the Actinide and Transactinide Elements,* (eds. L. R. Morss, N. M. Edelstein, and J. Fuger), Springer Publishing, New York, ch. 21.
Artyukhin, P. I., Gel'man, A. D., and Medvedovskii, V. I. (1958) *Doklady Akad. Nauk SSSR,* **120**, 98–100.
Artyukhin, P. I., Medvedovskii, V. I., and Gel'man, A. D. (1959) *Zh. Neorg. Khim.,* **4**, 1324–31.
Asanuma, N., Harada, M., Ikeda, Y., and Tomiyasu, H. (2001) *J. Nucl. Sci. Technol.,* **38**(10), 866–71.
Asprey, L. B., Keenan, T. K., and Kruse, F. H. (1964) *Inorg. Chem.,* **3**(8), 1137–240.
Asprey, L. B., Eller, P. G., and Kinkead, S. A. (1986) *Inorg. Chem.,* **25**(5), 670–2.
Atlas, L. M. and Schlehman, G. J. (1967) Defect Equilibria of Nonstoichiometric Plutonium dioxide 1045 to 1505 Deg. *Plutonium 1965, Proc. Third Int. Conf. on Plutonium* (eds. A. E. Kay and M. B. Waldron), Chapman and Hall, London, pp. 838–44.
Atlas, L. M., Schlehman, G. J., and Readey, D. W. (1966) *J. Am. Ceram. Soc.,* **49**(11), 624–5.
Audi, G. and Wapstra, A. H. (1995) *Nucl. Phys. A,* **595**(4), 409–80.
Audi, G., Bersillon, O., Blachot, J., and Wapstra, A. H. (1997) *Nucl. Phys. A,* **624**(1), 1–124.
Austin, A. E. (1959) *Acta Crystallogr.,* **12**, 159–61.
Avdeef, A., Raymond, K. N., Hodgson, K. O., and Zalkin, A. (1972) *Inorg. Chem.,* **11**(5), 1083–8.
Avens, L. R., Bott, S. G., Clark, D. L., Sattelberger, A. P., Watkin, J. G., and Zwick, B. D. (1994) *Inorg. Chem.,* **33**(10), 2248–56.
Avignant, D. and Cousseins, J. C. (1971) *Compt. Rend.,* **272**(26), 2151–3.
Avivi, E. (1964) *Etudes d'Alliages Plutonium - Fer at d'Alliages Uranium - Plutonium-Fer*, Thesis, Universite de Paris, 72 pp.
Awasthi, S. K., Chackraburtty, D. M., and Tondon, V. K. (1968) *J. Inorg. Nucl. Chem.,* **30**(3), 819–21.

Axler, K. M., Roof, R. B., and Foltyn, E. M. (1992) *J. Nucl. Mater.,* **189**(2), 231–2.
Baes, C. F. and Mesmer, R. E. (1976) *The Hydrolysis of Cations,* Wiley, New York, 489 pp.
Baglan, N., Fourest, B., Guillaumont, R., Blain, G., Le Du, J.-F., and Genet, M. (1994) *New J. Chem.,* **18**(7), 809–16.
Bagnall, K. W. (1967a) *Coord. Chem. Rev.,* **2**(2), 145–62.
Bagnall, K. W. (1967b) *Halogen Chem.,* **3**, 303–82.
Bagnall, K. W., Deane, A. M., Markin, T. L., Robinson, P. S., and Stewart, M. A. A. (1961) *J. Chem. Soc., Abstracts*: 1611–17.
Bagnall, K. W., Plews, M. J., and Brown, D. (1982a) *J. Organomet. Chem.,* **224**(3), 263–6.
Bagnall, K. W., Plews, M. J., Brown, D., Fischer, R. D., Klaehne, E., Landgraf, G. W., and Sienel, G. R. (1982b) *J. Chem. Soc., Dalton Trans.*, (10), 1999–2007.
Bagnall, K. W., Payne, G. F., and Brown, D. (1985a) *J. Less-Common Met.,* **109**(1), 31–6.
Bagnall, K. W., Payne, G. F., and Brown, D. (1985b) *J. Less-Common Met.,* **113**(2), 325–9.
Bagnall, K. W., Payne, G. F., and Brown, D. (1986) *J. Less-Common Met.,* **116**(2), 333–9.
Baily, H., Bernard, H., and Mansard, B. (1989) *Mater. Sci. Forum,* **48–49**(Nucl. Fuel Fabr.), 175–83.
Bairiot, H. and Deramaix, P. (1992) *J. Nucl. Mater.,* **188**, 10–18.
Bairiot, H., Blanpain, P., Farrant, D., Ohtani, T., Onoufriev, V., Porsch, D., Stratton, R., Brown, C., Deramaix, P., Golovnin, I., Haas, E., Laraia, M., Nagai, S., Pope, R., Sanchis, H., Shea, T., and Weston, R. (2003) *Status and Advances in MOX Fuel Technology*, Technical Report Series - International Atomic Energy Agency (415), Report 1-179.
Baker, R. D. (1946) *Preparation of Plutonium Metal by the Bomb Method*, Report LA-473, Los Alamos Scientific Laboratory, 65 pp.
Baker, R. D. and Maraman, W. J. (1960) *Extract. Phys. Met. Plutonium and Alloys, Symp.,* San Francisco, California, 43–59.
Balakrishnan, P. V. and Ghosh Mazumdar, A. S. (1964) *J. Inorg. Nucl. Chem.,* **26**(5), 759–63.
Baldwin, C. E. and Navratil, J. D. (1983) *ACS Symp. Ser.* **216** (Plutonium Chem.) (eds. W. T. Carnall and G. R. Choppin), American Chemcial Society, Washington, DC. pp. 369–80.
Bamberger, C. E. (1985) in *Handbook on the Physics and Chemistry of the Actinides* (eds. A. J. Freeman and C. Keller), Elsevier Science, New York, ch. 6, pp. 289–303.
Banks, R. H. (1979) *Preparation and Spectroscopic Properties of Three New Actinide(IV) Borohydrides*, Thesis, Report LBL-10292, Lawrence Berkeley Laboratory, University of California, 209 pp.
Banks, R. H. and Edelstein, N. M. (1980) *ACS Symp. Ser.* **131**(Lanthanide Actinide Chem. Spectrosc.), American Chemcial Society, Washington, DC. 331–48.
Banks, R. H., Edelstein, N. M., Rietz, R. R., Templeton, D. H., and Zalkin, A. (1978) *J. Am. Chem. Soc.,* **100**(6), 1957–8.
Banyai, I., Glaser, J., Micskei, K., Toth, I., and Zekany, L. (1995) *Inorg. Chem.,* **34**(14), 3785–96.

Bardelle, P. and Bernard, H. (1989) *Preparation of Uranium and/or Plutonium Nitride for Use as a Nuclear Reactor Fuel*, (Commissariat a l'Energie Atomique, France). Ep Patent 307311, 5 pp.

Barmore, W. L. and Uribe, F. S. (1970) *Mechanical Behavior of Pu-Ga, Proc. Fourth Int. Conf. on Plutonium and Other Actinides* (ed. W. N. Miner), Santa Fe, NM, The Metallurgical Society of AIME, 1, 414 pp.

Barney, G. S. (1976) *J. Inorg. Nucl. Chem.,* **38**(9), 1677–81.

Barton, C. J., Redman, J. D., and Strehlow, R. A. (1961) *J. Inorg. Nucl. Chem.,* **20**, 45–52.

Bartscher, W. (1996) *Diffusion and Defect Data–Solid State Data, Pt. B. Solid State Phenomena,* **49–50**(Hydrogen Metal Systems I), 159–238.

Bartscher, W., Boeuf, A., Caciuffo, R., Fournier, J. M., Haschke, J. M., Manes, L., Rebizant, J., Rustichelli, F., and Ward, J. W. (1985) *Physica B & C,* **130**(1–3), 530–2.

Baskes, M. I. (2000) *Phys. Rev. B: Condens. Matter,* **62**(23), 15532–7.

Baskes, M. I., Muralidharan, K., Stan, M., Valone, S. M., and Cherne, F. J. (2003) *JOM,* **55**(9), 41–50.

Baston, G. M. N., Bradley, A. E., Gorman, T., Hamblett, I., Hardacre, C., Hatter, J. E., Healy, M. J. F., Hodgson, B., Lewin, R., Lovell, K. V., Newton, G. W. A., Nieuwenhuyzen, M., Pitner, W. R., Rooney, D. W., Sanders, D., Seddon, K. R., Simms, H. E., and Thied, R. C. (2002) Ionic Liquids for the Nuclear Industry: A Radiochemical, Structural and Electrochemical Investigation, in *Ionic Liquids - Industrial Applications to Green Chemistry* (eds. R. D. Rogers and K. R. Seddon), American Chemical Society, Washington, DC, pp. 162–77.

Battles, J. E. and Blackburn, P. E. (1969) *Reactor Development Program Progress Report September 1969*, Report ANL-7618, Argonne National Laboratory, 141 pp.

Battles, J. E., Reishus, J. W., and Shinn, W. A. (1968) *Am. Ceram. Soc. Bull.,* **47**(4), 414.

Battles, J. E., Reishus, J. W., and Shinn, W. A. (1969) *Volatilization Studies of Plutonium Compounds by Mass Spectrometry, in Chemical Engineering Division, Annual Report 1968*, Report ANL-7575, Argonne National Laboratory, pp. 77–82.

Battles, J. E., Shinn, W. A., Blackburn, P. E., and Edwards, R. K. (1970) *Plutonium 1970 and Other Actinides, Proc. Fourth Int. Conf. on Plutonium and Other Actinides,* Santa Fe, NM, Oct. 5–9, 1970 (ed. W. N. Miner), AIME, New York, 733 pp.

Bauche, J., Blaise, J., and Fred, M. (1963) *Compt. Rend.,* **257**(16), 2260–3.

Bauer, E. D., Thompson, J. D., Sarrao, J. L., Morales, L. A., Wastin, F., Rebizant, J., Griveau, J. C., Javorsky, P., Boulet, P., Colineau, E., Lander, G. H., and Stewart, G. R. (2004) *Phys. Rev. Lett.,* **93**(14), 147005/1–4.

Baumgärtner, F., Fischer, E. O., Kanellakopulos, B., and Laubereau, P. (1965) *Angew. Chem.,* **77**(19), 866–7.

Bayoglu, A. S. and Lorenzelli, R. (1979) *J. Nucl. Mater.,* **79**(2), 437–8.

Bayoglu, A. S. and Lorenzelli, R. (1984) *Solid State Ionics,* **12**, 53–66.

Bayoglu, A. S., Giordano, A., and Lorenzelli, R. (1983) *J. Nucl. Mater.,* **113**(1), 71–4.

Bean, A. C., Campana, C. F., Kwon, O., and Albrecht-Schmitt, T. E. (2001) *J. Am. Chem. Soc.,* **123**(36), 8806–10.

Bean, A. C., Abney, K., Scott, B. L., and Runde, W. (2005) *Inorg. Chem.,* **44**(15), 5209–11.

Bearden, J. A. (1967) *Rev. Mod. Phys.,* **39**, 78–124.

Bearden, J. A. and Burr, A. F. (1967) *Rev. Mod. Phys.,* **39**, 125–42.

Beauvais, R. A. and Alexandratos, S. D. (1998) *React. Funct. Polym.,* **36**(2), 113–23.

Beitscher, S. (1970) *Hot Shortness in Plutonium-1 Weight Percent Gallium*, *Proc. Fourth Int. Conf. Plutonium - Other Actinides*, Santa Fe, NM (ed. W. N. Miner), The Metallurgical Society of AIME, 1, pp. 449–56.
Beitz, J., Jonah, C., Sullivan, J. C., and Woods, M. (1986) *Radiochim. Acta,* **40**(1), 7–9.
Benard, P., Brandel, V., Dacheux, N., Jaulmes, S., Launay, S., Lindecker, C., Genet, M., Louer, D., and Quarton, M. (1996) *Chem. Mater.,* **8**(1), 181–8.
Benedict, U. (1970) *J. Nucl. Mater.,* **35**(3), 356–61.
Benedict, U. (1979) *Solid Solubility of Fission Product and Other Transition Elements in Carbides and Nitrides of Uranium and Plutonium*, European Institute for Transuranium Elements, Report 6 pp.
Benedict, U. and Sari, C. (1969) *Ternary System Uranium dioxide-Uranium oxide (U_3O_8)-Plutonium dioxide*, Report EUR-4136, Transuranium Institute, European Atomic Energy Community, Karlsruhe, Germany, 38 pp.
Bennett, D. A., Hoffman, D., Nitsche, H., Russo, R. E., Torres, R. A., Baisden, P. A., Andrews, J. E., Palmer, C. E. A., and Silva, R. J. (1992) *Radiochim. Acta,* **56**(1), 15–19.
Benz, R., Kahn, M., and Leary, J. A. (1959) *J. Phys. Chem.,* **63**, 1983–4.
Benz, R. (1961) *J. Phys. Chem.,* **65**(1), 81–4.
Benz, R. (1962) *J. Inorg. Nucl. Chem.,* **24**(Dec), 1191–5.
Benz, R. and Douglass, R. M. (1961a) *J. Inorg. Nucl. Chem.,* **23**, 134–6.
Benz, R. and Douglass, R. M. (1961b) *J. Phys. Chem.,* **65**, 1461–3.
Benz, R. and Leary, J. A. (1961) *J. Phys. Chem.,* **65**(6), 1056–8.
Benz, R., Douglass, R. M., Kruse, F. H., and Penneman, R. A. (1963) *Inorg. Chem.,* **2**(4), 799–803.
Berg, J. M., Smith, C. A., Cisneros, M. A., Vaughn, R. B., and Veirs, D. K. (1998) *J. Radioanal. Nucl. Chem. Lett.,* **235**(1–2), 25–9.
Berg, J. M., Veirs, D. K., Vaughn, R. B., Cisneros, M. R., and Smith, C. A. (2000) *Appl. Spectrosc.,* **54**(6), 812–23.
Berger, R. and Gäumann, T. (1961) *Helv. Chim. Acta,* **44**(4), 1084–8.
Bergstresser, K. S. (1950) *Plutonium Electropolishing Cell*, Report LA-1106, Los Alamos Scientific Laboratory, 10 pp.
Bernard, H. (1989) *J. Nucl. Mater.,* **166**(1–2), 105–11.
Berndt, A. F. (1962) *On the Use of a Modified Radial Distribution Analysis for Indexing Powder Patterns*, Report ANL-FGF-360, Argonne National Laboratory, 12 pp.
Berndt, A. F. (1966) *J. Less-Common Met.,* **11**(3), 216–19.
Berndt, A. F. (1967) *J. Less-Common Met.,* **12**(1), 82–3.
Berthon, C. and Chachaty, C. (1995) *Solvent Extr. Ion Exc.,* **13**(5), 781–812.
Besmann, T. M. and Lindemer, T. B. (1983) *J. Am. Ceram. Soc.,* **66**(11), 782–5.
Bessonov, A. A., Krot, N. N., Budantseva, N. A., and Afonas'eva, T. V. (1996) *Radiokhimiya,* **38**(3), 223–5.
Betz, T. and Hoppe, R. (1984) *Z. Anorg. Allg. Chem.,* **512**, 19–33.
Beznosikova, A. V., Chebotarev, N. T., Luk'yanov, A. S., Chernyi, A. V., and Smirnova, E. A. (1974) *Sov. At. Energy,* **37**(2), 842–6.
Bhide, M. K., Kadam, R. M., Babu, Y., Natarajan, V., and Sastry, M. D. (2000) *Chem. Phys. Lett.,* **332**(1,2), 98–104.
Bjorklund, C. W. (1957) *J. Am. Chem. Soc.,* **79**, 6347–50.
Bjorklund, C. W., Reavis, J. G., Leary, J. A., and Walsh, K. A. (1959) *J. Phys. Chem.,* **63**(10), 1774–7.

Blaise, A., Collard, J. M., Fournier, J. M., Rebizant, J., Spirlet, J. C., and Vogt, O. (1985) *Physica B & C,* **130**(1–3), 99–101.

Blaise, J., Fred, M. S., Carnall, W. T., Crosswhite, H. M., and Crosswhite, H. (1983a) Measurement and Interpretation of Plutonium Spectra (ACS Symp. Ser. no. 216), (eds. W. T. Carnall and G. R. Choppin), American Chemical Society, Washington, DC, pp. 173–98.

Blaise, J., Fred, M., and Gutmacher, R. G. (1983b) *The Atomic Spectrum of Plutonium*, Report ANL-83-95, Argonne National Laboratory, 612 pp.

Blaise, J., Fred, M., and Gutmacher, R. G. (1986) *J. Opt. Soc. Am.,* **B3**(3), 403–18.

Blaise, J., Fred, M., and Gutmacher, R. G., unpublished results.

Blaise, J. and Wyart, J.-F. (1992) *Energy levels and atomic spectra of actinides,* Tables Internationales de Constantes, Paris, France, ISBN 2-9506414-0-7.

Blank, H. (1976) Transurane: Binare Legierungsysteme 1, in *Gmelin Handbuch der Anorganische Chemie* (ed. K.-C. Buschbeck), Springer-Verlag, Berlin, 38 pp.

Blank, H. (1977) Binary Alloys, in *Gmelin Handbuch der Anorganische Chemie Transurane: The Alloys* (ed. K.-C. Buschbeck), Springer-Verlag, Berlin, pp. 1–275.**39, B3:**

Blank, H. (1994) in *Nuclear Materials* (ed. B. R. T. Frost), VCH publishers, Weinheim, 203 pp.

Blank, H., Brossman, G., Kemmerich, M., and Weitzenmiller, F. (1962) *Zwei- und mehrstoffsysteme mit plutonium. Literaturubersicht, phasendiagramme und daten, teil 1, Pu-Ag bis Pu-Sn.* Karlsruhe, Kernreaktor Bau- und Betriebs-Gesellschaft, 243 pp.

Blank, H. R. and Lindner, R. (eds.) (1976a) *Plutonium 1975 and Other Actinides: Proc. Conf. in Baden-Baden*, Sept. 10–13, 1975/*Proc. Fifth Int. Conf. on Plutonium and Other Actinides*, 1975, American Elsevier Publication, New York; North-Holland, Amsterdam.

Blau, M. S. (1998) *J. Radioanal. Nucl. Chem.,* **235**(1–2), 41–5.

Blaudeau, J.-P. and Bursten, B. E. (2000) *Abstracts of Papers, 220th ACS National Meeting*, Aug. 20–24, 2000, Washington, DC, INOR-419.

Bleaney, B. (1955) *Discuss. Faraday Soc.,* **19**, 112–18.

Bluestein, B. A. and Garner, C. S. (1944) *The Preparation of Plutonium Tribromide*, Report LA-116, Los Alamos Scientific Laboratory, 7 pp.

Boatner, L. A. and Sales, B. C. (1988) in *Monazite,* (eds. W. Lutze and R. C. Ewing), Radioactive Waste Forms for the Future North-Holland, Amsterdam.

Bochvar, A. A., Konobeevsky, S. T., Kutaitsev, V. I., Menshikova, T. S., and Chebotarev, N. T. (1958) *Interaction of Plutonium and Other Metals in Connection with the Arrangement in Mendeleev's Periodic Table, Proc. Second UN Int. Conf. on the Peaceful Uses of Atomic Energy,* Geneva, Switzerland, 6, pp. 184–93.

Bodu, R., Bouzigues, H., Morin, N., and Pfiffelmann, J. P. (1972) *C. R. Acad. Sci., Ser. D,* **275**(16), 1731–2.

Boehlert, C. J., Schulze, R. K., Mitchell, J. N., Zocco, T. G., and Pereyra, R. A. (2001) *Scr. Mater.,* **45**(9), 1107–15.

Boerrigter, P. M., Baerends, E. J., and Snijders, J. G. (1988) *Chem. Phys.,* **122**(3), 357–74.

Boeuf, A., Caciuffo, R., Fournier, J. M., Manes, L., Rebizant, J., Roudaut, E., and Rustichelli, F. (1984) *Solid State Commun.,* **52**(4), 451–3.

Bohe, A. E., Nassini, H. E., Bevilacqua, A. M., and Pasquevich, D. M. (1997) *Chlorination Reactions Applied to Reprocessing of Aluminum–Uranium Spent Nuclear Fuels,*

1997 *Symp. on Scientific Basis for Nuclear Waste Management XXI* (eds. I. G. McKinley and C. McCombie), Materials Research Society, Davos, Switzterland, 506, pp. 535–42.
Boivineau, M. (2001) *J. Nucl. Mater.,* **297**, 97–106.
Bokelund, H. and Glatz, J. P. (1984) *Inorg. Chim. Acta,* **94**(1–3), 131–132.
Bolvin, H., Wahlgren, U., Moll, H., Reich, T., Geipel, G., Fanghaenel, T., and Grenthe, I. (2001) *J. Phys. Chem. A,* **105**(51), 11441–5.
Bonnelle, C. (1976) *Struct. Bond. I,* **31**, 23–48.
Boreham, D., Freeman, J. H., Hooper, E. W., Jenkins, I. L., and Woodhead, J. L. (1960) *J. Inorg. Nucl. Chem.,* **16**, 154–6.
Boring, M. and Hecht, H. G. (1978) *J. Chem. Phys.,* **69**(1), 112–16.
Boring, A. M. and Smith, J. L. (2000) *Los Alamos Science,* **26**(1), 90.
Borkowski, M., Chiarizia, R., Jensen, M. P., Ferraro, J. R., Thiyagarajan, P., and Littrell, K. C. (2003) *Separ. Sci. Technol.,* **38**(12–13), 3333–51.
Boucher, R. and Quere, Y. (1981) *J. Nucl. Mater.,* **100**(1–3), 132–6.
Boukhalfa, H., Reilly, S. D., Smith, W. H., and Neu, M. P. (2004) *Inorg. Chem.,* **43**(19), 5816–23.
Boulet, P., Wastin, F., Colineau, E., Griveau, J. C., and Rebizant, J. (2003) *J. Phys. Condens. Mat.,* **15**(28), S2305–S2308.
Bourges, J., Madic, C., Koehly, G., and Lecomte, M. (1986) *J. Less-Common Met.,* **122**, 303–11.
Bovey, L. and Gerstenkorn, S. (1961) *J. Opt. Soc. Am.,* **51**, 522–5.
Bovey, L. and Steers, E. B. M. (1960) *Spectrochim. Acta,* **16**, 1184–99.
Bowersox, D. F. and Leary, J. A. (1966) *The Solubilities of Selected Elements in Liquid Plutonium. X. Thulium*, Report LA-3623, Los Alamos Scientific Laboratory, 10 pp.
Bowersox, D. F. and Leary, J. A. (1967) *Trans. Amer. Nucl. Soc.,* **10**(1), 106.
Bowersox, D. F. and Leary, J. A. (1968) *The Solubilities of Selected Elements in Liquid Plutonium. XII Chromium*, Report LA-3850, Los Alamos Scientific Laboratory, 5 pp.
Bradley, D. C., Harder, B., and Hudswell, F. (1957) *J. Chem. Soc.*, *Abstracts*: 3318.
Brandel, V. and Dacheux, N. (2004a) *J. Solid State Chem.,* **177**, 4743–54.
Brandel, V. and Dacheux, N. (2004b) *J. Solid State Chem.,* **177**, 4755–67.
Brennan, J. G., Green, J. C., and Redfern, C. M. (1989) *J. Am. Chem. Soc.,* **111**(7), 2373–7.
Brett, N. H. and Fox, A. C. (1966) *J. Inorg. Nucl. Chem.,* **28**(5), 1191–203.
Brewer, L. (1953) *Chem. Rev.,* **52**, 1–75.
Brewer, L. (1965) in *High-strength Materials* (ed. V. F. Zackay), John Wiley, New York, 12.
Brewer, L. (1970) *Proc. Fourth Int. Conf. on Plutonium and Other Actinides,* (ed. W. N. Miner), The Metallurgical Society of AIME, Warrendale, PA, 650 pp.
Brewer, L. (1971a) *J. Opt. Soc. Am.,* **61**(8), 1101–11.
Brewer, L. (1971b) *J. Opt. Soc. Am.,* **61**(12), 1666–82.
Brewer, L. (1983) Systematics of the Properties of the Lanthanides, in *Systematics and the Properties of the Lanthanides* (eds. S. P. Sinha, D. Reidel), Hingham, MA, pp. 17–69.
Brewer, L. (2000) *Metall. Mater. Trans.,* **31B**(4), 603–7.

Brewer, L., Bromley, L., Gilles, P. W., and Lofgren, N. L. (1949) *Natl. Nucl. En. Ser.*, Div IV **14B**(Transuranium Elements, Pt. II) (eds. G. T. Seaborg, J. J. Katz and W. M. Manning), McGraw-Hill, New York, pp. 861–86.

Bridger, N. J. and Dell, R. M. (1967) *Research on Plutonium Nitride*, Report AERE-R-5441, UK Atomic Energy Research Group, Atomic Energy Research Establishment, 14 pp.

Bridger, N. J., Dell, R. M., and Wheeler, V. J. (1969) *Reactivity Solids, Proc. Sixth Int. Symp.*, pp. 389–400.

Brodsky, M. B. (1961) *Comment on J. Friedel Paper, Plutonium 1960,* Grenoble, France (eds. E. Grison, W. B. H. Lord, and R. D. Fowler), Cleaver-Hume Press, London, 1, 210 pp.

Brown, D. (1968) *Halides of the Lanthanides and Actinides.* Wiley-Interscience, New York, 290 pp.

Brown, F., Ockenden, H. M., and Welch, G. A. (1955) *J. Chem. Soc.*, *Abstracts*: 4196–201.

Brown, D., Fletcher, S., and Holah, D. G. (1968) *J. Chem. Soc.*, *(London)* (8), 1889–94.

Brown, D., and Edwards, J. (1972) *J. Chem. Soc., Dalton Trans.: Inorg. Chem.* (1972–1999) (16), 1757–1762.

Brown, D., Hurtgen, C., and Fuger, J. (1977) *Rev. Chim. Miner.,* **14**(2), 189–98.

Buchmeiser, M. R. (2001) *Macromol. Rapid Commun.,* **22**(14), 1081–94.

Budantseva, N. A., Shilov, V. P., and Krot, N. N. (1998) *Radiochemistry,* **40**(6), 565–7.

Budantseva, N. A., Fedosseev, A. M., Bessonov, A. A., Grigoriev, M. S., and Krupa, J. C. (2000) *Radiochim. Acta,* **88**(5), 291–5.

Bullock, J. I., Ladd, M. F. C., Povey, D. C., and Storey, A. E. (1980) *Inorg. Chim. Acta,* **43**(1), 101–8.

Büppelmann, L., Kim, J. I., and Lierse, C. (1988) *Radiochim. Acta,* **44–45**(Pt. 1), 65–70.

Burney, G. A. (1962) *Separation of Neptunium and Plutonium by Anion Exchange*, Report DP-689, E. I. du Pont de Nemours & Co., Aiken, SC, 33 pp.

Burney, G. A. and Thompson, G. H. (1972) *Radiochem. Radioanal. Lett.,* **12**(4–5), 207–14.

Burney, G. A. and Thompson, G. H. (1974) *Separation of Plutonium-238 from Neptunium-237 by Pressurized Anion Exchange*, Report DP-1331, Savannah River Laboratory, E. I. DuPont de Nemours and Co., Aiken, SC, 21 pp.

Burns, C. J. and Sattelberger, A. P. (2002) Organometallic and Nonaqueous Coordination Chemistry, in *Advances in Plutonium Chemistry 1967–2000* (ed. D. C. Hoffman), American Nuclear Society, La Grange Park, IL, pp. 61–76.

Burns, C. J., Neu, M. P., Boukhalfa, H., Gutowski, K. E., Bridges, N. J., and Rogers, R. D. (2004) *Comprehensive Coord. Chem. II,* **3**, 189–345.

Burns, C. J., Clark, D. L., and Sattelberger, A. P. (2005) Actinides: Organometallic Chemistry, in *Encyclopedia of Inorganic Chemistry 2nd Ed.* (ed. R. B. King), Wiley Interscience, New York, 33–59.

Burns, J. H., Peterson, J. R., and Stevenson, J. N. (1975) *J. Inorg. Nucl. Chem.,* **37**(3), 743–9.

Burns, R. C. and O'Donnell, T. A. (1977) *Inorg. Nucl. Chem. Lett.,* **13**(12), 657–60.

Bursten, B. E. and Strittmatter, R. J. (1991) *Angew. Chem., Int. Ed. Engl.,* **30**(9), 1069–85.

Burwell, C. C., Bidwell, R. M., Hammond, R. P., Kemme, J. E., and Thamer, B. J. (1962) *Nucl. Sci. Eng.,* **14**, 123–34.

Buscher, C. T., Donohoe, R. J., Mecklenburg, S. L., Berg, J. M., Tait, C. D., Huchton, K. M., and Morris, D. E. (1999) *Appl. Spectrosc.,* **53**(8), 943–53.

Buyers, W. J. L. and Holden, T. M. (1985) in *Handbook on the Physics and Chemistry of Actinides,* vol. 2, (eds. A. J. Freeman and G. H. Lander), North-Holland, Amsterdam, 239 pp.

Bychkov, A. V. and Skiba, O. V. (1999) Review of Non-aqueous Nuclear Fuel Reprocessing and Separation Methods, in *Chemical Separation Technologies and Related Methods of Nuclear Waste Management* (eds. G. R. Choppin and M. K. Khankhasayev), Kluwer Academic Publishers, Boston, MA, pp. 71–98.

Calder, C. A., Draney, E. C., and Wilcox, W. W. (1981) *J. Nucl. Mater.,* **97**, 126–36.

Campbell, G. M., Kent, R. A., and Leary, J. A. (1970) *Plutonium 1970 and Other Actinides, Proc. Fourth Int. Conf. on Plutonium and Other Actinides,* (ed. W. N. Miner), Santa Fe, NM, Oct. 5–9, 1970 Metallurgical Society of AIME, New York, 781 pp.

Cantrell, K. J. (1988) *Polyhedron,* **7**(7), 573–4.

Capdevila, H. and Vitorge, P. (1995) *Radiochim. Acta,* **68**(1), 51–62.

Capdevila, H. and Vitorge, P. (1998) *Radiochim. Acta,* **82**, 11–16.

Capdevila, H. and Vitorge, P. (1999) *Czech. J. Phys. Sect. B,* **49**(Suppl. 1, Pt. 2, 13th Radiochemical Conference, 1998, 603–9.

Capdevila, H., Vitorge, P., and Giffaut, E. (1992) *Radiochim. Acta,* **58/59**(Pt. 1), 45–52.

Capdevila, H., Vitorge, P., Giffaut, E., and Delmau, L. (1996) *Radiochim. Acta,* **74**, 93–8.

Capone, F., Colle, Y., Hiernaut, J. P., and Ronchi, C. (1999) *J. Phys. Chem. A,* **103**(50), 10899–906.

Carbajo, J. J., Yoder, G. L., Popov, S. G., and Ivanov, V. K. (2001) *J. Nucl. Mater.,* **299** (3), 181–98.

Carnall, W. T. (1989) *J. Less-Common Met.,* **156**, 221–35.

Carnall, W. T. (1992) *J. Chem. Phys.,* **96**(12), 8713–26.

Carnall, W. T., and Choppin, G. R. (eds.) (1983) *ACS Symp. Ser.*, **216**(Plutonium Chem.), American Chemical Society, Washington, DC. 484 pp.

Carnall, W. T., Liu, G. K., Williams, C. W., and Reid, M. F. (1991) *J. Chem. Phys.,* **95** (10), 7194–203.

Carniglia, S. C. (1953) *Vapor-pressures of Americium Trifluoride and Americium Metal*. Thesis, Report UCRL-2389, University of California, Berkeley, 76 pp.

Carniglia, S. C., and Cunningham, B. B. (1955) *J. Am. Chem. Soc.,* **77**(6), 1451–3.

Carre, D., Laruelle, P., and Besancon, P. (1970) *Cr. Acad. Sci. C Chim.,* **270**(6), 537–9.

Carroll, D. F. (1964) *J. Am. Ceram. Soc.,* **47**(12), 650.

Cassol, A., Di Bernardo, P., Portanova, R., and Magon, L. (1973) *Inorg. Chim. Acta,* **7**, 353.

Cauchetier, P. and Guichard, C. (1973) *Radiochim. Acta,* **19**(3), 137–46.

Cauchetier, P. and Guichard, C. (1975) *J. Inorg. Nucl. Chem.,* **37**(7–8), 1771–8.

Cauchois, Y. and Manescu, I. (1956) *Compt. Rend.,* **242**, 1433–6.

Cauchois, Y., Manescu, I., and Le Berquier, F. (1954) *Compt. Rend.,* **239**, 1780–2.

Cauchois, Y., Bonnelle, C., and Bersuder, L. (1963a) *Compt. Rend.,* **257**(20), 2980–3.

Cauchois, Y., Bonnelle, C., and de Bersuder, L. (1963b) *Compt. Rend.,* **256**, 112–14.

Cefola, M. (1958) *Microchem. J.,* **2**, 205–17.

Chackraburtty, D. M. and Jayadevan, N. C. (1964) *Indian J. Phys.,* **38**(11), 585–6.

Chackraburtty, D. M. and Jayadevan, N. C. (1965) *Acta Crystallogr.,* **18**, 811.

Chackraburtty, D. M., Jayadevan, N. C., and Swaramakrishnan, C. K. (1963) *Acta Crystallogr.,* **16**(Pt. 10), 1060–1.

Chang, Y. A., Chen, S. L., Zhang, F., and Oates, W. A. (2002) Improving Multicomponent Phase Diagram Calculations, in *CALPHAD and Alloy Thermodynamics* (eds. P. E. A. Turchi, A. Gonis and R. D. Shull), TMS-Minerals, Metals & Material Society, Warrendale, PA, 53 pp.

Charvillat, J. P. (1978) *Crystal Chemistry of Transuranium Pnictides*, Report CEA-R-4933, CEA, CEN, Fontenay-aux-Roses, France, 364 pp.

Charvillat, J. P. and Damien, D. (1973) *Inorg. Nucl. Chem. Lett.,* **9**(5), 559–63.

Charvillat, J. P., Damien, D., and Wojakowski, A. (1977) *Rev. Chim. Miner.,* **14**(2), 178–88.

Chebotarev, N. T. and Utkina, O. N. (1975) Relation between Structure and Some Properties of δ-plutonium and γ-uranium Alloys. *Plutonium 1975 and Other Actinides*, *Proc. Fifth Int. Conf.*, Baden-Baden, Germany (eds. H. Blank and R. Lindner), North-Holland Publishing Company, New York, pp. 559–66.

Cheetham, A. K., Fender, B. E. F., Fuess, H., and Wright, A. F. (1976) *Acta Crystallogr. B,* **B32**(1), 94–7.

Chereau, P. and Wadier, J. F. (1973) *J. Nucl. Mater.,* **46**(1), 1–8.

Chereau, P., Dean, G., De Franco, M., and Gerdanian, P. (1977) *J. Chem. Thermodyn.,* **9** (3), 211–19.

Chiarizia, R., Jensen, M. P., Borkowski, M., Ferraro, J. R., Thiyagarajan, P., and Little, K. C. (2003) *Separ. Sci. Technol.,* **38**(12–13), 3313–31.

Chikalla, T. D. (1968) *J. Am. Ceram. Soc.,* **46**(7), 328.

Chikalla, T. D., McNeilly, C. E., and Skavdahl, R. E. (1962) *The Plutonium-Oxygen System*, Report HW-74802, General Electric Company, Hanford Atomic Products Operation, 30 pp.

Chikalla, T. D., McNeilly, C. E., and Skavdahl, R. E. (1964) *J. Nucl. Mater.,* **12**(2), 131–41.

Chipaux, R., Bonnisseau, D., Boge, M., and Larroque, J. (1988) *J. Magn. Magn. Mater.,* **74**(1), 67–73.

Chipaux, R., Larroque, J., and Beauvy, M. (1989) *J. Less-Common Met.,* **153**(1), 1–7.

Chipaux, R., Blaise, A., and Fournier, J. M. (1990) *J. Magn. Magn. Mater.,* **84**(1–2), 132–42.

Choppin, G. R. (1983) *Radiochim. Acta,* **32**(1–3), 43–53.

Choppin, G. R. and Saito, A. (1984) *Radiochim. Acta,* **35**(3), 149–54.

Choppin, G. R. and Wong, P. J. (1998) *Aquat. Geochem.,* **4**(1), 77–101.

Choppin, G. R., Roberts, R. A., and Morse, J. W. (1986) *ACS Symp. Ser.* **305** (Org. Mar. Geochem.), American Chemical Society, Washington, D.C. 382–8.

Christensen, E. L. and Maraman, W. J. (1969) *Plutonium Processing at the Los Alamos Scientific Laboratory*, Report LA-3542, Los Alamos Scientific Laboratory, 85 pp.

Christensen, E. L. and Mullens, L. J. (1952) *Preparation of Anhydrous Plutonium trichloride*, Report LA-1431, Los Alamos Scientific Laboratory, Los Alamos, NM, 8 pp.

Christensen, D. C. and Mullins, L. J. (1983) *ACS Symp. Ser.* **216**(Plutonium Chem.) (eds. W. T. Carnall and G. R. Choppin), American Chemical Society, Washington, DC. pp. 409–31.

Christensen, D. C., Bowersox, D. F., McKerley, B. J., and Nance, R. L. (1988) *Wastes from Plutonium Conversion and Scrap Recovery Operations*, Report LA-11069-MS, Los Alamos National Laboratory, Los Alamos, NM, 96 pp.

Christoph, G. G., Larson, A. C., Eller, P. G., Purson, J. D., Zahrt, J. D., Penneman, R. A., and Rinehart, G. H. (1988) *Acta Crystallogr. B,* **B44**(6), 575–80.

Chudinov, E. G. and Choporov, D., Ya. (1970) *At. Energiya,* **28**(2), 151–3.
Cinader, G., Zamir, D., and Hadari, Z. (1976) *Phys. Rev. B,* **14**(3), 912–20.
Clark, H. K. (1981) *Nucl. Sci. Eng.,* **79**(1), 65–84.
Clark, D. L. (in preparation) Crystal structures of K(18-crown-6)$_2$AnO$_2$Cl$_4$, (An = Np, Pu), Los Alamos National Laboratory, for publication.
Clark, S. B. and Delegard, C. (2002) Plutonium in Concentrated Solutions, in *Advances in Plutonium Chemistry 1967–2000* (ed. D. C. Hoffman), American Nuclear Society, La Grange Park, IL, pp. 118–68.
Clark, D. L., Hobart, D. E., and Neu, M. P. (1995) *Chem. Rev.,* **95**(1), 25–48.
Clark, D. L., Conradson, S. D., Ekberg, S. A., Hess, N. J., Neu, M. P., Palmer, P. D., Runde, W., and Tait, C. D. (1996) *J. Am. Chem. Soc.,* **118**(8), 2089–90.
Clark, D. L., Conradson, S. D., Keogh, D. W., Palmer, P. D., Scott, B. L., and Tait, C. D. (1998) *Inorg. Chem.,* **37**(12), 2893–9.
Clark, D. L., Conradson, S. D., Donohoe, R. J., Keogh, D. W., Morris, D. E., Palmer, P. D., Rogers, R. D., and Tait, C. D. (1999a) *Inorg. Chem.,* **38**(7), 1456–66.
Clark, D. L., Conradson, S. D., Keogh, D. W., Neu, M. P., Palmer, P. D., Runde, W., Scott, B. L., and Tait, C. D. (1999b) *X-ray Absorption and Diffraction Studies of Monomeric Actinide Tetra-, Penta-, and Hexa-Valent Carbonato Complexes*. Speciation, Techniques and Facilities for Radioactive Materials at Synchrotron Light Sources, OECD Nuclear Energy Agency, pp. 121–33.
Clayton, E. D. (1965) *Phys. Today,* **18**(9), 46–8, 50–2.
Cleveland, J. M. (1979) *The Chemistry of Plutonium,* American Nuclear Society, La Grange Park, IL, 680 pp.
Cleveland, J. M. (1980) Section IV: Chemical Processing, in *Plutonium Handbook: A Guide to the Technology,* vol. 2, (ed. O. J. Wick), American Nuclear Society, LaGrange Park, IL, 966 pp.
Cleveland, J. M., Bryan, G. H., Heiple, C. R., and Sironen, R. J. (1974) *J. Am. Chem. Soc.,* **96**(7), 2285–6.
Cleveland, J. M., Bryan, G. H., Heiple, C. R., and Sironen, R. J. (1975) *Nucl. Technol.,* **25**(3), 541–5.
Coffinberry, A. S. and Miner, W. N. (eds.) (1961) *The Metal Plutonium,* University of Chicago Press, Chicago, 446 pp
Coffinberry, A. S. and Waldron, M. B. (1956) Metallurgy and Fuels in *Progress in Nuclear Energy,* (eds. J. P. Howe and H.M. Finniston), ser. V, vol. 1, Pergamon Press, London, pp. 354–410.
Coffinberry, A. S., Schonfeld, F. W., Cramer, E. M., Miner, W. N., Ellinger, F. H., Elliott, R. O., and Struebing, V. O. (1958) *The Physical Metallurgy of Plutonium and its Alloys*. Second United Nations International Conference on the Peaceful Uses of Atomic Energy, Geneva, Switzerland, United Nations, 6, 681 pp.
Cogliati, G., Recrosio, A., and Lanz, R. (1969) *Plutonium Compounds*, (Comitato Nazionale per l'Energia Nucleare) De Patent 1801682, 14 pp.
Cohen, D. (1961a) *J. Inorg. Nucl. Chem.,* **18**, 207–10.
Cohen, D. (1961b) *J. Inorg. Nucl. Chem.,* **18**, 211–18.
Coleman, C. F. and Leuze, R. E. (1978) *J. Tenn. Acad. Sci.,* **53**(3), 102–7.
Colinet, C. (2002) Phase Diagram Calculations: Contribution of *Ab initio* and Cluster Variation Methods, in *CALPHAD and Alloy Thermodynamics.* (eds. P. E. A. Turchi, A. Gonis and R. D. Shull), TMS-Minerals, Metals & Material Society, Warrendale, PA, 21 pp.

Comstock, A. A. (1952) *Measurement of Plutonium Liquid Density*, Report LA-1348, Los Alamos Scientific Laboratory, 23 pp.
Connick, R. E. (1949) *J. Am. Chem. Soc.,* **71**, 1528–33.
Connick, R. E. (1954) Oxidation States, Potentials, Equilibria, and Oxidation–Reduction Reactions of Plutonium, in *The Actinide Elements* (eds. G. T. Seaborg and J. J. Katz), McGraw-Hill, New York, pp. 221–300.
Connick, R. E. and McVey, W. H. (1949) *J. Am. Chem. Soc.,* **71**(5), 1534–42.
Conradson, S. D. (2000) *Los Alamos Science,* **26**(2), 356.
Conradson, S. D. (2003) personal communication, S. S. Hecker, Los Alamos, NM.
Conradson, S. D., Mahamid, I. A., Clark, D. L., Hess, N. J., Hudson, E. A., Neu, M. P., Palmer, P. D., Runde, W. H., and Tait, C. D. (1998) *Polyhedron,* **17**(4), 599–602.
Conradson, S. D., Begg, B. D., Clark, D. L., Den Auwer, C., Espinosa- Faller, F. J., Gordon, P. L., Hess, N. J., Hess, R., Keogh, D. W., Morales, L. A., Neu, M. P., Runde, W., Tait, C. D., Veirs, D. K., and Villella, P. M. (2003) *Inorg. Chem.,* **42**(12), 3715–17.
Conradson, S. D., Abney, K. D., Begg, B. D., Brady, E. D., Clark, D. L., Den Auwer, C., Ding, M., Dorhout, P. K., Espinosa- Faller, F. J., Gordon, P. L., Haire, R. G., Hess, N. J., Hess, R. F., Keogh, D. W., Lander, G. H., Lupinetti, A. J., Morales, L. A., Neu, M. P., Palmer, P. D., Paviet- Hartmann, P., Reilly, S. D., Runde, W. H., Tait, C. D., Veirs, D. K., and Wastin, F. (2004a) *Inorg. Chem.,* **43**(1), 116–31.
Conradson, S. D., Begg, B. D., Clark, D. L., Den Auwer, C., Ding, M., Dorhout, P. K., Espinosa- Faller, F. J., Gordon, P. L., Haire, R. G., Hess, N. J., Hess, R. F., Keogh, D. W., Morales, L. A., Neu, M. P., Paviet- Hartmann, P., Runde, W., Tait, C. D., Veirs, D. K., and Villella, P. M. (2004b) *J. Am. Chem. Soc.,* **126**(41), 13443–58.
Conway, J. G. and Rajnak, K. (1966) *J. Chem. Phys.,* **44**, 348–54.
Coogler, A. L., Craft, R. C., and Tetzlaff, R. N. (1963) *Proc. Conf. on Hot Laboratory Equipment*, vol. 11, pp. 75–87.
Cooper, B. R., Thayamballi, P., Spirlet, J. C., Mueller, W., and Vogt, O. (1983) *Phys. Rev. Lett.,* **51**(26), 2418–21.
Cooper, N. G. and Schecker, J. A. (eds.) (2000) *Los Alamos Science,* Vol. 26, Los Alamos Science, Los Alamos National Laboratory, 493 pp
Coops, M. S., Knighton, J. B., and Mullins, L. J. (1983) *ACS Symp. Ser.* **216**(Plutonium Chem.) (eds. W. T. Carnall and G. R. Choppin), American Chemical Society, Washington, DC. pp. 381–408.
Cope, R. G., Hughes, D. G., Loasby, R. G., and Miller, D. C. (1960) The Plutonium–Ruthenium and Plutonium–Neptunium Binary Phase Diagrams, in *Plutonium 1960,* Grenoble, France (eds. E. Grison, W. B. H. Lord and R. D. Fowler), Cleaver-Hume Publishing, London, 280 pp.
Cordfunke, E. H. P., and Konings, R. J. M., Editors (1990) *Thermochemical Data for Reactor Materials and Fission Products,* North-Holland, Amsterdam, 696 pp.
Cornet, J. A. (1971) *J. Phys. Chem. Solids,* **32**, 1489–506.
Cornet, J. A. and Bouchet, J. M. (1968) *J Nucl. Mater.,* **28**, 303–10.
Costa, P. (1960) *J. Nucl. Mater.,* **2**, 75.
Costanzo, D. A., Biggers, R. E., and Bell, J. T. (1973) *J. Inorg. Nucl. Chem.,* **35**(2), 609–22.
Covert, A. S. and Kolodney, M. (1945) *Protection of Plutonium against Atmospheric Oxidation*, Report LA-314, Los Alamos Scientific Laboratory, 38 pp.

Cowan, G. A. (1976) *Sci. Am.,* **235**(1), 36–47.
Cox, M. and Flett, D. S. (1983) Metal Extractant Chemistry, in *Handbook of Solvent Extraction* (eds. T. C. Lo, M. H. I. Baird, and C. Hanson), Wiley, New York, 980 pp.
Cox, L. E., Martinez, R., Nickel, J. H., Conradson, S. D., and Allen, P. G. (1995) *Phys. Rev. B,* **51**(2), 751–5.
Cox, L. E., Peek, J. M., and Allen, J. W. (1999) *Physica B,* **259–261**, 1147–8.
Cramer, E. M. and Wood, D. H. (1967) *J. Less-Common Met.,* **13**(1), 112–21.
Cramer, E. M., Ellinger, F. H., and Land, C. C. (1960) *Extractive and Physical Metallurgy of Plutonium and its Alloys* (ed. W. D. Wilkinson), Interscience Publishers, New York, 169 pp.
Cramer, E. M., Hawes, L. L., Miner, W. N., and Schonfeld, F. W. (1961) *The Dilatometry and Thermal Analysis of Plutonium Metal,* in *The Metal Plutonium.* (eds. A. S. Coffinberry and W. N. Miner), University of Chicago Press, Chicago, IL, pp. 112–22.
Cremers, T. L., Dworzak, W. R., Brown, W. G., Flamm, B. F., Sampson, T. E., Bronisz, L. E., Nelson, T. O., Bronson, M. C., Colmenares, C. A., and Merrill, R. D. (1995) *Proc. Fifth Int. Conf. on Radioactive Waste Management and Environmental Remediation*, vol. 1, Berlin, Sept. 3–7, 1995, pp. 553–6.
Crisler, L. R. and Eggerman, W. G. (1974) *J. Inorg. Nucl. Chem.,* **36**(6), 1424–6.
Crocker, A. G. (1971) *J. Nucl. Mat.,* **41**(2), 167.
Crocker, H. W. (1961) *Ammonium bifluoride Fusion of Ignited Plutonium dioxide*, Report HW-68655, General Electrical Company, Richland, Washington, 5 pp.
Croff, A. G. (1980) ORIGEN2: *A Revised and Updated Version of the Oak Ridge Isotope Generation and Depletion Code*, Report ORNL-5621, Oak Ridge National Laboratory, 62 pp.
Croff, A. G. (1983) *Nucl. Technol.,* **62**(3), 335–52.
Cromer, D. T. (1975) *Acta Crystallogr.* **B31**, 1760.
Cromer, D. T. (1976) *Acta Crystallogr.* **B32**, 1930.
Cromer, D. T. (1977a) *Acta Crystallogr.* **B33**, 1993.
Cromer, D. T. (1977b) *Acta Crystallogr.* **B33**, 1996.
Cromer, D. T. (1978) *Acta Crystallogr.* **B34**, 913.
Cromer, D. T. (1979a) *Acta Crystallogr.* **B35**, 14.
Cromer, D. T. (1979b) *Acta Crystallogr.* **B35**, 1945.
Cromer, D. T. and Larson, A. C. (1960) *Acta Crystallogr.,* **13**(11), 909–12.
Cromer, D. T. and Larson, A. C. (1975) *Acta Crystallogr.* **B31**, 1758.
Cromer, D. T. and Larson, A. C. (1977) *Acta Crystallogr.* **B33**, 2620.
Cromer, D. T. and Olsen, C. E. (1959) *Acta Crystallogr.,* **12**(9), 689–94.
Cromer, D. T. and Roof, R. B. (1959) *Acta Crystallogr.,* **12**(11), 942–3.
Cromer, D. T., Larson, A. C., and Roof, R. B. Jr., (1964) *Acta Crystallogr.,* **17**(8), 947–50.
Cromer, D. T., Larson, A. C., and Roof, R. B. (1973) *Acta Crystallogr.* **B29**, 564–7.
Cromer, D. T., Larson, A. C., and Roof, R. B. (1975) *Acta Crystallogr.* **B31**, 1756.
Cunningham, B. B. (1949) *Nucleonics,* **5**(No. 5), 62–85.
Cunningham, B. B. (1954) Preparation and Properties of the Compounds of Plutonium, in *The Actinide Elements* (eds. G. T. Seaborg and J. J. Katz), McGraw-Hill, New York, pp. 371–434.
Cunningham, B. B. and Werner, L. B. (1949a) *J. Am. Chem. Soc.,* **71**, 1521–8.
Cunningham, B. B. and Werner, L. B. (1949b) The First Isolation of a Synthetic Element 94Pu239, in *Natl. Nucl. Energy Serv.*, Div IV **14B**(Transuranium Elements,

Pt. I) (eds. G. T. Seaborg, J. J. Katz and W. M. Manning), McGraw-Hill, New York, 51–78.

Curtis, D., Fabryka- Martin, J., Dixon, P., and Cramer, J. (1999) *Geochim. Cosmochim. Acta,* **63**(2), 275–85.

Czerwinski, K. and Kim, J.-I. (1997) *Mater. Res. Soc. Symp. Proc.,* **465**(Scientific Basis for Nuclear Waste Management XX), 743–50.

Dacheux, N., Podor, R., Brandel, V. and Genet, C. R. (1998) *J. Nucl. Mater.,* **252,** 179–86.

Dai, X., Savrasov, S. Y., Kotliar, G., Migliori, A., Ledbetter, H., and Abrahams, E. (2003) *Science,* **300**(5621), 953–5.

Dalton, J. T. and Griffin, R. M. (1964) *The Thorium–Plutonium–Carbon System*, Report AERE-R-4742, Atomic Energy Reseach Establishment, Harwell, UK, 20 pp.

Dalton, J. T., Potter, P. E., and Shaw, J. L. (1967) *Plutonium 1965, Proc. Third Int. Conf.*, pp. 775–805.

Damien, D. (1973) *Inorg. Nucl. Chem. Lett.,* **9**(4), 453–6.

Damien, D. (1976) *Synthesis and Crystal Chemistry of Transuranium Element Chalcogenides. Contribution to the Study of the 5f Electron Localization*, Report CEA-R-4783, CEN, CEA, Fontenay-aux-Roses, France, 161 pp.

Damien, D. and De Novion, C. H. (1981) *J. Nucl. Mater.,* **100**(1–3), 167–77.

Damien, D., de Novion, C. H., and Thevenin, T. (1986) Crystal Chemistry of Actinide Chalcogenides and Pnictides, in *Handbook on the Physics and Chemistry of the Actinides* (eds. A. J. Freeman and C. Keller), Elsevier Science, Amsterdam, pp. 39–96.

Danis, J. A., Lin, M. R., Scott, B. L., Eichhorn, B. W., and Runde, W. H. (2001) *Inorg. Chem.,* **40**(14), 3389–94.

Darken, L. S. and Gurry, R. W. (1953) *Physical Chemistry of Metals,* McGraw-Hill, New York, 535 pp.

David, S. J. and Kim, K. C. (1988) *J. Chem. Phys.,* **89**(4), 1780–6.

Davidson, N. R. and Katz, J. J. (1958) *Plutonium halides*. US Patent no. 2859 097. (U.S. Atomic Energy Commission)

Davidson, N. R., Hagemann, F., Hyde, E. K., Katz, J. J., and Sheft, I. (1949) The Preparation and Properties of Plutonium Tribromide and Oxybromide. *Natl. Nucl. Energy Ser.*, Div IV **14B**(Transuranium Element, Pt. I) (eds. G. T. Seaborg, J. J. Katz and W. M. Manning), McGraw Hill, New York, 759–74.

Dawson, J. K. and Elliott, R. M. (1953) *The Thermogravimetry of Some Plutonium Compounds*, Report AERE-C/R-1207, Great Britain Atomic Energy Research Establishment, 20 pp.

Dawson, J. K. and Truswell, A. E. (1951) *The Preparation of Plutonium Trifluoride and Tetrafluoride by the Use of Hydrogen Fluoride*, Report AERE-C/R-662, Great Britain Atomic Energy Research Establishment, 6 pp.

Dawson, J. K., Mandleberg, C. J., and Davies, D. (1951) *J. Chem. Soc.*, 2047–50.

Dawson, J. K., D'Eye, R. W. N., and Truswell, A. E. (1954a) *J. Chem. Soc., Abstracts*: 3922–9.

Dawson, J. K., Elliott, R. M., Hurst, R., and Truswell, A. E. (1954b) *J. Chem. Soc.*, 558–64.

Dayton, R. W. and Tipton, C. R., Jr (1961) *Progress Relating to Civilian Applications during June 1961*, Report BMI-1524(Del.), Battelle Memorial Institute, 104 pp.

De Alleluia, I. B., Berndt, U., and Keller, C. (1983) *Rev. Chim. Miner.,* **20**(4–5), 441–8.

De Winter, F., Stapfer, G., and Medina, E. (1999) *The Design of a Nuclear Power Supply with a 50 Year Life Expectancy: the JPL Voyager's SiGe MHW RTG. Proc. 34th Intersociety Energy Conversion Engineering Conf.*, pp. 433–40.

Dean, G. and Boivineau, J. C. (1970b) *Plutonium 1970 and Other Actinides, Proc. Fourth Int. Conf. on Plutonium and Other Actinides*, Santa Fe, NM, Oct. 5–9, 1970 (ed. W. N. Miner), AIME, New York.

Dean, G., Boivineau, J. C., Chereau, P., and Marcon, J. P. (1970a) *Plutonium 1970 and Other Actinides, Proc. Fourth Int. Conf. on Plutonium and Other Actinides*, Santa Fe, NM, Oct. 5–9, 1970 (ed. W. N. Miner), AIME, New York, 753 pp.

Deaton, R. L. and Wiedenheft, C. J. (1973) *J. Inorg. Nucl. Chem.,* **35**(2), 649–50.

Deloffre, P. (1997) *Etude de la Stabilite de la Phase Delta des Alliages de Plutonium Obtenue par Additions d'elements Deltagenes,* Thesis, Universite de Paris-Sud, Department d'Etudes et Technologies Nucleaires, Paris, 152 pp.

Den Auwer, C., Revel, R., Charbonnel, M. C., Presson, M. T., Conradson, S. D., Simoni, E., Le Du, J. F., and Madic, C. (1999) *J. Synchrotron Radiat.,* **6**(2), 101–04.

Denning, R. G. (1991) *Eur. J. Solid State Inorg.,* **28**(Suppl.), 33–45.

Denning, R. G. (1992) *Structure and Bonding,* **79**(Complexes, Clusters Cryst. Chem.), 215–76.

Denning, R. G. (1999) *Spectrochim. Acta. A,* **55**(9), 1757–65.

Denning, R. G., Green, J. C., Hutchings, T. E., Dallera, C., Tagliaferri, A., Giarda, K., Brookes, N. B., and Braicovich, L. (2002) *J. Chem. Phys.,* **117**(17), 8008–20.

Denotkina, R. G., Moskvin, A. I., and Shevchenko, V. B. (1960) *Russ. J. Inorg. Chem.,* **5**, 387–9.

Denotkina, R. G., Shevchenko, V. B., and Moskvin, A. I. (1965) *Russ. J. Inorg. Chem.,* **10**, 1333–35.

Denotkina, R. G., and Shevchenko, V. B. (1967) *Russ. J. Inorg. Chem.,* **12**, 42–45.

Deron, S. and Vesnovskii, S. (1999) *Nucl. Instrum. Meth. A,* **438**(1), 20–2.

Dewey, H. J., Barefield, II, J. E., and Rice, W. W. (1986) *J. Chem. Phys.,* **84**(2), 684–91.

Dixon, P., Curtis, D. B., Musgrave, J., Roensch, F., Roach, J., and Rokop, D. (1997) *Anal. Chem.,* **69**(9), 1692–9.

Dmitriev, S. N., Oganessian, Y. T., Buklanov, G. V., Kharitinov, Y. P., Novgorodov, A. F., Salamatin, L. I., Starodub, G. Y., Shishkin, S. V., Yushkevich, Y. V., and Newton, D. (1993) *Appl. Radiat. Isot.,* **44**(8), 1097–100.

Dmitriev, S. N., Oganessian, Y. T., Starodub, G. Y., Shishkin, S. V., Bulanov, G. V., Kharitonov, Y. P., Novgorodov, A. F., Yushkevich, Y. V., Newton, D., and Talbot, R. J. (1995) *Appl. Radiat. Isot.,* **46**(5), 307–9.

Dmitriev, S. N., Zaitseva, N. G., Starodub, G. Y., Maslov, O. D., Shishkin, S. V., Shishkina, T. V., Buklanov, G. V., and Sabelnikov, A. V. (1997) *Nucl. Instrum. Methods Phys. Res., Sect. A,* **397**(1), 125–30.

Dodgen, H. W., Chrisney, J., and Rollefson, G. K. (1944) *The Spectrum of Plutonium*, Report ANL-JJK-14B-24, Argonne National Laboratory, 17 pp.

Dodgen, H. W., Chrisney, J., and Rollefson, G. K. (1949) *Natl. Nucl. Energy Ser.*, Div IV **14B**(Transuranium Elements, Pt. II) (eds. G. T. Seaborg, J. J. Katz and W. M. Manning), McGraw Hill, New York, 1327–36.

DOE (1987) *Atomic Power in Space: A History*, Report DOE/NE/32117-H1; DE87010618 (Mar. 1987), 189 pp.

Domanov, V. P., Buklanov, G. V., and Lobanov, Y. V. (2002) *Radiochemistry,* **44**(2), 114–20.

Dormeval, M. (2001) *Structure Electronique d'alliages Pu-Ce(-Ga) et Pu-Am(-Ga) Stabilises en Phase Delta*, Thesis, Chimie - Physique, Dijon, L'Universite de Bourgogne, 194 pp.
Dormeval, M., Baclet, N., and Fournier, J. M. (2000) *AIP Conf. Proc.* **532**(Plutonium Futures–The Science) (eds. K. K. S. Pillay and K. C. Kim), p. 33.
Dormeval, M., Baclet, N., Valot, C., Rofidal, P., and Fournier, J. M. (2003) *J. Alloys Compd.,* **350**(1–2), 86–94.
Douglass, R. M. (1962) *Acta Cryst.,* **15**, 505–6.
Drummond, J. L. and Welch, G. A. (1957) *J. Chem. Soc., Abstracts*: 4781–5.
Drummond, J. L., McDonald, B. J., Ockenden, H. M., and Welch, G. A. (1957) *J. Chem. Soc.*, 4785–9.
Duff, M. C., Newville, M., Hunter, D. B., Bertsch, P. M., Sutton, S. R., Triay, I. R., Vaniman, D. T., Eng, P., and Rivers, M. L. (1999) *J. Synch. Rad.,* **6**(3), 350–2.
Dunlap, B. D. and Kalvius, G. M. (1985) in *Handbook on the Physics and Chemistry of Actinides,* vol. 2, (eds. A. J. Freeman and G. H. Lander), North-Holland, Amsterdam, 329 pp.
Dupuy, M. and Calais, D. (1968) *T. Am. I. Min. Met. Eng.,* **242**, 1679.
Durakiewicz, T., Joyce, J. J., Lander, G. H., Olson, C. G., Butterfield, M. T., Guziewicz, E., Arko, A. J., Morales, L., Rebizant, J., Mattenberger, K., and Vogt, O. (2004) *Phys. Rev. B,* **70**(20), 205103/1–205103/11.
Duriez, C., Alessandri, J. P., Gervais, T., and Philipponneau, Y. (2000) *J. Nucl. Mater.,* **277**(2,3), 143–58.
Dwyer, O. E., Eshaya, A. M., and Hill, F. B. (1959) *Continuous Removal of Fission Products from Uranium-Bismuth Fuels*, *Proc. Second Int. Conf. on the Peaceful Uses of Atomic Energy*, 1958, Geneva, United Nations, New York, 17, pp. 428–37.
Dyall, K. G. (1999) *Mol. Phys.,* **96**(4), 511–18.
Eberle, S. H. and Wade, U. (1970) *J. Inorg. Nucl. Chem.,* **32**, 109.
Edelstein, N. M. (1991) *Eur. J. Solid State Inorg. Chem.,* **28**(Suppl.), 47–55.
Edwards, G. R., Tate, R. E., and Hakkila, E. A. (1968) *J. Nucl. Mater.,* **25**(3), 304–9.
Ehrhart, P., Jung, P., Schultz, H., and Ullmaier, H. (1991) *Atomic Defects in Metals,* vol. 25, (ed. H. Ullmaier), Springer-Verlag, Berlin, 437 pp.
Eichelsberger, J. F. (1961) *Mound Laboratory Progress Report for December 1960*, Report MLM-1108, Mound Laboratory, 16 pp.
Eick, H. A. (1965) *Inorg. Chem.,* **4**(8), 1237–9.
Eisenberg, D. C., Streitwieser, A., and Kot, W. K. (1990) *Inorg. Chem.,* **29**(1), 10–14.
Eller, P. G., Kinkead, S. A., and Nielsen, J. B. (1992) in *Transuranium Elements: A Half Century* (eds. L. R. Morss and J. Fuger), 202–12.
Ellinger, F. H. (1956) *J. Metals,* **8**(AIME Trans. 206), 1256–9.
Ellinger, F. H. (1961) A Review of the Intermetallic Compounds of Plutonium, in *The Metal Plutonium* (eds. A. S. Coffinberry and W. N. Miner), University of Chicago Press, Chicago.
Ellinger, F. H. and Land, C. C. (1968) *J. Nucl. Mater.,* **28**(3), 291–6.
Ellinger, F. H. and Zachariasen, W. H. (1954) *J. Phys. Chem.,* **58**, 405–8.
Ellinger, F. H. and Zachariasen, W. H. (1965) *Acta Crystallogr.,* **19**, 281–3.
Ellinger, F. H., Elliott, R. O., and Cramer, E. M. (1959) *J. Nucl. Mater.,* **1**(3), 233–43.
Ellinger, F. H., Land, C. C., and Miner, W. N. (1962a) *J. Nucl. Mater.,* **1**, 115.
Ellinger, F. H., Land, C. C., and Miner, W. N. (1962b) *J. Nucl. Mater.,* **5**(2), 165–72.

Ellinger, F. H., Land, C. C., and Struebing, V. O. (1964) *J. Nucl. Mater.,* **12**(2), 226–36.
Ellinger, F. H., Land, C. C., and Johnson, K. A. (1965) *Trans. Metall. Soc. AIME,* **233** (7), 1252–8.
Ellinger, F. H., Johnson, K. A., and Struebing, V. O. (1966) *J. Nucl. Mater.,* **20**(1), 83–6.
Ellinger, F. H., Land, C. C., and Johnson, K. A. (1967) *Trans. Metall. Soc. AIME,* **239**(6), 895.
Ellinger, F. H., Land, C. C., and Johnson, K. A., unpublished work, Los Alamos Scientific Laboratory.
Ellinger, F. H., Land, C. C., and Johnson, K. A. (1968a) *J. Nucl. Mater.,* **29**(2), 178–83.
Ellinger, F. H., Miner, W. N., O'Boyle, D. R., and Schonfeld, F. W. (1968b) *Constitution of Plutonium Alloys*, Report LA-3870, Los Alamos Scientific Laboratory, 185 pp.
Elliott, R. O. (1980) personal communication, S. S. Hecker, Los Alamos, NM.
Elliott, R. O. and Giessen, B. C. (1975) Splat Cooling, in *Plutonium and Other Actinides* (eds. H. Blank and R. Lindner), North-Holland, Amsterdam, p. 47.
Elliott, R. O. and Larson, A. C. (1961) Delta-prime Plutonium, in *The Metal Plutonium* (eds. A. S. Coffinberry and W. N. Miner), University of Chicago Press, Chicago, pp. 265–80.
Elliott, R. O., Gschneidner, K. A., and Kempter, C. P. (1960) Thermal Expansion. *Plutonium 1960, Proc. Second Int. Conf. on Plutonium and Other Actinides* (eds. E. Grison, W. B. H. Lord, and R. D. Fowler), Cleaver-Hume Press, London, 142 pp.
Elliott, R. O., Olsen, C. E., and Louie, J. (1962) *J. Phys. Chem. Solids,* **23**(AUG), 1029–44.
Engel, T. K. (1969) *J. Nucl. Mater.,* **31**(2), 211–14.
Engerer, H. (1967) *Phase Equilibrium in the Systems* ThO_2–$HoO_{1.5}$($LuO_{1.5}$, $ScO_{1.5}$) *and* $HoO_{1.5}$–UO_2, UO_{2+x}, NpO_{2+x}, PuO_{2+x}), Thesis, Report KFK-597, Kernforschungszentrum, Karlsruhe, Federal Republic of Germany, 59 pp.
Enriquez, A. E., Matonic, J. H., Scott, B. L., and Neu, M. P. (2003) *Chem. Commun.*, (15), 1892–3.
Ephritikhine, M. (1992) *New J. Chem.,* **16**(4), 451–69.
Erdmann, B. and Keller, C. (1973) *J. Solid State Chem.,* **7**(1), 40–8.
Erdmann, N., Nunnemann, M., Eberhardt, K., Herrmann, G., Huber, G., Kohler, S., Kratz, J. V., Passler, G., Peterson, J. R., Trautmann, N., and Waldek, A. (1998) *J. Alloys Compd.,* **271–273**, 837–40.
Erilov, P. E., Titov, V. V., Serik, V. F., and Sokolov, V. B. (2002) *Atomic Energy (Translation of Atomnaya Energiya),* **92**(1), 57–63.
Etter, D. E., Martin, D. B., Roesch, D. L., Hudgens, C. R., and Tucker, P. A. (1965) *Trans. Metall. Soc. AIME,* **233**(11), 2011–13.
Evans, J. S. O., Mary, T. A., Vogt, T., Subramanian, M. A., and Sleight, A. W. (1996) *Chem. Mater.,* **8**, 2809.
Fardy, J. J. and Buchanan, J. M. (1976) *J. Inorg. Nucl. Chem.,* **38**(3), 579–83.
Faris, J. P. and Buchanan, R. F. (1964) *Anal. Chem.,* **36**(6), 1157.
Farkas, M. S. (1966) *Preparation and Heat Content of Uranium-, Plutonium-, and Neptunium-Containing Microspheres for Use as Intrinsic Thermocouple Flux Probes*, Report BMI-X-10175, Battelle Memorial Institute, Columbus, OH, 19 pp.
Faure, P., Deslandes, B., Bazin, D., Tailland, C., Doukhan, R., Fournier, J. M., and Falanga, A. (1996) *J. Alloys Compd.,* **244**(1–2), 131–9.

Faust, L. G., Brackenbush, L. W., Heid, K. R., Herrington, W. N., Kenoyer, J. L., Munson, L. F., Munson, L. H., Selby, J. M., Soldat, K. L., Stoetzel, G. A., Traub, R. J. and Vallario, E. J. (1988) *Health Physics Manual of Good Practices for Plutonium Facilities*, Report PNL-6534, Pacific Northwest Laboratory, 251 pp.

Favas, M. C., Kepert, D. L., Patrick, J. M., and White, A. H. (1983) *J. Chem. Soc. Dalton Trans.*, (**3**), 571–81.

Fedosseev, A. M., Budantseva, N. A., Grigoriev, M. S., Bessonov, A. A., Astafurova, L. N., Lapitskaya, T. S., and Krupa, J. C. (1999) *Radiochim. Acta,* **86**(1–2), 17–22.

Feldman, C. (1960) *Anal. Chem.,* **32**, 1727–8.

Felmy, A. R., Rai, D., Schramke, J. A., and Ryan, J. L. (1989) *Radiochim. Acta,* **48**(1–2), 29–35.

Ferro, R. and Cacciamani, G. (2002) Chemical Criteria in the Assessment of Alloy Constitutional Properties, in *CALPHAD and Alloy Thermodynamics* (eds. P. E. A. Turchi, A. Gonis and R. D. Shull), TMS, Warrendale, PA, 177 pp.

Filin, V. M., Bulkin, V. I., Timofeeva, L. F., and Polyakova, M. Y. (1989) *Sov. Radiochem.,* **30**, 683–721.

Finch, C. B. and Clark, G. W. (1972) *J. Cryst. Growth,* **12**(2), 181–2.

Fink, J. K. (1982) *Int. J. Thermophys.,* **3**(2), 165–200.

Fink, J. K. (2000) *J. Nucl. Mater.,* **279**(1), 1–18.

Firestone, R. B., Shirley, V. S., Baglin, C. M., Chu, S. Y. F., and Zipkin, J. (eds.) (1996) *Table of Isotopes,* John Wiley & Sons, New York.

Firestone, R. B., Shirley, V. S., Baglin, C. M., Chu, S. Y. F., and Zipkin, J. (eds.) (1998) *Table of Isotopes,* 8th edn, John Wiley & Sons, New York.

Fischer, R. D. (1963) *Theor. Chim. Acta,* **1**(5), 418–31.

Fischer, R., Werner, G.-D., Lehmann, T., Hoffmann, G. and Weigel, F. (1981) *J. Less-Comm. Met.,* **80**, 121–32.

Fisher, E. S. (1974) Ultrasonic Waves in Actinide Metals and Compounds, in *The Actinides: Electronic Structure and Related Properties,* part II, vol. 2 (eds. A. J. Freeman and J. B. Darby), Academic Press, New York, pp. 289–343.

Flahaut, J. (1979) in *Handbook on the Physics and Chemistry of Rare Earths* (eds. K. A. Gschneidner, Jr., and L. Eyring), North-Holland, Amsterdam, p. 2.

Flamm, B. F., Isom, G. M., and Nelson, T. O. (1998) *Proc. Third Topical Meeting on DOE Spent Nuclear Fuel and Fissile Materials Management*, vol. 1, Sept. 8–11, 1998, Charleston, SC, pp. 191–2.

Fleming, W. H. and Thode, H. G. (1953a) *Phys. Rev.,* **90**, 857–8.

Fleming, W. H. and Thode, H. G. (1953b) *Phys. Rev.,* **92**, 378–82.

Fletcher, J. M., Hyde, K. R., and Roberts, F. P. (1967) Germany Patent no. 108 4338.

Florin, A. E. (1950a) *Plutonium Hexafluoride, Plutonium (VI) Oxyfluoride: Preparation, Identification, and Some Properties*, Report LAMS-1118, Los Alamos Scientific Laboratory, Los Alamos, NM, US, 24 pp.

Florin, A. E. (1950b) *Plutonium Hexafluoride: Second Report on the Preparation and Properties*, Report LA-1168, Los Alamos Scientific Laboratory, 18 pp.

Florin, A. E. (1953) *Thermodynamic Properties of Plutonium Hexafluoride: A Preliminary Report*, Report LAMS-1587, Los Alamos Scientific Laboratory, 9 pp.

Florin, A. E. and Tannenbaum, I. R. (1952) *An Improved Apparatus for the Preparation of Plutonium Hexafluoride*, Report LA-1580, Los Alamos Scientific Laboratory, 12 pp.

Florin, A. E., Tannenbaum, I. R., and Lemons, J. F. (1956) *J. Inorg. Nucl. Chem.,* **2**, 368–79.

Flotow, H. E. and Tetenbaum, M. (1981) *J. Chem. Phys.,* **74**(9), 5269–77.

Flotow, H. E., Osborne, D. W., Fried, S. M., and Malm, J. G. (1976) *J. Chem. Phys.,* **65**(3), 1124–9.

Flotow, H. E., Haschke, J. M., and Yamauchi, S. (1984) *The Chemical Thermodynamics of Actinide Elements and Compounds,* part 9, *The Actinide Hydrides,* International Atomic Energy Agency, Vienna, Austria, 115 pp.

Fomin, V. V., Reznikova, V. E., and Zaitseva, L. L. (1958) *Zh. Neorg. Khim.,* **3**, 2231–5.

Forbes, R. L., Fuhrman, N., Andersen, J. C., and Taylor, K. M. (1966) *Uranium-Plutonium Monoxides*, Report UNC-5144, United Nuclear Corporation, Elmsford, New York, 81 pp.

Fortner, J. A., Kropf, A. J., Finch, R. J., Bakel, A. J., Hash, M. C., and Chamberlain, D. B. (2002) *J. Nucl. Mater.,* **304**(1), 56–62.

Fournier, J. M. and Troc, R. (1985) in *Handbook on the Physics and Chemistry of Actinides,* vol. 2 (eds. A. J. Freeman and G. H. Lander), North-Holland, Amsterdam, 29 pp.

Fournier, J. M., Pleska, E., Chiapusio, J., Rossat- Mignod, J., Rebizant, J., Spirlet, J. C., and Vogt, O. (1990) *Physica B,* **163**(1–3), 493–5.

Fox, R. V. and Mincher, B. J. (2002) *ACS Symp. Ser.* **860**(Separ. Processes Using Supercritical Carbon Dioxide) (eds. A. S. Gopalan, C. M. Wai and H. K. Jacobs), American Chemical Society, Washington, DC, pp. 36–49.

Fradin, F. Y. (1970) *Plutonium 1970 and Other Actinides, Proc. Fourth Int. Conf. on Plutonium and Other Actinides*, Santa Fe, NM, Oct. 5–9, 1970 (eds. W. N. Miner), New York, 264 pp.

Fred, M., Blaise, J., and Gutmacher, R. (1966) *J. Opt. Soc. Am.,* **56**, 1416A.

Freedberg, N. A., Antonelli, D., Bloch, L., and Rosenfeld, T. (1992) *Pacing Clin. Electrophysiol.,* **15**(11), 1639–41.

Freeman, A. J. and J. B. Darby, J. (eds.) (1974) *The Actinides, Electronic Structure and Related Properties*, Academic Press, New York.

Fried, S. and Davidson, N. R. (1949) *Nat'l. Nucl. Energy Ser.,* Div IV **14B**(Transuranium Elements, Pt. I) (eds. G. T. Seaborg, J. J. Katz and W. M. Manning), McGraw-Hill, New York, pp. 784–92.

Fried, S., Westrum, Jr, E. F., Baumbach, H. L., and Kirk, P. L. (1958) *J. Inorg. Nucl. Chem.,* **5**, 182–9.

Frolov, A. A., Andreichuk, N. N., Ratmanov, K. V., Frolova, I. M., and Vasiliev, V. Y. (1990) *J. Radioanal. Nucl. Ch. Le.,* **143**(2), 433–44.

Fuger, J. (1992) *Radiochim. Acta,* **58–59**(1), 81–91.

Fuger, J. and Cunningham, B. B. (1963) *J. Inorg. Nucl. Chem.,* **25**(11), 1423–9.

Fuger, J., Oetting, F. L., Hubbard, W. N., and Parker, V. B. (1983) *Chemical Thermodynamics of Actinide Elements and Compounds. Pt. 8. The Actinide Halides.* IAEA, Vienna, Austria, 267 pp.

Fujiwara, K., Yamana, H., Fujii, T., and Moriyama, H. (2001) *Genshiryoku Bakkuendo Kenkyu (J. Nucl. Fuel Cycle Environ. (Japan)),* **7**(1), 17–23.

Fulton, R. B. and Newton, T. W. (1970) *J. Phys. Chem.,* **74**(8), 1661–9.

Gal, J., Hadari, Z., Bauminger, E. R., and Ofer, S. (1972) *Phys. Lett. B,* **41**(1), 53–4.

Galasso, F. S. (1968) *Structure, Properties, and Preparation of Perovskite-type Compounds,* Pergamon Press, Oxford, England.

Ganz, M., Barth, H., Fuest, M., Molzahn, D., and Brandt, R. (1991) *Radiochim. Acta,* **52–53**(Pt. 2), 403–4.
Gardner, H. (1965) Mechanical Properties *Plutonium 1965, Proc. Third Int. Conf.* (eds. A. E. Kay and M. B. Waldron), Chapman and Hall, London, 118 pp.
Gardner, H. R. (1980) Mechanical Properties *The Plutonium Handbook,* vol. 1, (ed. O. J. Wick), American Nuclear Society, La Grange Park, IL, pp. 59–100.
Gardner, E. R., Markin, T. L., and Street, R. S. (1965) *J. Inorg. Nucl. Chem.,* **27**(3), 541–51.
Garner, C. S. (1950) *Los Alamos Technical Series, Chemistry of Uranium and Plutonium*, Report LA-1100, Los Alamos Scientific Laboratory, Los Alamos, NM, pp. 110–16.
Garner, C. S., Bonner, N. A., and Seaborg, G. T. (1948) *J. Am. Chem. Soc.,* **70**, 3453–4.
Gel'man, A. D. and Zaitsev, L. M. (1958) *Zh. Neorg. Khim.,* **3**, 1304–11.
Gel'man, A. D. and Zaitseva, V. P. (1964) *Dokl. Akad. Nauk SSSR,* **157**(6), 1403–5.
Gel'man, A. D. and Zaitseva, V. P. (1965a) *Radiokhimiya,* **7**(1), 49–55.
Gel'man, A. D. and Zaitseva, V. P. (1965b) *Radiokhimiya,* **7**(1), 56–68.
Gendre, R. (1962) *Preparation of Plutonium hexafluoride: Recovery of Plutonium from Waste Dross*, Report CEA-2161, Commissariat a l'Energie Atomique, 109 pp.
Gens, T. A. (1961) *Nucl. Sci. Eng.,* **9**(4), 488–94.
Gens, R., Fuger, J., Morss, L. R., and Williams, C. W. (1985) *J. Chem.Thermodyn.,* **17**(6), 561–73.
Gevantman, L. H. and Kraus, K. A. (1949) *Natl. Nucl. Energy Ser.*, Div IV, **14B** (Transuranium Elements, Pt. I), (eds. G. T. Seaborg, J. J. Katz, and W. M. Manning), pp. 500–18.
Gibney, R. B. and Sandenaw, T. A. (1954) *Electrical Resistivity of Plutonium Metal and of Gallium–Plutonium Alloys over the Temperature Range of 26 K to ~773 K*, Report LA-1883, Los Alamos Scientific Laboratory, 26 pp.
Giessen, B. C., Elliott, R. O., and Struebing, V. O. (1975) *Mat. Sci. Eng.,* **18**(2), 239–43.
Gilman, W. S. (1965) *A Review of the Dissolution of Plutonium Dioxide*, Report MLM-1264, Mound Laboratory, Miamisburg, OH, 12 pp.
Gilman, W. S. (1968) *Review of the Dissolution of Plutonium Dioxide. II*, Report MLM-1513, Mound Laboratory, Miamisburg, OH, 12 pp.
Glazyrin, S. A., Rodchenko, P. Y., and Sokina, L. P. (1989) *Radiokhimiya,* **31**(4), 48–52 (pp 407–410 in English translation).
Glushko, V. P. (ed.) (1982) *Thermodynamic Properties of Individual Substances,* vol. 4, Nauka, Moscow, 623 pp.
Goldberg, A. and Massalski, T. (1970a) *Phase Transformations in the Actinides, Proc. Fourth Int. Conf. on Plutonium and Other Actinides,* Santa Fe, NM (ed. W. N. Miner), The Metallurgical Society of AIME, pp. 875–945.
Goldberg, A., Rose, R. L., and Matlock, D. K. (1970b) *The Delta and Epsilon Thermal Expansion Coefficients and the Delta-to-epsilon Contraction for Some Plutonium-rich Alloys, Proc. Fourth Int. Conf. on Plutonium and Other Actinides 1970, vol. 2,* (ed. W. N. Miner), The Metallurgical Society of AIME, Warrendale, PA, pp. 1056–68.
Gomez Marin, E. (1997) *Etude du Comportement de la Resistivite Electrique des Mono-Chalcogenures de Plutonium et des Alliages de Plutonium et Americium*, Thesis, l'Universite Grenoble, Grenoble.
Gorbunov, S. I. and Seleznev, A. G. (2001) *Radiochemistry,* **43**(2), 111–117.
Gordon, G. and Taube, H. (1961) *J. Inorg. Nucl. Chem.,* **19**, 189–91.

Gordon, J. E., Hall, R. O., Lee, J. A., and Mortimer, M. J. (1976) *Proc. R. Soc. London, Ser. A,* **351**(1665), 179–96.
Gorum, A. E. (1957) *Acta Crystallogr.,* **10**, 144.
Gouder, T., Wastin, F., Rebizant, J., and Havela, L. (2000) *Phys. Rev. Lett.,* **84**(15), 3378–81.
Gouder, T., Havela, L., Wastin, F., and Rebizant, J. (2002) *J. Nucl. Sci. Tech.*, (Suppl. 3), 49–55.
Gouder, T., (2005) *XPS studies of PuH_3 thin films, personal communication*, D. L. Clark, Los Alamos, NM.
Grachev, A. F., Maershin, A. A., Skiba, O. V., Tsykanov, V. A., Bychkov, A. V., Kormilitsyn, M. V., and Sokolvskii, Y. S. (2004) *At. Energ.,* **96**(5), 320–6.
Graf, W. L. (1994) *Plutonium and the Rio Grande: Environmental Change and Contamination in the Nuclear Age,* Oxford University Press, New York, 329 pp.
Green, J. L. and Leary, J. A. (1970) *J. Appl. Phys.,* **41**(13), 5121–4.
Green, D. W. and Reedy, G. T. (1978a) *J. Chem. Phys.,* **69**(2), 552–5.
Green, D. W. and Reedy, G. T. (1978b) *J. Chem. Phys.,* **69**(2), 544–51.
Green, D. W., Fink, J. K., and Leibowitz, L. (1983) *ACS Symp. Ser.* **216**(Plutonium Chem.) (eds. W. T. Carnall and G. R. Choppin), American Chemical Society, Washington, DC, pp. 123–43.
Greenwood, N. N. and Earnshaw, A. (1997) *Chemistry of the Elements,* Butterworth-Heinemann, Oxford, England, 1341 pp.
Grenthe, I., Riglet, C., and Vitorge, P. (1986a) *Inorg. Chem.,* **25**(10), 1679–84.
Grenthe, I., Robouch, P., and Vitorge, P. (1986b) *J. Less-Common Met.,* **122**, 225–31.
Grenthe, I., Fuger, J., Konigs, R. J. M., Lemire, R. J., Muller, A. B., Nguyen- Trung, C., and Wanner, H. (1992) *Chemical Thermodynamics of Uranium,* Elsevier Science Publishing Company, New York, 676 pp.
Grenthe, I., Puigdomenech, I., and Allard, B. (1997) *Modelling in Aquatic Chemistry,* Nuclear Energy Agency, OECD, Washington, DC, 724 pp.
Grigor'ev, M. S., Gulyaev, B. F., and Krot, N. N. (1986) *Sov. Radiochem.,* **28**(6), 630–4.
Grigor'ev, M. S., Baturin, N. A., Bessonov, A. A., and Krot, N. N. (1995) *Radiokhimiya,* **37**(1), 15–18.
Grison, E., Lord, W. B. H., and Fowler, R. D. (eds.) (1960) *Plutonium 1960, Proc. Second Int. Conf. on Plutonium Metallurgy,* Grenoble, France, Apr. 19–22, 1960, Cleaver Hume, London.
Griveau, J. C., Pfleiderer, C., Boulet, P., Rebizant, J., and Wastin, F. (2004) *J. Magn. Magn. Mater.,* **272/276**, 154–5.
Grove, G. R. (1966) *Reactor Fuels and Materials Development. Plutonium Research. April–Sept.*, Report MLM-1347, Mound Laboratory, pp. 11–18.
Grove, G. R., Goldenberg, J. A., Kelly, D. P., and Prosser, D. L. (1965) *Plutonium-238 Isotopic Power Sources, a Summary Report*, Report MLM-1270, Mound Laborabory, Miamisburg, OH, 234 pp.
Gruen, D. M. and deKock, C. W. (1967) *J. Inorg. Nucl. Chem.,* **29**(10), 2569–75.
Gruen, D. M., Malm, J. G., and Weinstock, B. (1956) *J. Chem. Phys.,* **24**(4), 905–6.
Gruen, D. M., McBeth, R. L., Kooi, J., and Carnall, W. T. (1960) *Ann. N.Y. Acad. Sci.,* **79**(11), 941–9.
Gschneidner, K. A., Jr (1980) Theory Alloy Phase Form., Proc. Symp, Meeting Date 1979, Metall. Soc. AIME, Warrendale, PA, 1–39.

Gschneidner, Jr, K. A., Elliott, R. O., and Struebing, V. O. (1960) *Pu Phase Diagrams Discussion, Proc. Second Int. Conf. on Plutonium and Other Actinides,* Grenoble, France (eds. E. Grison, W. B. H. Lord, and R. D. Fowler), Cleaver-Hume Press, London, 1, 166 pp.

Guerin, G. (1996) Research on Actinides. CLEFS/CEA. **31**, 1–71.

Guillaumont, R. and Adloff, J. P. (1992) *Radiochim. Acta,* **58–59**(Pt. 1), 53–60.

Guillaumont, R., Fanghaenel, T., Fuger, J., Grenthe, I., Neck, V., Palmer, D. A., and Rand, M. H. (2003) *Update on the Chemical Thermodynamics of Uranium, Neptunium, Plutonium, Americium, and Technetium,* Elsevier, Amsterdam, The Netherlands, 919 pp.

Güldner, R. and Schmidt, H. (1991) *J. Nucl. Mater.,* **178**(2–3), 152–7.

Hagan, P. G. and Miner, F. J. (1980) *ACS Symp. Ser.,* **117**(Actinide Sep.), 51–67.

Hagemann, F., Abraham, B. M., Davidson, N. R., Katz, J. J., and Sheft, I. (1949) The Preparation and Properties of Plutonium Iodide and Plutonium Oxyiodide, in *Natl. Nucl. Energy Ser.,* Div IV **14B**(*Transuranium Elements*, Pt. II), (eds. G. T. Seaborg, J. J. Katz, and W. M. Manning), McGraw-Hill, New York, pp. 957–63.

Haines, H. R. and Potter, P. E. (1975) *Thermodyn. Nucl. Mater*., Proc. Symp., 4th, Meeting Date 1974, **2,** pp. 145–73.

Haire, R. G. and Eyring, L. (1994) Comparison of the Binary Oxides, in *Handbook on the Physics and Chemistry of Rare Earths,* vol. 18, (eds. K. A. J. Gschneidner, L. Eyring, G. R. Choppin, and G. H. Lander), Elsevier Science, New York, pp. 413–505.

Haire, R. G., Heathman, S., Le Bihan, T., Lindbaum, A., and Iridi, M. (2004) *Mater. Res. Soc. Symp. Proc.,* **802**, (Actinides–Basic Science Technol.), 15–20.

Hall, R. O. A., Jeffery, A. J., Lee, J. A., Mortimer, M. J., and Lander, G. H. (1985) *Heat Capacity Measurements on Plutonium Phosphide*, Report AERE-R-11075, Atomic Energy Research Establishment, Harwell, UK, 24 pp.

Hammel, E. F. (1998) *Plutonium Metallurgy at Los Alamos, 1943–1945: Recollections of Edward F. Hammel,* Los Alamos National Laboratory, Los Alamos, NM, 173 pp.

Handa, M. and Suzuki, Y. (1984) *Nihon Genshiryoku Gakkaishi,* **26**(1), 2–7.

Handwerk, J. H. and Kruger, O. L. (1971) *Nucl. Eng. Des.,* **17**(3), 397–408.

Hanrahan, R. J., Boehlert, C., and McDeavitt, S. (2003) *J. Metals*, **55**(9).

Harland, C. E. (1994) *Ion Exchange: Theory and Practice*, 2nd Ed., The Royal Society of Chemistry, Cambridge.

Harmon, K. M. and Reas, W. H. (1957) *Conversion Chemistry of Plutonium Nitrate*, Report HW-49597 A, 15 pp.

Harmon, K. M., Judson, B. F., Lyon, W. L., Pugh, R. A., and Smith, R. C. (1961) in *Reactor Handbook,* 2nd edn, vol. II, (eds. S. M. Stoller and R. B. Richard), Interscience Publishers, New York, 680 pp.

Harper, E. A., Hedger, H. J., and Dalton, J. T. (1968) *Nature,* **219**(5150), 151.

Harrison, W. A. (2001) *Phys. Rev. B,* **64**(23), 235112/1–10.

Harrowfield, J. M. B., Kepert, D. L., Patrick, J. M., White, A. H., and Lincoln, S. F. (1983) *J. Chem. Soc. Dalton Trans.*, (2), 393–6.

Harvey, B. G., Heal, H. G., Maddock, A. G., and Rowley, E. L. (1947) *J. Chem. Soc.*, 1010–21.

Harvey, M. R., Doyle, J. H., Rafalski, A. L., and Riefenberg, D. H. (1971) *J. Less-Common Met.,* **23**, 446.

Hasbrouk, M. E. and Burns, M. P. (1965) *Plutonium Metallurgy Handbook*, Report BNWL-37, Pacific Northwest Laboratory.

Haschke, J. M. (1991) Actinide Hydrides, in *Topics in f-element Chemistry,* vol. 2 (eds. G. Meyer and L. R. Morss), Kluwer Academic Publishers, Boston, MA, pp. 1–53.

Haschke, J. M. (1992) *Hydrolysis of Plutonium. Plutonium–Oxygen Phase Diagram* in *Transuranium Elements: A Half Century* (eds. L. R. Morss and J. Fuger), pp. 416–25.

Haschke, J. M. (1999) Pu Oxidation, personal communication, J. C. Martz, Los Alamos, NM.

Haschke, J. M. (2005) *J. Nucl. Mater.,* **340**(2–3), 299–306.

Haschke, J. M. and Allen, T. H. (2001) *J. Alloys Compd.,* **320**(1), 58–71.

Haschke, J. M. and Haire, R. G. (2000) Crystalline Solids and Corrosion Chemistry, in *Advances in Plutonium Chemistry 1967–2000* (ed. D. C. Hoffman), The American Nuclear Society, La Grange Park, IL, pp. 212–59.

Haschke, J. M. and Martz, J. C. (1998a) *J. Alloys Compd.,* **266**(1–2), 81–9.

Haschke, J. M. and Martz, J. C. (1998b) *Encyclopedia of Environmental Analysis and Remediation, Plutonium Storage,* vol. 6, John Wiley, New York, pp. 3740–55.

Haschke, J. M. and Oversby, V. M. (2002) *J. Nucl. Mater.,* **305**(2–3), 187–201.

Haschke, J. M., Hodges, A. E., III, Bixby, G. E., and Lucas, R. L. (1983) *Reaction of Plutonium with Water. Kinetic and Equilibrium Behavior of Binary and Ternary Phases in the Plutonium + Oxygen + Hydrogen System*, Report RFP-3416, Rockwell International Corporation, Rocky Flats Plant, Golden, CO, 24 pp.

Haschke, J. M., Hodges, III, A. E., and Lucas, R. L. (1987) *J. Less-Common Met.,* **133**(1), 155–66.

Haschke, J. M., Allen, T. H., and Stakebake, J. L. (1996) *J. Alloys Compd.,* **243**(1–2), 23–35.

Haschke, J. M., Allen, T. H., and Martz, J. C. (1998) *J. Alloys Compd.,* **271**, 211–15.

Haschke, J. M., Allen, T. H., and Morales, L. A. (2000a) *Los Alamos Science,* **26**(1), 252–73.

Haschke, J. M., Allen, T. H., and Morales, L. A. (2000b) *Science,* **287**(5451), 285–7.

Haschke, J. M., Allen, T. H., and Morales, L. A. (2001) *J. Alloys Compd.,* **314**(1–2), 78–91.

Hasilkar, S. P., Khedekar, N. B., Chander, K., Jadhav, A. V., and Jain, H. C. (1994) *J. Radioanal. Nucl. Chem.,* **185**(1), 119–25.

Hass, P. A., Lloyd, M. H., Band, W. D., and McBride, J. P. (1966) *Sol-Gel Process Development and Microsphere Preparation*, Report ORNL-P-2159, Oak Ridge National Laboratory, 42 pp.

Haug, H. (1963) *The Systems Uranium Oxide–Europium Oxide and Plutonium Oxide–Europium Oxide*, Thesis, Report NP-13003, University of Munich, Germany, 97 pp.

Haug, H. and Weigel, F. (1963) *J. Nucl. Mater.,* **9**(3), 160–3.

Hawkins, N. J. (1956) *Report of the Chemistry and Engineering Section for February, March, April, 1956*, Report KAPL-1536, Knolls Atomic Power Laboratory, Schenectady, New York, 98 pp.

Hawkins, N. J., Mattraw, H. C., and Sabol, W. W. (1954) *Infrared Spectrum and Thermodynamic Properties of PuF_6*, Report KAPL-1007, Knolls Atomic Power Laboratory, 21 pp.

Hay, P. J. and Martin, R. L. (1998) *J. Chem. Phys.,* **109**(10), 3875–81.

Hay, P. J., Martin, R. L., and Schreckenbach, G. (2000) *J. Phys. Chem. A,* **104**(26), 6259–70.

Hayes, R. G. and Edelstein, N. (1972) *J. Am. Chem. Soc.,* **94**(25), 8688–91.
Hecker, S. S. unpublished work, Los Alamos National Laboratory.
Hecker, S. S. (2000) *Los Alamos Science,* **26**(2), 290.
Hecker, S. S. (2003) *JOM* **55**(9), 13–50.
Hecker, S. S. (2004) *Metall. Mater. Trans. A,* **35 A**(8), 2207–22.
Hecker, S. S. and Martz, J. C. (2000) *Los Alamos Science* **26**(1), 238–43.
Hecker, S. S. and Martz, J. C. (2001) Plutonium Aging: from Mystery to Enigma, in *Aging Studies and Lifetime Extension of Materials* (ed. L. G. Mallinson), Kluwer Academic, New York, pp. 23–52.
Hecker, S. S. and Morgan, J. R. (1976) *Effect of Strain Rate on the Tensile Properties of Alpha - and Delta - Stabilized Plutonium, Proc. Fifth Int. Conf. on Plutonium and Other Actinides 1975, Sept. 10–13, 1975,* Baden-Baden, West Germany, (eds. H. Blank and R. Linder), North-Holland, Amsterdam, The Netherlands, pp. 697–709.
Hecker, S. S. and Stevens, M. F. (2000) *Los Alamos Science* **26**(2), 336–55.
Hecker, S. S. and Timofeeva, L. F. (2000) *Los Alamos Science* **26**(1), 244–51.
Hecker, S. S., Zukas, E. G., Morgan, J. R., and Pereyra, R. A. (1982) *Temperature-Induced Transformation in a Pu-2 at.% Al Alloy. Proc. Int. Conf. on Solid to Solid Phase Transformations;* Pittsburgh, PA, Metallurgical Society of AIME, 1982, Warrendale, PA, pp. 1339–43.
Hecker, S. S., Harbur, D. R., and Zocco, T. G. (2004b) *Prog. Mater. Sci.,* **49**(3–4), 429–85.
Herbst, R. J. and Matthews, R. B. (1982) *Uranium–Plutonium Carbide as an LMFBR Advanced Fuel*, Report LA-9259-MS, Los Alamos National Laboratory, Los Alamos, NM, 24 pp.
Herrick, C. C., Olsen, C. E., and Sandenaw, T. A. (1959) *The Density of Liquid Plutonium Metal*, Report LA-2358, Los Alamos Scientific Laboratory, 17 pp.
Hidaka, H. (1999) *J. Radioanal. Nucl. Chem.,* **239**(1), 53–8.
Hidaka, H. and Holliger, P. (1998) *Geochim. Cosmochim. Acta,* **62**(1), 89–108.
Hill, O. F. and Cooper, V. R. (1958) *Ind. Eng. Chem.,* **50**(4), 599–602.
Hill, H. H. and Kmetko, E. A. (1976) *J. Phys. F: Me. Phys.,* **6**(6), 1025–37.
Hill, R. N. (2005), personal communication, G. Jarvinen.
Hilliard, J. E., Averbach, B. B., and Cohen, M. (1959) *Acta Met.,* **7**, 86.
Hincks, J. A. and McKinley, L. C. (1966) *Heat Source Fabrication*, Report MLM-1365, Mound Laboratory, 35 pp.
Hindman, J. C. (1954) Ionic and Molecular Species of Plutonium in Solution, in *The Actinide Elements* (eds. G. T. Seaborg and J. J. Katz), McGraw-Hill, New York, pp. 301–70.
Hinrichs, W., Melzer, D., Rehwoldt, M., Jahn, W., and Fischer, R. D. (1983) *J. Organomet. Chem.,* **251**(3), 299–305.
Hobart, D. E., Morris, D. E., Palmer, P. D., and Newton, T. W. (1989) *Formation, Characterization, and Stability of Plutonium (IV) Colloid: A Progress Report*, Report LA-UR-89-2541, Los Alamos National Laboratory, 9 pp.
Hocheid, B., Tanon, A., and Despres, J. (1965) *J. Nucl. Mater.,* **15**(3), 241–4.
Hocheid, B., Tanon, A., Bedere, S., Despres, J., Hay, S., and Miard, F. (1967) *Pu-Ga Phase Diagram,* Plutonium 1965, Proc. Third Int. Conf. on Plutonium (eds. A. E. Kay, and M. B. Waldron), Chapman-Hall, London, 321 pp.
Hodge, N. (1961) in *Advances in Fluorine Chemistry,* vol. 2 (eds. M. Stacey, J. C. Tatlow, and A. G. Sharpe), Butterworths, London, England, 138 pp.

Hoekstra, H. R. and Gebert, E. (1977) *J. Inorg. Nucl. Chem.,* **39**(12), 2219–21.
Hoffman, D. C. (ed.) (2000) *Advances in Plutonium Chemistry 1967–2000,* The American Nuclear Society, La Grange Park, IL, 320 pp.
Hoffman, D. C., Lawrence, F. O., Mewherter, J. L., and Rourke, F. M. (1971) *Nature,* **234**(5325), 132–4.
Hoffman, D. C., Ghiorso, A., and Seaborg, G. T. (2000) *The Transuranium People: The Inside Story,* Imperial College Press, London, England, 467 pp.
Holleck, H. (1975) *Proc. Fourth Symp. on Thermodyn. Nucl. Mater.,* vol. 2, pp. 213–64.
Holleck, H. and Kleykamp, H. (1972) *Gmelin Handbook of Inorganic Chemistry, Transuranium Elements, part C,* Verlag Chemie, Weinheim, 83 pp.
Holley, C. E., Jr (1974) *J. Nucl. Mater.,* **51**(1), 36–46.
Holley, C. E., Jr, Mulford, R. N. R., Huber, E. J., Jr, Head, E. L., Ellinger, F. H., and Bjorklund, C. W. (1958) *Proc. Second UN Int. Conf. Peaceful Uses Atomic Energy*, Geneva, 1958, vol. 6, pp. 215–20.
Holley, C. E., Rand, M. H., and Storms, E. K. (1984) The Actinide Carbides, in *Chemical Thermodynamics of Actinide Elements and Compounds: Part. 6,* IAEA, Vienna, Austria, 101 pp.
Holliger, P. and Devillers, C. (1981) *Earth Planet. Sc. Lett.,* **52**(1), 76–84.
Horner, D. E., Crouse, D. J., and Mailen, J. C. (1977) *Cerium-promoted Dissolution of Plutonium dioxide and Plutonium dioxide–Uranium dioxide in Nitric Acid*, Report ORNL/TM-4716, Oak Ridge National Laboratory, TN, 41 pp.
Hough, A. and Marples, J. A. C. (1965) *J. Nucl. Mater.,* **15**(4), 298–309.
Howell, R. H. and Sterne, P. A. (2002) Positron Annihilation Spectroscopy, personal communication, A. J. Schwartz, Livermore, CA.
Howell, R. H., Sterne, P. A., Hartley, J., and Cawan, T. E. (1999) *Appl. Surf. Sci.,* **149**, 103–5.
Hunt, D. C. and Boss, M. R. (1971) *J. Nucl. Energy,* **25**(6), 241–51.
Hunt, D. C. and Rothe, R. E. (1974) *Nucl. Sci. Eng.,* **53**(1), 79–92.
Hurst, H. J. and Taylor, J. C. (1970) *Acta Crystallogr.,* **B26**(Pt. 4), 417–21.
Hurst, R., Mandleberg, C. J., Rae, H. K., Davies, D., Francis, K. E., and Brooks, R. (1953) *Plutonium Hexafluoride*, part II, *Preparation and Some Physical Properties*, Report AERE-C/R-1312, Great Britain Atomic Energy Research Establishment.
Hyde, E. K., Davidson, N. R., Katz, J. J., and Wolf, M. J. (1944) *Chemical Research - Special Chemistry of Plutonium. Report for Month Ending April 1, 1944*, Report CK-1512, Metallurgical Laboratory, pp. 5–7.
Hyde, E. K., Perlman, I., and Seaborg, G. T. (1964) *The Nuclear Properties of the Heavy Elements Vol. I: Systematics of Nuclear Structure and Radioactivity. Vol. II: Detailed Radioactivity Properties*, Prentice-Hall, Englewood Cliffs, NJ, 400 pp.;36 pp.
IAEA (1967) *The Plutonium–Oxygen and the Uranium–Plutonium–Oxygen Systems. A Themochemical Assessment*, Report Tech. Rep Ser. No. 79, STI\DOC-10\79, International Atomic Energy Agency, 86 pp.
Iida, T., Guthrei, R. I. L., and Morita, Z. (1988) *Can. Metall. Quart.,* **27**(1), 1–5.
Iso, S., Uno, S., Yoshihiro, M., Sasaki, T., and Yoshida, Z. (2000) *Prog. Nucl. Energ.,* **37** (1–4), 423–8.
Iyer, P. N. and Natarajan, P. R. (1989) *J. Less-Common Met.,* **146**(1–2), 161–6.
Iyer, P. N. and Natarajan, P. R. (1990) *J. Less-Common Met.,* **159**(1–2), 1–11.

Jackson, E. F. and Rand, M. H. (1963) *Oxidation Behaviour of Plutonium Dioxide and Solid Solutions Containing Plutonium Dioxide*, Report AERE-R-3636, Atomic Energy Research Establishment, Harwell, UK, 13 pp.

Jacquemin, J. and Lallement, R. (1970) *Self-irrad Damage*, *Proc. Int. Conf. on Plutonium and Other Actinides 1970* (ed. W. N. Miner), The Metallurgical Society of AIME, pp. 616–22.

Jarvinen, G. D. (ed.) (2003) *AIP Conf. Proc.*, **673**(Plutonium Futures – The Science). 421 pp.

Jayadevan, N. C., Mudher, K. D. S., and Chackraburtty, D. M. (1982) *Z. Kristallogr.,* **161**(1–2), 7–13.

Jenkins, I. L., Moore, F. H., and Waterman, M. J. (1965) *J. Inorg. Nucl. Chem.,* **27**(1), 77–80.

Joel, J., Roux, C., and Rapin, M. (1971) *J. Nucl. Mater.,* **40**, 297–304.

Johns, I. B. (1944) *Plutonium Hydride And Deuteride*, Report LA-137, Los Alamos Scientific Laboratory, 12 pp.

Johns, I. B. and Moulton, G. H. (1944) *Large-scale Preparation of the Anhydrous Fluorides of Plutonium*, Report LA-193, Los Alamos Scientific Laboratory, Los Alamos, NM, 20 pp.

Johnson, K. W. R. (1954) *Preparation of High-purity Plutonium Metal*, Report LA-1680, Los Alamos Scientific Laboratory.

Johnson, K. A. (1964) *Homogenization of Gallium-stabilized Delta-phase Plutonium*, Report LA-2989, Los Alamos Scientific Laboratory, 43 pp.

Johnson, K. W. R. and Leary, J. A. (1964) *J. Inorg. Nucl. Chem.,* **26**(1), 103–5.

Johnson, K. W. R., Kahn, M., and Leary, J. A. (1961) *J. Phys. Chem.,* **65**, 2226–9.

Johnson, I., Chasanov, M. G., and Yonco, R. M. (1965) *Trans. Metall. Soc. AIME,* **233** (7), 1408–14.

Johnson, Q. C., Wood, D. H., and Smith, G. S. (1967) *The Crystal Structure of Pu_3Zn_{22}*, Report UCRL-70500.

Jones, M. M. (1953) *A Study of Plutonium Trifluoride Precipitated from Aqueous Solution*, Report HW-30384, Hanford Atomic Products Operation, 15 pp.

Jones, L. H. (1955) *J. Chem. Phys.,* **23**, 2105–7.

Jones, L. H. and Penneman, R. A. (1953) *J. Chem. Phys.,* **21**(3), 542–4.

Jones, L. V., Ofte, D., Rohr, L. J., and Wittenberg, L. J. (1962) *Am. Soc. Metals, Trans. Quart.,* **55**, 819–25.

Jones, L. V., Ofte, D., Phipps, K. D., and Tucker, P. A. (1964) *Ind. Eng. Chem. Prod. R. D.,* **3**(2), 78–82.

Jouniaux, B. (1979) *Study by Thermochromatography of Fluorides of Transuranium Elements*, Thesis, Report IPNO-T-79-05, Paris-6 Univ. 75; Paris-11 Univ. 91, Inst. de Physique Nucleaire, Orsay, France, 99 pp.

Jouniaux, B., Legoux, Y., Merinis, J., and Bouissieres, G. (1979) *Radiochem. Radioanal. Lett.,* **39**(2), 129–40.

Jove, J. and Cousson, A. (1977) *Radiochim. Acta,* **24**(2–3), 73–5.

Jove, J. and Pagès, M. (1977) *Inorg. Nucl. Chem. Lett.,* **13**(7), 329–34.

Jove, J., Pagès, M., and Freundlich, W. (1974) *Compt. Rend.,* **278**(12), 873–4.

Jove, J., Pagès, M., and Freundlich, W. (1976) *Inorg. Nucl. Chem. - Herbert H. Hyman Mem. Vol.*, 189–92.

Kabanova, O. L., Danuschenkova, M. A., and Paley, P. N. (1960) *Anal. Chim. Acta,* **22**, 66.

Kaltsoyannis, N. (2000) *Inorg. Chem.,* **39**(26), 6009–17.
Kaltsoyannis, N. and Bursten, B. E. (1997) *J. Organomet. Chem.,* **528**(1–2), 19–33.
Kalvius, G. M., Cohen, D., Dunlap, B. D., and Shenoy, G. K. (1978) *Phys. Rev. B,* **18**(9), 4581–7.
Kandan, R., Babu, R., Nagarajan, K., and Rao, P. R. V. (2004) *J. Nucl. Mater.,* **324**(2–3), 215–19.
Karraker, D. G. (1973) *Inorg. Chem.,* **12**(5), 1105–8.
Karraker, D. G. (1987) *Inorg. Chim. Acta,* **139**(1–2), 189–91.
Karraker, D. G. and Stone, J. A. (1974) *J. Am. Chem. Soc.,* **96**(22), 6885–8.
Karraker, D. G., Stone, J. A., Jones, E. R., Jr, and Edelstein, N. (1970) *J. Am. Chem. Soc.,* **92**(16), 4841–5.
Kasha, M. (1949) Reactions between Plutonium Ions in Perchloric Acid Solutions. Rates, Mechanisms, and Equilibria, in *Natl. Nucl. Energy Ser.*, Div IV **14B**(Transuranium Element, Pt. I) (eds. G. T. Seaborg, J. J. Katz, and W. M. Manning), McGraw-Hill, New York, ch. 3, 295–334.
Kasper, J. S. (1976) *J. Less-Common Met.,* **47**, 17–21.
Kassner, M. E. and Peterson, D. E. (1995) *Phase Diagrams of Binary Actinide Alloys.* ASM International, Materials Park, OH, 489 pp.
Katz, J. J. and Gruen, D. M. (1949) *J. Am. Chem. Soc.,* **71**, 2106–12.
Katz, J. J. and Sheft, I. (1960) Halides of the Actinide Elements, in *Advances in Inorganic Chemistry and Radiochemistry,* vol. 2, (eds. H. J. Emeleus and A. G. Sharpe), Academic Press, San Diego, pp. 195–236.
Katzin, L. I. (1944) *Survey of the Chemistry of Plutonium*, Report CK-2240(Del.), Chicago University Metallurgical Laboratory, 46 pp.
Kaufman, L. (2002) Keynote: Humerothery and Calphad Thermodynamics, in *CALPHAD and Alloy Thermodynamics* (eds. P. E. A. Turchi, A. Gonis and R. D. Shull), TMS, Warrendale, PA, 3 pp.
Kaufman, L. and Bernstein, H. (1970) *Computer Calculation of Phase Diagrams with Special Reference to Refractory Metals.* Academic Press, New York, 334 pp.
Kay, A. E. and Loasby, R. G. (1964) *Philos. Mag.,* **9**(97), 37–49.
Kay, A. E. and Waldron, W. B. (1967) *Plutonium 1965,* Proc. Third Int. Conf. on Plutonium, Institute of Metals, Chapman and Hall, London, 1114 pp.
Keenan, T. K. (1957) *J. Phys. Chem.,* **61**, 1117.
Keenan, T. K. (1965) *Inorg. Chem.,* **4**(10), 1500–1.
Keenan, T. K. (1966) *Inorg. Nucl. Chem. Lett.,* **2**(6), 153–6.
Keenan, T. K. (1967) *Inorg. Nucl. Chem. Lett.,* **3**(10), 463–7.
Keenan, T. K. and Asprey, L. B. (1969) *Inorg. Chem.,* **8**(2), 235–238.
Keiser, D. L. J., Hayes, S. L., Meyer, M. K., and Clark, C. R. (2003) *J. Metals,* **55**(9), 55.
Keller, C. (1962) *Nukleonik,* **4**, 271–7.
Keller, C. (1963) *Nukleonik,* **5**, 41–8.
Keller, C. (1964) *Solid-state Chemistry of the Actinide Oxides*, Thesis, Report KFK-225, Kernforschungszentrum, Karlsruhe, 261 pp.
Keller, C. (1965a) *J. Inorg. Nucl. Chem.,* **27**(6), 1233–46.
Keller, C. (1965b) *J. Inorg. Nucl. Chem.,* **27**(2), 321–7.
Keller, C. (1971) *The Chemistry of the Transuranium Elements* (*Nuclear Chemistry in Monographs,* vol. 3). Verlag Chemie, Weinheim, 675 pp.
Keller, C. and Salzer, M. (1967) *J. Inorg. Nucl. Chem.,* **29**(12), 2925–34.

Keller, C. and Schmutz, H. (1964) *Zeitschr. Naturfors.,* **19b**(11), 1080.
Keller, C. and Schmutz, H. (1966) *Inorg. Nucl. Chem. Lett.,* **2**(11), 355–8.
Keller, C. and Seiffert, H. (1969) *Angew. Chem., Int. Ed. Engl.,* **8**(4), 279–80.
Keller, C. and Walter, K. H. (1965) *J. Inorg. Nucl. Chem.,* **27**(6), 1253–60.
Keller, C., Koch, L., and Walter, K. H. (1965a) *J. Inorg. Nucl. Chem.,* **27**(6), 1205–23.
Keller, C., Koch, L., and Walter, K. H. (1965b) *J. Inorg. Nucl. Chem.,* **27**(6), 1225–32.
Keller, C., Berndt, U., Debbabi, M., and Engerer, H. (1972) *J. Nucl. Mater.,* **42**(1), 23–31.
Kelly, C. E. (1975) MHW [Multihundred Watt] converter (RTG) [radioisotope thermoelectric generator]. *Rec. Intersoc. Energy Convers. Eng. Conf*., 10, 880–6.
Kennedy, J. W., Seaborg, G. T., Segre, E., and Wahl, A. C. (1941) *Phys. Rev.,* **70**, 555–6.
Kent, R. A. (1968) *J. Am. Chem. Soc.,* **90**(21), 5657–9.
Kent, R. A. (1969) *High Temp. Sci.,* **1**, 169.
Kent, R. A. (1973) *Thermodynamic Analysis of MHW Space Electric Power Generator*, Report LA-5202-MS, Los Alamos Scientific Laboratory, Los Alamos, NM, 108 pp.
Kent, R. A. and Leary, J. A. (1968) *Mass Spectrometric Studies of Plutonium Compounds at High Temperatures, I: the Heats of Vaporization of Gold and Plutonium and the Heat of Decomposition of Plutonium Mononitride*, Report LA-3902, Los Alamos Scientific Laboratory, Los Alamos, NM, 20 pp.
Kent, R. A. and Zocher, R. W. (1976) *Reduction of Plutonia by Carbon Monoxide and Equilibrium Partial Pressures above Plutonia*, Report LA-6534, Los Alamos Scientific Laboratory, Los Alamos, NM, 27 pp.
Kessie, R. W. and Ramaswami, D. (1965) *Removal of Plutonium Hexafluoride from Cell Exhaust Air by Hydrolysis Filtration*, Report ANL-7066, Argonne National Laboratory, Argonne, IL,70 pp.
Khanaev, E. I., Teterin, E. G., and Luk'yanova, L. A. (1967) *Zh. Prikl. Spektrosk.,* **6**(6), 789–96.
Kiehn, R. M. (1961) Pu LAMPRE, in *The Metal Plutonium* (eds. A. S. Coffinberry and W. M. Miner), University of Chicago Press, Chicago, IL, 333 pp.
Kierkegaard, P. (1956) *Acta Chem. Scand.,* **10**(4), 599–616.
Kikuchi, T., Koyama, T., and Homma, S. (2003) *AIP Conf. Proc.,* **673**(Plutonium Futures – The Science), 42–4.
Kim, J. I. (1991) *Radiochim. Acta,* **52–53**(Pt. 1), 71–81.
Kim, J. I. (1994) *MRS Bull.,* **19**(12), 47–53.
Kim, K. C. and Campbell, G. M. (1985) *Appl. Spectrosc.,* **39**(4), 625–8.
Kim, K. C., Krohn, B. J., Briesmeister, R. A., and Rabideau, S. (1987) *J. Chem. Phys.,* **87**, 1538.
Kimura, T. and Choppin, G. R. (1994) *J. Alloys Compd.,* **213–214**, 313–17.
King, E., Lee, J. A., Mendelssohn, K., and Wigley, D. A. (1965) *Proc. R. Soc. Lond. Ser. A,* **284**(1398), 325–43.
Kittel, C. and Kroemer, H. (1980) *Thermal Physics,* Freeman and Company, San Francisco, CA, p. 196.
Kleinschmidt, P. D. (1988) *J. Chem. Phys.,* **89**(11), 6897–904.
Kleykamp, H. (1999) *J. Nucl. Mater.,* **275**, 1–11.
Knief, R. A. (1985) *Nuclear Criticality Safety: Theory and Practice,* American Nuclear Society, La Grange Park, IL, 233 pp.
Knighton, J. B., Auge, R. G., Berry, J. W., and Franchini, R. C. (1976) *Molten Salt Extraction of Americium from Molten Plutonium Metal*, Report RFP-2365, Rocky Flats Plant, Rockwell International, Golden, CO, 24 pp.

Knighton, J. B. and Steunenberg, R. K. (1965) *J. Inorg. Nucl. Chem.,* **27**(7), 1457–62.
Knoch, W., Knighton, J. B., and Steunenberg, R. K. (1969) *Nucl. Metall. Met. Soc. AIME,* **15**, 535–46.
Knopp, R., Neck, V., and Kim, J. I. (1999) *Radiochim. Acta,* **86**(3–4), 101–8.
Koch, L. (1964) *The Ternary oxide of Quinque- and Sexivalent Neptunium and Plutonium with Lithium and Sodium*, Thesis, Report KFK-196, Institute fur Radiochemie, Kernforschungszentrum, Karlsruhe, Germany, 74 pp.
Koch, G. (ed.) (1972) *Gmelin Handbook of Inorganic Chemistry*, vol. 4*: Transuranium Elements, C*, Verlag Chemie, Weinheim, 279 pp.
Koch, G. (ed.) (1973a) *Gmelin Handbook of Inorganic Chemistry*, vol. 7a, *Transuranium Elements, A1, I, The Elements*, Verlag Chemie, Weinheim.
Koch, G. (ed.) (1973b) *Gmelin Handbook of Inorganic Chemistry*, vol. 7b, *Transuranium Elements, A1, II, The Elements*, Verlag Chemie, Weinheim.
Koch, G. (ed.) (1973c) *Gmelin Handbook of Inorganic Chemistry*, vol. 8, *Transuranium Elements, A2, The Elements*, Verlag Chemie, Weinheim.
Koch, G. (ed.) (1976a) *Gmelin Handbook of Inorganic Chemistry, Supplementary Work*, vol. 31, *Transuranium Elements, B1, The Metals*, 8th edn, Springer-Verlag, Berlin.
Koch, G., Ed. (1976b) *Gmelin Handbook of Inorganic Chemistry. Supplementary Work,* vol. 38, *Transuranium Elements, B2: Binary Alloy Systems 1*, 8th edn, Springer-Verlag, Berlin.
Koelling, D. D., Ellis, D. E., and Bartlett, R. J. (1976) *J. Chem. Phys.,* **65**(8), 3331–40.
Koltunov, V. S. (1982a) *Radiokhimiya,* **23**(3), 462.
Koltunov, V. S., Frolov, K. M., Marchenko, V. I., Tikhonov, M. F., Zhuravleva, G. I., Kulikov, I. A., and Ryabova, A. A. (1982b) *Radiokhimiya,* **24**(5), 607–14 (508 pp. in English translation).
Koltunov, V. S. and Baranov, S. M. (1993) *Radiokhimiya,* **35**(6), 11–21.
Koltunov, V. S. and Marchenko, V. I. (1973) *Sov. Radiochem.,* **15**(6), 787–95.
Koltunov, V. S. and Mikhailova, N. A. (1977) *Radiokhimiya,* **19**(3), 342–8 (pp. 282–8 in English translation).
Koltunov, V. S. and Ryabova, A. A. (1980) *Sov. Radiochem.,* **22**(5), 481–7.
Koltunov, V. S. and Zhuravleva, G. I. (1968) *Radiokhimiya,* **10**(6), 662–9 (pp. 648–54 in English translation).
Koltunov, V. S. and Zhuravleva, G. I. (1973) *Sov. Radiochem.,* **15**(1), 73–6.
Koltunov, V. S. and Zhuravleva, G. I. (1974) *Sov. Radiochem.,* **16**(1), 80–3.
Koltunov, V. S. and Zhuravleva, G. I. (1978) *Sov. Radiochem.,* **20**(1), 73–80.
Koltunov, V. S., Frolov, K. M., Tikhonov, M. F., and Shapovalov, M. P. (1980a) *Radiokhimiya,* **22**(4), 491–8 (pp. 386–93 in English translation).
Koltunov, V. S., Tikhonov, M. F., Frolov, K. M., and Shapovalov, M. P. (1980b) *Radiokhimiya,* **22 (1)**, 65–74 (pp. 45–53 in English translation).
Koltunov, V. S., Kulikov, I. A., Kermanova, N. V., and Nikishova, L. K. (1981a) *Radiokhimiya,* **23**(3), 462–5 (pp. 384–6 in English translation).
Koltunov, V. S., Zhuravleva, G. I., and Shapovalov, M. P. (1981b) *Sov. Radiochem.,* **23** (4), 449–553.
Koltunov, V. S., Baranov, S. M., and Zhuravleva, G. I. (1989) *Sov. Radiochem.,* **31**(1), 47–52.
Koltunov, V. S., Pastushchak, V. G., Mezhov, E. A., and Koltunov, G. V. (2004) *Radiochemistry,* **46**(2), 125–30.

Komkov, Y. A., Krot, N. N., and Gel'man, A. D. (1968) *Radiokhimiya,* **10**(6), 625–9.
Komkov, Y. A., Peretrukhin, V. F., Krot, N. N., and Gel'man, A. D. (1969) *Radiokhimiya,* **11**(4), 407–12.
Konobeevsky, S. T. (1955) *Conf. Acad. Sci. USSR, Peaceful Uses of Atomic Energy*, vol. 4, Consultants Bureau, 207.
Korzhavyi, P. A., Vitos, L., Andersson, D. A., and Johansson, B. (2004) *Nat. Mater.,* **3** (4), 225–8.
Kotani, A. and Ogasawara, H. (1993) *Physica B,* **186–188**, 16–20.
Kotani, A., Ogasawara, H., and Yamazaki, T. (1993) *JJAP Series* **8**(Physical Properties of Actinide and Rare Earth Compounds), 117–28.
Kraus, K. A. (1956) *Proc. Int. Conf. Peaceful Uses Atomic Energy,* vol. 7, Geneva, pp. 245–57.
Kraus, K. A. and Dam, J. R. (1949) *in Natl. Nucl. Energy Ser.,* Div IV **14B**(*Transuranium Elements, Pt. I*) (eds. G. T. Seaborg, J. J. Katz, and W. M. Manning), McGraw-Hill, New York, 466.
Kraus, K. A. and Nelson, F. (1950) *J. Am. Chem. Soc.,* **72**(9), 3901–6.
Krikorian, O. H. and Hagerty, D. C. (1990) *J. Nucl. Mater.,* **171**(2–3), 237–44.
Krikorian, O. H., Fontes, A. S., Jr, Ebbinghaus, B. B., and Adamson, M. G. (1997) *J. Nucl. Mater.,* **247**, 161–71.
Krishnan, S., Weber, J. K. R., Anderson, C. D., Nordine, P. C., and Sheldon, R. I. (1993) *J. Nucl. Mater.,* **203**(2), 112–21.
Krot, N. N. (1975) *Radiokhimiya,* **17**(5), 677–83.
Krot, N. N. and Gel'man, A. D. (1967) *Dokl. Akad. Nauk SSSR,* **177**(1), 124–5; see also (1968) Chem. Abstr., **68,** 26372b.
Krott, N. N., Gel'man, A. D., Mefodeva, M. P., Shilov, V. P., Peretrukhin, V. F., and Zakharova, F. A. (1976) *Moscow Symp. on the Chemistry of the Transuranium Elements*, *V* (eds. I. Spitsyn and J. J. Katz), pp. 249–52.
Kruger, O. L. (1963) *J. Am. Ceram. Soc.,* **46**, 80–5.
Kruger, O. L. and Moser, J. B. (1966a) *J. Am. Ceram. Soc.,* **49**(12), 661–7.
Kruger, O. L. and Moser, J. B. (1966b) *J. Inorg. Nucl. Chem.,* **28**(3), 825–32.
Kruger, O. L. and Moser, J. B. (1967a) *J. Phys. Chem. Solids,* **28**(11), 2321–5.
Kruger, O. L. and Moser, J. B. (1967b) *Chem. Eng. Prog., Symp. Ser.,* **63**(80), 1–10.
Kruger, O. L. and Savage, H. (1968) *J. Chem. Phys.,* **49**(10), 4540–4.
Kruger, O. L., Moser, J. B., and Wrona, B. J. (1966a) *Preparation of Plutonium Monosulfide or Monophosphide*, (United States Atomic Energy Commission). US Patent no. 3282 656, 2 pp.
Kugel, R., Williams, C., Fred, M., Malm, J. G., Carnall, W. T., Hindman, J. C., Childs, W. J., and Goodman, L. S. (1976) *J. Chem. Phys.,* **65**(9), 3486–92.
Kuroda, P. K. (1960) *Nature,* **187**, 36–8.
Kuroda, P. K. and Myers, W. A. (1998) *J. Radioanal. Nucl. Chem.,* **230**(1–2), 175–95.
Kutaitsev, V. I., Chebotarev, N. I., Lebedev, I. G., Adrianov, M. A., Konev, V. N., and Menchikova, T. S. (1967) *Proc. Third Int. Conf. on Plutonium, Plutonium 1965,* (eds. A. E. Kay and M. B. Waldron), Chapman & Hall, London, England, pp. 429–30.
Lallement, R. (1963) *Phys. Chem. Solids* **24**, 1617.
Lallement, R. and Solente, P. (1967) *Low-Temperature Irradiation, Proc. Third Int. Conf. on Plutonium 1965* (eds. A. I. Kay and M. B. Waldron), Chapman and Hall for Institute of Metals, London, pp. 147–61.

Lam, D. J., Fradin, F. Y., and Kruger, O. L. (1969) *Phys. Rev.,* **187**(2), 606–10.
Lammermann, H. and Conway, J. G. (1963) *J. Chem. Phys.,* **38**(1), 259.
Land, C. C., Ellinger, F. H., and Johnson, K. A. (1965a) *J. Nucl. Mater.,* **16**(1), 87.
Land, C. C., Johnson, K. A., and Ellinger, F. H. (1965b) *J. Nucl. Mater.,* **15**(1), 23–32.
Land, C. C., Peterson, D. E., and Roof, R. B. (1978) *J. Nucl. Mater.,* **75**(2), 262–73.
Lander, G. H., Delapalme, A., Brown, P. J., Spirlet, J. C., Rebizant, J., and Vogt, O. (1984) *Phys. Rev. Lett.,* **53**(23), 2262–5.
Lander, G. H., Delapalme, A., Brown, P. J., Spirlet, J. C., Rebizant, J., and Vogt, O. (1985) *J. Appl. Phys.,* **57**(8, Pt. 2B), 3748–50.
Lander, G. H., Rebizant, J., Spirlet, J. C., Delapalme, A., Brown, P. J., Vogt, O., and Mattenberger, K. (1987) *Physica B & C,* **146**(3), 341–50.
Lange, R. G. and Mastal, E. F. (1994) A Tutorial Review of Radioisotope Power Systems, in *A Critical Review of Space Nuclear Power and Propulsion 1984–1993* (ed. M. S. El-Genk), American Institute of Physics, AIP Press, New York, pp. 1–20.
Larroque, J., Chipaux, R., and Beauvy, M. (1986) *J. Less-Common Met.,* **121**, 487–96.
Larson, D. T. (1980) *Effect of Vacuum Heat Treatment on Plutonium Oxide Surfaces as Studied by XPS and AES*, Report RFP-3108, Energy Systems Group, Rockwell International Corporation, Canoga Park, CA, 10 pp.
Larson, A. C. and Cromer, D. T. (1967) *Acta Crystallogr.,* **23**(1), 70–7.
Larson, D. T. and Haschke, J. M. (1981) *Inorg. Chem.,* **20**(7), 1945–50.
Larson, A. C., Cromer, D. T., and Stambaugh, C. K. (1957) *Acta Crystallogr.,* **10**(7), 443–6.
Larson, A. C., Roof, R. B., and Cromer, D. T. (1963) *Acta Crystallogr.,* **16**(8), 835–6.
Larson, A. C., Cromer, D. T., and Roof, R. B. (1965) *Acta Crystallogr.,* **18**(2), 294–5.
Lashley, J. C. (2003) *Cryogenics,* **43**, 369.
Lashley, J. C. (2004) Heat capacity, personal communication, S. S. Hecker, Los Alamos, NM.
Lashley, J. (2005) *Phys. Rev. B: Condens. Matter.*, **71**(17).
Lashley, J. C., Blau, M. S., Staudhammer, K. P., and Pereyra, R. A. (1999) *J. Nucl. Mater.,* **274**(3), 315–19.
Lashley, J. C., Moment, R. L., and Blau, M. S. (2000) *Los Alamos Science,* **26**(1), 226–32.
Lashley, J. C., Stout, M. G., Pereyra, R. A., Blau, M. S., and Embury, J. D. (2001) *Scripta. Mater.,* **44**(12), 2815–20.
Lashley, J. C., Migliori, A., Singleton, J., McQueeney, R. J., Blau, M. S., Pereyra, R. A., and Smith, J. L. (2003a) *J. Metals,* **55**(9), 34.
Lashley, J. C., Singleton, J., Migliori, A., Betts, J. B., Fisher, R. A., Smith, J. L., and McQueeney, R. J. (2003b) *Phys. Rev. Lett.,* **91**(20), 205901/1.
Lashley, J. C., Lawson, A. C., McQueeney, R. J., and Lander, G. H. (2004) *Absence of Magnetic Moments in Plutonium*, Report LA-UR-04-3439 Preprint Archive, Condensed Matter (2004), Los Alamos National Laboratory, pp. 1–30.
Lataillade, F., Pons, F., and Rapin, M. (1971) *J. Nucl. Mater.,* **40**(3), 284–8.
Laue, C. A., Gregorich, K. E., Sudowe, R., Hendricks, M. B., Adams, J. L., Lane, M. R., Lee, D. M., McGrath, C. A., Shaughnessy, D. A., Strellis, D. A., Sylwester, E. R., Wilk, P. A., and Hoffman, D. C. (1999) *Phys. Rev. C,* **59**(6), 3086–92.
Lavallee, C. and Newton, T. W. (1972) *Inorg. Chem.,* **11**, 2616.
Lawson, A. C. (2001) *Philos. Mag. B,* **81**(3), 255–66.
Lawson, A. C., Goldstone, J. A., Cort, B., Sheldon, R. I., and Foltyn, E. M. (1994) *J. Alloys Compd.,* **213/214**, 426–8.

Lawson, A. C., Goldstone, J. A., Cort, B., Martinez, R. J., Vigil, F. A., Zocco, T. G., Richardson, J. W., Jr, and Mueller, M. H. (1996) *Acta Crystallogr.,* **B52**, 32–7.

Lawson, A. C., Martinez, B., Roberts, J. A., and Bennett, B. I. (2000) *Philos. Mag. B,* **80** (1), 53–9.

Lawson, A. C., Roberts, J. A., Martinez, B., and Richardson, J. W. (2002) *Philos. Mag. B,* **82**(18), 1837–45.

Laxminarayanan, T. S., Patil, S. K., and Sharma, H. D. (1964) *J. Inorg. Nucl. Chem.,* **26** (6), 1001–9.

Leary, J. A. (1962) *Temperature-composition Diagrams of Pseudo-binary Systems Containing Plutonium (III) Halides*, Report LA-2661, Los Alamos Scientific Laboratory, Los Alamos, NM, 16 pp.

Leary, J. A. and Mullins, L. J. (1966) *Int. Atomic Energy Agency - Proc. Ser. Thermodynamics*, vol. 1, pp. 459–71.

Leary, J. A. and Mullins, L. J. (1974) *J. Chem.Thermodyn.,* **6**(1), 103–4.

Leary, J. A., Morgan, A. N., and Maraman, W. J. (1959) *Ind. Eng. Chem.,* **51**(1), 27–31.

Lechelle, J., Bleuet, P., Martin, P., Girard, E., Bruguier, F., Martinez, M. A., Somogyi, A., Simionovici, A., Ripert, M., Valdivieso, F., and Goeuriot, P. (2004) *IEEE Trans. Nucl. Sci.,* **51**(4, Pt. 1), 1657–61.

Ledbetter, H. (2004) Grüneisen constants, personal communication, S. S. Hecker, Los Alamos, NM.

Ledbetter, H. M. and Moment, R. L. (1976) *Acta Metall. Mater.,* **24**, 891–9.

Ledbetter, H., Migliori, A., Betts, J., Harrington, S., and El-Khatib, S. (2004) *Elastic Constant Measurements*, Report LA-UR-04-6980, Los Alamos National Laboratory.

Ledbetter, H., Migliori, A., Betts, J., Harrington, S., and El-Khatib, S. (2005) *Phys. Rev. B.*, **71**, 172101/1–4.

Ledbetter, H., and Migliori, A., (2005) Report LA-UR-05-1800, Los Alamos National Laboratory.

Lee, J. A. and Hall, R. O. A. (1959) *J. Less-Common Met.,* **1**, 356.

Lee, J. A. and Mardon, P. G. (1961) Thermal Conductivity, in *The Metal Plutonium* (ed. A. S. Coffinberry), Chicago University Press, Chicago, IL.

Lee, J. A., Hall, R. O. A., King, E., and Meaden, G. T. (1961) Electrical Resistivity, in *Plutonium 1960,* vol. 1, (eds. E. Grison, W. B. H. Lord, and R. D. Fowler), Cleaver-Hume Press Ltd., London, pp. 39–50.

Lee, J. A., Mendelssohn, K., and Wigley, D. A. (1962) *Phys. Lett.,* **1**(8), 325–7.

Lee, J. A., Marples, J. A. C., Mendelssohn, K., and Sutcliffe, P. W. (1965a) Thermal Expansion, in *Plutonium 1965* (eds. K. A. E. and R. G. Loasby), Chapman-Hall Publishers, London, England, pp. 176–88.

Lee, J., Mendelssohn, K., and Sutcliffe, P. (1965b) *Cryogenics,* **5**, 227.

Leibowitz, L., Fischer, D. F., and Chasanov, M. G. (1974) *Enthalpy of Molten Uranium–Plutonium Oxides*, Report ANL-8082, Argonne National Laboratory, Argonne, IL, 19 pp.

Leitner, L. (1967) *Quasibinary Phase Diagrams of the System Thulium Oxide–Actinide Oxide (ThO_2, UO_2, NpO_2, PuO_2) below 1700 deg*, Report KFK-521, Kernforschungszentrum, Karlsruhe, Germany, 86 pp.

Lemire, R. J., Fuger, J., Nitsche, H., Potter, P., Rand, M. H., Rydberg, J., Spahiu, K., Sullivan, J. C., Ullman, W. J., Vitorge, P., and Warner, H. (2001) *Chemical*

Thermodynamics of Neptunium and Plutonium, Elsevier, Amsterdam, The Netherlands, 845 pp.
Lesser, R. and Peterson, J. R. (1976) *Transurane: Die Metalle*, part B1, in *Transurane,* vol. 31, (ed. K.-C. Buschbeck), Springer-Verlag, Berlin, Germany, pp. 40–1.
Levine, C. A. and Seaborg, G. T. (1951) *J. Am. Chem. Soc.,* **73**, 3278–83.
Levitz, N. M., Vogel, G. J., Carls, E. L., Grosvenor, D. E., Murphy, W. F., Kullen, B. J., and Raue, D. J. (1968) *Engineering Development of Fluid-bed Fluoride Volatility Processes*, part 15, *Material Balance Demonstrations, Production Rates, and Fluorine Utilizations in Fluorination of Kilogram Quantities of PuF_4 to PuF_6 with Elemental Fluorine in a Fluid-bed Reactor*, Report ANL-7568, Argonne National Laboratory, Argonne, IL, 28 pp.
Lewis, H. D., Kerrisk, J. F., and Johnson, K. W. (1976) *Effect of a Delta-phase Stabilizer on the Thermal Diffusivity of Plutonium, Proc. 14th Int. Conf. on Therm Conduct,* Jun. 2–4, 1975, University of Connecticut, Storrs, Plenum Press, New York, pp. 201–8.
Li, J. and Bursten, B. E. (1998) *J. Am. Chem. Soc.,* **120**(44), 11456–66.
Lipis, L. V. and Pozharskii, B. G. (1960) *Zh. Neorg. Khim.,* **5**, 2162–6.
Liptai, R. G. and Friddle, R. J. (1967) *J. Nucl. Mater.,* **21**(1), 114.
Liptai, R. G., Lloyd, L. T., and Friddle, R. J. (1967) *J. Phys. Chem. Solids,* **1**, 573.
Littler, D. J. (1952) *Proc. Phys. Soc.,* **65A**, 203–8.
Lloyd, M. H. and Haire, R. G. (1968) *Nucl. Appl. Technol.,* **5**(3), 114–22.
Lloyd, M. H. and Haire, R. G. (1978) *Radiochim. Acta,* **25**(3–4), 139–48.
Long, J. T. (1978) *Engineering for Nuclear Fuel Reprocessing*, American Nuclear Society, La Grange Park, IL, 1025 pp.
Lorenzelli, R., Martin, A., and Schickel, R. (1966) *Reaction of Uranium and Plutonium Carbides with Nitrogen*, Report CEA-R 2997, 21 pp.
Louer, M., Brochu, R., Louer, D., Arsalane, S., and Ziyad, M. (1995) *Acta Crystallogr. B,* **51**(6), 908–13.
Louwrier, K. P. and Richter, K. (1976) *Des. Equip. Hot Lab.*, *Proc. Symp.*, pp. 3–12.
Louwrier, K. P., Ronchi, C., Steemers, T., and Zamorani, E. (1968) *Sol-gel Processes for Ceramic Nuclear Fuels*, *Proc. Panel on Sol-gel Processes for Ceramic Nuclear Fuels*, Report STI/PUB/207, International Atomic Agency, pp. 97–106.
Love, L. O. (1973) *Science,* **182**(4110), 343–52.
Love, L. O., Banic, G. M., Bell, W. A., and Prater, W. K. (1961) *Electromagnetic Separation Radioactive Isotopes, Proc. Int. Symp.,* Vienna, Austria, pp. 141–54.
Lupinetti, A. J., Fife, J. L., Garcia, E., Dorhout, P. K., and Abney, K. D. (2002) *Inorg. Chem.,* **41**(9), 2316–18.
Lynn, J., Kwei, G., Trela, W. J., Yuan, V. W., Cort, B., Martinez, R. J., and Vigil, F. (1998) *Phys. Rev. B,* **65**, 214107–1.
Lyon, W. L. and Baily, W. E. (1965) *Solid-liquid Phase Diagram for the Uranium Oxide–Plutonium Oxide System*, Report GEAP-4878, General Electric Company, 17 pp.
Lyon, W. L. and Baily, W. E. (1967) *J. Nucl. Mater.,* **22**(3), 332–9.
Madic, C., Begun, G. M., Hobart, D. E., and Hahn, R. L. (1984) *Inorg. Chem.,* **23**(13), 1914–21.
Madic, C., Berger, P., and Machuron-Mandard, X. (1992) in *Transuranium Elements: A Half Century*, American Chemical Society, Washington, DC, pp. 457–68.
Magon, L., Portanova, R., and Cassol, A. (1968) *Inorg. Chim. Acta,* **2**, 237.
Maillard, C. and Adnet, J.-M. (2001) *Radiochim. Acta,* **89**(8), 485–90.

Malm, J. G. and Weinstock, B. (1954) *Argonne Plutonium Hexafluoride Program*, Report ANL-5366, Argonne National Laboratory, 14 pp.
Malm, J. G., Eller, P. G., and Asprey, L. B. (1984) *J. Am. Chem. Soc.,* **106**(9), 2726–7.
Mandleberg, C. J. and Davies, D. (1954) *The Vapour Pressure of Plutonium Tetrafluoride*, Report AERE-C/R-1321, Great Britain Atomic Energy Research Establishment, 18 pp.
Mandleberg, C. J. and Davies, D. (1961) *J. Chem. Soc., Abstracts*: 2031–7.
Mandleberg, C. J., Rae, H. K., Hurst, R., Long, G., Davies, D., and Francis, K. E. (1953) *Plutonium Hexafluoride*, part I, *Preparation and Some Physical Properties*, Report AERE-C/R-1172, Great Britain Atomic Energy Research Establishment.
Mandleberg, C. J., Rae, H. K., Hurst, R., Long, G., Davies, D., and Francis, K. E. (1956) *J. Inorg. Nucl. Chem.,* **2**(5–6), 358–67.
Manley, M. E., Fultz, B., McQueeney, R. J., Brown, C. M., Hults, W. L., Smith, J. L., Thoma, D. J., Osborn, R., and Robertson, J. L. (2001) *Phys. Rev. Lett.,* **86**(14), 3076–9.
Maraman, W. J., Beaumont, A. J., Christensen, E. l., Henrickson, A. V., Hermann, J. A., Johnson, K. W. R., Mullins, L. J., and Winchester, R. S. (1954) *Calcium Oxalate Carrier Precipitation of Plutonium*, Report LA-1692, Los Alamos Scientific Laboratory, Los Alamos, NM, 10 pp.
Maraman, W. J., McNeese, W. D., and Stafford, R. G. (1975) *Health Phys.,* **29**(4), 469–80.
Marcon, J. P. (1969) *Actinide Sulfides*, Report CEA-R-3919, Commissariat al'Energie Atomique, France, 99 pp.
Marcon, J. P. and Pascard, R. (1966a) *J. Inorg. Nucl. Chem.,* **28**(11), 2551–60.
Marcon, J. P. and Pascard, R. (1966b) *CR Acad. Sci. C. Chim.,* **262**(24), 1679–81.
Marcon, J. P. and Pascard, R. (1968) *CR Acad. Sci. C. Chim.,* **266**(4), 270–2.
Mardon, P. G. and Potter, P. E. (1970) *Plutonium 1970 and Other Actinides, Proc. Fifth Int. Conf. on Plutonium and Other Actinides,* Baden-Baden, West Germany, (ed. W. N. Miner), North-Holland, New York, 809 pp.
Mardon, P. G., Haines, H. R., Pearce, J. H., and Waldron, M. B. (1957) *J. I. Met.,* **86** (Part 4), 166–71.
Mardon, P. G., Pearce, J. H., and Marples, J. A. C. (1961) *J. Less-Common Met.,* **3**(4), 281–92.
Markin, T. L. and McKay, H. A. C. (1958) *J. Inorg. Nucl. Chem.,* **7**, 298–999.
Markin, T. L. and Street, R. S. (1967) *J. Inorg. Nucl. Chem.,* **29**(9), 2265–80.
Marples, J. A. C. (1960) *J. Less-Common Met.,* **2**(5), 331–51.
Marples, J. A. C. and Hall, R. O. A. (1972) *J. Nucl. Mater.,* **42**(2), 212–16.
Marples, J. A. C., Hough, A., Mortimer, M. J., Smith, A., and Lee, J. A. (1970) *Self-irrad Damage*, in *Proc. Fourth Int. Conf. on Plutonium and Other Actinides 1970* (ed. W. N. Miner), The Metallurgical Society of AIME, pp. 623–34.
Marquart, R., Hoffmann, G., and Weigel, F. (1983) *J. Less-Common Met.,* **91**(1), 119–27.
Marsh, S. F., Day, R. S., and Veirs, D. K. (1991) *Spectrophotometric Investigation of the Pu(IV) Nitrate Complex Sorbed by Ion Exchange Resins*, Report LA-12070, Los Alamos National Laboratory, Los Alamos, NM, 22 pp.
Marsh, S. F., Veirs, D. K., Jarvinen, G. D., Barr, M. E., and Moody, E. W. (2000) *Los Alamos Science,* **26**(2), 454–63.

Martell, A. E. and Smith, R. M. (2001) *Critical Stability Constants,* Standard Reference Database 46, Version 6.0., National Institute of Standards, Gaithersburg, MD.
Martin, D. G. (1988) *J. Nucl. Mater.,* **152**(2–3), 94–101.
Marty, B. and Marti, K. (2002) *Earth Planet. Sc. Lett.,* **196**(3–4), 251–63.
Martz, J. and Haschke, J. (1998) *J. Alloys Compd.,* **266**(1–2), 90–103.
Martz, J. C. and Schwartz, A. J. (2003) *J. Metals,* **55**(9), 19–23.
Martz, J. C., Haschke, J. M., and Stakebake, J. L. (1994) *J. Nucl. Mater.,* **210**(1–2), 130–42.
Mary, T. A., Evans, J. S. O., Vogt, T., and Sleight, A. W. (1996) *Science,* **272**, 90.
Mashirev, V. P., Shatalov, V. V., Grebenkin, K. F., Zuev, Y. N., Panov, A. V., Subbotin, V. G., and Chuvilin, D. Y. (2001) *At. Energ.,* **90**(3), 235–42.
Massalski, T. B. (1996) *Physical Metallurgy* (eds. R. W. Cahn and P. Haasen), Elsevier Science, Amsterdam, The Netherlands, 136 pp.
Masters, B. J. and Rabideau, S. W. (1963) *Inorg. Chem.,* **2**, 1–5.
Matonic, J. H., Scott, B. L., and Neu, M. P. (2001) *Inorg. Chem.,* **40**(12), 2638–9.
Matsika, S., Zhang, Z., Brozell, S. R., Blaudeau, J. P., Wang, Q., and Pitzer, R. M. (2001) *J. Phys. Chem. A,* **105**(15), 3825–8.
Matsui, T. and Ohse, R. W. (1987) *High Temp.-High Press.,* **19**(1), 1–17.
Mattenberger, K., Vogt, O., Spirlet, J. C., and Rebizant, J. (1986) *J. Magn. Magn. Mater.,* **54–57**(1), 539–40.
Matthews, J. R. (1987) *J. Chem. Soc., Faraday Trans., 2,* **83**(7), 1273–85.
Matzke, H. (1982) *Mater. Sci. Monogr.,* **15**(Transp. Non-Stoichiom. Compd.), 203–31.
Matzke, H. (1984) *Solid State Ionics,* **12**, 25–45.
Matzke, H. (1986) *Science of Advanced LMFBR Fuels: Solid State Physics, Chemistry, and Technology of Carbides, Nitrides, and Carbonitrides of Uranium and Plutonium,* North-Holland, New York, 740 pp.
Mazumdar, A. S. G., Natarajan, P. R., and Vaidyanathan, S. (1970) *J. Inorg. Nucl. Chem.,* **32**, 3363.
McAlister, S. P. and Crozier, E. D. (1981) *Solid State Commun.,* **40**, 375.
McCreary, W. J. (1955) *J. Am. Chem. Soc.,* **77**, 2113–14.
McDonald, B. J. and Stuart, W. I. (1960) *Acta Crystallogr.,* **13**, 447.
McKay, H. A. C., Schulz, W. W., Navratil, J. D., Burger, L. L., and Bender, K. P. (1990) The PUREX Process. Part 1: Introduction. Science and Technology of Tributyl Phosphate, vol. 3, *Applications of Tributyl Phosphate in Nuclear Fuel Processing,* CRC Press, Boca Raton, FL, pp. 1–9.
McNally, Jr J. R., and Griffin, P. M. (1959) *J. Opt. Soc. Am.,* **49**, 162–6.
McNeese, J. A., Bowersox, D. F., and Christensen, D. C. (1986) *Proc. Electrochem. Soc.,* **86-1**(Molten Salts), 474–84.
McQueeney, R. J., Lawson, A. C., Migliori, A., Kelley, T. M., Fultz, B., Ramos, M., Martinez, B., Lashley, J. C., and Vogel, S. C. (2004) *Phys. Rev. Lett.,* **92**(14), 146401.
Meadon, G. T. and Lee, J. A. (1962) *Cryogenics,* **2**, 182.
Mendik, M., Wachter, P., Spirlet, J. C., and Rebizant, J. (1993) *Physica B,* **186–188**, 678–80.
Méot-Reymond, S. and Fournier, J. M. (1996) *J. Alloys Compd.,* **232**(1–2), 119–25.
Merciny, E., Gatez, J. M., and Duyckaerts, G. (1978) *Anal. Chim. Acta,* **100**, 329–42.
Merigou, C., Genet, M., Ouillon, N., and Chopin, T. (1995) *New J. Chem.,* **19**(3), 275–85.
Merrill, J. J. and Du Mond, J. W. M. (1958) *Phys. Rev.,* **110**, 79–84.

Merrill, J. J. and Du Mond, J. W. M. (1961) *Ann. Phys. (N.Y.)* **14**, 166–228.
Merz, M. D. (1970) *J. Nucl. Mater.,* **34**, 108–10.
Merz, M. D. (1971) *J. Nucl. Mater.,* **41**, 348–50.
Merz, M. D. (1974) *J. Nucl. Mater.,* **50**, 31–9.
Merz, M. D. and Allen, R. P. (1973) *J. Nucl. Mater.,* **46**, 110.
Merz, M. D. and Nelson, R. D. (1970) Alpha Plutonium, in *Plutonium 1970 and Other Actinides,* vol. 1 (ed. W. N. Miner), The Metallurgical Society of the AIME, Santa Fe, NM, 387 pp.
Merz, M. D., Hammer, J. H., and Kjarmo, H. E. (1974) *J. Nucl. Mater.,* **51**(3), 357–8.
Metivier, H. and Guillaumont, R. (1972) *Radiochem. Radioanal. Lett.,* **10**(1), 27–35.
Meyer, G. and Morss, L. R. (eds.) (1991) Synthesis of Lanthanide and Actinide Compounds, in *Topics in f-element Chemistry*, Kluwer Academic, Boston, MA.
Miedema, A. R. (1973) *J. Less-Common Met.,* **32**(1), 117–36.
Miedema, A. R. (1976) On the Heat of Formation of Plutonium Alloys. *Plutonium 1975 Other Actinides, Proc. Fifth Int. Conf.* (eds. H. Blank and R. Lindner), North-Holland, Amsterdam, The Netherlands, pp. 3–20.
Migliori, A., Baiardo, J. P., and Darling, T. W. (2000) *Los Alamos Science,* **26**(1), 209–25.
Migliori, A., Ledbetter, H., Betts, J., Ramos, M., Harrington, S., and El-Khatib, S. (2004) *Elastic Constants of Plutonium*, Report LA-UR-04-7419, Los Alamos National Laboratory.
Migliori, A., Ledbetter, H., Lawson, A. C., Ramirez, A. P., Miller, D. A., Betts, J. B., Ramos, M., and Lashley, J. C. (2006) *Phys. Rev. B.*, **73**, 052101/1–4.
Mikheev, N. B. and Myasoedov, B. F. (1985) Lower and Higher Oxidation States of Transplutonium Elements in Solutions and Melts, in *Handbook on the Physics and Chemistry of the Actinides* (eds. A. J. Freeman and C. Keller), Elsevier Science, New York, pp. 347–86.
Mikheev, N. B., Rumer, I. A., and Auerman, L. N. (1983) *Radiochem. Radioanal. Lett.,* **59**(5–6), 317–28.
Miles, J. H., Schulz, W. W., Navratil, J. D., Burger, L. L., and Bender, K. P. (1990) The PUREX Process. Part 2: Separation of Plutonium and Uranium. Science and Technology of Tributyl Phosphate, vol. 3. *Applications of Tributyl Phosphate in Nuclear Fuel Processing* (eds. W. W. Schulz and J. D. Navratil), CRC Press, Boca Raton, FL, pp. 11–54.
Mincher, B. J., Fox, R. V., Holmes, R. G. G., Robbins, R. A., and Boardman, C. (2001) *Radiochim. Acta,* **89**(10), 613–17.
Miner, W. N. (1970) *Plutonium 1970 and Other Actinides, Proc. Fourth Int. Conf. on Plutonium and Other Actinides,* Santa Fe, NM (ed. W. N. Miner), Metallurgical Society of AIME, New York, 2 v.
Miner, W. N. and Schonfeld, F. W. (1980) Physical Properties, in *Plutonium Handbook,* vol. 1 (ed. O. J. Wick), American Nuclear Society, La Grange Park, IL, pp. 31–59.
Miner, F. J. and Seed, J. R. (1967) *Chem. Rev.,* **67**, 299–315.
Miner, F. J., De Grazio, R. P., and Byrne, J. T. (1963) *Anal. Chem.,* **35**(9), 1218–23.
Mitchell, A. W. and Lam, D. J. (1971) *J. Nucl. Mater.,* **39**(2), 219–23.
Mitchell, A. W. and Lam, D. J. (1974) *The Actinides: Electronic Structure and Related Properties,* vol. II (eds. A. J. Freeman and J. B. J. Darby), Academic Press, New York, 139 pp.

Mitchell, J. N., Gibbs, F. E., Zocco, T. G., and Pereyra, R. A. (2001) *Metall. Mater. Trans. A,* **32**(3A), 649–59.
Mittal, R., Chaplot, S. L., Schober, H., and Mary, T. A. (2001) *Phys. Rev. Lett.,* **86**, 4692.
Moeller, R. D. and Schonfeld, F. W. (1950) *Alloys of Plutonium with Aluminum*, Report LA-1000, Los Alamos Scientific Laboratory, Los Alamos, NM, 87 pp.
Moll, H., Reich, T., and Szabo, Z. (2000) *Radiochim. Acta,* **88**(7), 411–15.
Moment, R. L. (1968) *J. Cryst. Growth,* **2**(1), 15–25.
Moment, R. (2000) *Los Alamos Science,* **26**(1), 233–7.
Mooney, R. C. L. and Zachariasen, W. H. (1949) *Natl. Nucl. Energy Ser.*, Div IV **14B** (Transuranium Elements, Pt. II) (eds. G. T. Seaborg, J. J. Katz and W. M. Manning), pp. 1442–7.
Moore, K. T., Wall, M. A., Schwartz, A. J., Chung, B. W., Shuh, D. K., Schulze, R. K., and Tobin, J. G. (2003) *Phys. Rev. Lett.,* **90**(19), 196404.
Morales, L. A., Lawson, A. C., Conradson, S., Butler, E. N., Moore, D. P., Ramos, M., Roberts, J. A., and Martinez, B. (2003) *AIP Conf. Proc.,* **673**(Plutonium Futures – The Science), 174–5.
Morgan, J. R. (1970) *Plutonium 1970 and Other Actinides, Proc. Fourth Int. Conf. on Plutonium and Other Actinides,* Santa Fe, NM (ed. W. N. Miner), Metallurgical Society of AIME, 669 pp.
Morgenstern, A. and Choppin, G. R. (1999) *Radiochim. Acta,* **86**(3–4), 109–13.
Morgenstern, A. and Kim, J. I. (1996) *Radiochim. Acta,* **72**(2), 73–7.
Morgenstern, A., Apostolidis, C., Carlos-Marquez, R., Mayer, K., and Molinet, R. (2002) *Radiochim. Acta,* **90**(2), 81–5.
Morss, L. R. (2005) PuF_6 gas pressure in aged cylinders, personal communication, D. L. Clark, Los Alamos, NM.
Morss, L. R. and Fuger, J. (eds.) (1992) *Transuranium Elements: A Half Century,* American Chemical Society, Washington, DC, 562 pp.
Morss, L. R. and Fujino, T. (1988a) *J. Solid State Chem.,* **72**(2), 338–52.
Morss, L. R. and Fujino, T. (1988b) *J. Solid State Chem.,* **72**(2), 353–62.
Morss, L. R., Appelman, E. H., Gerz, R. R., and Martin-Rovet, D. (1994) *J. Alloys Compd.,* **203**(1–2), 289–95.
Moser, J. B. and Kruger, O. L. (1966) *J. Less-Common Met.,* **10**(6), 402–7.
Moskvin, A. I. (1969) *Radiokhimiya,* **11**, 447.
Moskvin, A. I. (1971a) *Sov. Radiochemistry,* **13**, 688–93.
Moskvin, A. I. (1971b) *Radiokhimiya,* **13**, 641.
Moskvin, A. I. and Poznyakov, A. N. (1979) *Russ. J. Inorg. Chem.,* **24**, 1357–62.
Moulin, V. and Moulin, C. (2001) *Radiochim. Acta,* **89**(11–12), 773–8.
Moulin, C., Delorme, N., Berthoud, T., and Mauchien, P. (1988) *Radiochim. Acta,* **44–45**(1), 103–6.
Moulton, G. H. (1944) *Decomposition Products of Plutonyl Nitrate and Plutonium Oxalate*, Report LA-172, Los Alamos Scientific Laboratory, Los Alamos, NM, 10 pp.
Mudher, K. D. S., Krishnan, K., and Iyer, P. N. (1995) *NUCAR 95*, *Proc. Nuclear and Radiochemistry Symp.*, Feb. 21–24, 1995, Kalpakkam, India, pp. 228–9.
Mueller, M. H., Lander, G. H., Hoff, H. A., Knott, H. W., and Reddy, J. F. (1979) *J. Phys. Colloq.*, (4), 68–9.
Mulford, R. N. R. (1965) *Vapor Pressure, Joint Symp. of IUPAC and IAEA on Thermodynamics,* IAEA, Vienna, Austria 231 pp.

Mulford, R. N. R. and Ellinger, F. H. (1958) *J. Phys. Chem.,* **62**, 1466–7.
Mulford, R. N. R., Ellinger, F. H., Hendrix, G. S., and Albrecht, E. D. (1960) The Plutonium–Carbon System. *Plutonium 1960*, *Proc. Int. Conf. on Plutonium Metal*, Grenoble, France (eds. E. Grison, W. B. H. Lord and R. D. Fowler), pp. 301–11.
Mulford, R. N. R., Ellinger, F. H., and Johnson, K. A. (1965) *J. Nucl. Mater.,* **17**(4), 324–9.
Mulford, R. N. R., Ford, J. O., and Hoffman, J. J. (1963) *Thermodynamics of Nuclear Materials, Proc. Symp. on Thermodynamics of Nuclear Materials* 1962, pp.517–25.
Mulford, R. N. R. and Lamar, L. E. (1961) Volatility of Plutonium Oxide. *Plutonium 1960*, *Proc. Int. Conf. on Plutonium Metal*, Grenoble, France (eds. E. Grison, W. B. H. Lord and R. D. Fowler), pp. 411–21.
Mullins, L. J. and Foxx, C. L. (1982) *Direct Reduction of Plutonium-238 Dioxide and Plutonium-239 Dioxide to Metal*, Report LA-9073, Los Alamos National Laboratory, Los Alamos, NM, 19 pp.
Mullins, L. J. and Leary, J. A. (1965) *Ind. Eng. Chem., Process Design Develop.,* **4**(4), 394–400.
Mullins, L. J. and Morgan, A. N. (1981) *Review of Operating Experience at the Los Alamos Plutonium Electrorefining Facility, 1963–1977*, Report LA-8943, Los Alamos National Laboratory, Los Alamos, NM, 24 pp.
Mullins, L. J., Leary, J. A., and Bjorklund, C. W. (1960) *Large-Scale Preparation of High-purity Plutonium Metal by Electrorefining*, Report LAMS-2441, Los Alamos Scientific Laboratory, Los Alamos, NM, 16 pp.
Mullins, L. J., Leary, J. A., and Morgan, A. N. (1963a) *Large Scale Electrorefining of Plutonium from Plutonium–Iron Alloys*, Report LA-3029, Los Alamos Scientific Laboratory, Los Alamos, NM, 35 pp.
Mullins, L. J., Leary, J. A., Morgan, A. N., and Maraman, W. J. (1963b) *Ind. Eng. Chem., Process Design Develop.,* **2**, 20–4.
Mullins, L. J., Beaumont, A. J., and Leary, J. A. (1966) *Distribution of Americium between Liquid Plutonium and a Fused Salt: Evidence for Divalent Americium*, Report LA-3562, Los Alamos Scientific Laboratory, Los Alamos, NM, 26 pp.
Mullins, L. J., Beaumont, A. J., and Leary, J. A. (1968) *J. Inorg. Nucl. Chem.,* **30**(1), 147–56.
Mullins, L. J., Christensen, D. C., and Babcock, B. R. (1982) *Fused Salt Processing of Impure Plutonium dioxide to High-purity Plutonium Metal*, Report LA-9154-MS, Los Alamos National Laboratory, Los Alamos, NM, 26 pp.
Murch, G. E. and Catlow, C. R. A. (1987) *J. Chem. Soc. Faraday Trans. 2,* **83**(7), 1157–69.
Muromura, T. (1982) *J. Nucl. Sci. Technol.,* **19**(8), 638–45.
Muromura, T., Yahata, T., Ouchi, K., and Iseki, M. (1972) *J. Inorg. Nucl. Chem.,* **34**(1), 171–3.
Murzin, A. A., Babain, V. A., Shadrin, A. Y., Kamachev, V. A., Romanovskii, V. N., Starchenko, V. A., Podoinitsyn, S. V., Revenko, Y. A., Logunov, M. V., and Smart, N. G. (2002a) *Radiochemistry,* **44**(4), 410–15.
Murzin, A. A., Babain, V. A., Shadrin, A. Y., Smirnov, I. V., Lumpov, A. A., Gorshkov, N. I., Miroslavov, A. E., and Muradymov, M. A. (2002b) *Radiochemistry,* **44**(5), 467–71.
Musante, Y. and Ganivet, M. (1974) *J. Electroanal. Chem.,* **57**(2), 225–30.

Muscatello, A. C. and Killion, M. E. (1990) *Chloride Anion Exchange Coprocessing for Recovery of Plutonium from Pyrochemical Residues and Cs_2PuCl_6 Filtrate*, Report RFP–4325, EG & G Rocky Flats, Golden, CO, 19 pp.
Nachtrieb, N. H. and Lawson, A. W. (1955) *J. Chem. Phys.,* **23**(7), 1193–5.
Nagarajan, G. (1962) *Bull. Soc. Chim. Belg.,* **71**(1–2), 88–1.
Nair, G. M., and Joshi, J. K. (1981) *J. Indian Chem. Soc.,* **58**, 311.
Naito, K., Tsuji, T., Matsui, T., Fujino, T., Yamashita, T., and Ohuchi, K. (1992) *Defect Chemistry of Plutonium Oxides*, in *Transuranium Elem. Symp.* (eds. L. R. Morss and J. Fuger), American Chemical Society, Washington, DC, pp. 440–50.
Nakayama, Y. (1971) *J. Inorg. Nucl. Chem.,* **33**(12), 4077–84.
Nash, K., Noon, M. E., Fried, S., and Sullivan, J. C. (1980) *Inorg. Nucl. Chem. Lett.,* **16**(1), 33–5.
Nash, K. L. (1993) *Solvent Extr. Ion Exc.,* **11**(4), 729–68.
Nash, K. L. and Cleveland, J. M. (1983) *ACS Symp. Ser.,* **216**(Plutonium Chem.), 251–62.
Navratil, J. D. (1969a) *Dissolution of Impure Plutonium Tetrafluoride in Nitric Acid*, Report RFP-1118, Dow Chemical Company, Rocky Flats Division, Golden, CO, 4 pp.
Navratil, J. D. (1969b) *Dissolution of Plutonium Tetrafluoride in Nitric Acid*, Report RFP-1151, Dow Chemical Company, Rocky Flats Division, Golden, CO, 5 pp.
Navratil, J. D. (1969c) *J. Inorg. Nucl. Chem.,* **31**(11), 3676–80.
Neck, V. and Kim, J. I. (2001) *Radiochim. Acta,* **89**(1), 1–16.
Neeb, K.-H. (1997) *The Radiochemistry of Nuclear Power Plants with Light Water Reactors,* Walter de Gruyter, Berlin, New York, 725 pp.
Nelson, R. D. (1980) Solid State Reactions, in *Plutonium Handbook,* vol. 2, (ed. O. J. Wick), American Nuclear Society, La Grange Park, IL, 101 pp.
Nelson, T. O. (1998) *WM'98 Proc.*, Tucson, AZ, Mar. 1–5, 1998, pp. 1234–9.
Nelson, R. D., Bierlein, T. K., and Bowman, F. E. (1965) *The Steady-State Creep of High-Purity Plutonium*, Report BNWL-32, Battelle Pacific Northwest National Laboratory, 20 pp.
Nelson, G. C., Saunders, B. G., and John, W. (1969) *Phys. Rev.,* **188**(1), 4–6.
Nelson, G. C., Saunders, B. G., and Salem, S. I. (1970) *Z. Phys.,* **235**(4), 308–12.
Nelson, E. J., Blobaum, J. M., Wall, M. A., Allen, P. G., Schwartz, A. J., and Booth, C. H. (2003a) *AIP Conf. Proc.,* **673**(Plutonium Futures – The Science), 187–9.
Nelson, E. J., Blobaum, K. J. M., Wall, M. A., Allen, P. G., Schwartz, A. J., and Booth, C. H. (2003b) *Phys. Rev. B,* **67**(22), 224206.
Neu, M. P., Hoffman, D. C., Roberts, K. E., Nitsche, H., and Silva, R. J. (1994) *Radiochim. Acta,* **66–67**, 251–8.
Neu, M. P., Matonic, J. H., Smith, D. M., and Scott, B. L. (2000) *AIP Conf. Proc.,* **532** (Plutonium Futures – The Science), 381–2.
Neu, M., P., Ruggiero, C. E., and Francis, A. J. (2002) Bioinorganic Chemistry of Plutonium and Interactions of Plutonium with Microorganisms and Plants, in *Advances in Plutonium Chemistry 1967–2000* (ed. D. C. Hoffman), American Nuclear Society and the University Research Alliance, La Grange Park, IL, pp. 169–203.
Neuilly, M., Bussac, J., Frejacques, C., Nief, G., Vendryes, G., and Yvon, J. (1972) *C. R. Acad. Sci., Ser. D,* **275**(17), 1847–9.
Newton, T. W. (1958) *J. Phys. Chem.,* **62**, 943–7.
Newton, T. W. (1959) *J. Phys. Chem.,* **63**, 1493.

Newton, T. W. (1975) *Kinetics of the Oxidation–Reduction Reactions of Uranium, Neptunium, Plutonium, and Americium in Aqueous Solutions*, Los Alamos Scientific Laboratory, Report ERDA Critical Review Series, TID 26506, 131 pp.
Newton, T. W. (2002) Redox Reactions of Plutonium Ions in Aqueous Solutions, in *Advances in Plutonium Chemistry 1967–2000* (ed. D. C. Hoffman), American Nuclear Society and the University Research Alliance, La Grange Park, IL, pp. 24–60.
Newton, T. W. and Baker, F. B. (1956) *J. Phys. Chem.,* **60**, 1417–21.
Newton, T. W. and Baker, F. B. (1963) *J. Phys. Chem.,* **67**, 1425.
Newton, T. W. and Burkhart, M. J. (1971) *Inorg. Chem.,* **10**(10), 2323–6.
Newton, T. W. and Cowan, G. A. (1960) *J. Phys. Chem.,* **64**, 244.
Newton, T. W. and Hobart, D. E. (2004) *J. Nucl. Mater.,* **334**(2–3), 222–4.
Newton, T. W. and Montag, T. (1976) *Inorg. Chem.,* **15(11)**, 2856–61.
Newton, T. W. and Rundberg, V. L. (1984) *Mater. Res. Soc. Symp. Proc.,* **26**(Sci. Basis Nucl. Waste Manage. 7), 867–73.
Newton, T. W. and Sullivan, J. C. (1986) in *Handbook on the Physics and Chemistry of the Actinides* (eds. A. J. Freeman and C. Keller), Elsevier Science Publishers, Amsterdam, p. 387.ch. 10,
Newton, T. W., Hobart, D. E., and Palmer, P. D. (1986a) *The Preparation and Stability of Pure Oxidation States of Neptunium, Plutonium, and Americium*, Report LA-UR-86-967, Los Alamos National Laboratory, Los Alamos, NM, 11 pp.
Newton, T. W., Hobart, D. E., and Palmer, P. D. (1986b) *Radiochim. Acta,* **39**(3), 139–47.
Nikitenko, S. I. (1988) *Radiokhimiya,* **30**(4), 448–52.
Nikitenko, S. I. and Ponomareva, O. G. (1989) *Radiokhimiya,* **31**(2), 58–63 (pp 195–9 in English translation).
Nikitina, G. P., Ivanov, Y. E., Listopadov, A. A., and Shpunt, L. B. (1997a) *Radiochemistry,* **39**(2), 109–22.
Nikitina, G. P., Ivanov, Y. E., Listopadov, A. A., and Shpunt, L. B. (1997b) *Radiochemistry,* **39**(1), 12–25.
Nikonov, M. V., Gogolev, A. V., Tananaev, I. G., and Myasoedov, B. F. (2004) *Radiochemistry,* **46**(4), 340–2.
Nikonov, M. V., Gogolev, A. V., Tananaev, I. G., and Myasoedov, B. F. (2005) *Mendeleev Commun.,* **Mar–Apr 2005**(2), 50–2.
Nitsche, H. and Silva, R. J. (1996) *Radiochim. Acta,* **72**, 65–72.
Norling, B. K. and Steinfink, H. (1966) *Inorg. Chem.,* **5**(9), 1488–91.
Ockenden, D. W. and Welch, G. A. (1956) *J. Chem. Soc., Abstracts*: 3358–63.
Oetting, F. L. (1967) *Chem. Rev.,* **67**(3), 261–97.
Oetting, F. L. (1982) *J. Nucl. Mater.,* **105**(2–3), 257–61.
Oetting, F. L. and Adams, J. B. (1983) *J. Chem. Thermodyn.,* **15**(6), 537–54.
Oetting, F. L., Rand, M. H., and Ackerman, R. J. (1976) *The Chemical Thermodynamics of Actinide Elements and Compounds,* part 1, The Actinide Elements, IAEA, Vienna, Austria, 111 pp.
Ofte, D. and Rohr, W. G. (1965) *J. Nucl. Mater.,* **15**(3), 231.
Ofte, D. and Wittenberg, L. J. (1964) *Am. Soc. Metals, Trans. Quart.,* **57**(4), 916–23.
Ofte, D., Rohr, W. G., and Wittenberg, L. J. (1966) *Trans. Amer. Nucl. Soc.,* **9**, 5–6.
Ogard, A. E. (1970) High-Temperature Heat Content of Plutonium Dioxide. *Plutonium 1970, Proc. Fourth Int. Conf. on Plutonium and Other Actinides*, Santa Fe, NM (ed. W. N. Miner), pp. 78–83.

Ogard, A. E. and Leary, J. A. (1970) *Plutonium Carbides*, Report LA-4415, Los Alamos Scientific Laboratory, Los Alamos, NM, 6 pp.

Ogard, A. E., Pritchard, W. C., Douglass, R. M., and Leary, J. A. (1962) *J. Inorg. Nucl. Chem.,* **24**, 29–34.

Ogawa, T., Kobayashi, F., Sato, T., and Haire, R. G. (1998) *J. Alloys Compd.,* **271–273**, 347–54.

Ohse, R. W. and Olson, W. M. (1970) *Plutonium 1970 and Other Actinides, Proc. Fourth Int. Conf. on Plutonium and Other Actinides,* Santa Fe, NM, Oct. 5–9, 1970 (ed. W. N. Miner), AIME, New York, 743.

Oi, N. (1995) *Proc. Fifth Int. Conf. on Radioactive Waste Management and Environmental Remediation,* vol. 1, Berlin, Sept. 3–7, 1995, pp. 469–70.

Okajima, S. and Reed, D. T. (1993) *Radiochim. Acta,* **60**(4), 173–84.

Oldham, S. M., Schake, A. R., Burns, C. J., Morgan, III, A. N., Schnabel, R. C., Warner, B. P., Costa, D. A., and Smith, W. H. (2000) *AIP Conf. Proc.,* **532**(Plutonium Futures – The Science), 230–1.

Olsen, C. E. and Elliott, R. O. (1962) *J. Phys. Chem. Solids,* **23**, 1225.

Olsen, C. E., Sandenaw, T. A., and Herrick, C. C. (1955) *The Density of Liquid Plutonium Metal*, Report LA-2358, Los Alamos Scientific Laboratory, Los Alamos, NM, 17 pp.

Olsen, C. E., Comstock, A. C., and Sandenaw, T. A. (1992) *J. Nucl. Mater.,* **195**, 312.

Olson, G. B. and Adler, P. H. (1984) *Scripta Met.,* **18**(4), 401–6.

Olson, W. M. and Mulford, R. N. R. (1964) *J. Phys. Chem.,* **68**(5), 1048–51.

Olson, W. M. and Mulford, R. N. R. (1967) *Thermodynamics of the Plutonium Carbides*, Report LA-DC-8012, Los Alamos Scientific Laboratory, Los Alamos, NM, 19 pp.

Onoe, J. (1997) *J. Phys. Soc. Jpn.,* **66**(8), 2328–36.

Orlemann, E. F. (1944) *Distribution of 49 [Pu-239] between Aqueous and Non-Aqueous Phases*. Fundamental Chemistry of 49.

Orme, J. T., Faiers, M. E., and Ward, B. J. (1976) The Kinetics of the Delta to Alpha Transformation in Plutonium Rich Pu-Ga Alloys, *5th Int. Conf. on Plutonium and Other Actinides 1975,* Sept. 10–13, 1975, Baden-Baden, West Germany (eds. H. Blank and R. Linder), 1976, North-Holland, Amsterdam, The Netherlands, pp.761–73.

Paffett, M. T., Farr, D., and Kelly, D. (2003a) *AIP Conf. Proc.,* **673**(Plutonium Futures – The Science), 193–5.

Paffett, M. T., Kelly, D., Joyce, S. A., Morris, J., and Veirs, K. (2003b) *J. Nucl. Mater.,* **322**(1), 45–56.

Pagès, M. and Freundlich, W. (1976) Some Actinides Double Orthovanadates and Orthoarsenates: Structural "Evolution" Due to Cationic and Anionic Substitutions. *Plutonium 1975 Other Actinides*, *Proc. Fifth Int. Conf.* (eds. H. Blank and R. Lindner), North-Holland, Amsterdam, pp. 205–7.

Pagès, M., Nectoux, F., and Freundlich, W. (1971a) *Radiochem. Radioanal. Lett.,* **8**(3), 147–50.

Pagès, M., Nectoux, F., and Freundlich, W. (1971b) *CR Acad. Sci. C. Chim.,* **273**(16), 978–80.

Palmer, D. A. and Nguyen- Trung, C. (1995) *J. Solution Chem.,* **24**(12), 1281–91.

Pansoy-Hjelvik, M. E., Brock, J., Nixon, J. Z., Moniz, P., Silver, G., and Ramsey, K. B. (2001) Purification and Neutron Emission Reduction of Plutonium-238 Oxide by Nitrate Anion Exchange Processing. *Space Technology and Applications International Forum (STAIF-2001)*, Albuquerque, NM, American Institute of Physics, *AIP Conf. Proc.*, **52,** 770–3.

Paprocki, S. J., Keller, D. L., Alexander, C. A., and Pardue, W. M. (1962a) *Volatility of Plutonium Dioxide in Nonreducing Atmospheres*, Report BMI-1591, Battelle Memorial Institute, Columbus, OH, 16 pp.

Paprocki, S. J., Keller, D. L., and Purdue, W. M. (1962b) *The Chemical Reactions of Plutonium Dioxide with Reactor Materials*, Report BMI-1580, Battelle Memorial Institute, Columbus, OH, 12 pp.

Pardue, W. M. and Keller, D. L. (1964) *J. Am. Ceram. Soc.,* **47**(12), 610–14.

Pardue, W. M., Storhok, V. W., Smith, R. A., Bonnell, P. H., Gates, J. E., and Keller, D. L. (1964a) *Synthesis, Fabrication, and Chemical Reactivity of Pu Mononitride*, Report BMI-1693, Battelle Memorial Institute, Columbus, OH, 38 pp.

Pardue, W. M., Storhok, V. W., Smith, R. A., and Keller, D. L. (1964b) *An Evaluation of Plutonium Compounds as Nuclear Fuels*, Report BMI-1698, Battelle Memorial Institute, Columbus, OH, 22 pp.

Pardue, W. M., Storhok, V. W., and Smith, R. A. (1967) *Chemical Engineering Progress, Symposium Series,* **63**(80), 142–6.

Parsonnet, V. (2004) personal communication, L. R. Morss.

Parsonnet, V., Berstein, A. D., and Perry, G. Y. (1990) *Am. J. Cardiol.,* **66**(10), 837–42.

Pascard, R. (1962) *Plansee Proc.,* **1961**, 387–419.

Pashalidis, I., Czerwinski, K. R., Fanghanel, T., and Kim, J. I. (1997) *Radiochim. Acta,* **76**(1–2), 55–62.

Patil, S. K. and Ramakrishna, V. V. (1976) *J. Inorg. Nucl. Chem.,* **38**(5), 1075–8.

Paxton, H. C. (1975) *Los Alamos Critical-Mass Data*, Report LA-3067-MS, Los Alamos Scientific Laboratory, Los Alamos, NM, 57 pp.

Paxton, H. C. and Pruvost, N. L. (1987) *Critical Dimensions of Systems Containing Uranium-235, Plutonium-239 and Uranium-233: 1986 Revision*, Report LA-10860-MS, Los Alamos National Laboratory, Los Alamos, NM, 205 pp.

Peddicord, K. L., Lazarev, L. N., and Jardine, L. J. (eds.) (1998) *Nuclear Materials Safety Management, NATO Advanced Research Workshop on Nuclear Materials Safety Management* (*1997: Amarillo, TX*). NATO ASI series. Partnership sub-series 1, Disarmament technologies; vol. 20. Kluwer Academic, Boston, MA, 378 pp.

Pekarek, V. and Marhol, M. (1991) Historical Background of Inorganic Ion Exchangers, their Classification, and Present Status, in *Inorganic Ion Exchangers in Chemical Analysis* (eds. M. Qureshi and K. G. Varshney), CRC Press, Boca Raton, FL, pp. 1–32.

Penneman, R. A. and Paffett, M. T. (2004) personal communication, D. L. Clark.

Penneman, R. A. and Paffett, M. T. (2005) *J. Solid State Chem.,* **178**(2), 563–6.

Penneman, R. A., Sturgeon, G. D., Asprey, L. B., and Kruse, F. H. (1965) *J. Am. Chem. Soc.,* **87**(24), 5803–4.

Peppard, D. F., Studier, N. H., Gergel, N. V., Mason, G. W., Sullivan, J. C., and Mech, J. F. (1951) *J. Am. Chem. Soc.,* **73**, 2529–31.

Pepper, M. and Bursten, B. E. (1991) *Chem. Rev.,* **91**(5), 719–41.

Peretrukhin, V. F., Shilov, V. P., Pikaev, A. K., and Delegard, C. H. (1995) *Alkaline Chemistry of Transuranium Elements and Technetium Elements and Technetium and the Treatment of Alkaline Radioactive Wastes*, Report WHC-EP-0817, Westinghouse Hanford Company, 172 pp.

Peterson, J. R. (1995) *J. Alloys Compd.,* **223**, 180–4.

Peterson, D. E. and Kassner, M. E. (1988) *Bull. Alloy Phase Diagr.,* **9**, 261.

Peterson, S. and Wymer, R. G. (1963) *Chemistry in Nuclear Technology,* Pergamon Press, Oxford, England.
Petit, L., Svane, A., Szotek, Z., and Temmerman, W. M. (2003) *Science,* **301**(5632), 498–501.
Petit, L., Svane, A., Temmerman, W. M., and Szotek, Z. (2002) *Eur. Phys. J. B,* **25**(2), 139–46.
Pettifor, D. G. (1996) in *Physical Metallurgy* (eds. R. W. Cahn and P. Haasen), Elsevier Science, Amsterdam, The Netherlands, 47 pp.
Phipps, K. D. and Sullenger, D. B. (1964) *Science,* **145**(3636), 1048–9.
Phipps, T. E., Sears, G. W., Seifert, R. L., and Simpson, O. C. (1949) *Natl. Nucl. Energy Ser.*, Div. IV, **14B**(Transuranium Elements, Pt. I), (eds. G. T. Seaborg, J. J. Katz, and W. M. Manning), McGraw-Hill, New York, 682–703.
Phipps, T. E., Sears, G. W., Seifert, R. L., and Simpson, O. C. (1950a) *J. Chem. Phys.,* **18**(5), 713–23.
Phipps, T. E., Sears, G. W., and Simpson, O. C. (1950b) *J. Chem. Phys.,* **18**, 724–34.
Phipps, T. E., Sears, G. W., Seifert, R. L., and Simpson, O. C. (1955) *Vapor Pressure of Liquid Plutonium*, *Proc. Int. Conf. on the Peaceful Uses of Atomic Energy*, Geneva, 7, pp. 382–5.
Pijanowski, S. W. and DeLucas, L. S. (1960) *Melting Points in the System PuO_2-UO_2*, Report KAPL-1937, KAPL General Electric Co., Schenectady, N.Y., pp. 1–5.
Pitner, W. R., Bradley, A. E., Rooney, D. W., Sanders, D., Seddon, K. R., Thied, R. C., and Hatter, J. E. (2003) *NATO Sci. Ser. II: Math. Phys. Chem.,* **92**(Green Industrial Applications of Ionic Liquids), 209–26.
Pons, F., Barbe, B., and Roux, C. (1972) *J. Appl. Crystallogr.,* **5**, 47.
Poole, D. M. and Nichols, J. L. (1961) *The Plutonium Cobalt System*, Report AERE-R-3609, UK Atomic Energy Authority Research Group.
Poole, D. M., Williamson, G. K., and Marples, J. A. C. (1957) *J. I. Met.,* **86**(4), 172–6.
Poskanzer, A. M. and Foreman, B. M. (1961) *J. Inorg. Nucl. Chem.,* **16**(3–4), 323–36 and references therein.
Potter, P. E. (1975) *MTP Int. Rev. Sci.: Inorg. Chem., Ser.2,* **7**, 257–315.
Potter, P. E. (1991) The Actinide Borides, in *Handbook on the Physics and Chemistry of the Actinides,* (eds. A. J. Freeman and C. Keller), vol. 6, North-Holland, Amsterdam, The Netherlands, 39 pp.
Powell, R. F. (1960) Thermal Conductivity of Plutonium, in *Plutonium 1960,* (eds. E. Grison, W. B. H. Lord and R. D. Fowler), vol. 1, Cleaver-Hume Press, London, 107 pp.
Preston, J. S. and du Preez, A. C. (1995) *Solvent Extr. Ion Exch.,* **13**(3), 391–413.
Pustovalov, A. A., Shapovalov, V. P., Bovin, A. V., and Fedorets, V. I. (1986) *At. Energ.,* **60**(2), 125–9.
Rabideau, S. W. (1953) *J. Am. Chem. Soc.,* **75**, 798–801.
Rabideau, S. W. (1956) *J. Am. Chem. Soc.,* **78**(12), 2705–7.
Rabideau, S. W. (1957) *J. Am. Chem. Soc.,* **79**(24), 6350–3.
Rabideau, S. W. and Cowan, H. D. (1955) *J. Am. Chem. Soc.,* **77**(23), 6145–8.
Rabideau, S. W. and Kline, R. J. (1958) *J. Phys. Chem. A,* **62**, 617–20.
Rabideau, S. W. and Masters, B. J. (1963) *J. Phys. Chem.,* **67**, 318–23.

Rabideau, S. W., Bradley, M. J., and Cowan, H. D. (1958) *Alpha-particle Oxidation and Reduction in Aqueous Plutonium Solutions*, Report USAEC-LAMS-2236, Los Alamos Scientific Laboratory, 28 pp.

Rabideau, S. W., Asprey, L. B., Keenan, T. K., and Newton, T. W. (1959) *Proc. Second Int. Conf. Peaceful Uses of Atomic Energy,* vol. 28, Geneva, pp. 361–72.

Rafalski, A. L., Harvey, M. R., and Riefenberg, D. H. (1967) *ASM Trans. Q,* **60**(4), 721.

Rai, D., Hess, N. J., Felmy, A. R., Moore, D. A., Yui, M., and Vitorge, P. (1999) *Radiochim. Acta,* **86**(3–4), 89–99.

Rai, D., Bolton, Jr, H., Moore, D. A., Hess, N. J., and Choppin, G. R. (2001) *Radiochim. Acta,* **89**(2), 67–74.

Rainey, R. H. (1959) *Chemistry of Plutonium(IV) Polymer*, Report CF-59-12-95, Oak Ridge National Laboratory, 4.

Raj, D. D. A., Nalini, S., Viswanathan, R., and Balasubramanian, R. (1999) *Proc. Eighth ISMAS Symp. on Mass Spectrometry,* vol. II, Dec. 7–9, 1999 (ed. S. K. Aggarwal), Indian Institute of Chemical Technology, Hyderabad, Indian Society for Mass Spectrometry, Mumbai, p. 847.

Rance, P. and Zilberman, B. (2002) *J. Nucl. Sci. Technol.*, (Suppl. 3), 375–8.

Rand, M. H. (1966) *Atom. Energy Rev.,* **4**(1), 7–51.

Rao, P. R. V. and Kolarik, Z. (1996) *Solvent Extr. Ion. Exch.,* **14**(6), 955–93.

Rao, G. S., Subramanian, M. S., and Welch, G. A. (1963) *J. Inorg. Nucl. Chem.,* **25**(10), 1293–5.

Rao, P. R. V., Bagawde, S. V., Ramakrishna, V. V., and Patil, S. K. (1978) *J. Inorg. Nucl. Chem.,* **40**(1), 123–7.

Rasmussen, M. J. and Hopkins, H. H., Jr (1961) *J. Ind. Eng. Chem.,* **53**, 453–7.

Ravat, B., Jolly, L., Valot, C., and Baclet, N. (2003) *AIP Conf. Proc.,* **673**(Plutonium Futures – The Science), 7–8.

Raynor, J. B. and Sakman, J. F. (1965) Oxidation, in *Proc. Third Int. Conf. on Plutonium 1965* (eds. A. E. Kay and M. B. Waldron), Cleaver - Hume, London, England, 575 pp.

Reader, J. and Corliss, C. H. (1980) *Wavelengths and Transition Probabilities for Atoms and Atomic Ions*, part I, *Wavelengths*, Report NSRDS-NBS 68, Natl. Meas. Lab., Natl. Bur. Stand., Washington, DC, pp. 1–357.

Reavis, J. G. and Leary, J. A. (1970) *Plutonium 1970 and Other Actinides, Proc. Fifth Int. Conf. on Plutonium and Other Actinides,* Baden-Baden, West Germany (ed. W. N. Miner), North-Holland, New York, 809 pp.

Reavis, J. G., Johnson, K. W. R., Leary, J. A., Morgan, A. N., Ogard, A. E., and Walsh, K. A. (1960) *The Preparation of Plutonium Halides for Fused Salt Studies, Extractive and Physical Metallurgy of Plutonium and its Alloys, Symp.,* San Francisco, CA (ed. W. D. Wilkinson), Interscience Publishers, New York, pp. 89–100.

Rebizant, J., Bednarczyk, E., Boulet, P., Fuchs, C., and Wastin, F. (2000) *Single Crystal Growth of* $(U_{1-x}Pu_x)O_2$ *Mixed Oxides. AIP Conf. Proc.,* **532**(Plutonium Futures–The Science), 355–6.

Reilly, S. D., Neu, M. P., and Runde, W. (2000) *AIP Conf. Proc.,* **532**(Plutonium Futures – The Science), 269–71.

Reshetnikov, F. G. (2003) *Mendeleev Commun.*, (4), 155–6.

Reynolds, L. T. and Wilkinson, G. (1956) *J. Inorg. Nucl. Chem.,* **2**, 246.

Rice, R. W. (1983) *Am. Ceram. Soc. Bull.,* **62**(8), 889–92.

Richards, S. M. and Kasper, J. S. (1969) *Acta Crystallogr. B,* **B25**, 237.
Richmann, M. K., Reed, D. T., Kropf, A. J., Aase, S. B., and Lewis, M. A. (1999) *XAFS/XANES Studies of Plutonium-loaded Sodalite/glass Waste Forms*, *Annual Meeting Proc. Institute of Nuclear Materials Management*, 40, pp. 668–75.
Riha, J. and Trevorrow, L. (1965) *Chemical Engineering Division Semiannual Report, January – June 1967*, Report ANL-7375, Argonne National Laboratory, pp. 54–6.
Riley, B. (1970) *Sci. Ceram.,* **5**, 83–109.
Rinehart, G. H. (1992) *Space Nucl. Power Syst.,* **10**, 39–43.
Rinehart, G. H. (2001) *Prog. Nucl. Energ.,* **39**(3–4), 305–19.
Robbins, J. L. (2004) *J. Nucl. Mater.,* **324**(2/3), 125–33.
Robouch, P. and Vitorge, P. (1987) *Inorg. Chim. Acta,* **140**, 239–42.
Roepenack, H., Schneider, V. W., and Druckenbrodt, W. G. (1984) *Am. Ceram. Soc. Bull.,* **63**(8), 1051–3.
Rogers, R. D. and Seddon, K. R., Eds. (2002) *ACS Symp. Ser.* **118**(Ionic Liquids – Industrial Applications for Green Chemistry), American Chemical Society, Washington, DC.
Rogl, P. and Potter, P. E. (1997) *J. Phase Equilib,* **18**(5), 467–73.
Rogozina, E. M., Konkina, L. F., and Popov, D. K. (1973) *Radiokhimiya,* **15**(1), 61–3.
Rolland, B. L., Molinie, P., Colombet, P., and McMillan, P. F. (1994) *J. Solid State Chem.,* **113**(2), 312–19.
Rollefson, G. K. and Dodgen, H. W. (1943) *Report on Spectrographic Analysis Work*, Report CK-812.
Romanovski, V. V., White, D. J., Xu, J., Hoffman, D. C., and Raymond, K. N. (1999) *Solvent Extr. Ion Exch.,* **17**(1), 55–71.
Ronchi, C., Sheindlin, M., Musella, M., and Hyland, G. J. (1999) *J. Appl. Phys.,* **85**(2), 776–89.
Ronchi, C., Capone, F., Colle, J. Y., and Hiernaut, J. P. (2000) *J. Nucl. Mater.,* **280**(1), 111–15.
Roof, R. B., Jr. (1973) *Adv. X. Ray Anal.,* **16**, 396–400.
Roof, R. B. (1989) *X-ray Diffraction Data for Plutonium Compounds: Plutonium and Plutonium Binary Compounds*, Los Alamos National Laboratory, Report LA-11619, 3 volumes.
Rose, R. L., Robbins, J. L., and Massalski, T. B. (1970) *J Nucl. Mater.,* **36**(1), 99–107.
Rosen, S., Nevitt, M. V., and Mitchell, A. W. (1963) *J. Nucl. Mater.,* **10**(2), 90–8.
Rosen, S., Nevitt, M. V., and Mitchell, A. W. (1964) *U-Pu-C Ternary Phase Diagram Below 50 Atomic Percent Carbon*, Report ANL-6435, Argonne National Laboratory, Argonne, IL, 107 pp.
Rosen, M., Erez, G., and Shtrikman, S. (1969) *J. Phys. Chem. Solids,* **30**(5), 1063–70.
Rosenthal, M. W., Rahman, Y. E., Moretti, E. S., and Cerny, E. A. (1975) *Radiat. Res.,* **63**(2), 262–74.
Rossat-Mignod, J., Lander, G. H., and Burlet, P. (1984) in *Handbook on the Physics and Chemistry of Actinides,* vol. 1 (eds. A. J. Freeman and G. H. Lander), North-Holland, Amsterdam, 415 pp.
Rothe, J., Denecke, M. A., Neck, V., Mueller, R., and Kim, J. I. (2002) *Inorg. Chem.,* **41**(2), 249–58.
Rothe, J., Walther, C., Denecke, M. A., and Fanghaenel, T. (2004) *Inorg. Chem.,* **43**(15), 4708–18.

Ruggiero, C. E., Matonic, J. H., Neu, M. P., and Reilly, S. P. (2000) *AIP Conf. Proc.,* **532**(Plutonium Futures – The Science), 284–5.

Ruggiero, C. E., Matonic, J. H., Reilly, S. D., and Neu, M. P. (2002) *Inorg. Chem.,* **41**(14), 3593–5.

Rundberg, R. S., Mitchell, A. J., Triay, I. R., and Torstenfelt, N. B. (1988) *Mater. Res. Soc. Symp. Proc.,* **112**(Sci. Basis Nucl. Waste Manage. 11), 243–8.

Runde, W. (2005a) Preparation and characterization of tetravalent plutonium oxalate compounds, personal communication, D. L. Clark, Los Alamos, NM.

Runde, W. (2005b) Preparation and characterization of peroxocarbonato complexes of tetravalent plutonium, personal communication, D. L. Clark, Los Alamos, NM.

Runde, W., Conradson, S. D., Wes Efurd, D., Lu, N., Van Pelt, C. E., and Tait, C. D. (2002) *Appl. Geochem.,* **17**(6), 837–53.

Runde, W., Bean, A., and Scott, B. L. (2003a) *AIP Conf. Proc.,* **673**(Plutonium Futures – The Science), 23–5.

Runde, W., Bean, A. C., Albrecht-Schmitt, T. E., and Scott, B. L. (2003b) *Chem. Commun.*, 478.

Runnalls, O. J. C. (1956) *Can. J. Chem.,* **34**(2), 133–45.

Runnalls, O. J. C. (1958) *The Preparation of Plutonium–Aluminum and Other Plutonium Alloys*, Report AECL-543, Atomic Energy Canada Ltd., Chalk River, 25 pp.

Runnalls, O. J. C. (1965) *Phase-equilibrium Studies on the Aluminum–Plutonium System*, Report AECL-2275, Atomic Energy Canada Ltd., Chalk River, 20 pp.

Runnalls, O. J. C. and Boucher, R. R. (1955) *Acta Crystallogr.,* **9**, 592.

Russell, L. E., Harrison, J. D. L., and Brett, N. H. (1960) *J. Nucl. Mater.,* **2**, 310–20.

Russell, L. E., Brett, N. H., Harrison, J. D. L., and Williams, J. (1962) *J. Nucl. Mater.,* **5**, 216–27.

Russell, L. E. (1964) *Carbides in Nuclear Energy*, vol. 1, *Physical and Chemical Properties; Phase Diagrams;* vol. 2, *Preparation and Fabrication; Irradiation Behavior*, 966 pp.

Ryan, J. L. (1959) *Concentration and Final Purification of Neptunium by Anion Exchange*, Report HW-59193 Rev, Hanford Works, 22 pp.

Ryan, J. L. (1960) *J. Phys. Chem.,* **64**(10), 1375–85.

Ryan, J. L. (1975) Anion Exchange Reactions, in *Gmelin Handbook of Inorganic Chemistry, Transuranic Elements* (ed. G. Koch), Springer-Verlag, New York. [D2 Chemistry in Solution: 418 and 432.]

Ryan, J. L. and Bray, L. A. (1980) *ACS Symp. Ser.* **117**(Actinide Sep.), American Chemical Society, Washington, DC, 499–514.

Ryan, J. L. and Joergensen, C. K. (1964) *Mol. Phys.,* **7**(1), 17–29.

Rykov, A. G., Timofeev, G. A., and Yakovlev, C. N. (1969) *Radiokhimiya,* **11(4)**, 413–18 (pp 403–407 in English translation).

Sackman, J. F. (1960) The Atmospheric Oxidation of Plutonium Metal. *Plutonium 1960*, *Proc. Int. Conf. Plutonium Met.*, Grenoble, France (ed. E. Grison, W. B. H. Lord and R. D. Fowler), pp. 222–9.

Sadigh, B. and Wolfer, W. G. (2005) *Phys. Rev. B.* **70**(20), 205122/1–12.

Sakurai, S., Tachimori, S., Akatsu, J., Kimura, T., Yoshida, Z., Mutoh, H., Yamashita, T., and Ohuchi, K. (1989) *Nihon Genshiryoku Gakkaishi,* **31**(11), 1243–50.

Sakurai, S., Usuda, S., Ami, N., Hirata, M., Wakamatsu, S., and Tachimori, S. (1993) *Nihon Genshiryoku Gakkaishi,* **35**(2), 147–54.

Sandenaw, T. A. (1960a) *Phys. Chem. Solids,* **16**, 329.

Sandenaw, T. A. (1960b) *The Thermal Expansion of Plutonium Metal below 300 K, Proc. Second Int. Conf. on Plutonium Metallurgy: Plutonium 1960,* Grenoble, France vol. 1, (eds. E. Grison, W. B. H. Lord, and R. D. Fowler), Cleaver-Hume Press, London, pp. 79–90.

Sandenaw, T. A. (1961) *Results of Measurements of Physical Properties of Plutonium metal*. in *The Metal Plutonium* (eds. A. S. Coffinberry and W. N. Miner), University of Chicago Press Chicago, IL, 154 pp.

Sandenaw, T. A. (1962) *Phys. Chem. Solids,* **23**(Sep), 1241–8.

Sandenaw, T. A. (1963) *J. Nucl. Mater.,* **10**(3), 165–72.

Sandenaw, T. A. and Gibney, R. B. (1958) *Phys. Chem. Solids,* **6**, 81.

Sandenaw, T. A. and Gibney, R. B. (1971) *J. Chem. Thermodyn.,* **3**, 85.

Sandenaw, T. A. and Harbur, D. R. (1973) *J. Phys. Chem. Solids,* **34**(9), 1487–95.

Sano, T., Tanaka, O., Akimoto, I., Imoto, S., Kikuchi, T., Ichikawa, M., Watanabe, H., Nishio, G., and Shimokawa, J. (1971) *Nihon Genshiryoku Gakkaishi,* **13**(11), 642–67.

Santini, P., Lemanski, R., and Erdos, P. (1999) *Adv. Phys.,* **48**(5), 537–653.

Santoro, A., Marezio, M., Roth, R. S., and Minor, D. (1980) *J. Solid State Chem.,* **35**(2), 167–75.

Sari, C., Benedict, U., and Blank, H. (1968) *Metallographic and X-ray Investigations in the Plutonium–Oxygen and Uranium–Plutonium–Oxygen Systems*, *Proc. Symp. on Thermodynamics of Nuclear Materials*, Vienna, Austria, pp. 587–611.

Sari, C., Benedict, U., and Blank, H. (1970) *J. Nucl. Mater.,* **35**(3), 267–77.

Sarrao, J. L., Morales, L. A., Thompson, J. D., Scott, B. L., Stewart, G. R., Wastin, F., Rebizant, J., Boulet, P., Colineau, E., and Lander, G. H. (2002) *Nature,* **420**(6913), 297–9.

Sarrao, J. L., Morales, L. A., Thompson, J. D., Scott, B. L., Stewart, G. R., Wastin, F., Rebizant, J., Boulet, P., Colineau, E., and Lander, G. H. (2003a) *AIP Conf. Proc.,* **673** (Plutonium Futures – The Science), 12–14.

Sarrao, J. L., Morales, L. A., and Thompson, J. D. (2003b) *J. Metals,* **55**(9), 38–40.

Sasao, N. and Yamaguchi, H. (1991) *Apparatus for Laser Isotope Separation*, (Power Reactor and Nuclear Fuel Development Corp., Japan). Jpn. Patent 03068420, 10 pp.

Sastre, A. M., Kumar, A., Shukla, J. P., and Singh, R. K. (1998) *Sep. Purif. Methods,* **27**(2), 213–98.

Savage, D. J. and Kyffin, T. W. (1986) *Polyhedron,* **5**(3), 743–52.

Savrasov, S. Y., Kotliar, G., and Abrahams, E. (2001) *Nature,* **410**(6830), 793–5.

Scheitlin, F. M. and Bond, W. D. (1980) *Recovery of Plutonium from HEPA Filters by Cerium(IV)*, *Promoted Dissolution of Plutonium Dioxide and Recycle of the Cerium Promoter*, Report ORNL/TM-6802, Oak Ridge National Laboratory, Oak Ridge, TN, 58 pp.

Scheuer, U. and Lengeler, B. (1991) *Phys. Rev. B,* **44**(18), 9883–94.

Schlechter, M. (1970) *J. Nucl. Mater.,* **37**(1), 82–8.

Schlesinger, H. I. and Brown, H. (1943) *Chemical Separation of 94 from Uranium on the Basis of the Volatility of the Borohydrides*, Report CN-441, University of Chicago.

Schmutz, H. (1966) *System Alkali Fluoride–Lanthanide/Actinide Fluoride (Lithium, Sodium, Potassium, Rubidium–Lanthanum, Rare Earths, Yttrium/Neptunium, Americium)*, Report KFK-431, Kernforschungszentrum, Karlsruhe, Germany, 73 pp.

Schneider, V. W. and Roepenack, H. (1986) Fabrication of (U/Pu)O_2-mixed oxide Fuel Elements, in *Handbook on the Physics and Chemistry of the Actinides* (eds. A. J. Freeman and C. Keller), Elsevier Science, New York, 531–55.

Schonfeld, F. W. (1961) Pu Phase Diagrams, in *The Metal Plutonium* (eds. A. S. Coffinberry and W. N. Miner), University of Chicago Press, Chicago, 243.

Schonfeld, F. W. and Tate, R. E. (1996) *The Thermal Expansion Behavior of Unalloyed Plutonium*, Report LA-13034-MS, Los Alamos National Laboratory, pp. 1–34.

Schonfeld, F. W., Cramer, E. M., Miner, W. N., Ellinger, F. H., and Coffinberry, A. S. (1959) *Prog. Nucl. Energy* (eds. H. M. Finniston, and J. P. Howe, Pergamon Press) *Ser. V,* **2**, 579–99.

Schreckenbach, G., Hay, P. J., and Martin, R. L. (1999) *J. Comput. Chem.,* **20**(1), 70–90.

Schwartz, A. J., Wall, M. A., Zocco, T. G., and Wolfer, W. G. (2005) *Philos. Mag.,* **85**, 479–88.

Seaborg, G. T. (1958) *The Transuranium Elements*, Addison-Wesley, Reading, MA, 348 pp.

Seaborg, G. T. (1977) *History of Met Lab section C-I, April 1942 – April 1943*, Report PUB-112(vol.1), Lawrence Berkeley Laboratory, University of California, Berkeley, CA, 708 pp.

Seaborg, G. T. (1978) *History of Met Lab section C-I, May 1943 – April 1944*, Report PUB-112(vol.2), Lawrence Berkeley Laboratory, University of California, Berkeley, CA, 581 pp.

Seaborg, G. T. (1979) *History of Met Lab section C-I, May 1944 – April 1945*, Report PUB-112(Vol.3), Lawrence Berkeley Laboratory, University of California, Berkeley, CA, 625 pp.

Seaborg, G. T. (1980) *History of Met Lab section C-I, May 1945 – May 1946*, Report PUB-112(vol. 4), Lawrence Berkeley Laboratory, University of California, Berkeley, CA, 657 pp.

Seaborg, G. T. (1983) *ACS Symp. Ser.* **216**(Plutonium Chem.) (eds. W. T. Carnall and G. R. Choppin), American Chemical Society, Washington, DC, pp. 1–22.

Seaborg, G. T. (1992) *Transuranium Elements. A Half Century* (eds. L. R. Morss and J. Fuger), American Chemical Society, Washington, DC, pp. 10–49.

Seaborg, G. T. (1995) *Radiochim. Acta,* **70/71**, 69–90.

Seaborg, G. T. and Katz, J. J. (1990) *Proc. Robert A. Welch Found. Conf. Chem. Res.,* **34**, 224–51.

Seaborg, G. T. and Loveland, W. D. (1990) *The Elements beyond Uranium,* John Wiley & Sons, New York, 359 pp.

Seaborg, G. T. and Perlman, M. L. (1948) *J. Am. Chem. Soc.,* **70**, 1571–3.

Seaborg, G. T. and Wahl, A. C. (1948a) *J. Am. Chem. Soc.,* **70**, 1128–34.

Seaborg, G. T. and Wahl, A. C. (1948b) *J. Am. Chem. Soc.,* **70**(3), 1128–34.

Seaborg, G. T., Wahl, A. C., and Kennedy, J. W. (1946) *Phys. Rev.,* **69**, 367.

Seaborg, G. T., Wahl, A. C., and Kennedy, J. W. (1949a) *Natl. Nucl. Energy Ser.,* Div. IV **14B**(Transuranium Elements, Pt. I), (eds. G. T. Seaborg, J. J. Katz and W. M. Manning), McGraw-Hill, New York, 13–20.

Seaborg, G. T., Katz, J. J., and Manning, W. M. (eds.) (1949b) *Natl. Nucl. Energy Ser.,* Div IV **14**B (Transuranium Elements Pt. I), McGraw-Hill, New York.

Selle, J. E. and Etter, D. E. (1964) *Trans. Metall. Soc. AIME,* **230**(5), 1000–5.
Selle, J. E., English, J. J., Teaney, P. E., and McDougal, J. R. (1970a) *Compatibility of Plutonium-238 Dioxide with Various Refractory Metals and Alloys: Interim Report*, Report MLM-1706, Mound Laboratoary, Miamisburg, OH, 214 pp.
Selle, J. E., McDougal, J. R., and Schaeffer, D. R. (1970b) *Compatibility of Plutonium-238 Dioxide with Platinum and Platinum–Rhodium Alloys*, Report MLM-1684, Mound Laboratory, Miamisburg, OH, 124 pp.
Serpan, C. Z. and Wittenberg, L. J. (1961) *Trans. Metall. Soc. AIME,* **221**(5), 1017–20.
Seyferth, D. (2004) *Organometallics,* **23**(15), 3562–83.
Shacklett, R. L. and Du Mond, J. W. M. (1957) *Phys. Rev.,* **106**, 501–12.
Sheft, I. and Davidson, N. R. (1949a) Equilibrium in the Vapor-phase Hydrolysis of Plutonium Tribromide, in *Natl. Nucl. Energy Ser.,* Div **14**B, (Transuranium Elements Pt. I) (eds. G. T. Seaborg, J. J. Katz, and W. M. Manning), McGraw-Hill, New York, pp. 831–40.
Sheft, I. and Davidson, N. R. (1949b) Equilibrium in the Vapor-phase Hydrolysis of Plutonium Trichloride, in *Natl. Nucl. Energy Ser.,* Div **14**B, (Transuranium Elements Pt. I) (eds. G. T. Seaborg, J. J. Katz, and W. M. Manning), McGraw-Hill, New York, pp. 841–7.
Sheft, I., Andrews, H. and Katz, J. J. (1949) *Summary Report for July, August, and September 1949*, Report ANL-4379, Chemistry Division, Section C1, Argonne National Laboratory, Argonne National Laboratory, pp. 43–50.
Sheldon, R. I., Rinehart, G. H., Krishnan, S., and Nordine, P. C. (2001) *Mater. Sci. Eng.,* **B79**, 113–22.
Sherby, O. D. and Simnad, M. T. (1961) *Am. Soc. Metals, Trans. Quart.,* **54**, 227–40.
Shewmon, P. G. (1963) *Diffusion in Solids,* McGraw-Hill, New York, 134 pp.
Shick, A. B., Drchal, V., and Havela, L. (2005) *Europhys. Lett.,* **69**(4), 588–94.
Shilov, V. P. (1997) *Radiokhimiya,* **39**(4), 330–2 (pp. 328–31 in English translation.).
Shilov, V. P. (1998) *Radiochemistry,* **40**(1), 11–16.
Shilov, V. P. and Yusov, A. B. (2002) *Russ. Chem. Rev.,* **71**(6), 465–88.
Shorikov, A. O., Lukoyanov, A. V., Korotin, M. A., and Anisimov, V. I. (2005) *Los Alamos National Laboratory, Preprint Archive, Condensed Matter*: 1–21, arXiv:cond-mat/0412724 v2.
Shumakov, V. D., Kosulin, N. S., and Chebotarev, N. T. (1990) *Phys. Metal Metalloved (Russian),* **37**, 14.
Shvareva, T. Y., Almond, P. M., and Albrecht- Schmitt, T. E. (2005) *J. Solid State Chem.,* **178**(2), 499–504.
Silva, R. J. and Nitsche, H. (1995) *Radiochim. Acta,* **70/71**, 377–96.
Silva, R. J. and Nitsche, H. (2002) *Environmental Chemistry*, in *Advances in Plutonium Chemistry 1967–2000* (ed. D. C. Hoffman), American Nuclear Society and the University Research Alliance, La Grange Park, IL, pp. 89–111.
Silva, R. J., Bidoglio, G., Rand, M. H., Robouch, P. B., Wanner, H., and Puigdomenech, I. (1995) *Chemical Thermodynamics of Americium,* Elsevier Science Publishers, Amsterdam, Netherlands, 392 pp.
Silver, G. L. (1971) *J. Inorg. Nucl. Chem.,* **33,** 577–583.
Silver, G. L. (1997) *Radiochim. Acta,* **77**, 189.
Silver, G. L. (2002) *Appl. Radiat. Isot.* **57,** 1–5.
Silver, G. L. (2003) *Appl. Radiat. Isot.* **59,** 217–20.

Silver, G. L. (2004) *J. Radioanal. Nucl. Chem.* **262**(3), 779–781.
Silvestre, J. P., Freundlich, W., and Pagès, M. (1977) *Rev. Chim. Miner.,* **14**(2), 225–9.
Simakin, G. A., Volkov, Y. F., Visyashcheva, G. I., Kapshukov, I. I., Baklanova, P. F., and Yakovlev, G. N. (1974) *Sov. Radiochem.,* **16**(6), 838–41.
Simon, G. P. (1991) *Ion Exchange Training Manual.* Van Nostrand Reinhold, New York, pp. 1–47.
Skavdahl, R. E. (1963) *Plutonium–Boron System*, Report HW-76302, Article 2.4, US Atomic Energy Commission.
Skavdahl, R. E. (1964) *The Reactions between PuO_2 and Carbon*, Report HW-77906 12 pp.
Skavdahl, R. E. and Chikalla, T. D. (1964) *The Plutonium–Boron System*, Report HW-81602, Article 2.1, US Atomic Energy Commission.
Skavdahl, R. E., Chikalla, T. D., and McNeilly, C. E. (1964) *Trans. Am. Nucl. Soc.,* **7**, 403–4.
Skriver, H. L. (1985) *Phys. Rev. B,* **31**, 1909.
Smirnov, E. A. and Shmakov, A. A. (1999) *Defect Diffus. Forum,* **166**, 63–7.
Smith, J. L. (1980) No superconductivity in plutonium, personal communication, S. S. Hecker, Los Alamos, NM.
Smith, J. L. and Fisk, Z. (1982a) *J. Appl. Phys.,* **53(11)**, 7883–6.
Smith, J. L. and Haire, R. G. (1978) *Science,* **200**(4341), 535–7.
Smith, J. L. and Kmetko, E. A. (1983) *J. Less-Common Met.,* **90**(1), 83–8.
Smolders, A. and Gilissen, R. (1987) *Mater. Sci. Monogr.,* **38C**(High Tech Ceram., Pt. C), 2849–60.
Soderlind, P. (2001) *Europhys. Lett.,* **55**(4), 525–31.
Sokhina, L. P., Solovkin, A. S., Teterin, E. G., Bogdanov, F. A., and Shesterikov, N. N. (1978) *Radiokhimiya,* **20**(1), 28–34.
Solar, J. P., Burghard, H. P. G., Banks, R. H., Streitwieser, A., Jr, and Brown, D. (1980) *Inorg. Chem.,* **19**(7), 2186–8.
Solovkin, A. S. and Rubisov, V. N. (1983) *Radiokhimiya,* **25**(5), 625–8.
Sood, D. D., Jayadevan, N. C., Mudher, K. D. S., Khandekar, R. R., and Krishnan, K. (1992) *Transuranium Elements: A Half Century* (eds. L. R. Morss and J. Fuger), American Chemical Society, Washington, DC, pp. 524–32.
Sorantin, H. (1975) *Determination of Uranium and Plutonium in Nuclear Fuels,* Verlag Chemie, Weinheim, Germany, 285 pp.
Spear, K. E. (1976) *J. Less-Common Met.,* **47**, 195–201.
Spear, K. E. and Leitnaker, J. M. (1968) *Review and Analysis of Phase Behavior and Thermodynamic Properties of the Plutonium–Nitrogen System*, Report ORNL-TM-2106, Oak Ridge National Laboratory, Oak Ridge, TN, 24 pp.
Spedding, F. H., Kant, A., Wright, J. M., Warf, J. C., Powell, J. E., and Newton, A. S. (1945) *Extraction Purification of Thorium Nitrate*, Report CC-2393.
Spinks, J. W. T. and Woods, R. J. (1990) *An Introduction to Radiation Chemistry,* 3rd ed, John Wiley & Sons, New York, Ch. 7, 574 pp.
Spirlet, J. C. (1982) *Nucl. Instrum. Methods,* **200**(1), 45–53.
Spirlet, J. C. (1991) Synthesis of f-element Pnictides, in *Topics in f-element Chemistry,* vol. 2, (eds. G. Meyer and L. R. Morss), Kluwer Academic Publishers, Boston, pp. 353–67.

Spirlet, J. C. and Vogt, O. (1982) *J. Magn. Magn. Mater.,* **29**(1–3), 31–8.

Spirlet, M. R., Rebizant, J., Apostolidis, C., Kanellakopulos, B. K., and Dornberger, E. (1992) *Acta Crystallogr.,* **C48**(7), 1161–4.

Spitsyn, V. I., Gel'man, A. D., Krot, N. N., Mefod'eva, M. P., Zakharova, F. A., Komkov, Y. A., Shilov, V. P., and Smirnova, I. V. (1969) *J. Inorg. Nucl. Chem.,* **31**(9), 2733–45.

Spriet, B. (1963) *Mem. Etud. Sci. Rev. Met.,* **60**, 531.

Spriet, B. (1965) *J. Nucl. Mater.,* **15**(3), 220–30.

Spriet, B. (1967) Study of Allotropic Transformation of Plutonium, in *Plutonium 1965* (eds. A. E. Kay and M. B. Waldron), Chapman and Hall, London, England, pp. 88–117.

Sriyotha, U. (1968) *Phase Equilibrium in the UO_{2+x}-$LuO_{1.5}$($ErO_{1.5}$) and $LuO_{1.5}$-UO_2(NpO_2,NpO_{2+x},PuO_2,PuO_{2+x}) Systems*, Thesis, Report KFK-737, Kernforschungszentrum, Karlsruhe, Germany, 61 pp.

Stakebake, J. L., Larson, D. T., and Haschke, J. M. (1993) *J. Alloys Compd.,* **202**(1–2), 251–63.

Standifer, R. L. (1968) *Fluoride Volatility 1968, Proc. Rocky Flats Fluoride Volatility Conf.,* Jun. 24–25, 1968, (eds. J. M. Cleveland and M. A. Thompson), Dow Chemical Company, pp. 79–98.

Staritzky, E. (1956) *Anal. Chem.,* **28**(12), 2021–2.

Staritzky, E. and Singer, J. (1952) *Acta Crystallogr.,* **5**, 536–40.

Starks, D. F. and Streitwieser, A., Jr (1973) *J. Am. Chem. Soc.,* **95**(10), 3423–4.

Steindler, M. J. (1963a) *Laboratory Investigations in Support of Fluid-bed Fluoride Volatility Processes*, part II, *The Properties of Plutonium Hexafluoride*, Report ANL-6753, Argonne National Laboratory, 83 pp.

Steindler, M. J. and Gunther, W. H. (1964a) *Laboratory Investigations in Support of Fluid-bed Fluoride Volatility Processes*, part VI, *A. The Absorption Spectrum of Plutonium Hexafluoride. B. Analysis of Mixtures of Plutonium Hexafluoride and Uranium Hexafluoride by Absorption Spectrometry*, Report ANL-6817, Argonne National Laboratory, 16 pp.

Steindler, M. J. and Gunther, W. H. (1964b) *Spectrochim. Acta,* **20**(8), 1319–22.

Steindler, M. J., Steidl, D. V., and Steunenberg, R. K. (1958) *The Fluorination of Plutonium Tetrafluoride*, Report ANL-5875, Argonne National Laboratory, 29 pp.

Steindler, M. J., Steidl, D. V., and Steunenberg, R. K. (1959) *Nucl. Sci. Eng.,* **6**(4), 333–40.

Steindler, M. J., Steidl, D. V., and Fischer, J. (1963) *Laboratory Investigations in Support of Fluid-bed Fluoride Volatility Processes*, part V, *The Radiation Chemistry of Plutonium Hexafluoride*, Report ANL-6812, Argonne National Laboratory, 24 pp.

Stewart, D. C. (1956) *Absorption Spectra of Lanthanide and Actinide Rare Earths. III. Heavier Lanthanide Elements in Aqueous Perchloric Acid Solution*, Report ANL-5624, US Atomic Energy Commission, 16 pp.

Stewart, G. R. and Elliott, R. O. (1981) *Specific Heat Studies of Alpha and Delta Plutonium. Actinides - 1981*, Report LBL-12441, Lawrence Berkeley Laboratory, Berkeley, CA.

Stiffler, G. L. and Curtis, M. H. (1960) *The Preparation of Plutonium Powder by a Hydriding Process: Initial Studies*, Report HW-64, 289, US Atomic Energy Commission, 17 pp.
Stoll, W., Scheider, V., and Ost, C. (1982) German Patent 3, **101**, 505 A.
Storms, E. K. (1964) *A Critical Review of Refractories*, Report LA-2942, US Atomic Energy Commission, 245 pp.
Storms, E. K. (1967) *The Refractory Carbides,* vol. 2 (*Refractory materials series*) Academic Press, New York, 284 pp.
Stout, B. E., Choppin, G. R., Nectoux, F., and Pagès, M. (1993) *Radiochim. Acta,* **61**, 65.
Stout, M. G., Kachner, G. C., and Hecker, S. S. (2002) *Mechanical Behavior of Delta-Phase Plutonium–Gallium Alloys*, Report LA-994458-PR-Revised, Los Alamos National Laboratory, pp. 1–38.
Stöwe, K. (2000) *J. Solid State Chem.,* **149**, 155–66.
Stoyer, N. J., Hoffman, D. C., and Silva, R. J. (2000) *Radiochim. Acta,* **88**(5), 279–82.
Stradling, G. N., Stather, J. W., Gray, S. A., Moody, J. C., Ellender, M., Hodgson, A., Volf, V., Taylor, D. M., Wirth, P., and Gaskin, P. W. (1989) *Int. J. Radiat. Biol.,* **56**(4), 503–14.
Stratton, R. W., Ledergerber, G., Ingold, F., Nicolet, M., and Botta, F. (1987) *Improv. Water React. Fuel Technol. Util., Proc. Int. Symp.*, pp. 353–62.
Stumpe, R., Kim, J. I., Schrepp, W., and Walther, H. (1984) *Appl. Phys. B-Photo,* **34**(4), 203–6.
Sugar, J. (1973) *J. Chem. Phys.,* **59**(2), 788–91.
Sugar, J. (1974) *J. Chem. Phys.,* **60**(10), 4103.
Sullivan, J. C., Hindman, J. C., and Zielen, A. J. (1961) *J. Am. Chem. Soc.,* **83**(16), 3373–8.
Sullivan, J. C., Woods, M., Bertrand, P. A., and Choppin, G. R. (1982) *Radiochim. Acta,* **31**(1–2), 45–50.
Sullivan, J. C., Choppin, G. R., and Rao, L. F. (1991) *Radiochim. Acta,* **54**(1), 17–20.
Sundaram, S. (1962) *Z. Phys. Chem.,* **34**, 225–32.
Suzuki, Y., Arai, Y., and Sasayama, T. (1983) *J. Nucl. Mater.,* **115**(2–3), 331–3.
Swanson, J. L. (1964) *J. Phys. Chem.,* **68**(2), 438–9.
Swanson, J. L. (1990) The PUREX Process. Part 3: PUREX Process Flowsheets. Science and Technology of Tributyl Phosphate, vol. 3, *Applications of Tributyl Phosphate in Nuclear Fuel Processing* (eds. W. W. Schulz, J. D. Navratil, L. L. Burger and K. P. Bender), CRC Press, Boca Raton, FL, pp. 55–79.
Tabuteau, A. and Pagès, M. (1980) *J. Inorg. Nucl. Chem.,* **42**(3), 401–3.
Tabuteau, A., Pagès, M., and Freundlich, W. (1972) *Mater. Res. Bull.,* **7**(7), 691–7.
Tait, C. D., Donohoe, R. J., Clark, D. L., Conradson, S. D., Ekberg, S. A., Keogh, D. W., Neu, M. P., Reilly, S. R., Runde, W. H., and Scott, B. L. (2004) *Actinide Research Quarterly,* Report LA-LP-04-60, Los Alamos National Laboratory, **1,** 20–2.
Takano, M., Itoh, A., Akabori, M., Ogawa, T., Numata, M., and Okamoto, H. (2001) *J. Nucl. Mater.,* **294**(1,2), 24–7.
Tan, J.-h. (2003) *Sichuan Shifan Daxue Xuebao, Ziran Kexueban,* **26**(3), 297–9.
Tananaev, I. G. (1989) *Radiokhimiya,* **31**(3), 46–51.
Tananaev, I. G., Rozov, S. P., and Mironov, V. S. (1992) *Radiokhimiya,* **34**(3), 88–92.

Tate, R. E. and Anderson, R. W. (1960) Some experiments in zone refining plutonium, *Extract. Phys. Met. Plutonium and Alloys, Symposium,* San Francisco, CA, Interscience, New York, pp. 231–42.

Tate, R. E. and Cramer, E. M. (1964) *Trans AIME,* **230**, 639.

Tate, R. E. and Edwards, G. R. (1966) *Diffusion*. Symposium on thermodynamics with emphasis on nuclear materials and atomic transport, Vienna, Austria, 2, 105 pp.

Taube, M. (1964) *Plutonium,* Macmillan Publishing, New York, 258 pp.

Taylor, J. M. (1966) *Physical Properties of Several Pu-base Intermetallic Compounds*, Report BNWLSA-385, Pacific Northwest Laboratory, Battelle Memorial Institute, Richland, WA, 7 pp.

Taylor, D. M. (1998) *J. Alloys Compd.,* **271–273**, 6–10.

Taylor, J. C., Loasby, R. G., Dean, D. J., and Linford, P. F. (1965) Elastic Constants, *Plutonium 1965, Proc. Third Int. Conf.,* London, England (eds. A. E. Kay and M. B. Waldron), Chapman and Hall, New York, 162 pp.

Taylor, J. C., Linford, P. F. T., and Dean, D. J. (1968) *J. Inst. Metals,* **96**(Part 6), 178–82.

Taylor, K. M., Andersen, J. C., Strasser, A., Stahl, D., and Forbes, R. L. (1967) *J. Am. Ceram. Soc.,* **50**(6), 321–5.

Taylor, R. J., Mason, C., Cooke, R., and Boxall, C. (2002) *J. Nucl. Sci. Technol.* (Suppl. 3), 278–81.

Terada, K., Meisel, R. L., and Dringman, M. R. (1969) *J. Nucl. Mater.,* **30**(3), 340–2.

Terminello, L. J., Caturla, M. J., Fluss, M. J., Gouder, T., Haire, R. G., Haschke, J. M., Hecker, S. S., Lander, G. H., Muller, I., Nitsche, H., Rebizant, J., Schwartz, A. J., Silva, R. J., Wall, M. A., Wastin, F., Weber, W. J., Wirth, B. D., and Wolfer, W. G. (2001) *Mater. Res. Soc. Bull.,* **26**(9), 667–71.

Teterin, Y. A. and Teterin, A. Y. (2004) *Russ. Chem. Rev.,* **73**(6), 541–80.

Tetzlaff, R. N. (1962) *Chemical Processing of 238Pu*, E. I. du Pont de Nemours & Co., Aiken, SC, Report DP-729, US Atomic Energy Commission, 30 pp.

Thiyagarajan, P., Diamond, H., Soderholm, L., Horwitz, E. P., Toth, L. M., and Felker, L. K. (1990) *Inorg. Chem.,* **29**(10), 1902–7.

Thomas, C. A. (1944) *The Chemistry, Purification and Metallurgy of Plutonium*, Report MUC-JCW-223 (Books 1 and 2) (Dec. 1944).

Thomas, W. (1969) *Critical and Safe Parameters for Plutonium and Plutonium Compounds*, Report MRR-56, Inst Mess- Regelungstech., Tech. Hochsch. Muenchen, Munich, Germany, 40 pp.

Thompson, M. A. (1965) Plutonium Oxidation, in *Plutonium 1965* (eds. A. E. Kay and R. G. Loasby), London, England, 592 pp.

Thompson, G. H. (1972) *Radiochem. Radioanal. Let.,* **10**(4), 223–30.

Thompson, S. G. and Seaborg, G. T. (1956) First use of bismuth phosphate for separating plutonium from uranium and fission products, *Progress in nuclear energy-Series 3*, *Process chemistry* (eds. F. R. Bruce, J. M. Fletcher, H. H. Hyman, and J. J. Katz), pp. 163–71.

Thuemmler, F., Theisen, R., and Patrussi, E. (1967) *Phase Relations, Production, and Characteristics of Substoichiometric Uranium and Plutonium oxide Fuels* (UO_{2-x} *and* (*Uranium, Plutonium Uranium*)O_{2-x}), Report KFK-543, Kernforschungszentrum, Karlsruhe, Germany, 44 pp.

Timofeeva, L. F. (2001) Phase Diagrams, in *Ageing Studies and Lifetime Extension of Materials* (ed. L. G. Mallinson), Kluwer Academic Publishers, New York, 191 pp.
Timofeeva, L. F. (2003a) *J. Metals*, (September 2003), 51–4.
Timofeeva, L. F. (2003b) *At.Energ.,* **95**(2), 540–5.
Toevs, J. W. (1997) *Surplus Weapons Plutonium: Technologies for Pit Disassembly/ Conversion and MOX Fuel Fabrication*, Report LA-UR-97-4113, Los Alamos National Laboratory, 8 pp.
Tolley, W. B. (1953) *Plutonium Trichloride: Preparation by Reaction with Phosgene or Carbon Tetrachloride, and Bomb Reduction to Metal*, Report HW-30121, General Electric Company, Richland, WA, 28 pp.
Toth, L. M., Friedman, H. A., and Osborne, M. M. (1981) *J. Inorg. Nucl. Chem.,* **43**(11), 2929–34.
Trevorrow, L. E. and Shinn, W. A. (1960) *in Chemical Engineering Division Summary Report for October, November, December 1959* (eds. Lawroski, S, Roedge, W. A., Vogel, R. C., Munnecke, V. H.), Report ANL-6101, Argonne National Laboratory, 80 pp.
Trevorrow, L., Shinn, W. A., and Steunenberg, R. K. (1961) *J. Phys. Chem.,* **65**(3), 398–403.
Trevorrow, L. E., Kessie, R. W., and Steindler, M. J. (1965) *Laboratory Investigations in Support of Fluid-bed Fluoride Volatility Process*, part VIII, *Analysis of an Accidental Multigram Release of Plutonium Hexafluoride in a Glovebox*, Report ANL-7068, Argonne National Laboratory, 20 pp.
Triay, I. R., Hobart, D. E., Mitchell, A. J., Newton, T. W., Ott, M. A., Palmer, P. D., Rundberg, R. S., and Thompson, J. L. (1991) *Radiochim. Acta,* **52–53**(Pt. 1), 127–31.
Trofimov, T. I., Samsonov, M. D., Kulyako, Y. M., and Myasoedov, B. F. (2004) *CR Chim,* **7**(12), 1209–13.
Tuli, J. K. (ed.) (2004) *Nuclear Data Sheets,* Academic Press, San Diego.
Turchi, E. A., Gonis, A., and Shull, R. D. (eds.) (2002) *CALPHAD and Alloy Thermodynamics,* TMS-Minerals, Metals & Materials Society, Warrendale, PA, 281 pp.
Turchi, P. E. A., Kaufman, L., Lui, Z.-K., and Zhou, S. (2004) *Thermodynamics and Kinetics of Phase Transformations in Plutonium Alloys* - part I, Report UCRL-TR-206658, Lawrence Livermore National Laboratory,
Ueno, K. and Hoshi, M. (1970) *J. Inorg. Nucl. Chem.,* **32**, 381.
Ugajin, M. and Abe, J. (1973) *J. Nucl. Mater.,* **47**(1), 117–20.
Ullman, W. J. and Schreiner, F. (1986) *Radiochim. Acta,* **40**(4), 179–83.
Ullman, W. J. and Schreiner, F. (1988) *Radiochim. Acta,* **43**(1), 37–44.
Usami, T., Kurata, M., Inoue, T., Sims, H. E., Beetham, S. A., and Jenkins, J. A. (2002) *J. Nucl. Mater.,* **300**(1), 15–26.
Vaidya, V. N., Kamat, R. V., Joshi, J. K., Iyer, V. S., Suryanarayana, S., Srinivasan, N. L., Pillai, K. T., and Sood, D. D. (1983) *Proc. Nucl. Chem. Radiochem. Symp.*, pp. 549–51.
Van der Sluys, W. G., Burns, C. J., Huffman, J. C., and Sattelberger, A. P. (1988) *J. Am. Chem. Soc.,* **110**(17), 5924–5.
Van der Sluys, W. G., Burns, C. J., and Sattelberger, A. P. (1989) *Organometallics,* **8**(3), 855–7.

Varlashkin, P. G., Begun, G. M., and Peterson, J. R. (1984) *Radiochim. Acta,* **35**(4), 211–18.

Vdovenko, V. M., Vodovatov, V. A., Mashirov, L. G., and Suglobov, D. N. (1973) *Dokl. Akad. Nauk SSSR,* **209**(2), 352–5.

Veirs, D. K., Smith, C. A., Berg, J. M., Zwick, B. D., Marsh, S. F., Allen, P., and Conradson, S. D. (1994) *J. Alloys Compd.,* **213–214**, 328–32.

Vesnovskii, S. P. and Polynov, V. N. (1992a) in *Transuranium Elements: A Half Century* (eds. L. R. Morss and J. Fuger), American Chemical Society, Washington, DC, 131–6.

Vesnovskii, S. P. and Polynov, V. N. (1992b) *Nucl. Instrum. Methods Phys. Res., Sect. B,* **b70**(1–4), 9–11.

Viklund, C., Nordstrom, A., Irgum, K., Svec, F., and Frechet, J. M. J. (2001) *Macromolecules,* **34**(13), 4361–9.

Vladimirova, M. V. (1982) *Sov. Radiochem.,* **24**(4), 393–401.

Vladimirova, M. V. (1990) *J. Radioanal. Nucl. Chem.,* **143**(2), 445–54.

Vladimirova, M. V. (1998) *Sov. Radiochem.,* **40**(5), 395–404.

Vladimirova, M. V. and Kulikov, I. A. (2002) *Radiochemistry (Moscow, Russian Federation) (Translation of Radiokhimiya),* **44**(1), 86–90.

Vogt, O. and Mattenberger, K. (1993) *Handbook on the Physics and Chemistry of Rare Earths,* vol. 17 (eds. K. A. J. Gschneidner, L. Eyring, G. R. Choppin, and G. H. Lander), Elsevier Science, New York, 301 pp.

Vogt, O. and Mattenberger, K. (1995) *J. Alloys Compd.,* **223**(2), 226–36.

Volkov, Y. F., Kapshukov, I. I., Visyashcheva, G. I., and Yakovlev, G. N. (1974a) *Radiokhimiya,* **16**(6), 863–7.

Volkov, Y. F., Kapshukov, I. I., Visyashcheva, G. I., and Yakovlev, G. N. (1974b) *Radiokhimiya,* **16**(6), 868–73.

Volkov, Y. F., Visyashcheva, G. I., Tomilin, S. V., Kapshukov, I. I., and Rykov, A. G. (1981) *Radiokhimiya,* **23**(2), 254–8.

Vyatkin, V. E., Davidov, Y. P., and Shashukov, E. A. (1972) *Radiokhimiya,* **14**(2), 289–93 (pp 299–303 in English translation).

Waber, J. T. (1958) *Plutonium Oxidation*, *Proc. Second UN Int. Conf. Peaceful Uses Atomic Energy*, Geneva, Switzerland, United Nations, 6, 204 pp.

Waber, J. T. (1980) Corrosion and Oxidation, in *Plutonium Handbook,* vol. 1 (ed. O. J. Wick), American Nuclear Society, La Grange, IL, pp. 145–89.

Waber, J. T., Olson, W. M., and Roof, R. B. (1961) *J. Nucl. Mater.,* **3**, 205.

Wachter, P. (2003) *Solid State Commun.,* **127**(9–10), 599–603.

Wachter, P., Marabelli, F., and Bucher, B. (1991) *Phys. Rev. B,* **43**(13-B), 11136–44.

Wachter, P., Filzmoser, M., and Rebizant, J. (2001) *Physica B,* **293**(3&4), 199–223.

Wade, W. Z. (1971) *J. Nucl. Mater.,* **38**, 292.

Wade, W. Z., Short, D. W., Walden, J. C., and Magana, J. W. (1978) *Metall. Trans. A,* **9A**, 965.

Wadt, W. R. (1987) *J. Chem. Phys.,* **86**(1), 339–46.

Wagner, R. P., Shinn, W. A., Fischer, J., and Steindler, M. J. (1965) *Laboratory Investigations in Support of Fluid-bed Fluoride Volatility Processes*, part VII, *The Decomposition of Gaseous Plutonium Hexafluoride by Alpha Radiation*, Report ANL-7013, Argonne National Laboratory, 32 pp.

Wahlgren, U., Moll, H., Grenthe, I., Schimmelpfennig, B., Maron, L., Vallet, V., and Gropen, O. (1999) *J. Phys. Chem. A,* **103**(41), 8257–64.

Waldek, A., Erdmann, N., Gruning, C., Huber, G., Kunz, P., Kratz, J. V., Lassen, J., Passler, G. and Trautmann, N. (2001) *RIMS Measurements for the Determination of the First Ionization Potential of the Actinides Actinium up to Einsteinium.* Melville, NY, American Institute of Physics, *AIP Conf. Proc.,* **584**, 219–24.

Waldron, M. B., Garstone, J., Lee, J. A., Mardon, P. G., Marples, J. A. C., Poole, O. M., and Williamson, G. K. (1958) *Proc. Second Int. Conf. Peaceful Uses of Atomic Energy*, vol. 6, Geneva, United Nations, 162 pp.

Wallace, P. L. and Harvey, M. R. (1974) *J. Nucl. Mater.,* **54**(2), 171–4.

Walter, K. H. (1965) *Ternary oxides of Tri- to Sexivalent Americium. Thesis*, Report KFK-280, Kernforschungszentrum, Karlsruhe, 76 pp.

Walters, R. T. and Briesmeister, R. A. (1984) *Spectrochim. Acta,* **40A**, 587.

Wang, R. and Steinfink, H. (1967) *Inorg. Chem.,* **6**(9), 1685–92.

Ward, J. W. (1985) *Physica B & C,* **130**(1–3), 510–15.

Ward, J. W. and Haschke, J. M. (1994) Comparison of 4f and 5f Element Hydride Properties, in *Handbook on the Physics and Chemistry of Rare Earths,* vol. 18 (eds. K. A. J. Gschneidner, E. L., G. R. Choppin, and G. H. Lander), Elsevier Science, New York, pp. 293–363.

Ward, J. W., Cort, B., Goldstone, J. A., Lawson, A. C., Cox, L. E., and Haire, R. G. (1992) in *Transuranium Elements: A Half Century* (eds. L. R. Morss and J. Fuger), American Chemical Society, Washington, DC, 404–15.

Warf, J. C. (1945) *The Extraction Purification of Cerium*, Report CC-2402.

Warner, B. P., D'Alessio, J. A., Morgan, A. N., III, Burns, C. J., Schake, A. R., and Watkin, J. G. (2000) *Inorg. Chim. Acta,* **309**(1–2), 45–8.

Wastin, F., Spirlet, J. C., and Rebizant, J. (1995) *J. Alloys Compd.,* **219**(1–2), 232–7.

Weber, E. T., Chikalla, T. D., and McNeilly, C. E. (1964) *The Plutonium–Boron System*, Report HW-81603, Article 2.9, US Atomic Energy Commission, 80 pp.

Weger, H. T., Okajima, S., Cunnane, J. C., and Reed, D. T. (1993) *Mater. Res. Soc. Symp. Proc.*, **294**(Scientific Basis Nucl. Waste Manag.), 739–45.

Wei, Y. Z., Arai, T., Hoshi, H., Kumagai, M., Bruggeman, A., Gysemans, M., and Sawa, T. (2002) *JAERI-Conf* **2002–004**(Proc. Int. Symp. NUCEF 2001), 225–36.

Weigel, F. (1965) *Preparation and Roentgenographic Study of Highly Radioactive Material*, Thesis, Report NP-15826, Munich University, 301 pp.

Weigel, F., Wishnevsky, V., and Hauske, H. (1977) *J. Less-Common Met.,* **56**(1), 113–23.

Weigel, F., Güldner, R., and Wishnevsky, V. (1982) *J. Less-Common Met.,* **84**(1), 147–55.

Weinstock, B. (1944) *Vapor Pressure of Plutonium Trichloride*, Report LA-122, Los Alamos Scientific Laboratory, 9 pp.

Weinstock, B. and Goodman, G. L. (1965) *Adv. Chem. Phys.,* **9**, 169–316.

Weinstock, B. and Malm, J. G. (1956a) *J. Inorg. Nucl. Chem.,* **2**(5–6), 380–94.

Weinstock, B. and Malm, J. G. (1956b) *Proc. First Int. Conf. on the Peaceful Uses of Atomic Energy*, vol. 2, New York, pp. 380–94.

Weinstock, B., Weaver, E. E., and Malm, J. G. (1959) *J. Inorg. Nucl. Chem.,* **11**(2), 104–14.

Weiss, R. J. (1963) *Proc. Phys. Soc.,* **62**, 28.

Wells, A. F. (1984) *Structural Inorganic Chemistry,* Oxford University Press, Oxford, England, 1382 pp.
Wensch, G. W. and Whyte, D. D. (1951) *The Nickel Plutonium System*, Report LA-1304, Los Alamos Scientific Laboratory, 29 pp.
Werner, G. D. (1982) *Doctoral Dissertation*, Report, University of Munich.
West, M. H., Ferran, M. D., and Fife, K. W. (1988) *The Chlorination of Plutonium Dioxide*, Report LA-11256, Los Alamos National Laboratory, Los Alamos, NM, 13 pp.
Wester, D. W. (1983) *ACS Symp. Ser.,* **216**(Plutonium Chem.), (eds. W. T. Carnall and G. R. Choppin) American Chemical Society, Washington, DC 49–63.
Wester, D. W. and Sullivan, J. C. (1983) *Radiochem. Radioanal. Lett.,* **57**, 35.
Westrum, E. F., Jr (1949a) Preparation and Properties of Plutonium Oxides, in *Natl. Nucl. Energy Ser.*, Div IV **14**B (Transuranium Elements Pt. II) (eds. G. T. Seaborg, J. J. Katz, and W. M. Manning), McGraw-Hill, New York, pp. 936–44.
Westrum, E. F., Jr (1949b) Preparation and Properties of Plutonium Silicides, in *Natl. Nucl. Energy Ser.*, Div IV **14**B (Transuranium Elements Pt. I) (eds. G. T. Seaborg, J. J. Katz, and W. M. Manning), McGraw-Hill, New York, pp. 729–30.
Westrum, E. F., Jr (1949c) Heat of Formation of Plutonium Tribromide, in *Natl. Nucl. Energy Ser.*, Div IV **14**B (Transuranium Elements Pt. II) (eds. G. T. Seaborg, J. J. Katz and W. M. Manning), McGraw-Hill, New York, pp. 926–9.
Westrum, E. F., Jr and Robinson, H. P. (1949a) Heat of Formation of Plutonium Trichloride, in *Natl. Nucl. Energy Ser.*, Div IV **14**B (Transuranium Elements Pt. II) (eds. G. T. Seaborg, J. J. Katz, and W. M. Manning), McGraw-Hill, New York, pp. 914–21.
Westrum, E. F., Jr and Robinson, H. P. (1949b) Heat of Formation of Plutonium Oxychloride, in *Natl. Nucl. Energy Ser.*, Div IV **14**B (Transuranium Elements Pt. II) (eds. G. T. Seaborg, J. J. Katz, and W. M. Manning), McGraw-Hill, New York, pp. 930–5.
Westrum, E. F., Jr and Wallmann, J. C. (1951) *J. Am. Chem. Soc.,* **73**, 3530–1.
Wick, O. J. (ed.) (1980) *Plutonium Handbook: A Guide to the Technology,* American Nuclear Society, La Grange Park, IL, 992 pp.
Wigley, D. A. (1964) PhD thesis, Oxford University, Oxford, UK.
Wigley, D. A. (1965) *Proc. Roy. Soc. Lond. Ser. A,* **284**(1398), 344–53.
Wilkinson, W. D. (ed.) (1960) *Extractive and Physical Metallurgy of Plutonium and its Alloys,* Interscience Publishers, New York.
Williams, C. W., Blaudeau, J. P., Sullivan, J. C., Antonio, M. R., Bursten, B., and Soderholm, L. (2001) *J. Am. Chem. Soc.,* **123**(18), 4346–7.
Willis, J. O., Ward, J. W., Smith, J. L., Kosiewicz, S. T., Haschke, J. M., and Hodges, A. E., III (1985) *Physica B & C,* **130**(1–3), 527–9.
Wills, J. M. and Eriksson, O. (2000) *Los Alamos Sci.,* **26**(1), 128.
Winchester, R. S. and Maraman, W. J. (1958) *Proc. Second UN Int. Conf. Peaceful Uses Atomic Energy*, vol. 17,Geneva, pp. 168–71.
Wirth, B. D., Schwartz, A. J., Fluss, M. J., Cartula, M. J., Wall, M. A., and Wolfer, W. G. (2001) *Mat. Res. Soc. Bull.,* **26**(9), 679–84.
Wiswall, R. J., Jr, Egan, J. J., Ginell, W. S., Miles, F. T., and Powell, J. R. (1959) *Recent Advances in the Chemistry of Liquid Metal Fuel Reactors*, *Proc. Second Int. Conf. Peaceful Uses of Atomic Energy*, 1958, Geneva, Switzerland, 17, pp. 421–7.

Wittenberg, L. J. (1963) *Symp. on Research at Mound Laboratory,* June 6–7, 1963, Report MLM-1163, Mound Laboratory, 157 pp.

Wittenberg, L. J. (1975) A Model for Liquid Uranium and Plutonium with Implications on the Adjacent Solid Phases, in *Plutonium and Other Actinides,* Baden-Baden, Germany (eds. H. Blank and R. Lindner), North-Holland, New York, pp. 71–83.

Wittenberg, L. J. and Grove, G. R. (1963) *Reactor Fuels and Materials Development. Plutonium Research*, Report MLM-1184, Mound Laboratory, pp. 12–16.

Wittenberg, L. J. and Grove, G. R. (1964) *Reactor Fuels and Materials Development. Plutonium Research*, Report MLM-1244, Mound Laboratory, 56 pp.

Wittenberg, L. J., Jones, L.V., and Ofte, D. (1960) *The Viscosity of a Liquid Pu-Fe Eutectic Alloy, Proc. Second Int. Conf. Plutonium,* Grenoble, France (eds. E. Grison, W. B. H. Lord, and R. D. Fowler), Cleaver-Hume Press, London, 1, pp. 671–83.

Wittenberg, L. J., Ofte, D., and Curtiss, C. F. (1968) *J. Chem. Phys.,* **48**(7), 3253–60.

Wittenberg, L. J., Vaughn, G. A., and DeWitt, R. (1970) *Phase Relationships in Uranium, Neptunium and Plutonium, Proc. Fourth Int. Conf. on Plutonium and Other Actinides,* Santa Fe, NM (ed. W. N. Miner), The Metallurgical Society of the AIME, II, 659–68.

Wolfer, W. G. (2000) *Los Alamos Sci.,* **26**(2), 274–85.

Wong, J., Holt, M., Hong, H., Schwartz, A. J., Zschack, P., Chiang, T. C., and Wall, M. (2003a) *AIP Conf. Proc.,* **673**(Plutonium Futures – The Science), 221–3.

Wong, J., Krisch, M., Farber, D. L., Occelli, F., Schwartz, A. J., Chiang, T. C., Wall, M., Boro, C., and Xu, R. Q. (2003b) *Science,* **301**(5636), 1078–80.

Wood, D. H., Cramer, E. M., Wallace, P. L., and Ramsey, W. J. (1969) *J. Nucl. Mater.,* **32**(2), 193–207.

Worden, E. F., Carlson, L. R., Johnson, S. A., Paisner, J. A., and Solarz, R. W. (1993) *J. Opt. Soc. Am.,* **B10**(11), 1998–2005.

Wriedt, H. A. (1989) *Bull. Alloy Phase Diagr.,* **10**(5), 593–602, 615–16.

Wriedt, H. A. (1990) *Bull. Alloy Phase Diagr.,* **11**(2), 184–202.

Wroblewska, J., Dobrowolski, J., Pages, M., and Freundlich, W. (1979) *Radiochem. Radioanal. Lett.,* **39**(3), 241–6.

Wruck, D. A., Russo, R. E., and Silva, R. J. (1994) *J. Alloys Compd.,* **213–214**, 481–3.

Wyckoff, R. W. G. (1963) *Crystal Structures,* Interscience, New York, 289 pp.

Wymer, R. G. (1968) *Sol-gel Processes for Ceramic Nuclear Fuels*, *Proc. Panel on Sol-gel Processes for Ceramic Nuclear Fuels*, Report STI/PUB–207;CONF-680532, International Atomic Energy Agency, pp. 131–72.

Wymer, R. G. and Coobs, J. H. (1967) *P. Brit. Ceramic Soc.,* **7**, 61–79.

Wynne, K. J. and Rice, R. W. (1984) *Annu. Rev. Mater. Sci.,* **14**, 297–334.

Yamaguchi, T., Sakamoto, Y., and Ohnuki, T. (1994) *Radiochim. Acta,* **66/67**, 9–14.

Yamashita, T., Ohuchi, K., Takahashi, K., and Fujino, T. (1992) Formation of Lithium Plutonates by the Reaction of Lithium Nitrate and Lithium Hydroxide with Plutonium dioxide, in *Transuranium Elements, A Half Century* (eds. L. R. Morss and J. Fuger), American Chemical Society, Washington, DC, pp. 451–6.

Yarbro, S. L., Schreiber, S. B., Ortiz, E. M., and Ames, R. L. (1998) *J. Radioanal. Nucl. Chem.,* **235**(1–2), 21–4.

Zachariasen, W. H. (1944) *X-ray Diffraction Results for Uranium and Plutonium Compounds*, Report CK-1367, Report USAEC Manhattan Project, Metallurgical Laboratory.
Zachariasen, W. H. (1948a) *Acta Crystallogr.,* **1**, 265–8.
Zachariasen, W. H. (1948b) *J. Am. Chem. Soc.,* **70**, 2147–51.
Zachariasen, W. H. (1948c) *Acta Crystallogr.,* **1**, 268–9.
Zachariasen, W. H. (1949a) in *Natl. Nucl. Energy Ser., Div. IV,* **14B**(Transuranium Elements Pt. II), (eds. G. T. Seaborg, J. J. Katz, and W. M. Manning), McGraw-Hill, New York, 1451–3.
Zachariasen, W. H. (1949b) *Acta Crystallogr.,* **2**, 94–9.
Zachariasen, W. H. (1949c) in *Natl. Nucl. Energy Ser., Div. IV,* **14B**(Transuranium Elements Pt. II), (eds. G. T. Seaborg, J. J. Katz, and W. M. Manning), 1448–50.
Zachariasen, W. H. (1949d) *Acta Crystallogr.,* **2**, 388–90.
Zachariasen, W. H. (1951) *Acta Crystallogr.,* **4**, 231–6.
Zachariasen, W. H. (1952) *Acta Crystallogr.,* **5**, 17–19.
Zachariasen, W. H. (1954a) *Acta Crystallogr.,* **7**, 795–9.
Zachariasen, W. H. (1954b) Crystal Chemistry of the 5f Elements, in *The actinide elements* (eds. G. T. Seaborg and J. J. Katz), McGraw-Hill, New York, pp. 769–96.
Zacharaisen, W. H. (1961a) Crystal-structure Studies of Plutonium Metal, in *The Metal Plutonium* (eds. A. S. Coffinberry and W. N. Miner), University of Chicago Press, Chicago, IL, pp. 99–107.
Zachariasen, W. H. (1961b) Crystal-structure Studies of Plutonium Metal, in *The Metal Plutonium* (eds. A. S. Coffinberry and W. N. Miner), University of Chicago Press, Chicago, IL, pp. 104–7.
Zachariasen, W. H. (1973) *J. Inorg. Nucl. Chem.,* **35**(10), 3487–97.
Zachariasen, W. H. and Ellinger, F. H. (1955) *Acta Crystallogr.,* **8**(7), 431–3.
Zachariasen, W. H. and Ellinger, F. H. (1957) *J. Chem. Phys.,* **27**(3), 811–12.
Zachariasen, W. H. and Ellinger, F. H. (1959) *Acta Crystallogr.,* **12**, 175–6.
Zachariasen, W. H. and Ellinger, F. H. (1963a) *Acta Crystallogr.,* **16**(8), 777–84.
Zachariasen, W. H. and Ellinger, F. H. (1963b) *Acta Crystallogr.,* **16**(5), 369–75.
Zachariasen, W. H. and Ellinger, F. H. (1970) *Unit Cell of the Zeta Phase of the Plutonium Zirconium and the Plutonium Hafnium Systems*, Report LA-4367, Los Alamos Scientific Laboratory, 4 pp.
Zagrai, V. D. and Sel'chenkov, L. I. (1962) *Radiokhimiya,* **4**, 181–4.
Zaitseva, V. P., Alekseeva, D. P., and Gel'man, A. D. (1973) *Radiokhimiya,* **15**(3), 385–90.
Zakharova, F. A., Orlova, M. M., and Gel'man, A. D. (1972) *Sov. Radiochem.,* **14**(1), 121–22.
Zalkin, A. and Raymond, K. N. (1969) *J. Am. Chem. Soc.,* **91**(20), 5667–8.
Zhou, J. S. and Goodenough, J. B. (2005) *Phys. Rev. Lett.,* **94**(6), 065501/1–065501/4.
Zocco, T. G. and Schwartz, A. J. (2003) *JOM,* **55**(9), 24–7.
Zocco, T. G., Stevens, M. F., Adler, P. H., Sheldon, R. I., and Olson, G. B. (1990) *Acta Met. Mater.,* **38**(11), 2275–82.
Zocco, T. T. and Rohr, D. L. (1988) *Mater. Res. Soc. Symp. Proc.*, **115** (Specimen Prep. Transm. Electron Mircosc. Mater.), 259–64.

Zubarev, V. G. and Krot, N. N. (1984) *Radiokhimiya,* **26**(2), 176–80.
Zukas, E. G., Hecker, S. S., Morgan, J. R., and Pereyra, R. A. (1981) *Pressure-induced Transformation in a Pu-2.0 at.% Al Alloy*, *Proc. Int. Conf. Solid-Solid Phase Transform*., Pittsburgh, AIME, 1, 1333–7.
Zukas, E. G., Hecker, S. S., and Pereyra, R. A. (1983) *J. Nucl. Mater.,* **115**(1), 63–8.
Zunger, A., Wei, S. H., Ferreira, L. G., and Bernard, J. E. (1990) *Phys. Rev. Lett.,* **65**(3), 353–6.
Zwick, B. D., Sattelberger, A. P., and Avens, L. R. (1992) in *Transuranium Elements: A Half Century* (eds. L. R. Morss and J. Fuger), American Chemical Society, Washington, DC, 239–46.